NON-PROPRIETARY VERSION

SAFETY ANALYSIS REPORT
on
THE HI-STAR 180D PACKAGE

(Revision 6)

by

Holtec International
Krishna P. Singh Technology Campus
1 Holtec Boulevard
Camden, NJ 08104
(holtecinternational.com)

USNRC Docket No. : 71-9367
Holtec Report No. : HI-2125175
Quality Designation : Safety Significant*

* The safety designation is pursuant to Holtec International's Quality Assurance Program.

REVISION SUMMARY LOG
(SAR ORGANIZATION, REVISION STATUS AND CONFIGURATION CONTROL AND SUMMARY OF CHANGES)

SAR Title: Safety Analysis Report on HI-STAR 180D Package

SAR Report No.: HI-2125175	**SAR Revision Number:** 6

ABOUT THIS SAR

This SAR is submitted to the USNRC in support of Holtec International's application to secure a CoC under 10CFR Part 71.

ORGANIZATION OF THIS SAFETY ANALYSIS DOCUMENT

Within this safety analysis document, all figures and tables cited within a section are placed after the section text narrative and are identified by the double decimal system m.n.i, where m is the chapter number, n is the section number, and i is the sequential number. Thus, for example, Figure 1.2.3 is the third figure in Section 1.2 of Chapter 1. Similarly, the following deci-numeric convention is used in the organization of chapters:

a. A chapter is identified by a whole numeral, say m (i.e., m=3 means Chapter 3).
b. A section is identified by one decimal separating two numerals. Thus, Section 3.1 is a section in Chapter 3.
c. A subsection has three numerals separated by two decimals. Thus, Subsection 3.2.1 is a subsection in Section 3.2.
d. A paragraph is denoted by four numerals separated by three decimals. Thus, Paragraph 3.2.1.1 is a paragraph in Subsection 3.2.1.
e. A subparagraph has five numerals separated by four decimals. Thus, Subparagraph 3.2.1.1.1 is a part of Paragraph 3.2.1.1.

Chapters include chapter sections and may also include chapter appendices and chapter supplements. Each chapter section, each chapter appendix and each chapter supplement begins on a fresh page.

REVISION STATUS AND CONFIGURATION CONTROL

SAR review and verification are controlled at the chapter level and changes are annotated at the chapter level. The revision of this SAR is the same as the latest revision of any chapter in this SAR, except the whole SAR revision is leveled up when incorporating a new revision to a licensing drawing that did not require a corresponding change to the text of any SAR chapter. Licensing drawings are controlled individually within the Holtec's drawing configuration control system and therefore have their own revision level.

Unless indicated as a "complete revision" in the summary description of change below, SAR changes are indicated by a "bar" in the right page margin and the revision number (annotated in the footer) of the entire chapter is changed. Those whole chapters that remain unchanged by a SAR revision will indicate the revision level corresponding to the initial revision or the last revision in which changes were made and thus will not match the revision of the whole SAR. Revision bars of chapters that remain unchanged by a SAR revision may or may not be shown.

The revision number of the whole SAR is annotated in the footer of every page of the SAR.

REVISION SUMMARY

A summary description of change is provided below for each SAR chapter (by chapter section, chapter appendix, and chapter supplement as applicable). Minor editorial changes to this SAR may not be summarized in the description of change. The summary descriptions of change for each Section or Appendix of any previous chapter revision that is not affected by the chapter revision or by the overall SAR revision is replaced by "no changes".

Chapter 1: General Information (includes Glossary and Notation)	**Revision Number.: 6**
Section or App.	**Summary Description of Change**
Glossary	No changes.
1.0	No changes.
1.1	No changes.
1.2	Editorial change to add comma after the word "Thus" in Subparagraph 1.2.1.1.d. Editorial change to add comma after the word "Thus" in Paragraph 1.2.1.6.Editorial change to add comma after the word "Thus" and "Therefore" in Subparagraph 1.2.1.6(i). Reference to Section 2.2 of SAR added to Paragraph 1.2.1.9 for shim emissivity values. Editorial change to reference Chapter 8 of the SAR instead of Section 8 of the SAR in the last sentence of Section 1.2.4.
1.3	Cask and Basket Licensing Drawings have been revised.
1.4	Editorial corrections to Table 1.4.1 to use the correct Holtec formatting terminology and to correct a reference to Chapter 5.
1.5	Table 1.5.1 updated to add further referenced locations in the SAR where Properties of Special Purposed Materials are discussed.
1.6	No changes.
References	Editorial corrections to introductory paragraph and Reference [1.0.3].
1.A	No changes.
1.B	Editorial corrections made to Section 1.B.1. Reference to Chapter 2 corrected in Section 1.B.3. Editorial corrections made to Section 1.B.4.

Chapter 2: Structural Evaluation	Revision Number: 6
Section or App.	**Summary Description of Change**
2.0	The table of Comparison of Major Design of HI-STAR 180 and HI-STAR 180D casks is updated.
2.1	Reference [1.2.22] is replaced by [1.2.30] in Section 2.1.2.2.
2.2	No changes.
2.3	No changes.
2.4	No changes.
2.5	Calculated values and safety factors are updated in Table 2.5.1. Reference [1.2.13] is replaced by [1.2.12] in Table 2.5.1.
2.6	Table 2.6.6 is updated.
2.7	Table 2.7.1 is updated to reflect change in the cavity axial gap (50 mm).
2.8	No changes.
2.9	No changes.
2.10	No changes.
2.11	No changes.
References	The reference [2.1.13] is deleted.
2.A	No changes.

Chapter 3: Thermal Evaluation	Revision Number.: 5
Section or App.	**Summary Description of Change**
3.0	No changes
3.1	No changes
3.2	No changes.
3.3	No changes.
3.4	No changes.
References	No changes.

Chapter 4: Containment Evaluation	Revision Number.: 4
Section or App.	**Summary Description of Change**
4.0	No changes.
4.1	No changes.
4.2	No changes.
4.3	No changes.
4.4	No changes.
References	No changes.

Chapter 5: Shielding Evaluation	Revision Number.: 6
Section or App.	**Summary Description of Change**
5.0	No changes.
5.1	Updated dose rates in Tables 5.1.1 to 5.1.8.
5.2	No changes.
5.3	Figure 5.3.9 is updated.
5.4	Subsection 5.4.7.4 is revised to account for updated "Lead Slump Analysis". Updated dose rates in Tables 5.4.2 to 5.4.6 and in Tables 5.4.8 to Table 5.4.12.
References	No changes.
5.A	MCNP input file in Appendix 5.A is updated.
5.B	MCNP input file in Appendix 5.B is updated.
5.C	No changes.

Chapter 6: Criticality Evaluation	Revision Number.: 4
Section or App.	**Summary Description of Change**
6.0	No changes.
6.1	Editorial changes.
6.2	No changes.
6.3	No changes.
6.4	No changes.
6.5	No changes.
6.6	No changes.
6.7	No changes.
6.8	No changes.
References	No changes.
6.A	Criticality benchmark analysis has been revised by removing critical experiments.
6.B	Subsection 6.B.3.2, Table 6.B.5, and Table 6.B.6 have been updated to incorporate changes from Appendix 6.A.
6.C	No changes.
6.D	No changes.
6.E	No changes.
6.F	No changes.

Chapter 7: Package Operations	Revision Number.: 5
Section or App.	**Summary Description of Change**
7.0	No changes.
7.1	No changes.
7.2	No changes.
7.3	No changes.
7.4	No changes.

References	No changes.
7.A	No changes.
7.B	No changes.
7.C	No changes.
7.D	No changes.
7.E	No changes.

Chapter 8: Acceptance Tests and Maintenance Program	**Revision Number.: 6**
Section or App.	**Summary Description of Change**
8.0	No changes.
8.1	Note 2 added to Table 8.1.2.
8.2	No changes.
References	No changes.
8.A	No changes.

End of Change Descriptions

CHAPTER 1: GENERAL INFORMATION

CHAPTER 2: STRUCTURAL EVALUATION

CHAPTER 3: THERMAL EVALUATION

CHAPTER 5: SHIELDING EVALUATION

CHAPTER 6: CRITICALITY EVALUATION

CHAPTER 8: ACCEPTANCE TESTS AND MAINTENANCE PROGRAM

GLOSSARY AND NOTATION

GLOSSARY

AFR is an acronym for Away From Reactor.

ALARA is an acronym for As Low As Reasonably Achievable.

AL-STAR is the trademark name of the impact limiter design used in the family of HI-STAR dual-purpose casks.

Basket Shims are aluminum alloy parts (typically extrusions) that serve to maintain the fuel basket coaxial with the cask's storage cavity.

BWR is an acronym for Boiling Water Reactor.

Cask is a generic term used to describe a device that is engineered to hold high level waste, including spent nuclear fuel, in a safe configuration.

C.G. is an acronym for Center of Gravity.

Closure Lid is a generic term to indicate a gasketed flat cover that bolts to the top flange of the cask.

Commercial Spent Fuel (CSF) refers to nuclear fuel used to produce energy in a commercial nuclear power plant.

Containment Boundary means the enclosure formed by the cask inner shell welded to a bottom plate and top flange plus dual closure lids with seal(s) and associated penetration port closure(s) and seal(s).

Containment System means the assembly of containment components of the packaging intended to contain the radioactive material during transport.

Cooling Time (or post-irradiation decay time, PCDT) for a spent fuel assembly is the time between reactor shutdown and the time the spent fuel assembly is loaded into the cask. Cooling Time is also referred to as the "age" of the CSF.

Critical Characteristic means a feature of a component or assembly that is necessary for the component or assembly to render its intended safety function. Critical characteristics of a material are those attributes that have been identified, in the associated material specification, as necessary to render the material's intended safety function.

Criticality Safety Index (CSI) means the dimensionless number (rounded to up to the next tenth) assigned to and placed on the label of a fissile material package, to designate the degree of control of accumulation of packages containing fissile material during transportation.

Damaged Fuel Assembly is a fuel assembly with known or suspected cladding defects, as determined by a review of records, greater than pinhole leaks or hairline cracks, empty fuel rod locations that are not filled with dummy fuel rods, whose structural integrity has been impaired such that geometric rearrangement of fuel or gross failure of the cladding is expected based on engineering evaluations, or that cannot be handled by normal means. Also see fuel debris.

Damaged Fuel Container (or Canister) (DFC) means a specially designed vessel for damaged fuel or fuel debris, which may permit gaseous and liquid media to escape while minimizing dispersal of gross particulates or which may be hermetically sealed. The DFC features a lifting location, which is suitable for remote handling of a loaded or unloaded DFC.

DBE means Design Basis Earthquake.

DCSS is an acronym for Dry Cask Storage System.

Design Heat Load is the computed heat rejection capacity of the HI-STAR package with a specific fuel basket with CSF stored in uniform storage with the ambient at the normal temperature and the peak cladding temperature (PCT) at 400 ºC. The Design Heat Load is less than the thermal capacity of the system by a suitable margin that reflects the conservatism in the system thermal analysis.

Design Life is the minimum duration for which the component is engineered to perform its intended function if operated and maintained in accordance with the instructions provided by the system supplier.

Design Report is a document prepared, reviewed and QA validated in accordance with the provisions of Holtec's Quality Program. The Design Report shall demonstrate compliance with the requirements set forth in the Design Specification. A Design Report is mandatory for systems, structures, and components designated as *Important-to-Safety*. The SAR serves as the Design Report for the HI-STAR 180D package.

Design Specification is a document prepared in accordance with the quality assurance requirements of 10CFR71 Subpart H to provide a complete set of design criteria and functional requirements for a system, structure, or component, designated as *Important-to-Safety*. The SAR serves as the Design Specification for the HI-STAR 180D package.

Dose Blocker Parts means the shielding components installed outside the Containment Boundary to enable the cask to meet the dose requirements of 10CFR71 during transport.

Enclosure Vessel (or MPC Enclosure Vessel) (EV) means the pressure vessel defined by the cylindrical shell, baseplate, port cover plates, lid, closure ring, and associated welds that provides confinement for the helium gas contained within the MPC. The EV and the fuel basket together constitute the multi-purpose canister. See Multi-Purpose Canister (MPC).

Exclusive use means the sole use by a single consignor of a conveyance for which all initial, intermediate, and final loading and unloading are carried out in accordance with the direction of the consignor or consignee. The consignor and the carrier must ensure that loading or unloading personnel have radiological training and resources appropriate for safe handling of the consignment. The consignor must issue specific instructions, in writing, for maintenance of exclusive use shipment controls, and include them with the shipping paper information provided to the carrier by the consignor.

Expanded Containment Boundary means a second barrier against leakage of radiological contents of the package engineered into the system for added safety or to meet a specific jurisdictional regulation.

Fastener Strain Limiter is a device to protect the impact limiter fastener bolts from experiencing excessive axial strain.

Fracture Toughness is a material property, which is a measure of the ability of the material to limit crack propagation under a suddenly applied load.

FSAR is an acronym for Final Safety Analysis Report.

Fuel Basket means a honeycombed cavity structure with square openings that can accept a fuel assembly of the type for which it is designed.

Fuel Debris is ruptured fuel rods, severed rods and loose fuel pellets from damaged fuel assemblies, and fuel assemblies with known or suspected defects which cannot be handled by normal means due to fuel cladding damage, including containers and structures supporting these parts.

GTCC is an acronym for Greater Than Class C waste.

High Burnup Fuel (HBF) is a commercial spent fuel assembly with an average burnup greater than 45,000 MWD/MTU.

HI-STAR is a generic term used to denote the family of metal casks consisting of HI-STAR 60, HI-STAR 63, HI-STAR 100, HI-STAR 100Z, HI-STAR 180, HI-STAR 180D and HI-STAR HB.

HI-STAR 180D Cask or cask means the cask that receives and contains the spent nuclear fuel. It provides the containment system boundary for radioactive materials and fulfills all requirements of 10CFR71 to merit certification as a B(U) package.

HI-STAR 180D Package consists of the HI-STAR 180D cask and fuel basket with two impact limiters installed at the extremities, a personnel barrier if required, and the licensed radioactive contents loaded for transport.

HI-STAR 180D Packaging consists of the HI-STAR 180D Package without the licensed radioactive contents loaded.

Holtite™ is the trade name for the neutron shielding materials used in the HI-STAR/HI-STORM family of casks.

Impact Limiters means a set of fully enclosed energy absorbers that are attached to the top and bottom of the cask during transport. The impact limiters are used to absorb kinetic energy resulting from normal and hypothetical accident drop conditions. The HI-STAR impact limiters are called AL-STAR.

Important-to-Safety (ITS) means a function or condition required to transport spent nuclear fuel safely; to prevent damage to spent nuclear fuel; and to provide reasonable assurance that spent nuclear fuel can be received, handled, packaged, transported, and retrieved without undue risk to the health and safety of the public.

Incore Grid Spacers are fuel assembly grid spacers located within the active fuel region (i.e., not including top and bottom spacers).

Inner Closure Lid means the bolted plate-like structure that forms the Containment Boundary for the cask.

LLNL is an acronym for Lawrence Livermore National Laboratory.

Leaktight means the degree of package containment that, in a practical sense, precludes any significant release of radioactive materials. This degree of containment is achieved by demonstration of a leakage rate less than or equal to 1 x 10^{-7} ref-cm^3/s of air at an upstream pressure of 1 atmosphere (atm) absolute (abs) and a downstream pressure of 0.01 atm abs or less. (Note: Reference Cubic Centimeter per Second (ref-cm^3/s) means a unit of leakage rate of one cubic centimeter of dry air per second at 1 atmosphere absolute pressure (760 mm Hg) and 25°C and Reference Air Leakage Rate means the allowable leakage rate converted to reference cubic centimeters per second (ref-cm^3/s).)

License Life means the duration for which the system is authorized by virtue of its certification by the U.S. NRC.

Light Water Reactor (LWR): are nuclear reactors moderated by light water. Commercial LWRs typically utilize enriched uranium and/or the so-called MOX fuel for power generation.

Lowest Service Temperature (LST) is the minimum metal temperature of a part for the specified service condition.

Maximum Normal Operating Pressure (MNOP) means the maximum pressure that would develop in the containment system in a period of 1 year under the heat condition specified in 10CFR71.71(c)(1), in the absence of venting, external cooling by an ancillary system, or operational controls during transport.

Maximum Reactivity means the highest possible k-effective including bias, uncertainties, and calculational statistics evaluated for the worst-case combination of fuel basket manufacturing tolerances.

Metamic™ is a trade name for an aluminum/boron carbide composite neutron absorber material qualified for use in the HI-STAR/HI-STORM fuel baskets.

MGDS is an acronym for Mined Geological Depository System.

Minimum Enrichment is the minimum assembly average enrichment. Natural uranium blankets are not considered in determining minimum enrichment.

Moderate Burnup Fuel (MBF) is a commercial spent fuel assembly with an average burnup less than or equal to 45,000 MWD/MTU.

Moderator Exclusion means no moderator intrusion into the cask storage cavity under hypothetical accident conditions of transport.

Multi-Purpose Canister (MPC) means the sealed canister consisting of a honeycombed fuel basket for spent nuclear fuel storage, contained in a cylindrical canister shell (the MPC Enclosure Vessel). See Enclosure Vessel (EV).

NDT is an acronym for Nil Ductility Transition, which is defined as the temperature at which the fracture stress in a material with a small flaw is equal to the yield stress in the same material if it had no flaws.

Neutron Absorber Material is a generic term used in this SAR to indicate any neutron absorber material qualified for use in the HI-STAR/HI-STORM fuel basket.

Neutron Shielding means a material used to thermalize and capture neutrons emanating from the radioactive spent nuclear fuel.

Neutron Sources means specially designed inserts for fuel assemblies that produce neutrons for startup of the reactor.

Non-Fuel Hardware (NFH) means high-level waste not used to produce thermal energy in the reactor. Examples of NFH are Burnable Poison Rod Assemblies (BPRAs), Thimble Plug Devices (TPDs), Control Rod Assemblies (CRAs), Axial Power Shaping Rods (APSRs), Wet Annular Burnable Absorbers (WABAs), Rod Cluster Control Assemblies (RCCAs), Control Element Assemblies (CEAs), primary and secondary neutron source assemblies (NSAs), water displacement guide tube plugs, orifice rod assemblies, and vibration suppressor inserts.

Not-Important-to-Safety (NITS) is the term used where a function or condition is not deemed as *Important-to-Safety*. See the definition for *Important-to-Safety*.

O&M Manual is an abbreviation for operation and maintenance manual.

ORNL is an acronym for Oak Ridge National Laboratory

Outer Closure Lid means the bolted plate-like structure that forms the expanded Containment Boundary for the cask.

Overpack is an alternative term used to denote a cask that contains a basket with a separate enclosure vessel.

Planar-Average Initial Enrichment is the average of the distributed fuel rod initial enrichments within a given axial plane of the assembly lattice.

Post-Core Decay Time (PCDT) is synonymous with cooling time.

Pressure Relief Device means a mechanical component specifically designed to relieve excess internal pressure upon reaching or exceeding a design set point. In this SAR, the term pressure relief device refers to commercial poppet valves, commercial rupture disks or similar devices.

PWR is an acronym for Pressurized Water Reactor.

Reactivity is used synonymously with effective neutron multiplication factor or k-effective.

Regionalized Fuel Loading is a term used to describe an optional fuel loading strategy used in lieu of uniform fuel loading. Regionalized fuel loading allows higher heat emitting fuel assemblies to be stored in certain fuel storage locations provided lower heat emitting fuel assemblies are stored in other fuel storage locations.

SAR is an acronym for Safety Analysis Report.

Service Life means the duration for which the component is reasonably expected to perform its intended function, if operated and maintained in accordance with the provisions of this SAR. Service Life may be much longer than the Design Life because of the conservatism inherent in the codes, standards, and procedures used to design, fabricate, operate, and maintain the component.

Short-term Operations means those normal operational evolutions necessary to support fuel loading or fuel unloading operations.

Single Failure Proof means that the handling system is designed so that a single failure will not result in the loss of the capability of the system to safely retain the load. Single Failure Proof means that the handling system is designed so that all directly loaded tension and compression members are engineered to satisfy the enhanced safety criteria of Paragraphs 5.1.6(1)(a) and (b) of NUREG-0612.

SNF is an acronym for Spent Nuclear Fuel (also referred to as CSF in this SAR).

STP is Standard Temperature (298K) and Pressure (1 atm) conditions.

SSC is an acronym for Structures, Systems and Components.

Surface Contaminated Object (SCO) means a solid object that is not itself classed as radioactive material, but which has radioactive material distributed on any of its surfaces. See 10CFR71.4 for surface activity limits and additional requirements.

Transport Index (TI) means the dimensionless number (rounded up to the next tenth) placed on the label of a package, to designate the degree of control to be exercised by the carrier during transportation. The transport index is determined as the number determined by multiplying the maximum radiation level in millisievert per hour at one meter (3.3 ft) from the external surface of the package by 100 (equivalent to the maximum radiation level in millirem per hour at one meter (3.3 ft)).

Transport Package consists of a HI-STAR Package with a set of support saddles, a personnel barrier and licensed radioactive contents loaded for transport. It excludes all lifting devices, tie-downs, longitudinal stops, rigging, transporters, welding machines, and auxiliary equipment (such as the drying and helium backfill system) used during fuel loading operations and preparation for off-site transportation.

Transport Packaging consists of a Transport Package without licensed radioactive contents loaded.

Uniform Fuel Loading is a fuel loading strategy where any authorized fuel assembly may be stored in any fuel storage location, subject to other restrictions in the CoC, such as those applicable to non-fuel hardware, and damaged fuel containers.

Undamaged Fuel Assembly is defined as a fuel assembly without known or suspected cladding defects greater than pinhole leaks and hairline cracks, and which can be handled by normal means. Fuel assemblies without fuel rods in fuel rod locations shall not be classified as Undamaged Fuel Assemblies unless dummy fuel rods are used to displace an amount of water greater than or equal to that displaced by the original fuel rod(s).

Water Tight is defined as a degree of leaktightness that in a practical sense precludes any significant intrusion of water through all water exclusion barriers. This degree of leaktightness ranges from 1 x 10^{-2} std cm^3/s air to 1 x 10^{-4} std cm^3/s air in accordance with ASTM E1003-05 “Standard Test Method for Hydrostatic Leak Testing.”

ZPA is an acronym for Zero Period Acceleration.

Zr means any zirconium-based fuel cladding material authorized for use in a commercial nuclear power plant reactor. Any reference to Zircaloy fuel cladding in this SAR applies to any zirconium-based fuel cladding material.

NOTATION

α Mean Coefficient of thermal expansion, cm/cm-ºC x 10^{-6} (in/in-ºF x 10^{-6})

d_{max}: Maximum predicted crush of the impact limiters in a package free drop event

e: Elongation in percent (i.e., maximum tensile strain expressed in percentage at which the ASME Code test specimen will fail)

E Young's Modulus, MPa x 10^4 (psi x 10^6)

f: Factor-of-Safety (dimensionless)

m: Metric for bolted joint leakage

P_b Primary bending stress intensity

P_e Expansion stress

$P_L + P_b$ Either primary or local membrane plus primary bending

P_L Local membrane stress intensity

P_m Primary membrane stress intensity

Q Secondary stress

S_u Ultimate Stress, MPa (ksi)

S_y Yield Stress, MPa (ksi)

S_m Stress intensity values per ASME Code

T_c: Allowable fuel cladding temperature

T_p: Peak computed fuel cladding temperature

α_{max}: Maximum value measured or computed deceleration from a package drop event. α_{max} can be parallel or lateral to the centerline of the cask.

β: Weight percent of boron carbide in the neutron shield

β_{max}: The value of maximum deceleration selected to bound all values of α_{max} for a package drop event. Values for β_{max} in axial and lateral directions are selected from the population of drop scenarios for a particular regulatory drop event (such as §71.73, free drop).

Γ: Total gasket spring back in the unloading cycle

Δ: Initial inter-part gap immediately before impact

δ: Lateral (global) deflection of the basket panel

δ_g: Maximum permissible gasket relaxation to maintain leak tightness

δ_{max}: Maximum value of δ

$\in$: Charpy lateral expansion at -28.9 ºC (-20 ºF)

ξ: Weight percent of hydrogen in the neutron shield material

ρ: Density

φ: Coefficient of thermal expansion (average between ambient and the temperature of interest)

ψ: Thermal conductivity

θ Orientation of free drop

CHAPTER 1: GENERAL INFORMATION

1.0 OVERVIEW

This Safety Analysis Report (SAR)[1] for the HI-STAR 180D Package is a compilation of information and analyses in the format suggested in Reg. Guide 7.9 [1.0.1] to support a United States Nuclear Regulatory Commission (USNRC) licensing review for certification as a spent nuclear fuel transportation package pursuant to the provisions of 10CFR71 Subpart D [1.0.2] and 49CFR173 [1.0.3].

HI-STAR 180D is the model name of a transport cask engineered to serve as a type B(U)F-96 packaging for transporting radioactive material (including but not limited to commercial spent fuel (CSF) and low to high level non-fuel waste (NFW) which can encompass reactor-related GTCC waste) under exclusive use shipment pursuant to 10CFR71.47. This SAR considers only CSF as the package contents.

In this SAR, SI units are the official units of measure (values in U.S. units, if provided, are for information only when accompanied by the equivalent SI unit value).

Section 1.6 of this SAR discusses quality assurance program and package design control for the HI-STAR 180D Package.

[1] See Glossary for definition and abbreviation of terms used throughout this SAR.

1.1 INTRODUCTION TO THE HI-STAR 180D PACKAGE

The HI-STAR 180D Package is a cylindrical metal cask with impact limiters qualified to carry CSF and engineered to be shipped by rail, road and seagoing vessel. Several key design concepts of the HI-STAR 180D Package are directly adapted from or reflected in Holtec's various licensed transport packages (see Table 1.1.1).

Figures 1.1.1 and 1.1.2 provide pictorials of the exterior of the HI-STAR 180D Cask and HI-STAR 180D Packaging, respectively. The drawing package in Section 1.3 details the important-to-safety features considered in the packaging evaluation and also includes certain details on not-important-to-safety features.

The HI-STAR 180D Cask containment system is engineered to parallel the anatomical design and construction of the containment system of HI-STAR 180 Package [1.0.4]. More specifically, the containment system materials of construction, welding joint details, NDE requirements, seal joint type, and Code of construction for the HI-STAR 180D Packaging, are identical or similar to those of the HI-STAR 180 Packaging. Furthermore, the double closure lid system of the HI-STAR 180D is identical in concept to the HI-STAR 180 system.

The HI-STAR 180D Cask body extensive shielding system is engineered to parallel the anatomical design and construction features of HI-STAR 180 Package. A monolithic shield cylinder made of alloy steel suitable for low temperature service and other shielding components surround the full length of the HI-STAR 180D Cask's containment shell. The monolithic shield cylinder contains neutron shielding material in an arrangement designed to optimize the shielding of neutron and gamma radiation emitted from the package's radioactive contents. The monolithic shield cylinder, along with other packaging shielding components, provides for a cask system that fulfills 10CFR71 dose rate requirements and ALARA objectives.

The HI-STAR 180D Package employs a bare basket within a cask; however, the system also lends itself to be employed as an overpack over a sealed fuel canister (e.g. Enclosure Vessel or MPC). The certification for enclosing the basket into an Enclosure Vessel is not sought at this time. The enhanced protection against release of radionuclides that would be provided by an Enclosure Vessel is restored in the HI-STAR 180D cask by the use of two independent closure lids, where both closure lids are designated as containment boundary components. By ensuring that each bolted lid joint is engineered to meet the leaktight criterion of ANSI N14.5 [8.1.6] under the normal and hypothetical accident conditions of transport, each joint will also meet the much less severe water exclusion criterion with ample margin. The inner and outer closure lids each feature concentric annular metallic seals providing multiple barriers against leakage.

The HI-STAR 180D Package employs the same fuel baskets (see Table 1.1.2) employed in the HI-STAR 180 (the basket design, material and construction are identical) but with their lengths customized for fit-up with the HI-STAR 180D cask cavity. The material is a high temperature metal matrix composite (MMC) of aluminum and boron carbide, manufactured using the powder metallurgy process under the trade name Metamic-HT™, and used as the principal constituent material for the Fuel Basket. Metamic-HT has been qualified and licensed for use in transport, under HI-STAR 180 Docket No. 71-9325, and storage casks, under HI-STORM 100 Docket 72-1014 [1.2.7] and HI-STORM FW Docket 72-1032 [1.0.9]. MMCs are commonly used because of their high conductivity, uniform boron dispersion, chemical stability, and strength characteristics.

Finally, the structural design embodiment, construction, and materials for the HI-STAR 180D Package AL-STAR impact limiters are identical to those used in the HI-STAR 180 Package (Docket No. 71-9325) and are fully described in this SAR.

Table 1.1.3 provides general dimensional and weight data on the HI-STAR package. Safety analysis is performed to dimensional data in the drawing package and to weight data in Chapter 2 unless otherwise specified in this SAR.

The HI-STAR 180D Package complies with all of the requirements of 10CFR71 for a Type B(U)F-96 package. In particular, the prescribed maximum normal operating pressure (MNOP) of 700 kPa (100 lb/in^2) for a type B(U) package is observed. No pressure relief device or feature intended to allow continuous venting during transport is provided on the HI-STAR 180D containment boundary (10CFR71.43(e) and 10CFR71.43(h)). Therefore, there is no pressure relief device or feature that may permit release of radioactive material under the tests specified in 10CFR71.73. Analyses that demonstrate the compliance of the HI-STAR 180D Package with the requirements of Subparts E and F of 10CFR71 are provided in this SAR[1].

The criticality safety index (CSI) for the HI-STAR 180D Package is 0.0, as an unlimited number of packages will remain subcritical under the procedures specified in 10CFR71.59(a) (Subsection 6.1.3 provides the determination of the CSI). The transport index (TI) is in excess of 10 for the HI-STAR 180D Packaging with design basis fuel contents (Section 5.0 provides the determination of the TI). Therefore, the HI-STAR 180D Package must be transported by exclusive use shipment (10CFR71.47) for any shipment of spent nuclear fuel. An empty but previously loaded HI-STAR 180D Package may be shipped as an excepted package provided the descriptions and limits for surface contaminated objects (SCO) material set forth in 10CFR71.4 are satisfied.

The HI-STAR 180D Packaging is designed to ensure safe transport of SNF. Some of the key features of the HI-STAR 180D Packaging that enhance its effectiveness are:

- Honeycomb design of the fuel basket to achieve high structural rigidity
- Optimized arrangement of neutron and gamma shielding materials within the system to minimize dose and achieve ALARA objectives
- High heat rejection capability through the use of a highly conductive basket material
- High strength cryogenic material in the containment system boundary (as in HI-STAR 180) to assure protection from fracture under sub-zero transport conditions [1.2.3]

[1] The HI-STAR 180D package is also designed to comply with SSR-6 (2012) [1.1.1] Type B(U)F package requirements. Certain acceptable criteria, methodology etc. may be stated or specified to bound both 10CFR71 and SSR-6 requirements; however, no specific SSR-6 paras. are referenced in this SAR.

This SAR supports a licensed life of the HI-STAR 180D package of 5 years, after which a renewal by the USNRC is based upon an affirmative safety assessment to support such renewal. Even though the safety analysis is not required to address more than 5 years, all safety evaluations are based on a design or service life of at least 50 years to provide a suitable degree of conservatism. This is accomplished by using materials of construction that have been exhaustively tested and determined capable of withstanding HI-STAR 180D's operating environments without degradation and with negligible reduction if any, in their capability to render their intended function (materials of construction and testing are discussed in Section 1.2 and Section 2.2 of this SAR). A maintenance program, as specified in Chapter 8, is implemented to ensure the HI-STAR 180D Package will meet its Design Life. The technical considerations that assure the HI-STAR 180D performs its design functions throughout its Design Life include all areas germane to the long-term integrity of the system, such as:

- Consideration of Exposure to Environmental Effects
- Consideration of Material Corrosion, Degradation and Aging Effects
- Provision of Preventive Maintenance and Inspections
- Consideration of Structural Fatigue, Brittle Fracture and Creep Effects
- Maintenance of Helium Atmosphere
- Assurance of Fuel Cladding Temperatures below NRC Prescribed Limits
- Assurance of Long-Term Effectiveness of the Neutron Absorber

Table 1.1.1
HI-STAR Family of Transport Packages
(USNRC Docketed Only)

Model No.	USNRC Docket and SAR Reference	Year First Certified	Content (Fuel Type or NFW)	Approx. Cask Cavity Length (mm [inch])	Approx. Cask ID (mm [inch])	Fuel Package Type: Bare Basket (B) or Canisterized (M)
HI-STAR 100 (Classic)	71-9261 [1.0.5]	1998	BWR & PWR	4855 [191 1/8]	1747 [68 3/4]	M
HI-STAR 100 Version HB		2009	BWR	2929 [115 5/16]	1747 [68 3/4]	M
HI-STAR 100 Version HB GTCC		2018	NFW	2931 [115 3/8]	1747 [68 3/4]	N/A
HI-STAR 100MB	71-9378 [1.0.14]	Foreseen 2019	BWR & PWR	4201 [165 3/8 (SL)] 4855 [191 1/8 (XL)]	1747 [68 3/4]	M & B
HI-STAR 60	71-9336 [1.0.7]	2009	PWR	3547 [139 5/8]	1080 [42 1/2]	B
HI-STAR 180	71-9325 [1.0.4]	2009	PWR	3572 [140 5/8]	1850 [72 7/8]	B
HI-STAR 180D	71-9367 [this SAR]	2014	PWR	2944 [115 7/8]	1850 [72 7/8]	B
HI-STAR 180L	71-9381 [1.0.10]	Foreseen 2019	BWR	4543 [178 7/8]	1689 [66 1/2]	B
HI-STAR 190	71-9373 [1.0.11]	2017	BWR & PWR	4845 [190 3/4 (SL)] 5417 [213 1/4 (XL)]	1931 [76]	M
HI-STAR 80	71-9374 [1.0.12]	2018	BWR & PWR & NFW	4579 [180 1/4]	1242 [48 7/8]	B
HI-STAR ATB-1T	71-9375 [1.0.13]	Foreseen 2019	NFW	N/A	N/A	N/A

Note: Dimensions are taken from respective licensing drawing packages approved at the time of this writing. Dimensions are nominal and may be rounded. N/A stands for Not Applicable.

Table 1.1.2

Permissible "Waste Packages" for HI-STAR 180D (Note 1 and 2)

Waste Package Model No. (Notes 3 and 4)	Waste Package Type (Fuel Package or NFW Package)	Content Type	Canisterized or Bare Basket	Basket Structural Material and Neutron Absorber	Damaged Fuel Container or Other Secondary Packaging
F-32	Fuel Package	PWR	Bare Basket	Metamic-HT	None
F-37	Fuel Package	PWR	Bare Basket	Metamic-HT	None

Notes
1. Refer to SAR Subsection 1.2.2 and Chapter 7 for specific package contents corresponding to the listed waste packages.
2. Canister-based fuel packages and non-fuel waste packages are not qualified for transportation at this time.
3. See licensing drawing package in SAR Section 1.3.
4. The numerical identifier in the fuel basket model name indicates the number of fuel storage locations and the maximum number of assemblies permitted for transport.

Table 1.1.3

Overall Dimensions and Weights of HI-STAR 180D

Item	**Value** **mm [in]**
DIMENSIONS (Note 1)	
Inside Diameter of the Cask Cavity	Table 1.1.1
Outside Diameter of the Cask	2712 [106 3/4]
Length of the Cask	3691 [145 3/8]
Outside Enveloping Diameter of the Packaging	3251 [128]
Length of the Packaging	6536 [257 3/8]
WEIGHTS (Note 2)	
Maximum Gross Weight of HI-STAR 180D Package (no Personnel Barrier)	See Appendix 7.A
Nominal Empty Packaging Weight (with either F-32 or F-37 Fuel Basket and no Personnel Barrier)	See Appendix 7.A

Notes

1. All dimensions are approximate and may be rounded. Design basis safety analyses use dimensions provided in the drawing package and/or elsewhere in this SAR and may use upper or lower bound values, as appropriate, to ensure conservatism.
2. The actual as-built packaging (i.e. empty) weight will vary slightly due to dimensional tolerances and small variations in material density. A verification of the as-manufactured empty packaging weight is not strictly required because the safety analysis contained in this SAR considers such variations to ensure that the analyses are bounding.

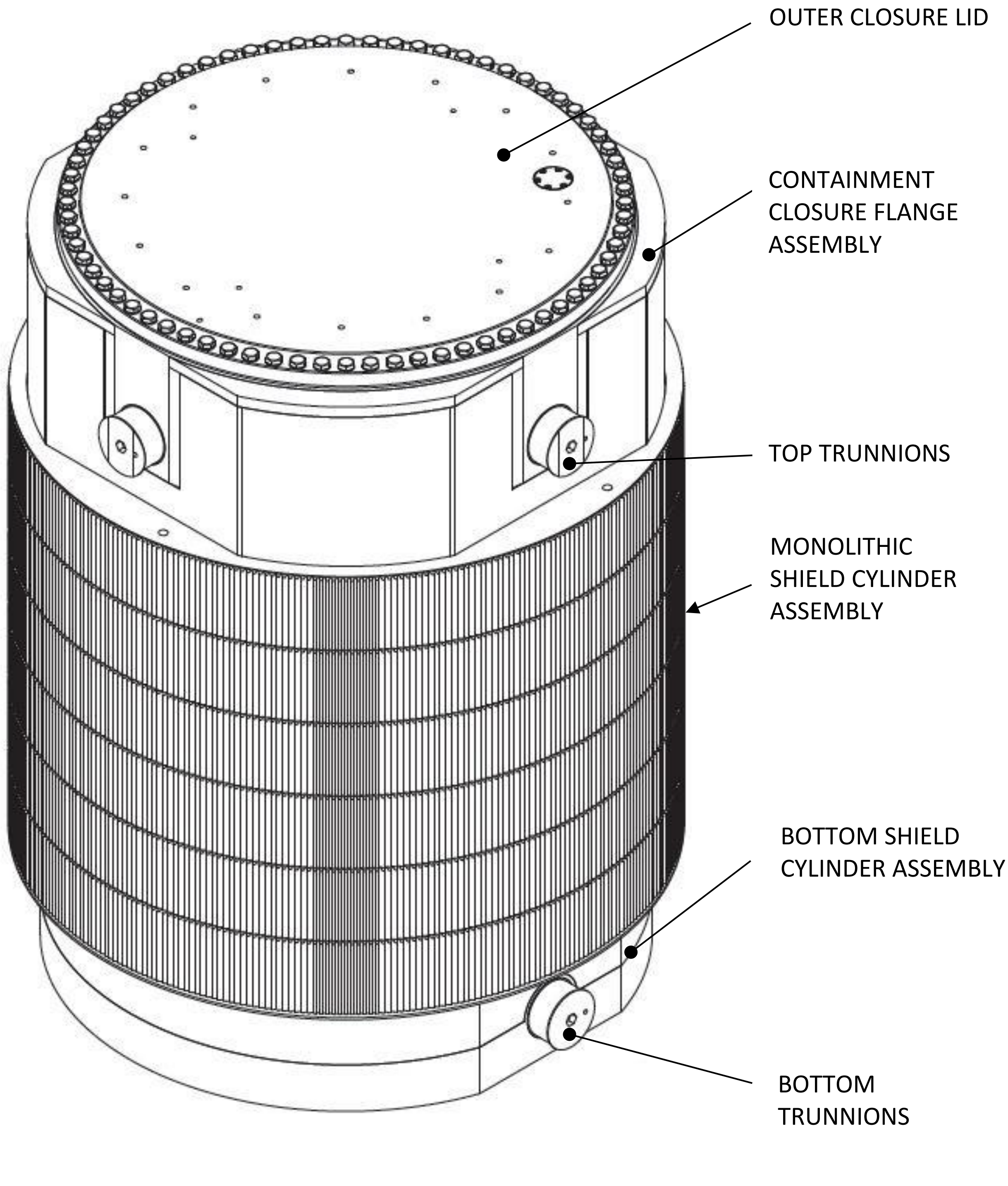

FIGURE 1.1.1 – EXTERIOR PICTORIAL VIEW OF THE HI-STAR 180D CASK

(Refer to Section 1.3 and the drawing package in Section 1.3 for details)

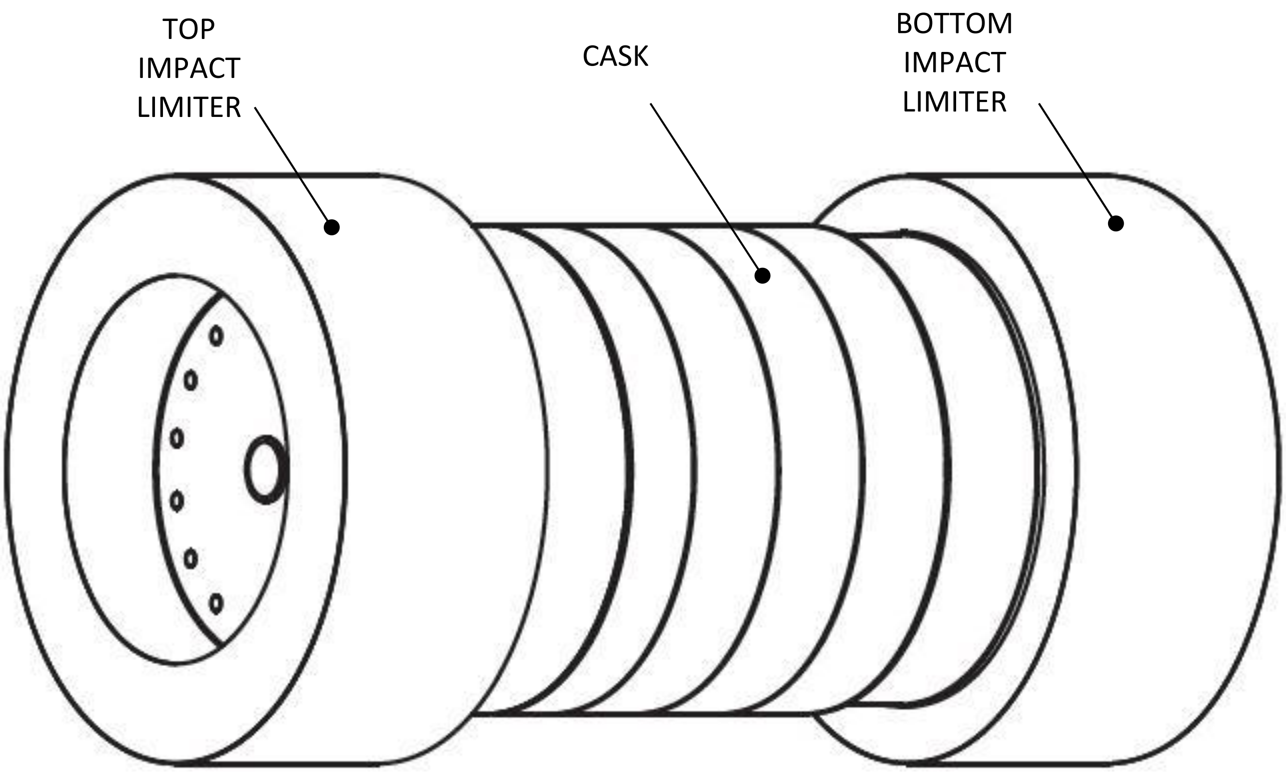

Note: Personnel Barrier Not Shown.

FIGURE 1.1.2 – EXTERIOR PICTORIAL VIEW OF HI-STAR 180D PACKAGING

(Refer to Section 1.3 and the drawing package in Section 1.3 for details)

1.2 DESCRIPTION OF PACKAGING COMPONENTS AND THEIR DESIGN & OPERATIONAL FEATURES

1.2.1 Packaging

1.2.1.1 Major Packaging Components and Packaging Supports and Restraints

The HI-STAR 180D Packaging consists of the four major components (Cask, Fuel Basket/Basket Shims, Impact Limiters and Personnel Barrier) discussed in (a) through (d) below. Additionally, auxiliary equipment, in the form of packaging supports and restraints typically necessary for package transport, is described in subparagraph (e) below.

a. Cask

The HI-STAR 180D Cask is a cylindrical metal cask designed and qualified to hold SNF in a subcritical "fuel package" configuration featuring a highly thermally conductive Metamic-HT fuel basket. The containment of the radiological contents is provided by a cryogenic nickel steel shell (the Containment Shell) welded to a nickel steel baseplate (the Containment Baseplate) at the bottom and a suitably machined nickel steel forging (the Containment Closure Flange) at the top. The Containment Closure Flange is equipped with machined surfaces to fasten two independent cryogenic steel closure lids, each equipped with concentric metallic seals. The fully cryogenic steel weldment and the cryogenic steel closure lid define the "Containment System Boundary" for the cask. The Containment System Boundary, including both closure lids, is designed and manufactured to ASME Section III Division 1, Subsection NB [1.2.1] as clarified in this SAR. Cask design details are shown in the drawing package in Section 1.3.

For purposes of description, the HI-STAR 180D cask is divided into six constituent parts, each with distinct roles and features, as follows:

1) The Cask Containment Shell (CCS): The innermost cylindrical member of the cask containment system made from cryogenic nickel steel forging or plate.
2) Cask Bottom Region (CBR): The CBR consists of a thick cryogenic nickel steel forging, namely the Containment Baseplate, featuring neutron and gamma shielding material for additional dose reduction. The CBR includes bottom trunnions used for cask rotation that are rendered inoperable during package transport.
3) Cask Top Region (CTR): The CTR consists of a massive cryogenic nickel steel forging, namely the Containment Closure Flange, featuring neutron shielding material for additional dose reduction. The CTR includes top trunnions (cask's interfacing lift points) which are rendered inoperable during package transport
4) Double Closure Lid System (DCLS): The DCLS consists of two specially shaped lids, the Inner and Outer Closure Lids, with two machined concentric grooves in each lid to provide containment protection. The bolted lid joints are "controlled compression" joints engineered to meet the leak-tight criterion of ANSI N14.5 [8.1.6] under the normal and hypothetical accident conditions of transport. See SAR Appendix 1.B for information on

Moderator Exclusion applicable only to Fuel Packages containing HBF. The inner closure lid features neutron shielding material for additional dose reduction.

5) Gamma Capture Space (GCS): The GCS refers to the monolithic shield cylinders which renders the principal function of blocking gamma radiation.
6) Neutron Capture Space (NCS): The NCS refers to the sector pockets within the monolithic shield cylinders that are filled with neutron shield material and whose principal function is to block the neutrons accreted by the contained waste package. This space itself is non-structural. The sector pockets are provided with pressure relief protection (as shown in the drawing package in Section 1.3) to prevent the over-pressurization of its enclosure (the monolithic shield cylinder weldment) in the case of off-gassing of the shield material.

The above description of the constituent parts is summarized in Table 1.2.1 for ease of reference.

As with the previously licensed HI-STAR 180 Cask, all materials used in the HI-STAR 180D Cask containment system boundary are widely used in low temperature applications and regardless of their product form, are of compatible metallurgical genre and thus are readily weldable to each other. While the HI-STAR 180D Cask containment system boundary renders the function of a high integrity pressure vessel by providing multiple highly reliable leakage barriers in its double lid closure, it does not possess the necessary shielding in the radial direction to attenuate the radiation dose sufficiently to meet the limits mandated in 10CFR71. Therefore, for shielding purposes, it is necessary to surround the containment shell with additional material optimized to reduce levels of gamma and neutron radiation. This additional shielding is achieved with a monolithic cylinder equipped with longitudinal through holes in the form of “sector pockets” near their outer boundary that provide the enclosure space for Holtite. The monolithic cylinder is made of alloy steel with excellent impact resistant properties at low temperatures. As shown in the drawing package in Section 1.3, the monolithic shield cylinder is configured from several short annular monolithic shield cylinders stacked on top of each other to provide gamma and neutron shielding around the containment shell and active fuel region to the maximum extent. Because of their complex geometry and large mass, it is necessary to produce the monolithic cylinders using the casting process. The casting technology to produce the low temperature alloy steel that yields the requisite properties (density, tensile strength, and impact strength at low temperatures) is well established in the U.S. Standards [1.2.2, 1.2.16] and has yet again proven successful with the fabrication of HI-STAR 180 monolithic shield cylinders. The HI-STAR 180D monolithic shield cylinder is identical to the HI-STAR 180 monolithic shield cylinder, in construction, material and design concept. The Holtite pocket width is optimized specifically for the package contents described in Subsection 1.2.2 of this SAR.

Use of alloy steels with excellent conductivity and impact strength properties helps render the HI-STAR 180D cask body into an efficient heat dissipater.

[

PROPRIETARY INFORMATION WITHHELD PER 10 CFR 2.390

]

Further, because the monolithic shield cylinders are not integral to the containment shell, a crack in the body of a monolithic shield cylinder will not radially propagate into the containment shell and in this manner the crack-arrest characteristic in HI-STAR 180D is similar to that in the previously licensed HI-STAR 180.

The monolithic shield cylinders are equipped with “sector pockets” that hold the Holtite neutron shielding material. The sector pockets contain pressure relief protection (as shown in the drawing package in Section 1.3) to prevent their overpressurization from off-gassing of the neutron shield material.

The HI-STAR 180D Cask features four removable top trunnions secured to the Containment Closure Flange for lifting and handling. In addition, the HI-STAR 180D Cask is equipped with two removable bottom trunnions connected to the Bottom Shield Cylinder. The bottom trunnions are qualified as cask rotation trunnions.

b. Fuel Basket and Basket Shims

Waste packages qualified for use with HI-STAR 180D are listed in Table 1.1.2. Waste packages may take various forms such as fuel packages or non-fuel waste (NFW) packages. Waste packages are also identified as either canisterized, where the waste package is sealed in a separate canister, or not canisterized (also referred to as a bare waste package). Therefore, the waste packaging discussed herein is dependent on the waste package type. The F-32 and F-37 are bare-basket PWR fuel packages currently available for the HI-STAR 180D Package.

The F-32 and F-37 fuel baskets are major components of the F-32 and F-37 fuel packages, respectively. Their design details, illustrated in the drawing package in Section 1.3, show that they are both of a honeycomb construction and feature 32 and 37 storage cavities accordingly.

[

PROPRIETARY INFORMATION WITHHELD PER 10 CFR 2.390

]

The honeycomb design of the fuel basket arrays the cell walls in two orthogonal sets of plates; consequently, the walls of the cells are either completely coplanar (no offset) or orthogonal with each other. The coplanar honeycomb design of the basket renders it extremely rugged under lateral drop scenarios. The final form of the fuel basket plates is extruded and has the dimensional precision that rivals machining. As a result, the fuel basket is assured to be a cellular structure with excellent dimensional precision, specifically regarding verticality and cross-sectional dimensions.

Finally, the cell-to-cell connectivity inherent in the honeycomb basket structure provides an uninterrupted heat transmission path, making the fuel baskets an effective heat rejection device.

The space between the fuel basket and the inside surface of the Containment Boundary is occupied by specially shaped basket shims made of high strength and creep resistant aluminum alloy sections and stainless steel sections as shown in the drawing package. The basket shims establish a near conformal contact interface with the fuel basket and the containment shell, thus prevent significant movement of the basket during all transport conditions. The aluminum portion of the basket shims are extruded and machined to a precise shape and high degree of accuracy. The clearance between the basket shims and the interfacing machined surface of the cask cavity is set to be sufficiently small such that the thermal expansion of the parts inside the containment space under Design Basis heat load conditions will minimize any macro-gaps at the interface and thus minimize any resistance to the outward flow of heat, yet ensure that there is no restraint against free thermal expansion. The major functions of the basket shims are heat transfer and lateral structural support to the basket; however, the stainless steel sections are used to enhance the shielding performance at the top and bottom regions of the cask. Pictorial top views of each fuel basket and basket shim assembly type are provided in Figures 1.2.1 and 1.2.2.

c. Impact Limiters:

Two impact limiters (also referred to as AL-STAR 180D) are installed at the two extremities of the HI-STAR 180D Cask and provide energy absorption capability for the normal and hypothetical accident conditions of transport. The impact limiters feature extremely rigid cylindrical barrels (backbone structures) that engage the top and bottom of the cask with a snug fit. Each impact limiter backbone is enveloped by crushable material, which in turn is enclosed by a stainless steel skin. The selection of the crushable material ensures that the performance of the impact limiters will be essentially insensitive to the ambient environment (temperature and humidity). The AL-STAR 180D impact limiters are of the same design genre as the AL-STAR 180 used in the HI-STAR 180 Package (Docket No. 71-9325). The following key design features typify the AL-STAR 180D impact limiters:

- Each impact limiter is configured in such a manner that under all potential free-fall scenarios, the collision of the package with the regulatory strike surface will always occur in the crush material space (i.e. will be cushioned by the impact limiter crush material).

- The impact limiter will protect the cask under all angular drop orientations onto the regulatory strike surface.

- External surface of the impact limiter surrounding the crushable material is made of stainless steel, a ductile, corrosion-resistant material.

- Axial (longitudinal) tension rods of high-strength material fasten the impact limiter to the two extremities of the cask body.
- Both impact limiters feature a skirt (shell) that fits the outside of the cask forging with a small radial clearance.
- The fasteners are engineered to be readily installable and removable for ALARA purposes.
- Each impact limiter is designed to render its intended function in the entire range of applicable ambient temperature conditions of the package.

Impact limiter details are shown in the drawing package in Section 1.3. The *critical characteristics* and the attainment of the required critical characteristics through a comprehensive qualification process and production testing are discussed in Chapters 2 and 8, respectively.

[

PROPRIETARY INFORMATION WITHHELD PER 10 CFR 2.390

]

d. Personnel Barrier:

During transport the cask lies in a horizontal orientation with the two impact limiters on its two extremities. Pursuant to 10CFR71.43(g), a personnel barrier is placed over the cask to provide a physical barrier against manual access to hot, 50°C (122°F) or higher, accessible areas of the package and limit hot accessible areas of the package to less than 85°C (185°F). According to Chapter 3 of this SAR the temperature of the accessible surfaces of the package exceeds 50°C (122°F) but is maintained less than 85°C (185°F) with the use of the personnel barrier; therefore, transport of the HI-STAR 180D Package must be performed under exclusive use shipment and with the personnel barrier installed.

The personnel barrier is not a structural part of the HI-STAR 180D Packaging but is designated as a packaging component when in use. Since the personnel barrier is not a structural part of the HI-STAR 180D Packaging, it is not required to remain in place under normal condition tests in 10CFR71.71.

Dose calculations in this SAR conservatively consider an open (flat-bed) conveyance and do not rely on conveyances that are “closed” or with “enclosures”. Moreover, it is conservatively shown, with the exception of the transport index, that the package design complies with the external surface radiation limits for a non-exclusive use shipment in accordance with 10CFR71.47(a). Thus, for the purpose of dose calculations/measurements that ensure compliance with regulatory radiation limits, the jurisdictional boundary of the HI-STAR 180D Packaging is the outer most external surfaces of the impact limiters and the cask. However, due to exceedance of the transport index (exclusive use shipment applies), the package is also shown to comply with the radiation limit at 2 meters from the vertical planes projected from the outer edges of the vehicle (excluding the top and underside of the vehicle) in accordance with 10CFR71.47(b)(3). See SAR Chapter 5 for complete acceptance criteria on radiation limits.

[

PROPRIETARY INFORMATION WITHHELD PER 10 CFR 2.390

]

e. Packaging Supports and Restraints:

The HI-STAR 180D Package lends itself to a horizontal packaging assembly for transport as shown in the drawing packaging in Section 1.3 and is engineered for shipment by seagoing vessel, railroads and roadways using appropriate supports and restraints. An illustrative example of packaging supports and restraints for rail transport is provided in Figure 1.3.2. The arrangement of packaging supports and restraints may vary as long as the package is properly secured and qualified for the specific mode of transport. Tapered wedge shims that close the gap between the impact limiters and the axial restraints (longitudinal stops) of the transport vehicle are examples of auxiliary equipment that may be used to restrain the package against axial movement. Non-integral appurtenances to the cask, such as the transport cradle, longitudinal stops, support saddles, tie down system and wedge shims are not structural parts of the HI-STAR 180D Package and, as such, are not designated as packaging components.

Packaging supports and restraints shall be designed as appropriate for either rail, road (i.e. public highway) or seagoing vessel transport applications in compliance with the applicable requirements of 10CFR Part 71 and the applicable 49CFR requirements as indicated by 10CFR71.5, with additional consideration to the applicable industry (railroad, road and sea transportation) standards. More specifically, 10CFR71.45(a) and (b) requirements must be complied with.

In the HI-STAR 180D transport package configuration, the cask trunnions are not qualified to be used to lift the HI-STAR 180D Package (i.e., loaded cask with impact limiters) and in fact the skirts on the impact limiters prevent access to all trunnion areas. Therefore, in the package transport configuration, there are no lifting attachments remaining that are a structural part of the package and there is no other structural part of the package that could be inadvertently used to lift the package that must be rendered inoperable per 10CFR71.45(a).

1.2.1.2 Overall Packaging Dimensions and Weight

An overview of approximate general dimensions and weights are provided in Table 1.1.3. Packaging dimensions are provided in the drawing package in Section 1.3. Overall nominal and/or maximum weights for operational purposes are provided in Appendix 7.A and the drawing package in Section 1.3. The nominal weights for the HI-STAR 180D Package main components, nominal weight of the cask and package at maximum capacity with design basis SNF are provided in Section 2.1 (and Table 2.1.11) for safety analysis purposes. The weight of the package contents is discussed in Subsection 1.2.2 below and Appendix 7.D as applicable.

The maximum gross transport weight of the HI-STAR 180D Package (without the personnel barrier) is marked on the packaging nameplate.

1.2.1.3 Containment Features

The Containment System forms an internal cylindrical cavity for housing the waste packages listed in Table 1.1.2. A schematic of containment system components is shown in the drawing package in Section 1.3 and also in Figures 4.1.1, 4.1.2, and 4.1.3 (all components with the primary function of containment are shown in these schematics). As shown in these schematics, the massive inner closure lid system defines the containment boundary. The outer closure lid system along with the inter-lid space also meets the design and manufacturing criteria to be merged with the inner containment space to define an expanded containment boundary. The expanded containment boundary will play its role only in the unlikely event that the boundary defined by the inner lid fails to hold.

Both closure lids have been engineered to perform the containment function with final qualification by leak testing according to ANSI N14.5 [8.1.6] as specified in Chapter 8, Table 8.1.2 and to the leakage acceptance criterion specified in Chapter 8, Table 8.1.1. Each closure lid joint features equally proficient seals, one seal serving as a back-up to the other seal.

1.2.1.4 High Burnup Fuel Transportation and Moderator Exclusion Features

The HI-STAR 180D packaging is designed to transport both moderate burnup (MBF) and high burnup fuel (HBF). To address concerns with the structural integrity of HBF under accident conditions, and its potential impact on criticality safety, the design of HI-STAR 180D provides utmost assurance of water exclusion under a postulated 10CFR 71.73 accident scenario. Details of the design measures and technical confirmation to meet the intent and performance objectives of ISG-19 are described in Appendix 1.B, where additional defense-in-depth measures to ensure sub-criticality compliance are also discussed. The overall licensing approach on HBF is summarized in Section 1.4.

Table 1.2.2 provides a reactivity limit compliance matrix to summarize compliance with 10 CFR 71.55 and 10 CFR 71.59 as discussed in Appendix 1.B Section 1.B.5 and Chapter 6, Subsection 6.3.5. Table 1.2.2 also acknowledges additional conservative defense-in-depth safety evaluations provided in Chapter 6, Subsection 6.3.5.

1.2.1.5 Neutron and Gamma Shielding Features

The HI-STAR 180D Package is equipped with appropriate shielding to minimize personnel exposure. The HI-STAR 180D Packaging (with or without the personnel barrier) ensures the external radiation standards of 10CFR71.47 under exclusive shipment are met when loaded with design basis fuel. The drawing package in Section 1.3 provides information on the configuration of neutron and gamma shielding features.

The initial attenuation of gamma and neutron radiation emitted by the radioactive spent fuel is provided by the fuel basket and the fuel basket shims. However, most of the shielding in the transport package is contained in the body of the cask and consists of neutron and gamma shielding. The majority of the neutron shielding is provided in two overlapping radial layers within the monolithic shield cylinder to maximize neutron capture. The placement of the two principal shielding materials, namely steel and Holtite, in the right sequence and the right quantity is optimized to maximize the attenuation of radiation emanating from the fuel. The arrangement of the shielding materials shown in the licensing drawings reflects the design optimization carried out for the HI-STAR 180D cask.

The HI-STAR 180D cask features enhanced shielding radially and axially at the top and bottom areas of the cask. These optimized shielding enhancements are used to achieve specific ALARA design objectives that do not necessarily pertain to 10CFR71 but have the added benefit of enhancing overall transport package shielding performance and margins to 10CFR71 transport package radiation level limits. At the top of the cask, the containment closure flange assembly features built-in neutron shielding (Holtite). The inner closure lid has imbedded supplemental neutron shielding (Holtite). Likewise, at the bottom of the cask, the bottom shield cylinder assembly features built-in supplemental neutron shielding (Holtite) and gamma shielding (lead) both layered around the containment shell and over the containment baseplate. The cask features enhanced shielding in local areas around the top and bottom trunnions using an optimized arrangement of neutron (Holtite) and gamma (lead) shielding with additional gamma shielding provided by the stainless steel basket shim sections at the top and bottom regions of the cask. Lead gamma shielding is installed in such a manner that macro-voids do not exist.

During transport, the impact limiters provide additional gamma shielding (steel) at the ends of the cask and help prevent loss of shielding as a result of normal and accident conditions of transport by complete enclosure of the containment closure flange assembly and the bottom shield cylinder assembly.

1.2.1.5.1 Holtite™ Neutron Shielding Material

(a) Qualification of the Holtite™ Neutron Shielding Material

The shielding against neutron radiation in HI-STAR 180D Packaging is provided by Holtite-B, the same material qualified as neutron shielding in the HI-STAR 180 Packaging under Docket 71-9325. Holtite™ is a hydrogen rich, radiation resistant, polymeric material impregnated with boron carbide. Holtite-A is the predecessor of Holtite-B which was developed by Holtec International in the early 90s as a part of the company's HI-STAR 100 design development program.

Holtite-A was subjected to extensive studies of its critical characteristics (viz., radiation resistance, physical stability at service temperature and homogeneity) during its evaluation and validation program [1.2.4, 1.2.5], which led to its regulatory approval in the HI-STAR 100 Docket (71-9261) and subsequent use in the manufactured HI-STAR 100 overpacks. Holtite-B is an improved version of Holtite-A in respect of its stability at higher temperatures.

Like Holtite-A, Holtite-B is a relatively poor conductor of heat and possesses limited gamma attenuation capability. Its main function is to provide neutron shielding which is enabled by a hydrogen rich polymeric matrix and spatially distributed particles of Boron Carbide. Holtite-B may also contain spatially distributed particles of copper to enhance thermal conductivity and/or gamma shielding. Boron carbide and copper content of the Holtite-B for the HI-STAR 180D are specified in this SAR as critical characteristics.

Holtite-B has been subjected to the same battery of tests to establish its radiation resistance, physical stability at service temperature and homogeneity as Holtite-A [1.2.17]. In contrast to Holtite-A which is qualified to operate under 149°C (300°F) temperature, Holtite-B is capable of operating at 204°C (400°F) in sustained use without a significant weight loss. Critical Characteristics of the Holtite-B neutron shielding material used in the safety analyses are provided in Table 2.2.13.

In this SAR, the terms Holtite-B and Holtite are used interchangeably.

1.2.1.6 Criticality Control Features

Criticality control in the HI-STAR 180D Packaging for SNF is provided by the coplanar grid work of the Fuel Basket honeycomb, made entirely of the Metamic™-HT extruded borated metal matrix composite plates. Metamic-HT is the neutron absorber in HI-STAR 180D fuel baskets. Thus, the neutron absorber is not attached to the cell walls by a mechanical means that may be vulnerable to detachment. Hence, the locational fixity of the neutron absorber is guaranteed.

[

PROPRIETARY INFORMATION WITHHELD PER 10 CFR 2.390

]

There are no moderators in the HI-STAR 180D Packaging.

1.2.1.6.1 Qualification of Metamic-HT

Metamic-HT is a composite of nano-particles of aluminum oxide (alumina) and finely ground boron carbide particles dispersed in the metal matrix of pure aluminum. Metamic-HT is the constituent material of the HI-STAR 180D fuel baskets. Metamic-HT neutron absorber is a successor to the Metamic (classic) product widely used in dry storage fuel baskets [1.2.7] and spent fuel storage racks [1.2.8, 1.2.9]. Metamic-HT is engineered to possess the necessary mechanical characteristics for structural application in spent nuclear fuel casks.

[

PROPRIETARY INFORMATION WITHHELD PER 10 CFR 2.390

]

[

PROPRIETARY INFORMATION WITHHELD PER 10 CFR 2.390

]

[

PROPRIETARY INFORMATION WITHHELD PER 10 CFR 2.390

]

[

PROPRIETARY INFORMATION WITHHELD PER 10 CFR 2.390

]

[

PROPRIETARY INFORMATION WITHHELD PER 10 CFR 2.390

]

[

PROPRIETARY INFORMATION WITHHELD PER 10 CFR 2.390

]

1.2.1.7 Lifting and Tie-Down Devices

Lifting trunnions are attached to the cask containment closure flange for lifting and also for rotating the cask body between vertical and horizontal positions. Four lifting trunnions are located 90° apart in the sides of the top flange. Two additional trunnions are attached near the bottom extremity of the cask and located 180° apart to provide a built-in pivoting axis for cask rotation. The bottom trunnions may be slightly off-center to facilitate the rotation direction of the cask. Each pair of top lifting trunnions is conservatively qualified to independently lift the cask in compliance with ANSI N14.6 increased stress margins as specified in Section 8.1.

Lifting trunnions are manufactured from a high strength alloy and designed in accordance with 10CFR71.45 and NUREG 0612 (per Chapter 2) with load testing performed in accordance with ANSI N14.6 [8.1.3] (per Chapter 8). The cask may be lifted from one pair of top trunnions qualified to increased stress margins for non-redundant lifting or from all four top trunnions, each pair qualified to appropriate increased stress margins for redundant lifting.

The lifting, upending, and downending of the HI-STAR 180D Package requires the use of external handling devices. A lift yoke is typically utilized when the cask is to be lifted and handled vertically and to perform upending and downending. Upending and downending are typically performed with the cask pivoting on an ancillary tilting device specifically designed for this purpose. Lift yokes, other purposed structural/mechanical lifting devices, and/or slings may be used to lift the cask in the horizontal orientation.

There is no system of tie-down devices that is a structural part of the package. For additional discussion on tie-downs, see Subparagraph 1.2.1.1(e) on package supports and restraints.

1.2.1.8 Heat Transfer Features

The HI-STAR 180D Package can safely transport SNF by maintaining the fuel cladding temperature below the limits for normal and accident conditions consistent with the guidance in the NRC Interim Staff Guidance, ISG-11 Rev. 3 [1.2.13]. The temperature of the fuel cladding is dependent on the decay heat and the heat dissipation capabilities of the cask. The SNF decay heat is passively dissipated without any mechanical or forced cooling. The primary heat transfer mechanisms in the HI-STAR 180D Package are conduction and thermal radiation.

The free volume of the space under the inner closure lid (storage cavity) and the cask inter-lid space are filled with high purity helium gas (see Chapter 7 of this SAR) during fuel loading operations. Besides providing an inert dry atmosphere for the fuel cladding, the helium gas also provides conductive heat transfer between each assembly and the surrounding basket walls and across any gaps between the metal surfaces inside the containment system. Metal conduction transfers the heat throughout the fuel basket, through the containment system boundary, and finally through the monolithic shield cylinder and other exterior cask components. The cask storage cavity and inter-lid spaces are backfilled with helium to pressures specified in Table 7.1.4.

The distinguishing features of the HI-STAR 180D cask that enables it to dissipate heat efficiently are:

i. A high conductivity basket material (Metamic-HT) and coplanar honeycomb basket design which facilitates an efficient transmission of heat along the fuel basket's walls.

ii. Use of extruded aluminum alloy shims to provide a near conformal contact between the periphery walls of the basket and the inner surface of the HI-STAR 180D containment shell.

iii. Use of monolithic, low temperature-qualified and high conductivity "shield cylinders" with embedded pockets for Holtite-B that do not interrupt the continuity of the conduction heat transfer path from the inside to the outside.

iv. Use of the shrink fit technology, used in ultra-high pressure vessel manufacturing, to mitigate contact resistance at the shield cylinder/containment shell interface.

[

PROPRIETARY INFORMATION WITHHELD PER 10 CFR 2.390

]

1.2.1.9 Internal Support Features

The HI-STAR 180D Package is equipped with basket shims engineered to provide near conformal support for the fuel basket and facilitate heat transfer. The center sections of the basket shims are fabricated from a high strength aluminum alloy by the extrusion process for maximum homogeneity, strength, and thermal conduction capability. [PROPRIETARY INFORMATION WITHHELD PER 10 CFR 2.390] Mechanical and thermal properties of the shim material are provided in Section 2.2 and Subsection 3.2.1. See additional description in Subparagraph 1.2.1.1 (b). The top and bottom sections of the basket shims are made from stainless steel as shown in the drawing package in Section 1.3.

[

PROPRIETARY INFORMATION WITHHELD PER 10 CFR 2.390

]

1.2.1.10 Anti-Rotation Devices

The HI-STAR 180D Package is equipped with internal anti-rotation devices to prevent the rotation of the fuel basket and basket shims within the cask. [PROPRIETARY INFORMATION WITHHELD PER 10 CFR 2.390]

1.2.1.11 Packaging Markings

Each HI-STAR 180D Packaging shall have a unique identification plate with appropriate markings per 10CFR71.85(c). The identification plate shall not be installed until each HI-STAR 180D Packaging component has completed the fabrication acceptance test program and been accepted by authorized Holtec International personnel.

1.2.2 Contents of Package

The HI-STAR 180D Package is classified as a Category I Type B package since the maximum activity of the contents to be transported in the HI-STAR 180D Package is above limits shown in Table 1 of Regulatory Guide 7.11 [1.2.3].

The allowable radioactive waste (i.e. allowable content) corresponding to each qualified waste package identified in Table 1.1.2 is specified in Appendix 7.D.

The HI-STAR 180D package when equipped with a fuel package is specifically designed for transportation of spent fuel from a nuclear power plant over the plant's entire life cycle, including transport of all fuel assemblies after the plant shutdown. The range of cask content does therefore need to encompass a wide range of fuel parameters, including the following:

- Lower burnup fuel with long cooling times from earlier cycles of the plant; and
- High burnup fuel with intermediate cooling times from current plant operations; and
- High and moderate burnup fuel with short cooling times to be transported after plant shutdown.

[

PROPRIETARY INFORMATION WITHHELD PER 10 CFR 2.390

]

Table 7.D.1 lists the acceptable physical characteristics of the fuel assemblies qualified for transportation in the HI-STAR 180D package. Assemblies are limited to the maximum initial enrichment given in Table 7.D.1 for both F-32 and F-37 baskets.

The maximum mass of radioactive material permitted for transport in the HI-STAR 180D Package is shown in Table 1.2.3. The maximum was calculated assuming the use of the F-37 basket completely filled with fuel assemblies at the maximum allowable fuel mass. For the F-32 basket the maximum will be lower.

The maximum mass of fissile material permitted for transport in the HI-STAR 180D Package is also shown in Table 1.2.3. The maximum was calculated assuming the use of the F-37 basket filled with 37 bounding UO_2 fuel assemblies. For the F-32 basket the maximum mass of fissile material will be lower due to the lower number of assemblies in that basket.

The radioactive and fissile material is in the form of solid fuel pellets with a maximum fuel density shown in Table 1.2.3. There are no moderating material or neutron absorbers in the contents, nor any other material that would create a chemical, galvanic or other reaction leading to the release of combustible gases.

The fuel assemblies are loaded into the basket cells. Each basket cell holds one fuel assembly. The fuel assemblies and the basket cells are approximately the same height. There is no secondary packaging in the contents that is not considered part of the packaging discussed in Section 1.2.1.

The maximum weight of the radioactive payload is shown in Table 1.2.3.

Figures 7.D.1 and 7.D.2 provide cross sectional views of the F-32 and F-37 baskets storage cell layouts. The storage cells are numbered and basket quadrants are specified as shown in these figures to facilitate fuel loading under regionalized storage. With regionalized loading there are eight regions defined for F-32 and nine regions defined for F-37. The storage cell numbers for each region are defined in Table 7.D.5 and Figures 7.D.1 and 7.D.2.

Table 7.D.6 specifies burnup requirements for UO_2 fuel in certain regions in the F-37 basket for two different configurations. These are required for the additional reactivity control in the F-37 basket using burnup credit. Only configuration 2 allows fresh fuel assemblies together with spent fuel assemblies. The fixed minimum burnup requirements in both cases are defined by the maximum permissible enrichment given in Table 7.D.1. Corresponding core operating requirements are listed in Table 7.D.7. There are no minimum burnup requirements for the F-32 basket.

Tables 7.D.2 and 7.D.3 list the specific minimum enrichment, maximum decay heat, maximum assembly average burnup and minimum cooling time limits for five loading patterns for the F-32 and for five loading patterns for the F-37 fuel basket.

In addition to the overall heat load limit specified in Table 7.D.1 for both the F-32 and F-37, there are also heat load limits for each basket cell location by regions as specified in Tables 7.D.2 and 7.D.3. Table 7.D.4 lists alternative maximum burnup/minimum enrichment/minimum cooling time combinations for most regions. These are referenced appropriately in Tables 7.D.2 and 7.D.3.

[

PROPRIETARY INFORMATION WITHHELD PER 10 CFR 2.390

]

1.2.3 Special Requirements for Plutonium

Plutonium (in any form) other than from spent fuel pellets is not authorized for transport.

1.2.4 Operational Features

The HI-STAR 180D Packaging has been developed to facilitate loading and unloading of fuel with ALARA protection against handling accidents and a minimum number of handling evolutions (i.e., simplicity of handling). There are no complex operational features that required a detailed exposition. Similar to the HI-STAR 180 cask, the HI-STAR 180D cask closure lids are equipped with penetrations (ports) for drying and inerting the cask's content. The port configuration on the inner closure lid is configured to minimize radiation streaming as indicated in the drawing package in Section 1.3. The inner closure lid ports shown in the drawing package in Section 1.3 are typical ports equipped with port plugs. Port caps, in lieu of plugs, are equally effective and may be used. The configuration of the outer closure lid access port cover and port cover subcomponents likewise have redundant closure. The HI-STAR 180D Packaging is a completely passive system once loaded and sealed in accordance with Chapter 7. The abbreviated narrative below on typical loading operations helps illustrate the overall simplicity of the loading process. Chapter 7 provides the essential elements of cask operations.

Typical Loading Operations

At the start of loading operations, the cask is configured with the closure lids removed and the fuel basket installed. The cask is lowered into the spent fuel pool for fuel loading. Pre-selected assemblies are loaded into the fuel basket cells and a visual verification of the assembly identification is performed.

While still underwater, the inner closure lid is installed. The cask is removed from the pool and placed in the designated preparation area.

The Forced Helium Dehydration (FHD) System is connected to the cask and used to remove all bulk water and water vapor so as to reduce the level of moisture in the cask cavity to acceptable levels. This is accomplished by recirculating dry, heated helium through the cask cavity to absorb the moisture. The HI-STORM FSAR [1.2.7] provides the Design Criteria for the FHD system.

Alternatively, cavity drying may be carried out using the classical vacuum drying system, if it is ensured that the fuel temperature remains within acceptable limits per the requirements in Chapter 3 and procedures in Chapter 7 of this SAR.

Following the fuel drying operations, the cask cavity is backfilled with helium gas and the vent/drain ports are sealed (quantity of helium is specified in Table 7.1.4). The inner Containment Boundary seals are then leak tested to the leakage acceptance criteria specified in Chapter 8 of this SAR.

The outer closure lid is installed, followed by evacuation of the inter-lid space using the outer lid's port openings and backfilling with helium (quantity of helium is specified in Table 7.1.4). The outer lid (expanded) containment boundary seals are then also leak tested to the leakage acceptance criteria specified in Chapter 8 of this SAR.

The cask is next secured on the transport vehicle with impact limiters attached, a security seal (tamper device) is attached, and the personnel barrier is installed (if required). The HI-STAR 180D Package is then ready for transport.

The inspections and tests (acceptance criteria and maintenance requirements) required to prepare the package for shipment are specified in Chapter 8 of this SAR.

Table 1.2.1

Major Constituent Parts of the HI-STAR 180D Cask

Item No.	Part Name	Principal Function	Comments
1	Cask Containment Shell (CCS)	Containment of radionuclides, pressure retention and radiation blockage	Containment parts in Items 1, 2, 3 and 4 comprise the cask's containment system; all containment parts must meet ASME Section III Subsection NB in all respects.
2	Cask Bottom Region (CBR)	Containment of radionuclides, pressure retention and radiation blockage; Mounting surface for the bottom impact limiter	The welded joint between the containment shell and the containment baseplate is a structural butt welded joint volumetrically examined to meet the ASME code. The Cask Bottom Region provides the location for the cask bottom trunnions.
3	Cask Top Region (CTR)	Containment of radionuclides, pressure retention and radiation blockage; seating surface for the Double Closure Lid system and mounting surface for the top Impact Limiter	The welded joint between the containment shell and the containment closure flange is a structural butt welded joint volumetrically examined to meet the ASME code. Top Forging provides the location for the cask top trunnions and the location for a fine-machined gasket seating surface for each Closure Lid.
4	Double Closure Lid System (DCLS)	Defines the top region of the Containment Boundary. Serves to provide access to the Waste Package within	Must meet Section III Subsection NB of the ASME Code and must be sufficiently robust to withstand loadings under accident conditions of transport.
5	Gamma Capture Space (GCS)	Blockage of gamma radiation, rendered by the mass of monolithic steel cylinders fabricated and installed to preclude macro-voids and large spatial discontinuities	The annular space defined by the external surface of the Containment Shell on its inside and the Monolithic Shield Cylinder on its outside. This annular space contains the Neutron Capture Space (NCS).
6	Neutron Capture Space (NCS)	Attenuation of neutrons, rendered by Holtite	The sector pockets within the monolithic shield cylinders that are filled with Holtite-B and whose principal function is to block the neutrons accreted by the contained CSF.

Table 1.2.2

[PROPRIETARY INFORMATION WITHHELD PER 10 CFR 2.390]

Table 1.2.3

[PROPRIETARY INFORMATION WITHHELD PER 10 CFR 2.390]

Tables 1.2.4 through 1.2.10 are left intentionally blank

Table 1.2.11 is intentionally left blank

See Table 2.2.8 for Metamic-HT properties.

Table 1.2.12 is intentionally left blank

See Table 2.2.13 for Holtite-B properties.

FIGURE 1.2.1
[PROPRIETARY INFORMATION WITHHELD PER 10 CFR 2.390]

FIGURE 1.2.2
[PROPRIETARY INFORMATION WITHHELD PER 10 CFR 2.390]

1.3 ENGINEERING DRAWINGS

This section contains a HI-STAR 180D Drawing Package prepared under Holtec's QA Program. This drawing package contains the details of the safety features considered in the analysis documented in this SAR. In particular, this drawing package includes:

- A list of materials and parts, including their safety significance status.
- All dimensions that define the package's *Critical Characteristics*.
- All interface dimensions to ensure fit-up between mating parts.
- Requisite information on *safety significant* parts such as the containment boundary parts as well as processes such as welding, non-destructive examinations, including appropriate weld symbols and NDE acceptance criteria.
- Details on configuration of gasket joints germane to their sealing function.
- Identification of the Containment System Boundary.
- Design details on the impact limiters.

The manufacturing of the HI-STAR 180D components is required to be in strict compliance with the Drawing Package in this section.

Figure 1.3.1 provides an illustration of the assembled HI-STAR 180D Package for transport. Figure 1.3.2 provides an illustration of the HI-STAR 180D Package on a railcar with personnel barrier, support saddles and other typical components.

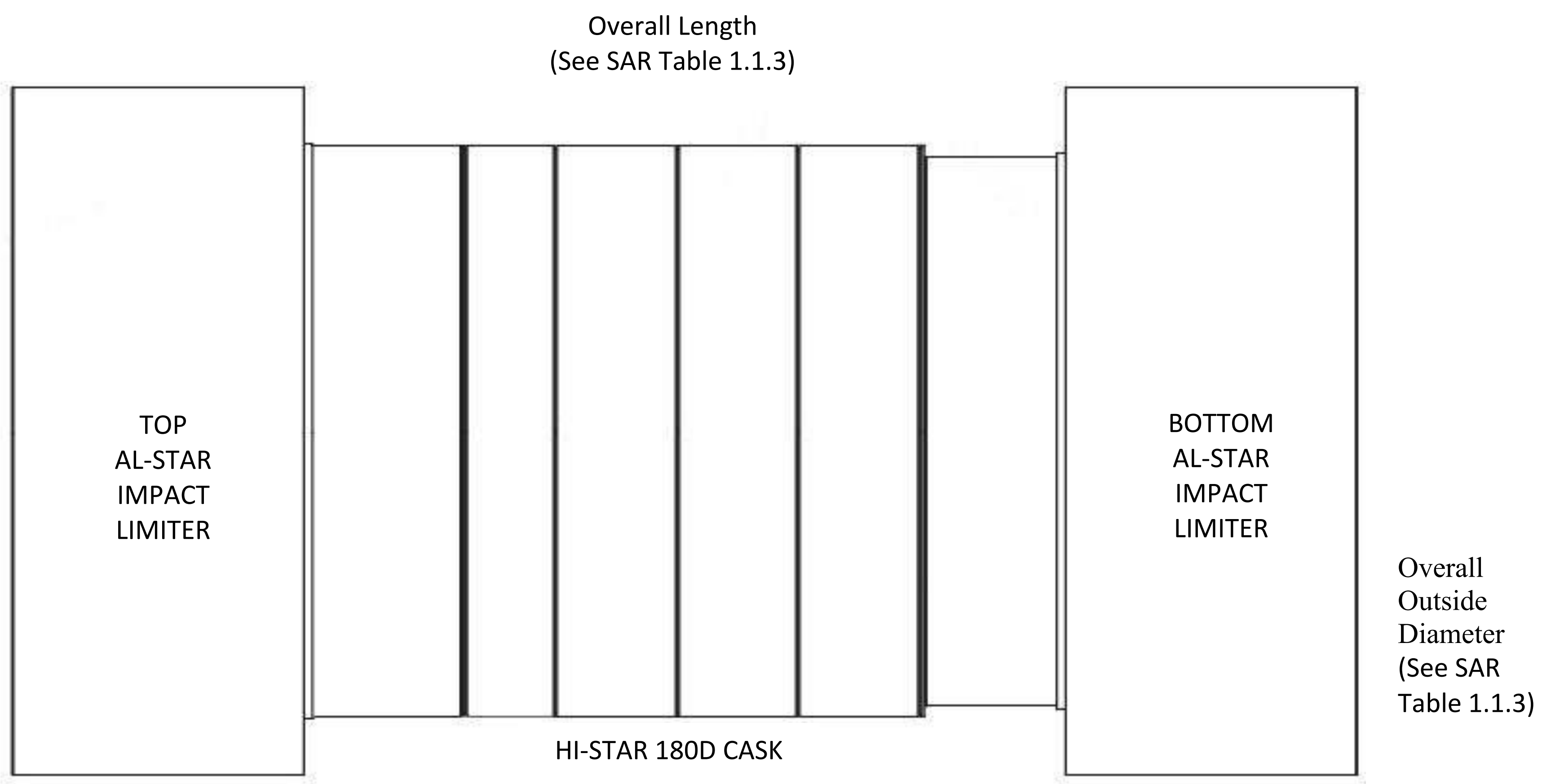

Note: Dimensions are nominal.

FIGURE 1.3.1: ILLUSTRATION OF HI-STAR 180D TYPICAL ASSEMBLY FOR TRANSPORT

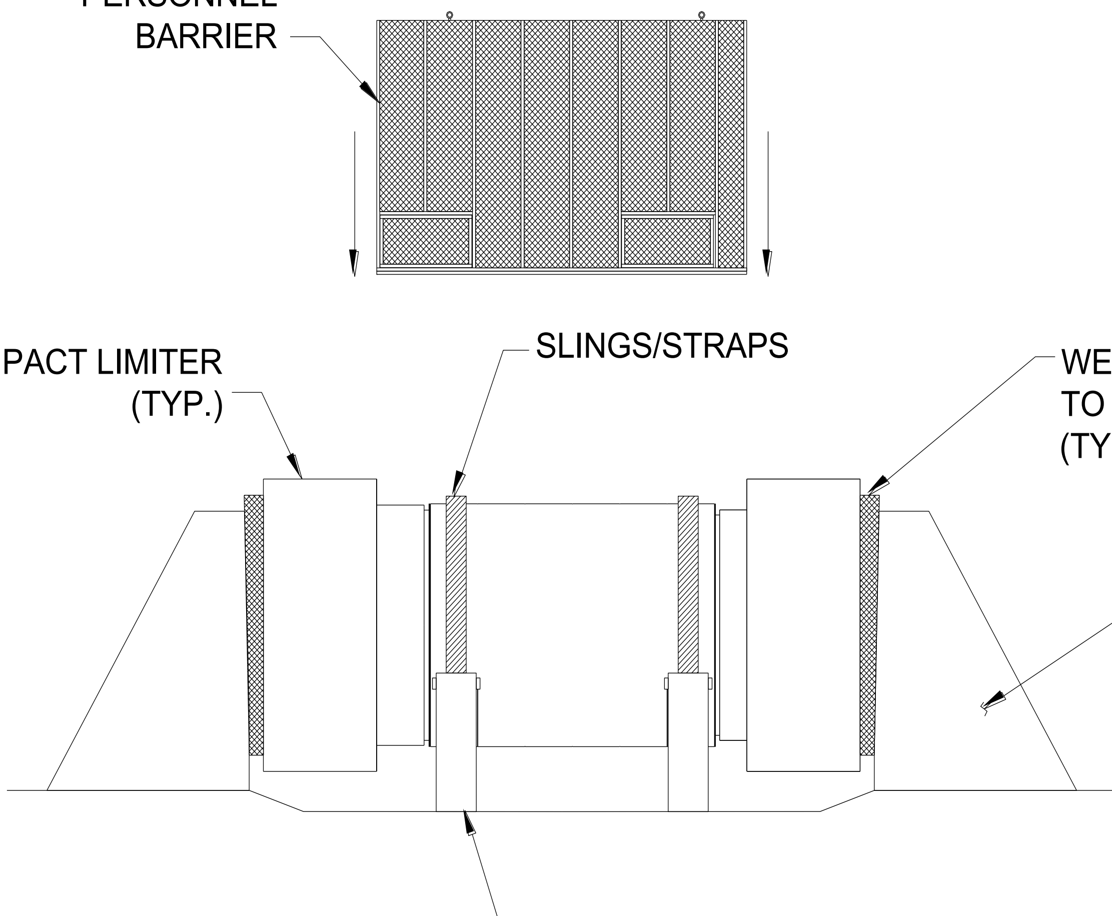

FIGURE 1.3.2: ILLUSTRATION OF HI-STAR 180D TYPICAL RAILCAR TRANSPORT CONFIGURATION

1.4 SUMMARY OF COMPLIANCE WITH 10CFR71 REQUIREMENTS

The HI-STAR 180D Package complies with the requirements of 10CFR71 for a Type B(U)F-96 package. Analyses which demonstrate that the HI-STAR 180D Package complies with the requirements of Subparts E and F of 10CFR71 are provided in this SAR. The HI-STAR 180D Package complies with the general standards for all packages, 10CFR71.43, as demonstrated in Chapter 2. Under the tests specified in 10CFR71.71 (normal conditions of transport) the HI-STAR 180D Package is demonstrated to sustain no impairment of its safety function capability, enabling the HI-STAR 180D Package to meet the requirements of 10CFR71, Paragraphs 71.45, 71.51, and 71.55 (see discussion on high burnup fuel below). Under the tests specified in 10CFR71.73 (hypothetical accident conditions) and 10CFR71.61 (special requirement for irradiated nuclear fuel shipments), the damage sustained by the HI-STAR 180D Package is shown to be within the permissible limits set forth in 10CFR71, Paragraphs 71.51, and 71.55 (see discussion on high burnup fuel below).

The HI-STAR 180D Package meets the structural, thermal, containment, shielding and criticality requirements of 10CFR71, as described in Chapters 2 through 6. The package operations; and acceptance tests and maintenance program provided in Chapters 7 and 8 ensure compliance of the package with the requirements of 10CFR71.

The following is a summary of the information provided in Chapter 1, which in conjunction with the information provided in Chapters 2, 7 and 8 is directly applicable to verifying compliance with 10CFR71:

- The HI-STAR 180D Packaging description including the drawing package provided in Section 1.3 provides an adequate basis for evaluation of the HI-STAR 180D Packaging against the 10CFR71 requirements for each technical criterion. Each drawing is identified, consistent with the text of the SAR, and contains appropriate annotations to explain and clarify information on the drawing.

- The NRC-approved Holtec International quality assurance program for the HI-STAR 180D packaging has been identified.

- The applicable codes and standards for the HI-STAR 180D Packaging design, fabrication, assembly, and testing have been identified in the drawing package in Section 1.3 and in Chapter 2.

- Allowable contents in the HI-STAR 180D Packaging are specified (in Section 1.2).

<u>High Burnup Fuel (HBF) Considerations</u>:

[

PROPRIETARY INFORMATION WITHHELD PER 10 CFR 2.390

]

[

PROPRIETARY INFORMATION WITHHELD PER 10 CFR 2.390

]

[

PROPRIETARY INFORMATION WITHHELD PER 10 CFR 2.390

]

Table 1.4.1
[PROPRIETARY INFORMATION WITHHELD PER 10 CFR 2.390]

1.5 LOCATION OF PROPERTIES OF SPECIAL PURPOSE MATERIALS

Requirements for special purpose materials and parts (essentially non-code materials) utilized in the HI-STAR 180D package such as Holtite, containment seals, impact limiter crush materials, etc., are provided in their proper context in this SAR and are thus scattered across this document. To ensure that the applicable properties of such materials used in the safety analyses are correctly extracted in the Purchasing Specification for each special purpose material, Table 1.5.1 provides the location where the required information can be found in this SAR.

Table 1.5.1: Location of Properties of Special Purpose Materials in This SAR

Item No.	Material	Location
1	Holtite-B	Subparagraph 1.2.1.5.1 Table 2.1.16 Table 2.2.13 Subsection 3.2.1 Table 3.2.1 Table 3.2.2 Table 3.2.7 Table 3.2.12Table 3.2.12 Table 5.3.3 Table 8.1.11 (including for B_4C and copper content)
2	Metamic -HT	Subparagraph 1.2.1.6.1 Section 1.3 (Drawing 8553) Table 2.1.16 Table 2.2.8 Subsection 3.2.1 Table 3.2.1 Table 3.2.5 Table 3.2.6 Table 3.2.7 Table 3.2.10 Table 5.3.2 Table 6.3.4 Table 8.1.3 (for B_4C and B-10 content) Table 8.1.5
3	Containment Seals	Section 1.3 (Drawing 8545) Subparagraph 2.2.1.1.6 Table 2.1.16 Table 2.2.12 Table 3.2.12 Appendix 8.A
4	AL-STAR Impact Limiter Crush Material	Section 1.3 (Drawing 8552) Subparagraph 2.2.1.1.5 Table 2.1.16 Table 2.2.10 Paragraph 2.7.1.1 Table 3.2.1 Table 3.2.2 Table 3.2.7 Table 3.2.10 Table 3.2.12

1.6 QUALITY ASSURANCE AND DESIGN CONTROL

1.6.1 Quality Assurance Program:

The HI-STAR 180D Package design, material acquisition, fabrication, assembly, and testing shall be performed in accordance with Holtec International's QA program. Holtec International's QA program was originally developed to meet NRC requirements delineated in 10CFR50, Appendix B, and was expanded in the early 90s to include provisions of 10CFR71, Subpart H, and 10CFR72, Subpart G, for structures, systems, and components (SSCs) designated as *important-to-safety*. NRC approval of Holtec International's QA program is documented by the Quality Assurance Program Approval for Radioactive Material Packages (NRC Form 311), Approval Number 0784, Docket No. 71-0784.

1.6.2 Package Design Control:

The design information presented in this SAR is subject to validation, safety compliance, and configuration control in accordance with Holtec's NRC-approved quality assurance (QA) program which comports with the provisions of 10CFR71.107. Chapters 7 and 8 and the licensing drawing package collectively contain conditions to the CoC, and as such, they can be modified only through an NRC licensing action. The other chapters contain substantiating information to support the safety case and can be amended subject to the stipulations of 71.107(c).

CHAPTER 1 REFERENCES

The following generic industry and Holtec produced references may have been consulted in the preparation of this document. Where specifically cited, the identifier is listed in the SAR text or table. Active Holtec Calculation Packages which are the repository of all relevant licensing and design basis calculations are annotated as “latest revision”. Submittal of the latest revision of such Calculation Packages to the USNRC and other regulatory authorities during the course of regulatory reviews are managed under the company’s Configuration Control system. Supporting documents submitted to the USNRC with the HI-STAR 180D LAR 9367-2 have been italicized.

[1.0.1] Regulatory Guide 7.9, "Standard Format and Content of Part 71 Applications for Approval of Packaging for Radioactive Material", Revision 2, USNRC, March 2005.

[1.0.2] 10CFR Part 71, "Packaging and Transportation of Radioactive Materials", Title 10 of the Code of Federal Regulations, Office of the Federal Register, Washington, D.C.

[1.0.3] 49CFR173, "Shippers - General Requirements for Shipments and Packagings", Title 49 of the Code of Federal Regulations, Office of the Federal Register, Washington, D.C.

[1.0.4] “Safety Analysis Report for the HI-STAR 180 Package”, Holtec Report HI-2073681, latest revision, Docket No. 71-9325.

[1.0.5] “Safety Analysis Report for the HI-STAR 100 Package”, Holtec Report HI-951251, latest revision, Docket No. 71-9261.

[1.0.6] “Final Safety Analysis Report for the HI-STAR 100 Package”, Holtec Report HI-2012610, latest revision, Docket No. 72-1008.

[1.0.7] “Safety Analysis Report for the HI-STAR 60 Package”, Holtec Report HI-951251, latest revision, Docket No. 71-9336.

[1.0.8] “Safety Analysis Report for the HI-STAR 63 Package”, Holtec Report HI-2073777, latest revision (design approval by MEST in South Korea).

[1.0.9] “Final Safety Analysis Report on the HI-STORM FW System”, Holtec Report HI-2114830. Latest revision, Docket No. 72-1032.

[1.0.10] “Safety Analysis Report for the HI-STAR 180L Package”, Holtec Report HI-2177805, latest revision, USNRC Docket No. 71-9381.

[1.0.11] "Safety Analysis Report for the HI-STAR 190 Package", Holtec Report HI-2146214, latest revision, USNRC Docket No. 71-9373.

[1.0.12] "Safety Analysis Report for the HI-STAR 80 Package", Holtec Report HI-2146261, latest revision, USNRC Docket No. 71-9374.

[1.0.13] "Safety Analysis Report for the HI-STAR ATB-1T Package", Holtec Report HI-2146312, latest revision, USNRC Docket No. 71-9375.

[1.0.14] "Safety Analysis Report for the HI-STAR 100MB Package", Holtec Report HI-2188080, latest revision, USNRC Docket No. 71-9378.

[1.1.1] IAEA Safety Standards, Safety Requirements, No. SSR-6, "Regulations for the Safe Transport of Radioactive Material", International Atomic Energy Agency, 2012 Edition.

[1.2.1] American Society of Mechanical Engineers, "Boiler and Pressure Vessel Code", Section III, Div. 1, Subsection NB 2007 Edition, 2008 Addenda.

[1.2.2] American Society for Testing and Materials, ASTM A-352-93, "Ferritic and Martensitic Steel Castings for Pressure-Containing Parts Suitable for Low-Temperature Service"

[1.2.3] Regulatory Guide 7.11, "Fracture Toughness Criteria of Base Material for Ferritic Steel Shipping Cask Containment Vessels with a Maximum Wall Thickness of 4 Inches (0.1m)", U.S. Nuclear Regulatory Commission, Washington, D.C., June 1991.

[1.2.4] Holtite-A: Development History and Thermal Performance Data, Holtec Report HI-2002396, 2002, Docket No. 72-1014. (Holtec Proprietary)

[1.2.5] Holtite-A: Results of Pre-and Post Irradiation Tests and Measurements, Holtec Report HI-2002420, 2003, Docket No. 72-1014. (Holtec Proprietary)

[1.2.6] "Qualification of METAMIC for Spent Fuel Storage Applications", Report 1003137, EPRI, Palo Alto, CA, October 2001.

[1.2.7] "HI-STORM 100 Final Safety Analysis Report", Holtec Report HI-2002444, latest revision, Docket No. 72-1014.

[1.2.8] USNRC Docket No. 72-1004 SER on NUHOMS 61BT (2002).

[1.2.9] "Safety Evaluation by the Office of Nuclear Reactor Regulation Related to Holtec International Report HI-2022871 Regarding Use of Metamic in Fuel Pool Applications," Facility Operating License Nos. DPR-51 and NPF-6, Entergy Operations, Inc., docket No. 50-313 and 50-368, USNRC, June 2003.

[1.2.10] "Sourcebook for Metamic Performance Assessment", by Dr. Stanley Turner, Holtec Report HI-2043215, Rev. 2, Docket No. 71-9261 (TAC L24029). (Holtec Proprietary)

[1.2.11] NUREG-0612, "Control of Heavy Loads at Nuclear Power Plants", U.S. Nuclear Regulatory Commission, Washington, D.C., July 1980.

[1.2.12] ANSI N14.6-1993, "Special Lifting Devices for Shipping Containers Weighing 10,000 Pounds (4500 Kg) or More", June 1993.

[1.2.13] Interim Staff Guidance ISG-11, Rev. 3, USNRC, November, 2003.

[1.2.14] American National Standards Institute, Institute for Nuclear Materials Management, ""American National Standard for Radioactive Materials Leakage Tests on Packages for Shipment", ANSI N14.5, 2014.

[1.2.15] Interim Staff Guidance ISG-19, Rev. 0, USNRC, May, 2003.

[1.2.16] ASME Boiler & Pressure Vessel Code, Section II, Part A, SA-352-LCC American Society of Mechanical Engineers, 2007 Edition, 2008 Addenda.

.

[1.2.17] *"Holtite-B Sourcebook", Holtec Report HI-2167314, Latest Revision. (Holtec Proprietary)*

[1.2.18] "Handbook of Aluminum - Alloy Production and Materials Manufacturing", Vol. 2, Edited by G.E. Totten and D.S. Mackenzie, CRC (Taylor and Francis Group), 2003.

[1.2.19] "Oxide Dispersion Strengthening" by Ansell et. als, ASME Convergence, Vol. 47, Gordon and Breach, NY (1966).

[1.2.20] "Increasing the Use of Fibre-Reinforced Composites in the Sasol Group of Companies: A Case Study", by Jacques Mouton, Ph.D. Dissertation, University of Durban, South Africa (2007).

[1.2.21] "Metals Handbook", Vol. 7, 9th Edition

[1.2.22] NUREG-1617, Standard Review Plan for Transportation Packages for Spent Nuclear Fuel, 2000.

[1.2.23] Turner, S.E., "Reactivity Effects of Streaming Between Discrete Boron Carbide Particles in Neutron Absorber Panels for Storage or Transport of Spent Nuclear Fuel," Nuclear Science and Engineering, Vol. 151, Nov. 2005, pp. 344-347.

[1.2.24] Natrella, M.G., “Experimental Statistics, “National Bureau of Standards Handbook 91, National Bureau of Standards, Washington, DC, 1963.

[1.2.25] “Metamic-HT Manufacturing Manual”, Latest Revision, Holtec International (Holtec Proprietary).

[1.2.26] “Metamic-HT Purchasing Specification”, Holtec Document ID PS-11, Latest Revision, (Holtec Proprietary).

[1.2.27] *“Metamic-HT Qualification Sourcebook”, Holtec Report No. HI-2084122, Latest Revision (Holtec Proprietary)*

[1.2.28] “Application of Time-Temperature-Stress Parameters to High Temperature Performance of Aluminum Alloys”, by J.G. Kaufman, Z. Long and S. Ningileri, Minerals, Metals & Materials Society, 2007.

[1.2.29] “Sampling Procedures and Tables for Inspection by Attributes”, Military Standard MIL-STD-105E, (10/5/1989).

[1.2.30] “Dynamic Mechanical Response and Microstructural Evolution of High Strength Aluminum-Scandium (Al-Sc) Alloy, by W.S. Lee and T.H. Chen, Materials Transactions, Vol. 47, No. 2(2006), pp 355-363, Japan Institute for metals.

Appendix 1.A: NOT USED

APPENDIX 1.B:

[PROPRIETARY INFORMATION WITHHELD PER 10 CFR 2.390]

CHAPTER 2: STRUCTURAL EVALUATION

2.0 INTRODUCTION

This chapter presents a synopsis of the Design Criteria relevant to the mechanical and structural characteristics of the HI-STAR 180D Package that ensure compliance with the performance requirements of 10CFR71, and it summarizes all structural evaluations and analyses of the package, pursuant to the provisions of 10CFR§71.61, 10CFR§71.71, and 10CFR§71.73.

In particular, the objectives of this chapter are twofold:

a. To demonstrate that the structural performance of the HI-STAR 180D Package has been adequately evaluated for the normal conditions of transport and for the hypothetical accident conditions set forth in 10CFR§71.61, 10CFR§71.71, and 10CFR§71.73.

b. To demonstrate that the HI-STAR 180D Package design has adequate structural integrity to meet the regulatory requirements of 10CFR§71.61, 10CFR§71.71, and 10CFR§71.73.

Among the topical areas addressed in this chapter are:

i. Structural characterization of the cask and its appurtenances.
ii. Identification of the materials used in the package and their *critical characteristics*.
iii. Identification of the loads applied on the package during handling, normal conditions of transport and accident conditions. Definition of miscellaneous bounding conditions for design such as a fire and immersion in water.
iv. Derivation of acceptance criteria for the package's performance under the aforementioned various conditions of service from the ASME B&PV Codes and other reference standards.
v. Analyses of the package using appropriate methodologies to establish the margins of safety under each condition of service. In addition to the typical evaluations for normal and accident conditions, these analyses include:
   - Evaluation of the physical integrity of the spent fuel under the postulated impactive loading events.
   - A demonstration of the adequacy of the minimum acceptable Charpy impact values specified for the parts subject to potential impact loadings. This is based on a methodology that determines the fracture strength of a material using the Charpy impact strength data.

Appendix 2.A provides introductory information on the principal codes used in the structural analysis (ANSYS and LS-DYNA). Appendix 2.B of HI-STAR 180 SAR [1.0.4] provides a comprehensive summary of the three-stage benchmarking effort by Holtec International to establish the veracity of the LS-DYNA solution for predicting the peak deceleration of the package and crush performance of the AL-STAR impact limiters. A discussion of the finite element discretization level to ensure that the solutions are fully converged is also provided.

To facilitate regulatory review, throughout this chapter, the assumptions and conservatism inherent in the analyses are identified along with a complete description of the analytical methods, models, and acceptance criteria. A summary of other considerations germane to satisfactory structural performance, such as protection against corrosion, creep (in the Metamic-HT fuel basket), and brittle fracture, is also provided.

Finally, the analysis methods, models and acceptance criteria utilized in the safety evaluation documented in this chapter mirror those used in the SAR for HI-STAR 180 certified in Docket #71-9325. Specifically, all the analysis methods (e.g., strength of materials and finite element analysis codes) employed to structurally qualify the two casks and the corresponding acceptance criteria are identical. The structural analysis models developed to analyze the two casks are very similar due to the similar design features of the two casks as listed in the following table.

Comparison of Major Design Features of HI-STAR 180 and HI-STAR 180D Casks

Cask Feature	HI-STAR 180	HI-STAR 180D
Containment Shell	[Withheld in Accordance with 10 CFR 2.390] SA203-E or SA350 LF3	[Withheld in Accordance with 10 CFR 2.390] SA203-E or SA350 LF3
Containment Closure Flange	[Withheld in Accordance with 10 CFR 2.390] SA350-LF3	[Withheld in Accordance with 10 CFR 2.390] SA350-LF3
Containment Baseplate	[Withheld in Accordance with 10 CFR 2.390] SA203-E or SA350 LF3	[Withheld in Accordance with 10 CFR 2.390] SA203-E or SA350 LF3
Monolithic Shield Cylinder	[Withheld in Accordance with 10 CFR 2.390] A352-93-LCC or SA352-LCC	[Withheld in Accordance with 10 CFR 2.390] A352-93-LCC or SA352-LCC
Inner Lid	[Withheld in Accordance with 10 CFR 2.390] SA203-E or SA350 LF3	[Withheld in Accordance with 10 CFR 2.390] SA203-E or SA350 LF3
Inner Lid Bolts	[Withheld in Accordance with 10 CFR 2.390] SA564-630 (H1025) or SA705-630 (H1025) or SB637-N07718	[Withheld in Accordance with 10 CFR 2.390] SA564-630 (H1025) or SA705-630 (H1025) or SB637-N07718
Outer Lid	[Withheld in Accordance with 10 CFR 2.390] SA203-E or SA350 LF3	[Withheld in Accordance with 10 CFR 2.390] SA203-E or SA350 LF3
Outer Lid Bolts	[Withheld in Accordance with 10 CFR 2.390] SA564-630 (H1025) or SA705-630 (H1025) or SA193-B7 or SB637-N07718	[Withheld in Accordance with 10 CFR 2.390] SA564-630 (H1025) or SA705-630 (H1025) or SB637-N07718

Inter-Lid Gap	[Withheld in Accordance with 10 CFR 2.390]	[Withheld in Accordance with 10 CFR 2.390]
Fuel-to-Cask Axial Gap Control	[Withheld in Accordance with 10 CFR 2.390]	[Withheld in Accordance with 10 CFR 2.390] See SAR Paragraph 1.2.1.9

2.1 STRUCTURAL DESIGN

2.1.1 Discussion

This subsection presents the essential characteristics of the principal structural members and systems that are important to the safe operation of the HI-STAR 180D Package. These members are the containment system components (together with those parts that render the radiation shielding function in the cask), the structural components that constitute the fuel basket and the surrounding support, and the impact limiters needed to protect the package in the event of a hypothetical accident event (§71.73).

2.1.1.1 Cask

The structural functions of the cask in the transport mode are:

- To provide a high integrity fuel basket.
- To serve as a penetration and puncture barrier for the fuel basket.
- To provide a high-integrity containment system.
- To provide a structurally robust support for the radiation shielding components.

The HI-STAR 180D cask consists of three discrete regions; namely:

1. the containment space
2. the inter-lid space
3. the supplemental shielding

The containment space (or space within the containment boundary as identified in the drawing package in Section 1.3 and described in Sections 1.2 and 4.1) is the heart of the package. It must ensure a leak-tight enclosure for its contents under all normal and accident conditions of transport.

Accordingly, it is designed to meet the most rigorous industry requirements, to the extent germane to its function, of Section III, Subsection NB of the ASME Boiler & Pressure Vessel Code [2.1.1]. Section 1.5.2.6 of NUREG-1617 [2.1.11] states the following:

“ASME has published Section III, Division 3, ASME Boiler and Pressure Vessel (B&PV Division 3) Code for the design and construction of the containment system of SNF transport packagings. NRC staff expects full compliance with the B&PV Division 3 Code for the containment system, including the services of an Authorized Inspection Agency. However, the SAR may justify alternatives as appropriate.”

In this SAR, ASME Section III, Division 1, Subsection NB is used for the design and construction of the HI-STAR 180D containment system, in lieu of the Division 3 Code, since Subsection NB has an established history of use and NRC approval for similar cask designs (e.g., HI-STAR 100, HI-STAR 60, HI-STAR 180).

The inter-lid space (or expanded containment space as described in Section 1.2 and Section 4.1) is the space between the outer closure lid and the inner closure lid. The inter-lid gap between the closure lids is sufficiently small as shown in the drawing package such that the outer closure lid reinforces the inner closure lid and and both lids can act in tandem in the event of a hypothetical drop accident when the fuel and the lid are potentially subjected to large impact forces. This feature limits the maximum deflection in the inner lid and keeps check on the demand on the inner lid bolting and the corresponding seals. The structural analysis models developed for analyzing the hypothetical drop accident condition (see Subsection 2.7.1.1) consider the structural interaction of the two closure lids by defining a surface-to-surface contact between the two lids to capture this design feature. The outer closure lid gasketed joint is accordingly designed to have the same level of sealing reliability as the inner closure lid joint. The double lid closure feature in the HI-STAR 180D Package is not a Part 71 requirement: It has been incorporated into the package to help establish the necessary level of technical confidence to rule out moderator intrusion into the space under the inner closure lid in the sequence of accident events set forth in §71.73, which culminates in water submergence (see Appendix 1.B).

The supplemental shielding consists primarily of the monolithic shield cylinders (or shield cylinders). The monolithic shield cylinders, with neutron shielding material installed in their sector pockets (as described in Section 1.2 and identified in the drawing package in Section 1.3), are dose blocker parts that provide gamma and neutron attenuation. To perform their function, they must not undergo body extensive damage resulting in an appreciable loss of shielding capacity under normal and accident conditions of transport.

To minimize the axial gap between the top of the fuel assemblies and the inner closure lid, the population of the fuel common to the host reactor plant is surveyed and the cask cavity length is accordingly controlled as discussed in Section 1.2. The cask cavity is sized such that the fuel assembly top nozzle hold-down springs may be in nominal contact with the bottom surface of the inner closure lid during transport. Fuel assembly hold-down spring travel is sufficiently large to accommodate differential thermal expansion (reported in Chapter 3 of this SAR) that can occur under normal and accident conditions of transport. Nonetheless, both the hypothetical drop accidents, as detailed in Section 2.7, and the fuel integrity evaluation, as discussed in Section 2.11, consider the maximum axial gap between the fuel assemblies and the containment cavity considering the minimum end of life (eol) fuel length (with hold-down springs) and the maximum differential thermal expansion.

2.1.1.2 Fuel Basket and Fuel Basket Support

The structural function of the fuel basket and fuel basket support (basket shims) (see drawing package in Section 1.3) in the transport mode is to maintain the position of the fuel in a sub-critical configuration. In its role as the guarantor of subcriticality, the fuel basket must exhibit global physical integrity (i.e., no potential for large plastic deformation or structural failure in the active fuel region) under the most structurally demanding conditions of transport (see 2.1.2.2 (ii) for acceptance criterion).

2.1.1.3 Impact Limiters

The impact limiters used in the HI-STAR family of transport casks utilize shaped blocks of a crushable material arrayed around an extremely stiff cylindrical core in such a manner that the cask is protected from excessive inertia forces under a (hypothetical) uncontrolled drop event *regardless* of the orientation of drop. The three defining characteristics of the HI-STAR impact limiter are:

(i) An essentially rigid steel cylindrical core,
(ii) A steel cylindrical skirt integrally welded to the core that girdles the cask's forging (at its two extremities) and thus prevents any significant rigid body rotation of the core under a drop event, and
(iii) A set of ductile alloy steel fasteners that provide the necessary connectivity between the cask and the impact limiter.

The impact limiter configured on the above design platform is referred to as "AL-STAR" and is used in all models of HI-STAR transport packages, including the first package (HI-STAR 100), and subsequent packages labeled HI-STAR HB, HI-STAR 60, HI-STAR 180 and the current package (HI-STAR 180D).

The structural function of the AL-STAR impact limiters (shown in the drawing package in Section 1.3) in the transport mode is to cushion the HI-STAR 180D cask and the contained fuel during normal transport package handling, and during a hypothetical drop accident. The AL-STAR impact limiters and other appurtenances such as the support saddles and the personnel barrier necessary for the transport package must also meet all applicable regulatory requirements.

In what follows, explicit design criteria for the components of the transport package and essential appurtenances are presented.

2.1.2 Design Criteria

Regulatory Guide 7.6 [2.1.2] provides guidance for design criteria for the structural analysis of shipping cask containment vessels. Loading conditions and load combinations for transport are defined in 10CFR71 [2.1.3] and in Regulatory Guide 7.8 [2.1.4]. Consistent with the provisions of these documents, the central objective of the structural requirements presented in this section is to ensure that the HI-STAR 180D Package possesses sufficient structural capability to meet the demands of both normal (§71.71) and hypothetical accident conditions (§71.73) of transport articulated in the regulatory guidance documents, specifically Reg. Guide 7.6. The following table provides a synoptic matrix to demonstrate the explicit compliance with the seven regulatory positions with respect to the Containment Boundary stated in Regulatory Guide 7.6.

USNRC's Regulatory Position regarding the Containment Boundary for the Transport Package
1. Material properties, design stress intensities, and fatigue curves are obtained from the ASME Code.
2. Under normal conditions of transport, the limits on stress intensity are those limits defined by the ASME Code for primary membrane and for primary membrane plus bending for Level A conditions.

USNRC's Regulatory Position regarding the Containment Boundary for the Transport Package
3. Perform fatigue analysis for normal conditions of transport using ASME Code Section III methodology (NB) and appropriate fatigue curves.
4. The stress intensity S_n associated with the range of primary plus secondary stresses under normal conditions should be less than $3S_m$ where S_m is the primary membrane stress intensity from the ASME Code.
5. Buckling of the containment vessel should not occur under normal or accident conditions.
6. Under accident conditions, the values of primary membrane stress intensity should not exceed the lesser of $2.4S_m$ and $0.7S_u$ (ultimate strength), and primary membrane plus bending stress intensity should not exceed the lesser of $3.6S_m$ and S_u.
7. The extreme total stress intensity range should be less than $2S_a$ at 10 cycles as given by the appropriate fatigue curves.

The following design requirements are applicable to the remainder of the transport package:

- The shield cylinders are required to remain in place and functional after all Normal and Hypothetical Accident Conditions of Transport.

- The fuel basket is required to maintain its shape so as to ensure reactivity control after all Normal and Hypothetical Accident Conditions of Transport.

- The fuel basket supports are required to maintain global positioning of the fuel basket after all Normal and Hypothetical Accident Conditions of Transport.

- The impact limiters are required to have an appropriate shape and energy absorption capacity to ensure that impacts, resulting from hypothetical accident events, do not cause any of the containment and shielding components to fail to meet their specified requirements.

2.1.2.1 Loading and Load Combinations

10CFR71 and Regulatory Guide 7.6 define two conditions that must be considered for qualification of a transport package. These are defined as "Normal Conditions of Transport" and "Hypothetical Accident Conditions".

The loadings applicable to the HI-STAR 180D package can be broadly divided into five categories, namely:

1. permanent loads
2. design condition loads
3. handling loads
4. normal condition of transport loads (§71.71)
5. hypothetical accident condition loads (§71.73)

1. Permanent Loads

Permanent loads in HI-STAR 180D arise from bolt pre-load to seat the gasketed joints. The preload applied to the cask lid bolts seats the metal seals and creates a contact pressure on the inside metal-to-metal annulus, referred to as the “land”, to protect the joint from leakage under postulated impact loading events. Bolt pre-load produces a state of stress in the closure lids, the cask closure flange, and the cask inner shell region adjacent to the flange.

The stress field in the cask body and the lids from the bolt pre-load combines with the stresses produced under a specific event such as during the hypothetical accident condition (item #5 above). Thus, the bolt pre-load induced stress participates in every load combination analyzed for the cask.

The initial preload should be set to maintain a seal under the action of the internal pressure plus the effective pressure calculated as the cask content weight times the maximum rigid body deceleration from the free 9-meter end drop (see discussion below). This preload is much larger than the preload needed to balance the maximum normal operating internal pressure (MNOP specified in Table 2.1.1).

Stresses from weld shrinkage endemic to every welded component also lie in the category of permanent stresses. However, because they are of the secondary genre (i.e., they arise to satisfy compatibility, not equilibrium) they are not computed or included in the load combinations.

Finally, the interface load produced between the shield cylinder and containment shell due to the method of assembly, causes the shield cylinder to add structural support to the containment shell. The beneficial effect of the interface load between the shield cylinder and the containment shell is conservatively neglected in the structural analyses.

2. Design Condition Loads

The ASME Codes [2.1.1] and [2.1.17] require that a pressure vessel be qualified to a design internal and external (if applicable) pressure. The Design Pressure should be selected to bound all normal operating condition pressures. The applicable Design Temperature, likewise, should be one that bounds the metal temperature of the affected pressure parts under all normal service conditions. For the HI-STAR 180D Package, the Design Internal Pressure and Design Temperatures, set down in Table 2.1.1, accordingly bound all service condition values.

Stress analysis of the containment system under the Design Pressure is required to demonstrate compliance with “NB” stress limits, as identified in [2.1.1], for the containment system material and to demonstrate the leak tightness of the bolted joints. The Design Temperature is utilized to establish the applicable allowable stress intensity, S_m, for the “pressure part” (a term used in the ASME B&PV Code). The following pressure loading scenarios are identified:

- Maximum Normal Operating Pressure (MNOP): The MNOP is defined in Table 2.1.1 for the containment system of the cask and bounds the calculated internal pressure values in Table 3.1.2. The coincident external pressure is atmospheric.

- Design Internal Pressure: A design internal pressure is defined in Table 2.1.1 for the containment system of the cask as a pressure vessel. The coincident external pressure is atmospheric.

- Accident Condition Internal Pressure: An accident condition internal pressure is defined in Table 2.1.1 for the containment cavity of the cask pressure vessel. The coincident external pressure is atmospheric.

- Accident Condition External Pressure: An accident condition external pressure with cavity depressurized is defined in Table 2.1.1. This loading, in conjunction with the buckling analysis of the cask containment shell, is intended to demonstrate that the containment system is in compliance with the requirements of 10CFR71.61. This loading bounds the external pressure specified by 10CFR71.73(c) (5) and (6); therefore, it is considered in Section 2.7.

Table 2.1.1 provides the above values of design basis internal and external pressures. The Design Internal Pressure of the Cask Cavity Space is conservatively set higher than the Cask Cavity Space MNOP.

The most adverse possible internal pressure state occurs under the simultaneous effect of fire and 100% rod rupture. This pressure is bounded by the accident condition internal pressure specified in Table 2.1.1.

The case of deep submergence (§71.61) is enveloped by the accident condition external pressure specified in Table 2.1.1.

As discussed in Paragraph 2.1.1.1, there is no additional restraint load from the fuel assemblies on the cask closure lid.

3. Handling Loads

The lifting devices in the HI-STAR 180D cask are subject to the specific stress limits set forth by NUREG-0612 [2.1.5], which require that the primary stresses in a lifting point must be less than the smaller of 1/10 of the material ultimate strength and 1/6 of the material yield strength while subject to the lifted load that includes an appropriate dynamic load amplifier. These limits apply to the cask lifting trunnions and to the threaded holes in the lids. An associated requirement is an evaluation of the stress intensity state in the cask baseplate when the package is being lifted. Baseplate loads considered are the self-weight of the baseplate plus attached shielding, the fuel, the fuel basket, and the fuel basket shims (and supports). Under lifting (and handling) condition a 15% load amplifier is applied as discussed in Section 2.5. The component acceptance limits are based on the Level A stress intensity allowables from ASME Code, Section III, Subsection NB.

Section 2.5 documents the lifting analyses applicable to the HI-STAR 180D package.

4. Normal Conditions of Transport Loads (§71.71)

The normal conditions of transport loads that warrant structural evaluation are:

a. Reduced external pressure 25 kPa (3.5 psia).
b. Increased external pressure (140 kPa or 20 psi absolute).
c. Free drop from 0.3-meter (1-foot) height in the most vulnerable orientation onto an essentially unyielding horizontal surface (henceforth called the “1- foot drop event”).
d. Normal vibratory loads incidental to transport.
e. Normal operating conditions (pressure and temperature).

External pressure loads ((a) and (b) above) are clearly enveloped by the design external pressure set by a deep submersion of the package (10CFR71.61). This condition is evaluated in Section 2.7. The normal operating conditions (e) are evaluated to demonstrate that the containment meets the requirements of the ASME Code (as clarified in Subsection 2.1.4) to be designated as a “pressure vessel”. The “1-foot drop event” (c) evaluation in this section is the “Side Drop”. The HI-STAR 180D Package is assumed to drop with its axis parallel with respect to the horizontal surface, such that the collision of the two impact limiters with the target is coincident in time. Vibratory loads transmitted to the HI-STAR 180D Package (d) by the transport vehicle will produce negligibly small stresses in comparison with stresses that will be produced by the loadings described previously. Therefore, vibratory loading is neglected in the analyses performed herein. Fatigue considerations due to mechanical vibrations are further discussed in Section 2.6.

Based on the above considerations, the governing Load Combinations to be considered in Section 2.6, for both Heat and Cold conditions, are:

- Load Combination N1:
  Bolt pre-load plus Design Internal pressure and Normal operating temperature
- Load Combination N2:
  Free drop from 1 foot plus Bolt pre-load and Maximum Normal Operating Pressure (MNOP).

5. Hypothetical Accident Condition Loads (§71.73)

These loads pertain to hypothetical accident conditions. Specifically, they are:

a. Free Drop of 9 m (30 ft) (§71.73 (c) (1))
b. Puncture (§71.73 (c)(3))
c. Engulfing fire @ 800ºC (1475ºF) (§71.73 (c)(4))
d. Immersion in 15 m (50 ft) head of water (§71.73 (c) (6)).

a. Free Drop

The free drop event can be broken down into seven candidate scenarios with potential to cause maximum damage:

- Bottom End Drop: The packaging is assumed to drop vertically with its cask containment baseplate sustaining the impulsive load transmitted by the contents. The weight of the package is included in all drop load cases.

- Top End Drop: This drop condition is the opposite of the preceding case. The outer closure lid withstands the impact load transmitted through the impact limiter, and the inner closure lid withstands the impact from the contained fuel, fuel basket, and fuel basket supports (basket shims).

- Side Drop: The cask along with its contents drops with its longitudinal axis horizontal. The contents of the cask bear down on the cask as it decelerates under the resistance offered by the two impact limiters pressing against an essentially unyielding surface.

- Bottom Center-of-Gravity Over-the-Corner Drop: In this drop scenario, the HI-STAR 180D Package is assumed to impact an essentially unyielding surface with its center-of-gravity directly above its initial point of contact in the drop event.

- Top Center-of-Gravity Over-the-Corner Drop: This loading case is identical to the preceding case, except that the package is assumed to be dropping with its top end down and its center-of-gravity is aligned over the initial point of contact.

- Slapdown – Initial Impact at Top End: In this case, the package drops with its axis at a small angle with the horizontal with the top end impacting first. Subsequent to the primary impact, the package begins to rotate with the bottom end impacting the target at a later time (secondary impact). Higher decelerations are experienced during the secondary impact. The governing slapdown angle, θ, is determined by a parametric analysis.

- Slapdown – Initial Impact at Bottom End: This case is the same as above, except for the location of primary and secondary impacts.

b. <u>Puncture</u>

The puncture event is broken down into two limiting scenarios, namely:

- Side Puncture Force Event: This event consists of a 1-m (40-in) free drop (impact limiters are ignored) onto a stationary and vertical mild steel bar of 15 cm (6 in) diameter with its leading edge (top edge) rounded to 6 mm (1/4-in) radius. The bar is assumed to be of such a length as to cause maximum damage to the cask. The package is assumed to be dropping horizontally with the penetrant force being applied at the mid-length of the cask.

- Top End Puncture Force: This event is similar to the preceding case except the penetrant force is assumed to act at the center of the outer closure lid. Because of the proximity of the bolted joints, this case is considered limiting for an end puncture.

The above loading events may occur under the so-called “hot” (maximum ambient temperature) or “cold” condition at -29ºC (-20ºF). In the latter thermal state, the effects of brittle fracture must also be evaluated.

Because the HI-STAR 180D Package operates at a relatively low internal pressure, the impact and puncture loadings under service conditions are orders of magnitude greater than pressure loadings. However, for completeness the (force/stress) results from pressure loads are directly added with the results from the drop and puncture analyses as applicable to maximize the force or stress results on the cask system.

c. Fire

Fire is not a mechanical loading event; its chief consequence is to challenge the integrity of the neutron shielding material. The results are presented in Chapter 3. The results show that the gas pressure inside the containment system remains below the accident pressure limit for the package (see Table 2.1.1). Based on the temperature changes established in Chapter 3, an evaluation is performed to demonstrate that the land compression load at the lid/flange joint does not degrade to an unacceptable value.

d. Immersion

Finally, from the structural standpoint, the 15-m (50-ft) immersion case is clearly bounded by the accident external pressure loading of 2 MPa (290 psi) deemed to satisfy the requirements of 10CFR71.61. The ability of the package to maintain moderator exclusion pursuant to §71.61 is discussed in Appendix 1.B and in Section 2.7.

Based on the above considerations, the Load Combinations that are considered in Section 2.7, for both Heat and Cold conditions, are:

Hypothetical Accident Load Cases*
9-m free drops
End and Side Puncture
Deep Submergence 2 MPa (290 psi)
Gasket Relaxation from Fire

* Permanent Loads are in-place at the start of every load case.

2.1.2.2 Acceptance Criteria

The constituent parts of the package, namely, (i) the containment system components, (ii) the fuel basket, (iii) the dose blocker parts, and (iv) the impact limiters must meet acceptance criteria specific to their function under each loading condition, as described below:

(i) Containment System

a. Design Pressure: The containment baseplate, containment closure flange, inner and outer closure lids, and the containment shell should meet minimum stress intensity limits of Subsection NB (Table 2.1.2) under the Design Pressure and Design Temperature conditions.

b. Free Drop: Under the normal handling event (0.3 m drop (§71.71) with impact limiters installed) and the hypothetical accident (9-meter drop (§71.73) with impact limiters installed), the containment system (including the inner and outer closure lids) should be shown to remain leaktight. In quantitative terms, leaktightness is guaranteed if the primary axial stress in the body bolts remains in the elastic range and the gaskets remain compressed after the event. An additional quantitative measure of margin-against unacceptable leakage from or into the containment space is presented in Section 2.6. As suggested in Reg. Guide 7.6, the components of the containment system should also meet the ASME Code, Section III, Level A and Level D stress intensity limits under the free drop events for normal and accident conditions, respectively.

c. Under the puncture event, the containment system must be demonstrated to remain unbreached, leaktightness must be maintained, and applicable Level D primary stress intensity limits should be met away from the location of the impact. (High stresses that inevitably develop in the region of impact are termed "local" stresses that belong to the secondary or peak stress categories in the ASME Code (Figure NB-3222-1)).

d. The closure lid seals must remain functional under all events to ensure "leak tightness" of the containment system. Specifically, at the end of the event, the seal surface must maintain a minimum compressive force recommended by the seal manufacturer. The specific bolted joint detail utilized for both closure lids is of the so-called "controlled compression" type, which is defined by three distinct characteristics:

i. The seal sits in a precisely machined groove such that the extent of compression of the seal is precisely controlled.

ii. The bolt force, in excess of the load required to "seat" the seal, is counteracted by the contact force over the surface, where the flange and the closure lid make conformal contact. The contact force on this surface, referred to as the "land" in the pressure vessel literature, must be overcome by any force trying to open the joint (such as internal pressure) before the seal can be made to relax.

iii. The joint is immune to over-compression and crushing of the seal by external pressure or any other type of force trying to compress the seal (a desirable feature in the deep submergence case).

Although meeting the above seal pressure limit would suffice, as discussed in Section 2.6, a much more stringent criterion for ascertaining loss of margin against joint sealworthiness, termed "margin-against-leakage", m, is utilized in this SAR.

e. Applicable minimum allowable stress intensity limits for the containment system, including closure bolts, are obtained from the ASME Code, Section III, Division 1, Subsection NB [2.1.1]. The limiting allowable stress intensity values are given in Tables 2.1.2 and 2.1.3.

Allowable stresses and stress intensities are calculated using the data provided in the ASME Code, Section II, Part D [2.1.6] and Tables 2.1.2 and 2.1.3. Tables 2.1.4 through 2.1.8 provide numerical values of the stress intensities, as a function of temperature, for the cask containment system materials, including lid closure bolts.

Throughout this chapter, the term "S_m" and "S_u" denote the design stress intensity and ultimate strength, respectively. Property values at intermediate temperatures that are not reported in the tables are obtained by linear interpolation as allowed by paragraph NB-3229 of the ASME Code.

Terms relevant to the analyses are extracted from the ASME Code (Figure NB-3222-1) as follows.

Symbol	Description	Notes
P_m	Average primary stress across a solid section.	Excludes effects of discontinuities and concentrations. Produced by pressure and mechanical loads.
P_L	Average stress across any solid section.	Considers effects of discontinuities but not concentrations. Produced by pressure and mechanical loads, including inertia earthquake effects.
P_b	Primary bending stress.	Component of primary stress proportional to the distance from the centroid of a solid section. Excludes the effects of discontinuities and concentrations. Produced by pressure and mechanical loads, including inertia earthquake effects.
P_e	Secondary expansion stress.	Stresses, which result from the constraint of free-end displacement. Considers effects of discontinuities but not local stress concentration. (Not applicable to casks.)
Q	Secondary membrane plus bending stress.	Self-equilibrating stress necessary to satisfy continuity of structure. Occurs at structural discontinuities. Can be caused by pressure, mechanical loads, or differential thermal expansion.

Summarizing the previous discussions, in accordance with Regulatory Guide 7.6 and ASME Code Section III, Subsection NB, the allowable stress limits for the cask containment system are based on design stress intensities (S_m), yield strengths (S_y), and ultimate strengths (S_u). These limits govern the design of the cask inner shell, the closure flange, the containment baseplate, and the two closure lids and are given in Tables 2.1.4 through 2.1.8 for normal and hypothetical conditions of transport as a function of temperature. As the ASME Code sections governing the containment system are stress based, there is no explicit maximum strain limit set down in this SAR for the containment system.

Certain parts of the HI-STAR 180D containment system are composed of ferritic steel materials, which may be subject to impact loading in a cold environment and, therefore, must be evaluated and/or subjected to impact testing in accordance with the ASME Code to ensure protection against brittle fracture.

Table 8.1.9 provides the fracture toughness test criteria for the HI-STAR 180D containment system components in accordance with the applicable ASME Codes and Regulatory Guide requirements for prevention of brittle fracture.

All containment system materials subject to impact loading in a cold environment must be evaluated and/or tested for their potential for brittle fracture. Containment boundary plate and forging materials have been selected based on the material's capability to perform at low temperatures with excellent ductility properties. These materials of construction are identical to the materials approved for use in the HI-STAR 180 (certified in USNRC Docket No. 71-9325). The lowest service temperature (LST) (where impactive or impulsive loads are present) is -29ºC (-20ºF) per Reg. Guide 7.8 [2.1.4]; however, HI-STAR 180D may be qualified to an LST of -40ºC (-40ºF). Table 8.1.9 provides the criteria for qualification to LST of either -29ºC (-20ºF) or LST of -40ºC (-40ºF). The appropriate Regulatory Guides are used to provide guidance on the test temperature to demonstrate appropriate resistance to brittle fracture. For component thicknesses greater than four-inches, such as cask baseplate, closure flange, inner closure lid and outer closure lid, the fracture arrest criteria of Reg. Guide 7.12 is used for component thicknesses up to 12 inches and a LST of -29ºC (-20ºF). In lieu of the fracture arrest criteria, the fracture initiation criteria from NUREG/CR-3826 is used to determine the required Nil Ductility Transition (NDT) temperature, “T_{NDT}” where the component thickness is greater than 4 inches at an LST of -40ºC (-40ºF). As an alternative for components whose thickness exceeds 4 inches at an LST of -40ºC (-40ºF), the guidance from Reg. Guide 7.12 may be followed by setting the required NDT temperature 11.1ºC (20ºF) below the NDT temperature applicable to an LST of -29ºC (-20ºF). For component thicknesses equal to or less than four-inches, such as the containment shell, the required Nil Ductility Transition (NDT) temperature, “TNDT” is determined based on the guidance from Regulatory Guide 7.11 and NUREG/CR-1815 [2.1.9].

The austenitic stainless steel inner closure lid port cover plate material provides immunity from brittle fracture concerns at cask LST of either -29ºC (-20ºF) or LST of -40ºC (-40ºF) per Section III of the ASME code and NUREG/CR-1815.

SB 637 bolt material (Table 2.2.2) for both the outer and inner lid joints provides immunity from brittle fracture concerns at cask LST of either -29ºC (-20ºF) or LST of -40ºC (-40ºF) per Section III of the ASME code and NUREG/CR-1815.

SA564 and SA 705 are also bolt materials for both the outer and inner lid joints (Table 2.2.2). Section 5 of NUREG/CR-1815 indicates that bolts are generally not considered susceptible to brittle fracture. However, for additional assurance, the following additional requirements are imposed in the procurement of the bolting material:

a. Reg. Guides 7.11 and 7.12 specify the LST of -29ºC (-20ºF) for the brittle fracture test methods (Charpy V-notch tests). Conservatively, an LST of -40ºC (-40ºF) may be selected for HI-STAR 180D, according to Table 8.1.9.

b. A volumetric examination of each bolt to ensure absence of voids.

Additionally, crack propagation analyses of the inner and outer closure lid bolts are performed to establish that an adversely oriented surface V-notch in the bolts will not grow under the most limiting impactive scenario. Section 2.7 contains a description of the methodology.

(ii) Fuel Basket

The *critical characteristics* of the Metamic-HT material discussed in Section 1.2 are central to the fuel basket to render its intended function. The properties of Metamic-HT are provided in Table 2.2.8. The essential predicates for ensuring that the fuel basket will meet or exceed its performance requirements are:

i. Lateral deflection of the basket panels must be within prescribed limits.
ii. Protection against crack propagation under all operating conditions including the hypothetical free drop event under the "cold" ambient condition (-40ºC (-40ºF)).
iii. Protection against local tearing of basket panel during an accident event.
iv. B-10 areal density in the basket panel required to meet the subcriticality requirement in this SAR is assured.
v. Mechanical strength and physical properties under normal conditions of transport (characterized by the dead load of fuel on the basket panels and heated thermal state) are preserved.
vi. Physical properties of the basket structural material under the neutron and gamma fluence from the contained SNF are preserved.

Each performance requirement is discussed below:

i. Lateral deflection of the fuel basket panels within prescribed limits:

Lateral deflection of the basket panels can occur from two mechanisms:

a. Creep, which is a long-term effect
b. Instantaneous deflection under mechanical loading

a. Creep

The lateral deflection of the Metamic-HT panels from the sustained weight of the SNF during transport must be negligible. A proposed criterion in Japan [1.2.30] is to limit the cumulative creep to 0.4% in sixty years. This criterion, spanning over twelve times the initial five year license life for transport is arguably too stringent. However, it is adopted herein as a requirement that Metamic-HT in HI-STAR 180D fuel basket must fulfill to ensure a large margin against creep.

Testing to determine the creep characteristics of the Metamic-HT under both unirradiated and irradiated conditions has been performed and reported in [1.2.27], which also provides an equation to provide a bounding estimate of total creep as a function of stress and temperature.

The creep equation (developed in [1.2.27]) is confirmed to provide a conservative prediction of accumulated creep strain by direct comparison to measured creep in unirradiated and irradiated coupons. The details of the creep tests, which were run at tensile stress levels ranging from 200 to 1000 psi and at metal temperatures of 300°C to 400°C, including creep vs. time plots are provided in [1.2.27].

The creep equation for the Metamic-HT obtained from [1.2.27], provides the means to compute a bounding estimate of creep that a Metamic-HT panel will accumulate due to the dead weight of the SNF lying on it with the basket in the horizontal disposition (during transport). (Evidently, in the vertical orientation, the creep effects are inactive because of the absence of any meaningful load on the panels.) The cumulative value of creep can be calculated assuming a conservatively computed Metamic-HT metal temperature variation with time starting with the maximum calculated value in Table 3.1.1. An upper bound estimate of the bending stress in an F-37 Metamic-HT panel is computed by considering a strip of unit width simply supported at the two ends subjected to uniform pressure from the SNF resting on the Metamic-HT panel. Strength-of-materials calculations using the creep model from [2.1.12] have been carried out to determine the uniform pressure and the corresponding bending stress. Subsequently, using the creep equation from [1.2.27], the total creep strain after five years of transport under the maximum basket temperature is computed. The table below summarizes the creep results for the basket after five years of transport.

Effective Pressure on the Basket Panel (psi)	Bending Stress in the Basket Panel (psi)	Corresponding Cumulative Creep Strain after 5 years of Transport (%)
0.994	143.3	0.1665

The table below provides the conservatively predicted creep strain assuming that the metal temperature of the panel starts at the maximum basket temperature reported in Table 3.1.1 and decreases with the passage of time due to fuel decay inside the cask under a hypothetical 60-year duration under transport.

Duration Under Load (Years)	Upper Bound Metamic-HT Temperature, °C Note 1	Cumulative Creep Strain (%) Note 2
0	338 (from Table 3.1.1)	0
20	239	0.21
40	209	0.225
60	204	0.232
Note 1: Linear interpolation is used to bound Metamic-HT temperature between 0 to 20, 20 to 40, and 40 to 60 years, respectively. Note 2: Cumulative strain computed by integrating the creep rate equation from [1.2.27] under the time dependent Metamic-HT temperature tabulated herein.		

As the above data shows, the cumulative predicted creep after sixty years of continuous transport is well below the Japanese recommended limit of 0.4% [1.2.30]. Furthermore, as documented in [1.2.27], the cumulative strain sustained under the accelerated test conditions already exceeds the predicted strain from five years (initial licensing period) of a continuous state of transport.

Examining the creep test data compiled in [1.2.27] and summarized above, it is observed that the normal conditions of transport (max. metal temperature and coincident stress) are bounded by the test conditions. The five-year cumulative creep reported above under normal transport conditions is also bounded by the accumulated creep in certain accelerated Metamic-HT creep tests. The above results suggest that creep in Metamic-HT is not a concern or a controlling mechanism in the HI-STAR 180D fuel baskets.

b. Instantaneous Deflection Under Mechanical Loadings

In order to render its intended function, namely, to maintain reactivity control, the fuel basket plates must not experience any damage that would invalidate the analysis basis configuration assumed in the criticality analysis. The acceptable limit on panel deformation is accordingly set down to maintain a reactivity control with appropriate margin to the limits.

For this purpose, the fuel basket panel deformation criterion, for both Normal and Hypothetical Accident Conditions of Transport, is expressed in dimensionless form as:

$$\theta = \frac{\delta_{\max}}{W} \leq 0.005$$

where δ_{max} equals the maximum total deflection of the basket panel (relative to the panel supports), and W equals the nominal width of the basket panel. Thus, for the F-37 and F-32 fuel baskets (W = 206 mm), the maximum total deflection at any point along the panel width must not exceed 1 mm. The maximum total deflection limit and the average deflection limit of the basket panel are key performance objectives provided in Table 2.7.9 that ensures a positive margin against the regulatory reactivity limit ($k_{eff} \leq 0.95$), and from a structural perspective it is more conservative than ASME Subsection NG stress intensity limits as shown in Holtec Position Paper DS-331 [2.1.16].

ii. Protection Against Crack Propagation

The material property used to determine whether a flaw in the basket panel would propagate under the most adverse dynamic stress scenario is the L-T fracture toughness, K_{JQ}. There exists a large safety margin against crack propagation in the basket under various loadings (viz. creep, fatigue and governing 9m (30 ft.) hypothetical drop accident) applicable to transportation of the package. The calculations related to the stability against crack propagation are documented in the Metamic-HT sourcebook [1.2.27].

iii. Protection Against Local Tearing of the Basket Panel

The “elongation” of the panel material (the cumulative strain at failure) specified in Table 2.2.8 is used in the structural analysis of the fuel basket using the LS-DYNA code. The acceptance criterion is a *complete absence of local or global tear*. The ultimate strength and Young’s Modulus of the Metamic-HT material are also required to perform the structural analysis so as to accurately prognosticate failure from excessive tensile strain in the LS-DYNA model.

iv. Assured B-10 Loading

The B_4C concentration and the spatially homogeneous distribution of B_4C particles is an essential basis for criticality safety analyses. The manufacturing steps for Metamic-HT are identical to Metamic (classic) in this respect. Hundreds of Metamic-HT coupons drawn from different batches have been tested by the neutron attenuation method without a single case of inhomogeneity discovered. Nevertheless, coupons drawn from production lots are required to be tested by the neutron attenuation method under the provisions of this SAR (see Chapter 8).

The gross weight compliance requirement is also verified by samples of Al-B_4C mixture analyzed by the "wet chemistry" method (see Chapter 8) [1.2.26].

v. Preservation of Mechanical Strength and Physical Properties Under Operating Conditions

The table below provides the maximum temperature attained by the Metamic-HT panels during transport conditions.

Summary of the Metamic-HT's Temperature State in HI-STAR 180D†

Condition	Maximum Temperature, °C	
	Panel Closest to the Basket Centerline	Weld Line (at the Basket Periphery)
Normal condition of transport if transport occurred on the first day permitted by the CoC	338	282
10CFR71 Fire Event	393	346

† Source: From [3.4.1]

It is evident from the above table that the maximum temperatures in the HI-STAR 180D fuel basket are quite modest and well below the material's recrystallization temperature (530°C).

Accelerated thermal aging tests on Metamic-HT coupons show that strength properties of Metamic-HT are not affected by exposure to high temperatures [1.2.27].

vi. Preservation of Physical Properties Under the Neutron and Gamma Fluence

The tests on unirradiated and radiated coupons, documented in [1.2.27], show that neutron fluence on the coupons exceed the value that will be sustained by the Metamic-HT panels in 56 years of SNF confinement. At these irradiation levels, the Metamic-HT strength is unaffected and its creep behavior is bounded by the Metamic-HT creep equation [1.2.27].

Therefore, as expected of aluminum-based materials, the radiation dose from the transported SNF will not degrade the strength and ductility properties of the Metamic-HT panels.

(iii) Dose Blocker Parts

The monolithic shield cylinders (that girdle the containment shell), the monolithic shield cylinder bottom, Holtite neutron and lead gamma shield materials in the confined cavities, and the plate that make up the assemblies that confine the Holtite and lead shield materials including the bottom steel cap plate, are examples of dose blocker parts in the HI-STAR 180D package. These parts are generally located at the exterior boundary of the cask, and hence are subject to a direct action of the impactive/impulsive service condition and/or handling mishap loads. To meet the performance mission of the package, the dose blocker parts should not permanently separate from the cask or suffer a body extensive damage. Furthermore, under cold conditions, the potential for brittle fracture leading to a separation and/or loss of function must also be addressed.

The dose blocker parts do not serve as pressure parts and are not part of the containment system. Nevertheless, to provide assurance of protection against brittle fracture, provisions of ASME Section III, Subsection NF for Class 3 components (NF-2300) are invoked to provide guidance in establishing requirements for those metallic parts where through-thickness cracks could result in a loss of function. The monolithic shield cylinder, where multiple through-thickness cracking could result in a separation and loss of function, is in this category. SA-352 LCC (equivalent to ASTM A 352-93-LCC) is the casting material specified for the monolithic shield cylinder and has been chosen because it is well suited for low temperature service (see the material specification in [2.1.1, Part A]). This Carbon-Manganese-Silicone steel casting material, which is also used for the HI-STAR 180 Transport Cask, is similar in chemistry and strength to the Carbon-Manganese-Silicone steel SA-537 plate material. Table 2311(b)-1 of ASME Code Section III, Subsection NF [2.1.14] provides the Nil-Ductility-Temperature (T_{NDT}) of SA-537 as -30 deg. F. This temperature is sufficient to ensure ample protection against brittle fracture for a Lowest Service Temperature (LST) of -29ºC (-20ºF) (which is the lowest service temperature where loadings that could cause a brittle fracture are applied (per Reg. Guide 7.8 [2.1.4])). Since SA-352 LCC is the casting equivalent of SA-537, it will also provide sufficient protection at an LST = -29ºC (-20ºF). For the monolithic shield cylinder, however, additional resistance to brittle fracture is provided by requiring the material to have sufficient resistance to brittle fracture under the extreme cold condition of -40 deg. F (even though no impactive or impulsive load is defined for the extreme cold condition). Therefore, the Charpy test temperature for the SA-352 LCC casting material is set at -40 deg. F in Table 2.1.9.

The minimum value for Charpy energy required from the tests follows the guidance of the ASME Section III Code, Subsection NF [2.1.14, Figure NF-2331(a)-2]. Table 2.1.9 summarizes the test requirements. In addition to the above, added assurance is provided by the physical configuration of the monolithic shield configuration. The presence of the Holtite cavities in the monolithic shield cylinders serve as crack arresters, and prevent complete through thickness cracking in the monolithic shield even if a crack were to be initiated.

While the practice of specifying a minimum Charpy strength using the guidance in Subsection NF of Section III of the ASME Code for the Dose Blocker parts is well established in the HI-STAR design practice (licensed and used to manufacture HI-STAR 100s since 1999 in Docket No. 71-9261), an independent analysis of the sufficiency of the Charpy strength requirement to ensure protection from a significant loss of shielding in an impact event is also performed in Section 2.7.

Brittle fracture of the Holtite or the bottom lead gamma shield is not a concern as the presence of a crack will not lead to separation of the Holtite or lead material from the cask nor will it cause a loss of function as the Holtite is completely confined by the monolithic shield cylinder, and the lead is completely confined by the bottom steel cover plate.

To provide assurance of ample resistance to brittle fracture of the plates that make up the weldments that confine the Holtite and lead shield materials including the bottom steel cap plate, these components are also subject to testing following the guidance of the ASME Section III Code, Subsection NF [2.1.14, Figure NF-2331(a)-2]. Table 2.1.9 summarizes the test requirements for these dose blocker parts.

(iv) Impact Limiters

Impact limiters are designed to absorb the impact energy during a drop event by plastic deformation. The crush strength and size of the impact limiters are sufficient to prevent bottoming out. The impact limiter must perform its energy absorption function over the range of environmental temperatures.

Under all postulated impact events applicable to the HI-STAR 180D Package, the impact limiter must stay attached to the package and mitigate the inertia forces such that:

i. The stress levels in the containment system do not exceed the Section III Subsection NB allowables for the applicable service condition.
ii. The deformation levels in the basket meet the limits set forth in the foregoing.
iii. The gasketed joints in the containment system remain fully functional to prevent leakage.
iv. The decelerations in the cask under the 9-meter drop are limited to ensure that the contained spent nuclear fuel cladding will not breach from excessive flexural strain.
v. The deformation of the crush material is limited to prevent contact between the cask and the target ("bottoming out of the package").
vi. The impact limiter(s) remain physically attached to the cask. In quantitative terms, this means that the impact limiter's skirt (which girdles the cask at both ends) does not come off the cask and the attachment fasteners do not undergo excessive strains.

2.1.3 Weights and Centers of Gravity

Table 2.1.11 provides the weights of the individual HI-STAR 180D components as well as the total Transport Package weights, and the weight of the heaviest loaded HI-STAR 180D Cask.

Table 2.1.12 provides the location of the center of gravity (CG) for the package relative to the bottom surface of the bottom impact limiter. The CG is assumed to be located on the cask centerline since the non-axisymmetric effects of the cask plus contents are negligible.

2.1.4 Identification of Codes and Standards for Package Design

The design of the HI-STAR 180D Package does not invoke ASME Code Section III in its entirety. Specific Code paragraphs in NB-3000 of Section III, Subsection NB of the ASME Boiler and Pressure Vessel Code (ASME Code) [2.1.1], and Appendix F [2.1.10] that are cited herein are invoked for design of the containment system of the HI-STAR 180D Package.

Table 2.1.13 lists each major structure, system, and component (SSC) of the HI-STAR 180D Packaging, along with its function, and applicable code or standard. The drawing package in Section 1.3 identifies whether items are "Important to Safety" (ITS) or "Not Important to Safety" (NITS); the identification is carried out using the guidance of NUREG/CR-6407, "Classification of Transportation Packaging and Dry Spent Fuel Storage System Components". Table 2.1.14 lists some alternatives to the ASME Code where appropriate. Table 2.1.15 provides applicable sections of the ASME Code and other documents for Material Procurement, Design, Fabrication, and Inspection, and Testing pursuant to the guidance in NUREG 1617 [2.1.11].

All materials and sub-components that do not constitute the containment system in the HI-STAR 180D cask are procured to ASTM or ASME Specifications, except for the fuel basket (made of Metamic-HT) and the neutron shield sold under the trade name Holtite B described in Chapter 1.

The *critical characteristics* of all materials set down in this SAR establish the minimum requirements that must be met by the material. The applicable *critical characteristics* for each part in the HI-STAR 180D cask are listed in Table 2.1.16 with the required limiting values, as applicable.

Table 2.1.1: Pressures and Temperatures for Normal and Accident Conditions

		Gauge Pressure kPa (psig)	Temperature
1.	Cask (Cavity Space) Maximum Normal Operating Pressure (MNOP) (bounds MNOP values in Table 3.1.2)	303 (44)	Table 3.2.10
2.	Design Internal Pressure for Cavity Space (covers MNOP above and all essential operations described in Chapter 7 of this SAR)	552 (80)	
3.	Accident Condition Internal Pressure for Cavity Space and Inter-Lid Space (bounds value in Table 3.1.4 for fire and rod rupture)	1277.6 (185.3)	
4.	Accident Condition External Pressure (deep submergence)	2000 (290)*	
5.	Cask Inter-Lid Space Maximum Operating Pressure	689.5 (100)	
6.	Accident Condition Pressure Limit for Holtite Enclosure Spaces in the Monolithic Shield Cylinder**	See cask drawing in Section 1.3	
7.	Accident Condition Pressure Limit for Holtite Enclosure Space in the Bottom End Assembly**	See cask drawing in Section 1.3	
8.	Accident Condition Pressure Limit for Holtite Enclosure Space in the Inner Closure Lid Assembly**	See cask drawing in Section 1.3	
9.	Accident Condition Pressure Limit for Holtite Enclosure Space in the Top Flange Assembly**	See cask drawing in Section 1.3	
10.	Accident Condition Pressure Limit for Holtite Enclosure Space in the Bottom Shield Cylinder Assembly**	See cask drawing in Section 1.3	

*Set to meet 10CFR71.61

**Holtite-B Enclosure Spaces are equipped with pressure relief devices set to open at pressures less than or equal to the Accident Condition pressure limits.

Table 2.1.2: Stress Intensity Limits for Different Service Conditions for Section III Class 1 Pressure Vessels (Elastic Analysis per NB-3220)

Stress Category	Level A	Level D
Primary Membrane, P_m	S_m	Lesser of $2.4S_m$ and $0.7S_u$
Local Membrane, P_L	$1.5S_m$	150% of P_m Limit
Membrane plus Primary Bending	$1.5S_m$	150% of P_m Limit
Primary Membrane plus Primary Bending	$1.5S_m$	150% of P_m Limit
Membrane plus Primary Bending plus Secondary	$3S_m$	N/A
Average† Primary Shear (Section in pure shear)	$0.6S_m$	$0.42S_u$

Notes:

1. Fatigue analysis (as applicable) also includes peak stress (denoted by "F" in the nomenclature of the ASME Code [2.1.1]).

† Governed by NB-3227.2 or F-1331.1(d) of the ASME Code, Section III (NB or Appendix F)

Table 2.1.3: Stress Limits for Lid Closure Bolts (Elastic Analysis per NB-3230)

Stress Category	Level A	Level D
Average Service Stress	$2S_m$	Cannot exceed Yield Strength
Maximum Service Stress (tension + bending but no stress concentrations)	$3S_m$	Joint Remains Leak Tight (see Note 2). Cannot exceed Ultimate Strength

Notes:

1. Stress limits for Level A loading ensure that bolt remains elastic.
2. Limit set on primary tension plus primary bending for Level D loading is based on an elastic stress evaluation; however, the overriding acceptability of the joint design is performance based on an assured absence of leakage.
3. The closure lid bolt joints are friction type joints due to the large preload stress, they are not subjected to shear per ASME Code, Section III, Division 1, Subsection NF, NF-3324.6(a)(3)(b). Therefore, there is no need to include the shear and combined tensile and shear stress allowables in this table.

Table 2.1.4: Design, Levels A and B: Stress Intensity – SA-203 E

Code: ASME NB
Material: SA-203 E
Item: Stress Intensity

Temperature °C (°F)	Classification and Value, MPa (ksi)					
	S_m	**P_m** (Note 1)	**P_L** (Note 1)	**$P_L + P_b$** (Note 1)	**$P_L + P_b + Q$**	**P_e** (Note 2)
-29 to 38 (-20 to 100)	160.6 (23.3)	160.6 (23.3)	241.3 (35.0)	241.3 (35.0)	481.9 (69.9)	481.9 (69.9)
93,3 (200)	160.6 (23.3)	160.6 (23.3)	241.3 (35.0)	241.3 (35.0)	481.9 (69.9)	481.9 (69.9)
149 (300)	160.6 (23.3)	160.6 (23.3)	241.3 (35.0)	241.3 (35.0)	481.9 (69.9)	481.9 (69.9)
204 (400)	157.9 (22.9)	157.9 (22.9)	237.2 (34.4)	237.2 (34.4)	473.7 (68.7)	473.7 (68.7)
260 (500)	148.9 (21.6)	148.9 (21.6)	223.4 (32.4)	223.4 (32.4)	446.8 (64.8)	446.8 (64.8)

Definitions:

S_m	=	Stress intensity values per ASME Code
P_m	=	Primary membrane stress intensity
P_L	=	Local membrane stress intensity
P_b	=	Primary bending stress intensity
P_e	=	Expansion stress
Q	=	Secondary stress
$P_L + P_b$	=	Either primary or local membrane plus primary bending

Notes:

1. Evaluation required for Design condition only per NB-3220.
2. P_e not applicable to vessels per Fig. NB-3221-1.
3. Values are in accordance with stress intensity limits provided in Table 2.1.2.

Table 2.1.5: Level D Stress Intensity – SA-203 E

Code: ASME NB
Material: SA-203 E
Item: Stress Intensity

Temperature °C (°F)	Classification and Value, MPa (ksi)		
	P_m	P_L	$P_L + P_b$
-29 to 38 (-20 to 100)	337.8 (49.0)	506.8 (73.5)	506.8 (73.5)
93.3 (200)	337.8 (49.0)	506.8 (73.5)	506.8 (73.5)
149 (300)	337.8 (49.0)	506.8 (73.5)	506.8 (73.5)
204 (400)	337.8 (49.0)	506.8 (73.5)	506.8 (73.5)
260 (500)	337.8 (49.0)	506.8 (73.5)	506.8 (73.5)

Notes:

1. Level D allowables per NB-3225 and Appendix F, Paragraph F-1331.
2. Average primary shear stress across a section loaded in pure shear may not exceed 0.42 S_u.
3. Values are in accordance with stress intensity limits provided in Table 2.1.2.
4. See Table 2.1.4 for stress classification definitions.

Table 2.1.6: Design, Levels A and B: Stress Intensity – SA-350 LF3

Code: ASME NB
Material: SA-350 LF3
Item: Stress Intensity

Temperature °C (°F)	Classification and Value, MPa (ksi)					
	S_m	P_m (Note 3)	P_L (Note 3)	$P_L + P_b$ (Note 3)	$P_L + P_b + Q$	P_e (Note 4)
-29 to 38 (-20 to 100)	160.6 (23.3)	160.6 (23.3)	240.9 (35.0)	240.9 (35.0)	481.9 (69.9)	481.9 (69.9)
93.3 (200)	157.9 (22.9)	157.9 (22.9)	236.9 (34.4)	236.9 (34.4)	473.7 (68.7)	473.7 (68.7)
149 (300)	152.4 (22.1)	152.4 (22.1)	228.6 (33.2)	228.6 (33.2)	457.2 (66.3)	457.2 (66.3)
204 (400)	147.5 (21.4)	147.5 (21.4)	221.3 (32.1)	221.3 (32.1)	442.5 (64.2)	442.5 (64.2)
260 (500)	140.0 (20.3)	140.0 (20.3)	210.0 (30.5)	210.0 (30.5)	420.0 (60.9)	420.0 (60.9)
316 (600)	129.6 (18.8)	129.6 (18.8)	194.4 (28.2)	194.4 (28.2)	388.8 (56.4)	388.8 (56.4)
371 (700)	116.5 (16.9)	116.5 (16.9)	174.8 (25.4)	174.8 (25.4)	349.5 (50.7)	349.5 (50.7)

Notes:

1. Source for S_m is Table 2A of ASME Section II, Part D.
2. Values are in accordance with stress intensity limits provided in Table 2.1.2.
3. Evaluation required for Design condition only per NB-3220.
4. P_e not applicable to vessels per Fig. NB-3221-1.
5. See Table 2.1.4 for stress classification definitions.

Table 2.1.7: Level D, Stress Intensity – SA-350 LF3

Code: ASME NB
Material: SA-350 LF3
Item: Stress Intensity

Temperature °C (°F)	Classification and Value, MPa (ksi)		
	P_m	P_L	$P_L + P_b$
-29 to 38 (-20 to 100)	337.8 (49.0)	506.8 (73.5)	506.8 (73.5)
93.3 (200)	337.8 (49.0)	506.8 (73.5)	506.8 (73.5)
149 (300)	337.8 (49.0)	506.8 (73.5)	506.8 (73.5)
204 (400)	337.8 (49.0)	506.8 (73.5)	506.8 (73.5)
260 (500)	335.8 (48.7)	506.8 (73.5)	506.8 (73.5)
316 (600)	311.0 (45.1)	462.6 (67.7)	462.6 (67.7)
371 (700)	279.9 (40.6)	419.9 (60.9)	419.9 (60.9)

Notes:

1. Level D allowables per NB-3225 and Appendix F, Paragraph F-1331.
2. Average primary shear stress across a section loaded in pure shear may not exceed 0.42 S_u.
3. Values are in accordance with stress intensity limits provided in Table 2.1.2.
4. See Table 2.1.4 for stress classification definitions.

Table 2.1.8: Design Stress Intensity – Bolting Material

Code: ASME NB
Material: SA-193 B7 (Bolt < 2.5 inch diameter),
SA-564/705 630 (H1025)
& SB-637 N07718 (Bolt ≤ 6 inch diameter),
Item: Stress Intensity

Temperature ºC (ºF)	Design Stress Intensity SA-193 B7 MPa (ksi)	Design Stress Intensity SA-564/705 630 MPa (ksi)	Design Stress Intensity SB-637 MPa (ksi)
-29 to 38 (-20 to 100)	241.3 (35)	333.0 (48.3)	344.7 (50)
93.3 (200)	224.8 (32.6)	333.0 (48.3)	330.9 (48)
149 (300)	216.5 (31.4)	333.0 (48.3)	323.4 (46.9)
204 (400)	210.3 (30.5)	324.1 (47.0)	317.8 (46.1)
260 (500)	203.4 (29.5)	317.8 (46.1)	314.4 (45.6)
316 (600)	195.8 (28.4)	313.0 (45.4)	310.95 (45.1)
343 (650)	-	309.6 (44.9)	-
371 (700)	185.5 (26.9)	-	308.9 (44.8)

Notes:

1. Level A and D limits per Table 2.1.3
2. Table 2.2.2 contains other mechanical and thermal properties of the bolting material.
3. Sources for design stress intensity values for SA-193 B7 and SB-637 N07718 is Table 4 and that for SA-564/705 630 material, is Table 2A of ASME Section II, Part D.
4. Values for SA-564/705 630 are conservatively based on age hardening at 1075ºF (H1075).

Table 2.1.9: Fracture Toughness Test Criteria for Dose Blocker Part Materials

Item/Component	Material	Charpy V-Notch Test Temperature	Remarks (Note 6)
Monolithic Shield Cylinder and Bottom Shield Cylinder	SA-352 LCC, ASTM A 352 93 LCC, SA350-LF2, SA350-LF3	Test at -40ºC (-40ºF)	Charpy for absorbed energy is 27.1 J (20 ft-lbf) (average of 3 specimens and minimum of 20.3 J (15 ft-lbf) for any single specimen) Charpy for lateral expansion is 0.38 mm (15 mils)
Plates that enclose Holtite and/or lead shielding (Notes 1 through 5)	SA-36/SA-516 Gr. 70	Test at -40ºC (-40ºF)	Charpy for absorbed energy is 20.3 J (15 ft-lbf) (average of 3 specimens and minimum of 13.6 J (10 ft-lbf) for any single specimen) Charpy for lateral expansion is 0.38 mm (15 mils)

Notes:

1. Impact testing only applies to ferritic steel dose blocker parts located at the exterior boundary of the cask that remain exposed in the transport configuration with impact limiters.
2. Material to be Charpy impact tested in accordance with NF-2320.
3. Components may be exempt from impact testing as allowed by NF-2311.
4. SA-516 Gr. 70 plate may be normalized.
5. Charpy energy absorbed value may be adjusted based on actual thickness and/or minimum specified yield strength per Figure NF-2331(a)-2.
6. Components shall meet the acceptance standard applicable to either Charpy for Absorbed Energy (Figure NF-2331(a)-2) or Charpy for Lateral Expansion (Table NF-2331(a)-3).

Table 2.1.10 is intentionally deleted

Table 2.1.11: Weight Data for HI-STAR 180D Package and Components

	Item	Nominal Weight†, metric tons (lbf)
1.	HI-STAR 180D cask body (without lids)	62.1 (136,900)
2.	Inner Closure Lid	6.981 (15,400)††
3.	Outer Closure Lid	3.641 (8,050)††
4.	F-32 Fuel Basket (empty)	3.13 (6,900)
5.	F-32 Fuel Basket (loaded with SNF)	15.9 (35,100)
6.	F-37 Fuel Basket (empty)	3.13 (6,900)
7.	F-37 Fuel Basket (loaded with SNF)	17.9 (39,500)
8.	Basket shims for F-32	4.771 (10,600)
9.	Basket shims for F-37	4.773 (10,600)
10.	Loaded HI-STAR 180D Cask with F-32 Fuel Basket	93.7 (206,600)
11.	Loaded HI-STAR 180D Cask with F-37 Fuel Basket	95.7 (211,000)
12.	Bottom Impact Limiter (Including Radial Spacers)	11.4 (25,100)
13.	Top Impact Limiter (Including Radial Spacers)	13.9 (30,700)
14.	Transport Package (cask plus both impact limiters) with F-32 Basket	119 (262,400)
15.	Transport Package (cask plus both impact limiters) with F-37 Basket	121 (266,800)
16.	Fuel Weight – 37 Assemblies	14.8 (32,600)
17.	Fuel Weight – 32 Assemblies	12.8 (28,200)
Note: The weights listed in parentheses in lbf are not an exact conversion of metric tons. They are rounded to the nearest 100 lbf multiple.		

† Bounding weights may be used for component analyses to provide additional safety margins.

†† Excludes lid bolts.

Table 2.1.12: Center of Gravity of HI-STAR 180D Configuration

Component	**Nominal Location of CG** mm (in)
Transport Package (with impact limiters without fuel)	3412 (134.3)
Transport Package (with impact limiters with fuel)	3212 (126.5)

Notes:

1. The CG is measured from the base of the Bottom Impact Limiter (see drawing package in Section 1.3).

Table 2.1.13: Applicable Codes and Standards for the Materials Used in The HI-STAR 180D Packaging

	Item	Principal Function	Applicable Codes and Reference Standard
1.	Containment Baseplate	Containment Boundary	ASME Code Section III Subsection NB
2.	Containment Shell	Containment Boundary	ASME Code Section III Subsection NB
3.	Containment Closure Flange	Containment Boundary	ASME Code Section III Subsection NB
4.	Inner Closure Lid	Containment Boundary	ASME Code Section III Subsection NB
5.	Outer Closure Lid	Containment Boundary	ASME Code Section III Subsection NB
6.	Inner Closure Lid Bolts	Containment Boundary	ASME Code Section III Subsection NB
7.	Outer Closure Lid Bolts	Containment Boundary	ASME Code Section III Subsection NB
8.	Vent and Drain Port Plugs	Containment Boundary	ASME Code Section II
9.	Seals and Gaskets	Containment Boundary	Non-Code (Manufacturer’s Catalog and Test Data)
10.	Fuel Basket (Metamic-HT)	Positioning of Fuel Assemblies/ Criticality Control	Non-Code (Manufacturer’s Test Data [1.2.27])
11.	Monolithic Shield Cylinders	Gamma Shielding	ASME Code Section II
12.	Dose Blocker Plates	Gamma Shielding	ASME Code Section II
13.	Holtite-B	Neutron Shielding	Non-Code (Manufacturer’s Test Data [1.2.17])
14.	Trunnions	Lifting and Handling	ASME Code Section II and NUREG-0612
15.	Monolithic Shield Cylinder Top Cap	Holtite Cavity Space Enclosure (non-structural)	ASME Code Section II
16.	Monolithic Shield Cylinder Bottom Cap	Holtite Cavity Space Enclosure (non-structural)	ASME Code Section II

Table 2.1.13: Applicable Codes and Standards for the Materials Used in The HI-STAR 180D Packaging (Continued)

	Item	Principal Function	Applicable Codes and Reference Standard
17.	Basket Shims	Positioning of Basket in the Containment Cavity	ASTM B221
18.	Impact Limiter Backbone Plate Material	Structural Support of Impact Limiter	ASME Code Section II
19.	Impact Limiter Attachment Rods and Nuts	Structural Support of Impact Limiter	ASME Code Section II
20.	Impact Limiter Crush Material	Impact Energy Absorption	Non-Code (Manufacturer's Catalog and Test Data)
21.	Impact Limiter Fastener Strain Limiter	Protection of Impact Limiter Fasteners Against Excessive Stress/Strain	Non-Code (Manufacturer's Catalog and Test Data)

Notes:

1. Materials for ITS components not listed above shall meet ASME, ASTM, or other standard industrial codes, as approved by Holtec International. Materials for NITS components shall meet standard industrial codes or the manufacturer's product sheets as approved by Holtec International.

Table 2.1.14: ASME Code Requirements and Alternatives for the HI-STAR 180D Package (Sheet 1 of 4)

Component	Code Section	Code Requirement	Alternative, Justification & Compensatory Measures
Cask Containment System	NB-1000	Statement of requirements for Code stamping of components.	Cask containment boundary is designed, and will be fabricated in accordance with ASME Code, Section III, Subsection NB to the maximum practical extent, but Code stamping is not required.
Cask Containment System	NB-2000	Requires materials to be supplied by ASME-approved material supplier.	Holtec approved suppliers will supply materials with CMTRs per NB-2000.
Cask Containment System	NB-7000	Vessels are required to have overpressure protection.	No overpressure protection is provided. Function of cask vessel is as a radionuclide containment boundary under normal and hypothetical accident conditions. Cask is designed to withstand maximum internal pressure and maximum accident temperatures.
Cask Containment System	NB-8000	States requirements for name, stamping and reports per NCA-8000.	HI-STAR 180D Package to be marked and identified in accordance with 10CFR71. Code stamping is not required. QA data package prepared in accordance with Holtec's approved QA program.

Table 2.1.14: ASME Code Requirements and Alternatives for the HI-STAR 180D Package (Sheet 2 of 4)

Component	Code Section	Code Requirement	Alternative, Justification & Compensatory Measures
Cask Containment System	NB-2330	Establish T_{NDT} and test base metal, heat affected zone and weld metal at T_{NDT} + 60°F	Rather than testing to establish the RT_{NDT} as defined in paragraph NB-2331, the guidance from Reg. Guide 7.11 and NUREG/CR 1815 are used for materials less than 4 inches thick and Reg. Guide 7.12 & NUREG/CR 3826 are used for materials from greater than 4 up to 12 inches thick. The provisions of Reg. Guide 7.11 are applicable for the containment shell material. Reg. Guide 7.11 for materials up to 4 inches thick does have a reference to SA203 material and requires the T_{NDT} to be less than -56.7°C (-70°F). Since the specified T_{NDT} for the shell material, as reflected in Table 8.1.9, is lower, then it is in compliance with NB-2330. Table 8.1.9 summarizes the specific impact testing requirements for the Containment Boundary components per Reg. Guide 7.11 and NUREG/CR-3826. The thickness of the containment welds on the HI-STAR 180D are less than or equal to the containment shell wall thickness. Therefore, the T_{NDT} for the containment welds will be the same as the T_{NDT} for the containment shell as reflected in Table 8.1.9. Drop weight testing is not required to determine the T_{NDT} for the confinement welds.

Table 2.1.14: ASME Code Requirements and Alternatives for the HI-STAR 180D Package (Sheet 3 of 4)

Component	Code Section	Code Requirement	Alternative, Justification & Compensatory Measures
Cask • Monolithic Shield Cylinders • Containment Closure Flange Assembly • Bottom Shield Cylinder • Bottom Shield Cylinder Assembly • Other	NB-4622	All welds, including repair welds, shall be post-weld heat treated (PWHT).	The following welds are exempt from PWHT: • Impact limiter attachment inserts to containment base plate • Inner closure lid lifting thread inserts to inner closure lid core • Inner closure lid gamma shielding stand-offs to inner closure lid core • Containment closure flange ribs to containment closure flange • Containment closure flange neutron shielding top plate to containment closure flange • Containment closure flange neutron shielding flat outer plate to containment closure flange • Bottom shield cylinder to containment base plate Since the welds are less than 13 mm and the containment boundary is over 16 mm thick, these welds are exempt from PWHT per Table NB-4622.7(b)-1.
Cask Containment System	NB-5120	Perform radiographic examination after post-weld heat treatment (PWHT).	Radiography of the helium retention boundary welds after PWHT is not required. All welds (including repairs) will have passed radiographic examination prior to PWHT of the entire containment boundary. Confirmatory radiographic examination after PWHT is not necessary because PWHT is not known to introduce new weld defects in nickel steels.

Table 2.1.14: ASME Code Requirements and Alternatives for the HI-STAR 180D Package (Sheet 4 of 4)

Component	Code Section	Code Requirement	Alternative, Justification & Compensatory Measures
Cask • Monolithic Shield Cylinders • Bottom Shield Cylinder	Section II, SA-352 and SA-350	Material to be Charpy Impact Tested at -50ºF and conform to specified absorbed energy requirements	SA-352 LCC and SA-350 LF2 and LF3 are normally used as pressure retaining material, but in this application, they are selected to provide a shielding and/or structural support function due to their low temperature fracture toughness properties. Because the components' primary function is as a structural support, Holtec has applied the requirements of ASME Section III, Subsection NF for the brittle fracture testing and is not relying on the Section II testing requirements applicable to pressure retaining parts. While the test temperature per NF is based on the Lowest Service Temperature (LST) and is 10ºF greater than the Section II test temperature, the absorbed energy value is also higher making the use of the NF criteria conservative relative to Section II. Impact testing will be performed at the LST (-40ºF) for the HI-STAR 180D Package. Per NF-2331, material acceptability may be based on Charpy absorbed energy values or Charpy lateral expansion values.

Table 2.1.15: ASME Code Boiler & Pressure Vessel Code and Other Standards Applicable to HI-STAR 180D

Component ID	Material Procurement	Design Criteria	Stress and Deformation Analysis	Welding	Inspection	Testing
Containment System (pressure vessel except closure seals)	ASME Code Section III Subsection NB-2000	ASME Code Section III Subsection NB-3000	ASME Code Section III Subsection NB-3000	ASME Code Section III Subsection NB-4000 and Chapter 8 of this SAR	ASME Code Section III Subsection NB-5000 and Chapter 8 of this SAR	ASME Code Section III Subsection NB-6000 and Chapter 8 of this SAR
Fuel Basket	Chapter 8 of this SAR	Deflection limited to ensure subcriticality	Deflection Evaluation	Holtec Manufacturing Manual (Note 1)	Holtec Manufacturing Manual	Chapter 8 of this SAR
Top Lifting Trunnions	ASME Code Section II	NUREG-0612	NUREG-0612	Not Applicable	Chapter 8 of this SAR	Chapter 8 of this SAR
Monolithic Shield Cylinders	ASME Code Section II Part A or ASTM	ASME Code Section III Subsection NF-3000	Primary Effective Stress Below Ultimate Strength	ASME Code Section IX	ASME Code Section V	Not Applicable
Basket Shims	ASME Section II or ASTM	Non-Code	No gross yielding and no rupture	ASME Section IX, AWS or Holtec approved procedure	Not Applicable	Not Applicable
Neutron Shielding Material	Holtec Manufacturing Manual	Holtec Qualification Sourcebook	Not Applicable	Not Applicable	Holtec Manufacturing Manual	Chapter 8 of this SAR
Dose Blocker Steel Plate and Impact Limiter Backbone Structures	ASME Code Section II	ASME Code Section III Subsection NF-3000	No gross yielding or rupture	ASME Code Section IX	ASME Code Section V	Chapter 8 of this SAR

Note 1: The Holtec Manufacturing Manual contains detailed instructions for manufacturing of the subassemblies and the complete component in accordance with the applicable Codes and Standards. The Holtec Manufacturing Manual is a compilation of procedures, travelers, weld maps, specifications, standards, and encompasses the Metamic-HT Manufacturing Manual and other documents as applicable, to ensure the manufacturing of the HI-STAR components are in full accord with the design conditions of the CoC. The latest issue of the manufacturing manual(s) are maintained in the company's network under Holtec's configuration control system.

Table 2.1.16: *Critical Characteristics* of the HI-STAR 180D Package Materials

	Part I.D.	Function	Applicable *Critical Characteristics*	Minimum Values
1.	Containment Shell and Baseplate (or Forging) Stock	Provide radiological containment	Yield strength, σ_y, and ultimate strength, σ_u, at ambient and maximum possible metal temperature under normal and hypothetical conditions of transport. Minimum Charpy lateral expansion at "cold" conditions (-40°C) (measure of protection against brittle fracture); thermal conductivity, ψ; thermal expansion coefficient	As specified in Section II of the ASME Code for the materials listed in the Drawing Package in Section 1.3.
2.	Inner Closure Lid Bolts	Provide means to maintain the seals in compressed condition to prevent leakage for the inner closure lid seals	Yield strength, σ_y, and ultimate strength, σ_u, at 375 degrees F	$\sigma_y \geq$ 862.0MPa (125.025 ksi) $\sigma_u \geq$ 1047.9 MPa (151.99 ksi)
3.	Outer Closure Lid Bolts	Provide means to maintain the seals in compressed condition to prevent leakage for the outer closure lid seals	Yield strength, σ_y, and ultimate strength, σ_u, at 300 degrees F	$\sigma_y \geq$ 885.1 MPa (128.4 ksi) $\sigma_u \geq$ 1068.7 MPa (155 ksi)
4.	Closure Lid Seals	Prevent leakage in the closure lid bolted joint for closure lids main seals	Maintain sealing	See Subsection 2.2.1.1.6
5.	Fuel Basket	Maintain subcriticality of the fuel basket and provide support to the fuel	Yield strength, $\sigma_{y;}$ ultimate strength, $\sigma_{u;}$ Young's modulus, E	See Table 2.2.8
6.	Holtite Neutron Shielding	Provide principal means to block neutron radiation	See Subparagraph 1.2.1.5.1	See Table 2.2.13 and 8.1.11
7.	Top and Bottom Trunnions	Provide means for lifting and/or pivoting the cask for upending/downending.	Yield strength, σ_y, and ultimate strength, σ_u, at 400 degrees F	$\sigma_y \geq$ 677.7MPa (98.3 ksi) $\sigma_u \geq$ 938.4 MPa (136.1 ksi)
8.	Fuel Basket Supports (Shims)	Provide positioning and cushioning of the fuel basket	Yield strength, σ_y, and ultimate strength, σ_u, at 500 degrees F	$\sigma_y \geq$ 154 MPa (22 ksi) $\sigma_u \geq$ 182 MPa (26 ksi)
9.	Monolithic Shield Cylinders	Provide gamma radiation shielding	Yield strength, σ_y, and ultimate strength, σ_u, at 400 degrees F	$\sigma_y \geq$ 234.4 Mpa (34 ksi) $\sigma_u \geq$ 482.6 Mpa (70 ksi)
10.	Impact Limiters	Provide resistance against excessive deceleration	Crush Strength; Crush strength tolerance; % crush before "lock-up; sensitivity to temperature and humidity changes in the transport condition operating range.	See Table 2.2.10
11.	Bottom Shield Cylinder	Provide gamma radiation shielding	Yield strength, σ_y, and ultimate strength, σ_u, at 400 degrees F	$\sigma_y \geq$ 234.4 Mpa (34 ksi) $\sigma_u \geq$ 482.6 Mpa (70 ksi)

Note: Values for critical characteristics based on evaluation of safety margins from analysis results.

2.2 MATERIALS

2.2.1 Mechanical Properties and Specifications

This subsection provides the mechanical properties used in the structural evaluations. The properties include, as appropriate, yield stress, ultimate stress, modulus of elasticity, strength, weight density, and coefficient of thermal expansion. The property values are presented for a range of temperatures for which structural calculations are performed.

2.2.1.1 Structural Materials

2.2.1.1.1 Nickel Alloy, Low-Alloy Steel

The nickel alloy and low-alloy steels used in the HI-STAR 180D packaging are SA-203E and SA-350 LF3, respectively. The material properties (used in structural evaluations) of SA-203 E and SA-350 LF3 are given in Table 2.2.1.

Properties of steel, which are not included in any of the tables at the end of the section, are weight density and Poisson's ratio. These properties are assumed constant for all structural analyses. The values used are shown in the table below.

Property	**Value**
Weight Density, kg/m^3 (lb/in^3)	7,833 (0.283) 8,027 (0.290) (for Stainless Steel)
Poisson's Ratio	0.30

2.2.1.1.2 Bolting and Trunnion Materials

Material properties (for structural evaluations) of the closure lid bolting and trunnion materials used in the HI-STAR 180D Package are given in Tables 2.2.2 and 2.2.3.

2.2.1.1.3 Fuel Basket

The Fuel Basket is made of Metamic-HT.

Metamic-HT, a high strength, nanotechnology-based counterpart of the classic Metamic neutron absorber material, is extensively characterized in the supplier's report [1.2.27]. Minimum guaranteed values (MGVs) of Metamic-HT, based on the supplier's test report (as adopted by Holtec) [1.2.27] are provided in Tables 2.2.8 and 8.1.5.

2.2.1.1.4 Weld Material

All weld filler materials utilized in the welding of the Code components, which excludes the Metamic-HT fuel basket, will comply with the provisions of the appropriate ASME Code Subsection (e.g., cited paragraphs of Subsection NB and with applicable paragraphs of Section IX). All non-Code welds and non-Metamic-HT welds will be made using weld procedures that meet ASME Section IX, AWS D1.1, D.1.2 or equivalent. The minimum tensile strength of the weld wire and filler material (where applicable) will be equal to or greater than the tensile strength of the base metal listed in the ASME Code.

All non-destructive examinations specifications will comply with Section V of the ASME Code.

Metamic-HT welding and examinations will be in accordance with Subparagraph 1.2.1.6.1, Subsection 8.1.2, and the drawing package in Section 1.3.

2.2.1.1.5 AL-STAR Impact Limiter

The AL-STAR impact limiter for the HI-STAR 180D Package is shown in the drawing package in Section 1.3. The impact limiter consists of a rigid cylindrical core, a cylindrical skirt that girdles the cask forging, the energy absorbing material, an outer skin, and attachment bolts. The energy absorbing material is positioned in the impact limiter to realize adequate crush modulus in all potential impact modes. The external surface of the impact limiter consists of a stainless steel skin to provide long-term protection against weather and inclement environmental conditions. Attachment bolts are also made of stainless steel, which imparts a high fracture toughness and high ductility in the entire temperature range of service.

Rail transport considerations limit the maximum diameter of the impact limiter. The axial dimension of the impact limiter is limited by the considerations of maximum permissible packaging weight for rail transport. Within the limitations of space and weight, the impact limiter should possess sufficient energy absorption capacity so as to meet the structural demands on the package under all postulated drop orientations. The sizing of the impact limiter internal structure is principally guided by the above considerations. For example, in order to ensure that a sufficient portion of the energy absorbing material participates in lateral impacts, a thick high strength steel shell, buttressed with gussets, provides a hard backing surface for the energy absorbing material to crush against.

The material properties for the stainless and carbon steels, for structural evaluations, are provided in Tables 2.2.4 and 2.2.5, respectively. Material properties for the stainless steel impact limiter attachment bolts are provided in Table 2.2.6.

Two properties of the energy absorbing material germane to its function are the crush strength and the nominal density. The crush strength is the more important of the two properties; the density is significant in establishing the total weight of the package. The crush strength increases monotonically with density. Energy absorbing materials with a wide range of density and crush strength are available. A characteristic load-displacement relation for an energy absorbing material is shown in Figure 2.2.1 for a constant crush area. The relation shows an initial sharp peak, then an essentially constant force over a large crush depth, and finally a significant increase of the force when the material becomes compacted. To eliminate the initial peak, which could potentially result in higher g-loads at the beginning of the impact, all crush material for the HI-STAR 180D is pre-crushed by the material supplier. Table 2.2.10 provides design property values of the impact limiter crush material in tabular form.

For the HI-STAR 180D cask, two crush strengths are utilized to optimize the impact limiter's performance. The drawing package in Section 1.3 shows the location of the crush materials for predominately lateral impact (designated as Type 1) and for predominately longitudinal impact (designated as Type 2); Table 2.2.10 provides the design values for the impact limiter crush material's crush strengths in tabular form. The crush strength, being a critical characteristic, will be specified in the purchase specification for material procurement.

Table 2.2.10 also contains the required properties of the Fastener Strain Limiters (FSL), which protect the impact limiter attachment bolts against excessive tensile strains during a drop accident.

The properties listed in Table 2.2.10 are categorized as *Primary* or *Secondary* properties based on their effect on the performance of the component. Primary properties are those whose variations have a direct impact on the performance. Secondary properties are those whose percentage variation results in at least a rough order of magnitude (i.e., more than a factor of 5) smaller percentage variation in the applicable critical performance parameters, such as the g-load and crush depth in the case of the impact limiters. A procured material will be rejected if the *primary* property is outside of the limits of Table 2.2.10. However, if a *secondary* property in a procured material lies outside the range in Table 2.2.10 then a reconciliation analysis using the methodology in this SAR may be performed to determine whether the as-manufactured property value is acceptable. The value is acceptable if the g-load remains below β_{max} (see Section 2.6) and the crush depth remains below the available stroke. The reconciliation analysis will become a part of the documentation package on the manufactured component.

Like all manufactured materials, the mechanical properties of the material are subject to slight variation due to manufacturing tolerances, characterization methods and material temperature. Accordingly, the acceptance criteria for the average crush strength of the crush material is expressed as tolerance bands in Table 2.2.10 for Type 1 and Type 2 crush materials. Material testing will be performed in accordance with Holtec approved procedures to demonstrate that the crush strength limits are satisfied over the entire operating temperature range (see Table 2.2.10). The range of crush strengths provided in Table 2.2.10 are sufficiently large to account for both the temperature effects and the manufacturing variations based on historical testing of similar crush materials [2.2.11]. Additional information on crush material testing is provided in Paragraph 8.1.5.2. The minimum and maximum crush strength values specified in Table 2.2.10 are explicitly analyzed in Section 2.7 for the 9-meter drop simulations (see Table 2.7.3).

2.2.1.1.6 Closure Lid Seals

The containment integrity of the HI-STAR 180D Package relies on a double closure lid system with metallic seals, as shown in the licensing drawings in Section 1.3. The sealing action against the release of the cask's contents is provided by the two self-energizing seals located in each of the two annular grooves per lid. Each seal acts autonomously, thus providing a double barrier against leakage for each closure lid.

To ensure that the effectiveness of the leak barriers is optimal, the grooves are machined in the precise configuration and surface finish called for the type of self-energizing gasket selected for this application. The gasket chosen for the HI-STAR 180D cask must fulfill the principal requirements set down in the following:

- A reasonably uniform compression/decompression characteristic over the temperature range of interest (-40ºC to 200ºC)
- Adequate springback upon withdrawal of the compression load
- Ability to withstand Borated water environment
- Ability to seal against light gases such as helium
- Excellent radiation resistance
- Well adapted for joints required to withstand impulsive and impactive loads

The load required to "seat" the gaskets is a small percentage of the total applied bolt preload force; hence the required "seating load" (an ASME Boiler & Pressure Vessel code term) is not an important parameter. The size of the gasket in relation to the size of the groove, on the other hand, is a critical dimension that is based on the gasket supplier's test data and which must be controlled through the gasket Procurement Specification. The critical sealing dimensions consistent with seal manufacturers' data are provided in Appendix 8.A. Other critical characteristics of the HI-STAR 180D gasket that must be controlled to ensure a robust joint performance are listed in Table 2.2.12. The gaskets will be procured as an *Important-to-Safety* part.

Using the governing design features from Table 2.2.12, the closure seals have been conservatively specified to provide a high degree of assurance of leak tightness under normal and accident conditions of transport so that package service conditions at normal or accident pressures under high and low temperatures will not challenge the capabilities of cask closure seals. Creep of the cask closure seals, even under long term use in a loaded cask (50 years), is not credible due to its materials of construction and the nickel alloy seal spring. The specifications for the closure lid seals are provided below:

Temperature and Pressure Specifications:
Temperature limits for inner and outer closure lid seals are specified in Table 3.2.12
Pressure range for the seal assembly: hard vacuum to 5.51 MPa (800 psi.)

Material Specifications:
See Chapter 8 for material specifications for inner and outer closure lid seals.

Seal Assembly Springback:
Table 2.2.12 provides the useful springback to maintain the leak tightness for both closure lid seals. The increased springback and larger diameter seal cross section (compared to HI-STAR 100) provide for a tighter seal and increased surface area contact with the cask sealing surfaces for enhanced leaktightness and protection from degradation.

Table 2.2.12 provides the data on the bolted joint loads, including the load needed to "seat" the closure plate gaskets.

2.2.1.2 Nonstructural Materials

2.2.1.2.1 Monolithic Shield Cylinder

The monolithic shield cylinder is not in the primary load path of the HI-STAR 180D cask during a lifting operation since it has no connection to the upper trunnions. The monolithic shield cylinders do, however, girdle the containment shell and thus may act in concert with the containment shell during Hypothetical Accident Conditions of Transport. Necessary structural properties for the monolithic shield, for analysis purposes, are the yield and ultimate strength; a representative set of properties is tabulated in Table 2.2.7, and *critical characteristics* are provided in Table 2.1.16.

2.2.1.2.2 Holtite Neutron Shielding Material

The non-structural properties of the neutron shielding material are provided in Section 1.2 and Table 2.2.13. Holtite B does not serve a structural function in the HI-STAR 180D package.

2.2.1.2.3 Fuel Basket Supports

The fuel basket supports (basket shims), made of aluminum alloy and stainless steel, provide the heat transfer bridge between the basket and the cask inside surface, and serve to position the fuel basket. Representative mechanical properties for the basket supports are tabulated in Table 2.2.9. Table 2.2.4 provides the mechanical properties for the stainless steel basket support.

The creep behavior of the fuel basket supports is a function of the level of stress in the component under Normal Conditions of Transport. As justified below, shims creep has no adverse effect on the basket geometry. When the loaded cask is resting in the horizontal orientation, the fuel basket supports are loaded under a low compressive stress (maximum stress is less than 690 kPa (100 psi)). The table below provides the predicted creep strain assuming (conservatively) that the metal temperature of the basket support starts at or above the maximum basket reported in Table 3.1.1 and decreases with the passage of time due to fuel decay inside the cask under a hypothetical 60-year duration under transport.

Duration Under Load (Years)	Upper Bound Basket Support Temperature, °C	Cumulative Creep Strain (%)[Note 1]
0	270	0
20	201	0.03997
40	191	0.04112
60	186	0.0414
Note 1: Cumulative strain computed by integrating the creep rate equation from [1.2.27] under the time dependent Metamic-HT temperature tabulated herein.		

Note that the creep in the basket shims is applicable only in presence of appreciable load on the basket shims under horizontal configuration of the Transport Package for an extended period. Since the Transport Package remains in horizontal configuration for relatively short durations, the creep in the basket shims calculated over a period of sixty years is very conservative.

2.2.1.2.4 Cask Coating

The HI-STAR 180D cask exterior steel surfaces are coated with a conventional surface preservative such as Carboguard® 890 (see www.carboline.com for product data sheet) and/or equivalent surface preservative. Carboguard ® 890 and equivalent surface preservatives have provided years of proven performance on HI-STAR 100 casks. In addition, exterior surfaces of the cask are easily inspected and recoated as necessary. For cask coatings, alternate surface preservatives are determined equivalent per the recommendation of a coating manufacturer and with Holtec approval. Carboguard 890 is the product name at the time of this SAR writing. Chemically identical products with different names are permitted. Other coatings that can be shown to have had proven performance in similar applications and environments are permitted.

2.2.1.2.5 Cask Liner

A cask liner is required to protect containment boundary steel components against increased corrosion from submersions into the spent fuel pools. The HI-STAR 180D cask cavity and inter-lid space carbon steel surfaces (except for threaded features) may be lined with either a) conventional surface preservative, b) an atomized deposit of a corrosion resistant layer such as aluminum oxide or c) other methods according to the drawing package in Section 1.3. Conventional surface preservative over aluminum oxide is also acceptable where supported by manufacturer recommendation.

a) Conventional Surface Preservative

The HI-STAR 180D cask interior steel surfaces may be coated with conventional surface preservatives such as Thermaline® 450 (see www.carboline.com for product data sheet) or equivalent surface preservative. Thermaline® 450 and equivalent surface preservatives have provided years of proven performance on HI-STAR 100 casks. Conventional surface preservatives refer to sprayed/rolled on and cured "paints". Although interior cask surfaces are not accessible for routine liner repair during loaded cask operation, the dry helium environment protects cask contents and internals, including cask liners from long-term degradation. Conventional surface preservatives shall be applied in accordance with the manufacturer's recommendation and to the recommended dry film thickness. Conventional surface preservatives shall not result in significant chemical reaction with borated water. Thermaline® 450 is the product name at the time of this SAR writing. Chemically identical products with different names are permitted. The following critical characteristics are specified conservatively for conventional surface preservatives and in order of importance to guide the in the selection of equivalent surface preservatives:

Acceptance Criteria for Conventional Surface Preservative Liner	
Rank	**Criteria**
1	Chemical Immersion Resistance (suitable for short-term immersion in borated water)
2	High Temperature Resistance (suitable for 220°C for the cask cavity surfaces and 150°C for the inter-lid space, long-term dry helium environment)
3	High Radiation Resistance (suitable for $1x10^8$ Rad)
4	Good Adhesion Characteristics (adhesion to steel or aluminum oxide as applicable)
5	Good Structural Performance (bendability/ductility/cracking resistance/abrasion resistance)
6	Emissivity (as specified in Chapter 3, Table 3.2.6)

b) Aluminum Oxide

Aluminum oxide provides excellent corrosion resistance and is compatible with the cask aluminum basket supports. An aluminum oxide veneer provides superior performance and durability over conventional surface preservatives and provides sufficiently high emissivity (as specified in Chapter 3, Table 3.2.6).

Aluminum oxide may be applied by the commonly used thermal spray method along the cask inner surfaces. Approved procedures will be developed for performing the operation taking into consideration or fully applying available guidance from recognized standards. The following standards are available for developing procedures and for qualifying thermal spray contractors or operators.

1) ANSI/AWS C2.18-93 "Guide for the Protection of Steel with Thermal Sprayed Coating of Aluminum and Zinc and Their Alloys and Composites"

2) NACE No. 12/AWS C2.23M/SSPC-CS 23.00 "Specification for the Application of Thermal Spray Coatings (Metallizing) of Aluminum, Zinc, and Their Alloys and Composites for the Corrosion Protection of Steel"

3) SSPC 04-13 SSPC-QP 6 "Standard Procedure for Evaluating the Qualifications of Contractors Who Apply Thermal Spray (Metallizing) for Corrosion Protection of Steel and Concrete Structures"

4) ANSI/AWS C2.16/C2.16M:2002 "Guide for Thermal Spray Operator Qualification"

Other standard processes for aluminum oxide thermal spray and its application, which are supported by recognized standards, may be used subject to a suitability assessment by Holtec International.

c) Other surface preservation methods.

The cask liner surfaces may be protected using other methods which provide suitable corrosion resistance along with the heat transfer characteristics used in the thermal analysis. These methods include weld overlay, explosive bonding, and lining with a thin corrosion resistant sheet material. Use of these alternate methods is permitted provided that the heat transfer effectiveness of the cask containment boundary with the liner maintains fuel cladding and cask component temperatures within the design limits. The heat transfer effectiveness is maintained provided the minimum emissivity valued for the cask interior surfaces meets or exceeds the value of listed in Table 3.2.6 and the through wall thermal conductivity of the cask is not significantly reduced.

2.2.1.2.6 Lead

Lead is not considered as a structural member of the HI-STAR 180D Package. However, it is included in the dynamic simulation models for Normal and Accident Conditions of Transport. Applicable mechanical properties of lead are provided in Table 2.2.11.

2.2.2 Chemical, Galvanic or Other Reactions

Similar to the HI-STAR 100 and HI-STAR 180 packaging, the HI-STAR 180D packaging combines low-alloy and nickel alloy steels, carbon steels, neutron and gamma shielding, and bolting materials. All of these materials have a long history of non-galvanic behavior within close proximity of each other. The external surfaces of the cask are coated to preclude surface oxidation. The internal surfaces of the cask are lined to preclude any significant surface oxidation. The coatings and liners do not chemically react significantly with borated water. The cask is dried and helium backfilled as discussed in Chapter 7 to eliminate any credible corrosion from moisture and oxidizing gases. Metamic-HT plate has high corrosion resistance, and anodizing to meet the required emissivity further enhances its corrosion resistance. Therefore, chemical, galvanic or other reactions involving the cask materials are unlikely and are not expected.

The interfacing seating surfaces of the closure lid metallic seals are clad with or stainless steel to assure long-term sealing performance and to eliminate the potential for localized corrosion of the seal seating surfaces. The closure seals do not have separate jackets that can collect moisture or debris; instead closure seals are cladded, coated, or plated with silver for the best possible long-term performance.

In accordance with NRC Bulletin 96-04 [2.2.4], a review of the potential for chemical, galvanic, or other reactions among the materials of the HI-STAR 180D Package, its contents and the operating environment, which may produce adverse reactions, has been performed. As a result of this review, no operations were identified which could produce adverse reactions. No closure welding is performed and thus hydrogen generation while the cask is in the pool is of minor consequence to cask operations based on previous experience with the same cask materials. Because no welding activities are involved in the cask closure operations, the potential of a hydrogen ignition event does not exist.

2.2.3 Effects of Radiation on Materials

The general physical effects of radiation of metals by fast neutrons and other high-energy particles are summarized in the following table taken from a DOE Handbook on Material Science [2.2.3].

General Effect of Fast Neutron Irradiation on Metals	
Property Increases	Property Decreases
• Yield Strength • Tensile Strength • NDT Temperature • Young's Modulus (Slight) • Hardness • High Temperature Creep Rate (During Irradiation)	• Ductility • Stress-Rupture Strength • Density • Impact Strength • Thermal Conductivity

The HI-STAR 180D Package is composed of materials that either have a proven history of use in the nuclear industry or have been extensively tested. The radiation levels from spent nuclear fuel do not affect the packaging materials. Gamma radiation damage to metals (e.g., aluminum, stainless steel, and carbon steel) does not occur until the fluence level reaches 10^{18} rads or more. The 50-year gamma fluence (assuming design basis fuel for 50 years without radioactive decay) from the spent nuclear fuel transported in the HI-STAR 180D Package is on the order of 1.25 x 10^9 rads and reduces significantly as it penetrates through cask components. Moreover, significant radiation damage due to neutron exposure does not occur for neutron fluences below approximately 10^{19} n/cm^2 [2.2.3, 2.2.4, 2.2.5], which is far greater than the 50-year neutron fluence from spent nuclear fuel transported in the HI-STAR 180D Package, which is on the order of 1.25 x 10^{16} n/cm^2 assuming design basis fuel for 50 years without radioactive decay. Also, as indicated in reference [2.2.3], "The effects listed in the table above are generally less significant at elevated temperatures for a given fluence and some defects can be removed by heating (annealing)."

As discussed in Section 1.2 and its references, the Metamic-HT neutron absorber and Holtite have been tested extensively to prove that it will not degrade over the service life of the package. With the high nickel content in its spring, the cask closure seal materials are also most resistant to radiation. No adhesives are used in the cask packaging and packaging coatings (especially cask liners) are selected for the high radiation environment.

Table 2.2.1: Mechanical Properties of SA-350 LF3/SA-203 E

Temperature °C (°F)	**SA-350 LF3/SA-203 E for Cask Containment Boundary**					
	S_y	S_u	E	α	S_y	S_u
-73.30 (-100)	258.6 (37.5)	482.6 (70.0)	19.72 (28.6)	-	275.8 (40.0)	482.6 (70.0)
37.78 (100)	258.6 (37.5)	482.6 (70.0)	19.03 (27.6)	11.7 (6.5)	275.8 (40.0)	482.6 (70.0)
93.33 (200)	235.8 (34.3)	482.6 (70.0)	18.68 (27.1)	12.06 (6.7)	252.3 (36.6)	482.6 (70.0)
148.89 (300)	228.9 (33.2)	482.6 (70.0)	18.41 (26.7)	12.42 (6.9)	244.1 (35.4)	482.6 (70.0)
204.4 (400)	220.6 (32.0)	482.6 (70.0)	18.07 (26.2)	12.78 (7.1)	235.8 (34.2)	482.6 (70.0)
260 (500)	209.6 (30.4)	482.6 (70.0)	17.72 (25.7)	13.14 (7.3)	224.1 (32.5)	482.6 (70.0)
316 (600)	194.4 (28.2)	482.6 (70.0)	17.31 (25.1)	13.32 (7.4)	207.5 (30.0)	482.6 (70.0)

Definitions:

S_y = Yield Stress MPa (ksi)
S_u = Ultimate Stress MPa (ksi)
α = Coefficient of Thermal Expansion, cm/cm-°C x 10^{-6} (in./in. per degree F x 10^{-6})
E = Young's Modulus MPa x 10^4 (ksi x 10^3)

Notes:
1. Source for S_y values is Table Y-1 of [2.1.6].
2. Source for S_u values is ratioing S_m values.
3. Source for α values is material group 1 in Table TE-1 of [2.1.6].
4. Source for E values is material group B in Table TM-1 of [2.1.6].

Table 2.2.2a: Mechanical Properties of SA-193 Grade B7

SA-193 Grade B7 [less than 64 mm (2.5 in) diameter] for Containment Boundary Port Cover Bolts					
Temperature, ºC (ºF)	S_y	S_u	**E**	α	S_m
38 (100)	724.0 (105.0)	861.8 (125.00)	20.3 (29.5)	11.7 (6.5)	241.3 (35.0)
93.3 (200)	675.9 (98.0)	861.8 (125.00)	19.99 (29.0)	12.06 (6.7)	224.8 (32.6)
149 (300)	648.8 (94.1)	861.8 (125.00)	19.65 (28.5)	12.42 (6.9)	216.5 (31.4)
204 (400)	630.9 (91.5)	861.8 (125.00)	19.31 (28.0)	12.78 (7.1)	210.3 (30.5)
260 (500)	610.2(88.5)	861.8 (125.00)	18.89 (27.4)	13.14 (7.3)	203.4 (29.5)
316 (600)	588.1 (85.3)	861.8 (125.00)	18.55 (26.9)	13.32 (7.4)	195.8 (28.4)
371 (700)	555.72 (80.6)	824.6 (119.6)	18.06 (26.2)	13.68 (7.6)	185.5 (26.9)

Definitions:

S_y = Yield Stress, MPa (ksi)
α = Mean Coefficient of thermal expansion, cm/cm-ºC x 10^{-6} (in/in-ºF x 10^{-6})
S_u = Ultimate Stress, MPa (ksi)
E = Young's Modulus, MPa x 10^4 (psi x 10^6)

Notes:

1. Source for S_y values is Table Y-1 of [2.1.6] for ferrous materials.
2. Source for S_u values is Table U of [2.1.6] for ferrous materials, or from Section II, Part A. Where ultimate strength is unavailable, values above 300 deg. F are based on 100 deg.F value multiplied by ratio of yield strength at room temperature to yield strength at desired temperature.
3. Source for α values is Tables TE-1 and TE-4 of [2.1.6] for ferrous materials.
4. SA-705 630/SA-564 630 (H1025) per Table 2.2.3 is optional material for Port Cover Lid Bolts.

Table 2.2.2b: Inner and Outer Closure Lid Bolt Material – Mechanical Properties

SA-705 630, SA-564 630 (H1025 Condition)				
Temperature, ºC (ºF)	S_y	S_u	E	α
38 (100)	999.5 (145.0)	1068.7 (155)	19.7 (28.5)	11.16 (6.2)
93.3 (200)	924.4 (134.1)	1068.7 (155)	19.1 (27.8)	11.34 (6.3)
149 (300)	885.1 (128.4)	1068.7 (155)	18.8 (27.2)	11.52 (6.4)
204 (400)	854.1 (123.9)	1039 (150.7)	18.4 (26.7)	11.70 (6.5)
260 (500)	827.9 (120.1)	1018 (147.7)	18. (26.1)	11.70 (6.5)
288 (550)	816.2 (118.4)	1011 (146.6)	17.8 (25.8)	11.88 (6.6)
SB-637 N07718 (less than or equal to 6 inches diameter)				
38 (100)	1034 (150.0)	1276 (185.0)	19.83 (28.76)	12.9 (7.1)
93.3 (200)	992.8 (144.0)	1225 (177.6)	19.51 (28.3)	13.0 (7.2)
149 (300)	970.1 (140.7)	1196 (173.5)	19.24 (27.9)	13.2 (7.3)
204 (400)	953.5 (138.3)	1176 (170.6)	18.96 (27.5)	13.4 (7.5)
260 (500)	943.2 (136.8)	1163 (168.7)	18.75 (27.2)	13.6 (7.6)
316 (600)	932.9 (135.3)	1151 (166.9)	18.48 (26.8)	13.9 (7.7)

Definitions:

S_m = Design stress intensity MPa (ksi)
S_y = Yield Stress MPa (ksi)
α = Mean Coefficient of thermal expansion (in./in. per degree F x 10^{-6})
S_u = Ultimate Stress MPa (ksi)
E = Young's Modulus MPa 10^4 (psi x 10^6)

Notes:

1. Source for S_m values is Table 4 of [3.3.1].
2. Source for S_y values is ratioing design stress intensity values and Table Y-1 of [3.3.1], as applicable.
3. Source for S_u values is ratioing design stress intensity values and Table U of [3.3.1], as applicable.
4. Source for α values is Tables TE-1 and TE-4 of [3.3.1], as applicable.
5. Source for E values is Tables TM-1 and TM-4 of [3.3.1], as applicable.
6. Source for α values is Table TE-1 of [2.1.6] for ferrous materials. Values for α are for H1075 condition in lieu of H1025 condition.
7. SA-705 630 and SA-564 630 (both UNS No. S17400) have the same chemistry requirements and are considered equivalent for the intended application.

Table 2.2.3: Mechanical Properties of SA-705 630, SA-564 630

SA-705 630, SA-564 630 for Trunnions† (H1100 Condition)				
Temperature, ºC (ºF)	S_y	S_u	E	α
38 (100)	792.9 (115)	965.3 (140)	19.8 (28.68)	11.16 (6.2)
93.3 (200)	732.9 (106.3)	965.3 (140)	19.1 (27.8)	11.34 (6.3)
149 (300)	701.9 (101.8)	965.3 (140)	18.8 (27.2)	11.52 (6.4)
204 (400)	677.8 (98.3)	938.4 (136.1)	18.4 (26.7)	11.70 (6.5)
260 (500)	656.4 (95.2)	919.8 (133.4)	18. (26.1)	11.70 (6.5)
288 (550)	647.8 (93.95)	912.9 (132.4)	17.8 (25.8)	11.88 (6.6)
† Material SB-637 N07718 is also a candidate trunnion material, which if used, must instead satisfy the strength requirement specified in Table 2.1.16.				

Definitions:

S_y = Yield Stress, MPa (ksi)

α = Mean Coefficient of thermal expansion, cm/cm-ºC x 10^{-6} (in/in-ºF x 10^{-6})

S_u = Ultimate Stress, MPa (ksi)

E = Young's Modulus, MPa x 10^4 (psi x 10^6)

Notes:

1. Source for S_y values is Table Y-1 of [2.1.6] for ferrous materials.
2. Source for S_u values is Table U of [2.1.6] for ferrous materials, or from Section II, Part A. Where ultimate strength is unavailable, values above 300 deg. F are based on 100 deg.F value multiplied by ratio of yield strength at room temperature to yield strength at desired temperature.
3. Source for α values is Table TE-1 of [2.1.6] for ferrous materials. Values for α are for H1075 condition in lieu of H1100 condition.
4. SA-705 630 and SA-564 630 (both UNS No. S17400) have the same chemistry requirements and are considered equivalent for the intended application.

Table 2.2.4: Stainless Steel – Mechanical Properties (Minimum Values of SA-240 304, 304LN, 316, 316LN)

Temperature ºC (ºF)	S_y	S_u	α	E
-40 (-40)	206.8 (30.0)	517.1 (75.0)	14.58 (8.1)*	19.91 (28.88)
38 (100)	206.8 (30.0)	517.1 (75.0)	15.48 (8.6)	19.44 (28.2)
65.6 (150)	186.8 (26.7)	-	15.84 (8.8)	-
93.3 (200)	172.4 (25.0)	489.5 (71.0)	16.02 (8.9)	18.96 (27.5)
121 (250)	162.8 (23.6)	-	16.38 (9.1)	-
149 (300)	155.1 (22.5)	456.4 (66.2)	16.56 (9.2)	18.62 (27.0)
204 (400)	142.7 (20.7)	441.3 (64.0)	17.1 (9.5)	18.2 (26.4)

Definitions:

S_y = Yield Stress, MPa (ksi)
α = Mean Coefficient of thermal expansion, cm/cm-ºC x 10^{-6} (in/in-ºF x 10^{-6})
S_u = Ultimate Stress, MPa (ksi)
E = Young's Modulus, MPa x 10^4 (psi x 10^6)

Notes:

1. Source for S_y values is Table Y-1 of [2.1.6].
2. Source for S_u values is Table U of [2.1.6].
3. Source for α values is Table TE-1, Group 3 of [2.1.6]. * Value at –40 deg. F is extrapolated.
4. Source for E values is material group G in Table TM-1 of [2.1.6].
5. The listed yield and ultimate stress is the minimum value of SA-240 304, 304LN, 316, and 316LN.

Table 2.2.5: Miscellaneous Steel – Mechanical Properties

Temperature ºC (ºF)	SA-36			
	S_y	S_u	α	E
37,8 (100)	248.2 (36.0)	399.9 (58.0)	11.7 (6.5)	20.17 (29.26)
93,3 (200)	227.5 (33.0)	399.9 (58.0)	12.06 (6.7)	19.86 (28.8)
149 (300)	219.3 (31.8)	399.9 (58.0)	12.42 (6.9)	19.51 (28.3)
204 (400)	212.4 (30.8)	399.9 (58.0)	12.78 (7.1)	19.24 (27.9)
260 (500)	202.0 (29.3)	399.9 (58.0)	13.14 (7.3)	18.82 (27.3)
316 (600)	190.3 (27.6)	399.9 (58.0)	13.32 (7.4)	18.27 (26.5)
371 (700)	177.9 (25.8)	399.9 (58.0)	14.04 (7.8)	17.58 (25.5)

Table 2.2.5 (Continued): Miscellaneous Steel – Mechanical Properties

Temperature °C (°F)	SA-516 Grade 70 or A516 Gr 70			
	S_y	S_u	α	E
38 (100)	262.0 (38.0)	482.6 (70.0)	11.7 (6.5)	20.17 (29.26)
93.3 (200)	239.9 (34.8)	482.6 (70.0)	12.06 (6.7)	19.86 (28.8)
149 (300)	231.7 (33.6)	482.6 (70.0)	12.42 (6.9)	19.51 (28.3)
204 (400)	224.1 (32.5)	482.6 (70.0)	12.78 (7.1)	19.24 (27.9)
260 (500)	213.7 (31.0)	482.6 (70.0)	13.14 (7.3)	18.82 (27.3)
316 (600)	200.6 (29.1)	482.6 (70.0)	13.32 (7.4)	18.27 (26.5)
371 (700)	187.5 (27.2)	482.6 (70.0)	14.04 (7.8)	17.58 (25.5)

Definitions:

S_y = Yield Stress, MPa (ksi)
α = Mean Coefficient of thermal expansion, cm/cm-°C x 10^{-6} (in/in-°F x 10^{-6})
S_u = Ultimate Stress, MPa (ksi)
E = Young's Modulus, MPa x 10^4 (psi x 10^6)

Notes:

1. Source for S_y values is Table Y-1 of [2.1.6].
2. Source for S_u values is Table U of [2.1.6].
3. Source for α values is material group 1 in Table TE-1 of [2.1.6].
4. Source for E values is "Carbon steels with C less than or equal to 0.30%" in Table TM-1 of [2.1.6].

Table 2.2.6: Yield and Ultimate Strength of Impact Limiter Attachment Bolts

SA-193 B8 Class 2 (3⁄4 in. < t ≤ 1 in.)		
Temp. °C (°F)	**S_y**	**S_u**
Room Temperature	551.6 (80.0)	792.9 (115.0)
165.6 (330)	402.4 (58.37)	692.9 (100.49)

Definitions:

S_y = Yield Stress, MPa (ksi)
S_u = Ultimate Stress, MPa (ksi)

Notes:

1. Source for S_y values is Table Y-1 of [2.1.6].
2. Source for S_u values is Table U of [2.1.6].
3. Since the SA 193-B8 Class 2 bolt material properties are not listed at the elevated temperatures, the elevated temperature material properties for SA 193-B8 Class 2 bolt properties are derived using the proportioning of the SA 193-B8 Class 1 bolting material at elevated temperature to the room temperature properties.

Table 2.2.7: Monolithic Shield Cylinder – Mechanical Properties

SA-352 LCC / A352-93 LCC				
Temp. ºC (ºF)	**S_y**	**S_u**	**E**	**α**
37.8 (100)	275.8 (40.0)	482.6 (70.0)	20.2 (29.3)	11.7 (6.5)
93.33 (200)	251.7 (36.5)	482.6 (70.0)	19.86 (28.8)	12.06 (6.7)
148.89 (300)	244.8 (35.5)	482.6 (70.0)	19.51 (28.3)	12.42 (6.9)
204.2 (400)	234.4 (34)	482.6 (70.0)	19.24 (27.9)	12.78 (7.1)
260 (500)	223.4 (32.4)	482.6 (70.0)	18.82 (27.3)	13.14 (7.3)

Definitions:

S_y = Yield Stress, MPa (ksi)
α = Mean Coefficient of thermal expansion, cm/cm ºC x 10^{-6} (in/in-ºF x 10^{-6})
S_u = Ultimate Stress, MPa (ksi)
E = Young's Modulus, MPa x 10^4 (psi x 10^6)

Notes:

1. Source for S_y values is Table Y-1 of [2.1.6].
2. Source for S_u values is Table U of [2.1.6].
3. Source for α values is Table TE-1 (for Group 1) of [2.1.6].
4. Source for E values is "Carbon Steels with C less than 0.25%" in Table TM-1 of [2.1.6].
5. ASTM A352-93 LCC is equivalent material per ASME Code Section II (same properties are considered to apply in any analysis).

Table 2.2.8: Metamic-HT: Ancillary and Invariant Material Properties[Note 8]

	Property	Temperature, °C	Design Value[Notes 5 & 7]	Type
1.	Elongation, δ (%)	Ambient/200/300/350/450	11.3/9.0/7.6/7.4/4.5	Ancillary
2.	Maximum Creep Strain, ε (%)	$T \leq 400$	See creep equation in Note 1 below	Ancillary
3.	Thermal conductivity, k (W/m°K)	Ambient/200/300/350/450	170/170/170/170/170 (Note 9)	Invariant
4.	Emissivity (dimensionless), e	$150 \leq T \leq 350$	See Notes 2 & 3	Invariant
5.	Nominal specific gravity (dimensionless), s (Note 6)	Ambient	2.705	Invariant
6.	Average thermal expansion coefficient, Γ ($°C^{-1}$) (Note 6)	$30 \leq T \leq 500$	21×10^{-6}	Invariant
7.	Specific Heat, C_p (J/kg-°C)	100/200/350 $350 < T \leq 500$	832.3/914.1/1024.2 (Note 4)	Invariant

<u>Note 1:</u> Creep Equation

$\varepsilon = \alpha \exp(-E/RT) \sinh(\gamma\sigma) \tau^{\beta}$

where: ε is Creep Strain (%), σ is stress (psi), T is temperature (°K), τ is time (hr) and constants are as follows:

α: 1.05E03 %/hr; E: 50000 J/gmol; γ: 1E-04 psi^{-1}; β: 0.5; R: 8.31 J/gmol-°K

<u>Note 2:</u> Emissivity Equation (Ebony Coat Anodized Metamic-HT)

e = 0.35 + 1.541E-03*(T-100) (100°F ≤ T ≤ 392°F); T in °F

e = 0.8 + 2.777E-4*(T-392) (392°F < T ≤ 752°F); T in °F

e = 0.9 (T > 752°F)

<u>Note 3:</u> Emissivity Equation (Dark Grey Anodized Metamic-HT)

e = 0.2 + 0.6 sin[π(T-100)/1304] (100°F ≤ T ≤ 752°F); T in °F

e = 0.8 (T > 752°F)

Either dark gray or ebony coat anodizing are acceptable options. The thermal evaluations in Chapter 3 of this SAR use the lower bound (Dark Gray Anodized) specification.

<u>Note 4:</u> Specific Heat Function

T: Temperature (°C)

$C_p = 1024.2 + 0.493(T-350)$

<u>Note 5:</u> Interpolating

When interpolating between data at different temperatures, 40°C will be used for ambient.

<u>Note 6:</u> Specific Gravity and Coefficient of Thermal Expansion

Mean value obtained from test data is tabulated herein.

<u>Note 7:</u> Source for Metamic-HT Properties is [1.2.27]

<u>Note 8:</u> See Table 8.1.5 for Primary Properties

<u>Note 9:</u> Thermal Conductivity

An understated thermal conductivity is defined herein for additional conservatism in the computed fuel cladding temperatures.

Table 2.2.9: Basket Shims – Nominal Mechanical Properties

Aluminum Alloy (B221 2219-T8511)					
Temp. ºC (ºF)	S_y	S_u	E	α	% Elongation
25 (75)	290 (42)	400 (58)	7.2 (10.5)	–	5
150 (300)	243 (35)	307 (44)	6.8 (9.8)	23.9 (13.3)	6.4
204 (400)	188 (27)	231 (34)	6.3 (9.1)	24.5 (13.6)	8.2
230 (450)	171 (25)	209 (30)	6.1 (8.8)	24.8 (13.8)	8.6
260 (500)	154 (22)	182 (26)	5.9 (8.5)	25.0 (13.9)	8.6
290 (550)	98 (14)	116 (17)	5.5 (8.0)	25.4 (14.1)	10.5

Definitions:

S_y = Yield Stress, MPa (ksi)
α = Mean Coefficient of thermal expansion, cm/cm-ºC x 10^{-6} (in/in-ºF x 10^{-6})
S_u = Ultimate Stress, MPa (ksi)
E = Young's Modulus, MPa x 10^4 (psi x 10^6)

Notes:

1. Source for E values is "Properties of Aluminum Alloys", page 82 [2.2.7] (properties listed in the table above are not affected by time at temperature).
2. Source for S_y, S_u, and % Elongation values at room temperature is ASTM Specification B221M [2.2.9]. Values at elevated temperatures are obtained by scaling the room temperature values using the data from [2.2.7].
3. Source for α is Table TE-2 of [2.1.6] (values listed in TE-2 are also considered representative of Aluminum Alloy (2219-T8511) (UNS No. A92219)).

Table 2.2.10: Design Properties of Impact Limiter Crush Material and Fastener Strain Limiters

Item & Property Category	Value	Comment
Crush strength (nominal), σ_c, of crush material, psi (Primary property) • Type 1 • Type 2	(Target volumetric average value) See impact limiter drawing in Section 1.3	Used in free drop analyses (Sections 2.6 and 2.7). The individual sectors' crush strengths may vary somewhat from the target value. The volumetric average, however, must lie within the range specified on the drawing.
Density (reference) of crush material, lb/ft^3 (kg/m^3) (Secondary property) • Type 1 • Type 2	20.52 – 23.01 (328.7 – 368.59) 16.77 – 19.27 (268.63 – 308.68)	Reference value is used in the "fire analysis".
Operating temperature range of crush material, ºF (ºC) (Primary property)	See Table 3.2.10	The aluminum crush material must be tested to the specified temperature limit.
Maximum axial load before failure of Fastener Strain Limiter, lbf (N) (Primary property)	7,799 (34.69)	In the event of a hypothetical drop accident the Fastener Strain Limiter must fail and limit force transmitted through the bolted joint. This design feature ensures limited plastic strain in the impact limiter attachment bolts if permissible.

Table 2.2.11: Mechanical Properties of Lead

LEAD:	-40°C (-40°F)	-29°C (-20°F)	21°C (70°F)	93°C (200°F)	149°C (300°F)	316°C (600°F)
Yield Strength, MPa (psi)	4.83 (700)	4.69 (680)	4.41 (640)	3.38 (490)	2.62 (380)	0.138 (20)
Modulus of Elasticity, MPa (ksi)	1.65E+4 (2.4E+3)	1.65E+4 (2.4E+3)	1.59E+4 (2.3E+3)	1.38E+4 (2.0E+3)	1.31E+4 (1.9E+3)	1.03E+4 (1.5E+3)
Coefficient of Thermal Expansion, cm/cm/°C (in/in/°F)	28.1E-6 (15.6E-6)	28.3E-6 (15.7E-6)	29.0E-6 (16.1E-6)	29.9E-6 (16.6E-6)	31.0E-6 (17.2E-6)	36.4E-6 (20.2E-6)
Poisson's Ratio	0.40					
Density, kg/m^3 (lb/cubic ft.)	11,340 (708)					

Note: Values in this table are taken from [2.2.6].

Table 2.2.12: Containment Boundary Bolted Joint Data

No.	Item	Value
1.	Minimum Total Axial Load Capacity - Inner Closure Lid Bolts, kN (lbf) - Outer Closure Lid Bolts, kN (lbf) - Inner Closure Lid Port Cover Bolts, kN (lbf)	 50,980 (1.146×10^7) 37,190 (8.361×10^6) 199.3 (4.48×10^4)
2.	Minimum Total Bolt Preload - Inner Closure Lid Joint, kN (lbf) - Outer Closure Lid Joint, kN (lbf) - Inner Closure Lid Port Cover Joint, kN (lbf)	See Table 7.1.1
3.	Maximum Total Load Needed to Compress Seals‡ - Inner Closure Lid Joint, kN (lbf) - Outer Closure Lid Joint, kN (lbf) - Inner Closure Lid Port Cover Joint, kN (lbf)	 6,723 (1.511×10^6) 7,581 (1.704×10^6) 95.87 (2.155×10^4)
4.	Minimum Total Load on Contact "Land" - Inner Closure Lid Joint, kN (lbf) - Outer Closure Lid Joint, kN (lbf) - Inner Closure Lid Port Cover Joint, kN (lbf)	 35,810 (8.05×10^6) 21,040 (4.73×10^6) 14.13 (3,177)
5.	Minimum "Useful" Springback to Maintain Leak Tightness, cm (in.) for the Inner/Outer Closure Lid Seals†	0.0254 (0.01)

Notes:
‡ Tables 8.A-1 and 8.A-2 list seal seating load per unit length.
† For the seal characteristics beyond the listed values, the equivalence seal criteria from Section 2.6 shall be met.

Table 2.2.13: Holtite-B Properties[Note 4]

Characteristic	Value[Notes 1,2,3]
Minimum Effective Thermal Conductivity (including contribution from conductivity enhancers)	0.4 W/m-K (0.23 Btu/ft-hr-°F)
Coefficient of Thermal Expansion at 50°C - 204°C	81-136 μm/m-K
Compressive Modulus at 23°C	5343.4 MPa (775 ksi)
Compressive Yield Strength at 23°C	75.2 MPa (10.9 ksi)
Poisson's Ratio at 23°C	0.459
Compressive Modulus at 204°C	1454.8 MPa (211 ksi)
Compressive Yield Strength at 204°C	10.4 MPa (1.51 ksi)
Poisson's Ratio at 204°C	0.489
Design Temperature	204°C (400°F)

Note 1: Composition: Nylon 66 with 2.5 wt. % (nominal) B_4C and the copper content specified in Table 8.1.11.

Note 2: Sources for Holtite-B properties are [1.2.17] and [2.2.10]

Note 3: All listed values are nominal values unless otherwise noted

Note 4: Critical characteristics for shielding function are provided in Table 8.1.11

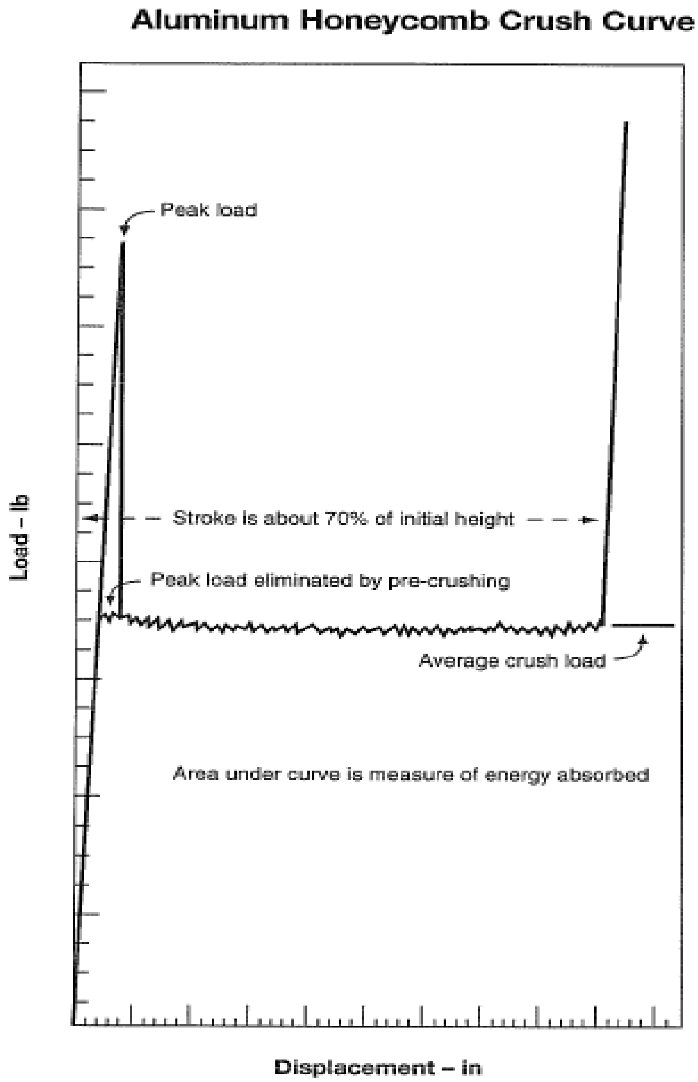

Figure 2.2.1: Load vs. Displacement Curve for Aluminum Crush Material (Typical, reproduced from [2.1.1])

2.3 FABRICATION AND EXAMINATIONS

2.3.1 Fabrication

Consideration of the manufacturing process of a cask must be an integral part of its design evolution to ensure that the as-engineered cask can be manufactured to meet the intents of the design. For HI-STAR 180D, as in all other cask models, Holtec International utilizes the following key criteria during the design stage to ensure that design objectives will be realized during manufacturing:

i. The tolerances specified for the sub-components are achievable with state-of-the-art equipment and machinery.

ii. The design is not overly reliant on tight tolerances to ensure functional compliance.

iii. Suitable (compatible) material combinations are specified whenever two dissimilar materials are to be welded.

iv. Post-weld heat treatment and other means to alleviate weld shrinkage stresses are specified, as appropriate, to enhance the quality of the hardware and to comply with the applicable ASME Code.

v. The manufacturing sequence must permit all required non-destructive examinations to be performed and remedial repairs to be made to ensure compliance with the applicable codes and standards. This requirement is particularly relevant to the Containment Boundary in which the butt-welded joints must undergo 100% volumetric examination.

vi. The manufacturing sequence must permit machining of critical surfaces, such as the gasket seating surfaces in the top flange, to be carried out after all welding and forming related operations (that inevitably produce distortion) have been completed.

vii. The manufacturing steps do not involve operations that entail unnecessary risk to worker safety.

The above objectives are fully realized in the manufacturing process envisioned for HI-STAR 180D. Of course, there are several candidate manufacturing sequences that will meet the above criteria. In the following, an overview of one such acceptable fabrication sequence for the HI-STAR 180D is presented to illustrate its fabricability while meeting the above objectives. Other sequences may be used provided they meet the above criteria for quality fabrication

[

PROPRIETARY INFORMATION WITHHELD PER 10 CFR 2.390

]

[

PROPRIETARY INFORMATION WITHHELD PER 10 CFR 2.390

]

[

PROPRIETARY INFORMATION WITHHELD PER 10 CFR 2.390

]

As shown in the basket drawings in the licensing drawing package in Section 1.3, certain peripheral junctions in the fuel basket grid work are welded to provide additional dimensional fixity to the basket. Strictly speaking, these welds are not required for the basket to render its structural function. Nevertheless, they are incorporated in the basket's design, included in the structural finite element evaluations, and specified as structural welds in the drawing package in Section 1.3 of the SAR. Extensive comparative evaluation of candidate welding processes has shown that the "Friction Stir welding" (FSW) provides at least 30% greater joint strength than classical welding methods in Metamic-HT joints. Accordingly, FSW has been specified as the mandatory welding process for basket weld joints. As can be deduced from the licensing drawing package, the weld configuration in the fuel basket welds is of Category E, Type VI per Section III Subsection NG. In the evaluation of the joint's structural strength, the weld joint is conservatively considered as a partial penetration weld with its thickness defined by the minimum depth of the friction stir zone per the licensing drawing package. Actual weld qualification testing on representative coupons prepared in accordance with the provisions of Section IX show section tensile strength of the FSW weld to be consistently in the range of the tensile strength of the base metal which provides the assurance that the weld joints internal to the fuel basket will have significant strength reserve compared to the structural demand placed on them. The bending and shear strength of the welded joints are computed using the weld tensile strength and weld depth determined from the coupon tests with the strength penalty factor applied in conformance with Table NG-3352-1.

Because of the extremely large thermal conductivity of the basket material (approximately 10 times that of austenitic stainless steel), the relatively thin wall of the Metamic-HT panels, and the slow rate of temperature changes in the containment cavity space due to the changes in the ambient conditions and the gradual decrease in the decay heat and absence of any constraints to the basket's free expansion, the cyclic stresses in the basket welds from thermal effects are assured to be minuscule. Likewise, the extent of fatigue expenditure in the basket due to vibration of the package during transport will be negligible because of the large section modulus of the basket structure (owing to its honeycomb construction) and small inertia loads associated with transportation. The structural stiffness of the basket, including its welds, is evidenced by its ability to withstand the inertia loads from the hypothetical accident condition (free drop from 9 meters) analyzed in Section 2.7. The vibration loads, which are a small fraction of the accident condition loads, can therefore be reasonably expected to produce cyclic stresses that are well below the endurance strength of the welds and panels in the basket. Therefore, it is concluded that the mechanical vibration and thermal effects are essentially ineffective as causative mechanisms for the loss of fatigue endurance capacity of the basket and the fatigue reduction factor for the corner welds in Table NG-3352-1 does not explicitly enter into the safety analysis. Thus, the conclusions reached in Subsection 2.6.5 with respect of absence of fatigue damage in the HI-STAR 180 transport package remain valid.

The basket shims used for the HI-STAR 180D are a combination of aluminum and stainless steel as shown in the drawing packages of Section 1.3. The aluminum shims are fabricated from a number of extrusions that are mated together to form the appropriate shape as shown in the drawings. The size and quantity of individual parts that form the cross section of the shim will vary depending upon the capacity of the extrusion press available for manufacture. The parts will be stacked together, mechanically joined together, or welded such that the overall shape is maintained, as shown in the drawing, and structural requirements are met. The stainless steel sections will be fabricated by welding stainless plate together to form an approximate shape and will then be finished machined to the proper profile. The shims will be installed in the cask after the basket has been positioned in the cask body and the bottom stainless steel shims will be installed first. The middle aluminum sections are then slid into place and then the top stainless steel section is installed.

The cask lid is fabricated as a separate assembly. The main center forging is first rough machined and then stainless steel weld overlay is applied to the sealing surface. The top lifting inserts and the Holtite outer ring plate are then welded to the main lid forging. The lid is then heat treated as required in accordance with the ASME code. The steel shielding plate and the Holtite are then placed into the cavity on top of the lid and the Holtite cover plate is then welded to the outer ring plate and the lifting inserts. After the lid is fully welded, the lid is finished machined to size and to incorporate the seal grooves in the overlay surface. After machining, the overlay is PT examined to verify that it is free of voids which could compromise the seal.

2.3.2 Examinations

The design, material procurement, fabrication, and inspection of the HI-STAR 180D are performed in accordance with applicable codes and standards. The following fabrication controls and required inspections shall be performed on the HI-STAR 180D in order to assure compliance with the SAR and the Certificate of Compliance.

1. Materials of construction specified for the HI-STAR 180D are identified in the drawings. Important-to-safety (ITS) materials shall be procured with certification

and supporting documentation as required by ASME Code, Section II (when applicable); the applicable subsection of ASME Code Section III (when applicable); and Holtec procurement specifications. Materials and components shall be receipt inspected for visual and dimensional acceptability, material conformance to specification requirements, and traceability markings, as applicable. Material traceability is maintained throughout fabrication for ITS items through a computerized process that has been implemented by Holtec International in the manufacture of all safety-significant components.

2. Welding of Code materials, shall be performed using welders and weld procedures that have been qualified in accordance with ASME Code Section IX and the applicable ASME Section III Subsections. Welding of welds identified as NITS welds may be performed as described above for code welds or using welders and weld procedures that have been qualified in accordance with AWS D1.1 or AWS D1.2 as applicable. The weld requirements for Metamic-HT are summarize below in item 14.

3. Welds shall be examined in accordance with ASME Code Section V with acceptance criteria per ASME Code Section III. Acceptance criteria for NDE shall be in accordance with the applicable Code for which the item was fabricated. Weld inspections shall be detailed in a weld inspection plan that identifies the weld and the examination requirements, the sequence of examination, and the acceptance criteria. The inspection plan is subject to mandatory review and approval by Holtec International in accordance with its QA program prior to its use. NDE inspections shall be performed in accordance with written and approved procedures by personnel qualified in accordance with SNT-TC-1A as specified in Holtec's QA program. The requirements stated in this paragraph are not applicable to NITS welds or Metamic-HT welds.

4. The HI-STAR 180D containment boundary shall be examined and tested by a combination of methods (including helium leak test, pressure test, UT, MT and/or PT, as applicable) to verify that it is free of cracks, pinholes, uncontrolled voids or other defects that could significantly reduce the effectiveness of the packaging. All Category A and B welds are subject to 100% volumetric examination per Subsection NB of the ASME Code.

5. Grinding and machining operations of the HI-STAR 180D containment boundary shall be controlled through written and approved procedures and quality assurance oversight to ensure that material removal operations do not reduce base metal wall thicknesses of the boundaries beyond that allowed by the design. The thicknesses of base metals shall be ultrasonically tested, as necessary, in accordance with written and approved procedures to verify base metal thickness meets design requirements.

6. Dimensional inspections of the HI-STAR 180D shall be performed in accordance

with written and approved procedures in order to verify compliance to design drawings and fit-up of individual components. All inspections of critical dimensions and functional fit-up tests shall be documented.

7. Lifting trunnions are provided for lifting and handling of the HI-STAR 180D. Although NUREG-0612 is applicable for interfacing lift points such as trunnions, they are designed, inspected, and tested following the guidance of both NUREG-0612 and ANSI N14.6, conservatively. A carefully engineered design to eliminate local stress risers in the highly-stressed regions of the trunnion during lift operations and excellent stress margins ensure that the lifting trunnions will work reliably. Further, pursuant to the defense-in-depth approach of NUREG-0612, acceptance criteria for the lifting trunnions have been established in conjunction with other considerations applicable to heavy load handling.

   In order to ensure that the lifting trunnions do not have any hidden material flaws, the lifting trunnions shall be tested at 300% of the maximum design (service) lifting load. The load shall be applied for a minimum of 10 minutes to the pair of lifting trunnions. The accessible parts of the trunnions (areas outside the HI-STAR cask), and the local HI-STAR 180D cask areas shall then be visually examined to verify no deformation, distortion, or cracking has occurred. Testing shall be performed in accordance with written and approved procedures.

8. The containment boundary shall be hydrostatically or pneumatically pressure tested, if necessary, in accordance with the requirements of the ASME Code and 10CFR71. The test shall be performed in accordance with written and approved procedures. The written and approved test procedure shall clearly define the test equipment arrangement and acceptance criteria.

   After completion of the pressure testing, the internal surfaces shall be visually examined for cracking or deformation. Any evidence of cracking or deformation shall be cause for rejection or repair and retest, as applicable. Test results shall be documented and shall become part of the final quality documentation package.

9. The majority of materials used in the HI-STAR 180D cask body are ferritic steels. ASME Code Section III and Regulatory Guides 7.11 and 7.12 require that certain materials be tested in order to assure that these materials are not subject to brittle fracture failures.

   Drop weight testing and Charpy impact testing of each plate and forging for the HI-STAR 180D containment boundary are carried out in accordance with Table 8.1.9. Weld material used in welding the containment boundary is also tested as specified in Table 8.1.9.

   Non-containment portions of the HI-STAR 180D, as required, shall be impact tested in accordance with Table 2.1.9. Test results shall be documented and shall become part of the final quality documentation record package.

10. A containment boundary leakage test of the welded structure shall be performed at any time after the containment boundary fabrication is complete. Preferably, this test should be performed at the completion of fabrication. The leakage test instrumentation shall have a minimum test sensitivity of one half of the leak test rate. Containment boundary welds shall have indicated leakage rates not exceeding leak test acceptance criteria. At the completion of fabrication, the helium leakage through all containment boundary penetrations shall be demonstrated to not exceed the leakage rate acceptance criteria. The leakage rate acceptance criteria is provided in Chapter 8.

11. All required inspections, examinations, and tests shall be documented. The inspection, examination, and test documentation shall become part of the final quality documentation package.

12. The HI-STAR 180D shall be inspected for cleanliness and proper preparation for shipping in accordance with written and approved procedures.

13. A completed quality documentation record package shall be prepared and maintained during fabrication of each HI-STAR 180D to include detailed records and evidence that the required inspections and tests have been performed for important to safety items. The quality document record package shall be reviewed to verify that the HI-STAR 180D has been fabricated and inspected in accordance with the governing Certificate-of-Compliance.

14. Metamic-HT welding and welder qualifications, requirements, and examinations will be in accordance with Paragraph 1.2.1.6, Subsection 8.1.2, and the drawing package in Section 1.3.

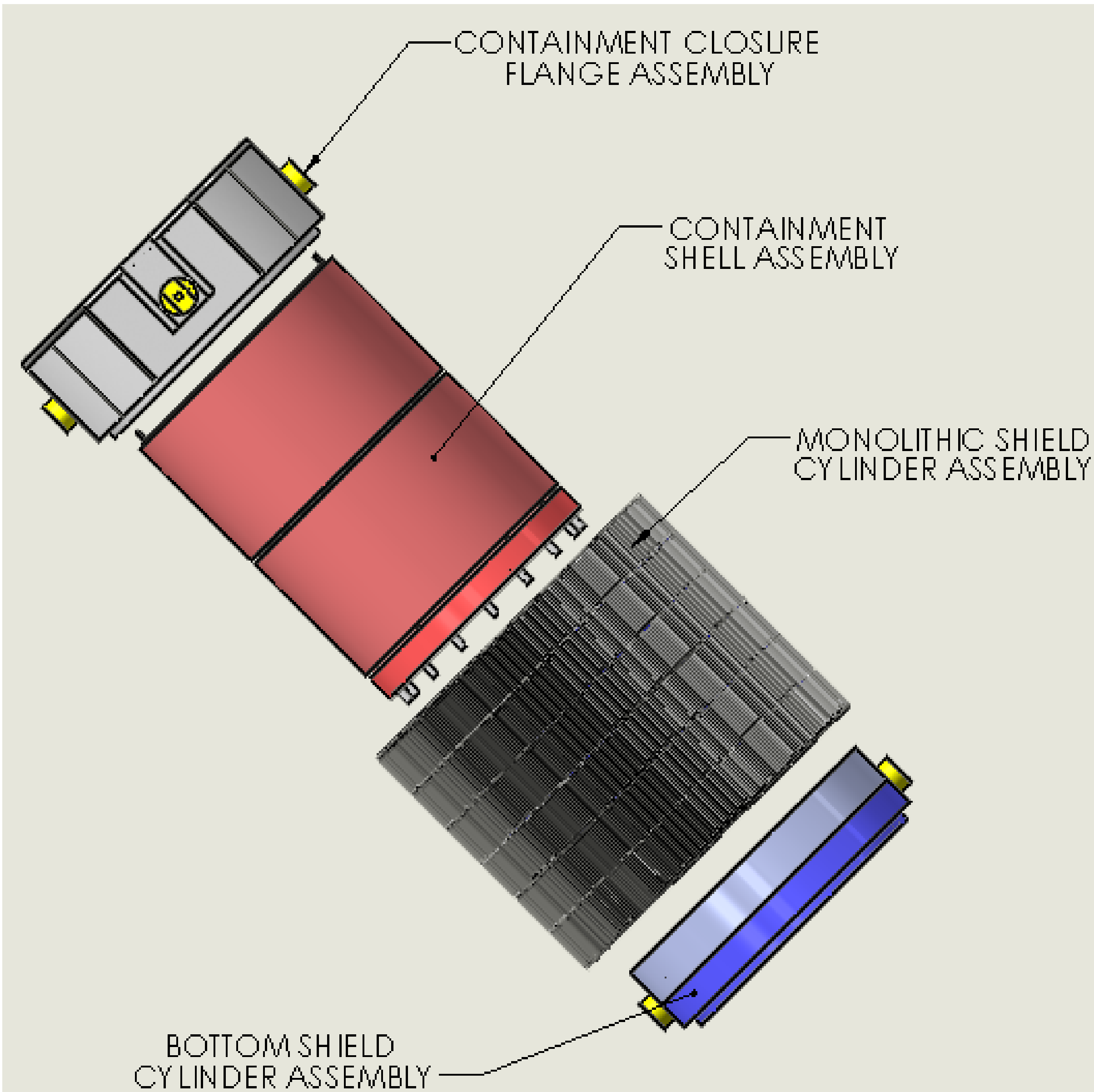

Figure 2.3.1: HI-STAR 180D in Exploded View Showing the Cask Body Assembly

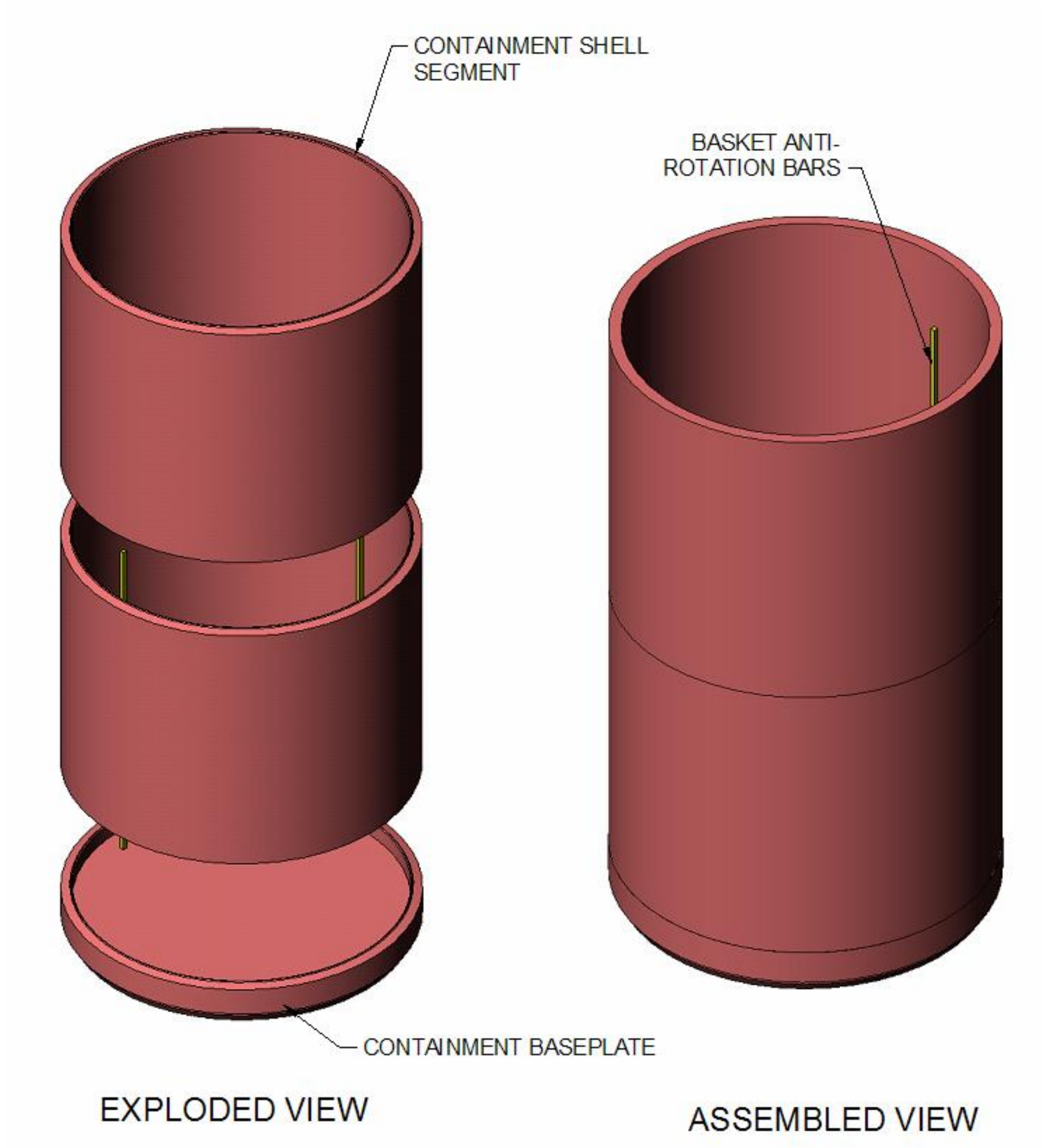

Note: The containment shell may be made from multiple pieces joined by longitudinal and circumferential welds

Figure 2.3.2: Containment Shell General Assembly

Figure 2.3.3: Monolithic Shield Cylinder Assembly

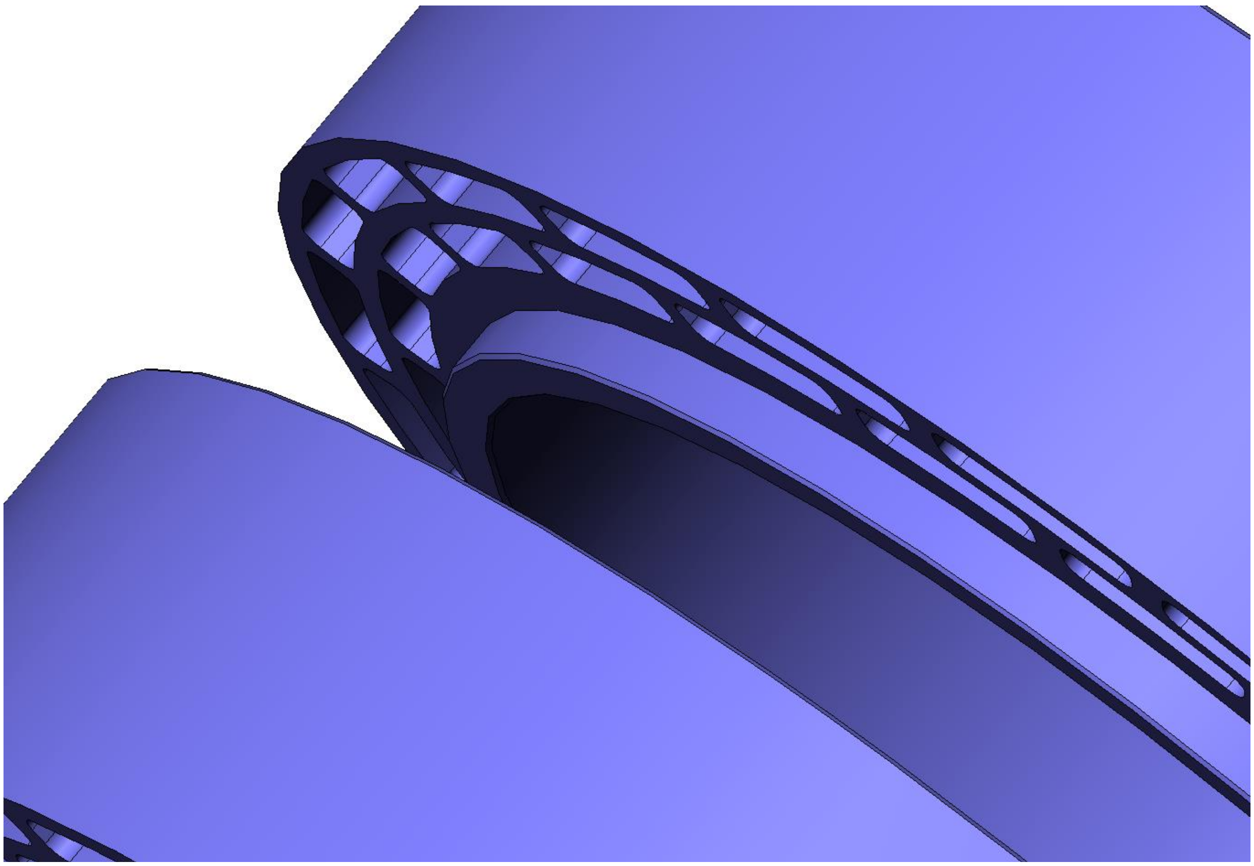

FIGURE 2.3.4: DETAILS OF THE MONOLITHIC SHIELD CYLINDERS SHOWING THE OVERLAPPING JOINT DETAIL (SURFACE FINS NOT SHOWN)

Figure 2.3.5: HI-STAR 180D Monolithic Shield Cylinder Installation

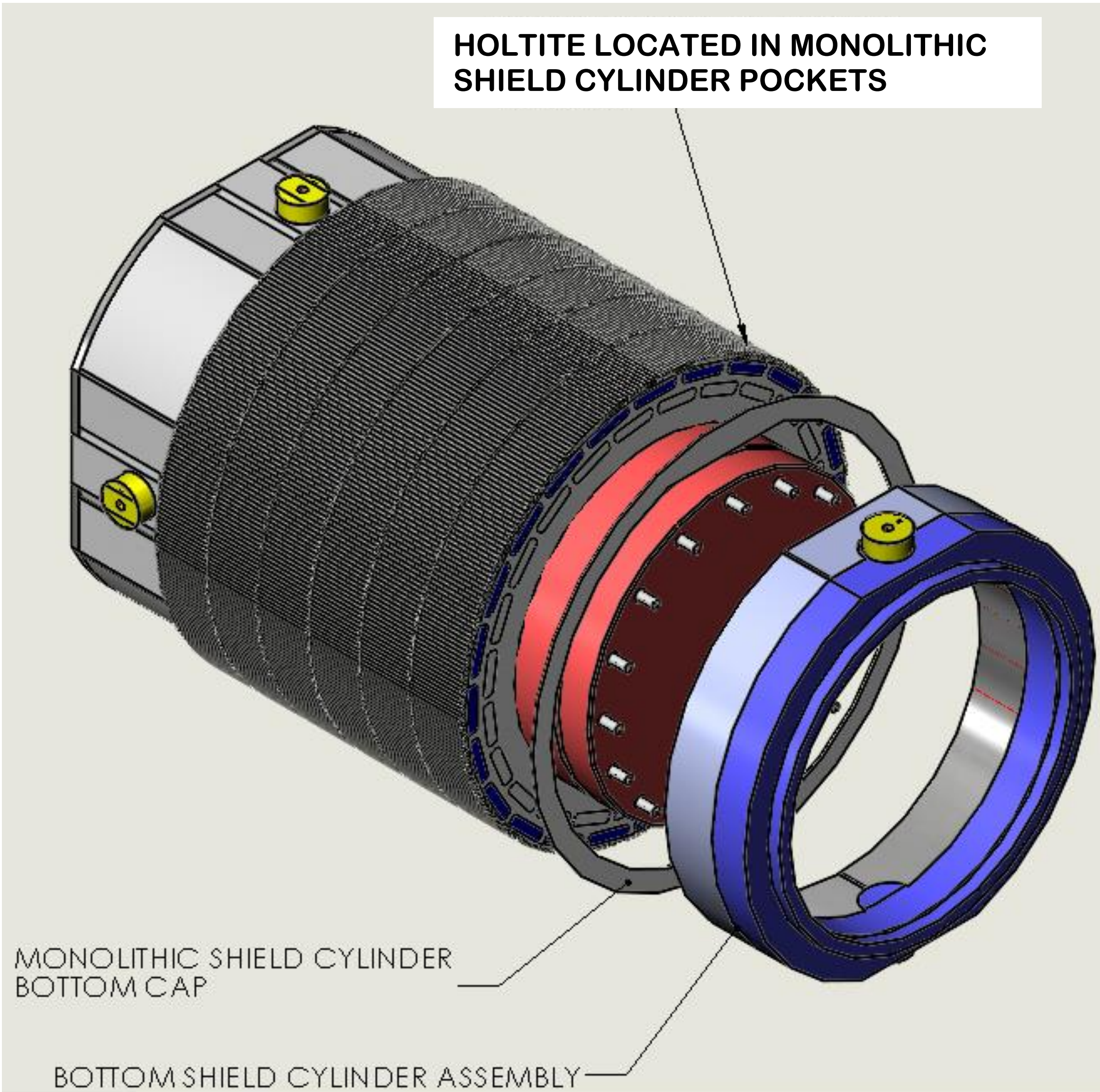

Figure 2.3.6: Bottom Shield Cylinder Installation

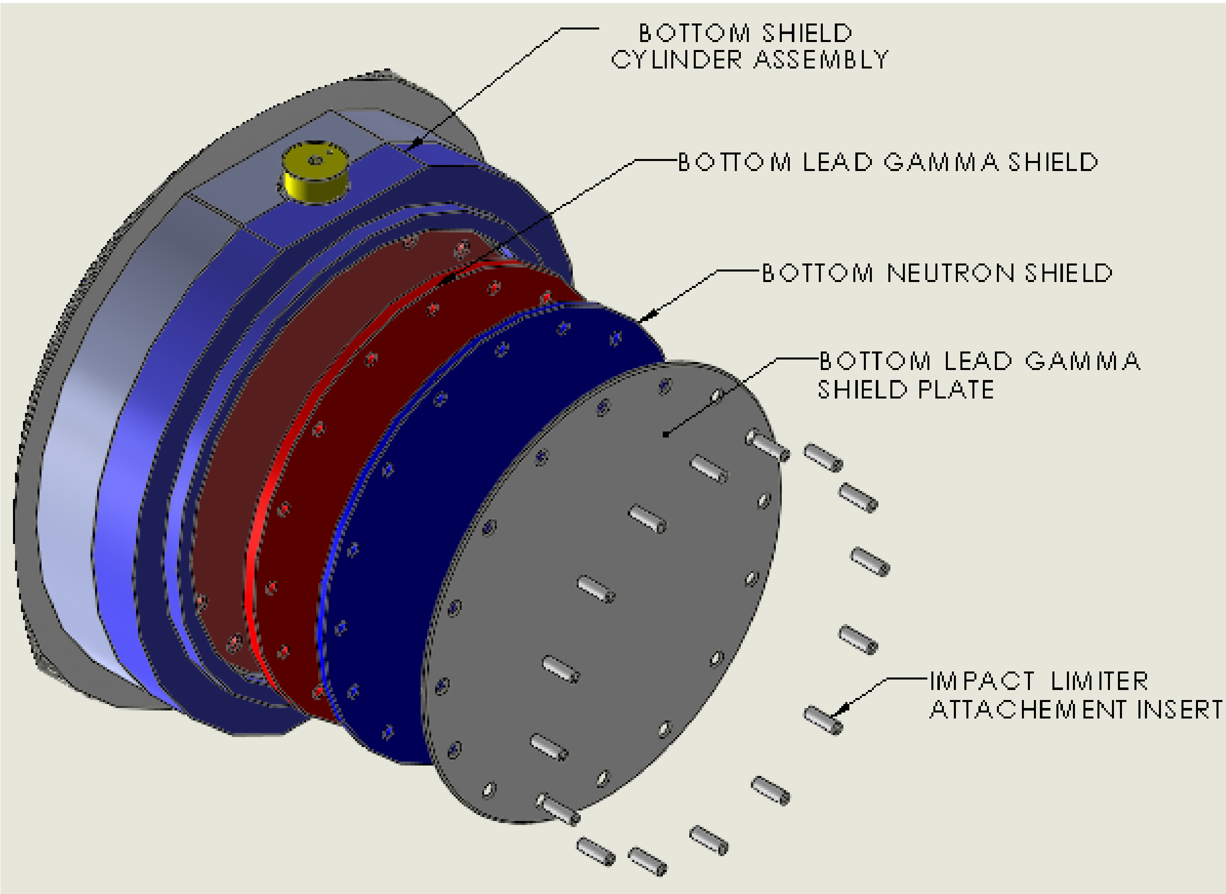

Figure 2.3.7: Cask Bottom Assembly Details

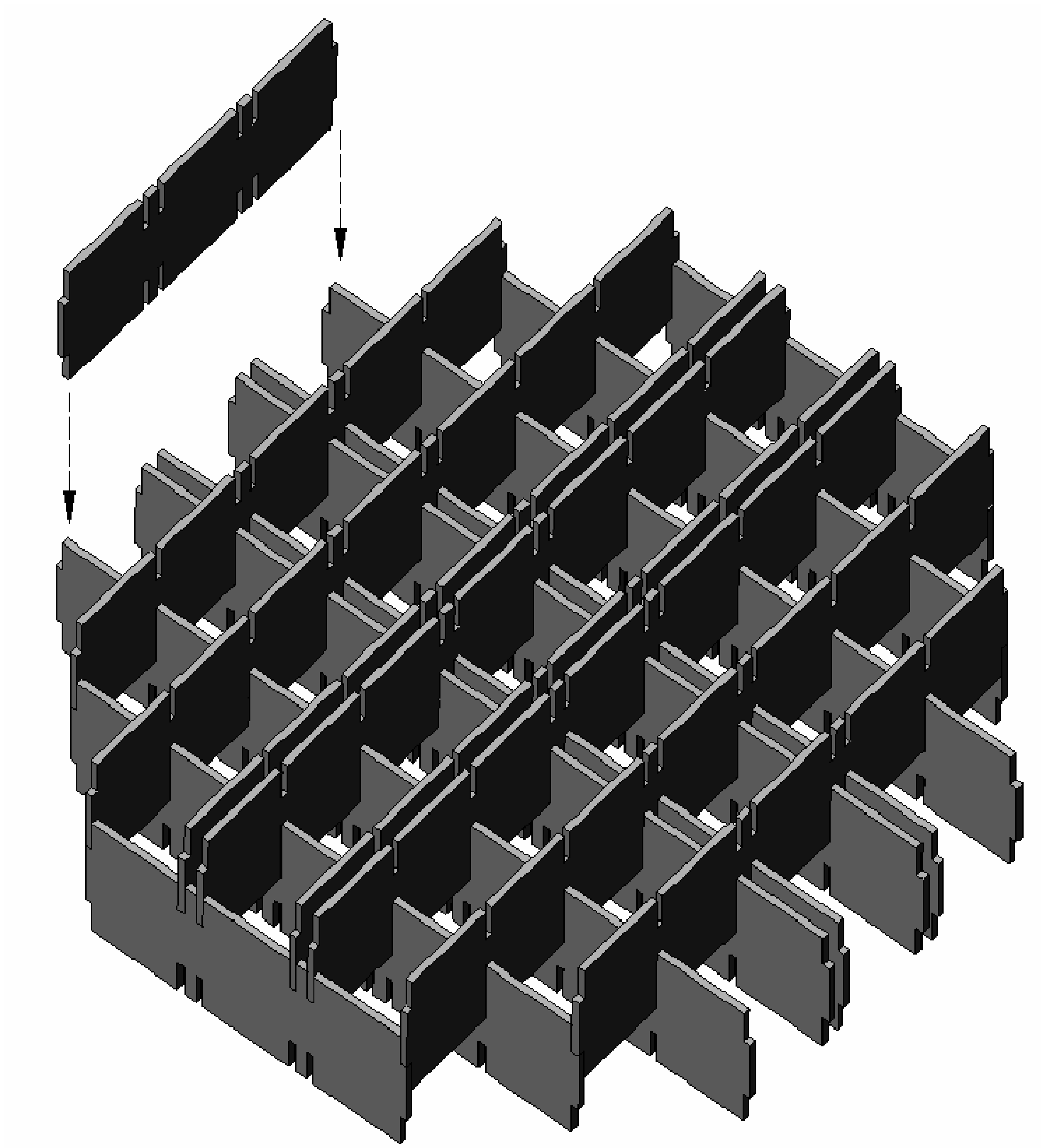

Figure 2.3.8: Slotted Plates Interlock to Form a Typical Segment of the HI-STAR 180D Basket

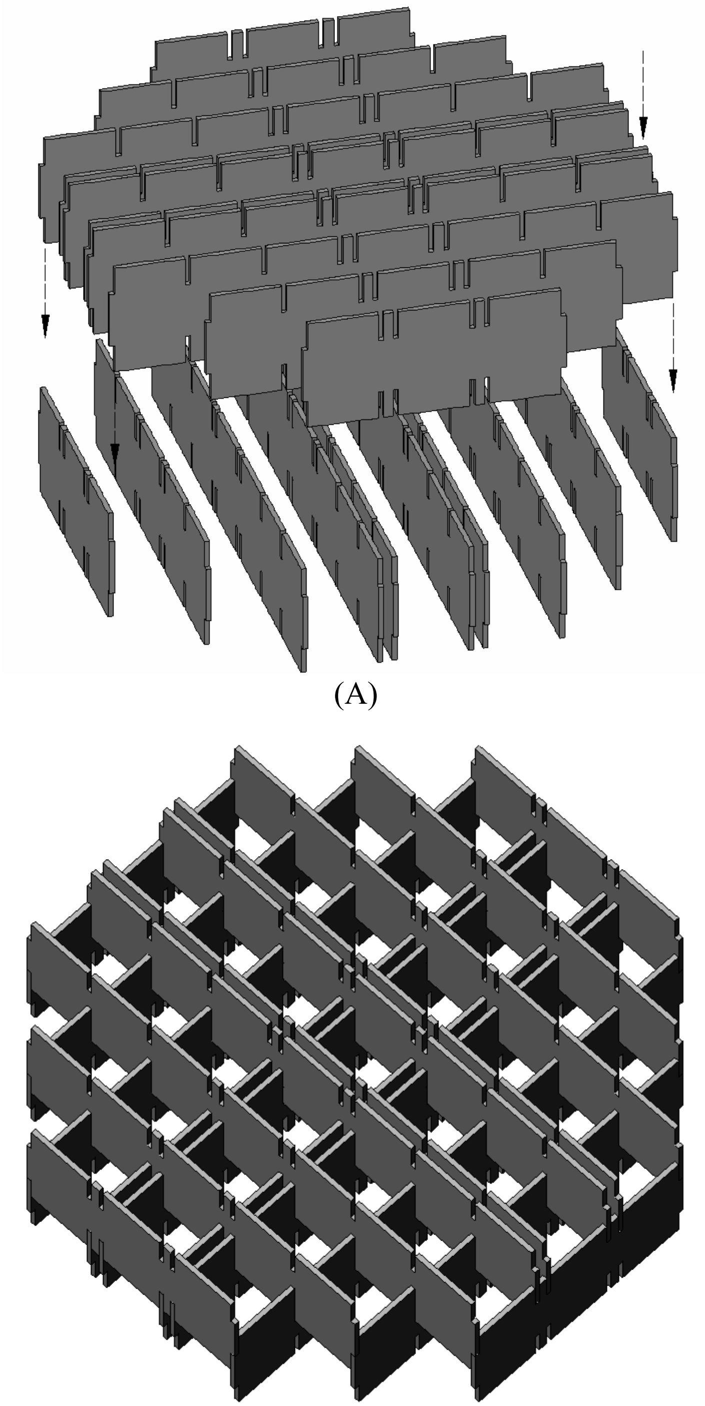

(A)

(B)

Figure 2.3.9: Slotted Plates (A) Interlock to Form a Typical Segment of the HI-STAR 180D Basket (B)

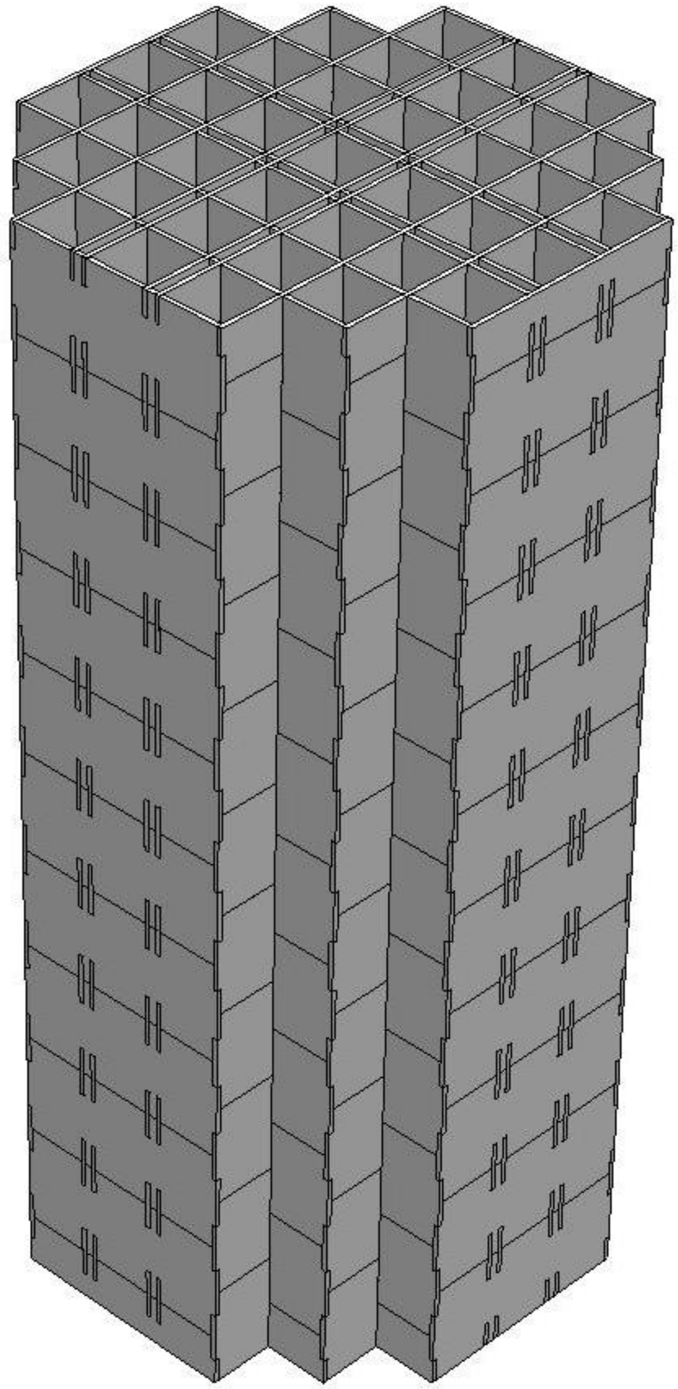

Figure 2.3.10: Isometric View of the Fully-Assembled HI-STAR 180D F-37 Basket

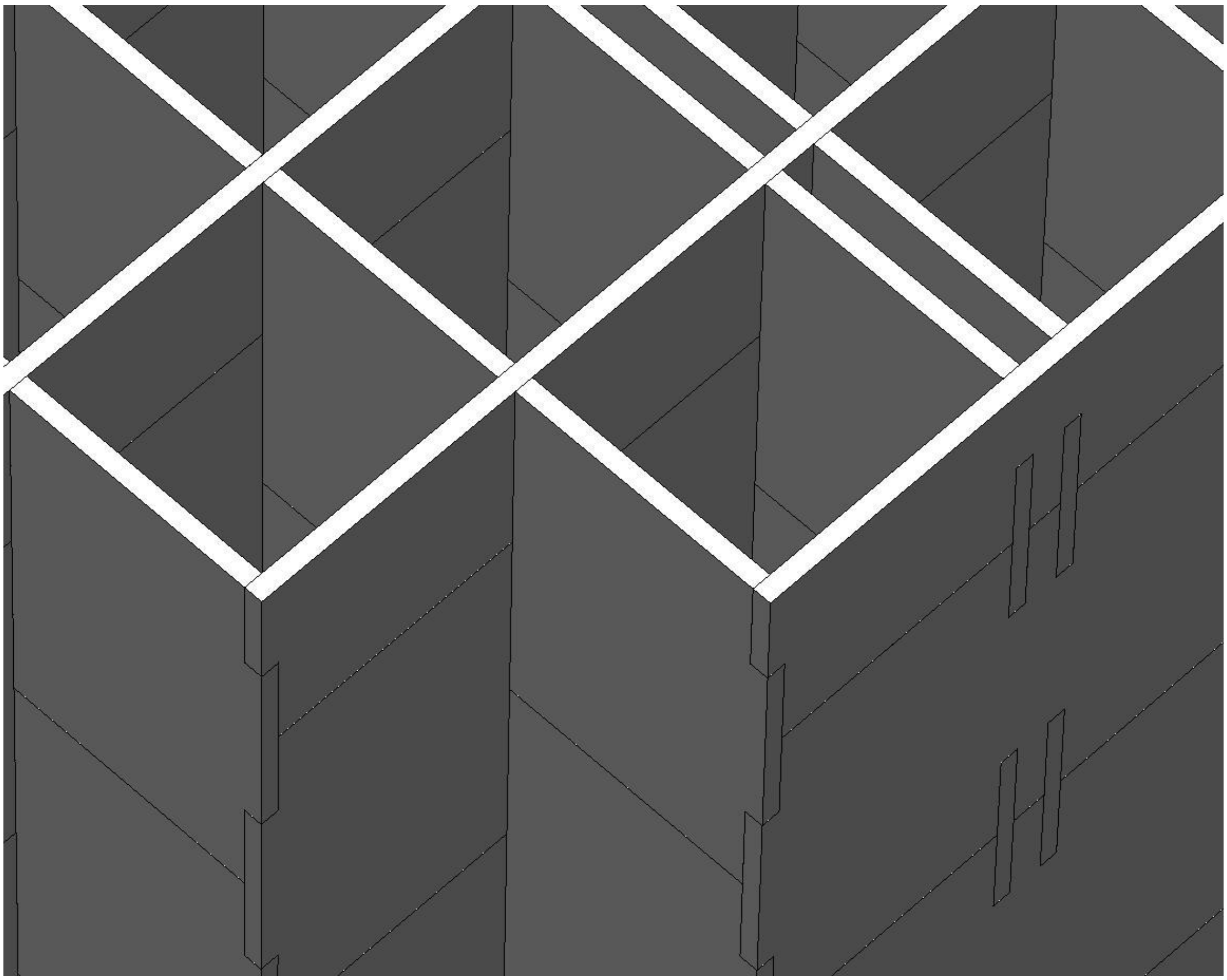

Figure 2.3.11: Close Up View of the Interlocking Plate Connections

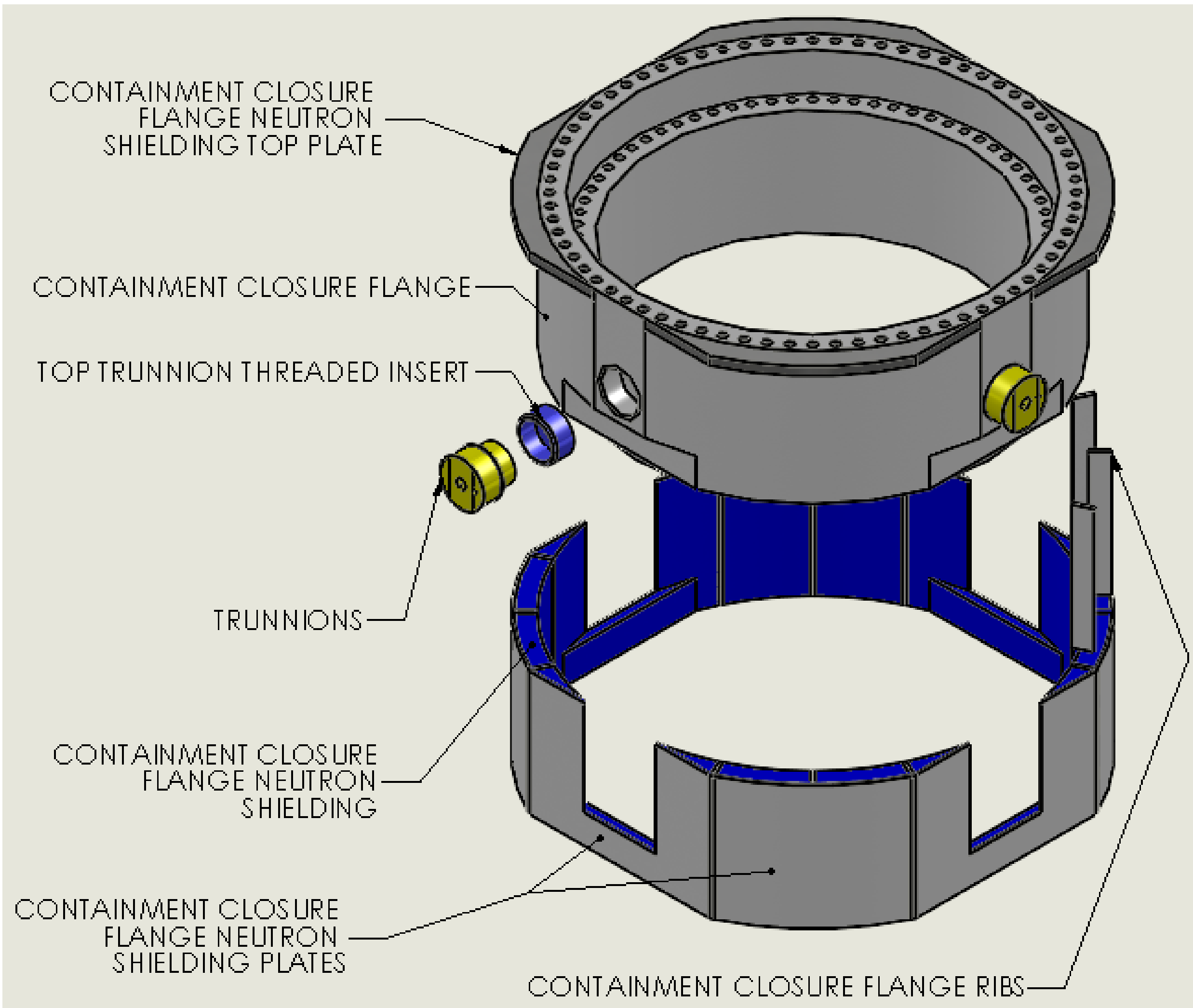

Figure 2.3.12: Containment Closure Flange Assembly

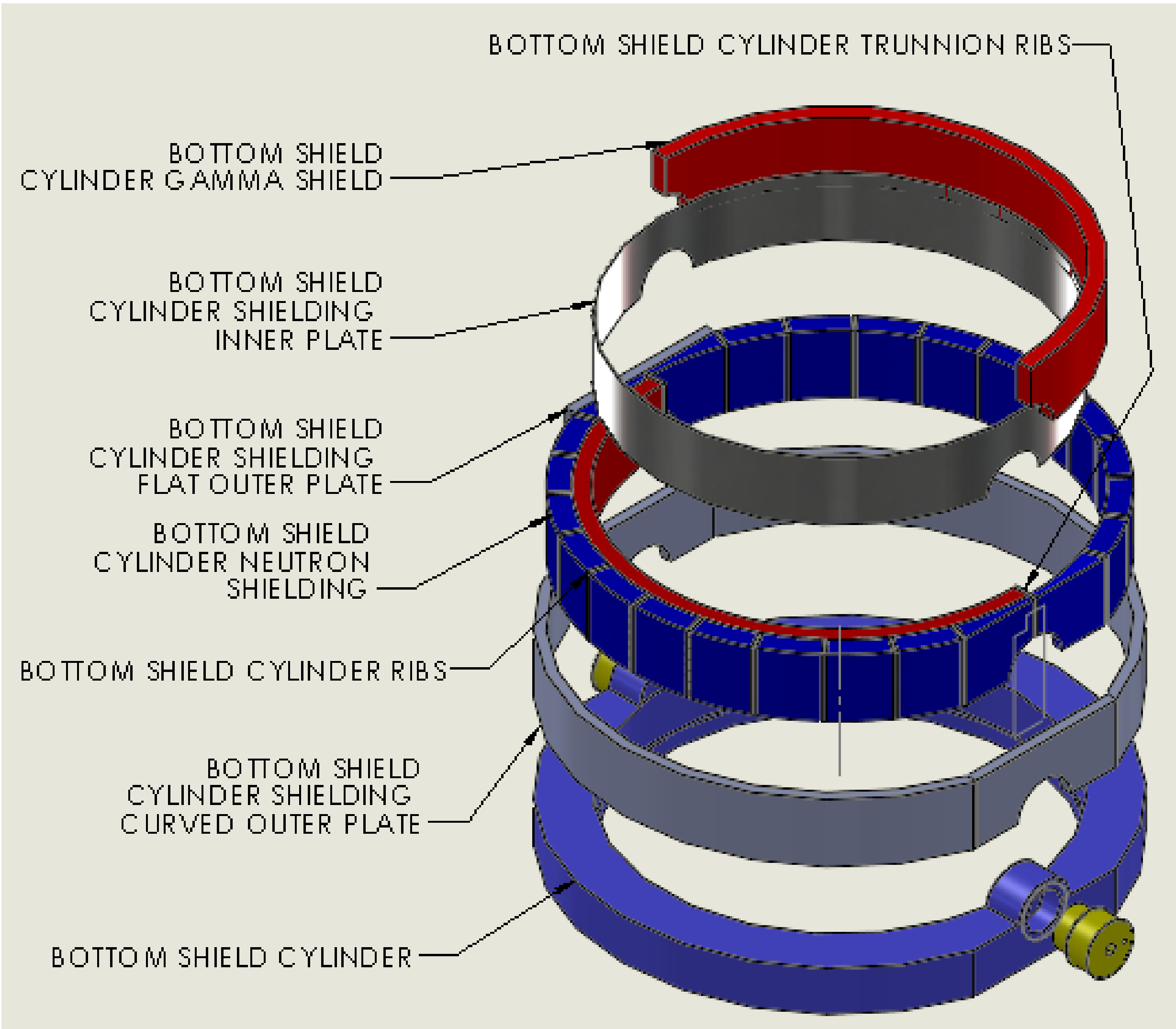

Figure 2.3.13: Bottom Forging Assembly

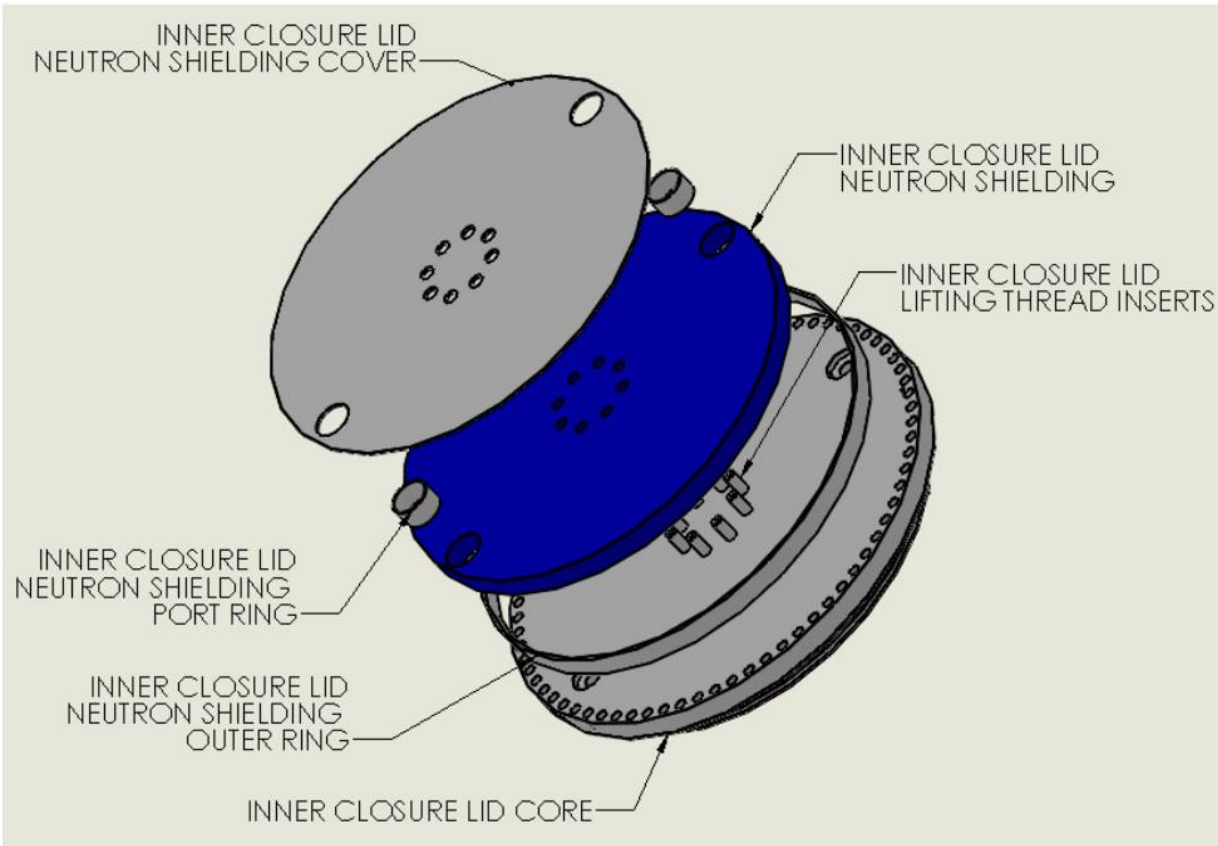

Figure 2.3.14: Inner Lid Assembly (shown only for illustrative purpose)

2.4 GENERAL REQUIREMENTS

The compliance of the HI-STAR 180D Packaging to the general standards for all packaging, specified in 10CFR71.43, is demonstrated in the following subsections.

2.4.1 Minimum Package Size

As can be seen from the external dimensions of the packaging, in Section 1.3, the HI-STAR 180D Packaging meets the requirements of 10CFR71.43(a).

2.4.2 Tamper-Indicating Feature

During transport operations, a cover is installed over the access tube above one of the impact limiter attachment bolts as shown in the drawing package for the impact limiters in Section 1.3. A wire tamper-indicating seal with a stamped identifier is attached to hold the cover in place to indicate possible tampering with the upper impact limiter. The upper impact limiter must be removed to gain access to the closure lid bolting and the radioactive contents; thus, the absence of tampering is an indication that the radioactive contents of the package have not been accessed. This tamper seal satisfies the requirements of 10CFR71.43(b).

As shown in the drawing package for the cask in Section 1.3, the cask closure lid bolts may include holes for installation of wire tamper-indicating seals (security seals). The use of the security seals on the cask closure lid bolts is specified by the user or may be mandated by the authority designated to enforce and inspect such security features.

2.4.3 Positive Closure

There are no quick-connect/disconnect valves in the containment boundary of the HI-STAR 180D Packaging. The only access to the cask internals is through the two closure lids, which are too heavy to be handled by manual means and require an especially engineered powered handling device; smaller openings (openings too small for manual access) in the cask are through the cask vent and drain ports, which are sealed and protected by bolted port covers and port caps/plugs. The closure lids are fastened to the cask flange with heavy bolts, which are torqued to create a high integrity seal. Opening of the cask vent and drain port would require removal of the bolted port cover and unthreading of the port cap/plug. Inadvertent opening of the cask is not feasible; opening a cask requires mobilization of special tools and a source of power. The cask containment boundary is analyzed for normal and accident condition internal pressure and is found to possess large margins with respect to both the sealworthiness of the bolted joints and stress intensity levels.

2.5 LIFTING AND TIE-DOWN STANDARDS

2.5.1 Lifting Devices

Per Reg. Guide 7.9, this subsection presents analyses for all lifting operations applicable to the transport of a HI-STAR 180D package to demonstrate compliance with requirements of paragraph 71.45(a) of 10CFR71.

The HI-STAR 180D Package has the following types of lifting devices: four lifting trunnions located on the cask top flange and threaded holes on each closure lid that serve as attachment locations to lift the cask closure lids. Only one pair of two top opposing trunnions are used to lift the entire loaded cask; however, if both pairs are enganged for lifting, then the second pair of trunnions may be considered as redundant lifting trunnions (see SAR Paragraph 8.1.3.1 for trunnion testing requirements). The drawing package in Section 1.3 shows the location of the Lifting Trunnions.

The evaluation of the adequacy of the lifting devices entails careful consideration of the applied loading and associated stress limits. The load combination D+H, where H is the "handling load", is the generic case for all lifting adequacy assessments. The term D denotes the dead load. Quite obviously, D must be taken as the bounding value of the dead load of the component being lifted. Table 2.1.11 provides package component weights. In all lifting analyses considered in this document, the handling load H is assumed to be equal to 0.15D. In other words, the inertia amplifier during the lifting operation is assumed to be equal to 0.15g. This value is consistent with the guidelines of the Crane Manufacturer's Association of America (CMAA), Specification No. 70, 1988 [2.5.5], Section 3.3, which stipulates a dynamic factor equal to 0.15 for slowly executed lifts. Thus, the "apparent dead load" of the component for stress analysis purposes is $D^* = 1.15D$. Unless otherwise stated, all lifting analyses in this chapter use the "apparent dead load", D^*, in the lifting analysis.

For use as part of a transportation package, the lifting trunnions that are a part of the HI-STAR 180D package are designed to meet the requirements of 10CFR71.45(a) and NUREG 1617 [2.1.11]. Accordingly, the lifting trunnions are required to maintain a safety factor of 3 based on trunnion material yield strength. The lifting attachments that are part of the HI-STAR 180D package are required to meet the design provisions of NUREG 1536 [2.5.6] and NUREG-0612 [2.1.5], which specify higher safety factor of 10 on ultimate strength to ensure safe handling of heavy loads in critical regions within nuclear power plants. Satisfying the more conservative design requirements of ANSI N14.6 ensures that the design requirements of 10CFR71.45(a) and NUREG-0612 are met. Hence, the lifting trunnions and the lifting attachments are conservatively analyzed to meet a minimum safety factor of 6 based on material yield strength and a safety factor of 10 based on material ultimate strength.

Unless explicitly stated otherwise, all stress results for lifting devices are presented in dimensionless form, as safety factors, defined as SF, where:

SF = (Allowable Stress Intensity in the Region Considered)/(Computed Maximum Stress

Intensity in the Region)

It should be emphasized that in the results for the trunnion stress levels, the safety factor, SF represents the additional margin that is over and beyond the margin built into ANSI N14.6 (e.g., a minimum safety factor of 10 on ultimate strength or 6 on yield strength).

2.5.1.1 Cask Trunnion Analysis

The lifting trunnion for the HI-STAR 180D cask is presented in the drawing package provided in Section 1.3. The four top lifting trunnions for HI-STAR 180D are circumferentially spaced at 90 degrees, however, only two top trunnions circumferentially spaced 180 degrees apart shall be engaged at any instant of time to perform the lifting operations. The trunnions are designed for a two-point lift and are sized to satisfy the aforementioned NUREG-0612 criteria. The trunnion material is identified in the drawing package shown in Section 1.3. There are also two (optional) trunnions at the base of the cask. These trunnions may be used as rotation supports when changing package orientation from vertical to horizontal (or vice- versa), or may be used to support 50% of the loaded cask when it is lifted in a horizontal orientation. In the former case, the lower trunnions may support 100% of the load but they are not acting as lifting trunnions so the requirements of a safety factor of 6 on yield strength need not be satisfied. In the latter case, the lower trunnions are acting as lifting trunnions and must show a minimum safety factor of 6 on yield strength, but the maximum lifted load is 50% of the total load.

The embedded trunnion is analyzed as a cantilever beam subjected to a line load applied at the outer edge of the trunnion (see Figure 2.5.1). This assumption is clearly very conservative because the moment arm of the load has been maximized. In reality the loading is distributed over the exposed surface of the trunnion with the resultant acting closer to the root of the cantilever than the mid-span location. A Strength of Materials methodology (classical beam theory) is used to represent the trunnion as a cantilever beam with a solid circular cross section. The bending moment and shear force at the root of the trunnion cantilever is compared against allowable values based on either yield or ultimate strength. Calculations demonstrate (Holtec Proprietary Report [2.1.12]) that the stresses in the upper and lower trunnions, computed in the manner of the foregoing, comply with requirements of paragraph 71.45(a) of 10CFR71 and also satisfy NUREG-0612 strength limits.

Key results are presented in Table 2.5.1 where it is shown that all safety factors meet the requirements for the trunnions as an ANSI N14.6-compliant handling appurtenance, conservatively.

2.5.1.2 Cask Closure Lids and Baseplate During Lifting

2.5.1.2.1 Closure Lid Lifting Holes

The closure lids contain tapped lifting holes used to move the lids over and onto the closure flange of the cask. Since the cask contains fuel during this movement, the tapped lifting holes in the closure lids are sized so that adequate thread strength and engagement length exist using allowable stresses in accordance with NUREG-0612 requirements (which are more severe than 10CFR71.45(a) requirements). The method of analysis is based on an industry standard approach to determine the capacity of a threaded connection.

Minimum safety factors are computed in the Holtec Proprietary Report [2.1.12], and are summarized in Table 2.5.2.

2.5.1.2.2 Baseplate

During lifting of a loaded HI-STAR 180D the containment baseplate is subject to amplified dead load, D* from the spent fuel, from the fuel basket, from the fuel basket supports, from the self-weight of the baseplate and any attached shielding, and from internal pressure. Note that the internal pressure loading bounds the weight of the water inside the cask, which acts during cask lifting from the loading pool, effective on the baseplate when the lifting operation is performed. To analyze this condition, the baseplate and a portion of the containment shell is modeled using the ANSYS finite element code [2.5.2] and a static analysis performed. The lid is included in the model, and the bolted connection is simulated by merged nodes (common nodes) at the lid to shell interface. The load case applies the loads from the fuel, the fuel basket, the fuel basket supports and the self-weight to the baseplate. Maximum normal operating pressure (MNOP) load is also applied normal to the inner surface of the containment boundary (viz. the baseplate, the containment shell and the primary lid) . In this load case, the 15% amplifier is applied to the lifted load. The fuel load is modeled as a uniform pressure on the baseplate, and the fuel basket and fuel basket supports are modeled as pressure loadings on an annulus adjacent to the outer edge of the baseplate. Figure 2.5.2a shows the model and applied loads. The distribution of temperature on the containment boundary is also shown in the figure.

Details of the evaluation and locations of maximum stress intensity are provided in the calculation package [2.1.12]. The calculation package contains additional plots of the stress distribution in the containment shell and baseplate. The results from the analysis of the top-end lift, subject to Level A service load conditions, are summarized in Table 2.5.3, where the minimum safety factors for components in the load path are computed using the ASME Level A allowable stress intensities from Table 2.1.2.

2.5.1.3 Failure of Lifting Devices

10CFR71.45 also requires that the lifting attachments permanently attached to the cask be designed in a manner such that a structural failure during lifting will not impair the ability of the transportation package to meet other requirements of Part 10CFR71. The ultimate load carrying capacity of the lifting trunnions is governed by the cross section of the trunnion external to the cask rather than by any section within the cask. Loss of the external shank of the lifting trunnion will not cause loss of any other structural or shielding function of the HI-STAR 180D cask; therefore, the requirement imposed by 10CFR71.45(a) is satisfied.

2.5.2 Tie-Down Devices

There are no tie-down devices that are a structural part of the package. Therefore, 10CFR71.45(b) is not applicable to the HI-STAR 180D Package.

The saddle supports under the cask, the straps, and the front and rear end structures that resist longitudinal load are not part of the HI-STAR 180D package. The loads used to design these components may be determined using the load amplifiers given by the American Association of Railroads (AAR) Field Manual, Rule 88 [2.5.4] or other appropriate standard.

2.5.3 Safety Evaluation of Lifting and Tie-Down Devices

Lifting devices have been considered in Subsection 2.5.1 and tie-down devices have been considered in Subsection 2.5.2. It is shown that requirements of 10CFR71.45(a)(lifting devices) and 10CFR71.45(b)(tie-down devices) are satisfied. All safety factors exceed 1.0.

No tie-down device is a permanent part of the cask. All tie-down devices (saddle, tie-down straps, etc.) are part of the transport conveyance and accordingly are not designed in this SAR.

Table 2.5.1: Key Safety Factors for HI-STAR 180D Trunnions

Item	Calculated Value	Safety Factor
Upper Trunnions		
Bending stress (Comparison with Yield Strength in Tension) - ksi (MPa)	4.70 (32.4)	3.49
Shear stress (Comparison with Yield Strength in Shear) - ksi (MPa)	2.18 (15.0)	4.53
Bearing Stress on Top Forging (Comparison with Yield Strength in Compression) - ksi (MPa)	33.79 (233)	1.11
Bearing Stress on Trunnion (Comparison with Yield Strength in Compression) - ksi (MPa)	33.79 (233)	3.41
Bending Moment (Comparison with Ultimate Moment) - kip-in (kN-m)	428 (48.4)	3.55
Shear Force (Comparison with Ultimate Shear Force) - kip (kN)	124 (550)	4.88

Notes:

As noted previously, safety factor in this table represents the margin above the mandated values of 6 on yield strength and 10 on ultimate strength. The requirement of a safety factor of 10 on ultimate strength is per NUREG-0612 and the requirement of a safety factor of 6 on yield strength is conservatively chosen. The actual safety factors for the trunnions are subjected to a 1/6th reduction for the material yield strength based safety factor quantification and a 1/10th reduction for the material ultimate strength based safety factor quantification. However, for the top forging, NUREG-0612 does not apply and the safety factors are not subject to any reduction factors.

The bearing (secondary) stress evaluation of forgings and trunnions is conservatively performed using a 400% load (vs. 300% load test as required by ANSI N14.6). A detailed finite element calculation in [2.1.12] demonstrates that no gross plastic deformation occurs at the trunnion-forging interface under test load for a similar design. Any bearing stresses at geometric discontinuities only lead to minor and extremely localized yielding in trunnion and forging but do not compromise their form, fit or function.

Governing transport package weight from Table 2.1.11 plus the weight of the water (while lifting from the spent fuel pool) is considered in this evaluation.

Table 2.5.2: Key Safety Factors for HI-STAR 180D Closure Lid Lifting Holes

Item	Value, kN (lbf)	Capacity, kN (lbf)	Minimum Safety Factor
Inner Closure Lid Direct Load	87 (19,550)	334 (75,110)	3.33

Notes:

Safety factor in this table represents the margin above the mandated value of 5 on ultimate strength per NUREG-0612 and the conservative value of 3 on yield strength.

Table 2.5.3: Top End Lift – Safety Factors

Item	Value- MPa (ksi) (see Figure 2.5.2b)	Allowable- MPa (ksi)	Safety Factor
Containment Shell, Primary Membrane Stress	< 23.2 (3.36)	143.8 (20.85)	> 6.19
Baseplate (Center), Membrane + Bending Stress	< 48.7 (7.06)	215.6 (31.275)	> 4.43
Baseplate (Joint with Shell), Membrane + Bending + Secondary Stress Intensity	< 275.4 (39.95)	431.3 (62.55)	> 1.57

Notes:

The loading case considers MNOP and temperature gradient on the applicable containment boundary in addition to the lifted load.

Conservatively, bounding temperature is used to obtain the allowable stress limits.

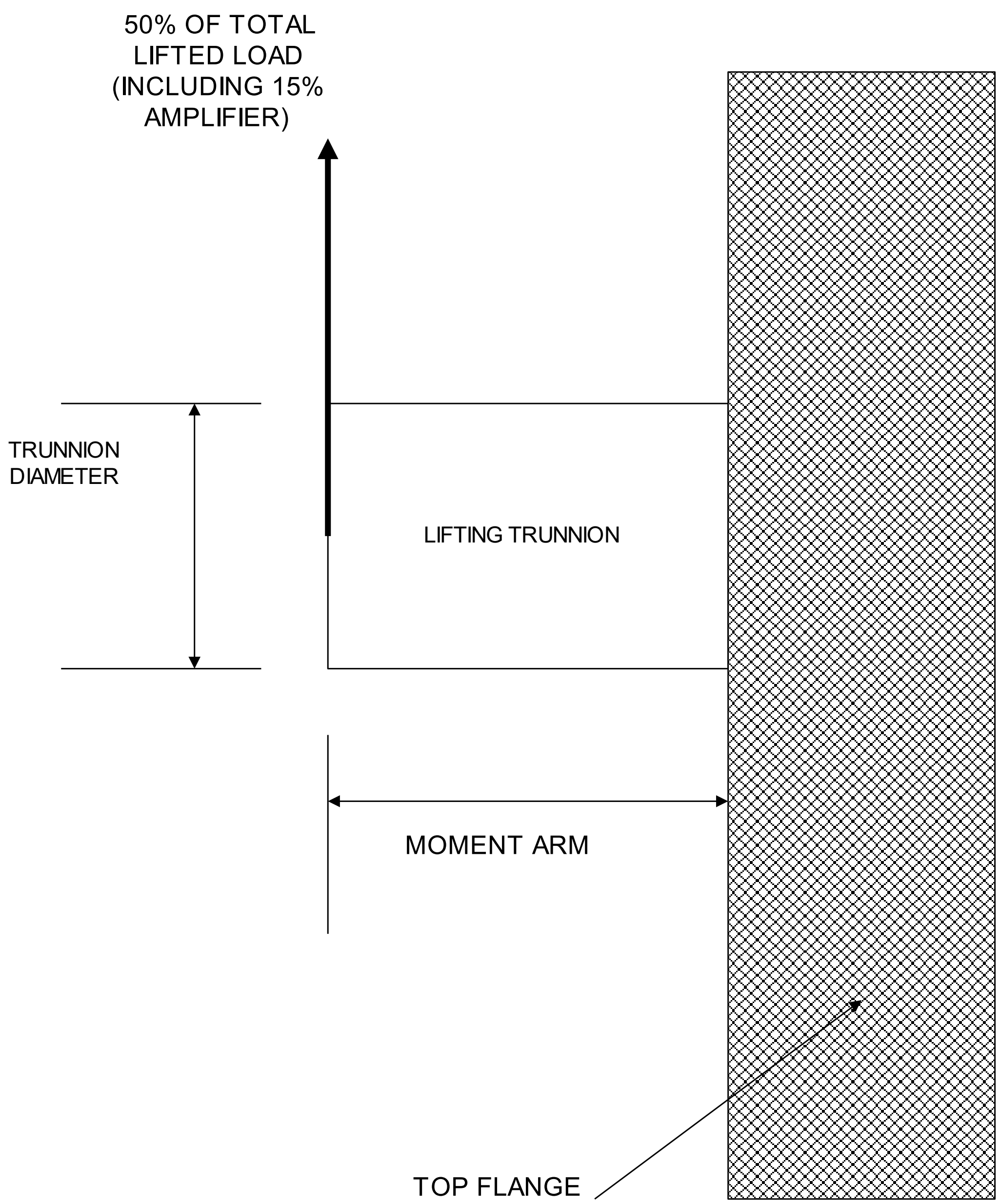

Figure 2.5.1: Top Lifting Trunnion with Applied Force

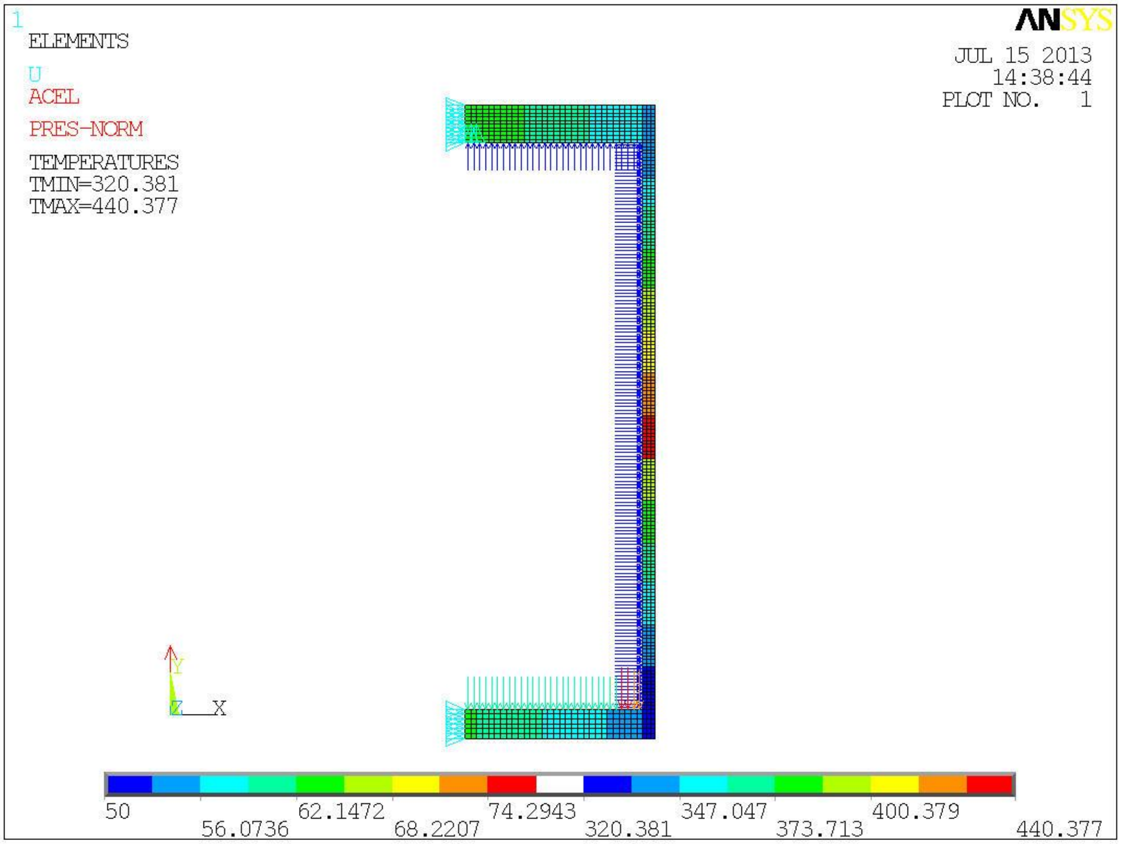

Figure 2.5.2a: Shell and Baseplate Finite Element Model for Lifting Load Case (Fuel, Self Weight, Fuel Basket, and Fuel Basket Supports)

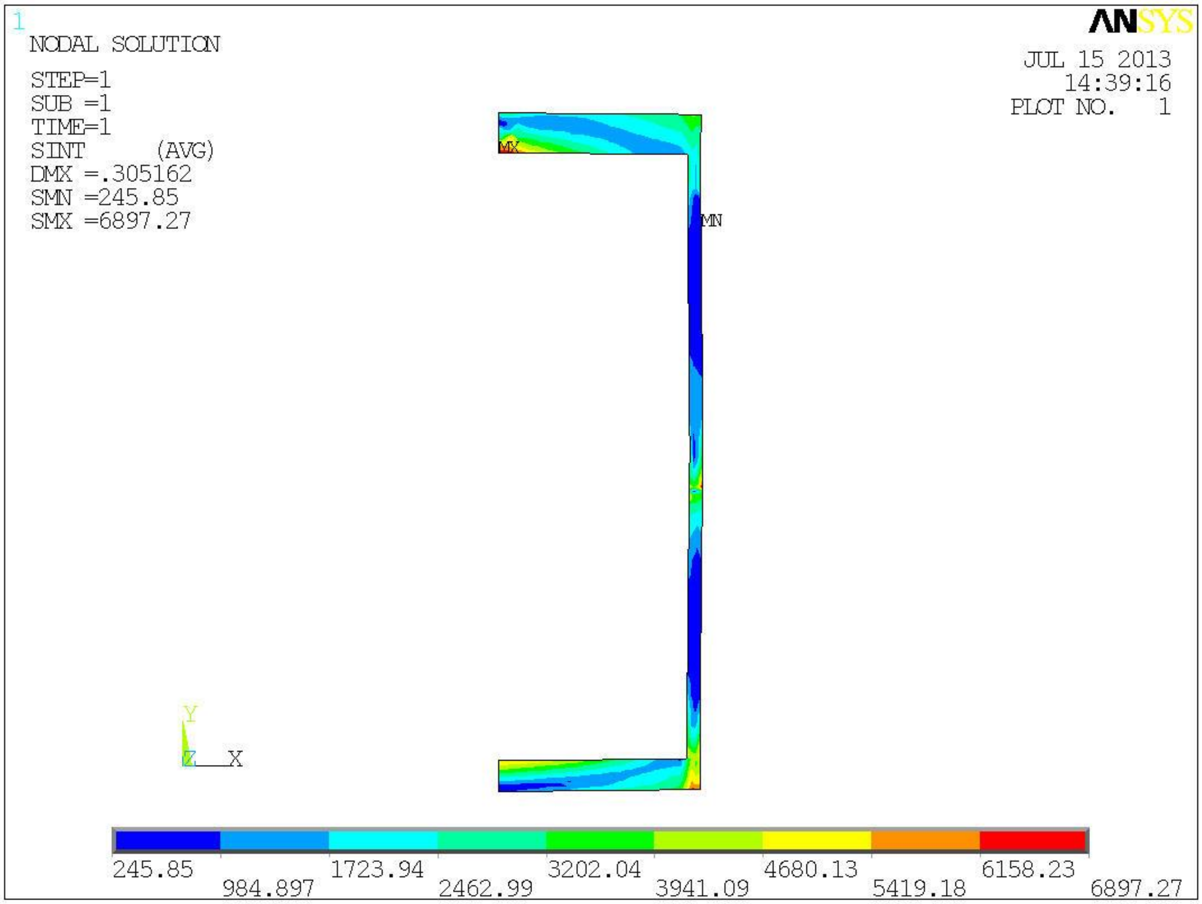

Figure 2.5.2b: Containment Boundary Under Normal Handling (with MNOP) - Stress Intensity Plot

2.6 NORMAL CONDITIONS OF TRANSPORT

In this section, the HI-STAR 180D package, consisting of the cask and the AL-STAR impact limiter, when subjected to the normal conditions of transport specified in 10CFR71.71, is shown to meet the design criteria in Section 2.1 (which are derived from the stipulations in 10CFR71.43 and 10CFR71.51). The vehicle utilized for the stress/deformation analysis is a comprehensive 3-D finite element simulation of the package on Q.A.-validated codes (see Appendix 2.A). 3-D finite element models of the cask, the fuel basket, and the two impact limiters have been prepared and assembled into a complete system to evaluate all of the Normal and Accident Conditions of Transport that involve an impact event. The stress analysis of the cask containment boundary is carried out using a 3-D finite element model or a simplified plate-and-shell theory solution, as appropriate. The stress intensity limits applicable to the containment boundary, as summarized below, are the central focus of the required qualifications.

i. The containment boundary must meet ASME Code Level A stress intensity limits under the design internal pressure and under operating internal pressure plus temperature appropriate to the normal condition of transport. For conservatism, only the containment boundary is considered, i.e., the strengthening effect of the Dose Blocker parts that girdle the containment shell is neglected.

ii. The containment boundary must also meet the same Level A stress limits when subject to a 0.3-meter (1 ft) side drop with impact limiters in place. For this dynamic analysis, the entire package is modeled and a comprehensive 3-D finite element simulation of the package drop performed using a public domain, QA validated computer code (Appendix 2.A). For this purpose, 3-D finite element models of the cask, the fuel basket, and the two AL-STAR impact limiters have been prepared.

As discussed in Appendix 2.B of HI-STAR 180 SAR [1.0.4], the AL-STAR impact limiter was subjected to a series of “9-meter drop tests” on quarter-scale models during the licensing of HI-STAR 100 in the late 90’s. The scale model was of the type A-4 in the parlance of Reference [2.7.11]. The quarter-scale drop test results were correlated with a classical contact mechanics-based simulation model to predict the HI-STAR 100 Package’s response under *any* drop orientation [2.2.2, 2.7.9]. The test data and the analytical correlation model provided the basis of NRC’s transport certification of the HI-STAR 100 package in the late 90s (Docket # 71-9261).

For the HI-STAR 180D, the simulation of the package drop event is carried out using the numerical dynamics approach implemented in LS-DYNA.

Previously, Classical Dynamics Approach (CDA) methodology was used to represent two-dimensional characterization of AL-STAR impact limiter, which was then calibrated and validated by static and scale model test data in the HI-STAR 100 docket (Docket No. 71-9261). The extensive body of material on the dynamic simulation of the HI-STAR 100 has been organized and condensed in [2.6.5]. The methodology described in this report is used to obtain the peak g-loads, α_{max}, and impact material crush, d_{max}, for the wide variety of impact scenarios considered in this safety analysis effort. These g-loads and crush data provide an independent means to assess the structural adequacy of the package.

The scale model test data from the H-STAR 100 certification effort has been used to develop an LS-DYNA-based dynamic simulation model to prognosticate the response of the AL-STAR impact limiter. As discussed in Appendix 2.B of [1.0.4], the LS-DYNA model simulates the scale model crush tests with acceptable accuracy. Because of the benchmarked LS-DYNA model, it has been possible to simulate a far greater number of drop scenarios than could be done by physical testing. Equally important, the LS-DYNA solution provides insights into the crush phenomena, such as margin to failure, which was only crudely inferable from scale model physical tests.

The benchmarking of the LS-DYNA model, by scale model testing, however, is limited to predicting the inertia loads (peak "g" value reached by the cask body) and extent of the crush sustained by the impact limiter. Strictly speaking, the LS-DYNA has not been benchmarked for its ability to simulate the transient stress or displacement field in the cask, which is influenced by the time-history (not only the peak value) of the impulse arising from the crushing of the impact limiter. To overcome this limitation in the state of LS-DYNA benchmarking, the analysis of the impactive events follows a two-step process, as follows:

i. In Step One, the LS-DYNA model is used to determine the peak value of the deceleration of the cask, α_{max} for the various candidate drop orientations.

ii. In Step Two, the HI-STAR 180D cask and the fuel basket are subjected to the static inertia load corresponding to β_{max} which is selected to be modestly larger than α_{max}. The stresses in the cask and displacements in the fuel basket under β_{max} are computed using a traditional finite element analysis procedure on ANSYS. This analysis procedure will be referred to as the "static analysis". Using the β_{max}-based static analysis solution is consistent with the approach used in the HI-STAR 100 and HI-STAR 180 dockets.

The two-step approach described above is used to analyze all of the 9-meter drop events in Section 2.7. Identical approach is used in this section to analyze the 1-foot free drop accident.

The internal and external external geometry of the HI-STAR 180D package is exactly the same as that of the HI-STAR 180 (an outer diameter sufficiently large to preclude target contact during drops, an internal backbone structure to provide an internal surface to crush against, and a skirt surrounding the cask upper and lower flanges). The configuration of the impact limiter attachment bolts for the HI-STAR 180D package is also the same as the HI-STAR 180 package. The impact limiter attachment bolts are high ductility members arranged in an orientation that is most favorable to maintaining their integrity during and after a drop. Ensuring that the impact limiter fasteners are not in the direct path of impact is an important feature in the design of this package. The number of attachment bolts is well in excess of the number needed to assure impact limiter retention under all transport modes.

The finite element models of the cask and the fuel basket are further described in Section 2.7 and have the following essential attributes:

- The finite element models of the cask and the fuel basket are implemented in ANSYS [2.5.2] and LS-DYNA [2.5.3], the former is used for static stress analysis purposes and the latter to prognosticate impact and crush response of the package. These two finite element codes are well established and are in wide use in the nuclear industry. The two codes have been validated for use at Holtec in accordance with Holtec's approved QA program. Appendix 2A describes the codes.

- The finite element discretization of the cask is sufficiently detailed to accurately articulate the primary membrane and bending stresses as well as secondary stresses at locations of gross structural discontinuity.

- Special emphasis is placed on a detailed modeling of the bolted joints; for example, the closure bolts are explicitly modeled and the gasket bearing and metal-to-metal contact interfaces are discretized in sufficient detail to capture the effect of deflections and rotations during the impact events on the seal-worthiness of the bolted joints.

- The finite element model is subjected to the *permanent loads* discussed in Section 2.1 (viz. the bolt pre-load). Interference fit self-limiting loads are conservatively neglected since they will strengthen the containment boundary during normal loading. The cask finite element model with a state of pre-stress from bolt preload is the starting point for all subsequent load analyses.

- All materials are represented by their bounding non-linear elastic-plastic true stress-strain relationships. Thus, the deformation of the fuel basket and the constituent parts of the cask under the various loadings is predicted with reliable accuracy.

- Mechanical and thermal property values of the materials used are those from robust sources (such as the ASME Code), as compiled in Chapters 2 and 3, respectively. The representative finite element models for the cask, fuel basket, and impact limiters are presented in detail in in Ref. [2.6.1].

The finite element model for the impact limiter for implementation on LS-DYNA is not only similar to the impact limiter used on the benchmarked HI-STAR 100 model [2.7.4]; it is near identical to the finite element model for the HI-STAR 180 impact limiter. The finite element model of the impact limiter has the following key features:

- The steel backbone of the impact limiter, including any buttress plate, is modeled as an elastic-plastic material.

- The energy absorbing material crush strength is a design parameter that can be varied to obtain optimal performance.

- Each of the attachment bolts that secure the impact limiters to the cask is explicitly modeled.

Section 2.7.1 contains a detailed discussion of the methodology and modeling associated with the package drop analyses. Analysis results germane to establish regulatory compliance are summarized in tabular form in this SAR. Details of the model input data and results can be perused in the Calculation Package [2.6.1].

2.6.1 Heat

This subsection, labeled "Heat", in the format of Regulatory Guide 7.9, contains information on all structural (including thermoelastic) analyses performed on the cask to demonstrate positive safety margins, except for lifting operations that are covered in Section 2.5. Accordingly, this subsection contains all necessary information on the applied loadings, differential thermal expansion considerations, stress analysis models, and results for all normal conditions of transport. Assessment of compliance under "Cold" conditions is presented in Subsection 2.6.2.

The thermal evaluation of the HI-STAR 180D package is reported in Chapter 3, wherein the material temperatures that are needed for the structural evaluations are discussed.

2.6.1.1 Summary of Pressures and Temperatures

Table 2.6.2 summarizes values for pressure and temperatures (based on the thermal analysis in Chapter 3) that are used as inputs, as necessary, for the analyses undertaken to structurally qualify the HI-STAR 180D under Normal (Hot) Conditions of Transport.

2.6.1.2 Differential Thermal Expansion

The effect of thermal expansion is closely related to the presence and consideration of gaps in the package, hence both thermal expansion and gaps are discussed together in this subsection.

The appropriate thermal solutions for the HI-STAR 180D fuel baskets, the fuel basket supports, and the cask are discussed in Chapter 3, for the Normal Conditions of Transport under hot conditions. Conservative estimates of free thermal expansion of the components in the HI-STAR 180D package are obtained using the computed temperatures, together with conservatively chosen coefficients of thermal expansion, and the calculations and results are documented in the thermal calculation package referenced in Section 3.4. Table 3.4.2 documents the radial and axial expansions prior to and after heat-up.

To provide for sufficient clearance during insertion of basket and assemblies, and to account for thermal expansion, carefully calibrated gaps are incorporated in the design between the various components of the package, i.e., the cask body, basket and assemblies. These gaps are small compared to other characteristic dimensions such as the cask diameter, or the crush depth of the impact limiters. Hence they are not expected to have a significant effect on the overall dynamic behavior of the package during transient events (drop conditions). However, during such events, those gaps can result in internal impacts, resulting in additional loads on the individual components involved. In the HI-STAR 180D, there are four locations of such engineered gaps. These are:

i. Axial gap between the fuel assembly and the containment cavity, either at the top (towards the inner closure lid) or the bottom (towards the containment baseplate).
ii. Axial gap between the fuel basket and the containment cavity, again either at the top or the bottom.
iii. Lateral gap between the fuel assembly and the storage cells.
iv. Small lateral gap between the fuel basket and the basket shims, and the shims and the containment cavity.

As heuristic reasoning would suggest, increased internal gaps would produce increased impact loads during impact events due to the rebound of the unfixed masses (fuel assemblies and/or basket) from their support surfaces during the package's free fall. For example, an elastic surface such as the baseplate or lid of the cask supports the weight of the fuel by flexural action when the cask is in a vertical orientation prior to the initiation of the drop event. As soon as the free fall begins, the "flexural spring" would begin to relieve its strain energy, resulting in the presence of a possible gap between the fuel assembly and the baseplate or lid surface at the moment of impact. The extent of separation depends on the flexibility of the support surface and weight of the supported mass. Scoping calculations show that the extent of separation between the fuel assembly and the cask and basket surfaces are rather minute at the instant of impact in any impact event. However, for conservatism, the initial gap is assumed to be at its *maximum geometrically feasible* value in any drop orientation. This is an evidently counterfactual assumption made to maximize the computed severity of the impact events.

Amongst the various drop orientations, the axial drops warrant additional attention, specifically the top end drop. Under this condition, the cask inner closure lid is impacted by the fuel and fuel basket, which challenges the sealing capacity of the containment system. Additionally, under both top end and bottom end drops, buckling of the fuel rods could lead to reconfiguration of the assembly geometry.

Fuel Assembly

The axial gap generated by the difference in length between the fuel assembly and cask cavity is minimized by controlling the cask cavity length during fabrication. The cask cavity is sized as indicated in Section 1.2 of this SAR such that the fuel assembly top nozzle hold-down springs may be in nominal contact with the bottom surface of the inner closure lid during transport. Fuel assembly hold-down spring travel is sufficiently large to accommodate differential thermal expansion (reported in Chapter 3 of this SAR) that can occur under normal and accident conditions of transport.

Nonetheless, informed by a survey of the population of fuel common to the host reactor plant, the structural analysis uses a conservative gap for the drop evaluations, as presented in Table 2.7.1. The gap results in a velocity differential for the fuel assembly relative to the cask, in the event of end drop accidents. This condition is evaluated in Sections 2.7 and 2.11, respectively, to determine the peak rigid body cask deceleration and the maximum strain in the fuel pins due to a 9-meter bottom end drop.

Additionally, any reaction force from the fuel assembly hold-down springs on the lid corresponding to the maximum differential thermal expansion is trivial (<0.5%) when compared to the total preload at the primary lid to top flange bolted joint. Therefore the safety factors remain unaffected by the lid to fuel assembly interface force.

Fuel Basket

The axial gap between the fuel basket and the cask cavity is dimensioned so that there is no restraint of free thermal expansion under hot conditions. The drop analyses in Section 2.7 assume the maximum gap at the beginning of the impact (per Table 2.7.1), and no impact attenuating devices are required.

Lateral Gaps

The lateral gaps between the fuel and the fuel basket, and between the fuel basket and the cask cavity are sufficient to preclude any restraint from thermal expansion under hot conditions. The drop analyses in Section 2.7 assume the maximum nominal gaps (per Table 2.7.1) in these areas, determined under cold conditions, at the beginning of the impact.

In summary, under Normal Hot Conditions of Transport, the HI-STAR 180D package internals are not subject to restraint of free thermal expansion. Therefore, subsequent buckling or significant fuel basket deformation due to differential thermal expansions that can afflict a transport package with heat producing contents is not credible for the HI-STAR 180D package. The drop analyses presented in Section 2.7 assume conservatively the maximum gaps present under normal conditions of transport.

2.6.1.3 Stress Calculations

In this subsection, the structural analysis of the package under the conditions of design pressure, normal operating pressure and temperature, together with the effects of bolt preload, is described. Also considered is the calculation of expenditure of fatigue life (usage factor) of the Containment Boundary parts under the above loads.

2.6.1.3.1 Structural Evaluation of the Package Subject to Pressure, Temperature, Bolt Preload – Normal Operating Condition and 1-foot Free Drop

The Package is analyzed for the Load Combinations N1 and N2 listed in Section 2.1 using the finite element codes ANSYS [2.5.2] and LS-DYNA [2.5.3], and the models described in Section 2.7 and in the Holtec Proprietary calculation packages [2.1.12] and [2.6.1]. For the simulation of the normal operating condition (Load Combination N1 consisting of design pressure and temperature), the package orientation is not significant. For the 1-foot free drop condition (Load Combination N2), the package is oriented at a 0-degree angle with respect to the horizontal rigid target, and the package has an initial downward vertical velocity given by

$V = \sqrt{2gH}$ H = 12 inches (0.3 meters)

so that V = 96.3 inch/sec (244.6 cm/sec)

The drop of the package is simulated on LS-DYNA with full representation of elastic-plastic response as discussed in Subsection 2.7.1. The details of the material models and contact surface definitions are documented in the Holtec Proprietary calculation package for the finite element analyses [2.6.1]. This same finite element model is used for both the Normal Condition of Transport (Load Combination N2) and the Hypothetical Conditions of Transport drop as well as puncture analyses reported in Section 2.7.

Results from the analysis of the one-foot drop case (Load Combination N2) are documented in the Holtec Proprietary finite element analysis calculation package [2.6.1]. A discussion of the analysis of the 1 foot drop event and key safety factors are reported in Subsection 2.6.1.4 below.

2.6.1.3.2 Fatigue Considerations

Regulatory Guide 7.9 [2.6.3] suggests consideration of fatigue due to cyclic loading under normal conditions of transport. Considerations of fatigue of individual components of the package, associated with long-term exposure to vibratory motion during normal conditions of transport, are presented below:

- Cask Fatigue Considerations

As shown in the following, the cask in the HI-STAR 180D Package does not require a detailed fatigue analysis because all applicable cyclic loadings are well within the range that permits exemption from fatigue analysis per the provisions of Section III of the ASME Code. Paragraph NB-3222.4 (d) of Section III of the ASME Code provides five criteria that are strictly material and design condition dependent to determine whether a component can be exempted from a detailed fatigue analysis. The sixth criterion is applicable only when dissimilar materials are involved, which is not the case in the HI-STAR 180D cask (the steel monolithic shield and the steel containment shell have essentially the same thermal expansion properties and the same Young's Modulus).

The Design Fatigue curves for the cask materials are given in Appendix I of Section III of the ASME Code. Each of the five criteria is considered in the following:

i. Atmospheric to Service Pressure Cycle

The number of permissible cycles, n, is bounded by $f(3S_m)$, where f(x) means the number of cycles from the appropriate fatigue curve at stress amplitude of "x" psi. In other words

$$n < f(3S_m)$$

From Tables 2.1.4 and 2.1.6 for normal conditions at a bounding temperature of 450°F, and from the fatigue curve in ASME Code Appendix I, the number of permissible cycles for the containment boundary is

n (cask) ≤ 1,600 ($3S_m$ = 62,500 psi) (Figure I-9.1 of ASME Appendix I)

Since 1,000 pressurizations in the 50-year life of the cask is an upper bound estimate, it is concluded that projected pressurizations of the HI-STAR 180D components do not warrant a usage factor evaluation.

ii. Normal Service Pressure Fluctuation

Fluctuations in the service pressure during normal operation of a component are considered if the total pressure excursion δ_p exceeds Δ_p.

where

Δ_p = Design pressure * S/($3S_m$)

S = Value of S_a for one million cycles.

Using the above mentioned tables and appropriate fatigue curves,

$$(\Delta_p)_{overpack} = \frac{(80)\,(12{,}500)}{(3)\,(20{,}850)} = 15.99\ psi\ \text{(0.11 MPa)}$$

During normal operation the pressure field in the cask is steady state. Therefore, pressure fluctuations during normal operation are negligibly small and nowhere approach the limit computed. Therefore, normal service pressure oscillations do not warrant a fatigue usage factor evaluation.

iii. Temperature Difference - Startup and Shutdown

Fatigue analysis is not required if the temperature difference ΔT between any two adjacent points on the component during normal service does not exceed $S_a/2E\alpha$, where S_a is the cyclic stress amplitude for the specified number of startup and shutdown cycles. E and α are the Young's Modulus and instantaneous coefficients of thermal expansion (at the service temperature). Assuming 1,000 startup and shutdown cycles, Table 2.2.1 (conservatively assuming a service temperature of 450°F) and the appropriate ASME fatigue curve in Appendix I of Section III of the ASME Code give:

$$(\Delta T)_{\text{overpack}} = \frac{83{,}000}{(2)\,(25.95)\,(7.2)} = 222.1°\,\text{F (123.4°C)}$$

There are no locations on the cask where ΔT between any two adjacent points approaches this value. Therefore, it is evident that this temperature criterion is satisfied for 1,000 startup and shutdown cycles.

iv. Temperature Difference - Normal Service

Significant temperature fluctuations that require consideration in this criterion are those in which the range of temperature difference between any two adjacent points under normal service conditions is larger than S/2Eα where S corresponds to 10^6 cycles. Substituting gives:

$$(\Delta T)_{overpack} = \frac{12{,}500}{(2)\,(25.95)\,(7.2)} = 33.45°F \;\; (18.6°C)$$

During normal operation, the temperature field in the cask is steady state. Therefore, normal temperature fluctuations are negligibly small. Therefore, normal temperature fluctuations do not warrant a fatigue usage factor evaluation.

v. Mechanical Loads

Mechanical loadings of appreciable cycling occur in the HI-STAR 180D Package only during transportation. The stress cycling under transportation conditions is considered significant if the stress intensity amplitude is greater than S_a corresponding to 10^6 cycles. It, therefore, follows that the stress intensity range that exempts the cask is 25,000 psi (172.4MPa).

Inertia loads typically associated with rail transport will produce stress intensity ranges in the cask that are a small fraction of the above limits. Therefore, the potential for large fatigue expenditure in the cask materials, under transportation conditions, is not credible.

In conclusion, the cask does not require fatigue evaluation under the exemption criteria of the ASME Code.

- Fatigue Analysis of Closure Bolts

The maximum tensile stress range, developed in the cask closure bolts during normal operating conditions, occurs during the preload operation. The maximum bolt stress is permitted to have the value $2S_m$ (Table 2.1.3). For the closure lids bolt material (SA-564 630/705 (H1025)), the value of S_m at 350°F (177°C) is 47.65 ksi (328.6 MPa) per Table 2.1.8, and the Young's modulus is 26,950 ksi (185,800 MPa). Therefore, incorporating a fatigue strength reduction factor of 4, the effective stress intensity amplitude using Figure I-9.4 (ASME Code, Section III Appendices [2.1.10]) is (ratioing the modulus used in the figure to the modulus used here):

$$S_a = \frac{(47.65)\,(4)\,(30\,e+06)}{26.95\,e+06}$$
$$= 212.2\text{ ksi} = 1463\,MPa$$

Using Figure I-9.4 of [2.1.10], the permissible number of cycles is 225; this sets a limit on the number of permitted loadings for a set of closure lid bolts.

A similar fatigue evaluation for an alternative closure lid bolting material SB-637 N07718 is performed and the correponding permissible number of cycles is determined as follows:

$$S_a = \frac{(46.5)\,(4)\,(29.8\,e+06)}{27.7\,e+06}$$
$$= 200.1\text{ ksi} = 1380\,MPa$$

Using Figure I-9.7 of [2.1.10], the permissible number of cycles is 277; this sets a limit on the number of permitted loadings if SB-637 N07718 material is used for the closure lid bolts.

- Fatigue Analysis of Inner Closure Lid Port Cover Bolts

The maximum tensile stress range, developed in the cask closure lid port cover bolts during normal operating conditions, occurs during the preload operation. The maximum bolt stress is permitted to have the value $2S_m$ (Table 2.1.3). At a temperature of 350°F (177°C), Table 2.1.8 shows that the closure lid port cover lid bolt material (SA-193 B7) may be pre-stressed to a value not to exceed 61.9 ksi (426.8MPa). The alternating stress intensity in the bolt is equal to 1/2 of the maximum stress intensity, or 30.95 ksi (213.4MPa). Per Table 2.2.2, the Young's modulus is 28,250 ksi (194,800 MPa). Therefore, incorporating a fatigue strength reduction factor of 4, the effective stress intensity amplitude using Figure I-9.4 (ASME Code, Section III Appendices) is (ratioing the modulus used in the figure to the modulus used here):

$$S_a = \frac{(30.95)\,(4)\,(30\,e+06)}{28.25\,e+06}$$
$$= 131.47\text{ ksi} = 906.5\,MPa$$

Using Figure I-9.4 of [2.1.10], the permissible number of cycles is 558; this sets a limit on the number of permitted loadings for the inner closure lid port cover bolts.

- Fatigue Considerations for the Containment Closure Flange Internal Closure Bolt Threads

Fatigue of the threads in the containment closure flange is also evaluated. Based on the nominal diameter and the thread engagement length, the total shear area of the cask closure bolt threads can be computed. The maximum shear stress on the threaded area of the flange is calculated as 91.7

ksi using the maximum Level A allowable bolt stress. The resulting shear tress is:

$$\tau = 18 \text{ ksi} \quad (124.1 \text{ MPa})$$

The primary membrane stress intensity in the closure flange threads is equal to twice the maximum shear stress, and the alternating stress intensity in the threads, S_a, is equal to 1/2 of the total stress. Conservatively, using the cask design temperature (per Table 3.2.10), the Young's Modulus (Table 2.2.1) is 26,200 ksi (180,700 MPa).

The effective stress amplitude accounting for the fatigue strength reduction and Young's Modulus effects is given by

$$S_a = \frac{(18)\,(4)\,(30)}{26.2} = 82.4\,\text{ksi} \qquad (568.1 MPa)$$

Using Figure I-9.1 of [2.1.10], the allowable number of cycles is approximately equal to 1000.

Therefore, the *maximum service life of the closure flange threads is 1000 cycles* of torque and un-torque of the cask closure system.

- Satisfaction of Regulatory Guide 7.6 Commitment (Condition 7 on Cyclic Stress Intensity Range

The minimum alternating stress range, S_a, at 10 cycles from all appropriate fatigue curves is 580 ksi. Calculated stress intensities in the containment boundary under any of the analyses performed in this SAR under the required load combinations for Normal Conditions of Transport are less than the ultimate strength of the containment vessel material (70 ksi). Conservatively assuming a stress concentration of 4 regardless of specific location produces a stress intensity range below 4 x (70 ksi) = 280 ksi (< 580 ksi). Therefore, satisfaction of the Regulatory Guide 7.6 commitment on alternating stress intensity range is assured.

2.6.1.3.3 Stability of the Metamic Fuel Basket Plates

Under certain conditions, the fuel basket plates may be under direct compressive load. Although the finite element simulations can predict the onset of an instability and post-instability behavior, the computation in this subsection uses (the more conservative) classical instability formulations to demonstrate that an elastic instability of the basket plates is not credible.

A solution for the stability of the fuel basket plate is obtained using the classical formula for buckling of a wide bar [2.6.4]. Material properties are selected corresponding to a metal temperature of 350ºC, which bounds the computed metal temperatures anywhere in the fuel basket (see Table 2.6.2). The critical buckling stress for a pin-ended bar is:

$$\sigma_{cr} = (\ \pi)^{\ 2} \frac{E}{12(1-\nu^2)}\left(\frac{h}{a}\right)^2$$

where h is the plate thickness, a is the unsupported plate length, E is the Young's Modulus of Metamic-HT at 350ºC, ν is Poisson's Ratio (use 0.3 for this calculation)

From the drawings in Section 1.3, h = 15 mm, a = 208 mm, and E = 6,900 ksi (Table 2.2.8). Then, the classical critical buckling stress is computed as 32.4 ksi, which exceeds the yield strength of the material. This demonstrates that basket plate instability by elastic buckling is not possible.

2.6.1.3.4 Closure Lid Flanged Joint

The closure lid-to-flange joint in all HI-STAR family of casks is engineered to be a "controlled compression joint" (see Figure 2.6.1) widely used in the pressure vessel industry (see [2.7.7, Chapter 3, pp 144-51]).

A "controlled compression" flanged joint is defined as a bolted closure wherein the extent of the pre-compression applied on the gasket is limited by geometric means. The controlled compression joint, illustrated in Figure 2.6.1, is widely used in the pressure vessel industry when the mechanical loads acting to actuate leakage are pulsating with time or are impulsive in nature. The controlled compression joint is particularly suited for those pressure vessels that are subject to severe impulsive or impactive loadings such as transport casks. As required by USNRC regulations (10CFR71) and IAEA Standards (TS-R-1), the containment space (the "pressure boundary" in the terminology of the ASME Code) must maintain the required leaktightness after an accident event that can produce significant inertia loadings from the contained fuel slamming against the lid (which would tend to pry open the gasketed joint). Accordingly, the closure lid-to-flange joints in the HI-STAR cask models (see Table below) have all been engineered to be of the "controlled compression joint" genre (see [2.7.7, Chapter 3, pp 144-151]). The defining features of a controlled compression joint are:

i. The extent of the gasket's compression is controlled by the metal-to-metal contact between the flange and the mating part inboard of the gasket circle. The surface where the contact occurs is referred to as the "*land*".

ii. There is a "relief" between the two surfaces outboard of the gasket contact annulus.

iii. The width of the land is maximized and the gasket annulus is located as close to the bolt circle as practicable.

Because the gasket sits in a machined groove, the seating force G on the gasket to compress it to the depth of the groove is known information. In a well designed joint, G should be much smaller than the bolt pull, B ($G \leq 0.4B$). The difference between the B and G is the contact force on the "land", which serves as the "force reserve" against the unloading of the gasket. Any external force acting to pry open the joint *must first overcome the contact interface force C before the gasket* *would begin to decompress.*

HI-STAR Transport Casks that Utilized Controlled Compression Joint	
Cask I.D.	**USNRC Docket No.**
HI-STAR 100	71-9261
HI-STAR 180	71-9325
HI-STAR 60	71-9336

The width of the land in the joint in the HI-STAR 180D has been carefully selected so that the contact stress (surface stress) due to the compression force does not cause local yielding in the mating parts.

The depth of the groove is a critical dimension because it establishes the extent of compression that is applied to "seat" the gasket. The following text matter on the mechanics of sealing action in a controlled compression joint and on the gasket deformation behavior is provided to identify the critical characteristics of the joint that must be controlled in the selection of the tubular gasket (seal).

(a) Mechanics of sealing action

In a controlled compression joint, the bolt pre-load B is equilibrated by the gasket "seating" force G and the contact force on the land C.

$$B = G + C \qquad (1)$$

The eccentricity between the bolt load circle B and the reaction circles G and C produces a rotational moment which tends to rotate both the flange and the lid towards each other. The edge "relief" between the two surfaces outboard of the bolt circle must be sufficient to prevent edge-to-edge contact.

During the "operating" condition (in the terminology of the ASME Code), wherein an axial load (impact or pressure load), H_p, acts on the inside surface of the inner closure lid, the axial force equilibrium changes to

$$B' = G' + C' + H_p \qquad (2)$$

It is shown in [2.7.7, Chapter 3, pp 104-151], that the bolt load $B' \cong B$, if no edge contact between the two bodies develops due to the added rotation of the two bodies due to increased offset between the opposing forces in the operating condition. (The "relief" must be sized to be large enough to prevent edge-to-edge contact. The design formulas in the ASME code for raised face flange design are predicated on assuming that $B = B'$.)

Furthermore, because of the joint geometry, the gasket will begin to relax only after the contact load on the land vanishes (i.e., $C' = 0$). A key consideration in the design of a high integrity closure joint is to ensure that the bolt pre-load B is large enough to prevent C′ from reaching zero and to ensure that there is sufficient relief outboard of the bolt circle to prevent the development of a contact reaction at the outer edge. If the above conditions are realized then the force equilibrium in the operating condition becomes

$$B = G + C' + H_p \tag{3}$$

Using Eq. (1) and (3), we have

$$C' = C - H_p \tag{4}$$

In other words the contact load at the “land” is reduced by the amount of the operating condition axial load.

Maintaining a positive C′ means that the compression of the gasket will remain unchanged, and, therefore, the sealing state of the gaskets will not be impaired.

To insure that the joint will not leak subsequent to an impulsive loading event, the following requirements have been imposed on the HI-STAR 180D cask:

i. The primary bending stress in the flange at all locations remains below the material’s yield strength under all normal and accident conditions of storage.

ii. The residual contact load on the land remains positive subsequent to the impact event.

iii. There is a complete absence of an edge-to-edge contact load outboard of the bolt circle during the pre-load and the operating conditions.

In the HI-STAR 180D cask, a sufficiently large C has been engineered in the design to prevent the opening of the joint altogether in the aftermath of an impact event. During the impact event, however, a slight transient gasket relaxation can occur, which is computed by the detailed finite element analysis, and the extent of gasket relaxation, δ′, is computed. The coincident (or residual) pressure on the gasket, p′, can be estimated by assuming a linear depressurization:

$$p' = \frac{p\,(\delta - \delta')}{\delta} \tag{5}$$

where

p: gasket pressure under the seating condition
δ: total springback available
δ′: amount of gasket relaxation
δ*: useful springback

For the joint to leak, the gasket must relax (i.e., the joint must open by a sufficient amount) more than the useful springback such that the pressure on the gasket drops to the point that it can no longer maintain the seal. Strictly speaking, leakage is likely to occur if both the inner and outer seals relax more than the useful springback provided in Table 2.2.12 (i.e., unload beyond the minimum compression determined by Eq. (5) for the gasket relaxiation equal to the useful springback). Typically, this condition is realized if the bolts begin to yield in sufficient amount (gross yielding) to permit a joint opening.

The above information can be cast into a metric, m, which serves to provide a quantitative assessment of the margin against leakage in the transport package in the wake of a drop event, as summarized in Table 2.6.1.

As indicated in Table 2.6.1, the maximum margin-against-leakage, *m*, which a joint can attain is 10; minimum is -10 (minus ten). A predicted value of *m* greater than zero means leakage is not indicated; a negative *m* indicates the likelihood of an unsealed state. The greater the value of m, the greater is the assurance of leaktightness. A value of 10 provides maximum assurance. Holtec International utilizes $m \geq 5$ as a conservative criterion for ensuring absence of leakage.

The total margin-against-leakage, *m*, is comprised of two indices, namely

i. m_g which indicates the margin against leakage by examining the post-impact decompression status of the gaskets and the "land".

ii. m_b which indicates the status of the post-impact joint by numerically relating the undamaged bolts to the continued viability of the joint.

$$m = m_b + m_g$$

The computed value of *m* can range from -10 (failed joint) to +10 (maximum assurance of absence of leakage). All assessments of the post-impact integrity of the containment boundary bolted joint presented in the SAR follow the above metric-based representation.

(b) Gasket characteristics germane to leaktightness

The selection of the gasket is critical to successful functioning of a gasketed joint. There are numerous textbooks [2.7.7, Section 3.5.2] and technical papers in the permanent literature that explain the properties and sealing behavior of gaskets. In the following, the essential concepts needed to design and analyze a controlled compression joint are presented:

i. <u>Loading and Unloading Curves</u>

Figure 2.6.2 illustrates a typical loading/unloading curve for a gasket. This curve provides the necessary insight into a gasket's mechanical behavior that is instrumental in the performance of the bolted joint.

- The loading curve tends to flatten out with increasing compression. The unloading curve emulates linear unloading indicating hysteresis. Thus, the gasket loaded from point 0 to point A in Figure 2.6.2 follows the unloading line AB. OB is the extent of the permanent set in the gasket from the loading cycle, and BA′ is the amount of "springback".

- Likewise, if the gasket is loaded to a higher compression level (point C), the unloading line is CD. OD represents the permanent set (loss in the gasket's thickness) and DC′ is the extent of "springback".

The single most important object in setting the groove depth for a gasket is to maximize the "springback", δ. Gasket suppliers provide the groove depth recommendation in their catalogs (or web site) that maximizes δ.

The minimum lineal pressure at which a tubular gasket may fail to maintain containment is referred to as the "threshold pressure", which can be established based on useful springback using Equation (5).

The self-energizing type gasket (see [2.7.7, pp 94]) often used in transport casks, is extremely effective in preventing leakage if the groove geometry and the flange face finish are correct for the species of gasket employed. The self-energizing gasket also possesses excellent springback characteristics, and maintains seal under axial loadings that tend to unload the joint, so long as the joint does not open up so much as to cause the gasket to lose its threshold pressure. A complete relaxation of the self-energizing gasket should be avoided by insuring that the preload C on the land is sufficiently large.

In HI-STAR 180D, both lids use the "controlled compression" feature. To provide stiff backing support to the inner lid and limit the deflection in the inner lid under a hypothetical free drop event, the inter-lid gap is minimized. This design feature together with the controlled compression type joint reinforces both the closure joints thereby providing a double barrier for any leakage.

(c) Seal equivalence

The above discussion of the bolted joint and seal behavior under loading events leads to the conclusion that a tubular metallic gasket can be replaced with an equivalent (or better) gasket if:

The minimum safety factor, defined as the ratio of the residual pressure (residual minimum compressive force) subsequent to the impact loading to the threshold pressure (specified for the equivalent seal), based on the analysis performed for the new gasket (seal) is greater than 1.1.

NRC concurrence is required for any change in seal design.

All seals, as specified in this SAR, are subjected to a proof test to insure that the groove dimensions and its surface finish are compatible with leak-tight performance.

2.6.1.3.5 Re-flood Event

During a cask re-flood event, water is introduced to the cask cavity through the lid drain line to cool-down the internals and support fuel unloading. This quenching operation induces thermal stresses and strains in the fuel rod cladding, which are at their maximum at the boundary interface between the rising water and the dry (gaseous) cavity. An analysis has been performed in Calculation 5 of [2.6.8], which shows that the maximum total strain in the fuel cladding due to the re-flood event is well below the failure strain limit of the material. Thus, the integrity of fuel rod cladding inside the HI-STAR 180D cask will be maintained in a re-flood event.

2.6.1.4 Comparison with Allowable Stresses

Following Regulatory Guide 7.9, calculated stress intensities in the containment component of the package from all analyses are compared with the allowable stress intensities defined in Section 2.1 (Tables 2.1.2 through 2.1.8) as applicable for conditions of normal transport. The results of these comparisons are presented in the form of factors of safety (SF) defined as:

$$SF = \frac{\text{Allowable Stress}}{\text{Calculated Stress}}$$

For convenience, those specific allowable strengths, loads, etc., that are used to develop the safety factors are summarized in Table 2.6.3. Data from Sections 2.1 and 2.2 are used to construct Table 2.6.3.

Safety factors associated components identified as lifting and tie-down devices have been presented in Section 2.5 as set forth by Regulatory Guide 7.9.

2.6.1.4.1 Results for Pressure Boundary Stress Intensity

Results from the finite element analyses for Load Combinations N1 and N2 are tabulated for normal heat conditions of transport in Holtec Proprietary calculation packages [2.1.12] and [2.6.1], respectively. For Load Combination N1, a static axi-symmetric finite element model is constructed using ANSYS [2.5.2] using layered Plane42 elements to model the through-thickness behavior of the containment shell and the baseplate. The tabular results include contributions from mechanical and thermal loading and are needed to insure satisfaction of primary and primary plus secondary stress limits for normal conditions of transport. For the purpose of this calculation only, the closure lid-shell junction is modeled assuming a clamped connection in recognition that the large preload from the closure lid bolts (see Table 2.2.12), necessary to insure continued sealing subsequent to the drop events, will preclude relative rotations at the joint under the internal pressure. The analysis considers the combined effects of the design internal pressure in Table 2.1.1 and the operating temperature distribution (Table 2.6.2). Figure 2.6.3 shows the axi-symmetric finite element model, and Figure 2.6.4 shows the graphical results, both reproduced from [2.1.12].

For Load Combination N2, a dynamic finite element model implemented in LS-DYNA [2.5.3] is used to determine the peak deceleration of the cask. Then a static stress analysis is performed in ANSYS [2.5.2] based on the bounding cask deceleration β_{max}.

Results are evaluated against Level A stress intensity limits for locations in the containment shell, and in the baseplate, which together with the closure lids, make up the containment boundary. The bolted connection of the lids to the closure flange is not modeled for Load Combination N1, as this solution is not meant to evaluate the sealing performance of the gaskets.

The key results for Load Combinations N1 and N2 are summarized, in Tables 2.6.5 and 2.6.6, respectively, wherein the minimum safety factor for different components of the cask for each of the load combinations is presented. All safety factors are conservatively computed using allowable stresses based on the maximum normal operating temperatures (see Tables 2.1.1 and Table 2.6.2, for component temperatures, and Table 2.1.6 for allowable stress intensity).

For all Holtite-B enclosure cavities, as a conservative measure, the accident pressure limit from Table 2.1.1 is utilized in analysis and it is demonstrated that the enclosure does not suffer large plastic deformation, i.e., the primary stresses are shown to be within elastic range. Pressure relief devices are designed for all Holtite-B cavities to relieve pressure at or below the accident pressure limits. The details of the calculations for all Holtite-B cavities are presented in [2.1.12].

Hazards from Holtite thermal degradation under routine conditions and normal conditions of transport have been evaluated in the Holtite Applications report [2.2.10]. Furthermore, all Holtite components/locations/regions in the cask are equipped with relief devices consistent with the cask licensing drawing.

Per [2.2.10] and [2.1.12], the cold (installation) condition gaps in all Holtite-B and lead cavities are sized such that there are no additional stresses in cavity enclosures (plates and welds) due to thermal expansion of Holtite-B and lead during normal (heat) condition of transport.

2.6.1.4.2 Result Summary for Normal Heat Condition for Transport

- Maximum Cask Deceleration from Load Combination N2

Table 2.6.4 lists the maximum cask deceleration calculated for the 0.3-meter side drop using the LS-DYNA model. Table 2.6.4 also defines the bounding value for β_{max}, which is used as input for the static stress analysis.

- Stress Intensity Results from Overall Finite Element Analysis of the Cask

Table 2.6.5 is a summary table that includes primary and primary plus secondary stress intensity safety factors (per Table 2.1.2) for Load Combination N1 associated with the Normal (Heat) Conditions of Transport. Table 2.6.6 provides similar results for Load Combination N2. The tabular results demonstrate that all safety factors exceed 1.0 at the key locations for each component of the containment boundary.

- Status of Lid Bolts and Seals

The principal means for the joint integrity evaluation is the so-called "static analysis" method described below. The dynamic results from the LS-DYNA solution serve to provide secondary validation of the conclusions from the primary (static analysis) solution.

The evaluation for the state of stress in the bolts and the state of compression in the seals is performed using the ANSYS finite element code. Note that Load Combination N1 and N2 do not govern as the bolts, gaskets, and the lands are preloaded to withstand the much larger loading from the hypothetical drop accidents.

The LS-DYNA finite element analysis for the cask also provides results at the lid-to-top forging interface. The results from the transient analysis indicate that all seal elements remain closed (i.e., the loading in the elements representing the seal remains compressive) and that the bolts remain elastic (stresses remain below the allowable limits per Table 2.1.3) for Load Combination N2, indicating that the sealworthiness of the bolted joint will not be adversely affected during normal heat conditions of transport. The measure of margin-against-leakage, m, defined in Table 2.6.1 is 10 (the maximum possible value).

The inner closure lid port cover seals are analyzed using classical methods to demonstrate that the torque requirement for the inner closure lid port cover bolts (Tables 2.2.12 and 7.1.1) is sufficient to seat the gasket and maintain a positive contact load on the land under Normal Conditions of Transport.

Based on the results of the above analyses for normal heat conditions of transport, the following conclusions are reached.

i. No bolt overstress is indicated under any loading event associated with Normal Conditions of Transport. As expected, the tensile stress in the bolts remains essentially unchanged from its initial preload state for reasons discussed in Subsection 2.6.1.

ii. The closure lid seals, including port cover seals, do not unload beyond the minimum force corresponding to the useful springback (per Table 2.2.12) required to maintain the leak tightness under Load Combinations N1 and N2; therefore, the seals continue to perform their function under Normal Conditions of Transport.

- ASME Pressure Test Condition

See Paragraph 8.1.3.2 for pressure test specifications.

- Performance of Non-Containment Components of Package

The Holtec Proprietary calculation package documenting all of the finite element solutions [2.6.1] contains graphical visualizations of the stress intensity and deformation for every component in the HI-STORM 180D package. In particular, the fuel basket and the monolithic shield surrounding the containment shell are surveyed to evaluate their performance and compare with the acceptance criteria in Section 2.1. Table 2.6.7 summarizes the acceptance criteria for performance of the non-containment components of the HI-STAR 180D. From Table 2.6.7, it is established that the surveyed components meet the acceptance requirements stated for Load Combination N2.

- Summary of Results for Normal Heat Conditions of Transport

Tables 2.6.4 through 2.6.7 present a concise summary of safety factors and performance results for the HI-STAR 180D for the Normal Heat Condition of Transport.

Based on the results of all analyses, it is concluded that:

i. All safety factors reported in the text and in the summary tables are greater than 1.0.

ii. There is no buckling or plastic deformation distortion of the cask internals.

iii. All performance requirements are met for the non-containment components.

iv. The containment boundary seals, which includes the closure lid seals and the vent and drain port cover seals, do not unload beyond the minimum force required to maintain leak tightness (per Table 2.12).

Therefore, the HI-STAR 180D Package, under the Normal Heat Conditions of Transport, has adequate structural integrity to satisfy the subcriticality, containment, shielding, and temperature requirements of 10CFR71.

2.6.2 Cold

The Normal Cold Condition of Transport assumes an ambient environmental temperature of -20°F (-29°C) and maximum decay heat. A special condition of extreme cold is also defined in Regulatory Guide 7.8 where the package and environmental temperature is at -40°F (-40°C) and the package is exposed to increased external pressure with minimum internal pressure. A discussion of the resistance to failure due to brittle fracture is provided in Section 2.1.

The value of the ambient temperature has two principal effects on the HI-STAR 180D Package, namely:

i. The steady-state temperature of all material points in the cask will go up or down by the amount of change in the ambient temperature.

ii. As the ambient temperature drops, the absolute temperature of the contained helium will drop accordingly, producing a proportional reduction in the internal pressure in accordance with the Ideal Gas Law.

In other words, the temperature gradients in the cask components under steady-state conditions will remain the same regardless of the value of the ambient temperature. The internal pressure, on the other hand, will decline with the lowering of the ambient temperature. Since the stresses under normal transport condition arise principally from pressure and thermal gradients, it follows that the stress field in the cask under a bounding "cold" ambient would be smaller than the "heat" condition of normal transport, treated in the preceding subsection.

In addition, allowable stresses generally increase with decreasing temperatures. Safety factors, therefore, will be greater for an analysis at cold temperatures than at hot temperatures. Therefore, the safety factors reported for the hot conditions in Subsection 2.6.1 provide the limiting margins. However, since the bolt preloads may be altered by a change in the environmental temperature, the effect of bolt temperature changes on the level of preload, subsequent to the initial application of preload, must be considered and is evaluated in the Holtec Proprietary calculation package [2.1.12]. The finite element analysis in [2.1.12] accounts for the maximum possible internal pressure and the relative growth (or shrinkage) of a preloaded bolt connecting the lid to the flange due to the change in elastic moduli and coefficients of thermal expansion. The results from that calculation are summarized below:

Evaluation of Environmental Temperature Changes on the Level of Preload	
Item	**Value**
Initial Bolt Prestress (Inner/Outer Lids) ksi (MPa)	76.5/76.5 (527.4/527.4)
% Change from Initial Condition to Cold (Inner/Outer Lids)	3.4/-6.3

The computed change in stress due to the assumption of a severe local low temperature condition is insignificant compared to the initial bolt stress and to the change in the allowable bolt stress because of the lowered temperature. It is concluded that the small change in bolt preload stress will have an insignificant effect on structural calculations and therefore safety factors and sealing are essentially unaffected by the environmental change.

As no liquids are included in the HI-STAR 180D Package design, loads due to expansion of freezing liquids are not considered.

The effect of environmental and component temperature changes on the stress from the interference between the monolithic shield and the inner containment shell is now considered. Because the coefficients of thermal expansion of the outer monolithic shield and the inner shell are essentially the same, the change of the cask's thermal state will not produce any significant internal or interface stresses under steady state conditions.

2.6.2.1 Differential Thermal Expansion

The methodology to determine differential thermal expansion in the Normal Heat Condition of

Transport is presented in Chapter 3. The same methodology is applied for the Normal Cold Condition of Transport, and results are summarized in Chapter 3.

It can be verified by referring to the drawing packages in Section 1.3 that the clearances between the fuel basket and cask inside surface are sufficient to preclude temperature induced interference in the cold condition.

No further analysis is warranted for the cold condition since (a) the restraint of free thermal expansion is less under cold conditions and (b) material strength properties tend to be greater at lower temperatures, resulting in higher allowable stress limits.

It is concluded that the HI-STAR 180D package meets the requirement that there be no restraint of free thermal expansion, under Normal Cold Conditions of Transport, that would lead to primary stresses greater than the applicable ASME Level A limit.

2.6.3 Reduced External Pressure

The effects of a reduced external pressure equal to 25 kPa (3.5 psia) are bounded by results from the design internal pressure analysis for the cask (Load Combination N1). This case does not provide any bounding loads for other components of the cask containment boundary.

2.6.4 Increased External Pressure

The effect of an external pressure equal to 140 kPa (20 psia) on the package, which is stated in USNRC Regulatory Guide 7.8 [2.1.4], is bounded by the effect of the large value for the external pressure specified by 10CFR71.61 (2 MPa (290 psia)). Instability of the containment boundary shell, under this external pressure is examined in Section 2.7. Therefore, no additional analyses are performed herein to demonstrate package performance.

2.6.5 Vibration

During transport, vibratory motions occur which could cause low-level stress cycles in the package due to beam-like deformations. If any of the package components have natural frequencies in the flexible range (i.e., below 33 Hz), or near the flexible range, then resonance may amplify the low level input into a significant stress response. Strength of materials calculations are performed to establish that vibrations are not an issue in transport of the HI-STAR 180D.

The lowest frequency of vibration during normal transport conditions may occur due to vibrations of a fuel basket cell wall. An analysis to determine the lowest frequency of vibration of the component has been performed. For this computation, the fuel basket plate (cell wall) is assumed to vibrate like a simply supported beam. Based on the plate mass density and the plate dimensions, the lowest natural frequency is well in the rigid range (see the Holtec Proprietary calculation package [2.1.12]).

When in a horizontal position, the cask is supported over a considerable length of the shield cylinder. Conservatively considering the HI-STAR as a supported beam at only the two ends of the shield cylinder, and assuming the total mass of the fuel basket and its contents moves with the cask, a computation of the lowest natural frequency of the structure during transport provides a result in the rigid range. (See calculation package [2.1.12]).

Based on these frequency calculations, it is concluded that vibration effects are inconsequential to the structural integrity of the cask.

The capacity of the stored fuel assemblies (i.e., fuel rods) to withstand vibratory loads during normal conditions of transport has also been evaluated. For this evaluation, the fuel rod is conservatively analyzed as a simply supported beam whose length is equal to the longest span between adjacent grid spacers. The section properties of the fuel rod beam are based solely on the thickness and diameter of the fuel rod cladding. The mass of the fuel pellets is smeared along the length of the fuel rod beam. The key input data that defines the fuel rod beam model is summarized in Table 2.6.9.
The lowest natural frequency of the fuel rod beam is reported in Table 2.6.10, which shows that the fuel rod beam is nearly rigid despite the fact that the beam ends are considered to be simply supported. In reality, the boundary conditions at the ends of the fuel rod beam fall somewhere between simply supported and clamped because the fuel rods are continuous (i.e., they extend beyond the grid spacers). Therefore, for the stress analysis of the fuel rod, the fuel rod beam is considered to be rigid, and the maximum bending stress in the fuel rod cladding is calculated using a quasi-static approach.

The load applied to the fuel rod beam is a transverse acceleration of 5-g, which is consistent with the design load applicable to the tie-down devices on the transport package per 10CFR71.45. Under this load, the maximum calculated bending stress in the fuel rod cladding is an order of magnitude less than the yield strength of Zircaloy. Furthermore, the calculated stress is well below the endurance limit of Zircaloy per NUREG/CR-1132 [2.6.6]. The stress analysis results for the fuel rod are summarized in Table 2.6.10.

In summary, the fuel rods will not rupture due to the vibratory loads associated with normal conditions of transport since the maximum calculated bending stress in the fuel rod cladding is less than the yield strength and the fatigue endurance limit of Zircaloy by a factor of 6 or more.

2.6.6 Water Spray

The condition is not applicable to the HI-STAR 180D Package per [2.1.4]. Additional discussion is provided in Appendix I of [2.6.1].

2.6.7 Free Drop

The structural analysis of a 0.3-meter (1-foot) side drop under the heat condition is documented in Paragraph 2.6.1.4. As demonstrated in Paragraph 2.6.1.4, safety factors are well over 1.0 (see Table 2.6.6 for Load Combination N2). The discussion in Subsection 2.6.2 demonstrates why the cold condition is not a bounding condition for the 0.3-meter (1-foot) side drop.

An additional 0.3-meter top down end drop evaluation is presented in Appendix I of [2.6.1] to bound all drop orientations.

2.6.8 Corner Drop

This condition is not applicable to the HI-STAR 180D Package per [2.1.3].

2.6.9 Compression

This condition is not applicable to the HI-STAR 180D Package per [2.1.3].

2.6.10 Penetration

This condition is not applicable to the HI-STAR 180D Package per [2.1.4]. Additional discussion is provided in Appendix I of [2.6.1].

2.6.11 Stacking

This test is not required for the HI-STAR 180D package because of its cylindrical shape and horizontal orientation during transport which prevents stacking.

Table 2.6.1: Metrics for Assessing the Post-Impact Margin-of-Safety, m, Against Leakage from the Containment Boundary Bolted Joint (max. possible value of m = 10; min. possible = -10)

Indicator (Metric)	Condition (Predicted by the LS-DYNA Solution)		
Status of gasket (symbol for status indicator metric: m_g)	A positive contact force, C means no gasket decompression	Contact force = 0, but the remaining gasket compression pressure is above the threshold value for joint leakage	Contact force = 0, and remaining gasket surface pressure is below the threshold value to prevent joint leakage.
Assigned points for gasket status indicator, m_g	5	1	-5
Status of body bolts (symbol for status indicator: m_b)	*No* bolts indicated by the stress analysis to result in primary direct load above that causing complete yielding over an entire cross-section.	n % of the body bolts have yielded over an entire cross-section under the operating condition (such as an impact event).	
Assigned metric points for bolt status indicator: m_b	5	$m_b = 5 - 0.1n$ (At 100% bolt thru-thickness yielding, i.e., n = 100, $m_b = -5$)	

Table 2.6.2: Summary of Operating Pressure Difference and Bounding Average Metal Temperatures for Normal Condition of Transport ("Heat" Condition)

Location	Pressure kPa (psig)	Min. Component Temperature Used in the Safety Factor Evaluation ºC (ºF) ††
Containment Shell (Top)	Refer to Table 2.1.1	196 (385)
Containment Shell (Middle)		224 (435)
Containment Shell (Bottom)		196 (385)
Containment Baseplate		196 (385)
Inner Closure Lid		196 (385)
Outer Closure Lid		149 (300)
Containment Closure Flange		204 (400)
Bottom Ring Forging		191 (375)
Monolithic Shield Inner Surface		216 (420)
Monolithic Shield Outer Surface		154 (310)
Fuel Basket – Top (Outer Edges)		302 (575)
Fuel Basket – Middle (Outer Edges)		316 (600)
Fuel Basket – Base (Outer Edges)		285 (545)
Fuel Basket – Top (Center)		321 (610)
Fuel Basket – Middle (Center)		343 (650)
Fuel Basket – Base (Center)		310 (590)

Notes:

††Temperatures listed bound the results in Chapter 3. Added conservatism may be noted in some of the structural calculations where bounding temperatures are considered while evaluating the minimum safety margins.

Table 2.6.3: Allowable Stresses for Level A and Level D Conditions (Normal Condition of Transport)

ITEM	LEVEL A†	LEVEL D†	TEMPERATURE
Inner Closure Lid – Primary Bending Stress Intensity – MPa (ksi)	221.3 (32.1)	506.8 (73.5)	204°C (400°F)
Outer Closure Lid – Primary Bending Stress Intensity – MPa (ksi)	228.6 (33.2)	506.8 (73.5)	149°C (300°F)
Containment Shell – Primary Membrane Stress Intensity – MPa (ksi)	143.76 (20.85)	336.8 (48.85)	232°C (450°F)
Containment Shell – Primary + Secondary Stress Intensity – MPa (ksi)	431.27 (62.55)	NA	232°C (450°F)
Baseplate – Primary Membrane + Bending Stress Intensity – MPa (ksi)	221.3 (32.1)	506.8 (73.5)	204°C (400°F)
Baseplate – Primary + Secondary Stress Intensity – MPa (ksi)	442.5 (64.2)	NA	204°C (400°F)
Inner Lid Bolts – Average Service Stress (Stress Intensity) – MPa (ksi)	601.2 (92.6)	862.0 (125.025)	191°C (375 °F)
Outer Lid Bolts – Average Service Stress (Stress Intensity) – MPa (ksi)	646.7 (93.8)	885.1 (128.4)	149°C (300 °F)
Inner Lid Bolts – Maximum Service Stress at Extreme Fiber (Stress Intensity) – MPa (ksi)	862(125.025) ††	1047.9 (151.99)	191°C (375 °F)
Outer Lid Bolts – Maximum Service Stress at Extreme Fiber (Stress Intensity) – MPa (ksi)	885.3 (128.4) ††	1068.7 (155.0)	149°C (300 °F)
Monolithic Shield Cylinder – Ultimate Strength – MPa (ksi)	NA	482.6 (70.0)	204.4°C (50 °F)

† Obtained from Section 2.1.
†† Lesser of 3Sm and S_y is used for conservatism.

Table 2.6.4: Maximum Deceleration Under 0.3 Meter Free Drop Condition (Side Drop)

Method	α_{max} (g's)
Numerical (LS-DYNA) Solution	24.1†
Notes: †A bounding acceleration of 30 g's (β_{max}) that exceeds the computed maximum dynamic deceleration (α_{max}) is conservatively used in the structural analysis of the cask components. This simulation considers the limiting upper bound crush strength for the impact limiter material.	

Table 2.6.5: Containment Boundary Stress Intensities and Safety Factors – Load Combination N1 (Static Analysis)

Location and Stress Intensity Component	Calculated Value
Inner Closure Lid – Primary Bending Stress Intensity – MPa (ksi)	33.23 (4.82) SF=6.66
Outer Closure Lid – Primary Bending Stress Intensity – MPa (ksi)	98.51 (14.29) SF=2.32
Containment Shell – Primary Membrane Stress Intensity – MPa (ksi)	20.46 (2.967) SF=7.03
Containment Shell – Primary + Secondary Stress Intensity – MPa (ksi)	271.7 (39.41) SF=1.59
†Baseplate – Primary Membrane + Bending Stress Intensity at Center – MPa (ksi)	40.09 (5.816) SF=5.37
†Baseplate – Primary + Secondary Bending Stress Intensity at Periphery – MPa (ksi),	45.0 (6.528) SF=9.58

Note:
"SF" means Safety Factor.
† The containment shell and the baseplate are conservatively evaluated @ 232 ºC (450 ºF) temperature.

Table 2.6.6: Results for 1-Ft (0.3 m) Drop Static Analysis

Item	Allowable from Table 2.6.3	Calculated Value	Safety Factor
Primary Membrane stress intensity in the containment shell – MPa (ksi)	143.76 (20.85)	34.5 (5)	4.1
Primary + Secondary stress intensity in the containment shell – MPa (ksi)	431.27 (62.55)	97.2 (14.1)	6.51

Note: "SF" means the Safety Factor. †As an example, the stress distribution in the containment shell under 1-Ft (0.3 m.) side drop is shown in Figure 2.6.5. Under 1-Ft (0.3 m.) top end drop is presinting in [2.6.1].

Table 2.6.7: Key Performance Objectives for Non-Containment Components of the HI-STAR 180D

Criterion	Load Combination N1	Load Combination N2
Stress Intensity in Monolithic Shield – Primary Stress Intensity Below Ultimate Strength	-	Yes
Fuel Basket Deformation – Maximum Total Deflection < 1 mm	Yes	Yes

Table 2.6.8 is intentionally left blank

Table 2.6.9: Key Input Data for Fuel Rod Vibration Analysis

Item	Value
Length of Fuel Rod	115.17 in (2925.4 mm)
Bounding Weight of a Single Fuel Rod	4 lbf (1.814 kg)
Maximum Distance between Grid Spacers	19.93 in (506.22 mm)
Cladding Thickness Considering Thinning due to In-Reactor Oxidation	0.02 in (0.516 mm)
Cladding OD	0.422 in (10.72 mm)
Lower-bound Elastic Modulus of Zircaloy Cladding	9.61×10^6 psi (6.626×10^4 MPa)

Table 2.6.10: Results for Fuel Rod Analysis Under Normal Vibration Load

Result	Calculated Value, Hz
Lowest Natural Frequency of Fuel Rod Beam	29.43

Result	Calculated Value, MPa (psi)	Fatigue Endurance Limit†, MPa (psi)	Safety Factor
Maximum Bending Stress in Fuel Rod	24.19 (3,509)	177.5 (25,730)	7.33

† Per Section 2.1 of NUREG/CR-1132 [2.6.6].

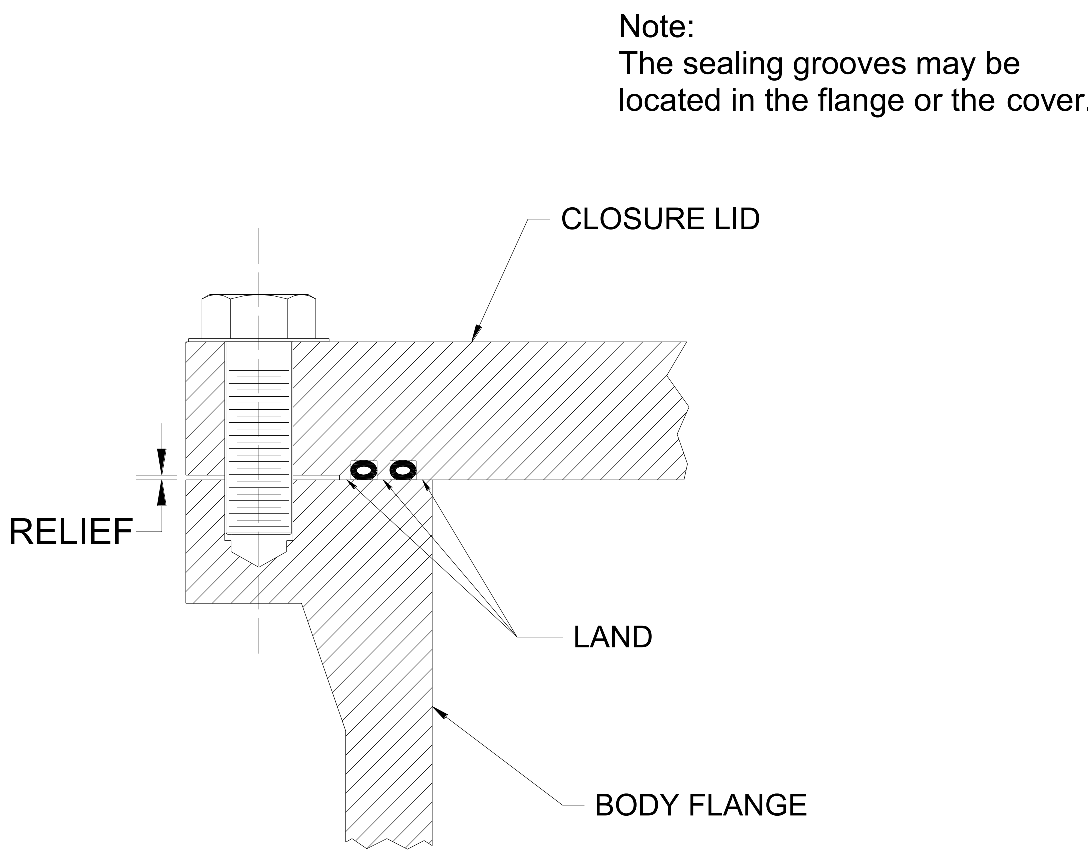

Figure 2.6.1: Essential Elements of a Classical "Controlled Compression Joint"

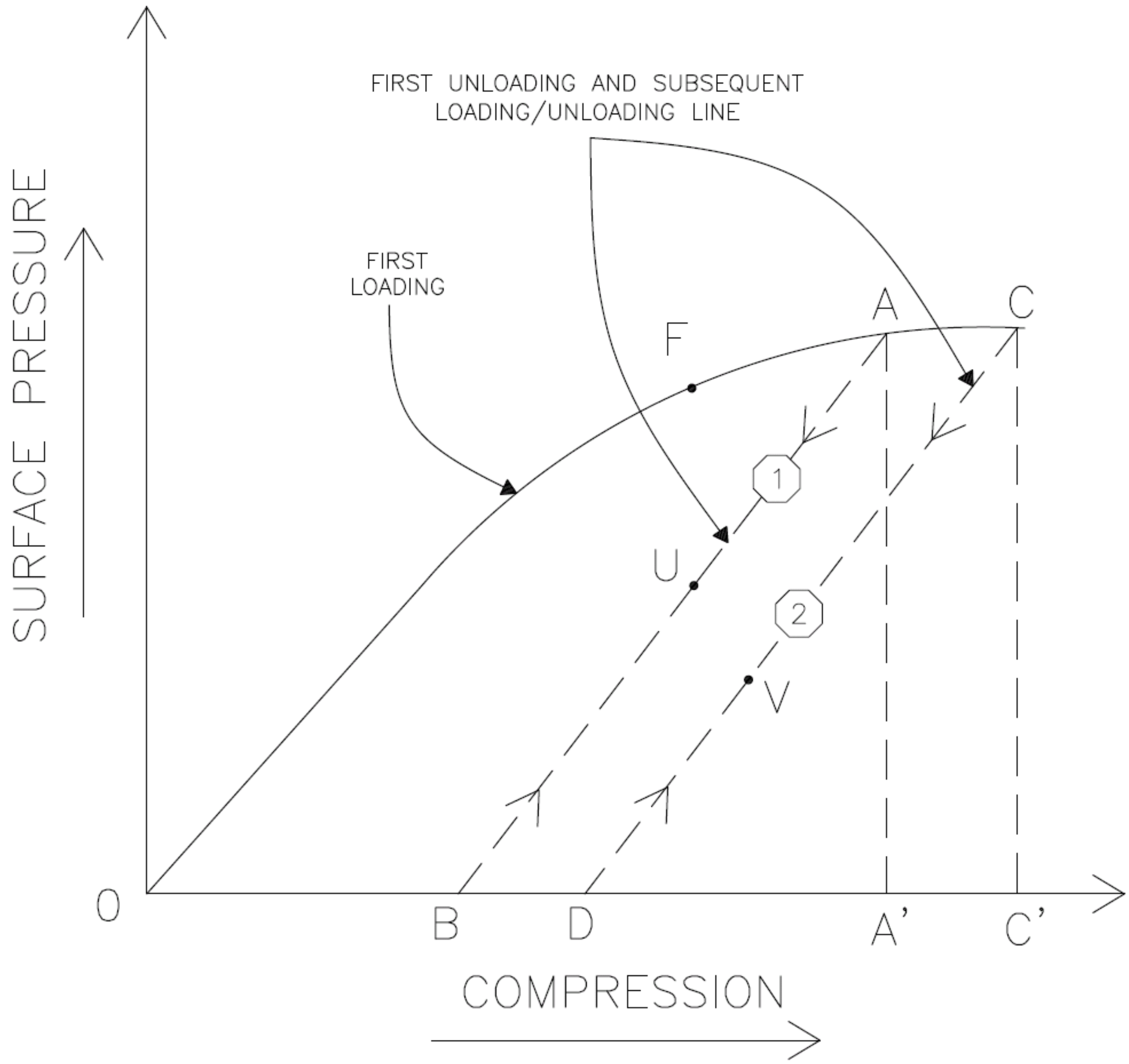

Figure 2.6.2: Loading and Unloading Curves for a Typical Gasket

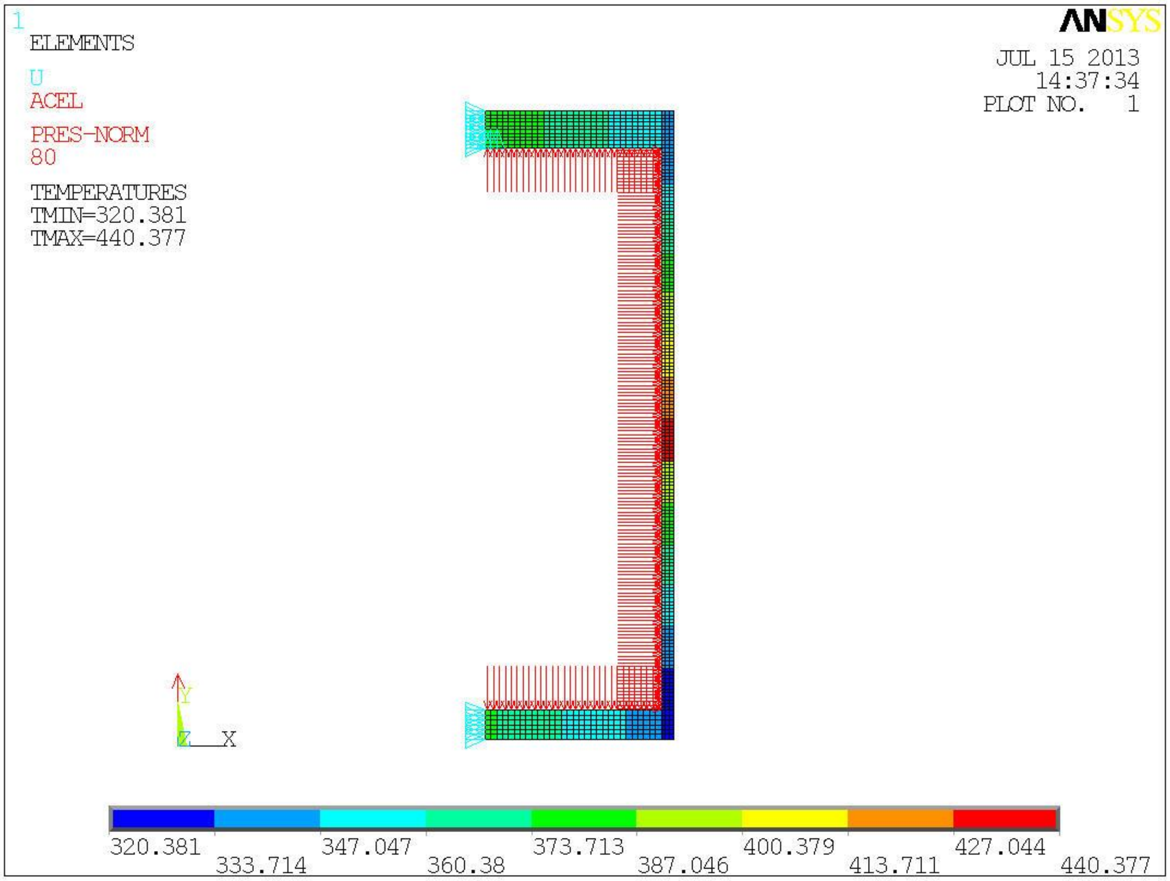

Figure 2.6.3: Finite Element Model for Load Combination N1

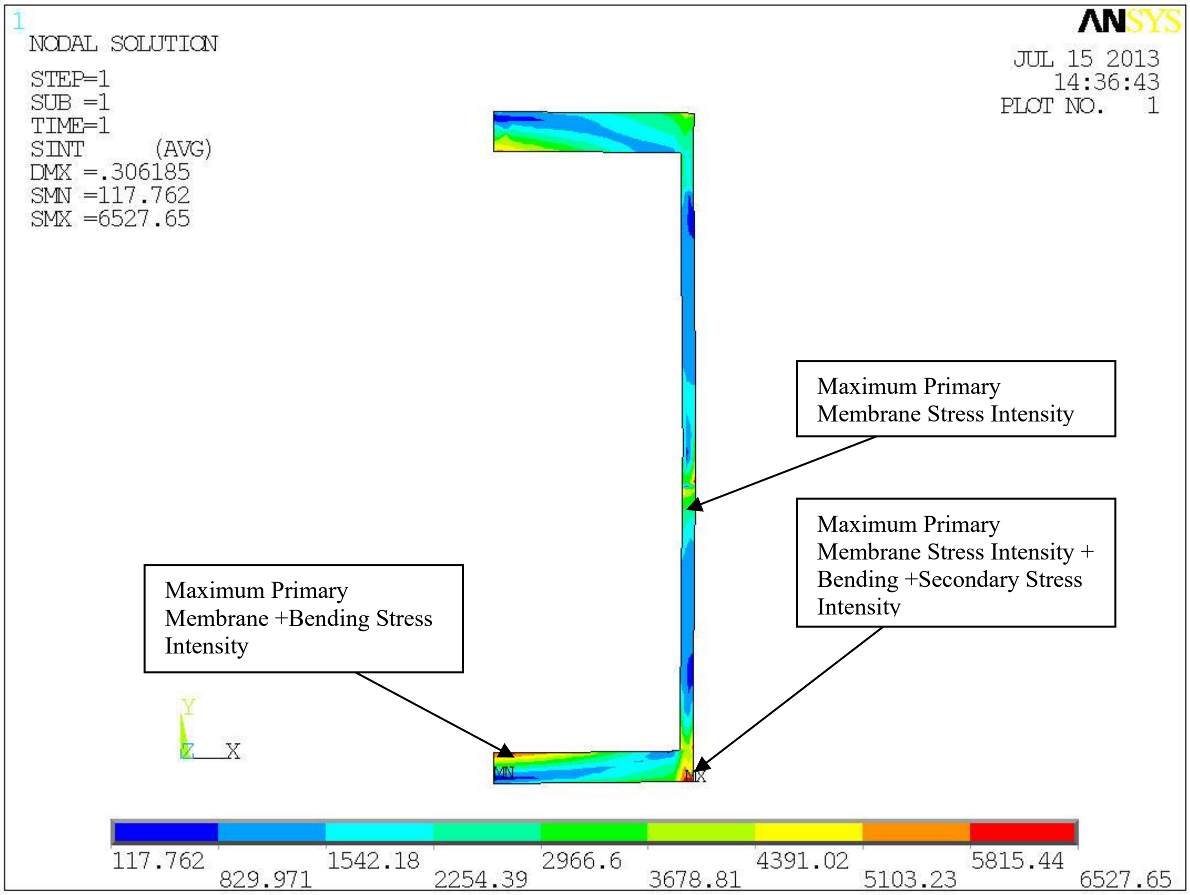

Figure 2.6.4: Results for Stress Intensity for Load Combination N1

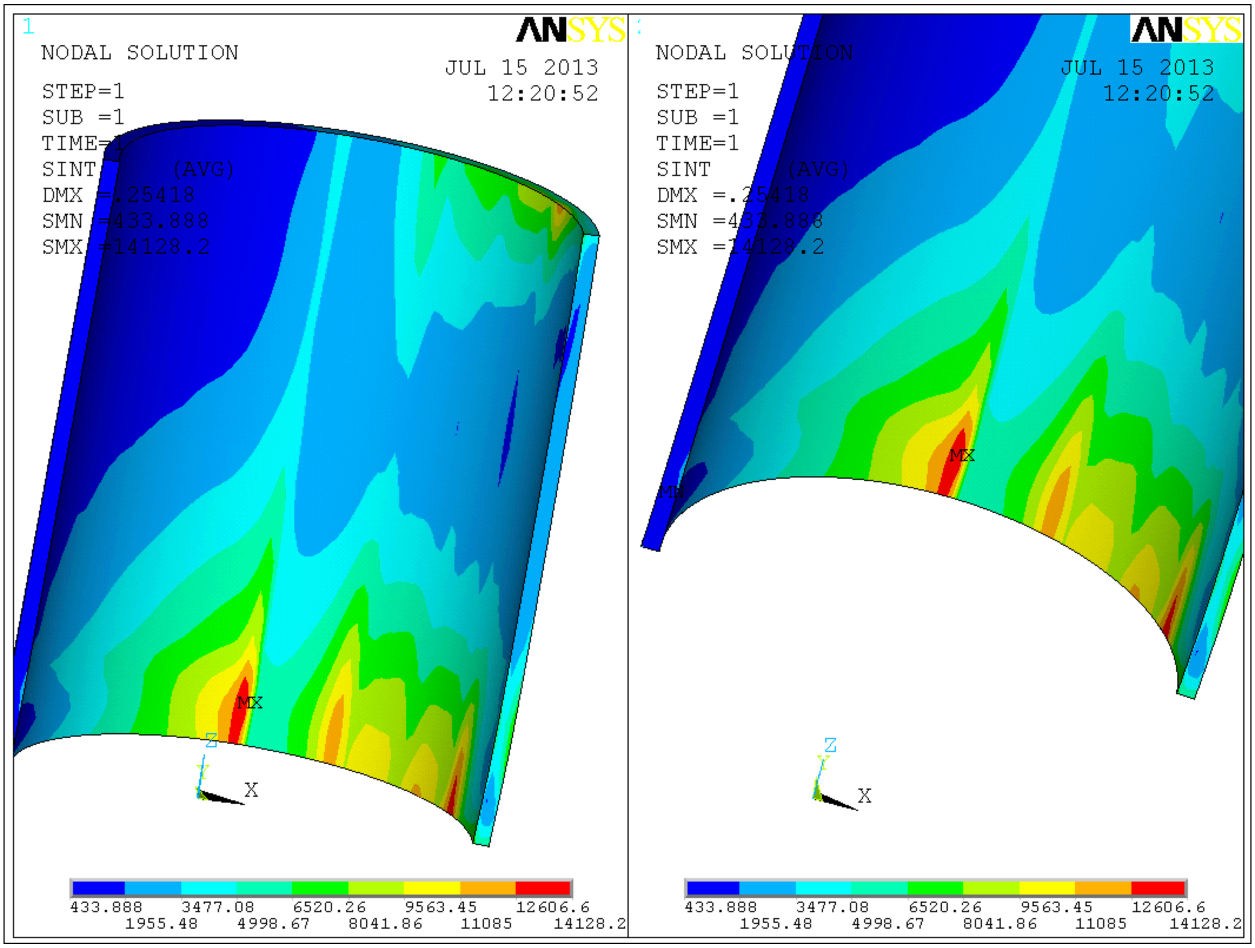

Figure 2.6.5: Stress Intensity Distribution in Containment Shell for 1-Ft Side Drop

2.7 HYPOTHETICAL ACCIDENT CONDITIONS

It is shown in the following subsections that the HI-STAR 180D Package meets the safety criteria set forth in 10CFR71 when it is subjected to the hypothetical accident conditions specified in 10CFR71.73. In particular, required technical data is presented herein to support the conclusion that HI-STAR 180D Package, when subjected to hypothetical accident conditions, will maintain its structural integrity to satisfy the subcriticality, containment, shielding, and temperature requirements of 10CFR71.

The hypothetical accident conditions, as defined in 10CFR71.73 and explained in Regulatory Guide 7.9, are applied to the HI-STAR 180D Package as a sequence of loading events. The package is first subject to a 9-meter (30-foot) drop. As required by the regulations, the "free drop" should be assumed to occur in the orientation that will cause maximum damage. To identify the most vulnerable orientation the drop simulation is performed in four candidate orientations. From the post-impact package configuration determined to have the most damaging orientation, the package is then subject to a 1-meter (40-inch) drop onto a 15 cm (6.0 inch) diameter mild steel pin (of length sufficient to impart the impact energy to the cask structure through penetrant action). In the third step, the package is subject to a 800°C (1475°F) temperature fire environment for 30 minutes. Finally the package is subject to water immersion.

As a separate loading event, the cask containment boundary is also subjected to deep immersion in accordance with 10CFR71.61.

As discussed in the preceding section, the evaluation of the maximum deceleration sustained by the package under a free drop event is determined. The methodology involves simulating of the free drops using the 3-dimensional dynamic finite element code LS-DYNA. The same methodology was previously used in the evaluation of the HI-STAR 180 package [1.0.4]. With respect to impact decelerations, the LS-DYNA method has been successfully benchmarked against the scale model drop tests, as detailed in Appendix 2.B of [1.0.4].

The LS-DYNA simulation also provides the time-history of the internal stresses in the cask. Since the scale model tests (described in Appendix 2.B of [1.0.4]) were not instrumented to measure internal stresses/strains, the LS-DYNA solution was previously used in the HI-STAR 180 docket [1.0.4] to predict only the impact limiter performance, such as the decelerations and the impact limiter crush. Subsequently, the ANSYS static analysis was used to quantify the stresses in the various components of the transportation cask.

Following an identical approach, the safety analysis for structural compliance of HI-STAR 180D follows a two-track approach, namely:

1. The package deceleration profile is obtained for each free drop scenarios using LS-DYNA.
2. A value of static deceleration, β_{max}, that exceeds the computed maximum dynamic deceleration, α_{max}, is used to perform static stress analyses to determine internal stresses and strains.

The "static analysis" approach adopted in this safety evaluation mimics the method used in the HI-STAR 100 and HI-STAR 180 dockets wherein the maximum deceleration of the package, α_{max}, obtained from the dynamic analysis was applied as a static inertia load to perform the stress and the bolted joint integrity analysis of the containment boundary. This so-called "static analysis" approach was previously discussed in Subsection 2.6.

The transient analysis results from LS-DYNA are used to provide the added (secondary) confirmation to the safety evaluation of the HI-STAR 180D Package. This second means of confirmation of safety could not be invoked in the HI-STAR 100 docket because LS-DYNA had not yet attained the necessary status of credibility in the mid-90s when HI-STAR 100 licensing occurred.

2.7.1 9-meter Free Drop

2.7.1.1 Problem Description and Dynamic Model

As specified in §71.73, the performance and structural integrity of the HI-STAR 180D Package must be evaluated for the most severe drop scenarios. The appurtenance that is critical to protecting the integrity of the containment boundary during a high momentum collision event is the AL-STAR impact limiter.

The central purpose of the impact limiter, defined as an essential package appurtenance in Section 1.2, is to limit the package maximum deceleration, α_{max}. The HI-STAR package, consisting of the loaded cask and top and bottom impact limiters, is essentially a cylindrical body with a very rigid interior (namely, the cask) surrounded by a pair of relatively soft crushable structures. The crushable structure (impact limiter) should deform and absorb the kinetic energy of impact without detaching itself from the cask, disintegrating, or otherwise malfunctioning. A falling cylindrical body may theoretically impact the target surface in an infinite number of orientations; the impact limiter must limit decelerations to insure that stress intensity and performance limits, as described in Section 2.1, are satisfied, and to ensure that the impact limiter does not detach from the cask, regardless of the impact orientation. In general, a drop event orientation is defined by the angle of the HI-STAR 180D longitudinal axis, "θ", with the impact surface. In this notation, $\theta = 0°$ means a side drop and $\theta = 90°$ implies a vertical or end drop scenario. In any orientation, the drop height is measured from the lowest point on the package.

An intermediate value of θ at which the point of impact is directly below the center of gravity (C.G.) of the HI-STAR package warrants special mention. This drop orientation is traditionally called the C.G.-over-corner (CGOC) configuration. The CGOC orientation, "θ_c", is the demarcation line between single and dual impact events. At $90° > \theta > \theta_c$ the leading end of the package (denoted as the "primary" impact limiter) is the sole participant in absorption of incident kinetic energy. At $\theta < \theta_c$ drop orientations, the initial impact and crush of the leading (primary) impact limiter is followed by the downward rotation of the package with the initial impact surface acting as the pivot, culminating in the impact of the opposite (secondary) impact limiter on the target surface. In the dual impact scenarios, the first and second impact limiter crush events are referred to as the "primary" and "secondary" impacts, respectively. It is reasonable to speculate that for certain values of θ, the secondary impact may be the more severe of the two. Figures 2.7.1 through 2.7.4 illustrate the orientation of a (generic) cask at the initiation of a drop event.

To meet the performance objective of the impact limiter, the attachment design should ensure that both impact limiters remain with the cask during and after the impact event, which is ensured in the AL-STAR impact limiter design by situating the fasteners in such a way that they are not in the primary path of impulse and momentum transfer during the impact event. The impact limiters are also required to have sufficient crush material to prevent cask body-to-unyielding target contact.

Finally, the package design must satisfy all criteria in ambient temperature conditions (temperature and humidity) that may prevail during transport. Therefore, the impact limiter design must be functionally insensitive to the ambient temperature and humidity.

As the drawings in Chapter 1 indicate, in addition to the crushable material, the impact limiter contains a cylindrical shell that is stiffened with internal gussets. This buttressed steel shell is sized to be sufficiently robust to preclude gross plastic deformation or buckling during impact events and thus serve as the backbone of the impact limiter.

To summarize, the performance objectives of the impact limiter are set down as five discrete items, namely:

i. Limit peak deceleration (α_{max}) to ensure satisfaction of: 1) stress intensity limits in the containment component under all limiting drop orientations; 2) functional performance requirements (closure lid seals do not leak, fuel basket plate global average permanent deformation (if any) remains within limits, fuel cladding shows no gross rupture and the effectiveness of the shielding surrounding the Containment Boundary is not significantly impaired) are met. In particular, the margin-against-leakage parameter, m (defined in Section 2.6 and Table 2.6.1) must remain ≥5 (a value of $m \geq 1$ is adequate to ensure leaktightness; requiring a higher value of m is in the spirit of conservatism).

ii. The impact limiters should not detach from the cask under a 9-meter drop event under any impact orientation.

iii. The impact limiters must bring the cask body to a complete stop prior to ground contact or lock-up of the crush material, else the potential for a large peak deceleration exists at the termination of the drop.

iv. Impact limiter crush material must be equally effective at upper and lower bound package operating temperatures, with humidity ranging from 0 to 100%.

v. All external surfaces must be corrosion-resistant.

The last two objectives are realized by utilizing crush material that is insensitive to the ambient psychrometric environment, and by using surface preservatives or corrosion resistant materials as indicated in the drawing package in Section 1.3. The stainless steel skin is procured to “bright annealed” finish to minimize absorption of solar thermal radiation.

To protect the studs that connect the impact limiters to the cask, a special washer named “Fastener Strain Limiter” (FSL) is employed under the nut of each stud. These FSLs are engineered to ensure that the impact limiter fasteners will not experience excessive plastic strains resulting in separation of the impact limiter from the HI-STAR package during a high impulse event such as a “free drop” (§71.73).

The remaining design objectives, namely, limiting of the maximum rigid body deceleration under the 9-meter drop event and preventing contact of the cask with the unyielding surface, is demonstrated by the LS-DYNA [2.5.3] finite element code, as discussed earlier. LS-DYNA has been benchmarked extensively by others [2.7.5, 2.7.6] and by Holtec using the test data from the static tests of the crush material and, more importantly, from the quarter-scale model 9-meter drop experiments carried out at the Oak Ridge National Laboratory in support of HI-STAR 100 Part 71 certification in the late 90s [2.7.4] (see Appendix 2.B of [1.0.4]). As discussed in Appendix 2.B of [1.0.4], the LS-DYNA simulation model for the family of AL-STAR impact limiters is a credible and reliable vehicle for determining the HI-STAR 180D Package’s impact performance *with respect to the extent of crush and the peak g-load.* LS-DYNA has been used by Holtec International in a wide variety of impact scenarios in dry storage projects [2.7.10].

Regulatory Guide 7.9 calls for evaluation of the response of the containment component in terms of stress intensity. Further, it requires investigation of structural stability as well as the consequences of the combined effects of temperature gradients, pressure, and other loads. The work effort to fulfill the above Reg. Guide 7.9 recommendation is carried out using the static analysis approach, as discussed in the foregoing.

The LS-DYNA model of the HI-STAR 180D package has been used to simulate the hypothetical drop accidents defined in Section 2.1to obtain α_{max} and to provide a reference result for the dynamic response of the cask. Details of the simulation model (figures showing the basics of the model for the fuel assemblies, the fuel basket, the basket supports, the containment boundary, the surrounding shield, the lids, and the detailed grid for the bolts and gaskets), and the graphical presentation of the results obtained for each drop considered are presented in the supporting Holtec Proprietary calculation package [2.6.1]. Summary description is provided below.

LS-DYNA Model Description

The LS-DYNA model constructed to analyze the HI-STAR 180D Package places considerable emphasis on modeling of the impact limiters, the gasketed joint, and the regions of the containment boundary subject to the direct brunt of the impact loads. The finite element articulation of the model must be refined enough to capture the essential characteristics of the package response, but not so fine as to lead to inordinately long computation times or to significant round-off errors. The HI-STAR 180D finite element model is aimed to realize the above mentioned balance between the minuteness of the discretized elements and efficiency of computation.

The LS-DYNA model of the HI-STAR 180D Package corresponds to the design drawings contained in Section 1.3. Because of the geometric symmetry of the physical problem, only half of the HI-STAR 180D Package (as well as its impact target) is modeled. Figures 2.7.5 through 2.7.11 show the LS-DYNA model of the HI-STAR 180D Package.

The LS-DYNA model of the HI-STAR 180D Package has the following key attributes:

- The finite element discretization of the cask containment members is sufficiently detailed to accurately articulate the primary membrane and bending stresses as well as the secondary stresses at locations of gross structural discontinuity. Table 2.7.1 provides reference data on the finite element model. The finite element layout of the cask is pictorially illustrated in Figures 2.7.5 through 2.7.11. For example, the containment shell represented by multi-layers of solid elements is shown in Figure 2.7.6.

- Special emphasis is placed on a detailed modeling of both bolted joints of the cask containment boundary. Tables 2.7.1 and 2.2.12 present some key data concerning the bolted joint and the surrounding containment. It is noted from the drawings in Section 1.3 that the lid-to-containment flange joints are of the classical "controlled compression" genre [2.7.7, pp 144-151]. In such joints, the bolt pull, B, is balanced by the reactive force on the gasket, G, and a contact force, C, at the so-called "land" surface (see Section 2.6 for additional details).

  $B = G+C$

  Because the gasket sits in a machined groove, the seating force G on the gasket to compress it to the depth of the groove is known information. As can be seen from Table 2.2.12, G is a relatively small force compared to the bolt pull, B. The difference between the B and G is the contact force on the "land", which serves as the "force reserve" against the unloading of the gasket. Any external force acting to pry open the joint must first overcome the contact interface force C before the gasket would begin to decompress. In order to predict the joint response in an accurate manner, the contact interface, with its pre-load C and gasket compression force G must be modeled with accuracy. To realize this modeling objective, as shown in Figure 2.7.7, the closure lid bolts are explicitly modeled and the gasket bearing and metal-to-metal contact interfaces are discretized in sufficient detail to capture the effect of deflections and rotations during the impact events on the seal-worthiness of the bolted joints. In addition to provide a high degree of assurance against leakage and to maintain seal-tightness, the following governing design parameters from Table 2.2.12 are used in the Finite Element model:

  i. The FE model of the seal uses the bounding seating load from Table 2.2.12. The upper-bound seating load used in the seal FE model ensures a lower contact interface force "C" thereby limiting the force reserve available before the seals undergo relaxation during a critical impactive loading such as the 30 ft (9 m) top end drop accident (see above discussion). Consequently, the seal-worthiness (effectiveness) is conservatively estimated.

ii. the use of minimum threshold pressure corresponding to the useful springback from Table 2.2.12 also renders additional conservatism to the analysis result. In the event that the total reserve "C" at the contact interface is overcome during the most critical impactive event, the minimum threshold pressure requires the least amount of bolt elongation before seal leakage is predicted.

Further, the linear elastic seal model will conservatively underestimate the remaining compressive deformation of an unloading gasket, which typically follows a nonlinear unloading path with a reducing stiffness. To ensure sealing, the gasket relaxiation (i.e., springback) must not exceed the useful springback listed in Table 2.2.12, which can be converted into an acceptable minimum compressive stress in the linear elastic gasket model. The sealing integrity of the HI-STAR 180D containment boundary in a drop event is evaluated by comparing the LS-DYNA predicted minimum compressive stress in the gasket with the acceptable minimum compressive stress. For additional assurance, analyses are also performed in ANSYS using all elastic material characteristics for the lid closure joint.

- Preloading of closure lid bolts is realized by using the *INITIAL_STRESS_SECTION command available in LS-DYNA [2.5.3] for each closure lid bolt during the dynamic relaxation phase prior to simulating the impact event (transient loading). An initial stress is also imposed on the seal elements to reflect the initial deformation of the seals after preloading, and an initial dynamic simulation performed to reach a steady state condition and establish the state of stress in the flange, lid, bolts, and seals. This solution becomes the starting point for any of the required drop and puncture analyses.

- To achieve a high level of accuracy with respect to the participation of the fuel assemblies in the impact event, *each* fuel assembly is modeled individually. Further, the axial stiffness of each assembly is maximized by representing it by an equivalent homogeneous rectangular solid of square cross section that has the same cross section as the fuel assembly. The elastic solid elements of the fuel model are specified with effective elastic moduli that correspond to the metal area of all fuel rods, the guide tubes and the instrument tubes. This method of representing the fuel assemblies renders them into relatively stiff perfectly elastic bodies, which absorb no energy from impact and thus maximize the impact loads. In reality, the fuel rods are free-floating between the top and bottom end fittings, and therefore don't fully participate in the axial strength of the fuel assembly. Thus by considering the fuel rods, the axial stiffness of the fuel assembly is over-estimated by several orders of magnitude which maximizes the deceleration experienced by the fuel during impact. For simulations where the fuel assembly primarily lies in a lateral plane, the effective modulus is set to ensure that the fundamental natural frequency of the rectangular solid is equal to that of the first mode beam frequency of the fuel assembly. The FEA calculation package [2.6.1] provides details of the calculation of the effective modulus for the elastic fuel assembly model in different impact orientations. For simulations where the fuel is primarily vertical, the modulus of the fuel assembly is based on the geometric arrangement of the rods (with the end fittings) acting as slender columns. The effective moduli of the fuel assembly, calculated in [2.6.1], are provided in Table 2.7.2.

- Following the design configuration, the fuel basket model (see Figure 2.7.10) which is assembled from intersecting plates per the drawings in Section 1.3, includes all potential contacts and allows relative rotations between individual basket intersecting plates. For conservatism, a bounding gap is assumed at contact interfaces between any two perpendicular basket plates to allow for any impacts and, therefore, maximize the stress and deformation of the fuel basket plate. The fuel basket plates are modeled by thick shell elements, which behave like solid elements in contact, but can also accurately simulate the bending behavior of the basket panel.

- All cask structural member materials are represented by their applicable nonlinear elastic-plastic true stress-strain relationships. This is important in order to accurately assess the behavior of the bolted joint connections. Details of the development of the true stress-strain relations are found in [2.6.1], which includes the methodology for obtaining a true stress-true strain curve from a set of data in terms of engineering stress-strain data. Non-structural members, such as Holtite, are characterized by the LS-DYNA bi-linear material model.

- Following the same approach as used in the benchmarking of the HI-STAR 100 [2.7.4] and HI-STAR 180 [1.0.4], the HI-STAR 180D Package impact limiter finite element model (see Figures 2.7.5 and 2.7.11) characterizes all steel backbone members based on true-stress-true-strain relationships developed with the LS-DYNA material model MAT_024 (*MAT_PIECEWISE_LINEAR_PLASTICITY), and crush material blocks by the LS-DYNA material model MAT_126 (*MAT_HONEYCOMB) with real orthotropic behavior. The material coordinate system for each crush material block is determined based on the drop orientation.

- The FSL's designed to protect the impact limiter attachment bolts from being overloaded are modeled as a cylinder of solid elements divided into two sections (see Figure 2.7.11C). The lower section of elements (closer to the cask) will fail if the axial load on the FSL exceeds the limit set forth to protect the attachment bolt. An elastic-perfectly-plastic material model (with a very small plastic failure strain) is used to characterize the FSL lower section; the yield stress of the material model is calculated in [2.6.1] based on the failure load of the FSL.

- Automatic "surface-to-surface" or "single-surface" contacts are defined at each of the potential contact surfaces between the HI-STAR 180D Package components, which include contacts involving fuel assemblies, fuel basket, seals, closure lids/bolts, impact limiter component, and other cask members. For example, the design feature of structural interaction between the two closure lids is captured by the surface-to-surface contact definition in the model as shown in Figure 2.7.20, where the gap between the closure lids closes momentarily during the top end vertical drop event.

- The coefficient of friction (COF) at all contact surfaces is set at 0.5, and material properties for each part are obtained from tables in Section 2.2 at the temperatures provided in Table 2.6.2.

- The simulation of the Normal and Hypothetical Accident Conditions of Transport that require dynamic analysis include an initial load state simulating the preloading of the seals by appropriate tensile loading of the lid bolts. The HI-STAR 180D has two seals on each of the lids, and a set of closure bolts for each lid.

The previously described key attributes implemented in the HI-STAR 180D LS-DYNA model take advantage of the state-of-art numerical analysis capability of the finite element code for simulating transient, nonlinear impact events. With good accuracy demonstrated in the benchmarking effort (Appendix 2.B of [1.0.4]) as well in the analysis independently performed by the NRC/PNNL investigators [2.7.5], the previously described HI-STAR 180D finite element model is deemed to be able to predict the impact performance of the package under various accidental drop conditions with reliable accuracy.

ANSYS Model Description

The LS-DYNA half model of the cask for the dynamic drop simulations is adapted for the ANSYS static analysis. Modifications are necessitated by the differences between the dynamic and the static analyses within two different environments. Specifically, the following changes are made to the LS-DYNA model:

- The top and bottom impact limiters are irrelevant and thus removed. Their effects are reflected with appropriate boundary conditions and pressure loadings at both ends. The non-structural shielding materials including lead and Holtite at top and bottom ends and in the monolithic shield cylinder pockets are also removed. Their weights are uniformly lumped into their containing cask components.

- The cask contents including the fuel basket and the loaded fuel assemblies are not explicitly modeled in the cask global model. For the end drops, the inertial load from the contents is applied as a uniform pressure to either the inner closure lid or the baseplate inner surface. For the side drop, the inertial load from the contents is applied as a uniform pressure to the supporting shims that are to be in contact with the containment shell.

- The normal pressure loading (MNOP) is uniformly applied on the interior boundary of the containment viz. the shell, the top flange, the inner closure lid and the baseplate.

- Solids are modeled with SOLID45 elements. The fuel basket, for the representative slice model, is modeled with SOLSH190 elements that are equivalent to thick shell elements in LS-DYNA.

- Preloading in closure lid bolts is realized by using PRETS179 elements that can be automatically inserted between the existing elements along the grip length of the bolts. Simultaneously, the initial compression on the closure lid seals is achieved through thermal growth by specifying certain thermal expansion coefficients for the inner and outer seals. Preloading is applied only for the 30-ft top end drop case wherein the closure lid is expected to experience the largest prying force resulting from the cask contents, which in turn will cause maximum bolt tension and seal opening, if any.

- Coefficient of friction at all contact interfaces is assumed to be 0.5. Bonded contact is always assumed at closure lid/lid bolt washer/bolt head interfaces. Separable contacts are defined at the interfaces of closure lid/top flange, closure lid seals/closure lid, and closure lid seals/top flange for the top end drop, and between the monolithic shield cylinder individual blocks, the containment shell/monolithic shield cylinder interface for the side drop. To save computational efforts, these separable contacts are turned into bonded for other drop cases where sliding and separation at these interfaces is either minimal or not physically credible for the particular drop event being analyzed. Closure lid seals are only modeled in the top end drop case.

- The materials used to represent the HI-STAR 180D package except for the fuel basket are assumed to be isotropic and elastic. Material properties for each component are defined at their corresponding ambient (hot) bounding temperatures as summarized in Table 2.6.2. Thermal expansion is not considered in drop events (see discussion in Section 2.6).

- A representative slice of the F-37 fuel basket, consisting of a smaller end section and a full section, is modeled in detail including the contained fuel assemblies and supporting basket shims. Per the licensing drawing, the nominal width of fuel basket panels in the vertical direction may be increased or decreased within a narrow range provided that the length of the panel slots is increased or decreased proportionally. This means that the fixed-height fuel basket may be assembled using more (or fewer) panels than the number depicted on the licensing drawing. The results of the ANSYS static analysis for the fuel basket presented herein are valid for the full range of panel widths permitted by the licensing drawings since (a) the lateral load on the fuel basket per unit (vertical) length remains the same and (b) the length of the slots measured as a percentage of the panel width remains the same.

- The fuel basket panels are modeled with SOLSH190 solid shell elements. The shims and each fuel assembly are modeled with SOLID45 solid elements. Standard contact pairs using CONTA173/TARGE170 elements are defined at the interfaces of fuel assembly/basket panel, shim/basket panel, and between stacked basket panels including all the intersecting slot locations. Plastic deformation is expected in the fuel basket panels that are made of Metamic-HT material. The fuel basket material model is implemented with true stress-true strain multi-linear isotropic hardening plasticity model. Elastic material model is defined for the basket shims since no plastic deformation is expected in the shims. To accommodate large deformation in the fuel basket panels, sufficiently small element sizes (< 11 mm) are used and 9 integration points through the thickness are specified. A mesh sensitivity study performed as part of the HI-STAR 180 license [1.0.4] shows that the panel stresses and displacements obtained using solid shell elements ensure a converged solution and indicate comparable results to those obtained using 5 solid elements through the thickness of the panel.

LS-DYNA Mesh Sensitivity and Assurance of Convergence

A converged solution is one that remains unaltered if the finite element grids are made more refined and the number of elements is accordingly increased. The area of the model where mesh quality is expected to be of highest importance is the crush material in the impact limiters. This is due to the highly non-linear behavior and the large deformation of this material. Of further interest are also the various shell element representations, in order to ensure these shell elements appropriately model the behavior of the actual three-dimensional part they represent. Meshing and modeling of these areas are discussed below.

An obvious approach to ensure that the meshing of the crush material in the impact limiter is appropriate would be to repeat the same drop calculation for the full cask and impact limiter model with different mesh densities and choose the meshing where further refinement would not lead to any significant changes of the results. However, this approach is not practical for two reasons: First, these studies would have to be repeated for every new impact limiter design, and second, for each design, the studies would have to be performed for each principal drop orientation, since it is not initially clear which orientation(s) is critical for determining mesh convergence. To overcome these problems, a more general approach is necessitated. In this context, LS-DYNA parametric studies were performed to evaluate the mesh sensitivity for representative blocks of crush material under impact conditions relevant for the drop test situations under the HI-STAR 180 Docket [1.0.4]. The details of this mesh sensitivity study is discussed here for completeness. The element sizes were chosen to be similar to the sizes of the material blocks in the impact limiters. The following conditions were specifically analyzed: compression in a direction normal to the block surface; compression in a direction slightly offset from the normal direction; and an impact that generates substantial shear load in the material. Element sizes were varied in several steps, with a total variation of factor 2 to 3. For the shear impact, a mesh with an optimized variable mesh is also included. The impact chosen was representative of the 30 ft drop condition. The cases were compared based on the overall deformation of the blocks. The studies showed that for all configurations, the deformation varies only slightly (by a few percent) over the range of element sizes (see Appendix 2.B of [1.0.4] for further details). These studies provided the basis for selecting the element sizes for the crush material in the impact limiter of the HI-STAR 180D. The studies yield a maximum acceptable mesh density (relative to the overall size of the crush material block) that assures a converged solution for all types of loading. For the HI-STAR 180D Impact Limiter, the number of element divisions in the finite element mesh for the aluminum crush material is chosen to be greater than the converged mesh density from the benchmark analysis.

Regarding the shell elements, the number of integration points through the thickness is chosen to be 10, which is the maximum value possible in LS-DYNA. This ensures converged and accurate solution for the shell elements.

2.7.1.2 Simulation of Drop Events

As discussed before, the free drop of the package from 9 meters onto an essentially unyielding surface is simulated for a number of orientations using LS-DYNA. The peak g-loads from each drop simulation, α_{max}, in both axial and lateral direction (to the cask's axis) are computed. The largest axial and lateral deceleration is then used to determine the regulatory compliance of the package using the so-called "static analysis" explained previously, with additional confirmatory results from the LS-DYNA analyses.

The postulated free drop events belong to four broad categories, namely:

1. Vertical-end drop
2. Lateral (side drop)
3. C.G.-over-corner
4. Oblique (slap down)

Under certain categories of events, there may be more than one drop "orientation". The orientation of drop, θ, is defined by the angle between the horizontal plane and the axis of the cask pointed from its base to its lid at the instant of impact. θ = 90º is a vertical-end drop event with bottom-down configuration (see Figure 2.7.1). Similarly, θ = 0 º means side (lateral) drop (see Figure 2.7.3).

The various drop orientations analyzed using LS-DYNA to identify the most damaging scenario with reasonable assurance are summarized in Table 2.7.3. Of these, the slap-down event warrants special mention because it often produces the bounding decelerations in transport packages and has two candidate orientations in an axially nonsymmetrical package, namely:

i. Wherein the top impact limiter strikes first, followed by the second impact at the bottom impact limiter.

ii. The obverse of case (i) wherein the primary impact occurs at the bottom impact limiter followed by a second impact at the top impact limiter.

As can be seen from Table 2.7.3, upper as well as lower bound properties of the crush material are analyzed in LS-DYNA to ensure that the largest value of α_{max} and maximum crush, d_{max}, have been identified and evaluated.

The initial velocity of the package corresponding to a free fall from 9 meters at impact in all impact scenarios is 13.392 m/sec (43.9 ft/sec).

2.7.1.3 Summary of Results

Table 2.7.3 summarizes the maximum values of α_{max} for the axial and lateral direction from all of the drop scenarios simulated on LS-DYNA.

Certain observations from the LS-DYNA numerical simulations provide valuable information with respect to the structural performance of the package.

i. For the dual impact scenarios (i.e. slapdown drop accident), the secondary impact is always more severe than the primary impact. The maximum deceleration and impact limiter crush occur in the region of the secondary impact.

ii. All body bolt stresses meet the acceptance criteria from Table 2.1.3 demonstrating that there is no risk of failure of any bolt fastened to the top forging.

iii. The bolts joining the impact limiters to the cask do not undergo catastrophic deformation/failure and remain connected to the impact limiter subsequent to the drop accident.

iv. The closure lid seals are fully seated after the the governing 9-m drop event since the closure lid bolts remain elastic.

The governing values of α_{max} (axial and lateral) culled from Table 2.7.3 are rounded up by a modest amount (for conservatism), henceforth referred to as "Design Basis" decelerations, β_{max}, and provided in Table 2.7.4. These design basis decelerations are used in the "static analyses" to determine the margins-of-safety in the different constituent parts of the package.

Evidently, the axial and lateral β_{max} values respectively challenge the top and bottom plate components, and the fuel basket panels in bending. Thus, β_{max} (axial) determines the margin-of-safety in the baseplate and inner closure lid (the outer closure lid does not experience the direct impact of the contents). The β_{max} (lateral) governs the lateral loading on and deflection of the fuel basket walls.

The axial deceleration, β_{max}, can be cast as a pressure loading on the inner closure lid (or the baseplate, depending on the assumed sense of action of the inertia load). The pressure p_{max} corresponding to β_{max} is given by

$$p_{max} = 4\, W_c \frac{\beta_{max}}{(\pi D^2)}$$

where W_c is the weight of the cask contents (basket and basket shims plus fuel) and D is the inside diameter of the containment closure flange.

In the "static analysis" procedure, p_{max} is applied as a pressure loading on the inner lid and the baseplate. Table 2.7.5 summarizes the value of p_{max} and identifies the most vulnerable locations and parts in the package that must be evaluated.

The effect of lateral deceleration is to cause flexing of the fuel basket cell panels transverse to the direction of the load under the magnified inertia load of the fuel, and to load the panels oriented in the direction of the inertia load in direct compression.

The outer closure lid, also a containment boundary part, does not experience the direct inertia load from β_{max} tending to unload the seals (as it does on the inner closure lid). Rather, a reaction load from the crushing of the impact limiter material acts on the outer surface of the outer lid, causing flexural action. While the gasketed joint is not directly challenged, the bending stress intensity in the outer lid must be shown to remain within Level D condition limits.

The finite element model of the HI-STAR 180D cask is based upon an earlier design of the inner closure lid which incorporated a lead gamma shielding cavity that has since been removed. The effect of new inner closure lid design on the governing hypothetical accident top end drop is evaluated in Appendix H of [2.6.1] and it is shown that the design change only has a second order effect on the results.

For convenience, the allowable stress limits necessary for the safety evaluation of each part are compiled in Table 2.6.3. The corresponding results from the ANSYS static analyses are listed in Table 2.7.6.

Based on the tabular results presented in Tables 2.7.6 and 2.7.9, it is concluded that:

- The primary stress intensities for the containment components are below the ASME NB limits for all drop configurations.

- The closure lid bolts show no gross yielding and the gaskets remain under a compressed state at the conclusion of the event. Therefore, continued bolted joint effectiveness in the wake of the 9-meter free drop event is assured.

- The monolithic shield surrounding the containment shell remains intact.

- The fuel basket does not undergo gross plastic deformation in the active fuel region, and the global average permanent deformation remains below the limit value established by the acceptance criteria in Section 2.1.

- The small quantity of lead, used for shielding in the HI-STAR 180D, is included in the LS-DYNA model. The lead is characterized by the properties given in Table 2.2.11. A review of all drop and puncture simulation results confirms that the predicted lead slump (Appendix G of [2.6.1]) in base plate assembly and bottom shield cylinder assembly is bounded by the shielding evaluations in Chapter 5. It is also confirmed that the lead enclosures and their weldments will maintain their structural integrity under all 9-meter hypothetical drop accidents, ensuring that the lead components continue to peform their intended function.

- The ability of the containment boundary and monolithic shield cylinders to maintain an adequate structural connection so that the monolithic shield cylinders are stable (i.e., remain attached to containment boundary) during hypothetical accident drops is demonstrated in [2.1.12].

- Since the ability to accurately predict and evaluate large displacements is included within the LS-DYNA algorithm, the effect of any instability is automatically accounted for. Based on the evaluated results, it is concluded that there is no buckling of the containment components during any of the postulated Hypothetical Accident events.

2.7.1.4 Fracture Analysis

To provide a reasonable confirmatory assurance that the closure lid bolts (viz. primary lid and secondary lid bolts) and the shield cylinder will not fracture under a severe Part 71 impactive event, resulting in a substantial loss of shielding material or a loss of seal integrity, the following analysis using LS-DYNA is performed.

i. The Charpy impact test for the material is simulated in LS-DYNA by modeling the edge-supported V-notched Charpy specimen and subjecting it to the blow of the hammer. The material stress-strain curve of the specimen is represented by its stress-strain relationship. For example, a material that can be represented by a bi-linear stress/strain relationship may be characterized by its material elastic modulus, elastic limit, tangent modulus, and failure strain (corresponding to the ultimate strength).

ii. The Charpy impact simulation is carried out several times, reducing the failure strain, ε_f, of the specimen's material in steps until the required amount of impact energy to break the specimen corresponds to the specified minimum Charpy absorbed energy for the part. The calibrated material property model established by this process ensures that a part made of such a material and equipped with a V-notch (to simulate a material defect) will fail at the strain level equal to that produced under the Charpy impact condition.

iii. In the next step, the region of maximum tensile stress in the cask from the Part 71 impactive event is identified. The location is easy to identify in loading events such as the puncture of side wall of the cask (§71.73(c)(3)) where the maximum tensile stresses develop on the opposite face of the shell's point of impact.

iv. A separate LS-DYNA model is then prepared, which is smaller in size than the full cask model and isolates the part under investigation (e.g., shield cylinder). The material properties of the part are input based on Charpy calibrated stress-strain relationship from step (ii). Further, a V-notch is introduced in the most vulnerable orientation at the location(s) of maximum tensile stress. A dynamic impact load is then applied to the LS-DYNA model, which bounds the maximum tensile stress and the load duration from the full cask model (step iii). The candidate regions of crack propagation (V-notched locations) are examined to determine if a crack has developed and, if so, the extent of the crack propagation that has occurred.

v. The acceptance criterion for this crack propagation evaluation is no significant loss of shielding or loss of seal integrity due to fragmentation or dismemberment of the analyzed part.

Using the approach described above, the potential fracture of the closure lid bolts and the monolithic shield cylinder under cold conditions at -40 degrees F is investigated. By simulating the standard Charpy V-notch impact test using the minimum Charpy energy specified in Section 2.1, the failure strains of the SA-564/705 630 bolting materials and SA-352 LCC shield cylinder material are calibrated.

To examine the propensity for crack propagation in the inner and outer closure bolts, a solid round bar representing about 1/3rd length of a closure bolt is modeled and a straight notch with similar shape as the Charpy V-notch (i.e., a 45^{o} tip opening angle and 2 mm maximum depth) is carved into one side of the bar. The finite element mesh size in the vicinity of the notch in both the Charpy test specimen and the round bar are similar. The maximum axial stress resulting from the dynamic event (top end drop) is conservatively applied on the SA-564/705 630 bolting material. The impact load is ramped to its peak within 0.002 seconds and is sustained for 0.055 seconds, which is consistent with the solution for the 9-meter top end drop using LS-DYNA. The other end of the bolt is fixed. To eliminate artificial end effects that will cause premature failure at both ends, a small section at the loaded end is defined as rigid, and three layers of nodes at the other end are all fixed. The LS-DYNA simulations show that a few elements at the notch tip failed when the impact load reached its peak. However, the crack did not propagate any further afterwards and the simulation was manually terminated at 0.0025 seconds since stress in the bolts became stable. The details of the calculation are provided in the Holtec proprietary calculation package [2.1.12]. Since the alternative material SB637-N07718 selected for closure lid bolting (as specified in the drawing package litsed in Section 1.3) are not susceptible to brittle fracture, this material, as specified in the ASME section NB, is exempted from fracture toughness testing.

To evaluate the propensity for crack propagation in the shield cylinder during the most severe accident of a 1 m side puncture (see Subsection 2.7.2), a section of the shield cylinder plus the containment shell is modeled in LS-DYNA as shown in Figure 2.7.13. For conservatism, the model neglects the outer region of the shield cylinder, where the neutron shielding pockets are located. The containment shell extreme radial edges are rigidly connected to a mass element on the centerline of the cask to account for the total mass of the HI-STAR 180D Package in the puncture simulation. Since the maximum tensile stress would develop on the opposite face of the shield cylinder's point of impact, the Charpy V-notch is introduced on the inside surface of the shield cylinder representing a longitudinal oriented crack. The entire model, except for the puncture bar which is fixed, is given an initial bounding velocity of 176 in/sec at time zero to simulate a 1-meter drop onto the puncture bar. The LS-DYNA simulation shows that:

i. the puncture bar does not penetrate the inner solid portion of the shield cylinder (see Figure 2.7.14);
ii. the embedded crack does not propagate and the crack tip strain is well below the calibrated material failure strain;
iii. the primary membrane plus bending stress intensity in the containment shell is less than the ASME Level D allowable stress intensity per Table 2.6.39.

The erosion detected in the puncture bar can be explained as follows. The erosion of the puncture bar elements is initially observed at the top and bottom edges of the contact interface (edges first contacting with the monolithic cylinder) where the elements are overstressed due to edge effects. The erosion extends further to other periphery surface elements of the puncture bar until the conformal contact between the monolithic cylinder and the puncture bar is established. Once the conformal contact is established, the center elements beneath the puncture bar contact surface fail due to excessive shear stress, according to a well-known phenomenon in contact mechanics.

Unlike the LS-DYNA simulation result, erosion of the puncture bar material might not happen in a real puncture test even though the effective stress exceeds the failure limit (leading to surface cracks and even cracks below contact surface). However, to eliminate the erosion of overstressed puncture bar elements observed in the original simulation, an additional LS-DYNA simulation has been performed in which no failure strain is specified in the puncture bar material model (see Figure 2.7.15).

Results from this simulation indicate no erosion on the puncture bar (see Figure 2.7.16), which is consistent with the new material definition. As shown in Figures 2.7.17 and 2.7.18, the time history of the impact force at the contact interface obtained from the additional simulation is similar to the original simulation, suggesting that element erosion in the puncture bar does not affect the loading on the cask surface.

The additional simulation also indicates that the predicted damage on the impacted monolithic cylinder surface is significantly reduced if the puncture bar elements are not allowed to erode. Only a few elements on the monolithic cylinder erode along the edge of the contact interface (see Figure 2.7.19) due to edge effects (i.e., stress concentration). Significant erosion of the monolithic cylinder, on the other hand, is observed in the original simulation (see Figure 2.7.14), since the puncture bar element erosion effectively reduces the overall contact area.

From the above simulations, it can be concluded that the minimum Charpy value prescribed for the shield cylinder is adequate to prevent a significant loss of shielding under all governing Part 71 impact events, and the minimum Charpy values prescribed for the closure lid bolts are adequate to prevent a loss of seal integrity. The details of this evaluation are documented in the Holtec proprietary calculation package [2.1.12].

2.7.2 Crush

An evaluation of package crush is not required for the HI-STAR 180D.

2.7.3 Puncture

10CFR71 specifies that a puncture event be considered as a hypothetical accident condition subsequent to the hypothetical 9-meter drop event. For this event, it is postulated that the package falls freely through a distance of 1 meter (40 inch) and impacts a 15 cm (6 inch) diameter mild steel bar. The effects of the puncture drop will, quite ostensibly, be most severe when the steel bar is perpendicular to the impact surface. Therefore, all puncture analyses assume that the bar is perpendicular to the impact surface. Puncture is considered on the sidewall, as discussed in

Subsection 2.7.1.4, and on the top end (a puncture on the bottom end is not bounding since there is a full welded connection, rather than a bolted connection that needs to remain intact).

Two independent methods are used to analyze the hypothetical puncture event. The first method uses the LS-DYNA simulation model to examine the puncture accidents. The same FE model used for top-end drop is retained for the top end puncture analysis. A mild steel bar, having the appropriate dimensions, is added to the model, placed in the proper orientation, and fixed to the ground. The package is then assumed to have a known initial velocity at contact with the bar. For conservatism, the side puncture model only credits the solid portion of monolithic shield, which is inboard from the neutron shield cavities. Further details of the simulation model and the results (all output figures) for the top end puncture and side puncture are provided in the Holtec Proprietary calculation packages [2.6.1] and [2.1.12], respectively.

The second method uses energy principles and strength of materials formula to determine the primary stress intensities in the containment boundary. In particular, local penetration is examined by comparing the potential energy of the falling cask with the strain energy required to shear a circular plug of material from an otherwise rigid plate. For the top end puncture, the Impact Limiter is conservatively ignored. The primary stress intensity in the containment shell due to the side puncture is calculated assuming that the shell deflects like a cantilever beam, which is fixed at the shell cross-section through the cask centroid. The stress in the closure lid away from the immediate vicinity of the impact is calculated by considering a simply supported circular plate under a concentrated load at its center. Details of the analysis and the results from each puncture accident are provided in the Holtec Proprietary calculation package [2.1.12]. The key results of the puncture analysis are summarized in Table 2.7.7.

The results from the puncture analyses yield the following conclusions:

i. The bolted joint maintains its integrity; the margin-against-leakage parameter, m, (defined in Table 2.6.1) remains at the maximum possible value of 10.

ii. No thru-wall penetration of the containment boundary or dose blocker parts (shield cylinder) is indicated. The total depth of local indentation is a fraction of the available material thickness in the path of the penetrant. Although the outer region of the monolithic shield (where the neutron shield cavities are located) is not credited in the model, the steel bar is expected to penetrate this region in the case of a side puncture event (see Figure 2.7.14).

iii. The stress levels in the closure lid, containment shell, and baseplate remain below their respective Level D condition limits.

iv. The monolithic shield cylinder continues to maintain its shielding effectiveness (i.e., no thru-wall cracks).

The above results confirm the structural adequacy of the package under the “puncture” event of §71.73.

2.7.4 Thermal

In this subsection, the structural consequences of the 30-minute fire event, which occurs after hypothetical drop and puncture events, are evaluated using the metal temperature data from Chapter 3 where a detailed analysis of the fire and post-fire condition is presented. Specifically, the evaluations show that:

1. The metal temperature, averaged across any section of the containment boundary, remains below the maximum permissible temperature for the Level A condition in the ASME Code for NB components. Strictly speaking, the fire event is a Level D condition for which Subsection NB of the ASME Code, Section III does not prescribe a specific metal temperature limit. The Level A limit is imposed herein for convenience because it obviates the need for creep considerations to ascertain post-fire containment integrity.

2. The outer surface of the cask, directly exposed to the fire does not slump (i.e., suffer primary or secondary creep). This condition is readily ruled out for steel components since the metal temperature remains below 50% of the metal melting point (approximately 3000ºF).

3. Internal interferences among the constituents of the HI-STAR 180D Package do not develop due to their differential thermal expansion during and after the fire event.

4. Cask closure lid bolts do not unload; therefore, there is no reduction of compression load on the gasket surfaces to a level that may precipitate leakage of gaseous contents from the containment boundary.

Table 2.7.8 provides a summary of the key results obtained from the continued sealing analysis under the fire accident; the details of the finite element solution are documented in the Holtec Proprietary calculation package [2.1.12]. The primary loadings are the initial preload, the internal pressure, and the temperature change of the bolted connection due to the fire event. Because the coefficients of thermal expansion of the lid and flange and the bolt are not significantly different, and because of the large preload on the bolts, the bolt loads do not change significantly from their starting value. As a result, the change in compression on the lands is also not significant. Therefore, the fire event, occurring after a 9-meter drop accident or a puncture, does not lead to loss of seal integrity in either lid. The package, therefore, meets all acceptance criteria set down in Section 2.1 for the postulated fire event.

2.7.4.1 Summary of Pressures and Temperatures

Section 3.4 contains a discussion of the peak temperatures occurring during and after the fire event. It is concluded in that section that:

1. The containment boundary, protected by the monolithic shield, remains below 500 degrees F (SA-203 E material).
2. The containment boundary that is within the confines of the impact limiters remains below 700 degrees F (SA-350 LF3 material).
3. The portion of the containment boundary directly exposed to the fire may have local outer surface temperatures in excess of 700 degrees F, but the bulk metal temperature of the material volume remains under 700 degrees F. All metal temperatures remain well below the "threshold damage temperature".
4. The Holtite-B neutron shield material experiences temperatures in excess of its design limit, leading to a ,minor loss in the cask's neutron shielding capacity.

2.7.4.2 Differential Thermal Expansion

Differential thermal expansions under the limiting conditions of the fire event are evaluated in Subsection 3.4.4. The analyses show that, under the fire condition, there is no restraint of free thermal expansion of the fuel basket.

2.7.4.3 Stress Calculations

Strength of materials calculations are used to evaluate the performance of the bolted joint in the Containment Boundary. Analyses show that:

i. The primary stress intensities in the Containment Boundary remain well below the Level D (Faulted Condition) limits.

ii. The bolt stresses in the Containment Boundary joint, due to differential thermal expansion, rise but remain within Level D limits.

iii. The temperature of the Holtite material exceeds its recommended operating limit for a very short duration; hence, a minor amount of loss of neutron shielding will occur.

2.7.5 Immersion - Fissile Material

10CFR71.73(c)(5) specifies that fissile material packages, in those cases where water leakage has not been assumed for criticality analysis, must be evaluated for immersion under a head of water of at least 0.9 m (3 ft) in the attitude for which maximum leakage is expected. Accordingly, the analysis is performed to demonstrate that there will be no water leakage in the package subsequent to the fire.

A head of water at a depth of 0.9 m (3 ft) is equal to 1.3 psi. The head of water (1.3 psi) is bounded by the hypothetical accident condition external pressure for the cask (10CFR71.61), which is considered later. Analyses summarized in this chapter demonstrate the containment component meets the applicable stress intensity allowables for normal conditions of transport and for hypothetical accident conditions (both conditions impose pressures larger than 1.3 psi on the components). Further, it is demonstrated that the sealing function is not impaired under these conditions. Therefore, there is no in-leakage of water into the cask under a head of water at a depth of 0.9 m (3 ft).

2.7.6 Immersion - All packages

This external pressure condition is bounded by the analysis in Subsection 2.7.7.

2.7.7 Deep Water Immersion Test

The HI-STAR 180D containment boundary is subject to an all-around external pressure of 2.0 MPa (290 psi) after applying initial bolt preload. Code Case N-284 is used to evaluate the propensity for containment shell instability assuming the monolithic shielding does not prevent the 290 psi pressure from acting directly on the outer surface of the containment shell. The Holtec Proprietary calculation package [2.1.12] contains the supporting details; it is demonstrated there that there is no yielding of the vessel and that there is no elastic or plastic instability of the containment shell. Since the external pressure acts in a direction to add additional pressure to the lands of the lids, seal opening is not a concern for this accident. The primary stress intensity in the lids, assuming that the lids are subject to 290 psi and are conservatively considered as simply supported plates at the bolt circle, meet the Level D ASME Code limits (this is easily demonstrated by examining the results for the N1 normal load condition summarized in Section 2.6). In-leakage of water through the containment system boundary seals is confirmed to be non-credible to satisfy the intent of ISG-19 [1.2.15]. Therefore, the package meets all acceptance criteria given in Section 2.1 under this immersion condition.

2.7.8 Summary of Damage

The results presented in Subsections 2.7.1 through 2.7.7 show that the HI-STAR 180D Package meets the requirements of 10CFR71.61 and 10CFR71.73. All (plausibly) vulnerable orientations of free drop have been analyzed. Two puncture events have also been considered and reported in the tables in Section 2.7. All safety factors are greater than 1.0 for the hypothetical accident conditions of transport, and the sealing function is maintained at the end of each event and at the end of the sequence. The fuel basket does not experience any primary plastic strain after any of the accidents simulated in this safety analysis effort. Therefore, the HI-STAR 180D package, under the hypothetical accident conditions of transport, has adequate structural integrity to satisfy the subcriticality, containment, shielding, and temperature requirements of 10CFR71.

Specifically, the analyses summarized in this section show that:

i. The HI-STAR 180D containment space will remain inaccessible to the moderator under the immersion event of §71.73, which follows free drop, puncture, and fire.

ii. Both lids will continue to maintain a positive contact load at their interfaces with the flange subsequent to the hypothetical accident event, indicating that both primary and secondary lid gaskets will remain functional to contain the radioactive material and as effective leakage barriers to moderator intrusion into the containment cavity. The torque requirement for the inner closure lid port cover bolts (Table 7.1.1) is also adequate to maintain compression on the port cover seals under Hypothetical Accident Conditions.

iii. Localized plastic deformation under the stabbing action of the mild steel bar is indicated. However, there is no through-wall puncture and the damage is superficial.

iv. The primary stresses in the Metamic-HT panels remain essentially elastic even under the inertia loads from the 9-meter drop event. (Maintaining elastic response, i.e., full deflection recovery after a drop event, imposed on the HI-STAR 180D fuel baskets is a far more stringent criterion than the ASME Level D service condition used in most packages).

Table 2.7.1: Key Modeling Data

Item	Inner Lid Joint	Outer Lid Joint
Bolt pre-stress†† – psi (MPa)	81,000 (558.48)	81,000 (558.48)
Number of bolts represented in the FE models	68†	68†
Representative fuel to containment cavity axial gap (mm)	50	
Axial gap between the cask cavity and the fuel basket (mm)	21	
Axial gap between the cask cavity and the basket supports/shims (mm)	21	
Representative basket to shim and shim to containment cavity radial gap (mm)	6	
Number of elements of the HI-STAR 180D package half model	>500,000	
Number of nodes of the HI-STAR 180D package half model	>488,706	
Metamic-HT Yield and Ultimate Strengths for Fuel Basket	Obtained from Table 2.2.8	

†The total number of bolts for the primary and secondary lid bolting, as shown in the drawing package contained in Section 1.3, is 72. In the FE drop simulation models only 68 bolts are explicitly modeled for the primary and secondary closure lid bolting, however, the stiffness (viz. elastic moduli) and the strength properties (viz. strain vs strain curves) are scaled to account for the unmodeled bolts. Correspondingly, the allowable bolt stress limits are scaled by a factor 1.0588 (72/68) to adjust for the unaccounted 4 bolts.

†† The preload stress listed above considers a factor of 1.0588 to make up for the 4 bolts not explicitly modeled in the FE simulations. Thus the effective preload on each bolt is 76.5 ksi (81 x 68/72).

Table 2.7.2: Effective Moduli of the Design Basis Fuel Assembly

Modulus in the vertical (axial) direction psi (MPa)	1.024×10^6 (7,060)
Modulus in the horizontal (lateral) direction psi (MPa)	†8.5×10^4 (586.05)

†Bounding elastic modulus value is conservatively used in the applicable drop simulations.

Table 2.7.3: Nine-Meter Free Drop Simulations Results Using LS-DYNA

Case No.	Drop Scenario	θ	Maximum Computed Deceleration in g's α_{max}		Maximum Crush Inch		Reference Figure	Comments
			Axial	Lateral	Allowable* Value	Computed Value		
1.	End drop – bottom down (UB**)	90	82.4***	-	15.12	6.42	2.7.1	
2.	End drop – top down (UB)	90	119.6***	-	15.12	6.73	2.7.1	
3.	Side drop (UB)	0	-	60	10.95	10.2	2.7.3	
4.	C.G.-over-corner drop – top down (UB)	62.4	45.2	23.63	30.44	20.8	2.7.2	
5.	Oblique drop (slap down) – primary impact at the top end (UB)	6	-	74	10.95	9.15	2.7.4	Bounding results of the primary and secondary impacts are reported
6.	Oblique drop (slap down) – primary impact at the bottom end (UB)	6	-	65	10.95	9.06	2.7.4	Bounding results of the primary and secondary impacts are reported
7.	Side drop (LB)	0	-	57.6	10.95	10.77	2.7.3	

* Allowable crush based on distance to closest point on steel backbone, except for end drop where allowable crush is 63% of the distance to closest point.

** "UB" indicates Upper Bound crush strength values are used in drop simulation; "LB" indicates Lower Bound crush strength values are used in drop simulation.

*** The maximum deceleration reported in this table is the maximum cask deceleration over the entire drop event. The LS-DYNA model developed for fuel integrity analysis is based on the peak cask deceleration before the fuel assemblies rebound and lose contact with the cask in Cases 1 and 2 (see Section 2.11). The corresponding peak decelerations in the two vertical drop scenarios are 82.4 g's and 75 g's, respectively, per the drop analyses reported in [2.6.1].

Table 2.7.4: Design Basis Decelerations*, β_{max} , for "Static Analysis" of 9-Meter Free Drop

Direction		Deceleration (in g's)	Controlling Drop Scenario
Axial	Top End	120	Top End Drop
	Bottom End	92	Bottom End Drop
Lateral		85	Oblique Drop

* Design Basis Deceleration in each direction is set down to be greater than the largest value of α_{max} from Table 2.7.3 in that direction by a modest percentage (for conservatism).

Table 2.7.5: Equivalent Load from the Design Basis Decelerations, β_{max}

Direction		β_{max} (in g's)	Equivalent Load psi (kPa)	Type of Stress and Location of Maximum Stress
Axial	Top End	120	1,440 (9.93)	Flexure of baseplate, flexure of inner and outer lids, unloading of gasket seals, possible overstressing of bolts, axial in-plane compression of Metamic-HT panels in the fuel basket.
	Bottom End	92	1,104 (7.61)	
Lateral		86	654.5 lbf/inch (114.63 kN/m) per panel	Flexure of Metamic-HT panels, in-plane compression of Metamic-HT panels, flexure of containment shell, monolithic shield cylinder strength.

Table 2.7.6: - Results from 30-Ft Drop Simulations Using ANSYS Static Analysis

Item	ALLOWABLE STRESS†	TOP END DROP	BOTTOM END DROP	SIDE DROP
Inner or Outer Closure Lid Top – Primary Bending Stress Intensity – MPa (ksi)	506.8 (73.5)	386.8 (56.1) SF = 1.31	NA	NA
Containment Shell – Primary Membrane Stress Intensity – Mpa (ksi)	336.8 (48.85)	40 (5.8) SF = 8.42	148.93 (21.6) SF = 2.27	122.0 (17.7) SF = 2.76
Baseplate – Primary Membrane + Bending Stress Intensity – Mpa (ksi)	506.8 (73.5)	NA	288.89 (41.9) †† SF = 1.75	NA
Fuel Basket Panel Lateral Deformation – Maximum Total Deflection < 1 mm?	NA	NA	NA†††	Yes (0.47 mm)
Inner Lid Bolts – Average Service Stress (Stress Intensity) – MPa (ksi) ∗	862.0 (125.025)	727.4 (105.5) SF = 1.19	NA	NA
Inner Lid Bolts – Maximum Service Stress at Extreme Fiber (Stress Intensity) – MPa (ksi) ∗	1047.9 (151.99)	930.8 (135.0) SF = 1.13	NA	NA
Outer Lid Bolts – Average Service Stress (Stress Intensity) – MPa (ksi) ∗	885.1 (128.4)	558.5 (81) SF = 1.58	NA	NA
Outer Lid Bolts – Maximum Service Stress at Extreme Fiber (Stress Intensity) – MPa (ksi) ∗	1068.7 (155.0)	632.3 (91.7) SF = 1.69	NA	NA
Lid Seals Remain Sufficiently Compressed?	NA	Yes	NA	NA
Monolithic Shield Cylinder – Primary Effective Stress (Compared to Ultimate Strength) – MPa (ksi)	482.6 (70.0)	47.4 (6.87) SF = 10.19	97.91 (14.2) SF = 4.9	253.7 (36.8) SF = 1.90

Note: "SF" means Safety Factor. "NA" means Not Applicable or Not Bounding.

† See also Table 2.6.3.

†† As an example, the stress distribution in the baseplate under 30-ft bottom end drop is shown in Figure 2.7.12.

††† During an end drop, the lateral pressure exerted on the fuel basket panels is negligibly small, and therefore the panel deformations are bounded by the side drop results.

∗ The listed allowable limits for the bolting are nominal values from ASME Section II Part D, as summarized in Table 2.6.3. As previously noted in Table 2.7.1, these listed allowable limits can be scaled for the unaccounted bolts in the FE (both LS-Dyna and ANSYS) models. In other words the calculated safety factors for the primary and secondary closure lid boltings are underestimated by a factor of 1.0588.

Table 2.7.7: Minimum Safety Factors for Containment Boundary Components Due to Puncture Event

ITEM	CALCULATED VALUE, MPa (ksi)	ALLOWABLE LIMIT, MPa (ksi)	SAFETY FACTOR
Side Puncture – Primary Membrane Stress Intensity in Containment Shell	239.524 (34.74)†	337.3 (48.9)	1.41
Top End Puncture – Primary Membrane Plus Bending Stress Intensity in Outer Closure Lid	330.95 (48.0)	506.8 (73.5)	1.53

Note:
† The maximum stress result from the FE analysis, as discussed in Subection 2.7.1, is used to quantify the safety factor under the 1m side puncture drop.

Table 2.7.8: Bolted Joint Performance Under the Fire Event

ITEM	CALCULATED VALUE†, MPa (ksi)	ALLOWABLE VALUE, MPa (ksi)
Inner Closure Lid Bolt – Average Service Stress MPa (ksi)	514.3 (74.6)	841.2 (122)
Outer Closure Lid Bolt – Average Service Stress MPa (ksi)	460.6 (66.8)	841.2 (122)

† The tensile stresses in inner and outer closure bolts under the preload condition are 78,860 psi and 76,500 psi, respectively. A load reduction of 50% is assumed for all previous accidents.

Table 2.7.9: Key Performance Objectives for Non-Containment Components of the HI-STAR 180D

Criterion	Result
Effective Stress in Monolithic Shield – Primary Effective Stress Below Ultimate Strength	Yes
Fuel Basket Deformation – Maximum Total Deflection† < 1 mm	Yes

† It is further shown that the average deflection of the basket panel remains below 0.5 mm.

Table 2.7.10: Intentionally Deleted

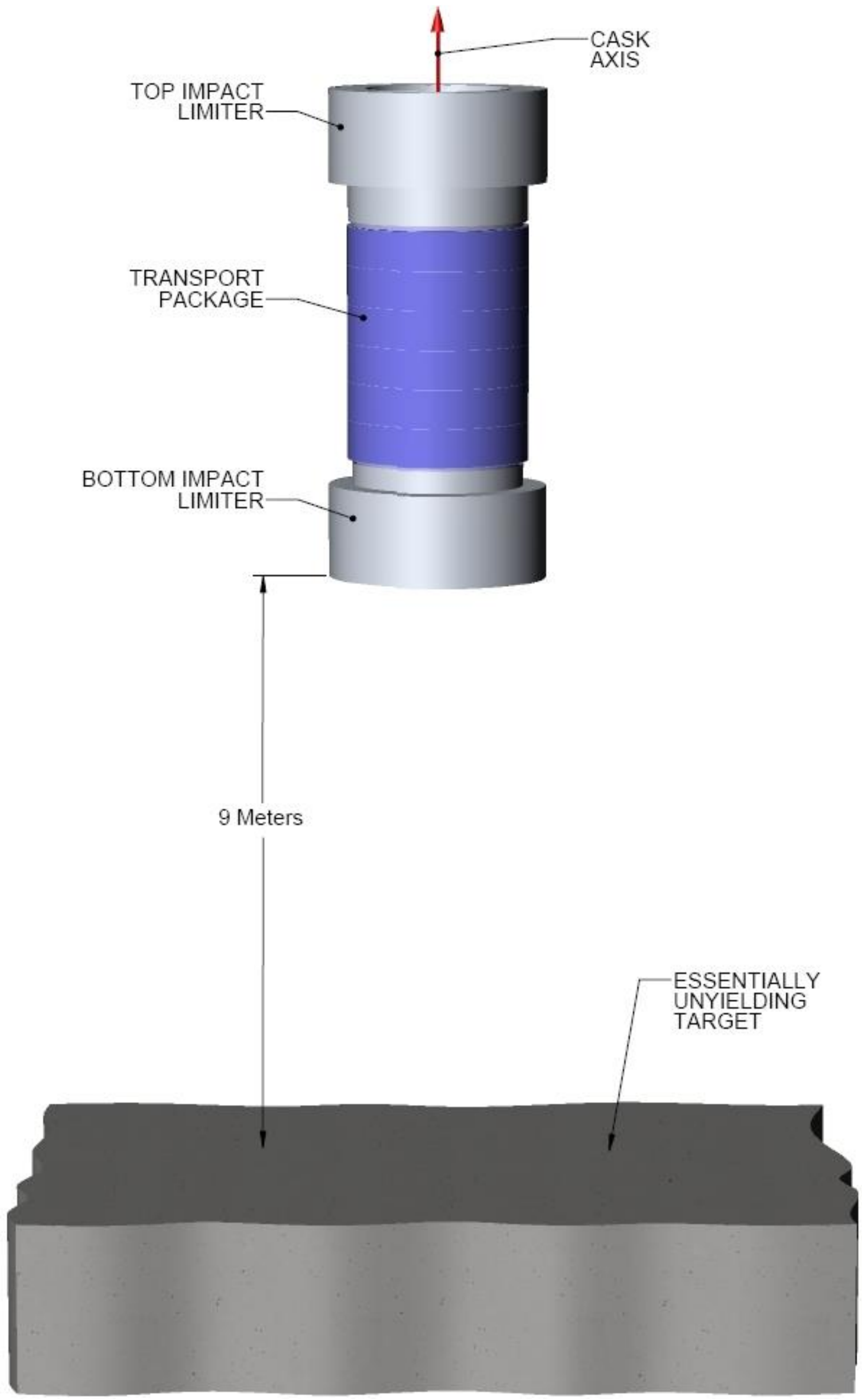

Figure 2.7.1: End Drop, θ = 90

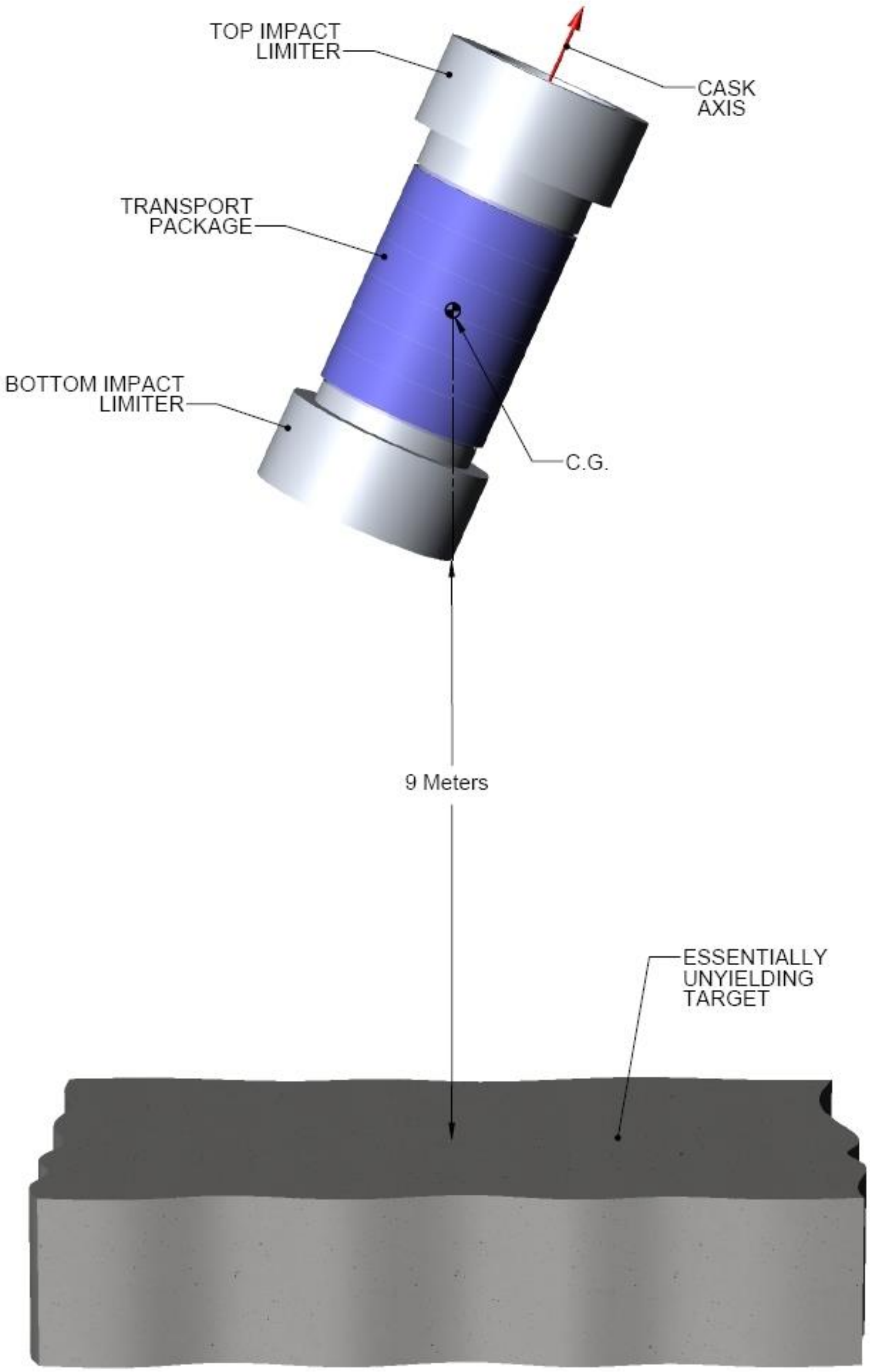

Figure 2.7.2: Center-of-Gravity-Over-Corner Drop

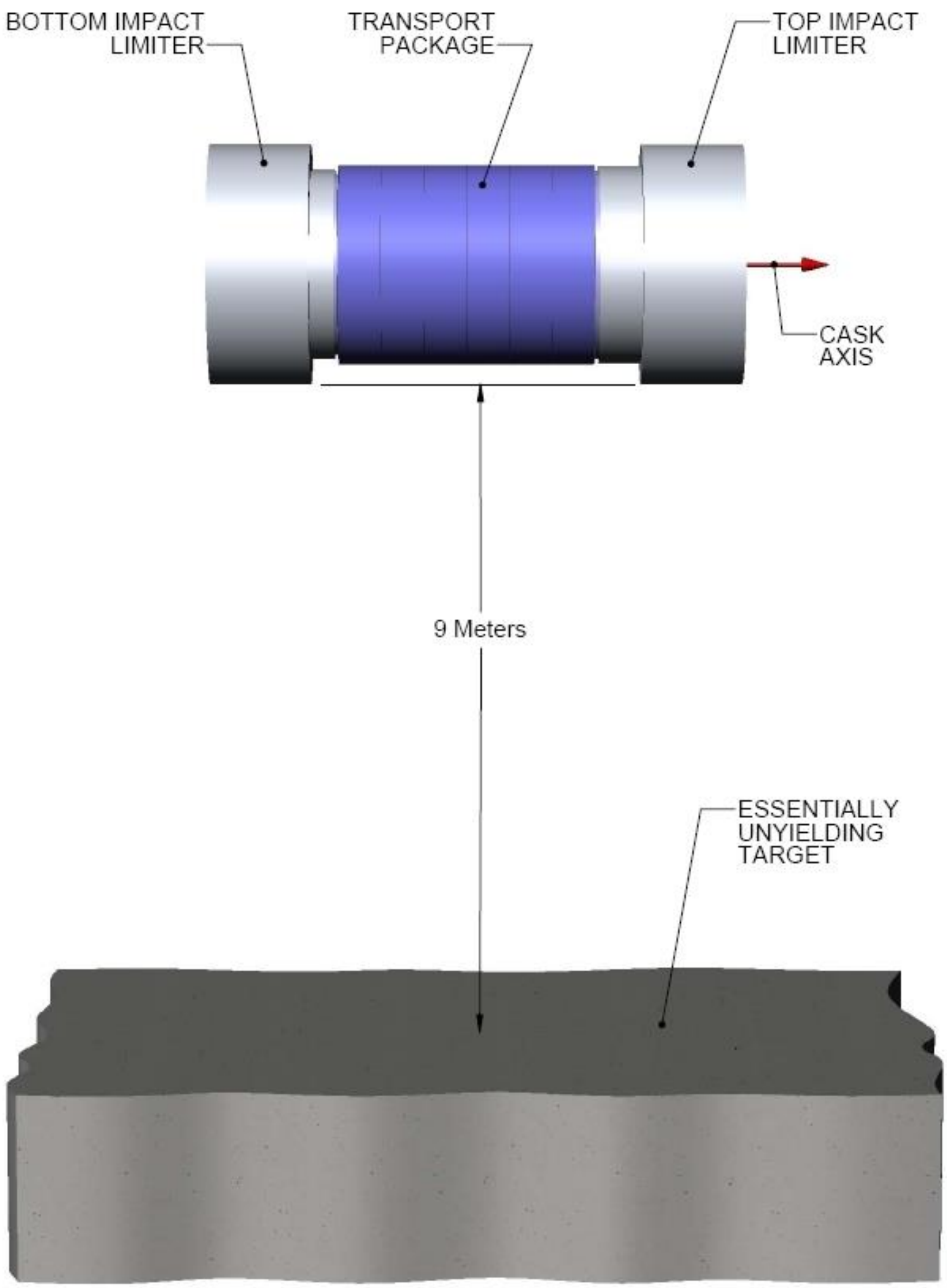

Figure 2.7.3: Side Drop, θ = 0 Degrees

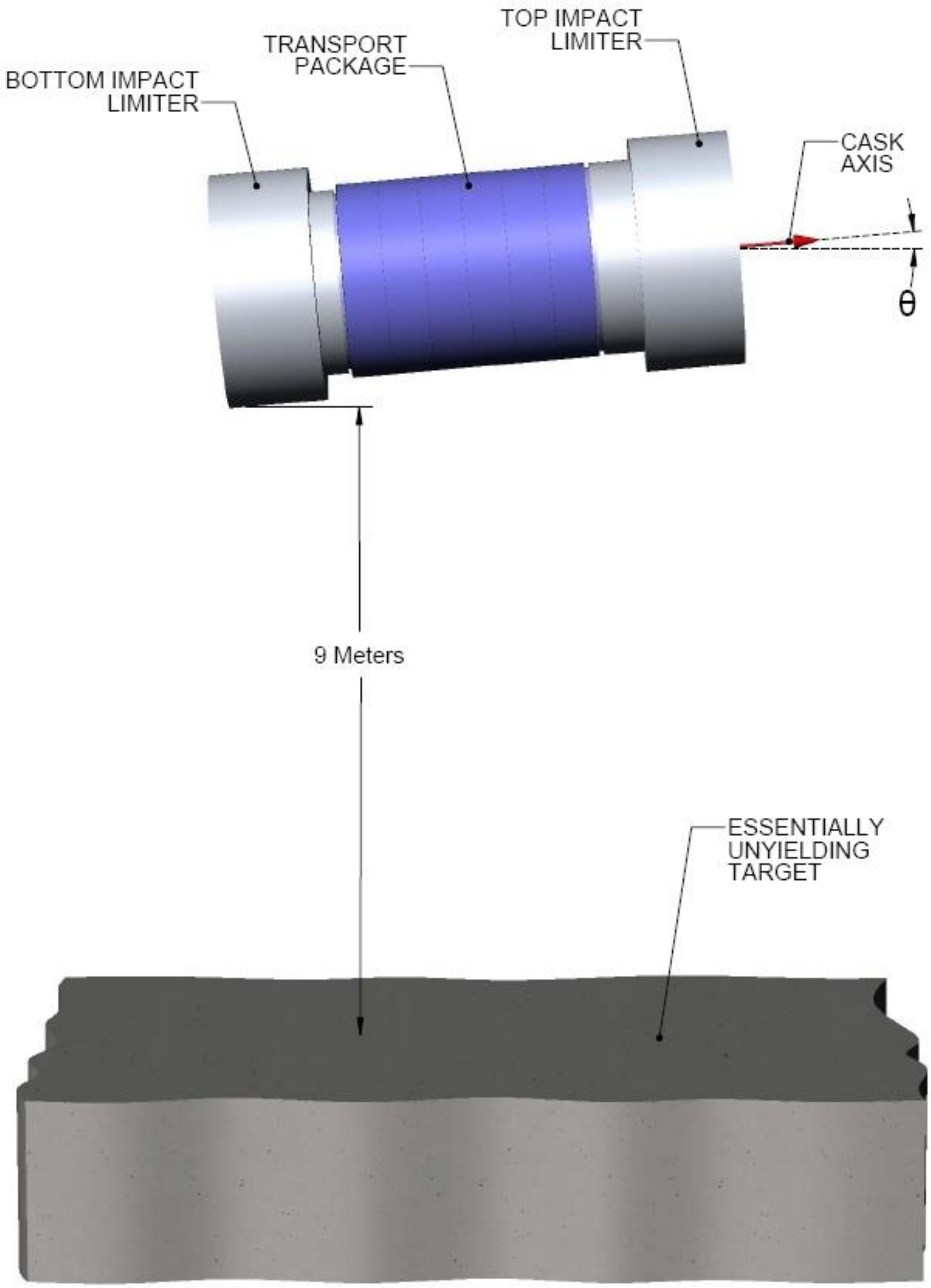

Figure 2.7.4: Oblique Drop (Slapdown), θ Selected to Maximize Secondary Impact

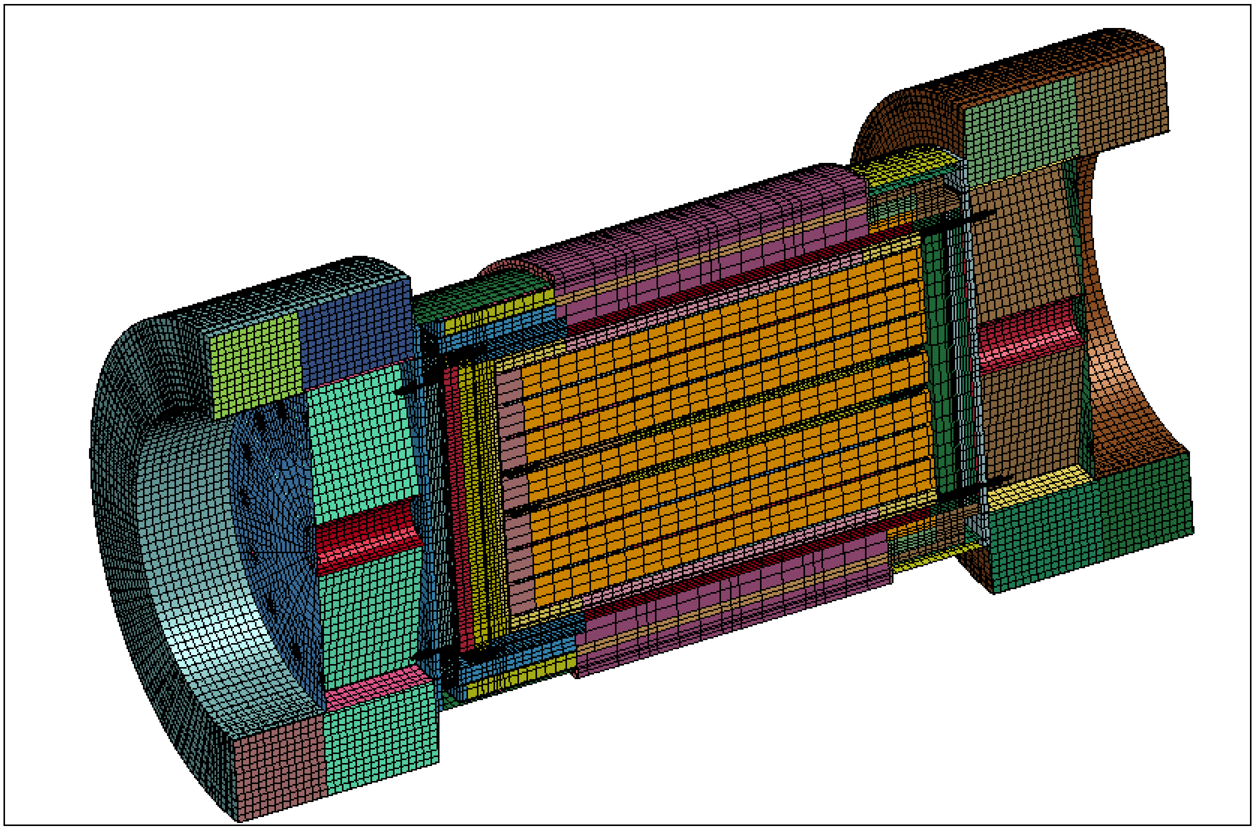

Figure 2.7.5A: HI-STAR 180D Package LS-DYNA Half Model – for Top End & CGOC Drops

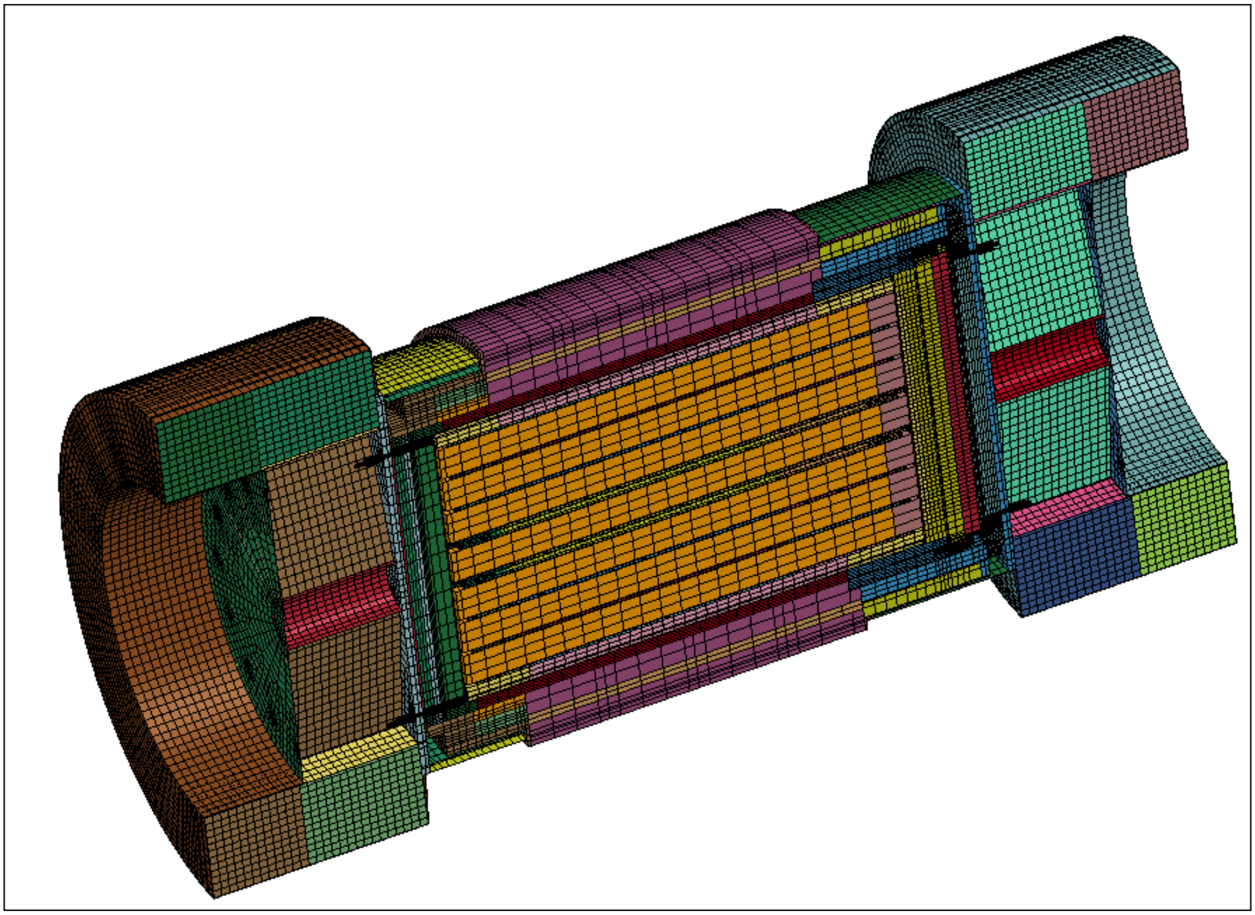

Figure 2.7.5B: HI-STAR 180D Package LS-DYNA Half Model – for Bottom End Drop

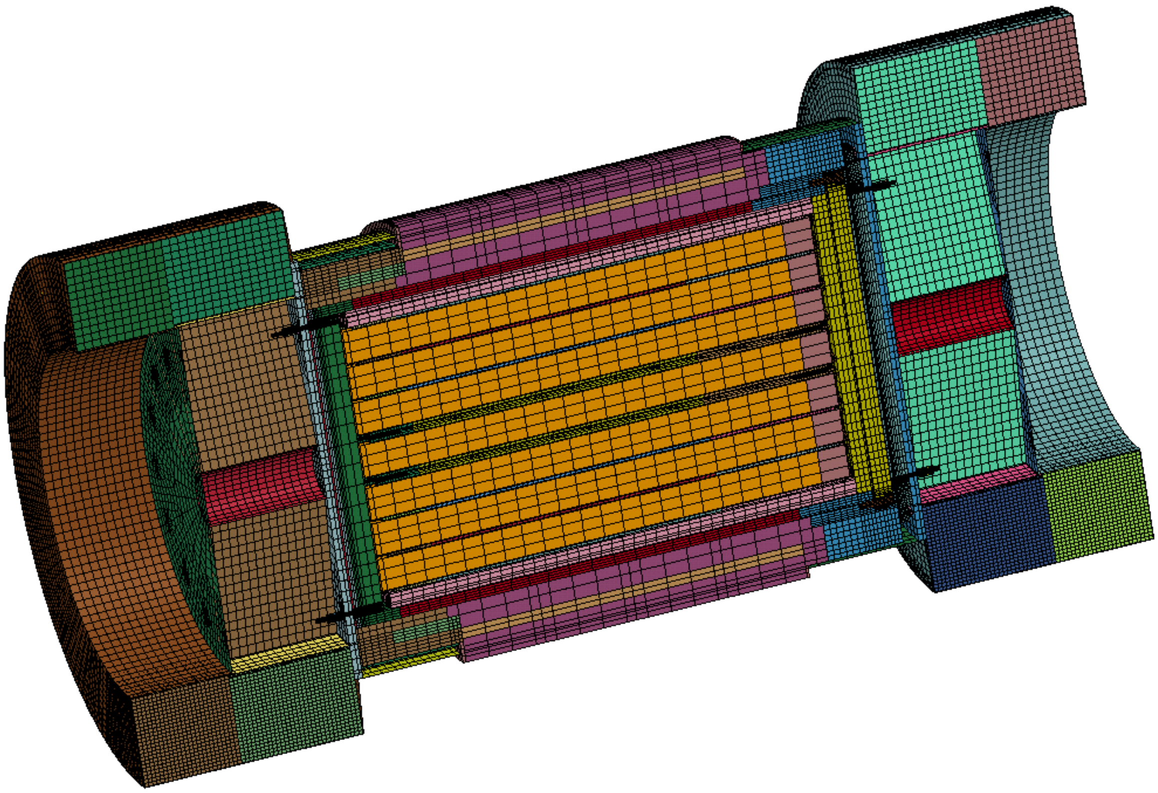

Figure 2.7.5C: HI-STAR 180D Package LS-DYNA Half Model – for Side Drops

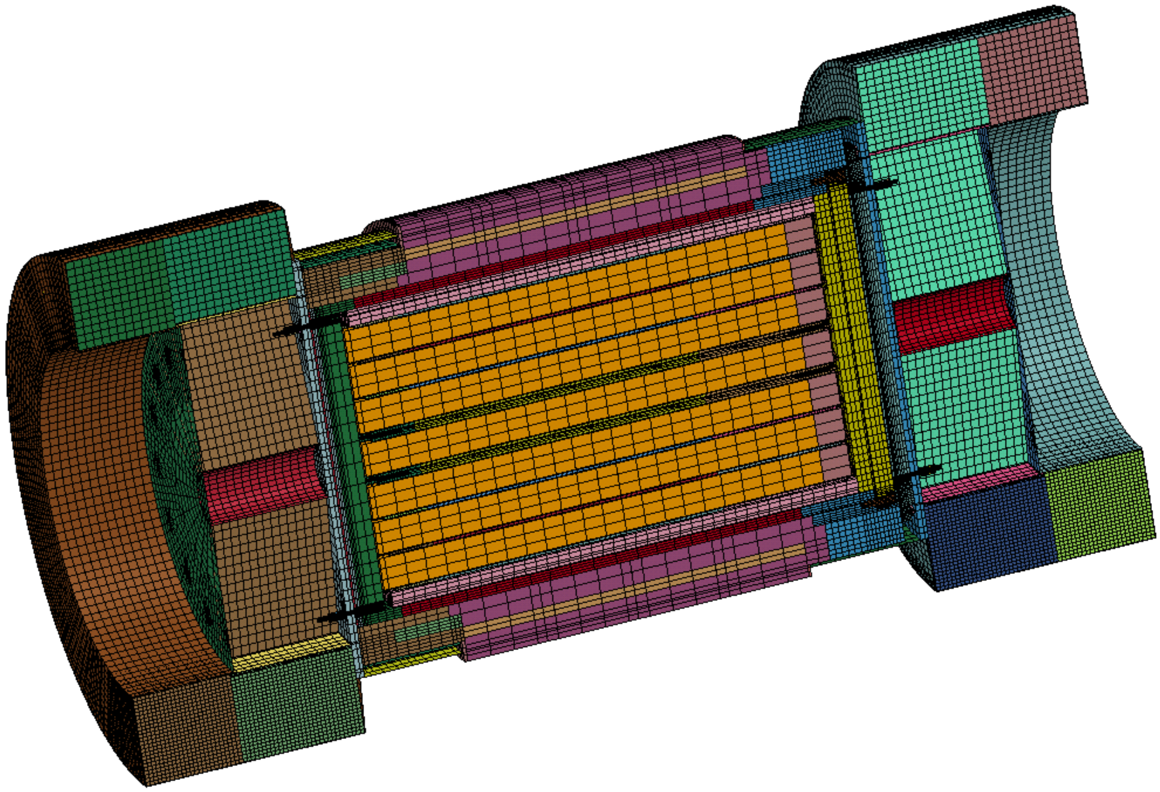

Figure 2.7.5D: HI-STAR 180D Package LS-DYNA Half Model – for Oblique Drops

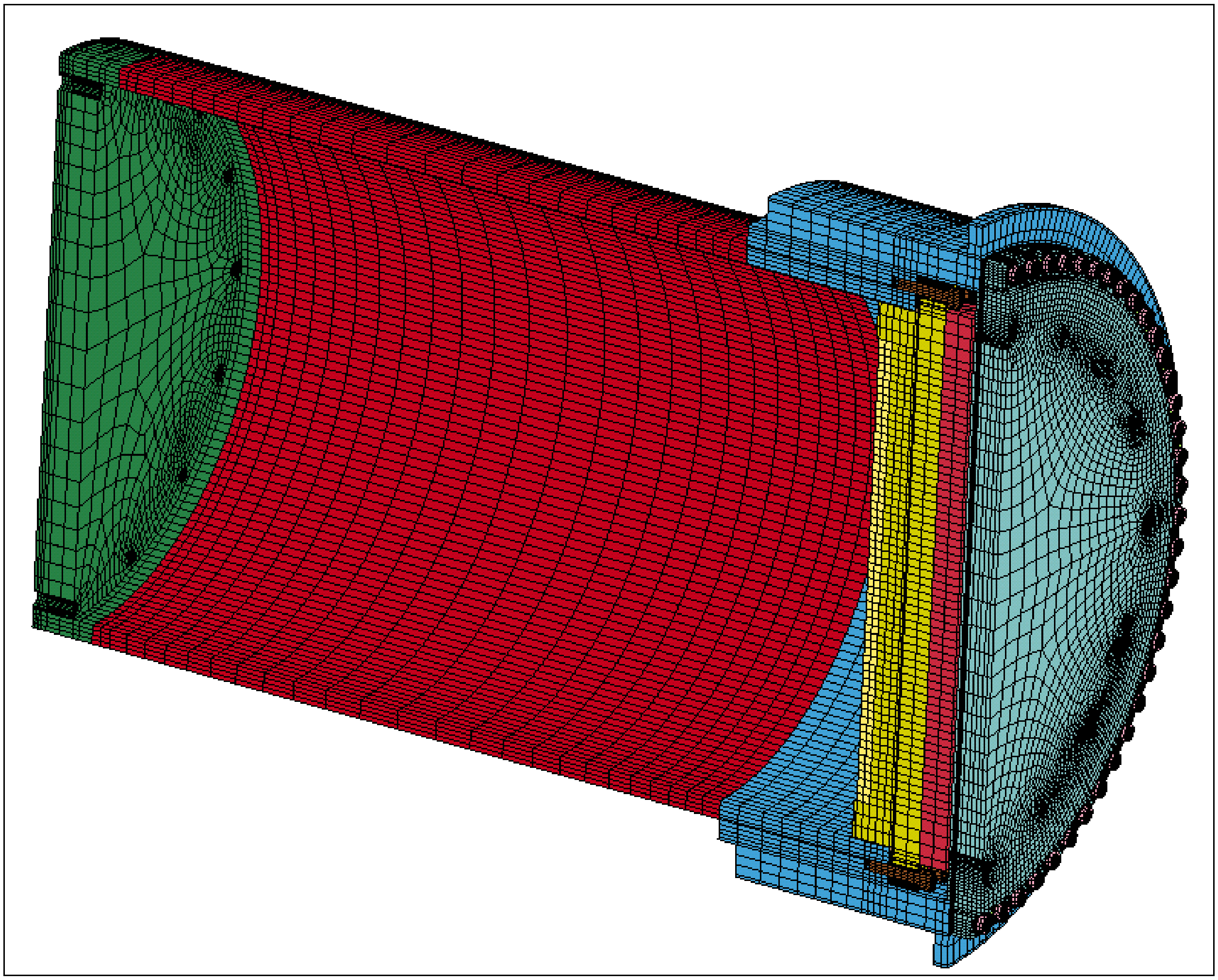

Figure 2.7.6: Finite Element Grid for HI-STAR 180D Containment Components

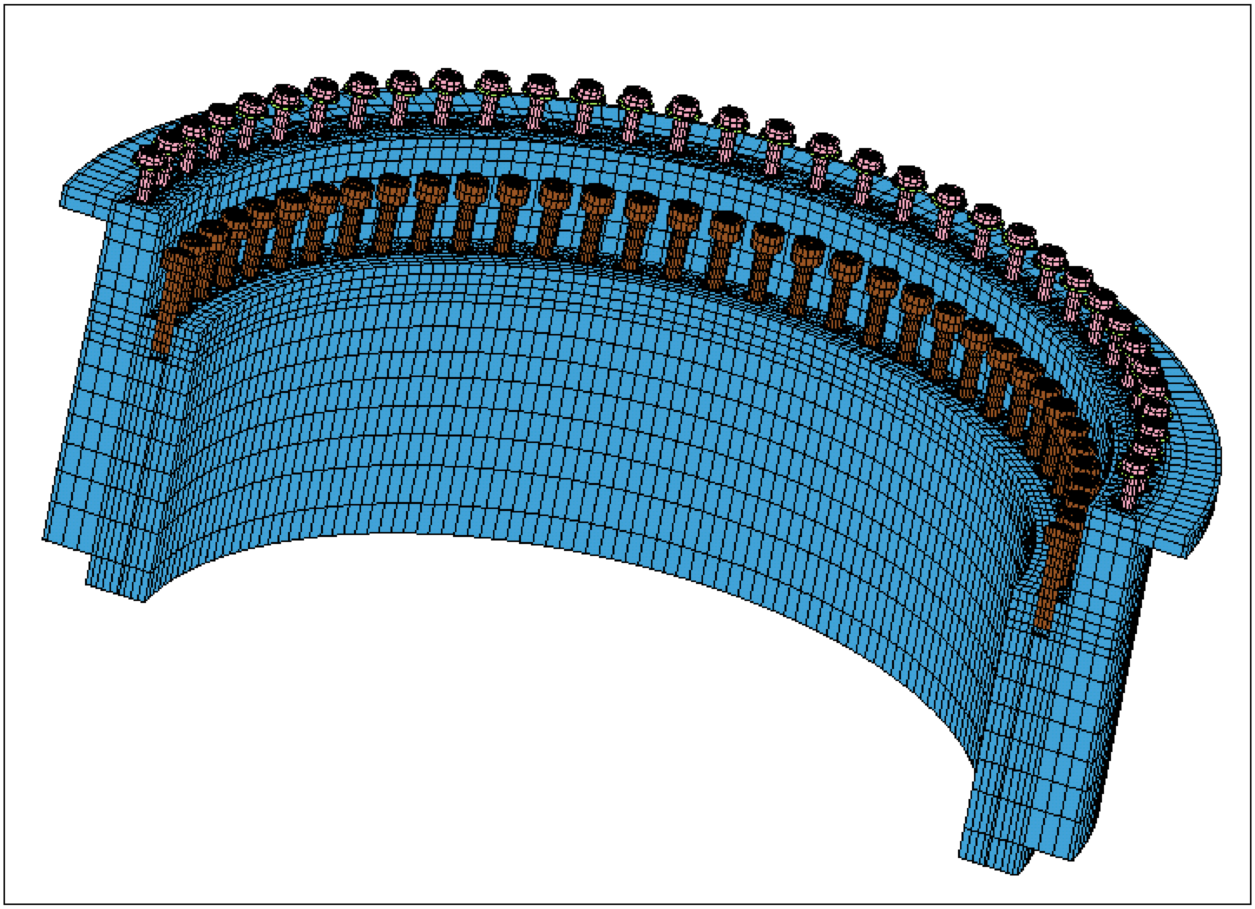

Figure 2.7.7: Finite Element Grid for HI-STAR 180D Top Forging (Containment Closure Flange)

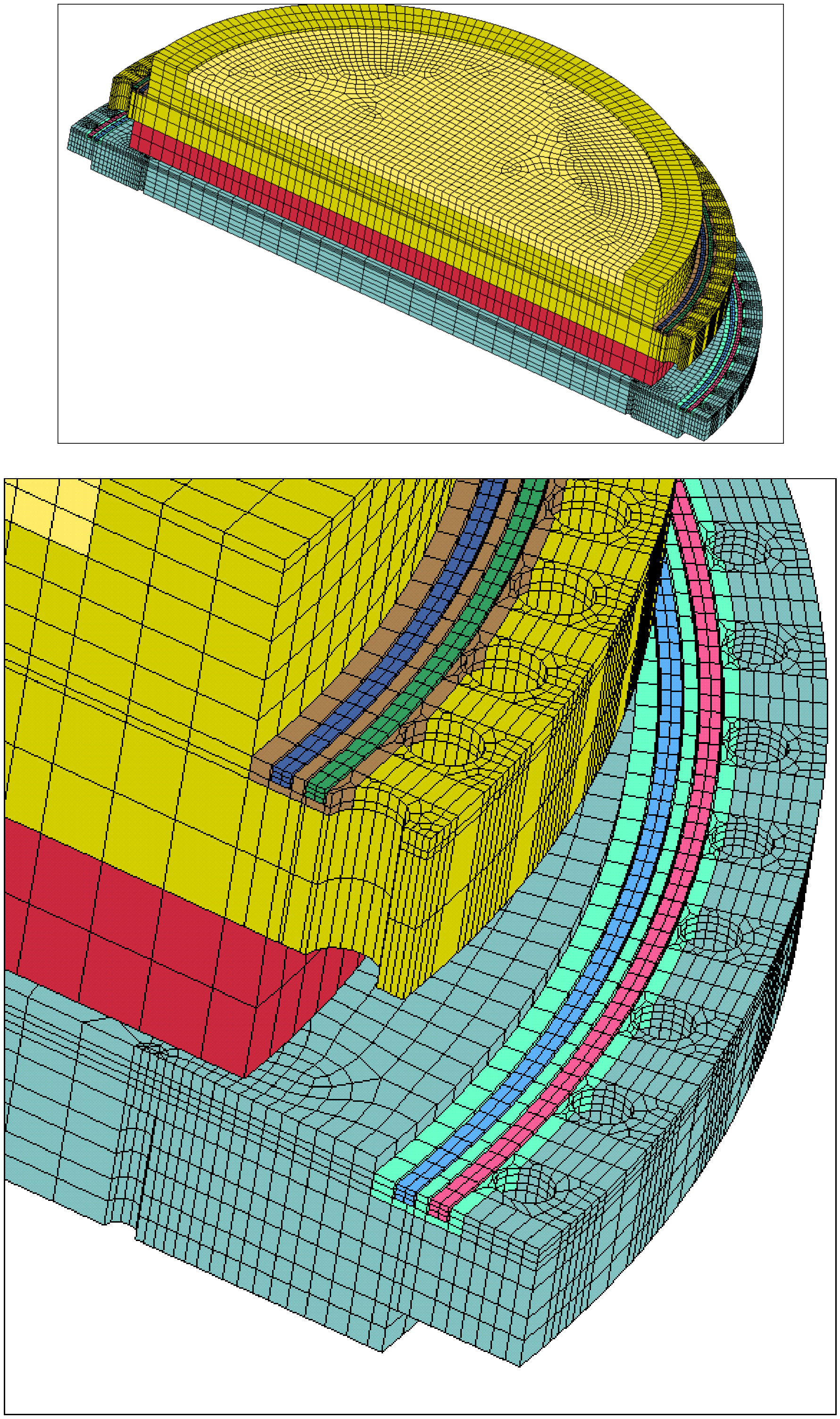

Figure 2.7.8: Finite Element Grid for HI-STAR 180D Closure Lids and Seals

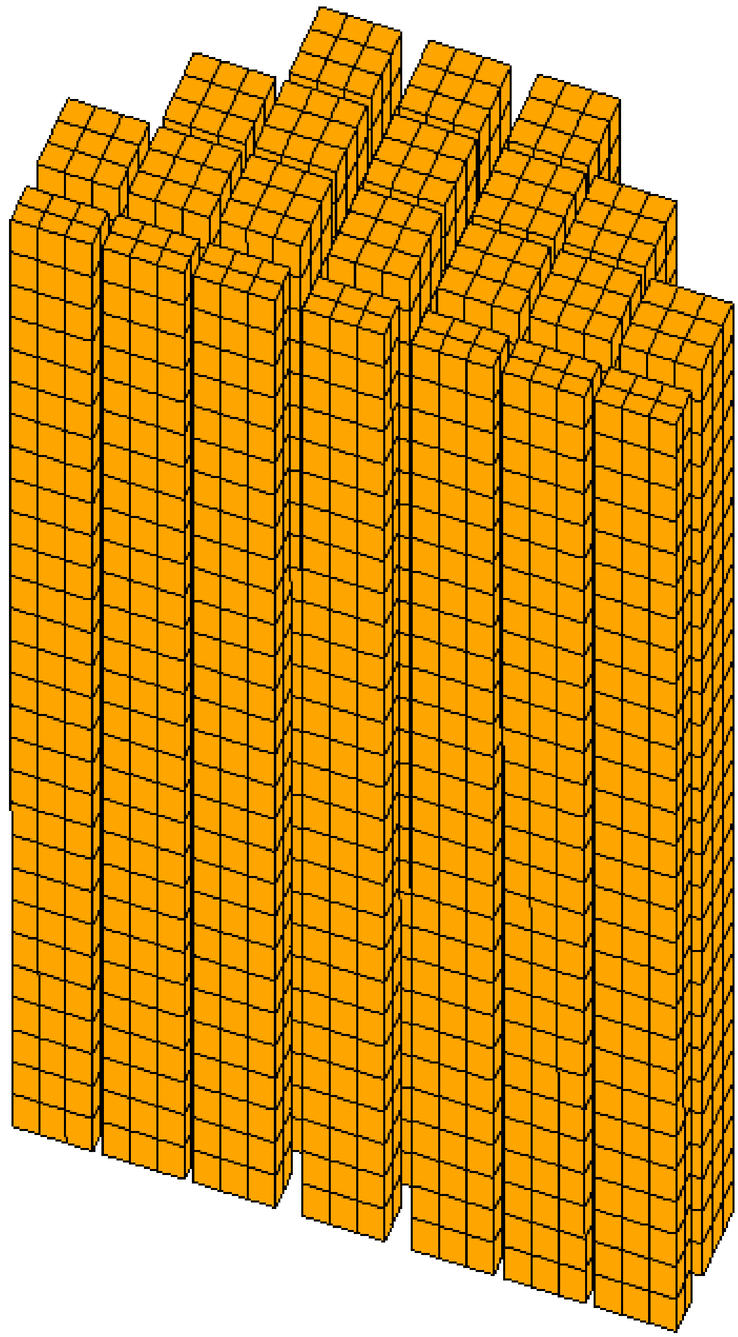

Figure 2.7.9: 37 Fuel Assembly Array Model

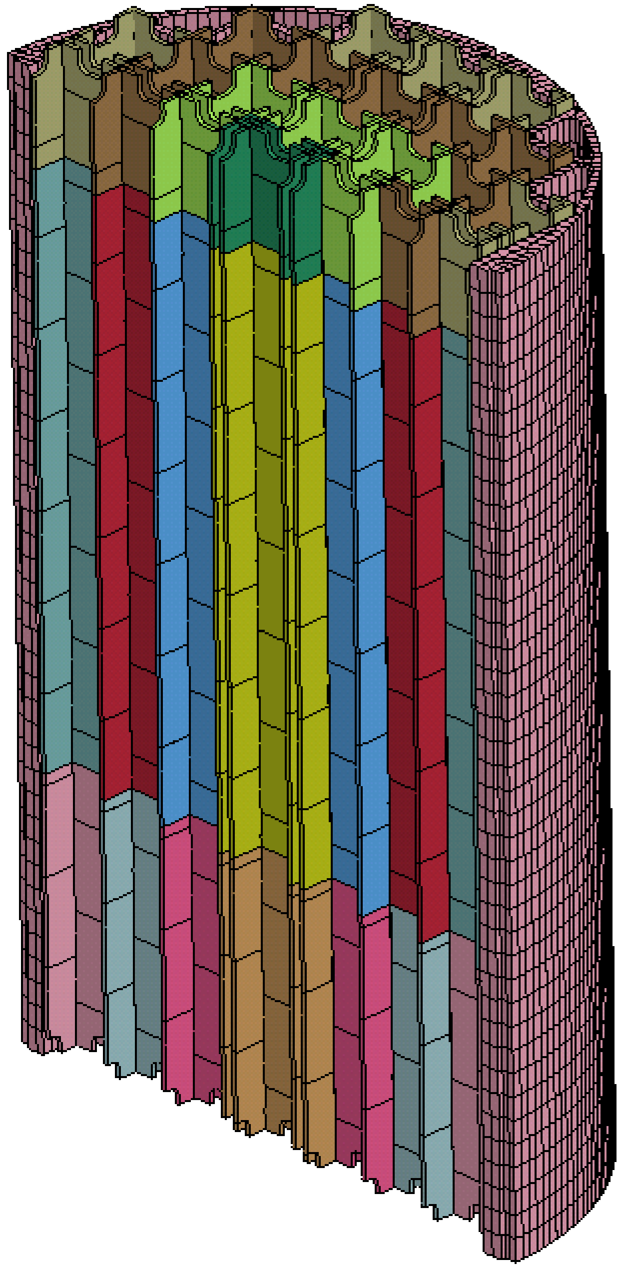

Figure 2.7.10: LS-DYNA Model of F-37 Fuel Basket and Basket Support

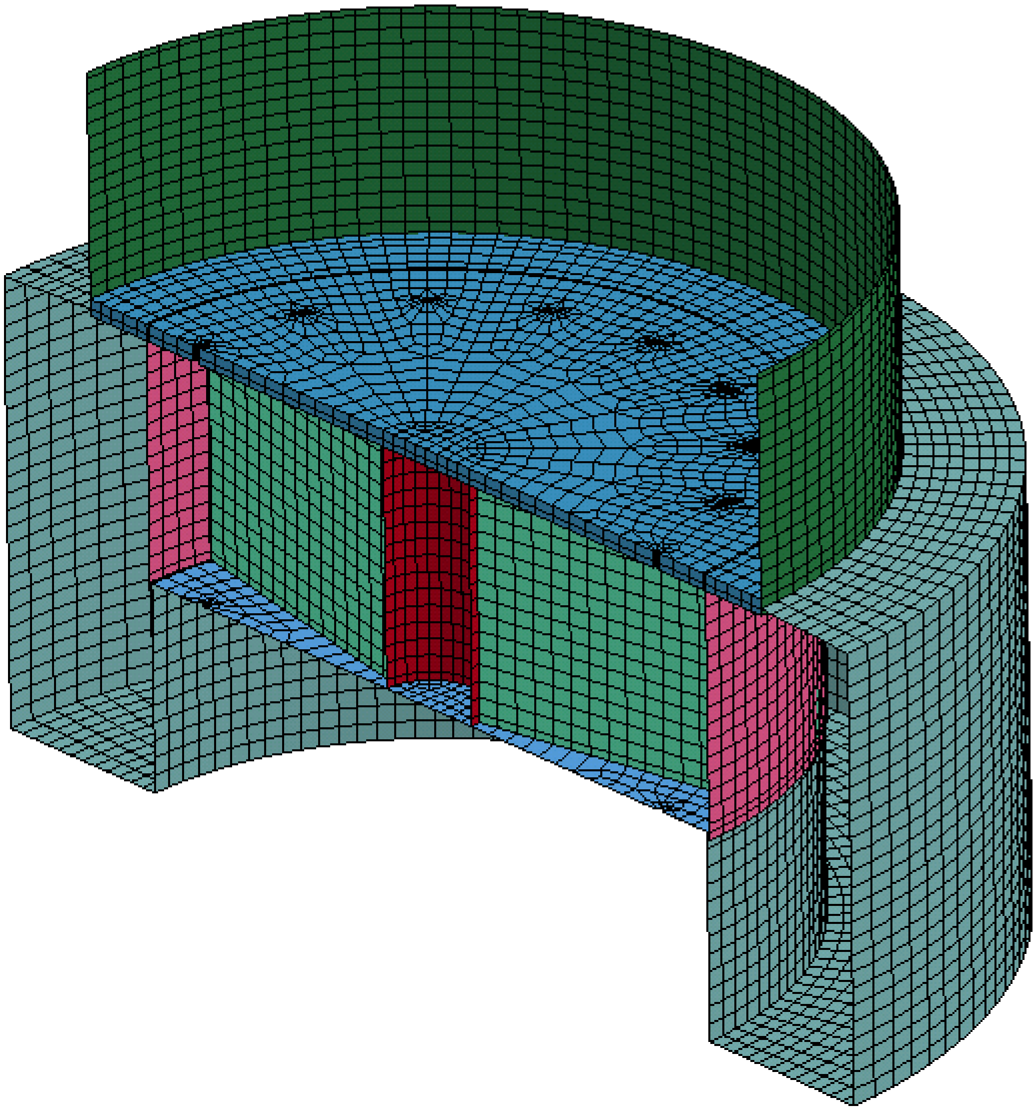

Figure 2.7.11A: LS-DYNA Model of Bottom Impact Limiter (w/o Crush Material Blocks)

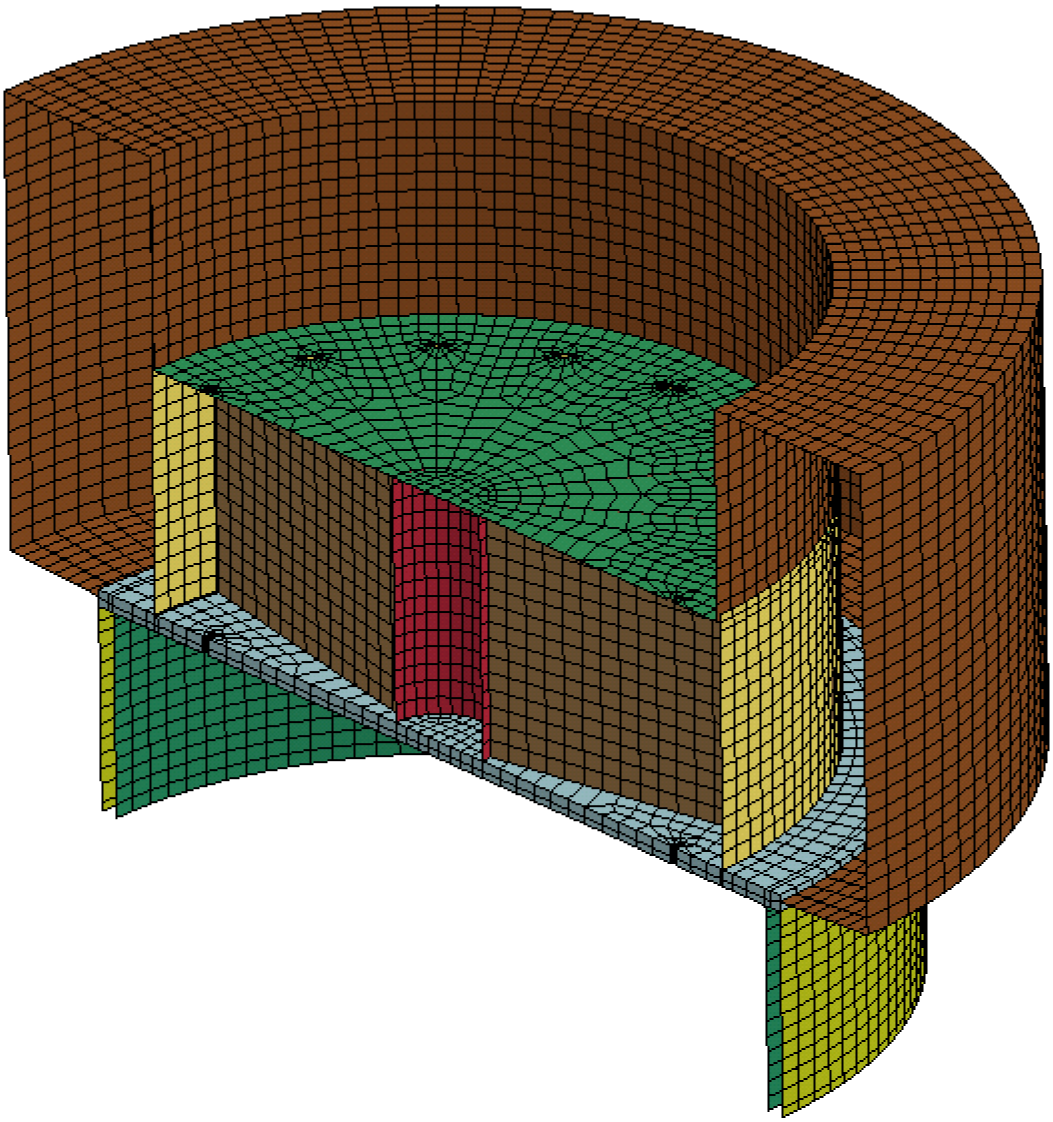

Figure 2.7.11B: LS-DYNA Model of Top Impact Limiter (w/o Crush Material Blocks)

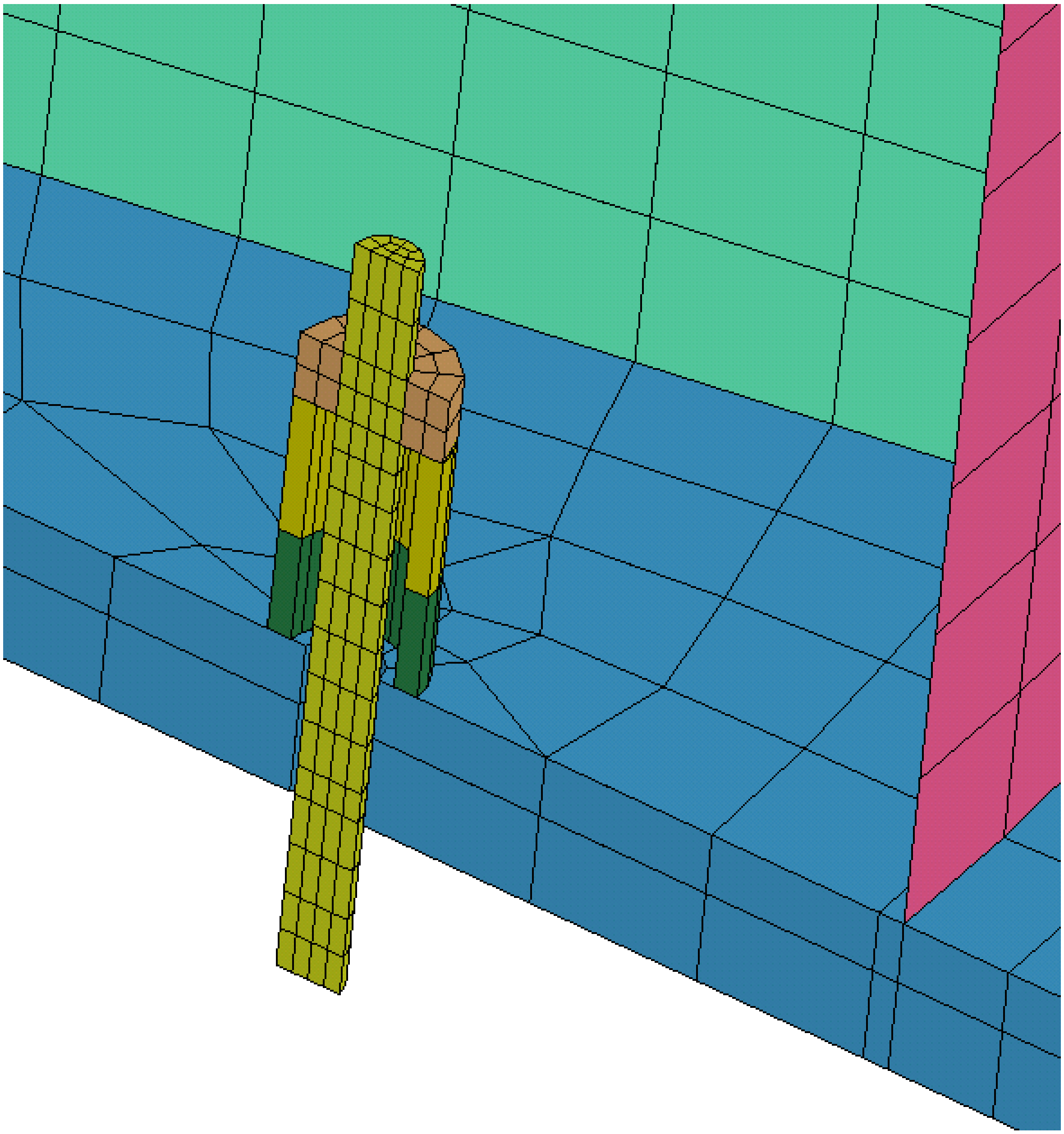

Figure 2.7.11C: LS-DYNA Models of the FSL (in Top Impact Limiter)

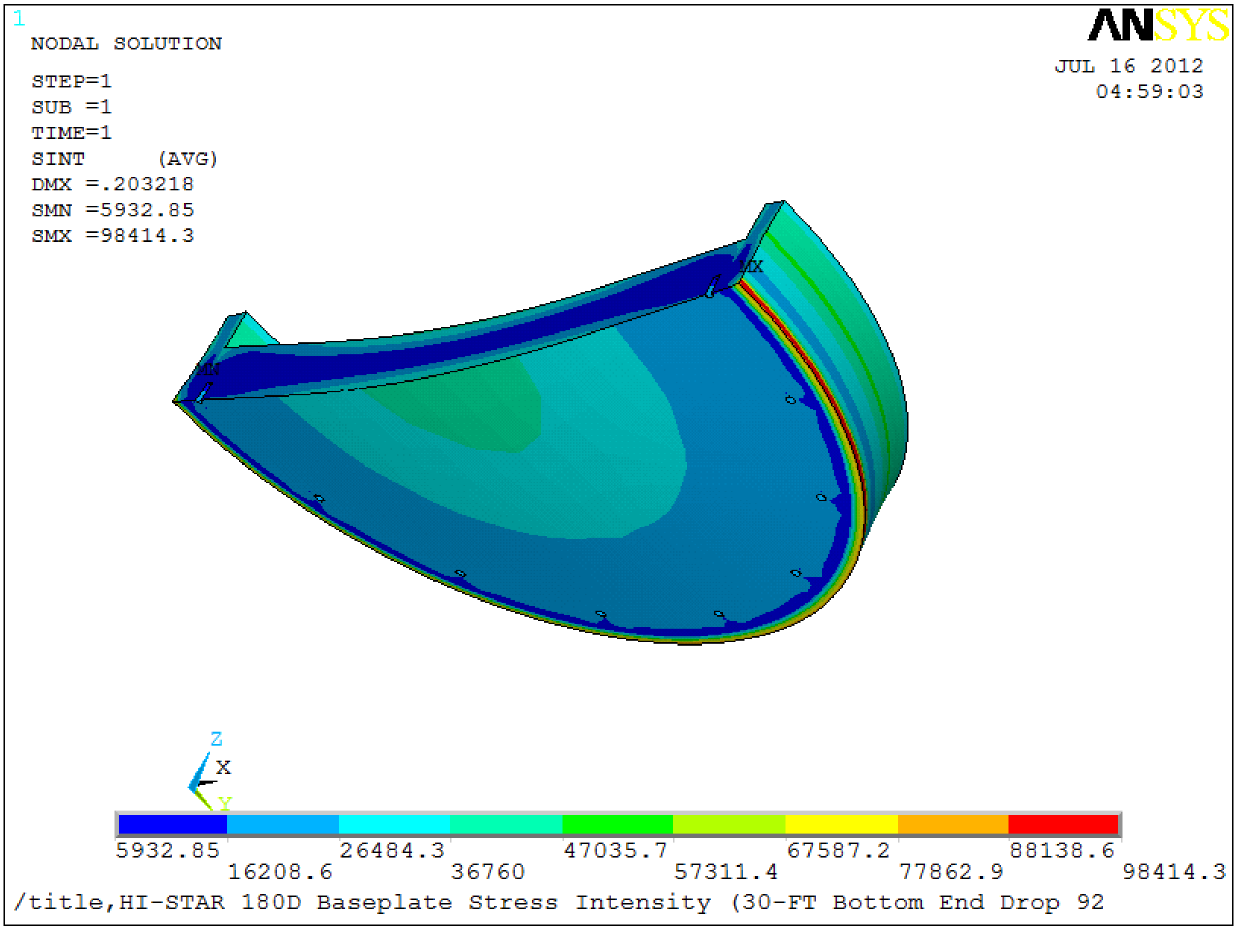

Figure 2.7.12: Baseplate Stress Intensity – 30-FT Bottom End Drop

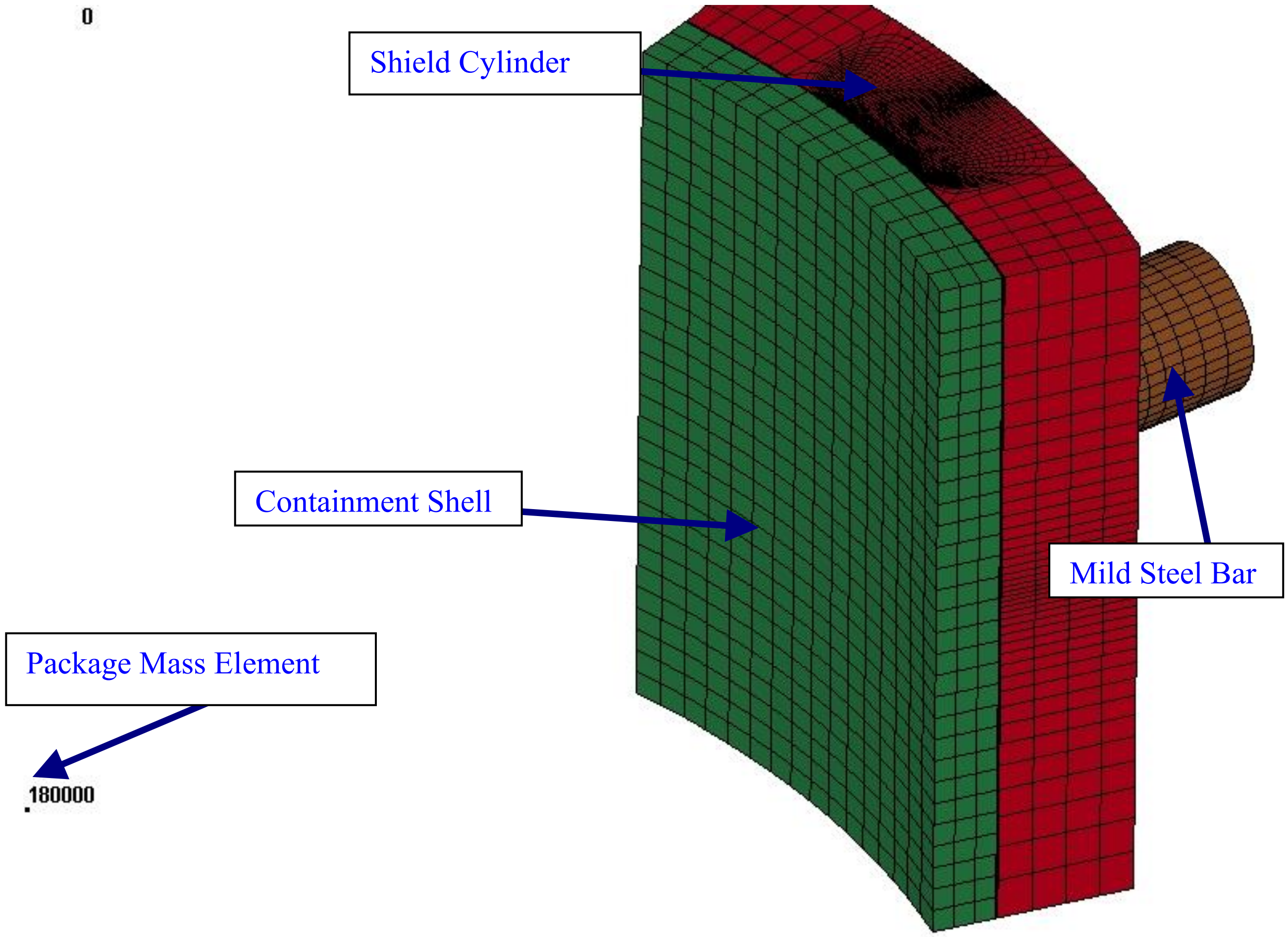

Note that the entire mass of the HI-STAR 180D package is lumped at the node 180000 and the node is rigidly attached to the extreme radial edges of the containment shell.

Figure 2.7.13: LS-DYNA Model for Crack Investigation and Puncture Evaluation

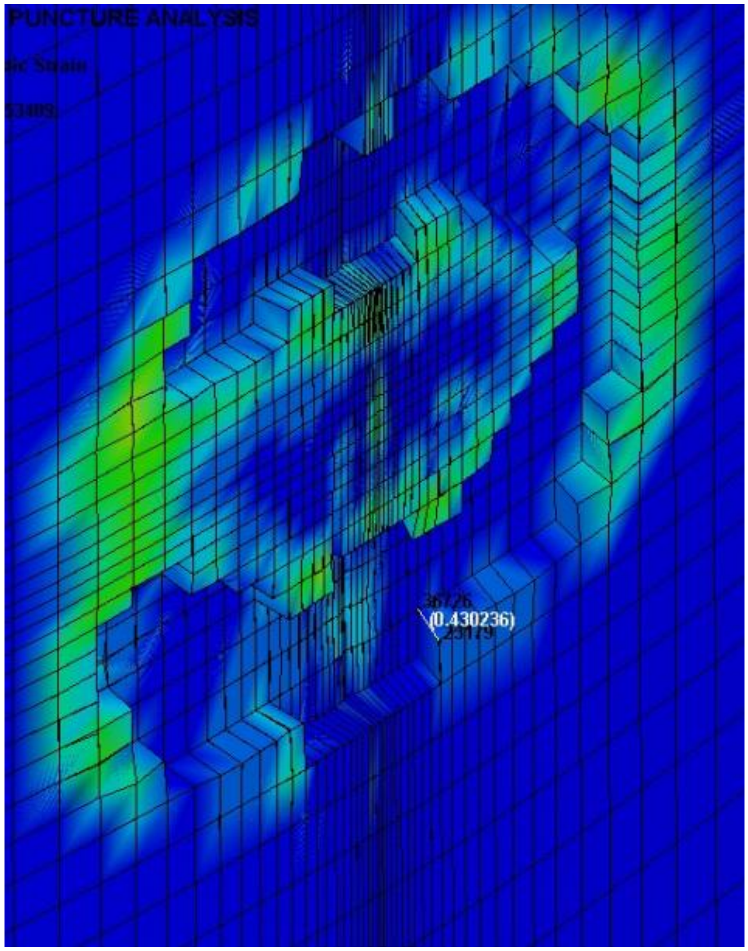

Outer Surface of the Shield Cylinder Depicting the Depth of Indent/Penetration (0.43 in.)

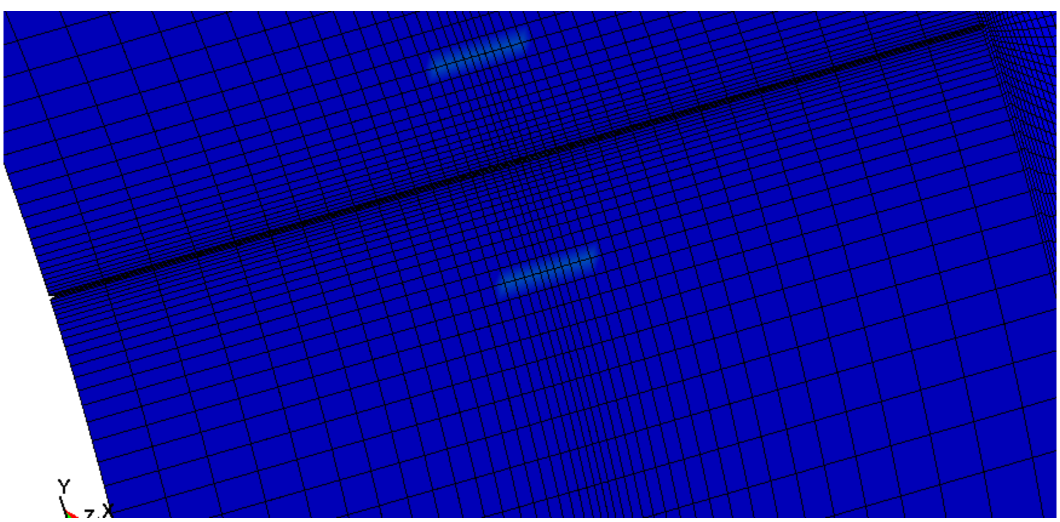

Inner Surface of the Shield Cylinder Depicting No Crack Propagation

Figure 2.7.14: Local Puncture Indentation and Intact Crack Region on the Shield Cylinder (With Puncture Bar Erosion)

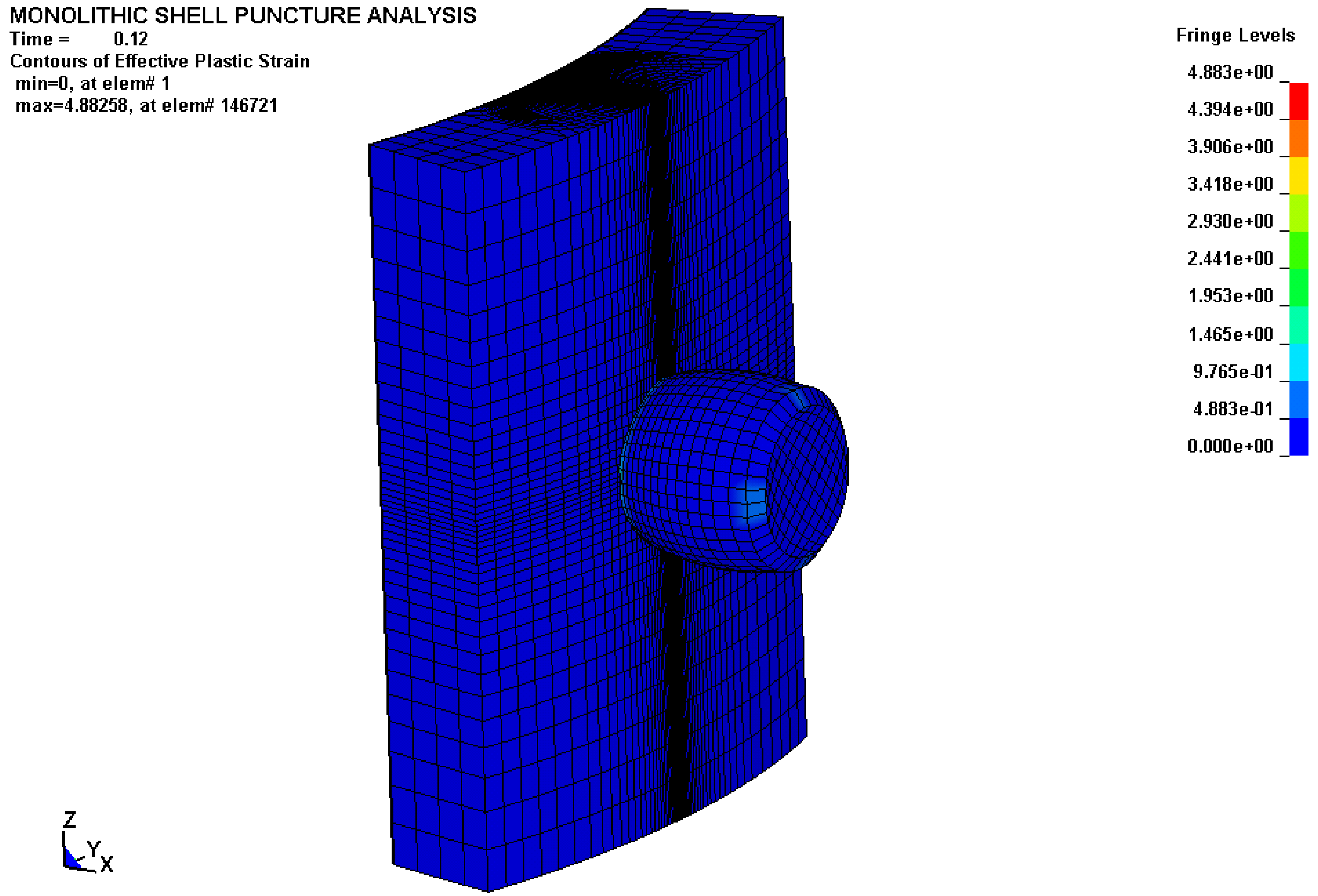

Figure 2.7.15: Puncture Bar and Monolithic Cylinder at the End of Simulation (No Puncture Bar Erosion)

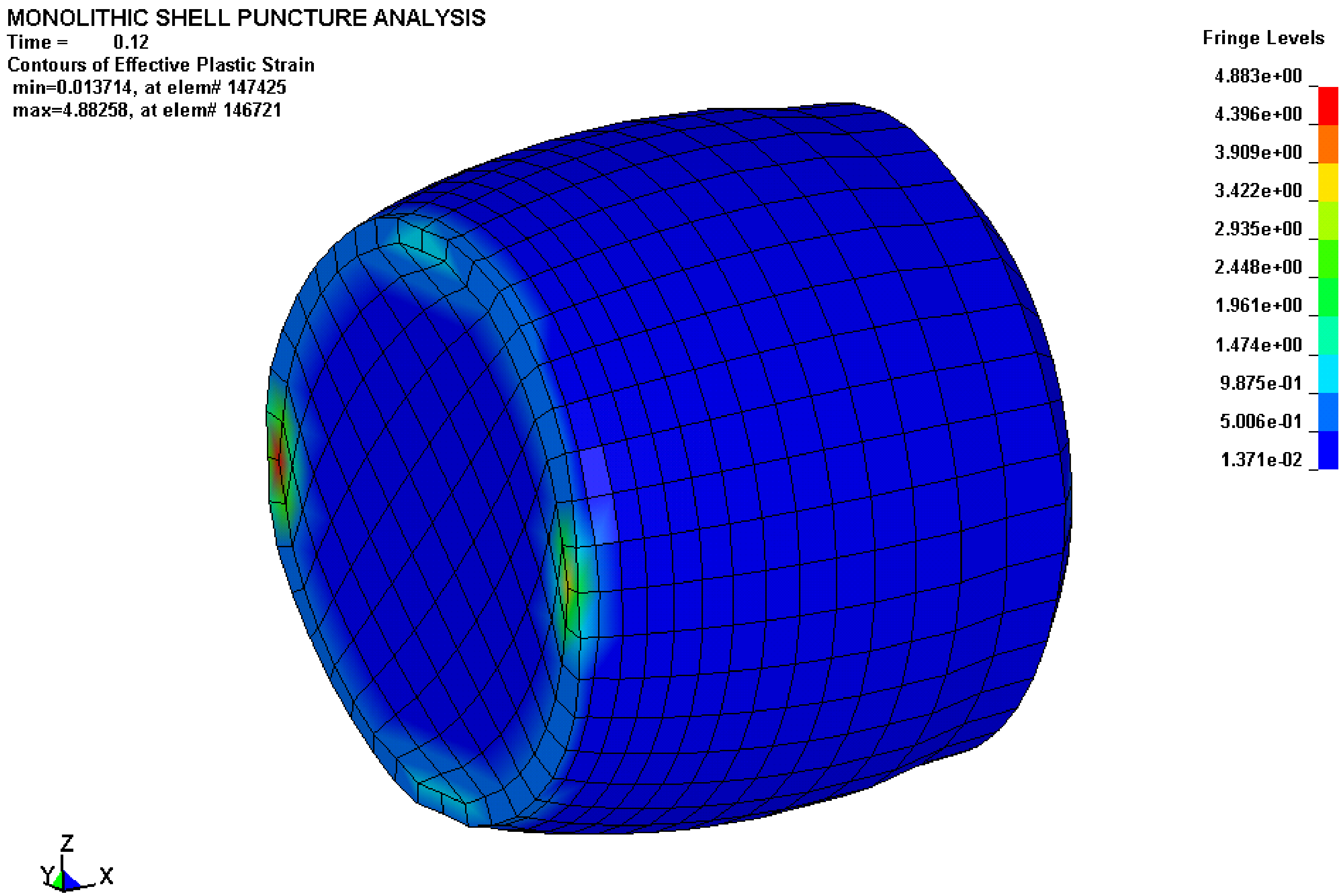

Figure 2.7.16: Final Deformed Shape of Puncture Bar (No Puncture Bar Erosion)

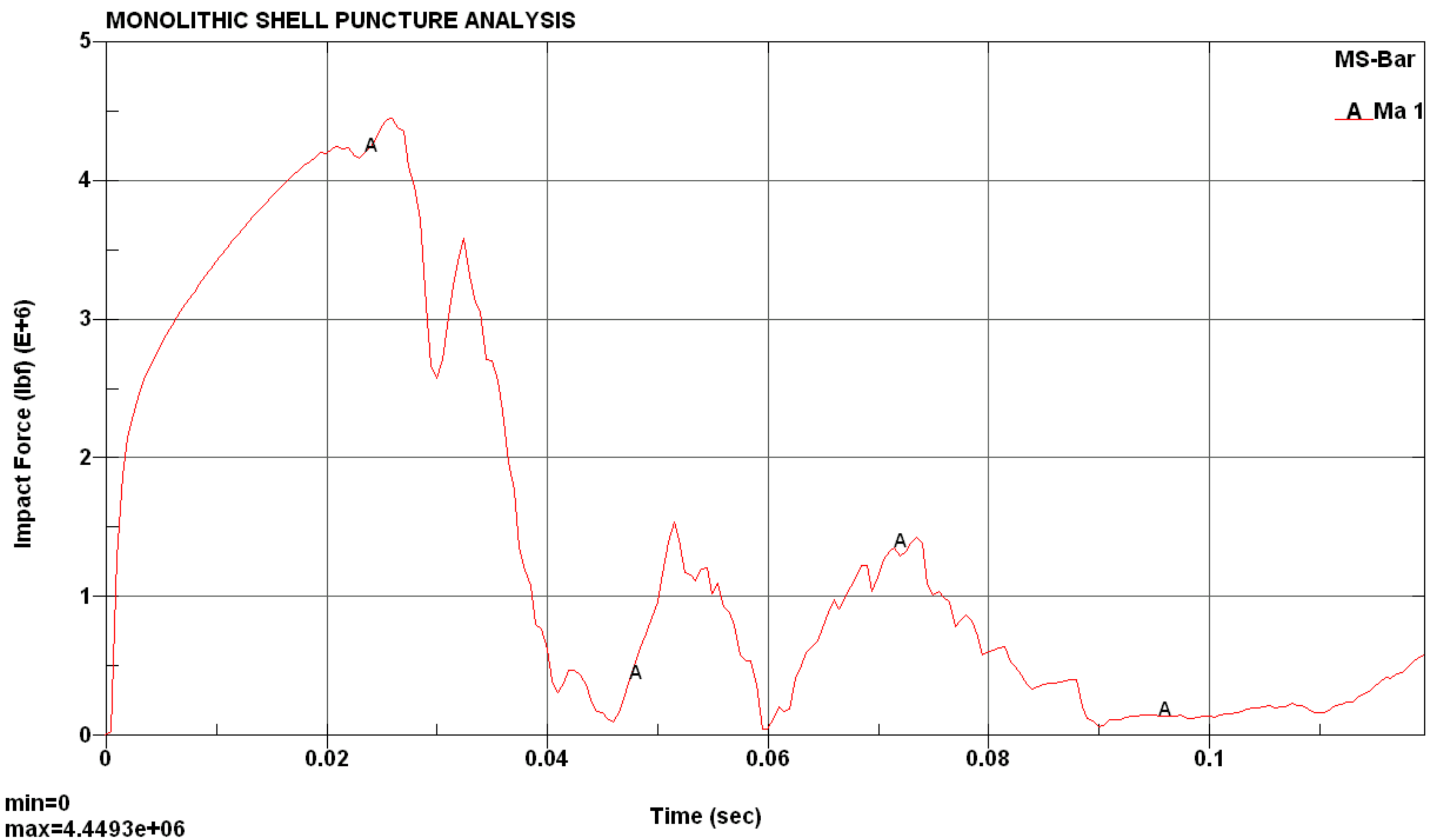

Figure 2.7.17: Impact Force Time-History (With Puncture Bar Erosion)

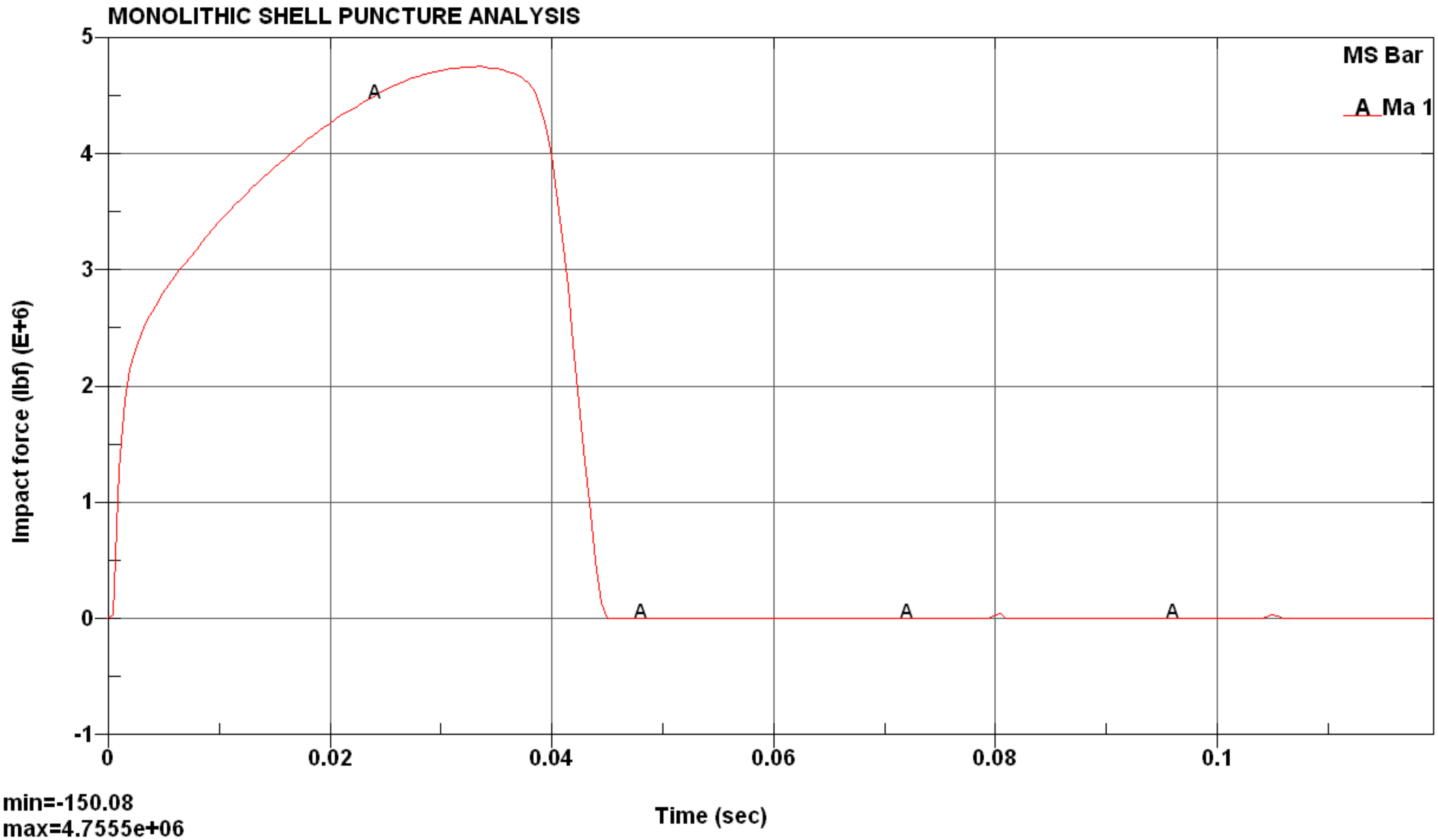

Figure 2.7.18: Impact force Time-History (No Puncture Bar Erosion)

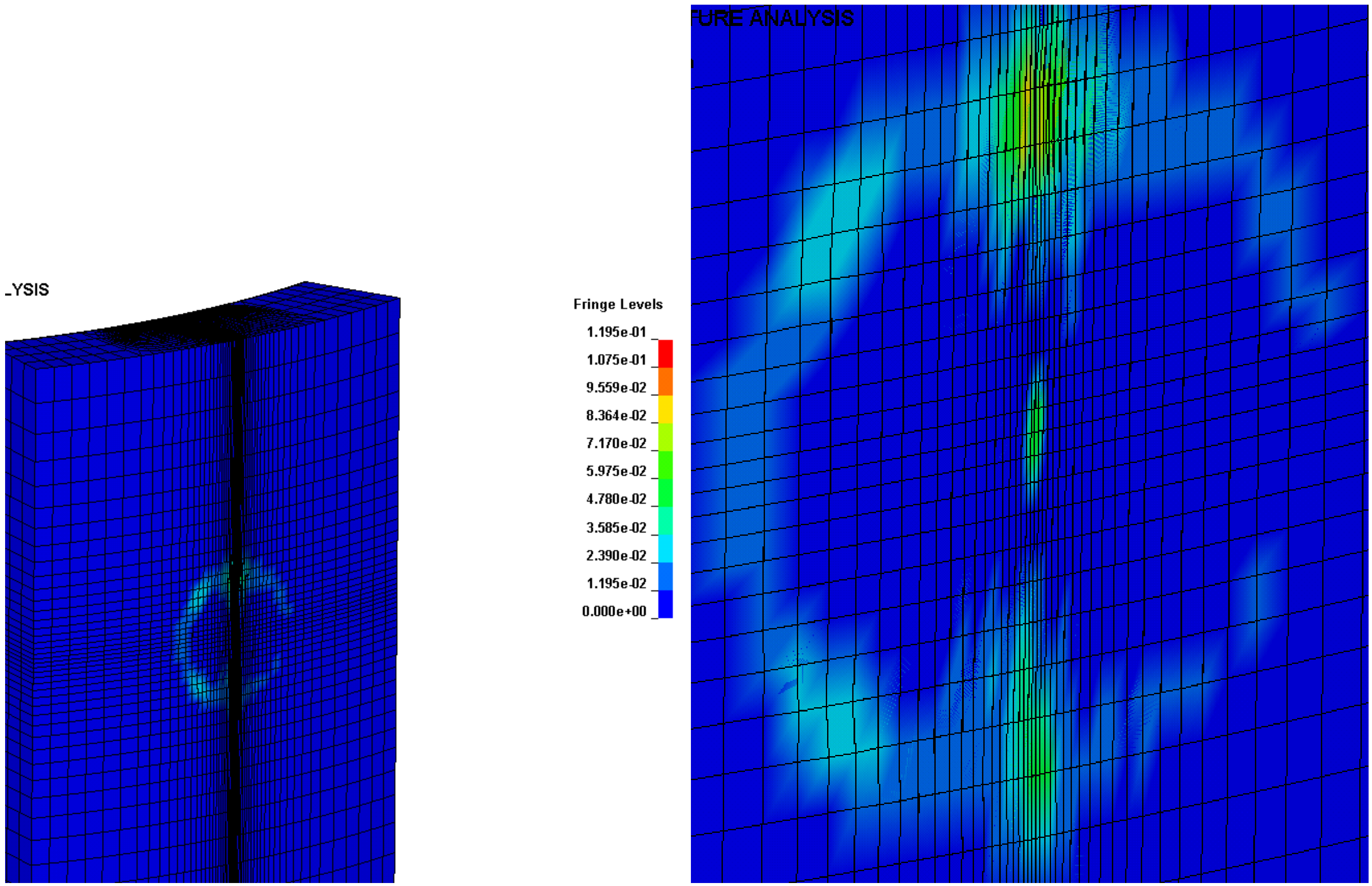

Figure 2.7.19: Plot Showing the Erosion on the Monolithic Cylinder (No Puncture Bar Erosion)

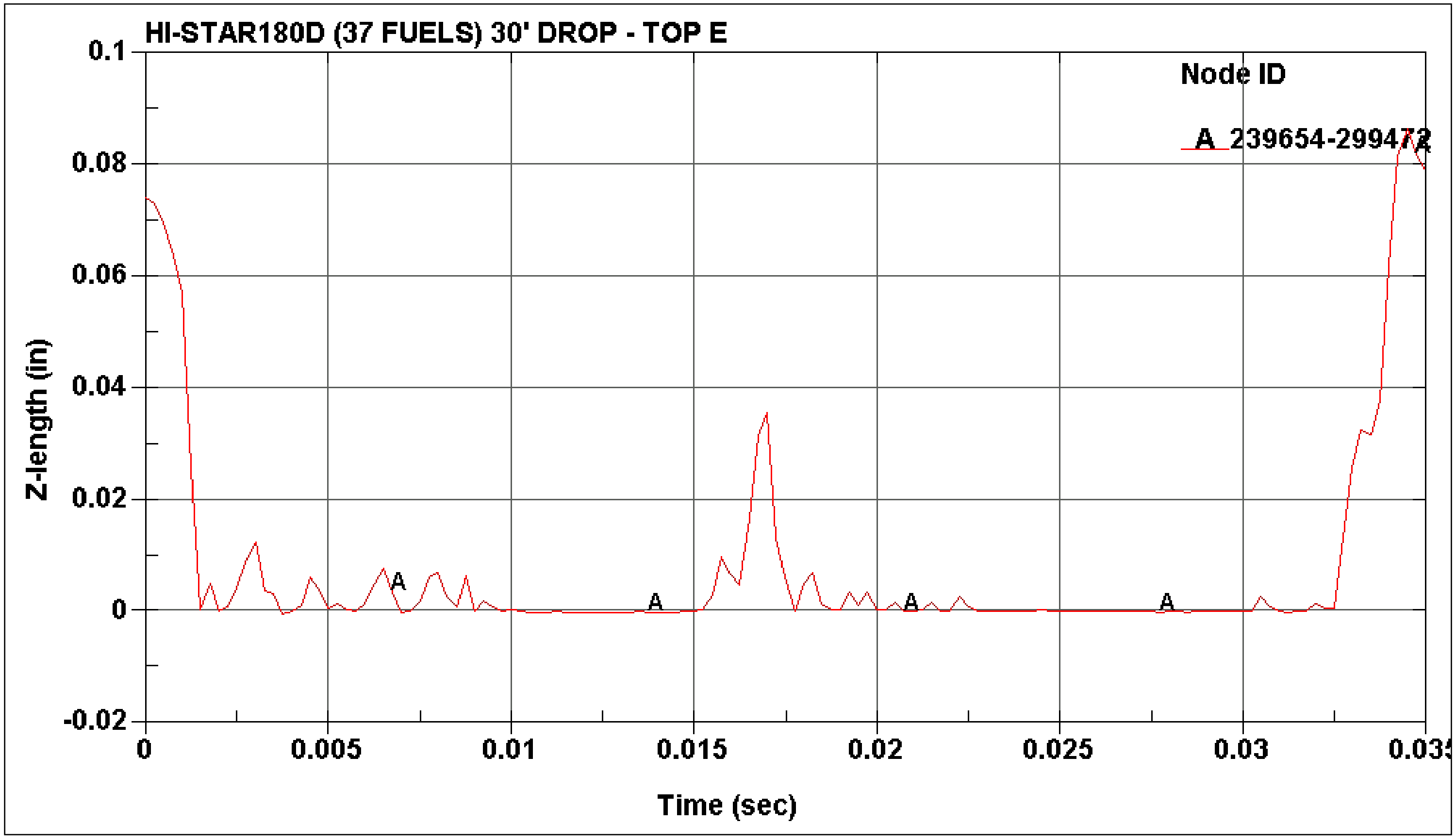

Figure 2.7.20: Time History of the Gap Between the Two Cask Closure Lids (Predicted by LS-DYNA for the Top End Vertical Drop Accident)

2.8 ACCIDENT CONDITIONS FOR AIR TRANSPORT OF PLUTONIUM

This section is not applicable to the HI-STAR 180D Package. This application does not seek approval for air transport of plutonium and, therefore, does not address the accidents defined in 10CFR71.74.

2.9 ACCIDENT CONDITIONS FOR FISSILE MATERIALS FOR AIR TRANSPORT

This section is not applicable to the HI-STAR 180D Package. This application does not seek approval for air transport of fissile materials and, therefore, does not address the accidents defined in 10CFR71.55(f).

2.10 SPECIAL FORM

This section is not applicable to the HI-STAR 180D Package. This application does not seek approval for transport of special form radioactive material; therefore, the requirements of 10CFR71.75 are not applied.

2.11 FUEL RODS

The cladding of the fuel rods is the first boundary for confining radiological matter in the HI-STAR 180D Transport Cask. Analyses have been performed in Chapter 3 to ensure that the maximum temperature of the fuel cladding is well below ISG-11, Rev. 3 regulatory limits [2.11.1].

The vertical drop of the package, leading to a rapid axial deceleration of the stored fuel and the consequent flexural strains, is recognized as the most vulnerable free drop configuration from the standpoint of potential damage to the fuel [2.11.2, 2.11.3]. Fortunately, the problem of large inertial loading of fuel has been comprehensively studied in the published NUREG [2.11.5] and studies conducted by Pacific Northwest National Laboratory (PNNL) and USNRC [2.11.4], which obsolesces prior analyses and provides a robust and conservative basis for prognosticating fuel damage under vertical drop events.

The analysis presented herein utilizes the finite element analysis model developed by PNNL and the NRC staff [2.11.4] with appropriate modifications to simulate the HI-STAR 180D Design Basis Fuel. Most notably the HI-STAR 180D fuel rod model includes an initial gap, δ, between the top/bottom of the fuel pin and point mass representing the cask to account for the axial clearance between the stored spent fuel assemblies and the cask internal cavity. The reference value of the prescribed gap δ is given in Table 2.11.1.

The analysis for the HI-STAR 180D fuel is divided into the following discrete steps:

i. Replicate the LS-DYNA model of a single fuel rod based on the detailed description provided [2.11.4]. Figure 2.11.1 (which is reproduced from [2.11.4]) illustrates the single fuel rod model and defines the key terminology. This model is referred to hereinafter as “Model 1”.

ii. Verify the accuracy of the LS-DYNA fuel rod model by simulating a vertical drop of a Transport Cask from a height of 30-feet above the target surface and compare the results with those from [2.11.4].

iii. Modify the mass and the dimensional properties of the fuel rod model to reflect the HI-STAR 180D Design Basis Fuel. Also modify the cask mass, the cask-to-ground spring representing the impact limiter, and the initial velocity of the fuel pin and the cask to simulate a 9 meter (30 ft) end drop of the HI-STAR 180D Package. This model is referred to hereinafter as “Model 2”. Model 2 also considers the maximum axial gap ‘δ’ between the fuel and the cask cavity.

iv. Simulate 9 meter vertical end drop (critical of top or bottom) of the HI-STAR 180D Package in LS-DYNA using Model 2.

v. Obtain the results for Model 2 and evaluate the strain ductility demand on the fuel cladding.

The value assumed for the dimension of the interstitial space between the single pin fuel model and the contact boundary is consistent with the methodology set forth in the joint paper by PNNL and the USNRC [2.11.4], in which the gap dimension is calculated as:

$$gap = \frac{W_{compartmen} - n_{pin} \cdot D_{pin}}{2}$$

where $W_{compartment}$ equals the inside dimension of the storage cell, n_{pin} equals the number of fuel pins across an assembly, and D_{pin} equals the outside diameter of a single fuel pin. The above equation gives the maximum distance that a center fuel pin can deform assuming that all pins deform identically in the in-plane direction.

Figure 2.11.2 shows the benchmark LS-DYNA model of a single fuel rod per the description in [2.11.4] (Step i). In order to verify that this model (Model 1) is an accurate replica of the original LS-DYNA model from NUREG-1864, Model 1 is used to analyze a vertical drop of a Transport Cask from a height of 30-feet above the target surface following guidelines from [2.11.4] (Step ii). Figure 2.11.3 shows the deceleration time history for the fuel pin and the cask obtained using Model 1, and Figure 2.11.4 shows the peak cladding axial strain from the same solution. Table 2.11.2 compares the key results from [2.11.4] and the new solution using Model 1 (Step ii) for the 30-feet drop event. As evident from Table 2.11.2, all the results for Model 1 are in good agreement with the corresponding results from [2.11.4]. Specifically, the cask and fuel dynamic results from the two solutions agree within 1%, however, the maximum compressive strain for Model 1 envelopes the corresponding value predicted from [2.11.4]. Hence, it is determined that Model 1 is sufficiently accurate and can serve as a baseline model to evaluate the structural integrity of the HI-STAR 180D design basis fuel under the 30 foot (9 m) drop accident.

It is to be noted that the analysis approach considered previously is very conservative in the sense that the fuel contributes only mass effects and no flexural rigidity to the cladding. It is concluded in [2.11.4] that the strains observed in the cladding would be much less if the fuel pellet is assumed fully intact and fully adhered to the cladding and adjacent fuel pellets. However, to overcome unrealistic ovalization of the open cross section of the fuel cladding, nonlinear single degree-of-freedom springs are included to represent Hertzian-type radial contact between the cladding and the fuel during lateral loading for the current fuel model.

It is further verified from the benchmark analysis (Step ii) that, without the fuel rod end caps included in the model, the internal pressure is applied only in the radial direction on the cladding. The end pressure load (or axial pressure) is conservatively ignored for the representative fuel drop accident [2.11.4]. However, in order to take credit for longitudinal tensile stress in the cladding that counters the stresses from impact, the axial pressure load is considered in the HI-STAR 180D drop simulations (Model 2) and applied as an equivalent nodal load on the cladding end nodes. However, for added conservatism, an additional simulation is performed, based on the governing model, excluding the fuel rod internal pressure load. This is based on a conservative assumption that all cladding internal gases have escaped due to a postulated leakage. This simulation model is hereafter referred to as Model 3.

The key input data that characterizes the HI-STAR 180D Design Basis Fuel is listed in Table 2.11.3. To construct the dynamic impact model for the HI-STAR 180D fuel (Model 2), the mass and dimensional properties of the fuel rod in Model 1 are revised to reflect the data in Table 2.11.3 (Step iii). The fuel cladding material for the HI-STAR 180D Design Basis Fuel is Zircaloy, which is the same cladding material, analyzed in [2.11.4]. Therefore, the material properties given in [2.11.4] for Zircaloy may be used for the HI-STAR 180D fuel model.

There have been ongoing efforts for the last decade to investigate the cladding material property degradation for the high burn-up fuel (burnups greater than 45 GWd/MTU) due to hydride dissolution at high temperatures and subsequent radial reorientation. Specifically, higher concentrations of radial hydrides indicate significant loss of ductility (hydride initiated cladding embrittlement) in the fuel cladding. The publications [2.11.10], [2.11.11] and [2.11.12] provide some insights into the hydride reorientation and its consequence on the spent fuel interim storage and transport conditions.

ISG-11 [2.11.1] also indicates uncertainty with respect to the material properties of the high burn-up fuel cladding. The following conservative approach is considered in this evaluation for the HI-STAR 180D fuel cladding to address the issues related to the high burn-up fuel and to show with reasonable assurance that there is no significant cladding failure:

(i) High burn-up fuel (i.e., fuel with burnups generally exceeding 45 GWd/MTU) may have cladding walls that have become relatively thin from in-reactor formation of oxides or zirconium hydride. The analysis thus considers the effective cladding thickness, per the guidance from ISG-11 [2.11.1], to account for any loss of thickness from oxidation.

(ii) The true-stress vs. true-strain curves surveyed from various publications and journals such as [2.11.8] and [2.11.9] show a minimum elastic modulus of 9.61×10^6 psi and a minimum yield strength of 76,870 psi for the high burn-up fuel cladding. The minimum cladding properties obtained from [2.11.8] correspond to a temperature of 673°K (400°C) with a fast fluence of 11.7×10^{25} n/m^2, hydrogen concentration of 360 ppm and 50% cold worked (in terms of ratio of areas). A similar study for high burn-up fuel by Electric Power Research Institute [2.11.9], based on three-phase mixture model, essentially predicts the minimum properties as discussed above. This three-phase mixture model enables the treatment of the interaction between the radial and the circumferential hydrides, which provides a tool for the development of a failure criterion for high burn-up spent fuel rods subjected to dynamic loading after being exposed to the effects of decades of dry storage..

The fuel integrity analysis therefore considers the thinning of the fuel cladding per the guidance from ISG-11 [2.11.1] and the lower-bound material properties for the Zircaloy cladding to account for uncertainties related to high burn-up as listed below:

Elastic Modulus of the Cladding = 9.61×10^6 psi
Yield Strength of Cladding = 76,870 psi

For Model 2, the cask represented by a mass element is modified to represent the mass of the HI-STAR 180D Transport Package excluding the stored fuel mass per Table 2.11.2. Specifically, the

HI-STAR 180D package mass per fuel rod is used in this model. The cask-ground spring, which represents the behavior of the impact limiter, is adjusted so that it transmits a constant crush force corresponding to the peak cask deceleration obtained from full 3D LS-DYNA drop simulations (see Table 2.11.4). The input values for the cask-ground spring for Model 2 are substantiated using the full 3-D LS-DYNA model of the HI-STAR 180D Transport Package explained in Section 2.7 (with summary results in Table 2.7.3 and 2.7.4). The fuel to cask spring stiffness used in simulation Model 2 is consistent with that specified in [2.11.4]. Finally, the velocity corresponding to the 9-meter (30 ft) free drop is used as the initial input for the cask and the fuel pin in this evaluation.

The following conservatisms are inherent in the explicit fuel cladding integrity simulation as observed below:

(i) The Fuel cladding, as observed from Figure 2.11.5a, is subjected to a constant crush force (corresponding to the peak deceleration of the cask during the intial impact with the rigid target obtained from the full 3D hypothetical drop simulation). It is to be noted from Figure 2.11.5b that the peak deceleration of the cask from the full 3D simulation is not constant for the entire impact duration. By setting the constant crush force equal to the peak cask deceleration (prior to rebound of the fuel), the differential velocity between the cask and the fuel at the time of impact is maximized, which in turn causes a higher impact load on the fuel rod.

(ii) Figures 2.11.5a and 2.11.5c also depict that the deceleration of the fuel assembly from the full 3D simulation models is lower than the simplified fuel cladding only simulation model. The resulting deceleration response from the cladding only model (from Figure 2.11.5a) compared against the full 3D drop simualtions model (see Figure 2.11.5c), is much lower indicating the inherent conservatism in predicting the strains in the cladding.

Table 2.11.5 summarizes the peak principal strain for the HI-STAR 180D design basis fuel for different drop models (Models 2 and 3). Note that the peak principal strains listed in the table correspond to the tensile strains. Compressive strains are slightly larger. However, the primary failure mode of the fuel cladding is tensile loading. Also, the compressive strains are still below the maximum limits discussed in the following section. Peak principal strains are therefore the appropriate measure for cladding integrity. Figures 2.11.6 and 2.11.7 show the peak cladding strain in Model 2 and Model 3, respectively. Since the simulation results indicate no contact between the representative fuel rod and cell wall, contact friction between the fuel cladding and the cell wall is not applicable.

According to PNNL and USNRC findings [2.11.4], the maximum permissible strain for high-burnup fuel is between 1.7% and 3%. It is worth noting that the failure strain limit established in [2.11.4] is applicable for high burn-up fuel, which is the design basis fuel in HI-STAR 180D.

The Nuclear Fuel Safety Criteria Technical Review [2.11.6] distinguishes the fuel cladding tangential strain limit as 1% and the equivalent strain limit (a vector sum of tangential and axial strains) as 2.5%. Further, for the high burn-up fuel this limit is increased from 2.5% to 3.5%.

However, for the HI-STAR 180D Package, a lower strain limit of 1% is conservatively used per NUREG 1864 [2.11.5]. Note that a proposed lower failure limit for the fuel cladding underestimates the maximum load sustained by the fuel before failure.

Based on some insights from [2.11.10], [2.11.11] and [2.11.12], the fuel integrity analysis documented in this calculation is conservative for the following reasons:

a. As investigated in publication [2.11.10], the normal conditions of storage, viz. the initial temperature limit of 400ºC during beginning of storage (BOS) and the reduced hoop stresses at the end of storage (EOS) due to cladding creep, are not sufficient to promote massive hydrides reorientation. Under the normal conditions of storage, the hydride reorientation is limited to roughly 20 ppm. Further it is shown that a bounding 60 ppm radial hydride concentration causes a hoop strain reduction from 17.5% to 1.5%.

b. Radial hydrides mostly affect the hoop strength of the fuel cladding. The vertical end drop of the package, however, tends to produce longitudinal bending stresses and strains in the fuel cladding. Nonetheless, the hoop strain reduction due to the radial hydrides is conservatively imposed on the results of the vertical end drop irrespective of the strain orientation.

The results in this evaluation, for various vertical end drops, clearly show that the induced strain in the fuel cladding is significantly lower than the conservatively established failure strain limit of 1.0%. In fact the strain calculated for the HI-STAR 180D fuel, using the lower-bound cladding material properties (as discussed in item (ii) above), is well below the elastic limit.

In summary, the results indicate that the HI-STAR 180D design basis fuel cladding is not vulnerable to failure (rupture or breach) as result of a -9-meter end drop accident.

It can further be concluded that the loads sustained by the fuel, under normal conditions of transportation, remain inconsequential for the following reasons:

i. The load sustained by the fuel from the 1-ft (0.3 m) side drop, applicable for the normal conditions of transport, is significantly lower than the corresponding 30-ft (9 m) side drop accident. In addition, the most vulnerable 30-ft (9 m) vertical drop accident (in the preceding sections) produces fuel cladding strains significantly lower than the conservatively established failure limit.

ii. Under normal conditions of transport since the HI-STAR 180D package is transported in horizontal orientation, the fuel axis lies parallel to the impact target. Consequently, the load sustained by the fuel rod is further distributed across the length of the fuel assembly by means of intermittent grid spacers.

Table 2.11.1: Values of Gaps in Fuel Assembly Impact Analyses

GAP (δ)	VALUE (mm)
Bounding Axial Gap	See Table 2.7.1

Table 2.11.2: Results for 30-Ft End Drop of Transport Cask from the Benchmark LS-Dyna Model

Item	From [2.11.4]	From LS-DYNA Solution Using "Model 1"
Max. Cask Deceleration (g's)	60	60
Max. Fuel Deceleration (g's)	135	136.7
Max. Cask Displacement (in)	7.0	7.23
Max. Fuel Rod Displacement (in)	7.0	7.27
Peak Cladding Axial Compressive Strain (%)	2.85	3.38

Table 2.11.3: Key Input Data for HI-STAR 180D Design Basis Fuel

Input Parameter	Value
Fuel Rod Height (mm)	Refer to Table 2.6.9
Fuel Rod Diameter (mm)	
Minimum Fuel Clad Thickness (mm)	
Fuel Rod Maximum Pressure (MPa)	14.37††
Loaded HI-STAR 180D Package Mass (including Impact Limiters) kg (lb)	117,934 (260,000)†
Total Mass of Fuel Assembly (kg)	396.4

† The transport package with F-32 fuel basket is selected for the fuel rod integrity evaluation for the following reasons:

1. Note that the F-32 transport package has a larger mass per fuel rod, which yields larger crush force for a given cask deceleration. Larger crush force implies larger response deceleration of the fuel cladding and the resulting strain in the cladding. Accordingly, the transport package with F-32 fuel basket including the impact limiters from Table 2.1.11 is used.

†† The value of maximum pressure in the fuel rod at room temperature (65 bar) is incremented proportionally to the fuel average temperature of 650 ^{o}K (bounding) [2.1.12].

Table 2.11.4: Key Dynamic Results for 9 Meter End Drop of HI-STAR 180D Transport Package

Key Results	Full 3-D Drop† Simulation	Model 2 (25 mm Gap)
Max. Cask Deceleration (g's)	82.4	85
Max. Cladding Deceleration (g's)	338	370
† Note that the maximum cask deceleration during the initial impact obtained from the Full 3D drop simulations, as discussed in Section 2.7, must be considered for the fuel rod integrity evaluation. As shown in Figure 2.11.5b, the peak deceleration during the initial impact (impact duration before the fuel rebounds), is observed for the 30 ft (9m) hypothetical bottom end drop accident.		

Table 2.11.5: Peak Principal Strains for 9 Meter End Drop of HI-STAR 180D Transport Package

Drop Case	Axial Strain
Model 2, Pressure and Impact††	0.44
Model 3, Impact Only†††	0.56
Notes: 1. The strain results in the Table are expressed in %. 2. Conservatively, the maximum absolute strain is reported.	

†† **Pressure and Impact**: The pressure and the impact are simulated as one solution. The pressure is ramped rapidly during the initial time steps so that the maximum pressure is active throughout the impact duration.

††† **Impact Only**: This is a drop scenario wherein the gases in the fuel rod are assumed to have escaped through the end leak and there is no pressure during the impact event.

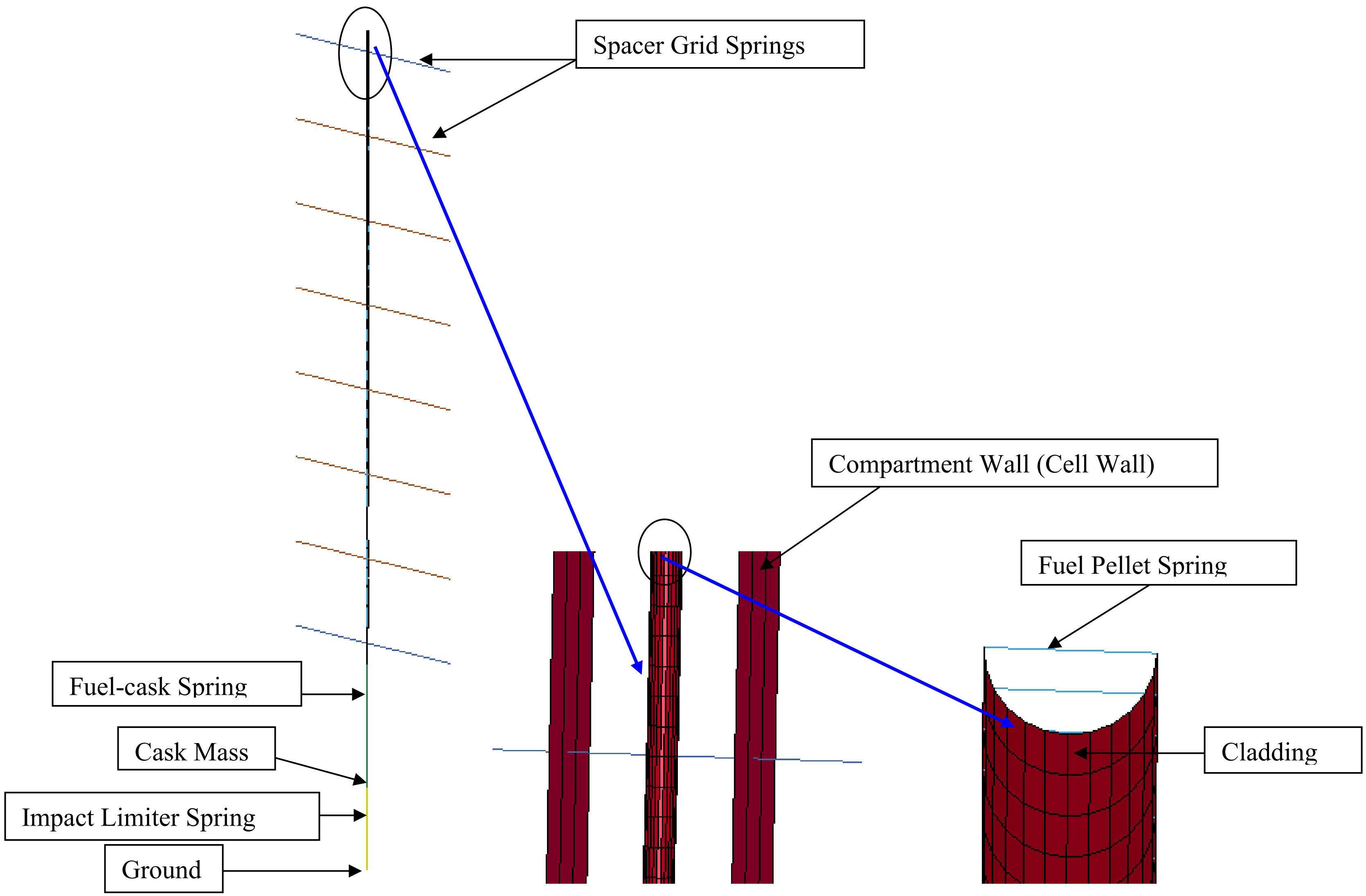

Figure 2.11.1: Finite Element Model of NUREG 1864 Fuel (Model 1)

Figure 2.11.2: Finite Element Model of HI-STAR 180D Design Basis Fuel (Model 2)

THIS FIGURE IS PROPRIETARY IN ITS ENTIRETY

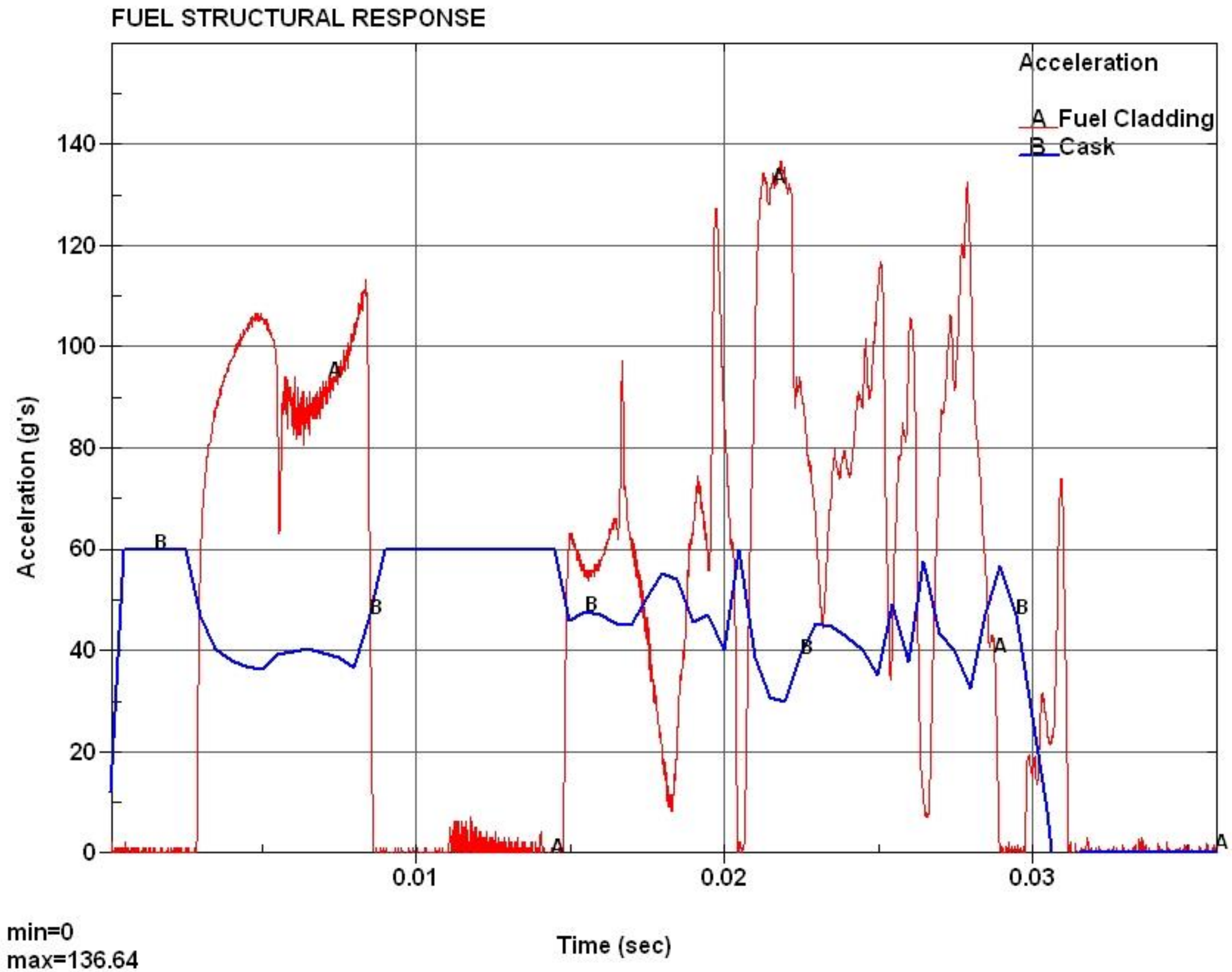

Figure 2.11.3: Cask and Cladding Deceleration – Model 1

THIS FIGURE IS PROPRIETARY IN ITS ENTIRETY

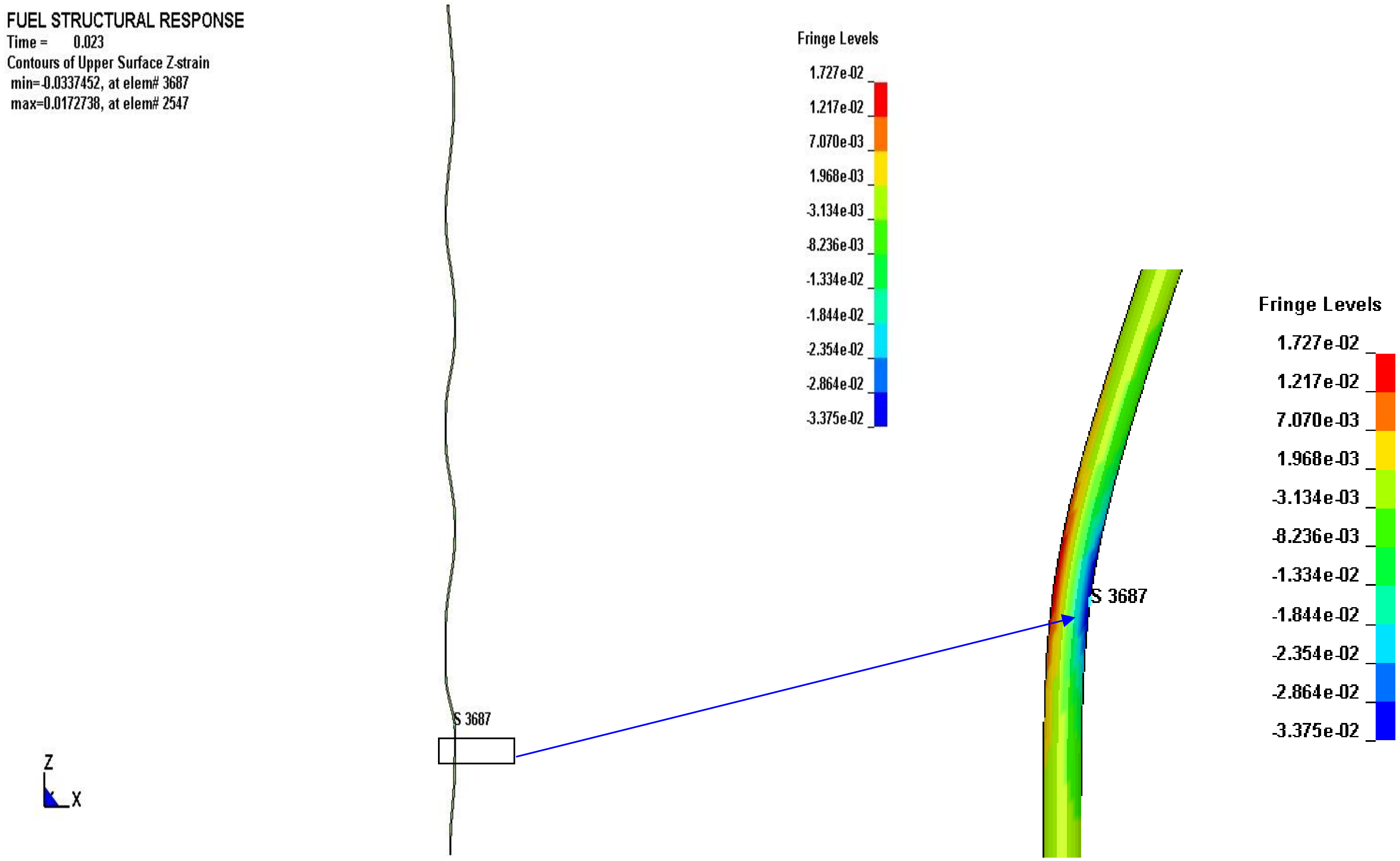

Figure 2.11.4: Cask and Cladding Deceleration – Model 1

THIS FIGURE IS PROPRIETARY IN ITS ENTIRETY

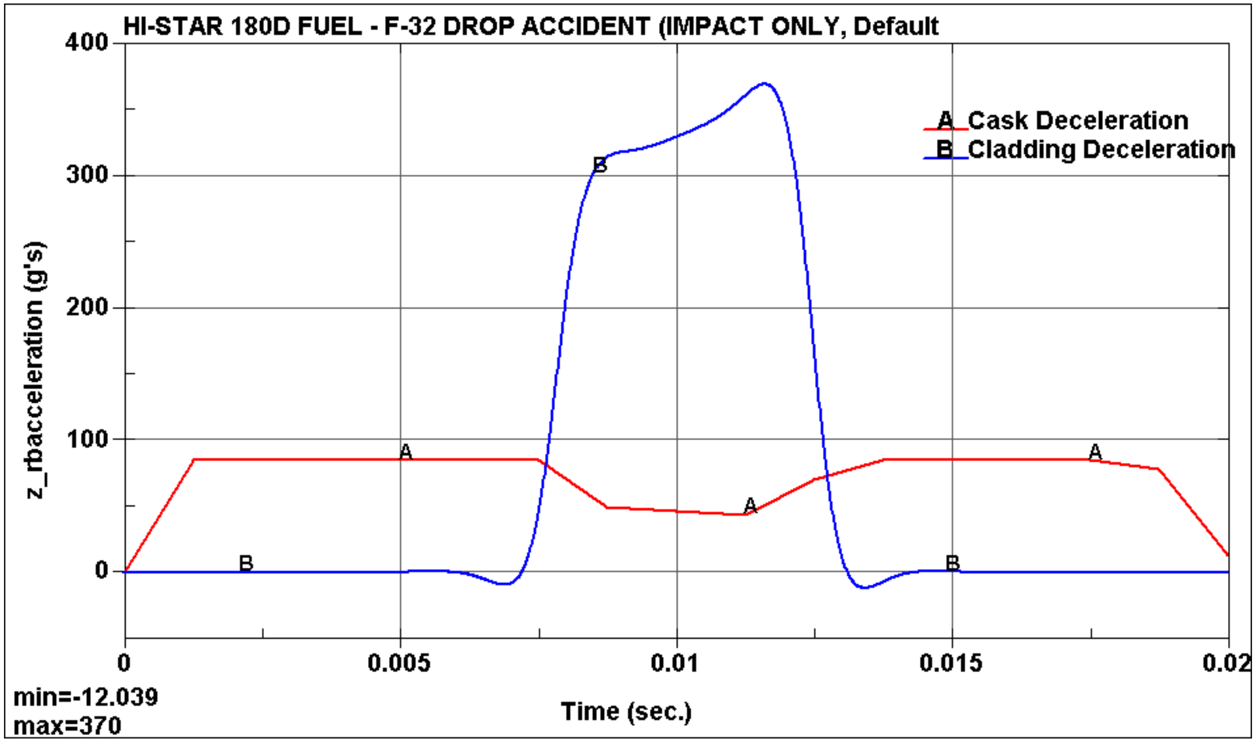

Figure 2.11.5a: Cask and Cladding Deceleration – Model 2

THIS FIGURE IS PROPRIETARY IN ITS ENTIRETY

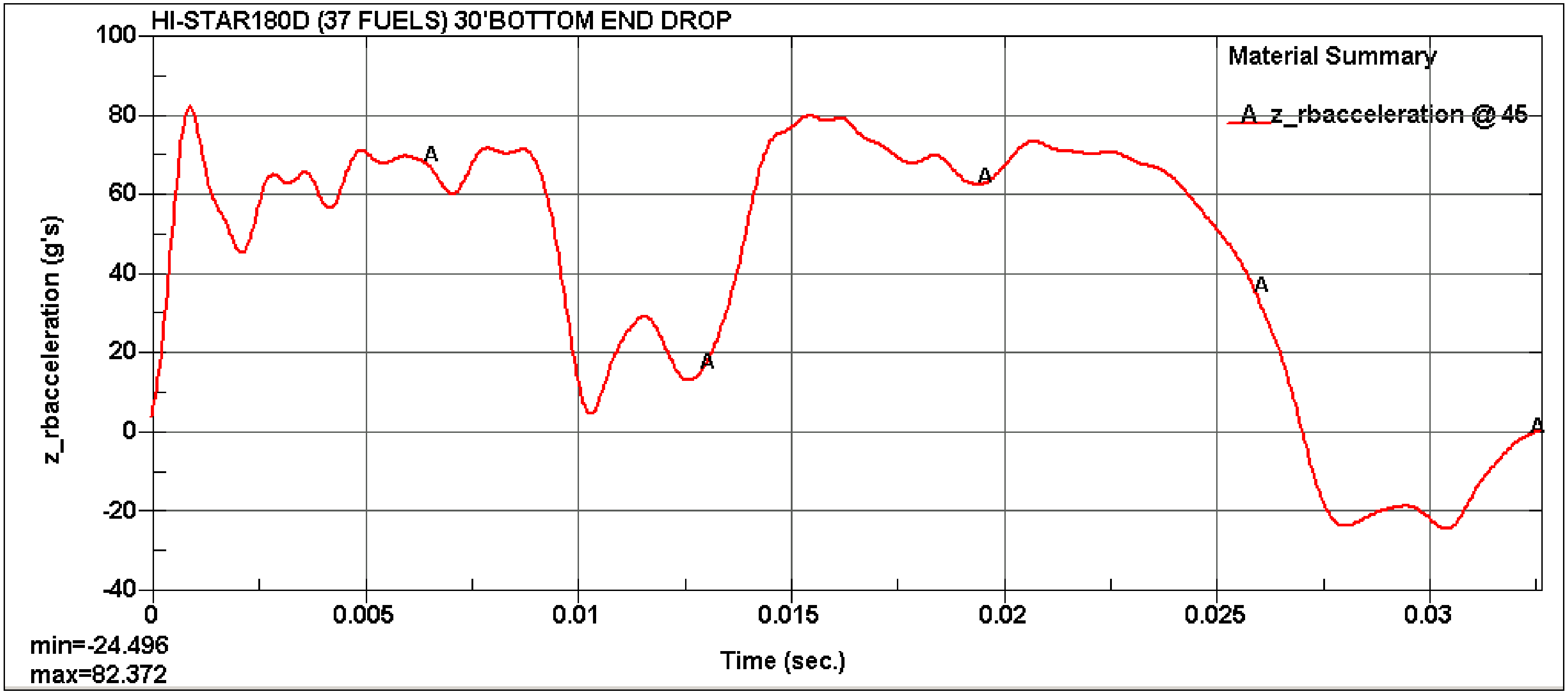

Figure 2.11.5b: CaskDeceleration – Full 3D 30 ft. Governing Bottom End Drop Simulation

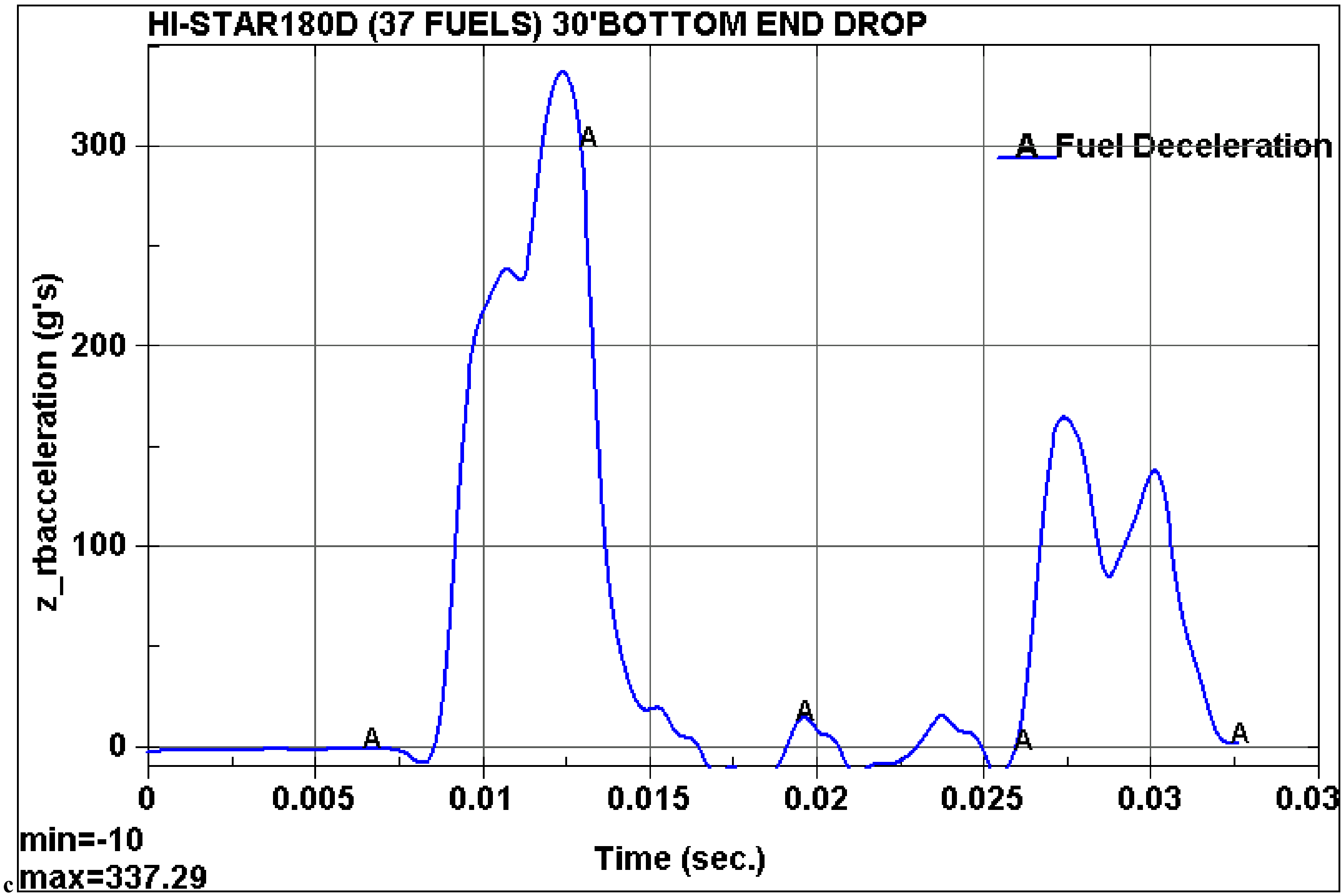

Figure 2.11.5c: Fuel Deceleration– Full 3D 30 ft Governing Bottom End Drop Simulation

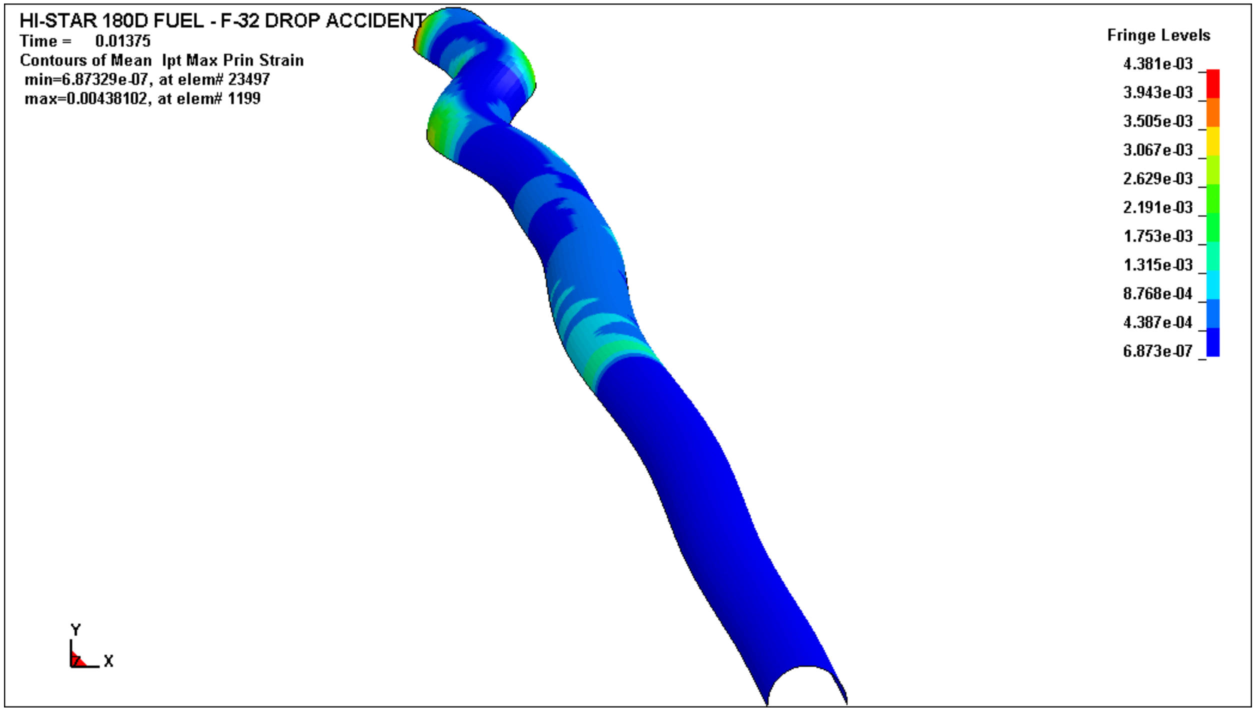

Figure 2.11.6: Maximum Principal Strain – Model 2

THIS FIGURE IS PROPRIETARY IN ITS ENTIRETY

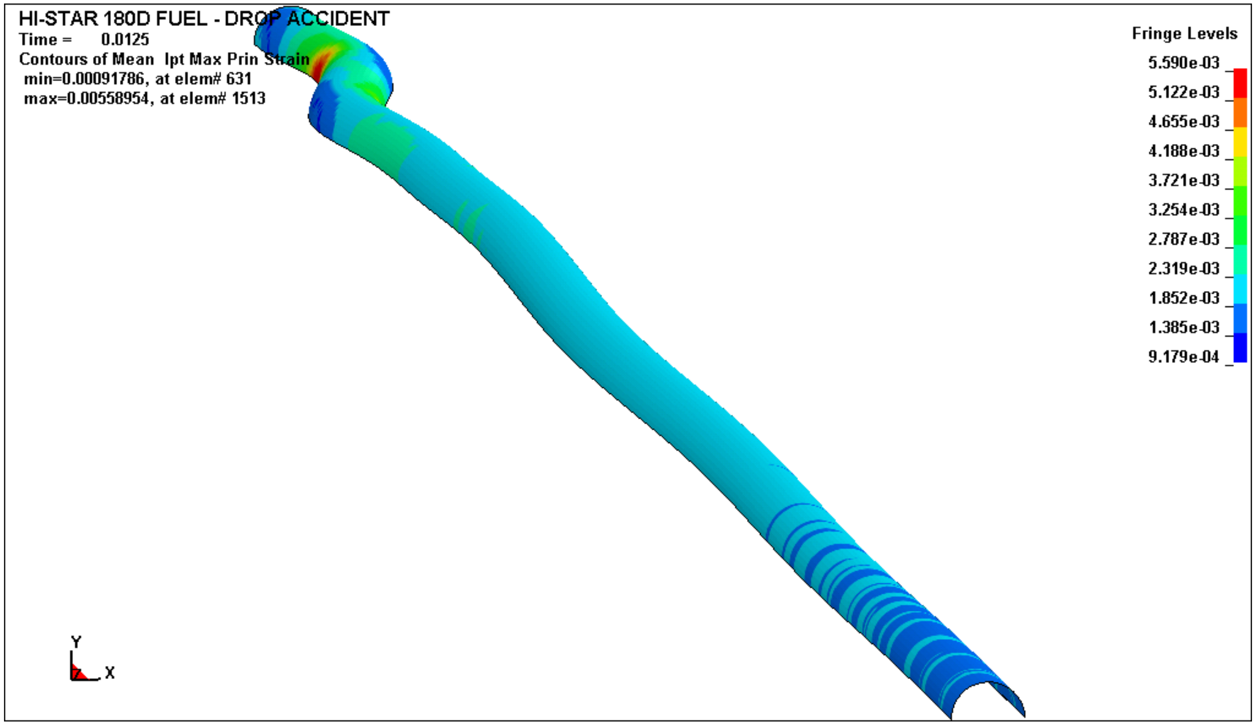

Figure 2.11.7: Maximum Principal Strain – Model 3

CHAPTER 2 REFERENCES

The following generic industry and Holtec produced references may have been consulted in the preparation of this document. Where specifically cited, the identifier is listed in the SAR text or table. Active Holtec Calculation Packages, which are the repository of all relevant licensing and design basis calculations, are annotated as "latest revision". Submittal of the latest revision of such Calculation Packages to the USNRC and other regulatory authorities during the course of regulatory reviews is managed under the company's Configuration Control system. Supporting documents submitted to the USNRC with the HI-STAR 180D LAR 9367-2 have been italicized.

[2.1.1] ASME Boiler & Pressure Vessel Code, Section III, Subsection NB, American Society of Mechanical Engineers, 2007 Edition, 2008 Addenda.

[2.1.2] Regulatory Guide 7.6, "Design Criteria for the Structural Analysis of Shipping Cask Containment Vessels", Revision 1, March, 1978, U.S. Nuclear Regulatory Commission.

[2.1.3] 10CFR Part 71, "Packaging and Transportation of Radioactive Materials", Title 10 of the Code of Federal Regulations, Office of the Federal Register, Washington, D.C.

[2.1.4] Regulatory Guide 7.8, "Load Combinations for the Structural Analysis of Shipping Casks for Radioactive Material", Revision 1, March, 1989, U.S. Nuclear Regulatory Commission.

[2.1.5] NUREG-0612, "Control of Heavy Loads at Nuclear Power Plants," United States Nuclear Regulatory Commission, July, 1980.

[2.1.6] ASME Boiler & Pressure Vessel Code, Section II, Parts A and D, American Society of Mechanical Engineers, 2007 Edition, 2008 Addenda.

[2.1.7] Regulatory Guide 7.11, "Fracture Toughness Criteria of Base Material for Ferritic Steel Shipping Cask Containment Vessels with a Maximum Wall Thickness of 4 Inches", United States Nuclear Regulatory Commission, June, 1991.

[2.1.8] Regulatory Guide 7.12, "Fracture Toughness Criteria of Base Material for Ferritic Steel Shipping Cask Containment Vessels with a Wall Thickness Greater Than 4 Inches But Not Exceeding 12 Inches", United States Regulatory Commission, June, 1991.

[2.1.9] NUREG/CR-1815, "Recommendations for Protecting Against Failure by Brittle Fracture in Ferritic Steel Shipping Containers Up to Four Inches Thick".

[2.1.10] ASME Boiler & Pressure Vessel Code, Section III, Appendices, American Society of Mechanical Engineers, 2007 Edition, 2008 Addenda.

[2.1.11] NUREG-1617 Standard Review Plan for Transportation Packages for Spent Nuclear Fuel, USNRC, (2000).

[2.1.12] *Calculation Package for the HI-STAR 180D Transport Cask System, Holtec International Proprietary Report HI-2125252, Latest Revision.*

[2.1.13] Deleted.

[2.1.14] ASME Boiler & Pressure Vessel Code, Section III, Subsection NF, American Society of Mechanical Engineers, 2007 Edition, 2008 Addenda.

[2.1.15] Not Used.

[2.1.16] Holtec Position Paper DS-331, “Structural Acceptance Criteria for the Metamic-HT Fuel Basket”, Revision 1.

[2.1.17] NUREG/CR-3826, "Recommendations for Protecting Against Failure by Brittle Fracture in Ferritic Steel Shipping Containers Greater than Four Inches Thick."

[2.2.1] Hexweb Honeycomb Attributes and Properties, HEXCEL Corp, Pleasanton, CA., 2006. (web site is www.hexcel.com).

[2.2.2] “Safety Analysis Report for the HI-STAR 100 Package”, Holtec Report HI-951251, Latest Revision, Docket No. 71-9261.

[2.2.3] DOE-HDBK – 1017/2-93, DOE Fundamentals Handbook, Material Science, Vol. 2 of 2.

[2.2.4] NRC Bulletin 96-04: Chemical, Galvanic or Other Reactions in Spent Fuel Storage and Transportation Casks, July 5, 1996.

[2.2.5] L.W. Ricketts, Fundamentals of Nuclear Hardening of Electronic Equipment, Robert E. Krieger Publishing Company, Malabar, FL, 1986.

[2.2.6] J.H. Evans, "Structural Analysis of Shipping Casks, Volume 8, Experimental Study of Stress-Strain Properties of Lead Under Specified Impact Conditions", ORNL/TM-1312, Vol. 8, ORNL, Oak Ridge, TN, August, 1970.

[2.2.7] Properties of Aluminum Alloys, Tensile, Creep, and Fatigue Data at High and Low Temperatures, ASM International, November 2006.

[2.2.8] Letter (transmitted September 3rd, 2009) from Mark Armitage, Engineering Manager, American Seal and Engineering Inc. to John Griffiths, Design Manager, Holtec International (Including Proprietary American Seal Drawings - Internal and External Spring Energized C-Ring Drawing Numbers 050056 and 050057, respectively).

[2.2.9] ASTM Specification B221M-07, “Standard Specification for Aluminum and Aluminum-Alloy Extruded Bars, Rods, Wire, Profiles, and Tubes (Metric)”.

[2.2.10] *Holtec Report HI-2177786, “Holtite-B Application Report for HI-STAR 180D”, Latest Revision.*

[2.2.11] Alcore Order No. SP-11201, Holtec Purchase Order No. 1630AICO #3, Crush Material Test Reports, M. C. Gill Corporation, 2009.

[2.5.1] ANSI N14.6-1993, “American National Standard for Special Lifting Devices for Shipping Containers Weighing 10,000 Pounds (4,500 kg) or More for Nuclear Materials”, American National Standards Institute, Inc.

[2.5.2] ANSYS, Version 13.0, Ansys Inc., Copyright 2010 SAS IP, Inc.

[2.5.3] LS-DYNA, Version 971, LSTC Software, 2006.

[2.5.4] Field Manual of the A.A.R. Interchange Rules, Rule 88, American Association of Railroads, 1996.

[2.5.5] Crane Manufacturer's Association of America (CMAA), Specification No. 70, 1988.

[2.5.6] NUREG 1536, Standard Review Plan for Dry Cask Storage Systems, USNRC, Rev. 1

[2.6.1] *Finite Element Analyses for the HI-STAR 180D, Holtec Proprietary Report, HI-2125251, Latest Revision.*

[2.6.2] Calculation Package of Humboldt Bay Impact Limiters, Holtec Proprietary Report HI-2063486, latest revision (Docket # 71-9261, TAC L24029).

[2.6.3] Regulatory Guide 7.9, “Standard Format and Content of Part 71 Applications for Approval of Packaging for Radioactive Material”, Revision 2, USNRC, March 2005.

[2.6.4] Buckling of Bars, Plates, and Shells, D.O. Brush and B.O. Almroth, McGraw-Hill, 1975, p.22.

[2.6.5] Holtec Proprietary Report HI-2084137, “A Classical Dynamics Based and Experimentally Benchmarked Impact Response Computation Methodology for AL-STAR Equipped Casks”, Latest Revision.

[2.6.6] NUREG/CR-1132, “A Survey of Potential Light Water Reactor Fuel Rod Failure Mechanisms and Damage Limits”, Courtright, E.L., July 1979.

[2.6.7] HI-STORM FW FSAR, Holtec Report HI-2114830, Latest Revision.

[2.6.8] *Holtec Report HI-2146017, "Calculation Package for HI-STAR 180D Storage Cask System", Latest Revision.*

[2.7.1] Holtec Proprietary Report HI-981891, "Impact Limiter Test Report - Second Series", Revision 3, 1998.

[2.7.2] Holtec Proprietary Report HI-2063591, "Benchmarking of LS-DYNA for Simulation of Hypothetical Drop Conditions of Transport", Revision 1, 2007.

[2.7.3] Not Used.

[2.7.4] Holtec Proprietary Report HI-2073743, "Benchmarking the LS-DYNA Impact Response Prediction Model for the HI-STAR Transport Package Using the AL-STAR Impact Limiter Test Data", Rev. 1, 2008.

[2.7.5] Shah, M.J., Klymyshyn N.A., and Kreppel B.J., "HI-STAR 100 Spent Fuel Transport Cask Analytic Evaluation for Drop Events", Packaging, Transport, and Security of Radioactive Materials, Vol. 18, No. 1, W.S. Maney & Sons (2007).

[2.7.6] Containment Performance of Transportable Storage Casks at 9-m Drop Test, Hitoshi Tobita and Kenji Araki, PATRAM 2004, Berlin, Germany, 9/2004.

[2.7.7] "Mechanical Design of Heat Exchangers and Pressure Vessel Components", by K.P. Singh and A. I. Soler, Arcturus Publishers, Cherry Hill, New Jersey, 1100 pages, hardbound (1984).

[2.7.8] Holtec Proprietary Report HI-2073715, Benchmarking of LS-DYNA For Use With Polyurethane Foam Filled Impact Limiter, 2007, Revision 0.

[2.7.9] "Validation of an Impact Limiter Crush Prediction Model with Test Data: The Case of the HI-STAR 100 Package", K.P. Singh, A.I. Soler, and C. Bullard, PATRAM 2004, Berlin, Germany, September 20-24, 2004.

[2.7.10] USNRC ASLB, "Final Partial Initial Decision on F-16 Aircraft Accident Consequences", Docket No. 72-22-ISFSI, ASLB# 97-732-02-ISFSI, dated2/24/2005.

[2.7.11] "Guidelines for Conducting Impact Tests on Shipping Packages for Radioactive Material", Mok, Carlson, Lu, and Fischer, UCRL-ID-121673, Lawrence Livermore National Laboratory, September 1995.

[2.7.12] QA Documentation Package for ANSYS (Versions 11.0 and Higher), HI-2012627, Revisison 9, 2012.

[2.7.13] QA Documentation for LS-DYNA3D, HI-961519, Revision 6, 2008.

[2.7.14] Holtec Proprietary Report HI-2094393, "Calculation Package for HI-STAR 180 Drop Simulations Using Classical Dynamics Method", Latest Revision.

[2.11.1] SFPO-ISG-11, Revision 3, "Cladding Considerations for the Transportation and Storage of Spent Fuel"

[2.11.2] The Buckling of Fuel Rods in Transportation Casks Under Hypothetical Accident Conditions, G.S. Bjorkman, PATRAM 2004, Berlin, Germany, 9/2004.

[2.11.3] Spent Nuclear Fuel Structural Response When Subject to an End Impact Accident, D. Tang, J. Guttmann, B. Koeppel, and H. Adkins, PATRAM 2004, Berlin, Germany, 9/2004.

[2.11.4] PVP2004-2804, "Spent Nuclear Fuel Structural Response When Subject to an End Impact Accident", PVP-Vol 483, Transportation, Storage and Disposal of Radioactive Materials-2004, Adkins, Koeppel, and Tang.

[2.11.5] NUREG/CR-1864, "A Pilot Probabilistic Risk Assessment of a Dry Cask Storage System at a Nuclear Power Plant", USNRC, Washington D.C., 2007.

[2.11.6] Nuclear Fuel Safety Criteria Technical Review, Second Edition, 2012.

[2.11.7] NUREG/CR-1132 PNL-2787, "A Survey of Potential Light Water Reactor Fuel Rod Failure Mechanisms and Damage Limits".

[2.11.8] PNNL-17700, "PNNL Stress/Strain Correlation for Zircaloy", July 2008.

[2.11.9] Electric Power Research Institute-1015048, "Spent Fuel Transportation Applications - Assessment of Cladding Performance" A Synthesis Report.

[2.11.10] "Threat of Hydride Re-oreintation to Spent Fuel Integrity During Transportation Accidents: Myths or Reality?", Proceedings of the 2007 International LWR Fuel Performance Meeting.

[2.11.11] Hydride-Related Degradation of Spent-Fuel Cladding Under Repository Conditions, Energy Technology Division, Argonne National Laboratory, Argonne, IL.

[2.11.12] 15th International Symposium on Zirconium in the Nuclear Industry, June 2007, "Evaluation of Hydride Reorientation Behavior and Mechanical Property for High Burnup Fuel Cladding Tube in Interim Dry Storage".

Appendix 2.A: Description of Computer Codes for Structural Evaluation†

Two commercial computer programs, both with a well established history of usage in the nuclear industry, have been utilized to perform structural and mechanical numerical analyses documented in this submittal. These codes are ANSYS Mechanical and LS-DYNA. A brief synopsis of the capabilities of each code is presented below:

ANSYS Mechanical

ANSYS is the original (and commonly used) name for ANSYS Mechanical general-purpose finite element analysis software. ANSYS Mechanical is the version of ANSYS commonly used for structural applications. It is a self contained analysis tool incorporating pre-processing (geometry creation, meshing), solver, and post processing modules in a unified graphical user interface. ANSYS Mechanical is a general purpose finite element modeling package for numerically solving a wide variety of mechanical problems. These problems include: static/dynamic structural analysis (both linear and non-linear), heat transfer and fluid problems, as well as acoustic and electro-magnetic problems.

ANSYS Mechanical has been independently QA validated by Holtec International and used for structural analysis of casks, fuel racks, pressure vessels, and a wide variety of SSCs, for over twenty years.

LS-DYNA

LS-DYNA is a general purpose finite element code for analyzing the large deformation static and dynamic response of structures including structures coupled to fluids. The main solution methodology is based on explicit time integration and is therefore well suited for the examination of the response to shock loading. A contact-impact algorithm allows difficult contact problems to be easily treated. Spatial discretization is achieved by the use of four node tetrahedron and eight node solid elements, two node beam elements, three and four node shell elements, eight node solid shell elements, truss elements, membrane elements, discrete elements, and rigid bodies. A variety of element formulations are available for each element type. Adaptive re-meshing is available for shell elements. LS-DYNA currently contains approximately one-hundred constitutive models and ten equations-of-state to cover a wide range of material behavior.

In this safety analysis report, LS-DYNA is used to analyze all loading conditions that involve short-time dynamic effects.

† This appendix contains generic information and is identical to the one submitted in the HI-STAR 60 SAR and HI-STAR 180 SAR. Under Holtec's configuration control, this appendix will be immediately revised in all submitted SARs if a USNRC request-for-additional-information (RAI) necessitates a change to its contents.

CHAPTER 3: THERMAL EVALUATION

3.0 INTRODUCTION

In this chapter, compliance of the HI-STAR 180D Package to 10CFR Part 71 [1.0.2] and ISG-11, Rev. 3 [3.3.3] thermal requirements is evaluated for normal transport and hypothetical accident conditions of transport. The analysis considers passive rejection of decay heat from the Spent Nuclear Fuel (SNF) to a 10CFR71- mandated environment for normal transport and hypothetical fire accident conditions.

The 10CFR Part 71 regulations define the thermal requirements of transport packages. The requirements are as follows:

1. A package must be designed, constructed, and prepared for shipment so that in still air at 38ºC (100°F) and in the shade, no accessible surface of the package would have a temperature exceeding 85ºC (185°F) in an exclusive use shipment [§71.43(g)].

2. With respect to the initial conditions for the events of normal conditions of transport and hypothetical accident conditions, the demonstration of compliance with the requirements of 10CFR71 must be based on the ambient temperature preceding and following the event remaining constant at that value between a bounding -40ºC (-40°F) and 38ºC (100°F) which is most unfavorable for the feature under consideration. The initial internal pressure within the containment must be considered to be the maximum normal operating pressure [§71.71(b) and §71.73(b)].

3. For normal conditions of transport, a heat event consisting of an ambient temperature of 38ºC (100°F) in still air and prescribed insolation must be evaluated [§71.71(c)(1)].

4. For normal conditions of transport, a cold event consisting of an ambient temperature of -40°C (-40°F) in still air and shade must be evaluated [§71.71(c)(2)].

5. Evaluation for hypothetical accident conditions is to be based on sequential application of the specified events, in the prescribed order, to determine their cumulative effect on a package [§71.73(a)].

6. For hypothetical accident conditions, a thermal event consisting of a fully engulfing hydrocarbon fuel/air fire with an average emissivity coefficient of at least 0.9, with an average flame temperature of at least 802ºC (1475°F) for a period of 30 minutes [§71.73(c)(4)].

Section 3.1 describes the thermal design features of the HI-STAR 180D Package. Section 3.2 lists the material properties data required to perform the thermal analyses and the applicable temperature limits criteria required to demonstrate the adequacy of the HI-STAR 180D Package design under normal and hypothetical accident conditions. Thermal analyses to evaluate the normal transport are described and evaluated in Section 3.3. Thermal analyses for hypothetical accident conditions are described and evaluated in Section 3.4.

Finally, the analysis methods, models and acceptance criteria utilized in the safety evaluation for normal conditions of transport documented in this chapter mirror those used in the SAR for HI-STAR 180 certified in Docket #71-9325.

3.1 DESCRIPTION OF THERMAL DESIGN

3.1.1 Design Features

Design details of the HI-STAR 180D Package are presented in Chapter 1 and structural and mechanical features are described in Chapters 1 and 2. The HI-STAR 180D Package geometry is detailed in Holtec drawings included in Section 1.3. All materials of construction are itemized in the drawings. The assembled packaging with impact limiters installed is shown in Figure 1.3.2. As shown in this figure, the HI-STAR 180D Package is equipped with a personnel barrier to prevent access to hot cask surfaces. The package consists of a Metamic-HT fuel basket inside a thick steel cask with twin (inner and outer) bolted closure lids. Two basket designs, the F-32 and F-37 baskets are available for storing up to 32 and 37 PWR fuel assemblies. The fuel basket is a honeycomb structure engineered with square-shaped compartments to store PWR fuel. Prior to lid closure, the cask cavity is backfilled with helium. This provides a stable and inert environment for the transport of the SNF. Heat is transferred from the cask to the environment by passive heat transport mechanisms only.

The HI-STAR 180D Package is designed to safely dissipate heat under passive conditions (no wind). During transport, the HI-STAR 180D Package is placed in a horizontal position with impact limiters installed at both ends of the cask. Under normal transport conditions, the cask contents (fuel basket, fuel and basket shims) rest on solid surfaces. Direct contact between the cask and its contents enhance heat dissipation. Prior to cask closure, the cask cavity is backfilled with helium. A double-lid design is engineered to eliminate air in-leakage during transport and to prevent water ingress under a hypothetical water immersion accident. Presence of a substantially more conductive medium (helium) relative to air in the cavity spaces aids heat transfer by minimizing gap resistances and dissipating heat by natural convection in the cavity peripheral spaces.

The fuel basket is a matrix of square-shaped fuel compartments sized to store PWR Spent Nuclear Fuel (SNF). The basket is formed by a honeycomb structure of thick Metamic-HT plates. The fuel basket is surrounded by an array of shaped aluminum and stainless steel spacers (basket shims) inserted in the cask cavity peripheral spaces. Cross-sectional views of the two fuel basket designs are provided in Chapter 1. Heat is dissipated in the fuel basket principally by conduction of heat in the highly conductive Metamic-HT plates arrayed in two orthogonal directions. Heat dissipation in the fuel basket peripheral spaces is by a combination of contact heat transfer, helium conduction and radiation across narrow peripheral spacer gaps and by conduction through the basket shims. The fuel basket and the basket shims reside in a containment boundary formed by the containment shell, baseplate and two closure lids. The containment shell is enclosed in a shrink fitted thick-section cask body engineered with neutron shield pockets. The cask body exterior is engineered with low profile fins to enhance heat transfer area and concomitant dissipation of heat. In the interest of conservatism dissipation of heat by fins is ignored. However, insolation heat due to higher surface area of the fins is included in the thermal model.

The helium backfill gas is an integral part of the HI-STAR 180D thermal design. The helium fills all the spaces between solid components and provides an improved conduction medium (compared to air) for dissipating decay heat. Additionally, helium in the spaces between the fuel basket and the cask cavity is heated differentially and dissipates heat by the so-called “Rayleigh” convection. To ensure that the helium gas is retained and not diluted by lower conductivity air, the cask containment boundary is designed as an ASME Section III pressure vessel equipped with high integrity double seals in *both* the inner and outer closure lids. This ensures the presence of helium during transport. The helium gas is therefore retained in an undiluted state, and may be credited in the thermal analyses.

An important thermal design criterion imposed on the HI-STAR 180D Package is to ensure that the peak fuel cladding temperatures are below regulatory limits. An equally important design criterion is to minimize temperature gradients within the fuel basket to minimize thermal stresses. In order to meet these design objectives, the HI-STAR 180D fuel basket is designed to possess certain distinctive characteristics, which are summarized in the following.

The cask design minimizes resistance to heat transfer within the basket and basket periphery regions. This is ensured by designing the fuel basket with highly conductive Metamic-HT plates. In the fuel basket peripheral spaces thick Aluminum basket shims are inserted to facilitate basket-to-cask heat transfer. The cask design incorporates top and bottom plenums with interconnected downcomer paths to facilitate heat dissipation by internal helium circulation. This mode of heat transfer is active when the cask is tilted a few degrees from horizontal orientation. The top and bottom plenums are formed between the cask ends and fuel basket lateral flow holes in the top and bottom sections of each fuel cell wall. The fuel basket is designed to minimize structural discontinuities (i.e., gaps), which can introduce large thermal resistances to heat flow. Consequently, temperature gradients are minimized in this design, which results in lower thermal stresses within the basket. Low thermal stresses are also ensured by provisions in the cask design that permit unrestrained axial and radial thermal growth of the basket.

The HI-STAR 180D Package is designed to transport PWR spent fuel assemblies. As explained next, thermal analysis of the HI-STAR 180D Package considers all three fundamental modes of heat transfer: conduction, natural convection and thermal radiation. On the outside surface of the package, heat is dissipated to the environment by buoyancy induced convective air-flow (natural convection) and thermal radiation. Within the cask body, heat dissipation is principally by heat conduction. Inside the cask cavity heat dissipation is conservatively limited to conduction and radiation. Between surfaces (e.g., between neighboring fuel rods) heat is transported by a combination of conduction through a gaseous medium (helium) and thermal radiation. Finally buoyancy-induced convective heat transport occurs within the open spaces of the cask cavity. Heat transfer between the fuel basket external surface and enclosure shell inside wall is enhanced by the so-called “Rayleigh” effect in differentially heated cavities [3.1.1]. In the interest of conservatism convective heat transfer in the cavity spaces is neglected.

In Section 3.2 the thermal criteria for ensuring Spent Nuclear Fuel (SNF) integrity and cask effectiveness are provided. To ensure SNF integrity, the ISG-11 recommended cladding temperature limits [3.3.3] are adopted (Table 3.2.11). To ensure cask effectiveness the cask materials and components are required to be below the pressure and temperature limits for creep, yield, decomposition and melting (Tables 2.1.1, 3.2.10 and 3.2.12).

3.1.2 Contents Decay Heat

The fuel loading is required to comply with both the decay heat and burnup limits in Tables 7.D.2 and 7.D.3. The HI-STAR 180D Package is designed to allow fuel loading under different regionalized loadings. The cask and assembly design heat loads are defined in Chapter 1, Tables 7.D.2 and 7.D.3. These tables define the permissible heat load patterns for the F-32 and F-37 baskets. The aggregate cask heat load, Q_d, under all storage configurations is limited to the value specified in Table 7.D.1.

3.1.3 Summary Table of Temperatures

The HI-STAR 180D Package temperatures are analyzed for normal transport condition for both F-32 and F-37 fuel baskets. All the permissible loading patterns for each basket are evaluated and details on the bounding pattern are discussed in Section 3.3. The hypothetical fire accident event is evaluated for thermally bounding scenario i.e. F-37 fuel basket with the bounding loading pattern. The modeling of the thermal problem is discussed in Sections 3.3 and 3.4. The analysis results are provided in Tables 3.1.1 and 3.1.3. The HI-STAR 180D normal transport and hypothetical accident temperatures comply with the normal and accident temperature limits specified in Tables 3.2.10, 3.2.11 and 3.2.12.

3.1.4 Summary Table of Maximum Pressures

The HI-STAR 180D Package containment boundary pressures are computed for normal transport condition and hypothetical fire accident event. The numerical modeling is discussed in Sections 3.3 and 3.4. The analysis results are provided in Tables 3.1.2 and 3.1.4. The HI-STAR 180D normal transport and hypothetical accident containment pressures comply with the pressure limits specified in Chapter 2, Table 2.1.1.

3.1.5 Cask Surface Temperature Evaluation

In accordance with the regulatory requirement specified in 10CFR71 (§71.43(g)), the cask surface temperature is computed in still air at 38ºC (100ºF) and in the shade. Under this scenario the maximum computed cask surface temperature reported in Table 3.1.5 is above the allowable surface temperature limit of 85ºC (185ºF). To meet the accessible surface temperature limit, a personnel barrier as defined in Chapter 1 will be required. The personnel barrier must be engineered to provide personnel protection without adversely impacting cask and fuel temperatures. In Section 3.3 a personnel barrier is conservatively defined and evaluated for the package at design basis heat load.

Table 3.1.1: HI-STAR 180D Normal Transport Maximum Temperatures

Material/Component	F-37 Basket Temperature °C (°F)	F-32 Basket Temperature °C (°F)
Fuel Cladding	363 (685)	352 (666)
Fuel Basket	338 (640)	327 (621)
Containment Shell	221 (430)	208 (406)
Neutron Shield[Note 1]	199 (390)	188 (370)
Lead	185 (365)	186 (367)
Cask Surface	144 (291)	138 (280)
Containment Baseplate[1]	181 (358)	172 (342)
Inner Closure Lid[1]	187 (369)	181 (358)
Outer Closure Lid[1]	112 (234)	108 (226)
Inner Closure Lid Seals[Note 2]		
Inner Closure Lid Inner Seal	169 (336)	162 (324)
Vent/Drain Port Cover Plate Inner Seal	172 (342)	165 (329)
Outer Closure Lid Seals[Note 2]		
Outer Closure Lid Inner Seal	119 (246)	114 (237)
Access Port Plug Seal	111 (232)	107 (225)
Basket Shims	256 (493)	254 (489)
Impact Limiter Type 1 Crush Material		
Bottom		
• Bulk	91 (196)	89 (192)
• Maximum	120 (248)	115 (239)
Top		
• Bulk	86 (187)	84 (183)
• Maximum	107 (225)	103 (217)
Impact Limiter Type 2 Crush Material		
Bottom		
• Bulk	80 (176)	79 (174)
• Maximum	84 (183)	83 (181)
Top		
• Bulk	77 (171)	75 (167)
• Maximum	81 (178)	79 (174)
Note 1: The temperature of the neutron shield component with the highest temperature is reported. Note 2: The temperatures on lid seals relied upon for containment function are reported herein. The containment boundary seals are identified in Chapter 4.		

[1] In accordance with temperature limits Table 3.2.10 Note (a) the maximum section temperatures of structural members are reported.

Table 3.1.2: HI-STAR 180D Maximum Operating Pressures

Condition	F-37 Basket		F-32 Basket	
	Absolute Pressure[1] kPa (psia)	Bulk Temperature ºC (°F)	Absolute Pressure[1] kPa (psia)	Bulk Temperature ºC (°F)
Fuel Storage Cavity MNOP[2]				
Initial Backfill (at 21.1ºC (70°F))	199.9 (29)[3]	288 (550)	199.9 (29)[3]	273 (523)
Normal Condition	381.2 (55.3)		370.8 (53.8)	
With 3% Rods Rupture(Note 1)	402.5 (58.4)		388.8 (56.4)	
Inter-Lid Space	155.8 (22.6)	114 (237)	154.4 (22.4)	110 (230)

Note 1: In accordance with NUREG-1617 [3.1.3], 3% of the rods are assumed to be breached releasing 100% fill gas and 30% fission gas to containment.

1 The coincident gage pressure defined as pressure above 1 atm ambient pressure is below the gage pressure limit under normal transport specified in Table 2.1.1.

2 Pressure analysis in accordance with heat condition specified in 10 CFR 71.71(c)(1) in the absence of venting, external ancillary cooling or operational controls.

3 The HI-STAR 180D helium backfill pressure limits are specified in Table 7.1.4. For a bounding evaluation the upperbound limit is used in the pressure calculations.

Table 3.1.3: Hypothetical Fire Accident Maximum HI-STAR 180D Temperatures

Material/Component	Initial Condition[1] ºC (°F)	During Fire ºC (°F)	Post Fire Cooldown ºC (°F)
Fuel Cladding	363 (685)	363 (685)	393 (739)
Fuel Basket	338 (640)	338 (640)	370 (698)
Containment Shell	221 (430)	222 (432)	255 (491)
Containment Baseplate[Note 1]	181 (358)	181 (358)	240 (464)
Inner Closure Lid[Note 1]	187 (369)	187 (369)	230 (446)
Inner Closure Lid Seals[Note 2]			
Inner Closure Lid Inner Seal	169 (336)	170 (338)	210 (410)
Vent/Drain Port Cover Plate Inner Seal	172 (342)	172 (342)	213 (415)
Outer Closure Lid Seals[Note 2]			
Outer Closure Lid Inner Seal	119 (246)	150 (302)	219 (426)
Access Port Plug Seal	111 (232)	113 (235)	189 (372)
Basket Shims	256 (493)	256 (493)	290 (554)
Note 1: In accordance with temperature limits Table 3.2.10 Note (a) the maximum section temperatures of structural members are reported. Note 2: The temperatures on lid seals relied upon for containment function are reported herein. The containment boundary seals are defined in Chapter 4.			

1 The initial condition is the bounding F-37 basket reported in Table 3.1.1.

Table 3.1.4: Maximum HI-STAR 180D Hypothetical Fire Accident Pressures

Condition	Absolute Pressure[1] kPa (psia)	Cask Cavity Bulk Temperature °C (°F)
No fuel rods rupture	400.5 (58.1)	317 (603)
With assumed 100% fuel rods rupture[2]	1154.6 (167.5)[Note 1]	
Note 1: The HI-STAR 180D fuel cavity accident pressure bounds the inter-lid pressure.		

1 The coincident gage pressure defined as pressure above 1 atm ambient pressure is below the accident condition fuel cavity and inter-lid space gage pressure limits specified in Table 2.1.1.

2 Pressure analysis is based on NUREG 1617 [3.1.3] requirements: Release of 100% of the rods fill gas and 30% of the significant radioactive gases from ruptured rods.

Table 3.1.5: HI-STAR 180D Normal Transport Surface Temperature in Shade

Material/Component	Temperature °C (°F)
Surface Temperature	128 (262)

3.2 MATERIAL PROPERTIES AND COMPONENT SPECIFICATIONS

3.2.1 Material Properties

Materials present in the HI-STAR 180D Packaging include structural steels, aluminum, lead, neutron shielding material (Holtite-B), neutron absorber (Metamic-HT), impact limiter crush material and helium. In Table 3.2.1, a summary of references used to obtain cask material properties for performing all thermal analyses is presented.

Thermal conductivity data of cask structural steels, neutron shielding materials, impact limiters, lead, insulation and helium are provided in Table 3.2.2. Thermal conductivities of fuel, aluminum basket shims, stainless steel basket shims and fuel basket (Metamic-HT) are provided in Tables 3.2.3, 3.2.4 and 3.2.5.

Surface emissivity data for key materials of construction are provided in Table 3.2.6. The emissivity properties of painted surfaces are generally excellent. Kern [3.2.5] reports an emissivity range of 0.8 to 0.98 for a wide variety of paints. In the HI-STAR 180D Package thermal analysis, an emissivity specified in Table 3.2.6[†] is applied to exterior painted surfaces. A theoretical bounding solar absorbtivity coefficient of 1.0 is applied to all exposed cask surfaces.

In Table 3.2.7, the specific heat and density data of cask materials is presented. These properties are also used in performing transient (hypothetical fire accident condition) analyses. The viscosity of helium is presented in Table 3.2.8.

The HI-STAR 180D Package exposed surfaces heat transfer coefficient is calculated by accounting for both natural convection heat transfer and radiation. Natural convection from a heated horizontal cylinder depends upon the product of the Grashof (Gr) and Prandtl (Pr) numbers. Following the approach developed by Jakob and Hawkins [3.2.8], GrPr is expressed as $L^3 \Delta T\ Z$, where L is the diameter of the cask, ΔT is the cask surface-to-ambient temperature differential and Z is a parameter which is a function of air properties evaluated at the average film temperature. The temperature dependence of Z for air is provided in Table 3.2.9.

The long-term thermal stability and radiation resistance of Holtite-B is discussed in Section 1.2.1.5. The Holtite-B thermal stability test temperature, reported in Table 2.2.13, is above the maximum operating temperature of Holtite-B (See Table 3.1.1). Holtite-B is capable of operating at this temperature in sustained use without a significant weight loss.

3.2.2 Component Specifications

The HI-STAR 180D Package materials and components which are required to be maintained

[†] This is conservative with respect to prior cask industry practice, which has historically accepted higher emissivities. For example, the TN-32 TSAR (Docket 72-1021) uses 0.95 emissivity and HI-STAR SAR (Dockets 72-1008 and 71-9261) uses 0.85 emissivity for painted surfaces.

below maximum pressure and temperature limits for safe operation, to ensure their intended functions, are summarized in Chapter 2 (Table 2.1.1) and Chapter 3 (Tables 3.2.10, 3.2.11 and 3.2.12). These materials and components do not degrade under exposure to extreme low temperatures. As defined by transport regulations, the HI-STAR 180D Package cold service temperature is conservatively limited to –40ºC (-40ºF).

Long-term stability of the neutron shield material (Holtite-B) under normal transport conditions is ensured when material exposure temperatures are maintained below the permissible limits. The cask metallic seals ensure leak tightness of the closure plates if the manufacturer's recommended design temperature limits are not exceeded. Integrity of SNF during transport requires demonstration of HI-STAR 180D Package fuel cladding temperatures below regulatory limits for Moderate Burnup Fuel (MBF) and High Burnup Fuel (HBF). In the HI-STAR 180D thermal evaluation, the cladding temperature limits of ISG-11, Rev. 3 [3.3.3] are adopted (See Table 3.2.11). These limits are applicable to all fuel types, burnup levels and cladding materials approved for power generation. Neutron absorber material (Metamic-HT) used for criticality control is stable in excess of 538°C (1000°F). For conservatism temperature limits well below the threshold of material integrity† are adopted (See Tables 3.2.10, 3.2.11 and 3.2.12).

For evaluation of the HI-STAR Package's thermal performance under hypothetical accident conditions, lowerbound material temperature limits for short-duration events are defined in Tables 3.2.10, 3.2.11 and 3.2.12.

† Neutron absorber materials are manufactured using B_4C and aluminum. B_4C is a refractory material that is unaffected by high temperatures and aluminum is solid at temperatures in excess of 538ºC (1000°F).

Table 3.2.1: Summary of HI-STAR Packaging Materials Thermal Property References

Material	Emissivity	Conductivity	Density	Heat Capacity
Helium	NA	Handbook [3.2.2]	Ideal Gas Law	Handbook [3.2.2]
Zircaloy Cladding	EPRI [3.2.3]	NUREG [3.2.6]	Rust [3.2.4]	Rust [3.2.4]
UO_2	Not Used	NUREG [3.2.6]	Rust [3.2.4]	Rust [3.2.4]
Stainless Steel (machined forgings)	Kern [3.2.5]	ASME [3.2.7]	Marks' [3.2.1]	Marks' [3.2.1]
Stainless Steel Plates	ORNL [3.2.13], [3.2.14]	ASME [3.2.7]	Marks [3.2.1]	Marks [3.2.1]
Carbon Steel	Kern [3.2.5]	ASME [3.2.7]	Marks [3.2.1]	Marks [3.2.1]
Aluminum Basket Shims	Note 1	ASM [3.2.12]	ASM [3.2.12]	ASM [3.2.12]
Holtite-B	Not Used	Table 2.2.13		Polymer Handbook [3.2.15]
Metamic-HT	Note 1	Note 1	Note 1	Note 1
Impact Limiter Crush Material	NA	Note 2	Table 2.2.10	ASME [3.2.7]
Lead	NA	Handbook [3.2.2]	Handbook [3.2.2]	Handbook [3.2.2]
Air	NA	Handbook [3.2.2]	Ideal Gas Law	Handbook [3.2.2.]
Note 1: The thermal properties of Metamic-HT used in the safety analysis are presented in Table 2.2.8. Note 2: Nominal values of thermal conductivity are specified in Table 3.2.2.				

Table 3.2.2: Thermal Conductivity of HI-STAR 180D Cask Materials

Material	@ 93.3ºC (200°F) W/m-ºK (Btu/ft-hr-°F)	@ 232.2ºC (450°F) W/m-ºK (Btu/ft-hr-°F)	@ 371.1ºC (700°F) W/m-ºK (Btu/ft-hr-°F)
Helium	0.1686 (0.0976)	0.2227 (0.1289)	0.2722 (0.1575)
Stainless Steel	14.5 (8.4)	17.0 (9.8)	19.0 (11.0)
Carbon Steel	47.7 (27.6)	45.5 (26.3)	41.5 (24)
Cryogenic Steel	41.1 (23.8)	41.0 (23.7)	38.5 (22.3)
Lead	33.6 (19.4)	31.0 (17.9)	29.2 (16.9)
Air	0.0299 (0.0173)	0.0389 (0.0225)	0.047 (0.0272)
Impact Limiters[1] Type 1 Crush Material	Axial	84.8 (49)	
	Radial	5.78 (3.34)	
Impact Limiters Type 2 Crush Material	Axial	81.3 (47)	
	Radial	5.16 (2.98)	
Holtite-B[1]	Table 2.2.13		
Note: Since the impact limiters are located at cask ends and peak temperatures are seen at approximately fuel mid height, the thermal conductivity of impact limiter does not affect the cask peak temperatures significantly. For modeling completeness, reasonable values are used in thermal evaluations [3.4.1].			

1 Reasonably bounding values under normal and fire accident conditions are tabulated herein. During post-fire cooldown conductivity is understated (See Table 3.4.1).

Table 3.2.3: Thermal Conductivity of Fuel Assembly Materials

Fuel Cladding		Fuel (UO_2)	
Temperature ºC (°F)	Conductivity W/m-ºK (Btu/ft-hr-°F)	Temperature ºC (°F)	Conductivity W/m-ºK (Btu/ft-hr-°F)
200 (392)	14.3 (8.28)	37.8 (100)	6.02 (3.48)
300 (572)	15.1 (8.76)	231.1 (448)	6.02 (3.48)
400 (752)	16.6 (9.60)	298.9 (570)	5.60 (3.24)
500 (932)	18.06 (10.44)	422.8 (793)	3.94 (2.28)

Table 3.2.4: Thermal Conductivity of Aluminum (Basket Shims Material)

Material	Conductivity W/m-ºK (Btu/ft-hr-°F)
Alloy 2219-T8511	120 (69.3)

Table 3.2.5: Metamic-HT Thermal Conductivity Data

Material	Conductivity W/m-ºK (Btu/ft-hr-°F)
Metamic-HT	Table 2.2.8

Table 3.2.6: Summary of Materials Surface Emissivity Data

Material	Emissivity
Fuel cladding	0.80
Painted surfaces	0.85
Stainless Steel (Machined Forgings)	0.36
Stainless Steel Plates	0.587
Carbon steel	0.66
Aluminum (Basket Shims)	Note 1
Metamic-HT	Note 1
Cask Interior Surfaces	0.2 (refer to Chapter 2, Subsection 2.2.1)
Polished Stainless Steel[1] (Impact Limiter Surfaces)	Emissivity: 0.11 Absorbtivity: 0.42
Note 1: Aluminum shims and Metamic-HT surfaces are hard anodized to yield high emissivities. The surface emissivity specified in Table 2.2.8 applies to both Metamic-HT and Aluminum (basket shims) surfaces. Conservatively, lowerbound emissivity values are used in the thermal analyses.	

[1] Surface properties from NASA technical report [3.2.10].

Table 3.2.7: Materials Density and Specific Heat Properties Summary

Materials		Density kg/m^3 (lbm/ft^3)	Specific Heat J/kg-°C (Btu/lbm-°F)
Helium		(Ideal Gas Law)	5183 (1.24)
Air		(Ideal Gas Law)	1006 (0.0421)
Zircaloy Cladding		6553 (409)	304 (0.0728)
Fuel (UO_2)		10959 (684)	234 (0.056)
Stainless Steel		8025 (501)	502 (0.12)
Structural Steel		7835 (489)	418 (0.1)
Metamic-HT		Table 2.2.8[1]	Table 2.2.8
Aluminum Crush Material	Type 1	352 (22)	961 (0.23)[Note 1]
	Type 2	304 (19)	961 (0.23)[Note 1]
Aluminum Basket Shims		2840 (178)	864 (0.207)
Holtite-B		Table 1.2.12	836 (0.2)[Note 2]
Lead		11000 (686)	129 (0.031)

Note 1: Heat capacity of Aluminum tabulated herein. Aluminum crush material heat capacity is computed by the volume weighted heat capacity of impact limiter components and air.
Note 2: A reasonably lowerbound specific heat of polymer [3.2.15] is used in the thermal evaluations.

[1] Conservatively understated for fire accident analysis.

Table 3.2.8: Helium and Air Viscosity Variation with Temperature[1]

Temperature (°F)	Helium Viscosity (Micropoise)	Temperature (°F)	Air Viscosity (Micropoise)
167.4	220.5	32.0	172.0
200.3	228.2	70.5	182.4
297.4	250.6	260.3	229.4
346.9	261.8	338.4	246.3
463.0	288.7	567.1	293.0
537.8	299.8	701.6	316.7
737.6	338.8	1078.2	377.6

1 Obtained from Rohsenow and Hartnett [3.2.2].

Table 3.2.9: Variation of Natural Convection Properties Parameter "Z" for Air with Temperature[1]

Temperature (°F)	Z (ft^{-3} $°F^{-1}$)
40	2.1×10^{6}
140	9.0×10^{5}
240	4.6×10^{5}
340	2.6×10^{5}
440	1.5×10^{5}

[1] Obtained from Jakob and Hawkins [3.2.8].

Table 3.2.10: HI-STAR 180D Structural Materials Temperature Limits

Component	Material	Normal Condition Temperature Limits[a] °C (°F)	Short Term Operations & Accident Temperature Limits[a] °C (°F)
Fuel Basket	Metamic-HT	350 (662)[b]	475 (887)[e]
Basket Shims	Aluminum Alloy	271 (520)[f]	371 (700)[e]
Basket Shims	Stainless Steel	271 (520)[c]	371 (700)[e]
Containment Shell	Cryogenic Steel	232 (450)[c]	371 (700)[d]
Containment Baseplate and Closure Flange	Cryogenic Steel	204 (400)[c]	371 (700)[d]
Inner and Outer Closure Lids	Cryogenic Steel	204 (400)[c]	371 (700) (Structural Accidents)[d] 420 (788) (Fire Accident[e]
Monolithic Shield Surface	Carbon Steel	204 (400)[c]	371 (700) (Structural accidents)[d] 788 (1450) (Fire Accident)[e]
Impact Limiter	Crush Material (Types 1 and 2)	-40 – 121 (-40 – 250)	-40 – 121 (-40 – 250) (Structural Accidents) N/A (Fire Accident)

Notes

(a) The ASME Code requires that the vessel design temperature be established with appropriate consideration of internal or external heat generation. In accordance with ASME Section III Code, Para. NCA-2142 the design temperature is set at or above the structural members' section temperature defined as the maximum through thickness mean metal temperature of the part under consideration. The section temperatures of the structural members shall not exceed the temperatures limits tabulated herein.
(b) The temperature limits of Metamic-HT are bounded by the maximum material qualification test temperatures [1.2.27].
(c) The normal condition temperature limits conservatively bound the ASME Code temperature limits.
(d) The accident temperatures of structural members must not exceed the ASME code temperature limits.
(e) To preclude melting the short term and fire accident temperature limits are set well below the melting temperature of structural steel, Metamic-HT and Aluminum Alloys.
(f) Supported by Table 2.2.9.

Table 3.2.11: Fuel Cladding Temperature Limits

Component	Material	Normal Condition Temperature Limits ºC (ºF)	Short Term Operations & Accident Temperature Limits ºC (ºF)
Fuel Cladding (Moderate Burnup Fuel)	See Note 1	400 (752)	570 (1058)
Fuel Cladding (High Burnup Fuel)	See Note 1	400 (752)	400 (752) (Short Term Operations) 570 (1058) (Accident)

<u>Notes</u>

1. Fuel cladding temperature limits are applicable to all cladding materials approved for power generation [3.3.3].

Table 3.2.12: HI-STAR 180D Component Temperature Limits

Component	Material	Normal Condition Temperature Limits °C (°F)	Short Term Operations & Accident Temperature Limits °C (°F)
Inner and Outer Closure Lid Seals	Note 1	200 (392)	Note 5
Closure Lids Port Cover and Port Plug Seals	Note 1	200 (392)	371 (700)
Neutron Shield	Holtite-B	Table 2.2.13	Note 2
Gamma Shield	Lead	316 (600)	316 (600)[Note4]
Impact Limiter Bulk	Aluminum Alloy Crush Material	Table 2.2.10	NA[Note 3]

Notes

1. Metallic seals as described in Chapter 2 and licensing drawings are standard materials used by seal manufacturers for high integrity (leaktight) sealing. The temperature limits tabulated herein bound the manufacturers recommended limits.
2. Neutron shield temperature limits are applicable during normal transport and short-term operations. During fire no reduction in Holtite-B heat conduction effectiveness is assumed. During post-fire cooldown conductivity of air is assumed.
3. Structural integrity of the crush material is not relied to comply with transport regulations during or after the fire accident.
4. To preclude melting the short term and fire accident temperature limits are set well below the melting temperature of lead.
5. The Inner Closure Lid Inner Seal will remain leaktight for at least 1 week for temperatures less than or equal to 450 °C, will remain leaktight for at least 1 year for temperatures less than or equal to 250 °C and will remain leaktight for at least 50 years for temperatures less than or equal to 200 °C

3.3 THERMAL EVALUATION UNDER NORMAL CONDITIONS OF TRANSPORT

The HI-STAR 180D Package is designed to safely dissipate heat under passive conditions (no wind). Under normal transport conditions, the cask contents (fuel basket, fuel and basket shims) rest on solid surfaces. Direct contact between the cask and its contents enhances heat dissipation. Nevertheless to engineer a robust measure of conservatism a hypothetical bounding configuration (levitating fuel basket) is assumed. Under this assumption, the fuel, fuel basket, basket shims and cask are in concentric alignment (i.e. they do not make physical contact).

The HI-STAR 180D Package consists of two distinct fuel basket geometries, the F-32 and F-37 designs engineered to hold 32 and 37 PWR fuel assemblies. The cask is rated for different heat loads for different basket types, as discussed in Chapter 1. Apart from their storage capacity, the two fuel basket designs are similar with respect to the basket material (Metamic-HT), basket construction (interlocking honeycomb panels) and thickness of the Metamic-HT plates. From a thermal-hydraulic standpoint both the two fuel baskets give similar cask and fuel temperatures. However as higher temperatures are reached in the F-37 basket (See Table 3.3.4), an F-37 equipped HI-STAR 180D Package is evaluated for compliance with transport regulations.

The HI-STAR 180D Package thermal analysis is performed using the FLUENT CFD code [3.3.2]. FLUENT is a well-benchmarked CFD code validated by the code developer with an array of theoretical and experimental works from technical journals. Additionally, Holtec has Q.A. validated FLUENT within the company's quality assurance program and confirmed the code's capability to reliably predict temperature fields in dry storage [3.3.4] using independent full-scale test data from a loaded cask [3.2.3]. The code has a long history of usage for obtaining NRC approval of fuel storage in transport and storage casks. A list of dockets wherein USNRC relied on FLUENT thermal models for cask certification is given in Table 3.3.3.

The HI-STAR 180D cask is designed to allow fuel loading under different regionalized loading conditions. The maximum aggregate cask decay heat is limited to the values specified in Table 7.D.1. Under regionalized loading, the fuel storage cells (Figures 7.D.1 and 7.D.2) are grouped in eight regions in F-32 basket and nine regions in F-37 basket (Table 7.D.5) and regionalized fuel decay heat limits are defined in Tables 7.D.2 and 7.D.3 under an array of fuel loading patterns A through C for F-37 basket and A through B for F-32 fuel basket. Loading patterns B and C for F-37 basket and loading pattern B for F-32 basket have the same two options, 1S and 2S. As explained next, the fuel loading patterns optimize shielding and thermal design of the HI-STAR 180D Package. To define a limiting pattern, an array of bounding fuel storage configurations is analyzed using 3D thermal models of the F-32 and F-37 baskets, as discussed later in this section. The results of pattern screening evaluation are presented in Table 3.3.4. As highlighted in Table 3.3.4 the highest cladding temperatures are reached in heat load distribution corresponding to Option 2S in F-37 fuel basket. Modeling details of the principal thermal transport mechanisms are provided in the following.

Fuel Region Effective Planar Conductivity

In the HI-STAR 180D thermal modeling, the cross section bounded by the inside of a storage cell is replaced with an "equivalent" square section characterized by an effective thermal conductivity in the planar and axial directions. Figure 3.3.1 pictorially illustrates this concept. The two conductivities are unequal because while in the planar direction heat dissipation is interrupted by inter-rod gaps; in the axial direction heat is dissipated through a continuous medium (fuel cladding). The equivalent planar conductivity of the storage cell space is obtained using a 2D conduction-radiation model of the fuel (PWR 14x14 assembly). The fuel geometry is constructed using the FLUENT's pre-processor GAMBIT [3.3.1]. The 2-D model, consisting of an array of fuel rods with helium gaps between them residing in a storage cell is illustrated in Figure 3.3.2. In the axial direction, an area-weighted average of the cladding and helium conductivities is computed. These calculations are presented in Reference [3.3.7].

The fuel region effective planar conductivity is defined as the calculated equivalent conductivity of the fuel storage cell by including conduction and radiation heat transfer. Because radiation is proportional to the fourth power of absolute temperature, the effective conductivity is a strong function of temperature. The 2-D CFD model is used to characterize fuel resistance at several representative storage cell temperatures and the effective thermal conductivity as a function of temperature obtained and presented in Table 3.3.1.

Heat Rejection from Cask and Impact Limiter Surfaces

The exposed surfaces of the HI-STAR 180D Package dissipate heat by radiation and external natural convection heat transfer. Radiation is modeled using classical equations for radiation heat transfer (Incropera and DeWitt [3.2.11]). Jakob and Hawkins [3.2.8] recommend the following correlations for natural convection heat transfer to air from heated vertical surfaces (flat impact limiter ends) and from horizontal cylinders (cask and impact limiter cylindrical surfaces):

Turbulent range:

$$h = 0.19\,(\Delta T)^{1/3}\ (\text{Vertical, GrPr} > 10^9)$$
$$h = 0.18\,(\Delta T)^{1/3}\ (\text{Horizontal Cylinder, GrPr} > 10^9)$$
$$(\text{in conventional U.S. units})$$

Laminar range:

$$h = 0.29\,\left(\frac{\Delta T}{L}\right)^{1/4}\ (\text{Vertical, GrPr} < 10^9)$$
$$h = 0.27\,\left(\frac{\Delta T}{D}\right)^{1/4}\ (\text{Horizontal Cylinder, GrPr} < 10^9)$$
$$(\text{in conventional U.S. units})$$

where ΔT is the temperature differential between the package exterior surface and ambient air and GrPr is the product of Grashof and Prandtl numbers. During normal transport conditions, the surfaces to be cooled are the impact limiter and cask cylindrical surfaces, and the flat vertical faces of the impact limiters. The corresponding length scales L for these surfaces are the impact limiter diameter, cask diameter, and impact limiter diameter, respectively. As described in Section 3.2, Gr×Pr can be expressed as $L^3 \Delta TZ$, where Z (from Table 3.2.9) is at least 2.6×10^5 at a conservatively high surface temperature of150ºC (302°F). It is thus apparent that the turbulent condition is always satisfied assuming a lowerbound L (8 ft) and a small ΔT (~10ºF). For conservatism the more limiting turbulent correlation ($h = 0.18\ \Delta T^{1/3}$) is used in the thermal analysis.

Determination of Solar Heat Input

The intensity of solar radiation incident on exposed surfaces depends on a number of time varying parameters. The solar heat flux strongly depends upon the time of the day as well as on latitude and day of the year. Also, the presence of clouds and other atmospheric conditions (dust, haze, etc.) can significantly attenuate solar intensity levels. In the interest of conservatism, the solar attenuation effects of dust, haze, angle of incidence and latitude are neglected.

The insolation energy absorbed by the HI-STAR 180D Package is the product of incident insolation and the package absorbtivity. For conservatism theoretical bounding absorbtivity equal to unity is assumed for the cask surfaces. For polished surfaces solar absorbtivity obtained from robust sources is applied (See Table 3.2.6). The HI-STAR 180D Package thermal analysis is based on 12-hour daytime insolation specified in 10CFR71. During normal transport conditions, the HI-STAR Package is cyclically subjected to solar heating during the 12-hour daytime period followed by cooling during the 12-hour nighttime. However, due to the large mass of metal and the size of the Package, the dynamic time lag exceeds the 12-hour heating period. Accordingly, the HI-STAR Package model includes insolation at exposed surfaces averaged over a 24-hour time period. The 10CFR71 12-hour insolation is summarized in Table 3.3.2.

To demonstrate the reasonableness of this approach, a sensitivity study is performed to evaluate cyclic effects of solar heating. A three-dimensional 12-hour cyclic transient analysis (referred to henceforth as the transient analysis) is performed while the three-dimensional 24-hour average steady-state analysis (referred to henceforth as the steady-state analysis) discussed above remains the licensing basis evaluation.

The transient analysis has the same inputs and boundary conditions as the steady-state analysis, the only difference being the introduction of the cyclic solar insolation. The transient analysis is performed until a “steady cyclic behavior” was obtained. The Holtite-B temperature result from the transient analysis with sufficiently large number of cycles that show steady cyclic behavior is graphed in Figure 3.3.9. Margins to MSC Holtite-B temperatures are lowest and is therefore adopted for comparison. The results between the transient analysis and the steady-state analysis are summarized in Table 3.3.13. Results from the transient analysis demonstrates that all components include MSC Holtite temperature remains below its design temperature limit.

Since the cyclic transient effect of solar insolation on the cask is small compared to steady state 24-hour average solar insolation, the method of applying solar insolation averaged over 24-hour period is reasonable.

HI-STAR 180D 3D Model

The HI-STAR 180D fuel baskets are essentially an array of square cells within an irregularly shaped basket outline. The fuel basket is confined inside a cylindrical cavity of the HI-STAR 180D containment shell. Between the fuel basket-to-cask cavity spaces, thick basket shims are installed to facilitate heat dissipation. To ensure an adequate representation of the fuel basket a geometrically accurate 3D model of the array of square cells and Metamic-HT plates is constructed using the FLUENT CFD code pre-processor. Other than the representation of fuel assemblies inside the storage cell spaces as a solid region with effective properties, the 3D model explicitly includes the cask components as described next. The basket shims are explicitly modeled in the peripheral spaces. The fuel basket is surrounded by the HI-STAR 180D cask body embedded with neutron shield pockets, outfitted with two bolted lids and impact limiters installed on both ends. All of these physical details are explicitly included in a quarter-symmetric 3D thermal model of the HI-STAR 180D Package. An overview of the principal features of the 3D thermal model is provided in the following.

(i) The fuel basket is modeled as a quarter-symmetric array of fuel storage cells formed by a honeycomb matrix of Metamic-HT plates.
(ii) The spent nuclear fuel is assumed to be levitating in the fuel storage cells with a uniform gap (See Figure 3.3.1). A sensitivity study is performed to evaluate the effect of asymmetry between the fuel basket components and cask cavity and presented in Paragraph 3.3.1.4.
(iii) As illustrated in Figure 3.3.1 the fuel cell storage spaces are replaced with a solid having equivalent temperature dependent planar and axial conductivities (See Table 3.3.1).
(iv) In the normal transport condition (horizontal orientation) the basket shims, fuel basket and cask cavity are in gap-free contact. For conservatism, the aluminum basket shims external surfaces and fuel basket external surfaces are modeled with hypothetical large interface resistances equivalent to 3 mm helium gap. The resistances are applied at the shims-to-basket and shims-to-cavity interfaces using FLUENT conduction walls in the HI-STAR 180D thermal model. Based on prior studies on the gap between the basket-basket shims-containment shell [3.3.6], a uniform gap of 3 mm each between the basket and basket shims and between basket shims and containment shell is modeled since it results in bounding fuel and basket temperatures [3.3.6]. The maximum total radial cold gap is specified in Table 3.3.7. The net radial thermal expansion of the basket (Table 3.4.2) combined with the total gap of 6 mm present in the thermal model bounds the maximum radial gap specified in Table 3.3.7.
(v) The modeling input parameters used in the thermal model are summarized in Table 3.3.7.
(vi) The HI-STAR 180D containment shell, baseplate, inner and outer lids, cask body, the staggered array of neutron shield pockets, monolithic cylinders and the two end

impact absorbers are explicitly included in the 3D model (See Figure 3.3.5).

(vii) To evaluate the hot transport condition, the appropriate external loads (38ºC (100ºF)) ambient air temperature and solar insolation (Table 3.3.2)) are applied on all external surfaces of the package.

(viii) The limiting decay heat distribution (See Table 3.3.4) is applied to the fuel storage cells as axially distributed heat sources with peaking in the active fuel mid-section.

(ix) The gas in the plenum areas between the basket and closure lid, and the basket and containment baseplate can move freely. However, internal convection heat transfer in the cask cavity (Rayleigh effect) is conservatively neglected. This maximizes the peak temperatures since heat transfer from the basket to the closure lid or containment baseplate due to helium movement is completely ignored.

The HI-STAR 180D Package thermal analysis is based on a 3D thermal model of the HI-STAR 180D cask that properly accounts radiation, conduction and external natural convection modes of heat transfer. The model is constructed using an array of conservative assumptions to bias the results of the thermal analysis towards much reduced computed margins. The thermal assumptions are listed below.

1. No credit for contact heat transfer. The cask contents are assumed to be in an adverse configuration (levitating fuel, fuel basket and shims).

2. The fuel basket peripheral gaps are overstated.

3. Internal natural convection heat transfer in the cask cavity is neglected.

4. Conductivity of neutron shielding materials understated.

5. Axial heat transfer through fuel pellets is neglected.

6. Design maximum heat load and a bounding decay heat distribution pattern defined in Section 3.3 are assumed.

7. The spent fuel decay heat of all the fuel assemblies in the cask is conservatively assumed to have the same bounding maximum burnup profile (Table 5.4.1(a)) thereby maximizing the fuel temperatures.

8. Heat dissipation by fuel assembly grid spacers neglected.

9. The solar attenuation effects of dust, haze, angle of incidence and latitude are neglected.

10. All the thermal analysis conservatively adopts lowerbound emissivity of dark grey anodized surfaces as specified in Table 2.2.8.

11. Removal of the lead shielding feature from the Inner Closure Lid Core and its replacement with steel (i.e. solid core) has no material impact on fuel cladding or package

component temperatures. The thermal conductivity of steel is higher than that of lead and the change in thermal resistance is negligible. Furthermore, the overall package heat transfer through the top end of the package is a fraction of that heat transfer through the entire package.

Sectional and isometric views of the HI-STAR 180D thermal model are presented in Figures 3.3.3, 3.3.4 and 3.3.5 respectively.

Screening Calculations to Ascertain Limiting Scenario

To define the thermally most limiting HI-STAR 180D transport scenario the following cases are evaluated:

(i) All patterns of F-32 basket defined in Table 7.D.2
(ii) All patterns of F-37 basket defined in Table 7.D.3

To evaluate the above scenarios, 3D FLUENT screening models of the HI-STAR 180D cask are constructed, Peak Cladding Temperatures (PCT) computed and tabulated in Table 3.3.4. The results of the calculations yield the following conclusion:

(a) Fuel transport in F-37 produces a higher PCT than that in F-32
(b) Option 2S in fuel loading patterns B and C for F-37 results in the highest PCT and cask component temperatures than the other loading patterns

To conservatively predict the HI-STAR 180D transport temperatures, the limiting scenario ascertained above is adopted for evaluation of all normal, short-term and accident conditions.

Grid Sensitivity Studies

To ensure mesh independent CFD results, a grid sensitivity study of the thermal model of the bounding F-37 basket in the HI-STAR 180D cask is performed with particular attention to mesh density in areas of high thermal resistance. The grid refinement is performed in the entire domain i.e. for both fluid and solid regions in both axial and radial directions.

A number of grids are generated to study the effect of mesh refinement on the fuel and component temperatures. All sensitivity analyses were carried out for the case of F-37 with thermally bounding loading pattern. Per ASME V&V [3.3.5], it is recommended that the mesh refinement in 3D be at least 2.2 times the previous mesh. This recommended criterion is satisfied by the meshes specified in Table 3.3.5 that gives a brief summary of the different sets of grids evaluated and PCT results.

As can be seen from the above table, the PCT is essentially the same for all the four meshes. The small PCT difference between the meshes is negligible compared to the available PCT safety margin. To provide further assurance of convergence, the sensitivity results are evaluated in accordance with the ASME V&V 20-2009 [3.3.5]. Towards this end, the apparent order of the method is calculated for Meshes 0, 1 and 2 and Meshes 1, 2 and 3. It is determined to be approximately the same for the simulation series and also close to theoretical value of 2. A constant order of method for the simulation series demonstrates mesh convergence. The Grid Convergence Index (GCI) is computed to be 0.245%. Based on these results, Mesh 1 grid layout is adopted for the thermal analysis of the HI-STAR 180D Package.

To this model insolation heat (Table 3.3.2) is applied on all external surfaces of the HI-STAR 180D Package assuming 100% absorption for cask external surfaces. Natural convection and radiation from exposed surfaces is enabled to model heat dissipation to ambient air. Using this model, steady state HI-STAR 180D Package temperatures in still air for the limiting decay heat distribution defined in Section 3.3 are computed and evaluated in the next section.

3.3.1 Heat and Cold

3.3.1.1 Maximum Temperatures

As required by transport regulations the HI-STAR 180D Package is evaluated under hot ambient conditions defined in 10CFR71. These conditions are 38°C (100°F) ambient temperature, still air and insolation (Table 3.3.2). To ensure a bounding evaluation, design heat load and a limiting heat load distribution (See Section 3.1.2) are assumed. Under this array of adverse conditions, the maximum steady state temperature of the package structural members and its contents (SNF) are computed. The temperatures are computed using the 3D thermal model described in Section 3.3 and results reported in Subsection 3.1.3. The following observations are derived by inspecting the temperature field obtained from the thermal analysis:

- The maximum fuel cladding temperature (Table 3.1.1) is well within the ISG-11, Rev. 3 temperature limit (Table 3.2.11).
- The maximum temperature of fuel basket (Table 3.1.1) is well within the design temperatures (Table 3.2.10).
- The maximum temperatures of the containment boundary and lid seals (Table 3.1.1) are well below the design temperatures (Tables 3.2.10 and 3.2.12, respectively).
- The maximum temperatures of the basket shims (Table 3.1.1) are well below the design temperature limits (Table 3.2.10).
- The neutron shielding material (Holtite-B) temperature (Table 3.1.1) is within its design limit (Table 3.2.12).

The temperatures of the HI-STAR 180D Package during normal transport are reported in Section 3.1.3. The temperatures are below the regulatory temperature limits (Table 3.2.11), ASME Code temperature limits (Table 3.2.10) and components safe operating temperature limits (Table 3.2.12). The above observations lead us to conclude that the temperature field in the HI-STAR 180D Package loaded with heat emitting SNF complies with all regulatory requirements for normal conditions of transport. In other words, the thermal environment in the HI-STAR 180D Package is conducive to safe transport of spent nuclear fuel.

3.3.1.2 Minimum Temperatures

As specified in 10CFR71, the HI-STAR 180D Package is evaluated for a cold environment at -40°C (-40°F). The HI-STAR Package design does not require minimum decay heat load restrictions for transport. Therefore zero decay heat load and no solar input are bounding conditions for cold evaluation. Under these conditions, the temperature distribution in the HI-STAR 180D Package uniformly approaches the cold ambient temperature. All HI-STAR 180D Package materials of construction satisfactorily perform their intended function in the transport mode at this minimum postulated temperature condition. Evaluations in Chapter 2 demonstrate the acceptable structural performance of the package materials at low temperature. The HI-STAR 180D shielding and criticality materials (Holtite-B and Metamic-HT) are unaffected by exposure to cold temperatures.

3.3.1.3 Personnel Barrier Evaluation

As defined in Chapter 1, personnel barrier is an open lattice cage placed around the HI-STAR 180D cask to prevent access to the hot surfaces (See Figure 1.3.2). The open structure ensures that movement of ambient air is not unduly restricted and the cask temperatures are not impacted. To provide an additional layer of assurance a thermal calculation was performed assuming bounding personnel barrier characteristics defined in Table 3.3.8. The thermal calculation deployed the same 3D HI-STAR 180D thermal model articulated in this section above except for the following major differences:

1. The thermal model is half-symmetric (see Figure 3.3.6)
2. Gas motion inside the cask cavity is included
3. An enveloping porous cylinder having the flow characteristics of the personnel barrier defined in Table 3.3.8 is modeled

To ensure mesh independent CFD results, a grid sensitivity study of the thermal model of the HI-STAR 180D cask equipped with a personnel barrier is performed similar to that discussed in this section. The grid refinement is performed in the entire domain i.e. for both fluid and solid regions in both axial and radial directions.

A number of grids are generated to study the effect of mesh refinement on the fuel and component temperatures. All sensitivity analyses were carried out for the case of F-37 with thermally bounding loading pattern. Per ASME V&V [3.3.5], it is recommended that the mesh refinement in 3D be at least 2.2 times the previous mesh. This recommended criterion is satisfied by the meshes specified in Table 3.3.12 that gives a brief summary of the different sets of grids evaluated and PCT results.

As can be seen from the above table, the small PCT difference between the meshes is negligible compared to the available PCT safety margin. To provide further assurance of convergence, the sensitivity results are evaluated in accordance with the ASME V&V 20-2009 [3.3.5]. The PCT results from these three grids demonstrate an asymptotic range of convergence. In addition, the apparent order of the method is calculated for the simulation series and is determined to be equal to 2, which is the same as the theoretical order. The Grid Convergence Index (GCI) is computed to be 0.365%. A three-grid solution for the observed order equal to 2 is adequate since the predicted PCT on the three grids are in the asymptotic region for the simulation series. Based on these results, Mesh 1 grid layout is adopted for the thermal analysis of the HI-STAR 180D Package.

The cask temperatures with and without the personnel barrier are tabulated in Table 3.3.9. The results show that the cask temperatures are essentially unchanged by the deployment of the personnel barrier.

3.3.1.4 Evaluation of Asymmetry during Transport Condition

During transport, the HI-STAR 180D is positioned horizontally. Therefore, the fuel assemblies are not centered in the fuel cell, and the basket and shim are not centered in cavity of containment shell. Licensing basis evaluations assume levitating condition. A sensitivity study is performed in this section to evaluate the effects of asymmetry due to gravity during transport condition.

Under this real condition, the fuel assemblies rest on the bottom side panel of the basket cells during horizontal transport which results in the center of the fuel assembly not aligned with the center of the basket cell. Consequently, the gap between the fuel assembly and the basket cell is larger on the top side than that on the bottom side. This causes a higher heat resistance between the fuel assembly and the basket panel on the top side and a lower heat resistance between the fuel assembly and the basket panel on the bottom side. The 2D effective properties thermal model discussed in Section 3.3 is modified to evaluate this condition, as shown in Figure 3.3.10. Steady State simulations are performed on this configuration at three different basket panel temperatures similar to that described in Section 3.3. The resultant effective fuel planar thermal conductivities are presented in Table 3.3.14 for helium filled condition. The results show that the effective properties under the real scenario are bounded by the scenario (Table 3.3.1) adopted in licensing basis evaluations.

In the thermal model of normal transport condition in Reference [E-2], it is assumed that the basket and shim are centered in cavity of containment shell. A uniform gap of 3 mm is modeled between the basket external wall and the aluminum shims, and a uniform gap of 3 mm is modeled between the aluminum shims and the containment shell.

During horizontal transport, the basket is in partial contact with the containment shell, and the aluminum shims are either resting on the containment shell or on the basket. This real scenario results in some contact between basket, basket shims and containment shell and smaller gaps between these components towards the bottom side than on the top side of the cask. Under this configuration, resistance to heat from the fuel assemblies to the containment shell is higher on the top side and lower on the bottom side. To study the effect of this real configuration, a half-symmetric model is developed, and bounding condition as detailed in [3.4.1]. A steady state evaluation of this configuration is performed for the bounding fuel loading pattern and F-37 fuel basket without considering convection inside the cask cavity. The peak cladding temperature result from this study is presented as Case 1 in Table 3.3.15. Results demonstrate that assuming levitating condition between basket, basket shims and cask cavity results in bounding temperatures.

3.3.1.5 Effect of Natural Convection in Cask Cavity during Transport

As described earlier in Section 3.3.1, all evaluations of transport condition do not credit heat convection by helium flow inside the cask cavity. A steady state evaluation of the real condition described in Paragraph 3.3.1.4 is performed with credit for convection in all open areas within the cask cavity except the fuel assemblies. The peak cladding temperature result from this study is reported as Case 2 in Table 3.3.15. The PCT in this evaluation is much lower than the computed PCT in the licensing basis thermal model (Table 3.1.1). The PCT is expected to be even lower when helium flow thru the fuel assemblies is also included.

3.3.2 Maximum Normal Operating Pressure (MNOP)

The HI-STAR 180D cavity is de-moisturized and backfilled with dry helium after fuel loading and prior to lid closures. The MNOP evaluation considers the following source of gases:

Initial Backfill:
The HI-STAR 180D cavity is assumed to be backfilled to the maximum permissible pressure (Table 7.1.4).

Water Vapor:
The HI-STAR 180D cavity and its stored fuel are de-moisturized to a very low vapor pressure (Table 7.1.2). As this pressure is dwarfed by the helium backfill pressure it is neglected in the MNOP calculations.

Helium from radioactive decay:
The helium from radioactive decay is dwarfed by the generation of fission products during power generation. These products are assumed to be released into the HI-STAR 180D cavity under hypothetical rod ruptures. As radioactive decay is a small fraction of the fission gas releases it is neglected in the MNOP calculations.

Generation of flammable gases:
The HI-STAR 180D Package uses non-reactive materials of construction. Generation of flammable gases is not credible.

Fuel Rod Failures:
In accordance with NUREG 1617 [3.1.3], 3% of the fuel rods are assumed to be breached.

During normal transport conditions, the gas temperature within the cavity rises to its maximum operating temperature as determined by the thermal evaluation described earlier. The gas pressure inside the cavity increases monotonically with rising temperature. The pressure rise is determined using the Ideal Gas Law.

The HI-STAR 180D Maximum Normal Operating Pressure (MNOP) is calculated for the §71.71(c)(1) heat condition (38ºC (100ºF) ambient, still air & insolation) and design maximum heat load. Based on a 30% release of the significant radioactive gases and 100% release of the rod fill gas from postulated cladding breaches (3%) the cask cavity space MNOP is computed and reported in Subsection 3.1.4. The HI-STAR 180D cavity pressures presented in Table 3.1.2 show that the MNOP is well below the design pressure of the containment boundary (Table 2.1.1).

The evaluation of pressures and temperatures reached during transport provides reasonable assurance of safe transport of spent nuclear fuel packaged in a HI-STAR 180D Package. This conclusion is based on the technical data and analyses presented in this chapter in conjunction with provisions of 10 CFR Part 71, appropriate regulatory guides, applicable codes and standards, and accepted engineering practices.

3.3.3 Time-to-Boil Limits

In accordance with NUREG-1536 [3.1.2], water inside the HI-STAR 180D cavity is not permitted to boil during fuel loading operations. In this manner operational concerns due to vapor formation and two-phase conditions are avoided. To meet this requirement time limits are defined herein for completion of wet operations upon removal of a loaded HI-STAR 180D cask from the pool.

When the HI-STAR 180D cask is removed from the pool, the combined water, fuel and cask metal mass absorb the decay heat emitted by the fuel assemblies. This results in a slow temperature rise of the cask with time, starting from an initial temperature of the contents. The rate of temperature rise is limited by the thermal inertia of the HI-STAR 180D. To obtain a heat-up rate, a conservative adiabatic heat up calculation may be adopted or alternatively the 3-D Fluent methodology articulated in this section may be deployed.

(a) Adiabatic Heatup Method

The adiabatic heat up calculation assumes the following:

i. Obtain the heat input Q from the fuel assemblies loaded in the cask.
ii. Heat dissipation to air by natural convection and radiation from the cask is neglected.
iii. Water mass in the cask cavity is understated by 50% for conservatism.

The rate of temperature rise of the cask under adiabatic heat up (assumption (ii) above) is computed as follows:

$$\frac{dT}{dt} = \frac{Q}{C_h}$$

where:

Q = cask heat load, W (Btu/hr) (Table 1.2.3)
C_h = thermal inertia of the loaded cask, J/°C (Btu/°F)
T = cask temperature, °C (°F)
t = time after inner closure lid is placed on the loaded cask while under water OR time after time to boil clock has been reset, s (hr)

The maximum permissible time duration, t_{max} for fuel to be submerged in water is computed as follows:

$$t_{max} = \frac{T_{boil} - T_{initial}}{(dT/dt)}$$

where:

T_{boil} = lowerbound boiling temperature of water (100°C (212°F) at the water surface)
$T_{initial}$ = initial cask temperature (pool temperature during in-pool fuel loading operations)

Example values of t_{max} under design maximum heat load are tabulated in Table 3.3.6 at several representative $T_{initial}$ temperatures.

(b) CFD Method

To obtain a heat-up rate, the 3-D FLUENT thermal model articulated in this section may be deployed with following modifications:

i. Cask is placed in vertical orientation.
ii. Secondary lid and impact limiters are not included since they are not present during wet transfer operations.
iii. Water motion inside the cask is enabled and is modeled as laminar.
iv. Heat dissipation by radiation and external natural convection from the cask external surfaces is included.
v. Fuel in the basket cell is modeled as a porous media with thermal properties presented in Table 3.3.1.

A transient CFD evaluation shall be performed using the above model with initial water temperature as the initial condition. The bulk water temperature inside the cask must remain below the boiling temperature i.e. 100°C.

3.3.3.1 Additional Measures During Extended Duration Operations

In the unlikely event that the maximum allowable time provided in Table 3.3.6 is found to be insufficient to complete wet transfer operations, forced water circulation may be provided to remove the decay heat from the cask cavity. During forced circulation relatively cooler water enters the inner closure lid drain port connection and heated water exits from the vent port. The minimum water flow rate required to maintain the water temperature below boiling is determined as follows:

$$M_W = \frac{Q_c}{C_{pW}\,(T_{max} - T_{in})}$$

where:

Q_c	= cask decay heat, W (Btu/hr)
M_W	= minimum water flow rate, kg/s (lb/hr)
C_{pw}	= water heat capacity, J/kg-°C (Btu/lb-°F)
T_{max}	= cask user selected maximum cavity water temperature, °C (°F) (must be less than 100°C (212°F))
T_{in}	= water supply temperature, °C (°F)

3.3.4 Fuel Temperatures During Moisture Removal Operations

The initial loading of SNF in the HI-STAR 180D requires that the water within the cask cavity be drained and replaced with helium. Since the design heat loads are high, this operation may be carried out using the cyclic vacuum drying approach as described in Section 3.3.4.1 limiting the fuel temperature excursions to ISG-11 criteria of 65°C under cyclic drying or by a forced flow helium drying process as described in Subsection 3.3.4.2. In the vacuum drying method evaluated in Subsection 3.3.4.1, removal of the last traces of residual moisture from the HI-STAR 180D is accomplished by evacuating the cavity after draining the cask. Based on the cask heat load, the time duration for vacuum drying cycles will vary for cask containing one or more high burnup fuel assemblies.

3.3.4.1 Vacuum Drying

Prior to the start of the HI-STAR 180D draining operation, the cask cavity is flooded with water. The presence of water in the cask cavity ensures that the fuel cladding temperatures are lower than design basis limits by large margins. As the heat generating active fuel length is uncovered during the draining operation, the fuel and basket mass undergo a gradual heat up from the initially cold conditions when the heated surfaces were submerged under water. Following the draining operation the HI-STAR 180D cavity is lined up to vacuum pump and the cavity pressure substantially lowered to facilitate fuel drying. However, at the Design Basis heat loads in HI-STAR 180D cask, the peak cladding temperature cannot be maintained below the ISG-11, Revision 3 limit of 400°C (752°F) under a vacuum condition of infinite duration. Under this scenario, cycles of vacuum drying resulting in heatup followed with cooling by helium are performed until drying criteria specified in Chapter 7 is achieved. The purpose of this evaluation is to compute permissible time duration available to perform the heatup/cooldown cycles for a cask with design maximum heat load. It must be noted that the permissible time for heatup/cooldown cycles is a function of cask specific heat loads. At lower heat loads the duration of vacuum drying cycles is increased and if the heat load is low enough, then the peak cladding temperature may remain below the ISG-11 limit under vacuum conditions indefinitely eliminating the need for cycling.

Following is a summary of the methodology and assumptions used in the thermal evaluation for multiple vacuum drying cycles performed for both F-32 and F-37 fuel baskets:

1. The HI-STAR 180D cavity is initially filled with water. The initial condition of the cask for vacuum drying is conservatively assumed to be at boiling temperature of water i.e. 100°C (212°F).

2. No impact limiters are present during loading operations.

3. F-37 heat distribution pattern with maximum decay heat defined in Tables 7.D.1 and 7.D.3 assumed. Similarly F-32 heat distribution pattern with maximum decay heat defined in Tables 7.D.1 and 7.D.2 assumed.

4. The cask bottom is assumed to be insulated.

5. The cask is assumed to be placed in still air and hot (38°C (100°F)) ambient temperature.

6. Cycle 1 (Heatup) – A transient thermal evaluation is performed for the bounding decay heat load pattern with the cask cavity under vacuum condition. The time required for the fuel to heatup from an initial temperature of 100°C (212°F) to 365°C (689°F)† is determined. If drying completion criteria is not met, then the cask cavity must be backfilled with helium for cooldown before it reaches the temperature limit of 400°C (752°F).

7. Cycle 1 (Cooldown) – The cask cavity is backfilled with helium to 1 atm absolute pressure. Fuel cooling under helium is evaluated until the fuel temperature decreases by 65°C (117°F) and the maximum permissible time is obtained from the transient evaluation.

8. The drying process should return to vacuum drying again which now is the beginning of second cycle. Up to 9 additional multiple cycles of drying may be performed until the drying completion criteria is not met.

9. If a total of 10 drying cycles fail to meet drying criteria then other competent means to dry fuel (like FHD discussed in subsection 3.3.4.2) must be used or the cask must be de-fueled.

10. Only two cycles are evaluated as an example in this subsection to provide an estimate on the time available for drying and cooling.

† A sufficient margin to temperature limit of 400°C is maintained.

The variation of fuel temperature with time under vacuum and helium conditions is shown in Figures 3.3.7 and 3.3.8 for F-37 and F-32 baskets respectively. The maximum permissible time for each heatup and each cooldown cycle for two complete cycles is provided in companion Table 3.3.10 for both F-37 and F-32 baskets.

3.3.4.2 Forced Helium Dehydration

Demoisturization of the HI-STAR 180D cask loaded with high burnup fuel is conducted by the Forced Helium Dehydration (FHD) system. The FHD is a conventional, closed loop dehumidification system consisting of a condenser, a demoisturizer, a compressor, and a pre-heater. The FHD is utilized to extract moisture from the HI-STAR 180D cavity through forced circulation of dry heated helium. During fuel drying operations the FHD system provides concurrent fuel cooling by forced convection heat transfer. The enhanced heat transfer occurring during operation of the FHD system ensures that the fuel cladding temperature will remain well below the peak cladding temperatures under normal conditions of transport, which is below the high burnup cladding temperature limit 400ºC (752ºF) for all combinations of SNF type, burnup, decay heat, and cooling time authorized for loading in the HI-STAR 180D cask. Because the FHD operation induces a state of forced convection heat transfer in contrast to the quiescent mode of cooling under normal transport it is readily concluded that the peak fuel cladding temperature under the latter condition will be greater than that during the FHD operation phase. In the event that the FHD system malfunctions, the forced convection state will degenerate to natural convection in the vertical orientation, which bounds the condition of normal transport in the horizontal orientation. As a result, the peak fuel cladding temperatures will approximate the values reached during normal transport as described elsewhere in this chapter.

3.3.5 Fuel Reconfiguration

Fuel assemblies are loaded in the fuel basket as intact and remain intact prior to and during normal conditions of transport. However, there is a potential (based on uncertainties) that the fuel may reconfigure during transportation. A vibration analysis and other structural evaluations according to the approach summarized in Table 1.4.1 show that there is no damage to the fuel assemblies during normal conditions of transport or hypothetical accident conditions. However, as a defense-in-depth, thermal analysis is performed assuming a punitive hypothetical fuel reconfiguration during normal conditions of transport and hypothetical accident conditions (see Subsection 3.4.5) to analyze its impact on the containment boundary and its components. The details of the analysis are summarized below:

- Fuel assemblies in every fuel storage location are assumed to compact to a reasonably conservative value of 75% of its original length.
- Fuel is assumed to shift towards the cask inner lid to maximize the predicted seal temperatures which is a part of the containment boundary.

- A steady state thermal analysis is performed for the bounding fuel loading pattern and fuel basket.

- The heat load per assembly is assumed to be uniformly distributed along the active height of a fuel assembly.

The temperature results of such a steady state analysis for a defense-in-depth hypothetical scenario are reported in Table 3.3.11. The results show that the temperatures of all package components (except containment seal) are below their respective normal condition temperature limits and containment seal temperatures are below the limit that is established to ensure the cask remains leaktight for at least 1 year (Table 3.2.12). The cavity temperature and hence the cavity pressure during normal conditions of transport remains unaffected due to fuel reconfiguration. Therefore, the containment boundary remains intact during normal conditions of transport with non-mechanistic fuel reconfiguration. The licensing approach to address the potential for high burnup fuel reconfiguration is delineated in Section 1.4.

Table 3.3.1: PWR 14x14 Fuel Effective Conductivities

Temperature ºC (ºF)	Helium Backfilled Conditions Thermal Conductivity W/m-ºC (Btu/ft-hr-ºF)	Vacuum Drying Conditions Thermal Conductivity W/m-ºC (Btu/ft-hr-ºF)	Temperature ºC (ºF)	Waterfilled Condition Thermal Conductivity W/m-ºC (Btu/ft-hr-ºF)
Planar Conductivity				
93 (200)	0.444 (0.257)	0.156 (0.09)	38 (100)	1.044 (0.603)
232 (450)	0.727 (0.420)	0.382 (0.221)	66 (150)	1.090 (0.629)
371 (700)	1.152 (0.666)	0.765 (0.442)	93 (200)	1.115 (0.644)
-	-	-	121 (250)	1.137 (0.656)
Axial Conductivity				
93 (200)	1.365 (0.789)	1.275 (0.737)	37 (99)	1.529 (0.883)
232 (450)	1.517 (0.877)	1.402 (0.810)	67 (153)	1.588 (0.917)
371 (700)	1.707 (0.986)	1.571 (0.908)	97 (207)	1.637 (0.945)
-	-	-	127 (261)	1.680 (0.970)

Table 3.3.2: 10CFR71 Insolation Data

Surface Type	12-Hour Insolation	
	(g-cal/cm^2)	(W/m^2)
Horizontally Transported Flat Surfaces		
- Base	None	None
- Other Surfaces	800	774.0
Non-Horizontal Flat Surfaces	200	193.5
Curved Surfaces	400	387.0

Table 3.3.3: History of FLUENT for Securing Transport and Storage Cask Certifications

USNRC Docket Number	Project
72-1008	HI-STAR 100 Storage
71-9261	HI-STAR 100 Transport
72-1014	HI-STORM Storage
72-22	Private Fuel Storage Facility
72-27	Humboldt Bay ISFSI
72-26	Diablo Canyon ISFSI
72-17	Trojan ISFSI
71-9325	HI-STAR 180 Transport
71-9336	HI-STAR 60 Transport
72-1032	HI-STORM FW Storage

Table 3.3.4: Fuel Loading Pattern Screening Evaluations

Loading Pattern	Max. Fuel Cladding Temperature, ºC (ºF)
F-32 Fuel Basket	
A	352 (666)
Option 1S	344 (651)
Option 2S	344 (651)
F-37 Fuel Basket	
A	351 (664)
Option 1S	362 (684)
Option 2S	**363 (685)**

Notes:
(1) Fuel loading patterns with options are defined in Tables 7.D.2 and 7.D.3.
(2) The PCT for Option 2S in F-37 fuel loading patterns B and C is the bounding scenario. Therefore, the limiting fuel loading configuration, Option 2S in the fuel basket F-37 as highlighted above, is used for all the licensing basis calculations.

Table 3.3.5: Mesh Sensitivity Studies

Mesh No	Total Mesh Size	PCT, ºC (ºF)	Permissible Limit ºC (ºF)	Cladding Temperature Margin ºC (ºF)
0	272,944	362 (684)	400 (752)	38 (68)
1	595,250	363 (685)	400 (752)	37 (67)
2	1,348,329	363 (685)	400 (752)	37 (67)
3	2,852,324	364 (687)	400 (752)	36 (65)

Table 3.3.6: Maximum Allowable Time for Completion of Wet Transfer Operations

Pool Water Temperature, °C (°F)	F-32 Basket Time to Boil Limit, hours	F-37 Basket Time to Boil Limit, hours
30 (86)	27	25
35 (95)	25	23
40 (104)	23	21
45 (113)	21	19
50 (122)	19	17
55 (131)	17	16
60 (140)	15	14

Notes:
1. Reference time to boil limits are based on design basis cask heat load presented in Table 7.D.1 and the methodology presented in Section 3.3.3.
2. Users may use the reference time limits given in this table or calculate their own time limits according to Section 3.3.3.

Table 3.3.7: Modeling Input Data

Item	Input
Reference axial gap between the cask cavity and the fuel basket (mm)	21
Minimum axial gap between the cask cavity and the fuel basket	Table 3.4.2
Minimum total combined radial gap between the basket & the basket shim and the basket shim & inside diameter of containment shell	Table 3.4.2
Maximum total combined radial gap between the basket & the basket shim and the basket shim & inside diameter of containment shell (mm)	8
Difference between the basket panel thickness and the notch width of the intersecting panel (mm)	1.6
Average radial gap between monolithic shield cylinder segments (mm)	3
Average axial gap between monolithic shield cylinder segments (mm)	1

Table 3.3.8: Bounding Personnel Barrier Characteristics

Minimum Percent Open Area	50
Maximum Wire Thickness	1.6 mm (0.0625 inch)

Table 3.3.9: Personnel Barrier Thermal Evaluation

Material/Component	Temperature without the Personnel Barrier °C (°F)	Temperature with the Personnel Barrier Deployed °C (°F)
Fuel Cladding	363 (685)	368 (694)[Note 3]
Fuel Basket	338 (640)	344 (651)[Note 3]
Basket Shims	256 (493)	264 (507)[Note 3]
Containment Shell	221 (430)	230 (446)[Note 3]
Neutron Shield	199 (390)	209 (408)[Note 4]
Cask Surface	144 (291)	162 (324)[Note 5]

Notes:

(1) The cask temperatures tabulated herein are under the 10CFR71, §71.43(g) scenario (hot ambient, still air and in the shade). The maximum computed personnel barrier temperature (60°C (140°F)) complies with the accessible surface temperature limit (85°C (185°F)).

(2) The results tabulated herein show that HI-STAR 180D maximum cask temperatures have a small effect with the deployment of the Personnel Barrier.

(3) The slightly higher cask temperatures in the Personnel Barrier deployed configuration are as expected due to the presence of a personnel barrier that offers slightly higher resistance to air flow around the cask.

(4) Holtite temperature limit in a highly localized region is nominally exceeded under personnel barrier deployed configuration. The shielding performance of the package is not affected.

(5) The higher cask surface temperature in the Personnel Barrier deployed configuration is a highly localized temperature reached at the bottom of the horizontally oriented cask surface. The bulk of the barrier surface is at 43°C (109°F).

Table 3.3.10: Permissible Time Durations for Multiple Vacuum Drying Cycles

Description	Permissible Time for Operation in F-37 Basket, hours	Permissible Time for Operation in F-32 Basket, hours
Cycle 1 – Heatup [Notes 1 and 2] (Vacuum Drying Condition)	15	18
Cycle 1 – Cooldown (Gas Backfilled Condition [Note 3])	7	6
Cycle 2 – Heatup (Vacuum Drying Condition)	4	5
Cycle 2 – Cooldown (Gas Backfilled Condition [Note 3])	8	9

Notes:
1. Example case evaluated under heatup from a bounding 100^{o}C (212^{o}F) initial condition upon completion of cask dewatering operation.
2. Example case is evaluated assuming fuel cladding temperature excursions are limited to 65^{o}C.
3. Example case assumes helium as the cover gas at standard atmospheric pressure.

Table 3.3.11: HI-STAR 180D Maximum Temperatures Due to Fuel Reconfiguration

Component	Normal Conditions of Transport[Note 1], °C (°F)	Normal Conditions of Transport with Fuel Reconfiguration, °C (°F)
Fuel Cladding	363 (685)	398 (748)[Note 4]
Fuel Basket	338 (640)	371 (700)
Containment Shell	221 (430)	237 (459)
Neutron Shield[Note 2]	199 (390)	232 (450)[Note 5]
Lid Seals[Note 3]	172 (342)	229 (444)

Note 1: These temperature results are extracted from Table 3.1.1.
Note 2: The temperature of the neutron shield component with the highest temperature is reported.
Note 3: The temperature of the containment seal with the highest temperature is reported.
Note 4: This estimated temperature is reported for information only since under the postulated fuel reconfiguration, the ISG-11 cladding temperature limits are not germane to the safety evaluation.
Note 5: The conservative defense-in-depth study of fuel reconfiguration at design basis heat load indicates that up to 25mm (1 inch) thick layer of Holtite in the inner lid may exceed its temperature limit. The dose margin in the normal condition analyses for the dose point location at the top of the cask, when compared to the transportation dose limits, is sufficient to accommodate the dose increase due to the higher temperatures in an inch thick Holtite of the lid region. More information is provided in Chapter 5.

Table 3.3.12: Mesh Sensitivity Studies for HI-STAR 180D Thermal Model Equipped with a Personnel Barrier

Mesh No	Total Mesh Size	PCT, ºC (ºF)	Permissible Limit ºC (ºF)	Cladding Temperature Margin ºC (ºF)
1	1,977,315	368 (694)	400 (752)	32 (58)
2	4,433,928	371 (700)	400 (752)	29 (52)
3	9,669,942	372 (702)	400 (752)	28 (50)

Table 3.3.13: Effects of Cyclic Solar Heating – Holtite-B Maximum Temperature at the End of Each Transient Cycle

Cycle No. (Time Duration)	Maximum Temperature (^oC)
Steady State (t = 0)[Note 1]	198.65
1 (t = 0 to 24 hrs)	200.34
2 (t = 24 to 48 hrs)	200.92
3 (t = 48 to 72 hrs)	201.18
4 (t = 72 to 96 hrs)	201.35
5 (t = 96 to 120 hrs)	201.47
6 (t = 120 to 144 hrs)	201.52
7 (t = 144 to 168 hrs)	201.55
8 (t = 168 to 192 hrs)	201.56
Note 1: The maximum Holtite-B temperature from the licensing-basis steady-state thermal analysis (Table 3.1.1) is used as the starting point for the transient analysis.	

Table 3.3.14: PWR 14x14 Fuel Effective Planar Thermal Conductivities under Asymmetric Conditions

Temperature °C (°F)	Helium Backfilled Conditions Thermal Conductivity W/m-°C (Btu/ft-hr-°F)
93 (200)	0.446 (0.258)
232 (450)	0.731 (0.422)
371 (700)	1.157 (0.669)

Table 3.3.15: Peak Cladding Temperature (PCT) Under Normal Transport Condition

Scenario	Description	PCT (°C)
Licensing Basis	1. Levitating condition between basket, basket shims and containment shell 2. No credit for natural convection inside cask cavity	345 Note 1
Case 1	1. Asymmetric condition between basket, basket shims and containment shell 2. No credit for natural convection inside cask cavity	342
Case 2	1. Asymmetric condition between basket, basket shims and containment shell 2. Credit for natural convection inside cask cavity	336
Note 1: This PCT result is obtained from Table 3.1.1.		

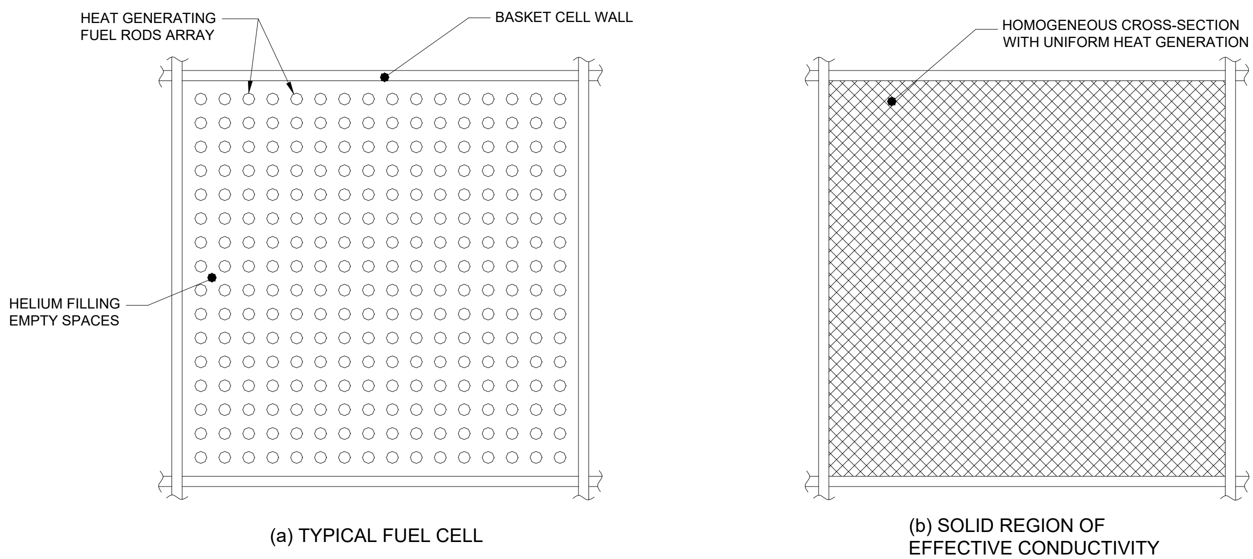

FIGURE 3.3.1: HOMOGENIZATION OF THE STORAGE CELL CROSS-SECTION

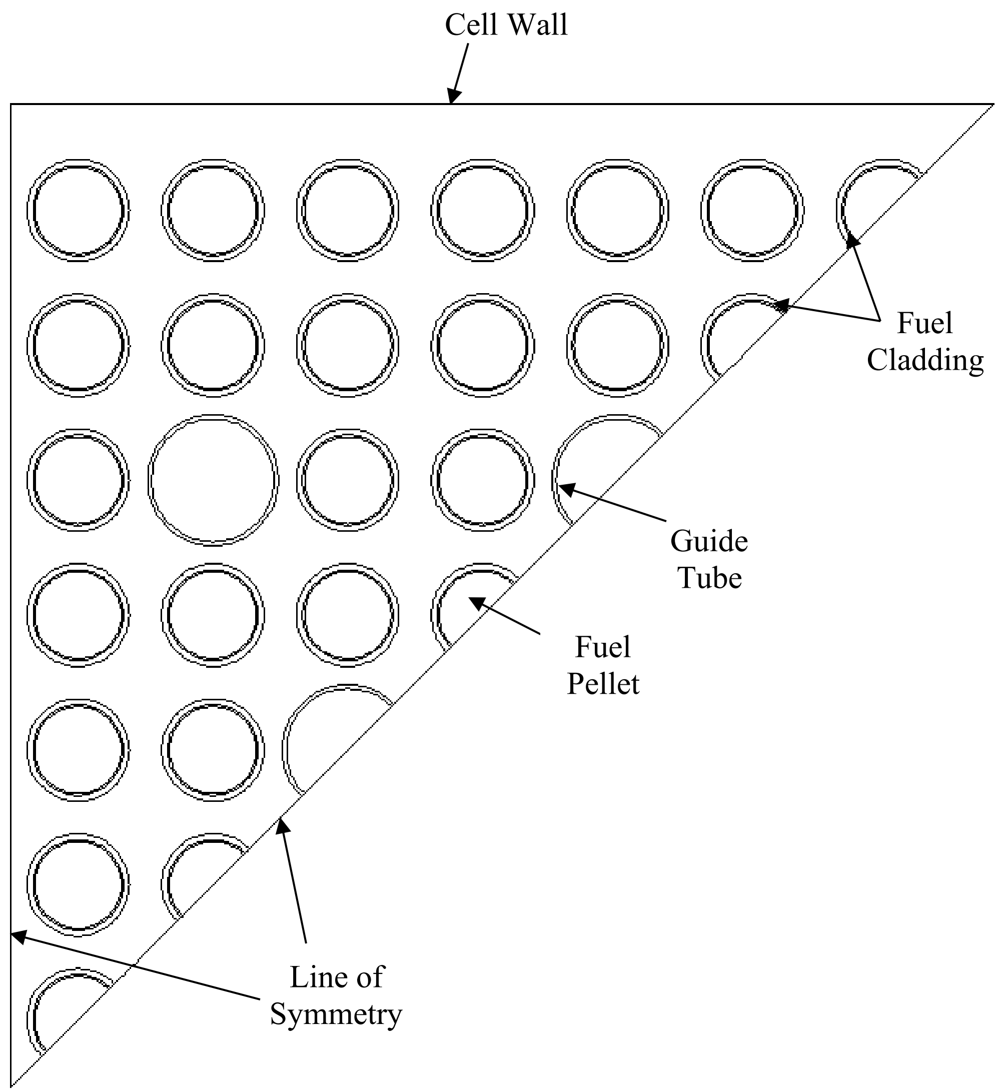

FIGURE 3.3.2: ONE-EIGHTH SYMMETRIC TWO-DIMENSIONAL CFD MODEL OF THE PWR 14x14 FUEL ASSEMBLIES

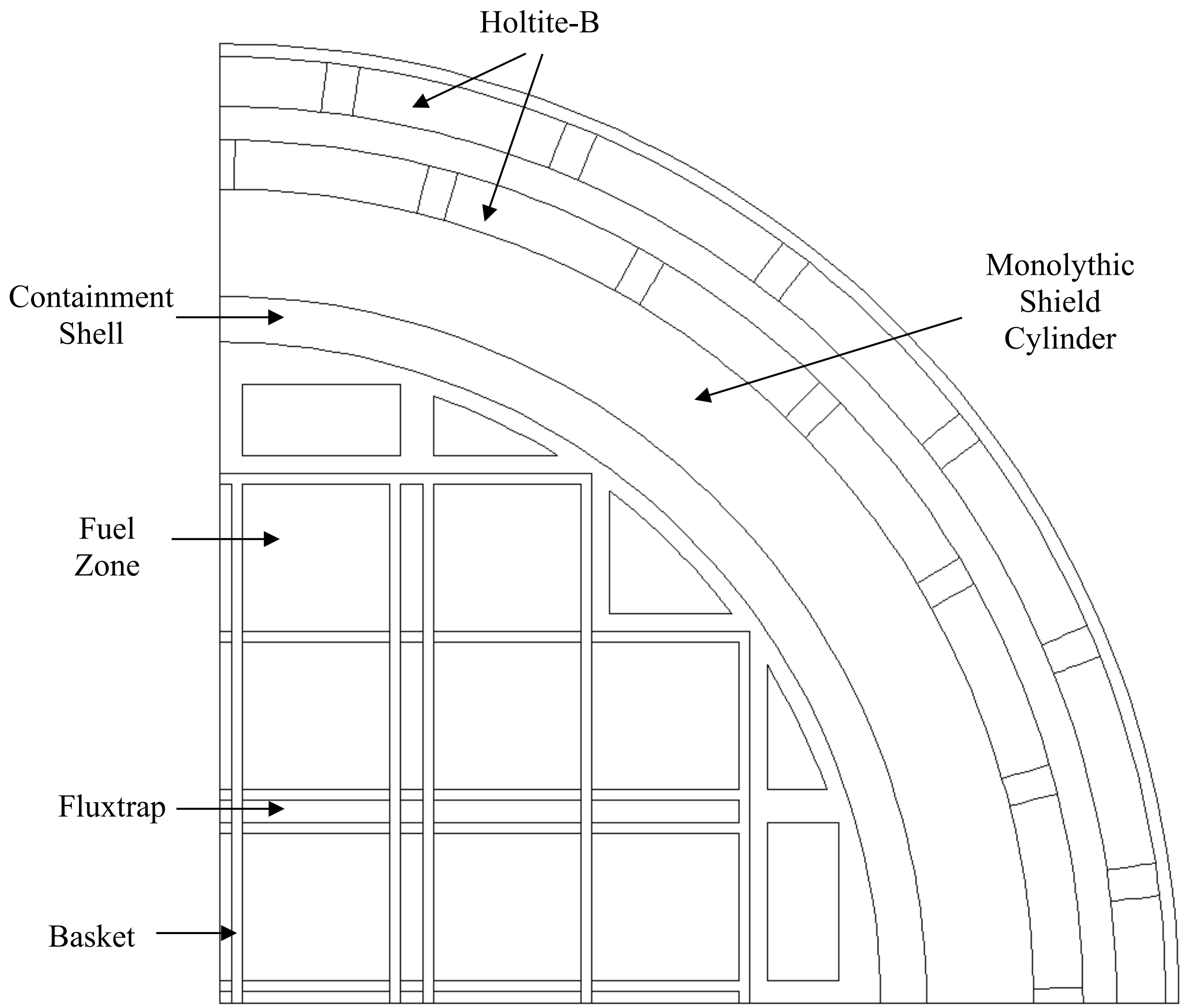

FIGURE 3.3.3: PLANAR VIEW OF F-32 BASKET IN THE HI-STAR 180D
3-D QUARTER-SYMMETRIC THERMAL MODEL
(IMPACT LIMITER, MESH OMITTED FOR CLARITY)

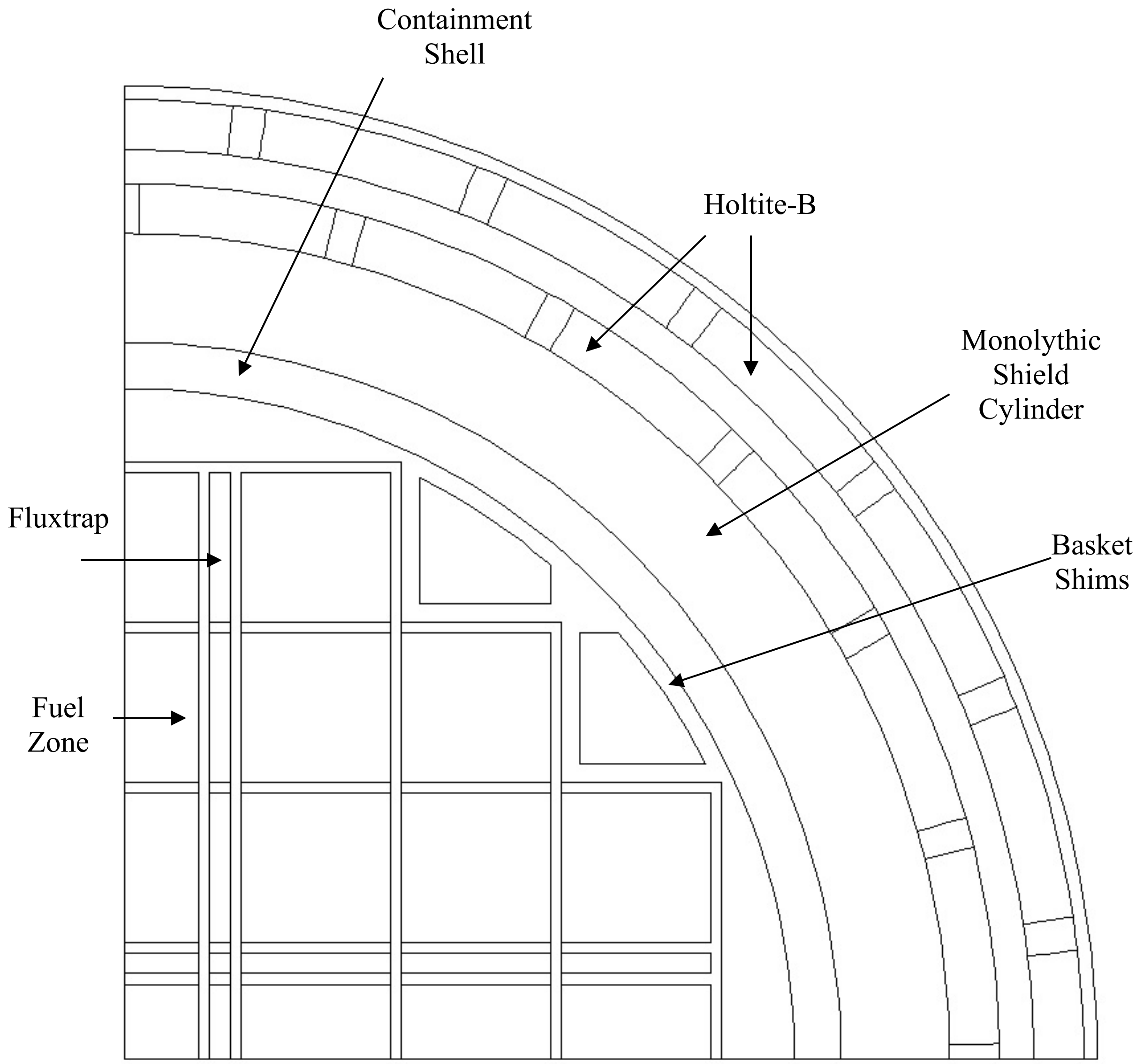

FIGURE 3.3.4: PLANAR VIEW OF F-37 BASKET IN THE HI-STAR 180D
3-D QUARTER-SYMMETRIC THERMAL MODEL
(IMPACT LIMITER, MESH OMITTED FOR CLARITY)

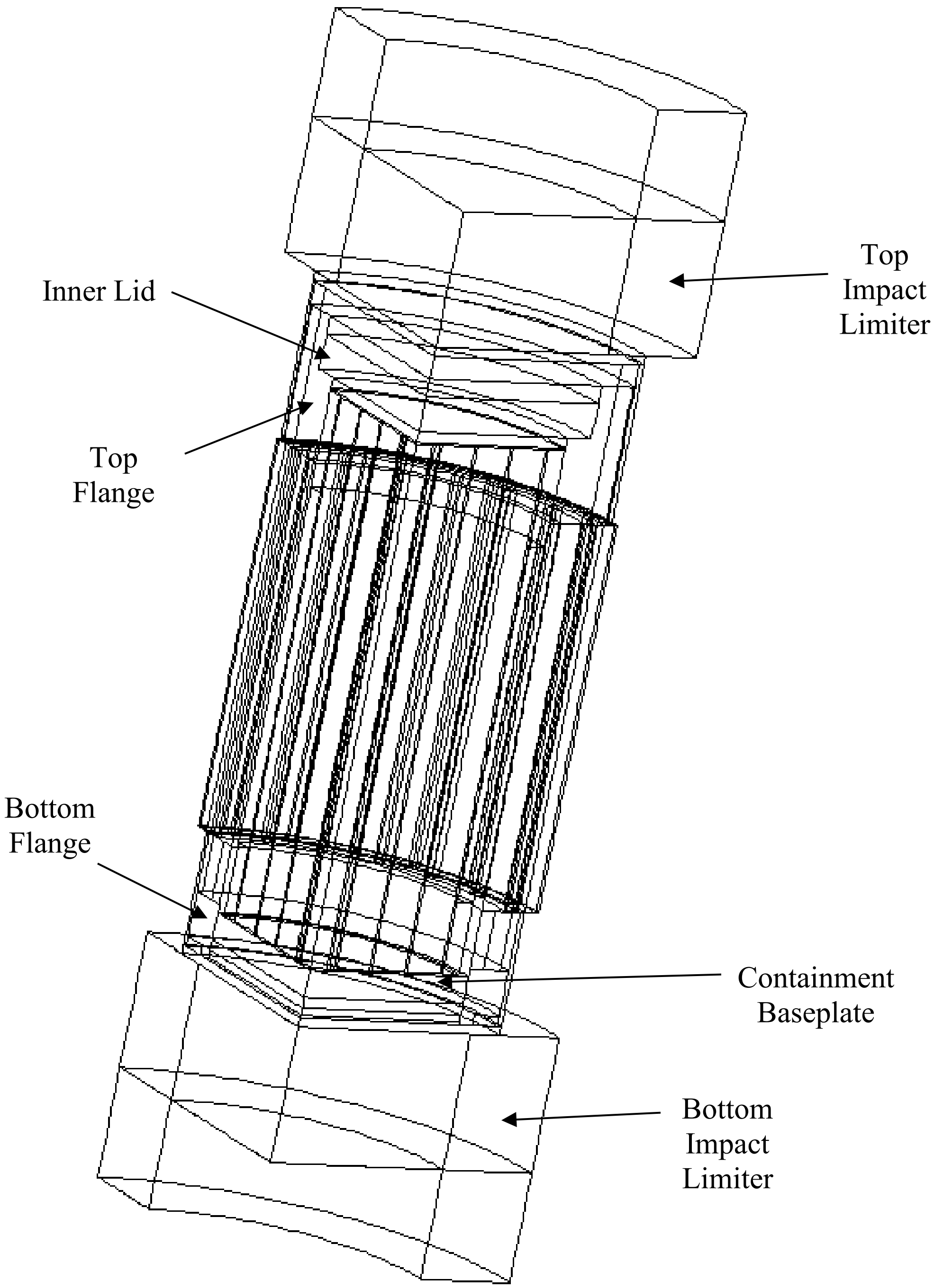

FIGURE 3.3.5: THREE-DIMENSIONAL VIEW OF THE HI-STAR 180D THERMAL MODEL (F-37 FUEL BASKET, MESH OMITTED FOR CLARITY)

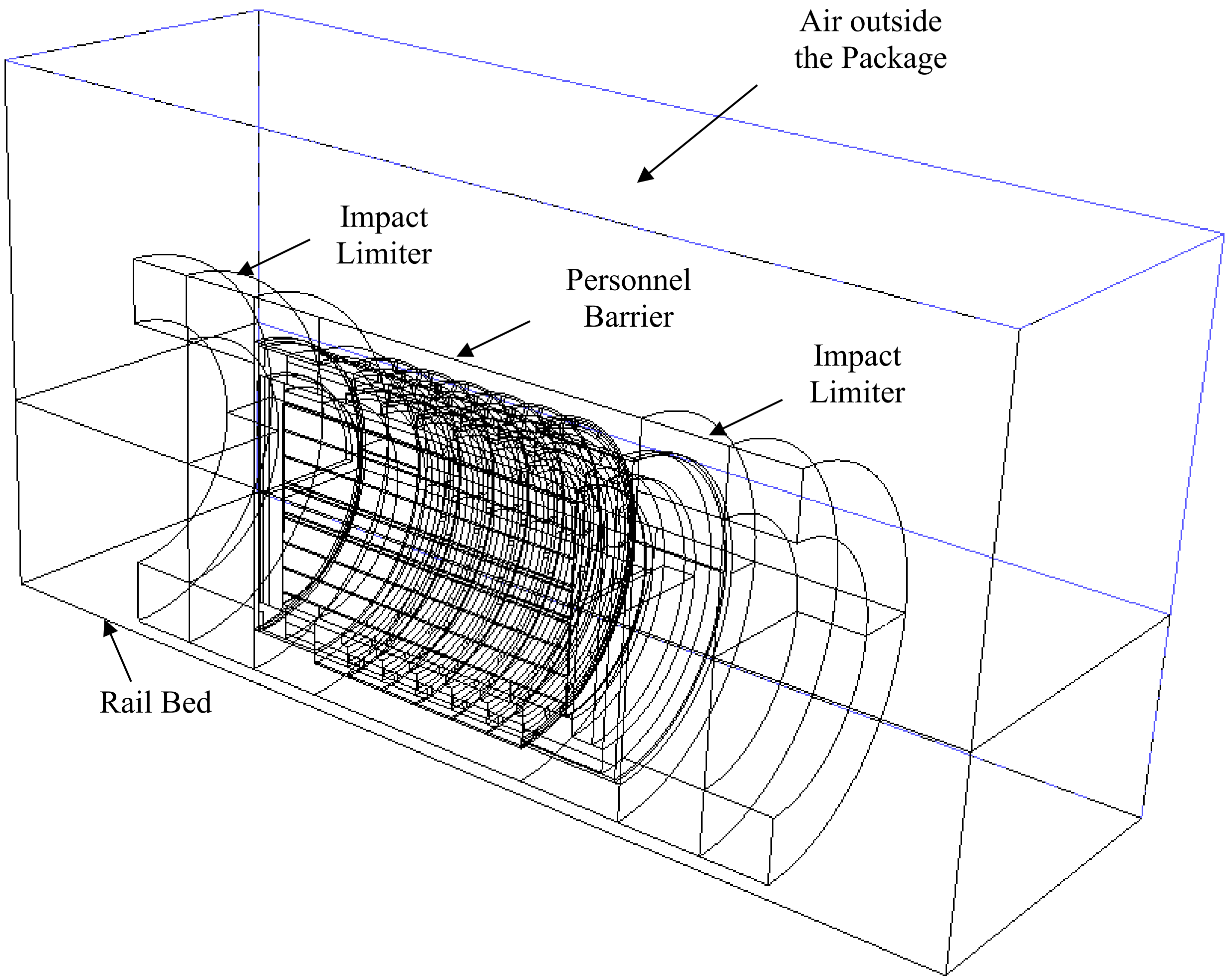

FIGURE 3.3.6: HALF-SYMMETRIC THREE-DIMENSIONAL HI-STAR 180D THERMAL MODEL EQUIPPED WITH A PERSONNEL BARRIER (MESH OMITTED FOR CLARITY)

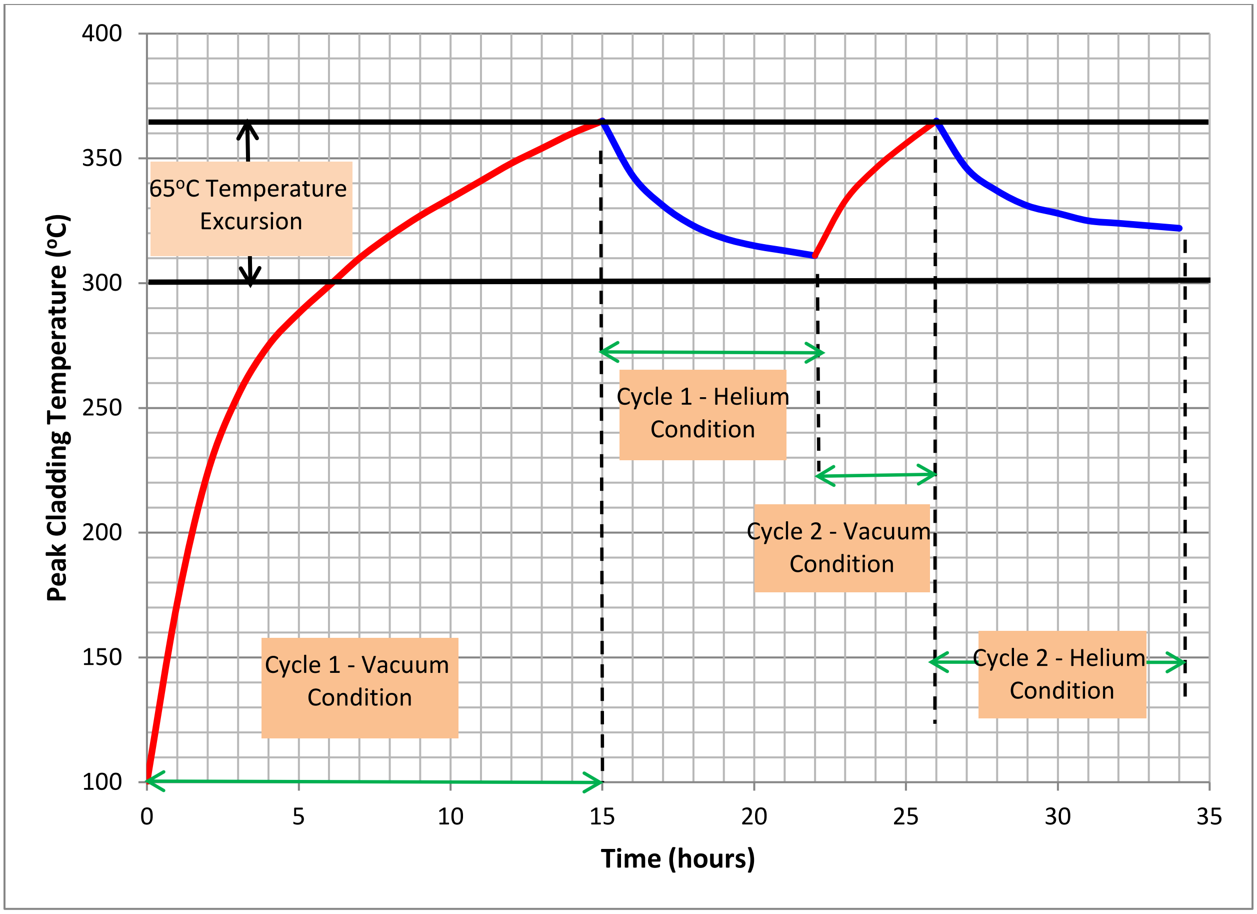

FIGURE 3.3.7: VARIATION OF PEAK CLADDING TEMPERATURE WITH TIME UNDER MULTIPLE VACUUM DRYING CYCLES FOR F-37 BASKET (SEE TABLE 3.3.10)

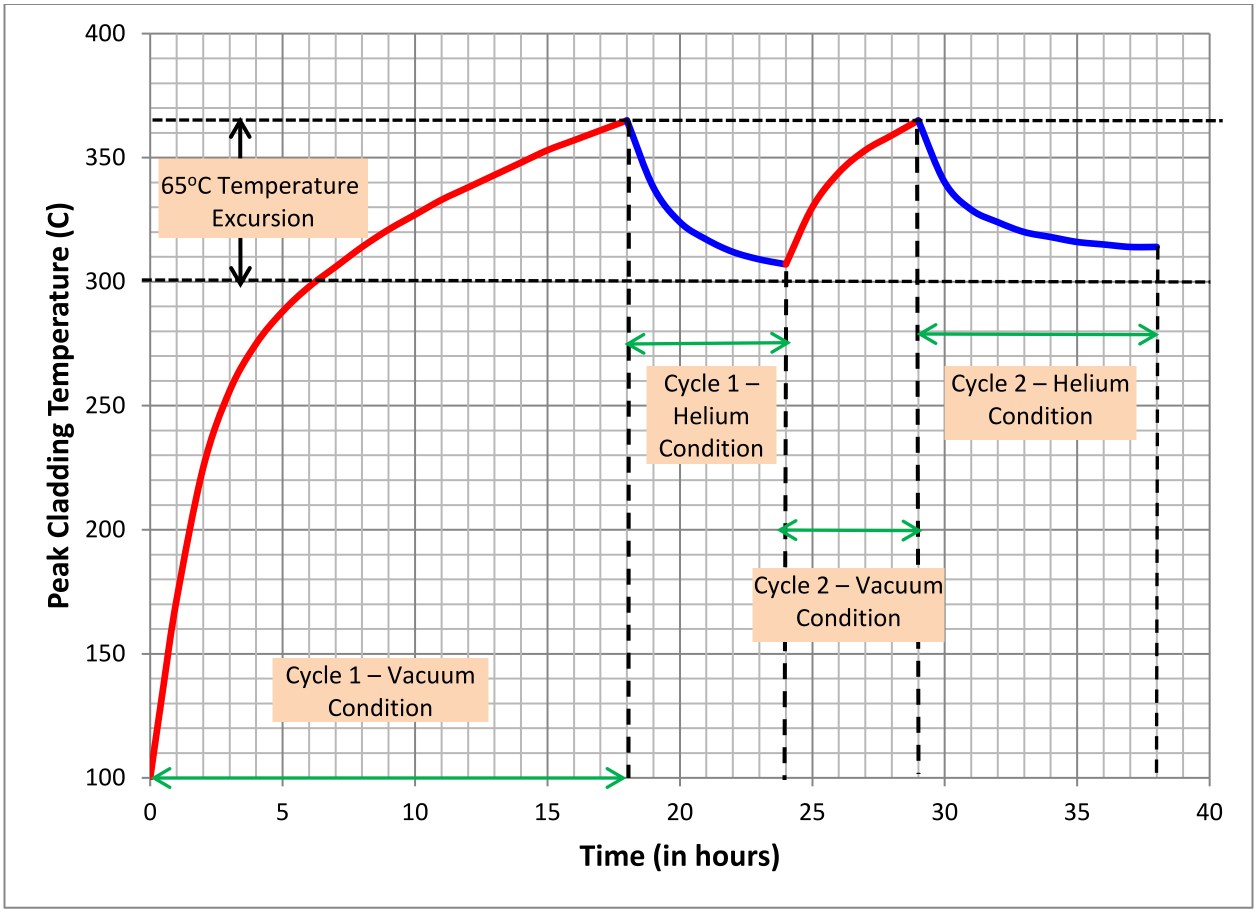

FIGURE 3.3.8: VARIATION OF PEAK CLADDING TEMPERATURE WITH TIME UNDER MULTIPLE VACUUM DRYING CYCLES FOR F-32 BASKET (SEE TABLE 3.3.10)

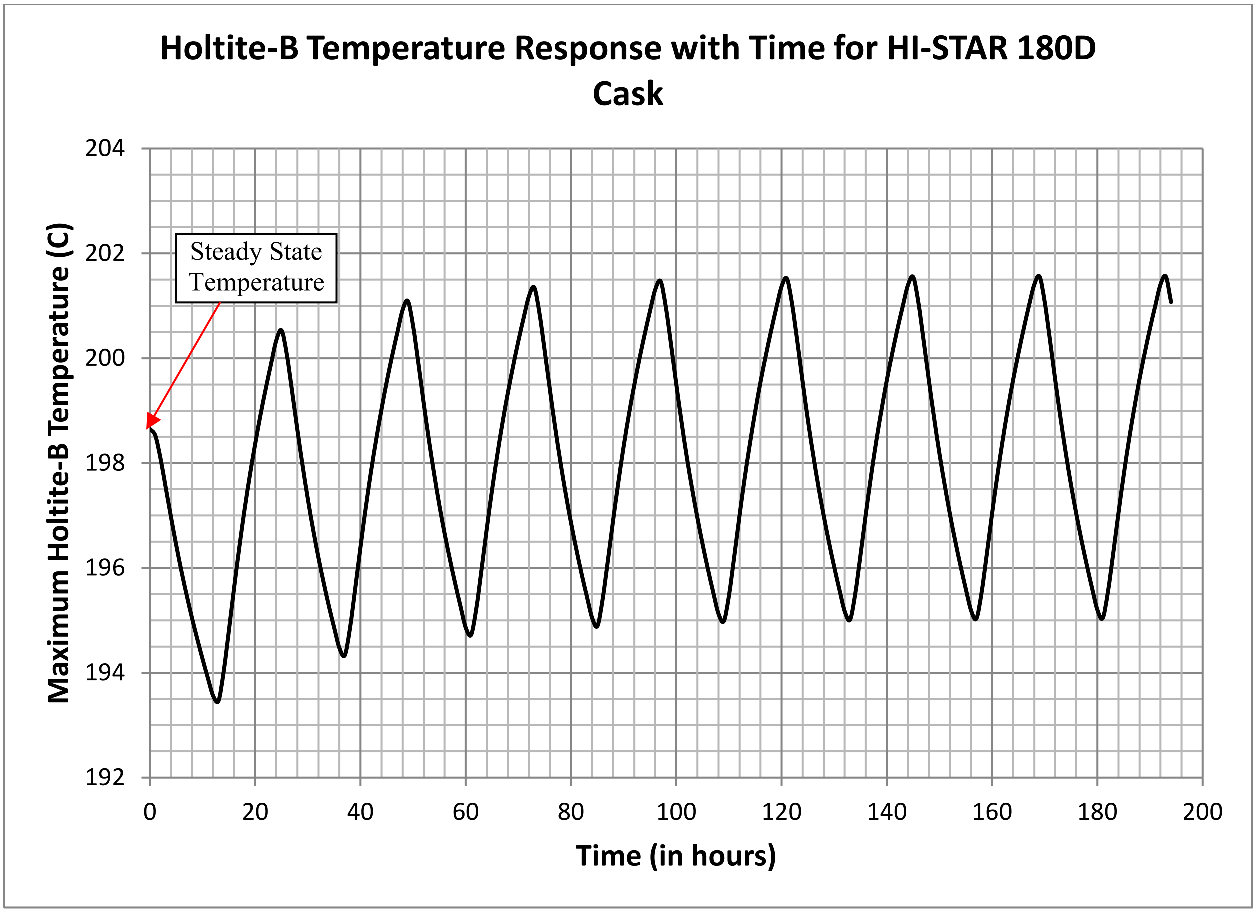

FIGURE 3.3.9: TEMPERATURE RESPONSE OF HOLTITE-B IN HI-STAR 180D CASK

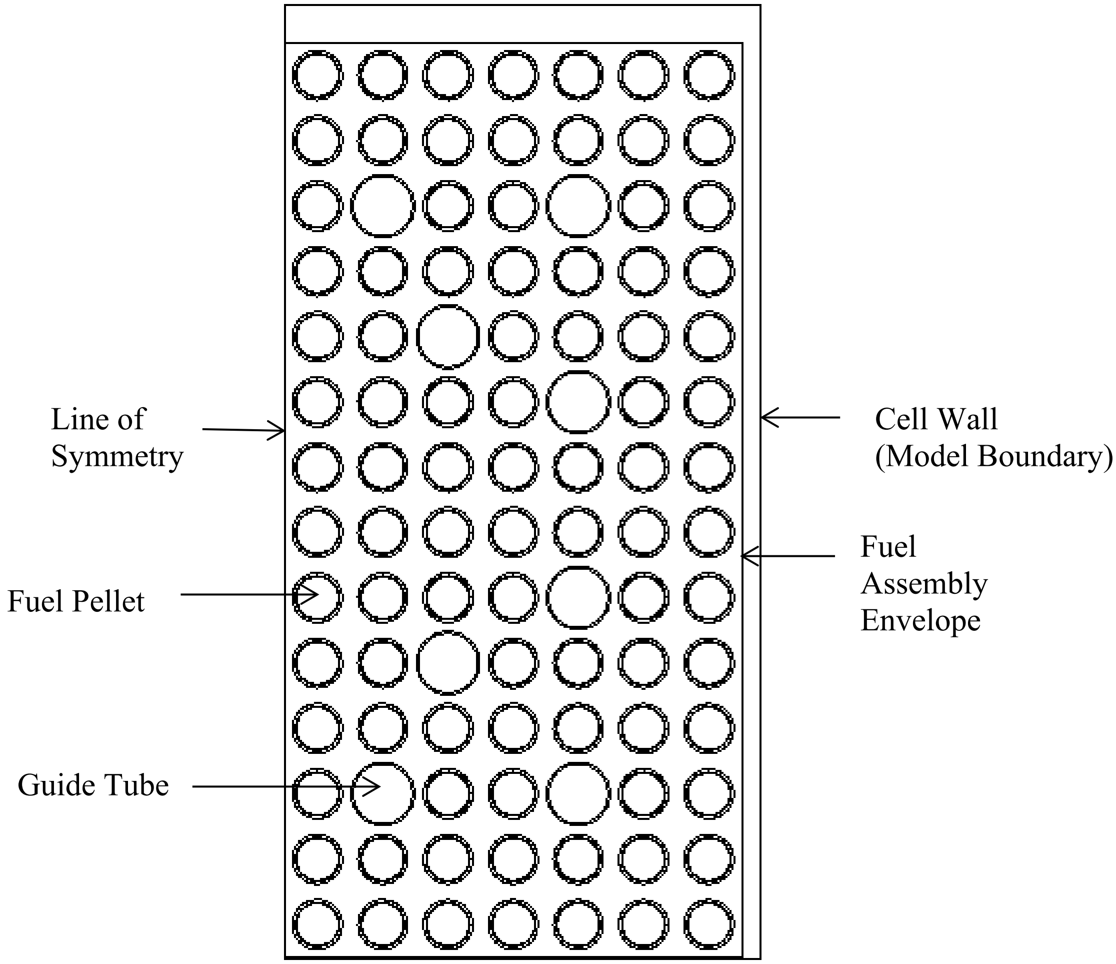

FIGURE 3.3.10: HALF CROSS-SECTION OF THE PWR 14X14 FUEL ASSEMBLIES THERMAL MODEL TO STUDY THE IMPACT OF ASYMMETRY DURING NORMAL TRANSPORT

3.4 THERMAL EVALUATION UNDER HYPOTHETICAL ACCIDENT

As mandated by 10 CFR Part 71 requirements, the HI-STAR 180D Package under the limiting F-37 fuel basket thermal loading is subjected to a sequence of hypothetical accidents. The objective is to determine and assess the cumulative damage sustained by the package. The accident scenarios specified in order are: (1) a 9 m (30 foot) free drop onto an unyielding surface; (2) a 1 m (40-inch) drop onto a mild steel bar; (3) exposure to a 30-minute fire at 802ºC (1475°F) and (4) immersion under a 0.9 m (3 ft) head of water. The initial conditions for the fire accident specify steady state at an ambient temperature between -40ºC (-40°F) and 38ºC (100°F). In the HI-STAR 180D Package hypothetical fire accident evaluation, insolation with a theoretical bounding absorbtivity equal to unity is applied. The effects of the accidents (1), (2) and (4) are evaluated in Chapter 2. In this section, the effects of accident (3) are evaluated. The initial condition prior to fire accident is the hot ambient environment for normal transport and design heat load for F-37 basket (See Section 3.3). The fire accident evaluation is performed assuming an adverse combination of factors that overestimate heat input during fire followed by an underestimation of heat rejection to the environment after the fire.

During drop and puncture accidents some neutron shield pockets can rupture thereby reducing the ability of the package to reject heat after the fire. To conservatively evaluate this hypothetical accident condition, the neutron shield thermal conductivity is assumed during fire to maximize heat input and thermal conductivity of air is applied to the neutron shield pockets during post-fire cooldown to minimize post-fire cooling. During drop events the crush material in the impact limiter is locally crushed. However, the impact limiters survive the drop events without structural collapse and remain attached to the cask during and after the event. During a puncture event the cask's exterior shell may be locally pierced but with no gross damage to the cask or its internals. Because of these reasons the global thermal performance of the HI-STAR 180D cask is unaffected by the drop events.

During fire some portions of the neutron shield will be exposed to high temperatures. In computing the heat input to the package during fire the undegraded neutron shield thermal conductivity is assumed. During the post-fire cooldown phase, thermal conductivity of air is applied to the neutron shield pockets to minimize heat dissipation and thermal inertia properties of undegraded neutron shield material is assumed to maximize fire accumulated thermal energy. During fire a 10 CFR Part 71 mandated cask surface absorbtivity is assumed to maximize radiant heat input to the cask. During fire the resin bonding the impact limiter's corrugated aluminum layers is destroyed thus severely degrading the normal-to-layers direction conductivity. In the interest of conservatism the undegraded crush material conductivity is assumed during fire to maximize heat input and an opposite assumption is used to minimize post-fire heat dissipation by applying air conductivity for the normal-to-layers direction (see Table 3.4.1).

The temperature history of the HI-STAR Package is monitored during the 30-minute fire and during post-fire cooldown for a sufficient length of time for the cask and fuel to reach maximum temperatures. The impact of transient temperature excursions on HI-STAR 180D Package materials is evaluated.

3.4.1 Initial Conditions

In accordance with transport regulations the HI-STAR 180D Package fire accident is evaluated under hot ambient initial conditions (§10CFR71.71(c)(1) and §10CFR71.73(b)). These conditions are 38°C (100°F) ambient temperature, still air and insolation. The HI-STAR 180D bounding steady state temperature distribution under hot ambient conditions reported in Section 3.1.3 is adopted as the initial condition for fire accident evaluation.

3.4.2 Fire Conditions

As required by transport regulations the HI-STAR 180D Package is evaluated under an all-engulfing fire at 802°C (1475°F) lasting for 30 minutes (§10CFR71.73(c)(4)). The regulations specify a minimum fire emissivity (0.9) and lowerbound package absorbtivity (0.8) for hypothetical accident evaluation. In the HI-STAR 180D fire accident evaluation, the minimum specified emissivity and conservatively postulated absorbtivity are adopted.

Heat input to the HI-STAR 180D Package while engulfed in a fire is from a combination of radiation and forced convection heat transfer. This can be expressed by the following equation:

$$q_F = h_{fc}(T_F - T_s) + \sigma\alpha\,\varepsilon\,[T_F^4 - T_s^4]$$

where:

- q_F = fire heat input, W/m^2 (Btu/ft^2-hr)
- T_F = fire condition temperature 1075°K (1935°R)
- T_S = package surface temperature °K (°R)
- h_{fc} = forced convection heat transfer coefficient W/m^2-°K [Btu/ft^2-hr-°F] (See Table 3.4.3)
- ε = flame emissivity (0.9 (min.) in accordance with transport regulations)
- a = package absorbtivity (0.8 (min.) in accordance with transport regulations)
- σ = Stefan-Boltzmann Constant 5.67x10^{-8} W/m^2-°K^4 (0.1714×10^{-8} Btu/ft^2-hr-°R^4)

For conservatism, the reported Sandia large pool fires forced convection heat transfer coefficient (See Table 3.4.3) is adopted. In Table 3.4.1 the principal fire accident assumptions are summarized.

The HI-STAR 180D package fire accident analysis is based on a 3D thermal model that properly accounts for radiation, conduction and external natural convection modes of heat transfer. The thermal model incorporates several conservative assumptions listed below.

1. The undegraded neutron shield conductivity is assumed during fire to maximize heat input to the cask body.
2. To maximize initial temperatures, the limiting decay heat pattern defined in Section 3.3 and bounding (steady state) temperatures are assumed.
3. To maximize the rate of heat input from the ends during fire the undegraded conductivity of impact limiters aluminum crush material is assumed (See Table 3.4.1).

4. To maximize fire heating of the cask, an all-engulfing fire, a high flame emissivity (e = 0.9) and a theoretically bounding package absorbtivity are assumed.
5. To minimize heat dissipation from the cask during post fire cooldown, the thermal conductivity of air is applied to the neutron shield pockets and complete destruction of the resin material bonding the corrugated Aluminum layers of the impact limiters material is assumed.
6. The Sandia laboratories reported forced convection heat transfer during large pool fires (See Table 3.4.3) is adopted.
7. To maximize fire accumulated thermal energy the thermal inertia properties of undegraded neutron shield and Aluminum crush materials are assumed during post fire cooldown.

The fire accident thermal analysis is performed for the HI-STAR 180D Package with F-37 basket. An explicit thermal analysis of the accident conditions for F-32 basket is not required due to the following reasons:

1. The thermal inertia of the cask with F-32 basket is approximately only 1.1% lower than the limiting scenario i.e. F-37 basket [3.4.1]. Such an extremely small difference in the thermal inertia does not have a material effect on the temperature field during short-term and accident conditions.

2. The maximum permissible heat load in F-32 basket is significantly lower than that companion F-37 basket (See Table 7.D.1). Therefore, the temperatures in F-37 basket are expected to increase to higher values than F-32 basket during accident conditions.

3. Fuel and containment seal temperatures have significant margins (more than 140^{o}C) to temperature limits during fire accident.

Therefore, for all the above reasons, a thermal analysis of the cask with F-32 basket under accident conditions is not merited.

Using this model of HI-STAR 180D with F-37 basket, the transient heat up of the cask and it's internals during the 30-minute fire is computed. At the end of the fire the hot ambient condition is restored and a post fire cooldown of the cask for a period of 21 hours is computed. As shown in Figure 3.4.1, this period is sufficient for the cask internals (principally the SNF) to reach their maximum temperatures and begin to recede. The results of the analysis are evaluated in the next section.

3.4.3 Maximum Temperatures and Pressures

3.4.3.1 Maximum Temperatures

The HI-STAR 180D Package is evaluated under a hypothetical fire accident at 802^{o}C (1475^{o}F) lasting for 30 minutes. To ensure a bounding evaluation, the limiting decay heat pattern (See

Subsection 3.1.2) and hot initial conditions are assumed. Under this array of adverse conditions, the maximum temperatures reached in the cask structural members and its contents (SNF) are computed. The temperatures are computed using the 3D thermal model described in Section 3.3, applying the fire accident thermal loads and computing the time-dependent response of the package to the 30-minute fire followed by a post fire cooldown for a sufficient duration to allow the cask and its contents to reach their maximum temperatures. The results of the critical components (cladding, basket, seals and containment shell) are graphed in Figure 3.4.1 and maximum temperatures reached during fire and post-fire cooldown are reported in Subsection 3.1.3. The following observations are derived by inspecting the temperature field obtained from the thermal analysis:

- The maximum fuel cladding temperature (Table 3.1.3) is well within the ISG-11, Rev. 3 accident temperature limit (Table 3.2.11).

- The maximum temperature of fuel basket (Table 3.1.3) is well within its accident design temperature (Table 3.2.10).

- The maximum temperatures of the containment boundary and lid seals (Table 3.1.3) are well below the ASME Code limits (Tables 3.2.10 and 3.2.12, respectively).

- The maximum temperatures of the basket shims (Table 3.1.3) are well below the accident temperature limits (Table 3.2.10).

- The maximum temperatures of the lid seals (Table 3.1.3) are well below the accident temperature limit (Table 3.2.12).

The HI-STAR 180D Package fire accident temperatures are reported in Section 3.1.3. The temperatures are below the regulatory temperature limits (Table 3.2.11), ASME Code temperature limits (Table 3.2.10) and components safe operating temperature limits (Table 3.2.12). The thermal evaluation provides reasonable assurance of safety in the event of a fire. This conclusion is based on the technical data and analyses presented in this chapter in conjunction with provisions of 10 CFR Part 71, appropriate regulatory guides, applicable codes and standards, and accepted engineering practices.

3.4.3.2 Maximum Pressures

The HI-STAR 180D containment pressure is computed based on the maximum temperatures of the cask contents (fuel basket and fuel) reached during the fire accident. The calculations use an array of conservative assumptions listed below:

i) Maximum initial fill pressure (See Table 7.1.4)
ii) 100% rods rupture
iii) 100% release of rods fills gas and 30% release of fission gases
iv) Lowerbound cavity free volume

The maximum containment pressures are tabulated in Subsection 3.1.4. The results show that the pressures are well below the containment boundary design pressure (Table 2.1.1).

3.4.4 Maximum Thermal Stresses

The HI-STAR 180D Package is designed to ensure a low state of thermal stress in the structural members. This is ensured by using high conductivity materials (Metamic- HT and low alloy steels) to minimize temperature gradients and large fit-up gaps to allow unrestrained thermal expansion of the package internals (fuel basket) during normal transport. The differential thermal expansion of the fuel basket during normal transport is calculated in Reference [3.4.1] and results provided in Table 3.4.2. The normal transport gaps are bounding during fire because of the expansion of the cask body under direct fire heating. As thermal interference is precluded during fire a low state of thermal stress prevails in the cask.

3.4.5 Fuel Reconfiguration Post Hypothetical Accident Drops

Though the structural evaluations, as delineated in Section 1.4, show there will be no damage to fuel assemblies, a hypothetical scenario is postulated that assumes punitive fuel reconfiguration as described in Section 3.3.5 coincident with hypothetical fire accident condition and 100% rod rupture. Based on the results of normal conditions of transport in Table 3.3.11 and hypothetical fire accident in Table 3.1.3, the package component temperatures for the postulated fuel reconfiguration, with coincident fire are reported in Table 3.4.4. The results show that the containment boundary components including seals are well below their temperature limit. Since the bulk cavity space temperature remains unchanged, the containment pressure is also below the limit reported in Table 3.1.4. Therefore the containment boundary remains intact during hypothetical accident conditions of transport with non-mechanistic fuel reconfiguration.

Table 3.4.1: Hypothetical Fire Accident Assumptions

	Initial Condition	30-minute Fire	Post-Fire Equilibrium
1.Neutron shield conduction	Yes (Understated Conductivity)	Yes (Undegraded material Conductivity)	No (Air conductivity applied to the neutron shield pockets)
2. Insolation	Yes	Yes	Yes
3. Surface Convection	Natural	Forced	Natural
4. Impact limiter conduction [Note A] Axial direction Radial direction	 Table 3.2.2 Table 3.2.2	 Table 3.2.2 Table 3.2.2	 Table 3.2.2 Air conductivity
5. Cask Surface Solar Absorbtivity	1.0	1.0	1.0
6. Emissivity Cask surface Polished Surfaces (impact limiter)	 0.85 Table 3.2.6	 0.9 (fire emissivity) 0.9 (fire emissivity)	 0.66 Table 3.2.6

Note A: Parallel-to-layers direction crush material conductivities are not affected by fire. However, normal-to-layers direction conductivity is severely degraded because the resin bonding the corrugated Aluminum layers is destroyed. To maximize heat input during fire the normal-to-layers direction conductivity is assumed to be unaffected and during post-fire cooldown theoretical lowerbound conductivity of air assumed to minimize post-fire cooldown heat dissipation.

Table 3.4.2: Thermal Expansion of the Fuel and Fuel Basket during Normal Transport

	Differential Expansion (mm)	Minimum Cold Gap (mm)
Basket Radial	3.89	4
Basket Axial	11.88	14
Fuel Axial	0.67	3.1

Notes:
1) The cold gaps are greater than the differential expansion of the fuel basket in axial and radial directions.
2) The normal transport condition gaps bound the fire accident gaps from below.

Table 3.4.3: Sandia Pool Fire Test Data[1]

Test equipment	3 m (10 ft) OD propane railcar
Fuel	JP-4
Pool Size	9 m x 9 m (30 ft x 30 ft)
Fire Temperature	649ºC to 1093ºC (843ºC avg.) 1200ºF to 2000ºF (1550ºF avg.)
Convective Coefficient	25.5 W/m^2-ºK (4.5 Btu/ft^2-hr-ºF)

[1] From Sandia large pool fires report [3.4.2], Page 41.

Table 3.4.4: HI-STAR 180D Hypothetical Accident Maximum Temperatures Due to Fuel Reconfiguration

Component	Fire Accident[Note 1] °C (°F)	Fire Accident Coincident with Fuel Reconfiguration[Note 2] °C (°F)
Fuel Cladding	393 (739)	428 (802)
Fuel Basket	370 (698)	403 (757)
Containment Shell	255 (491)	271 (520)
Lid Seals[Note 3]	219 (426)	276 (529)

Note 1: These maximum temperature results are extracted from Table 3.1.3.
Note 2: These temperatures are conservatively obtained by adding the difference in temperatures due to fuel reconfiguration as reported in Table 3.3.11 to the temperatures reported in Table 3.1.3.
Note 3: The temperature of the containment seal with the highest temperature is reported.

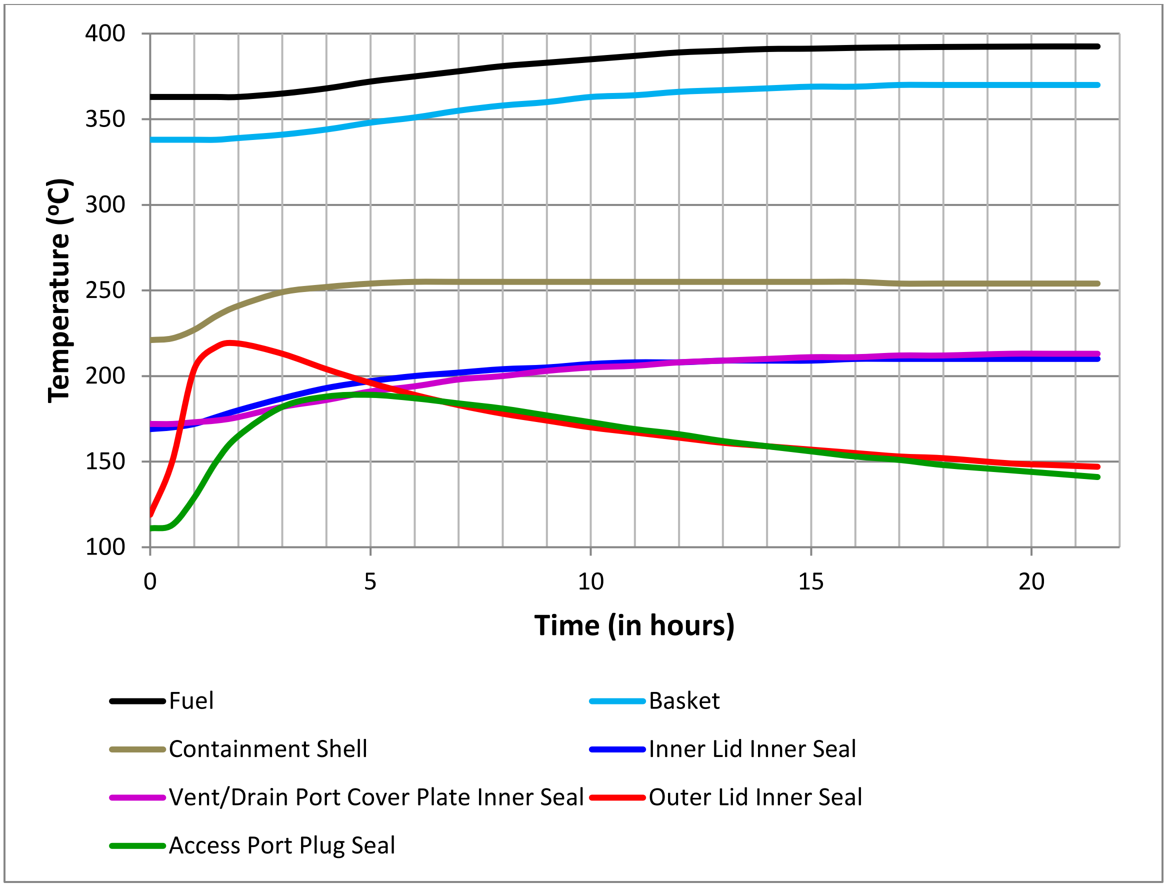

FIGURE 3.4.1: HI-STAR 180D FIRE AND POST FIRE COOLDOWN TEMPERATURE HISTORY

CHAPTER 3 REFERENCES

The following generic industry and Holtec produced references may have been consulted in the preparation of this document. Where specifically cited, the identifier is listed in the SAR text or table. Active Holtec Calculation Packages which are the repository of all relevant licensing and design basis calculations are annotated as "latest revision". Submittal of the latest revision of such Calculation Packages to the USNRC and other regulatory authorities during the course of regulatory reviews is managed under the company's Configuration Control system. Supporting documents submitted to the USNRC with the HI-STAR 180D LAR 9367-2 have been italicized.

[3.1.1] Gebhart, B., Jaluria, Y., Mahajan, R.L. and Sammakia, B., "Buoyancy Induced Flows and Transport", Hemisphere Publishing Corporation, NY, (1988).

[3.1.2] NUREG-1536, "Standard Review Plan for Dry Cask Storage Systems," USNRC, (January 1997).

[3.1.3] NUREG-1617, "Standard Review Plan for Transportation Packages for Spent Nuclear Fuel", USNRC, March 2000.

[3.2.1] Baumeister, T., Avallone, E.A. and Baumeister III, T., "Marks' Standard Handbook for Mechanical Engineers", 8th Edition, McGraw Hill Book Company, 1978.

[3.2.2] Rohsenow, W.M. and Hartnett, J.P., "Handbook of Heat Transfer," McGraw Hill Book Company, New York, 1973.

[3.2.3] Greer et al., "The TN-24P Spent Fuel Storage Cask: Testing and Analyses," EPRI NP-5128, PNL-6054, UC-85, (April 1987).

[3.2.4] Rust, J.H., "Nuclear Power Plant Engineering," Haralson Publishing Company, (1979).

[3.2.5] Kern, D.Q., "Process Heat Transfer," McGraw Hill Kogakusha, (1950).

[3.2.6] "A Handbook of Materials Properties for Use in the Analysis of Light Water Reactor Fuel Rod Behavior", NUREG/CR-0497, (August 1981).

[3.2.7] ASME Boiler and Pressure Vessel Code, Section II, Part D, 2007 Edition, 2008 Addenda.

[3.2.8] Jakob, M. and Hawkins, G.A., "Elements of Heat Transfer," John Wiley & Sons, New York, 1957.

[3.2.9] Not Used

[3.2.10] Kauder, L., “Spacecraft Thermal Control Coatings References,” NASA Technical Procedure, NASA/TP-2005-212792, NASA/Goddard Space Flight Center, Greenbelt, MD, July 2005.

[3.2.11] “Fundamentals of Heat and Mass Transfer”, 4th Edition, F.P. Incropera and D.P. DeWitt, John Wiley & Sons, Inc., New York, 1996.

[3.2.12] Aluminum Alloy 2219 Material Data Sheet, ASM Aerospace Specification Metals, Inc., Pompano Beach, FL.

[3.2.13] “Nuclear Systems Materials Handbook, Vol. 1, Design Data”, ORNL TID 26666.

[3.2.14] “Scoping Design Analyses for Optimized Shipping Casks Containing 1-, 2-, 3-, 5-, 7-, or 10-Year-Old PWR Spent Fuel”, ORNL/CSD/TM-149 TTC-0316, (1983).

[3.2.15] “Physical Properties of Polymers Handbook”, James E. Mark, 2nd Edition.

[3.3.1] ANSYS Finite Element Modeling Package, Swanson Analysis Systems, Inc., Houston, PA, 1993.

[3.3.2] FLUENT Computational Fluid Dynamics Software (Fluent, Inc., Centerra Resource Park, 10 Cavendish Court, Lebanon, NH 03766).

[3.3.3] “Cladding Considerations for the Transportation and Storage of Spent Fuel”, Interim Staff Guidance – 11, Rev. 3, (11/17/03).

[3.3.4] “Topical Report on the HI-STAR/HI-STORM Thermal Model and its Benchmarking with Full-Size Cask Test Data,” Holtec Report HI-992252, Rev. 1, Holtec International, Marlton, NJ, 08053. (Holtec Proprietary).

[3.3.5] “Standard for Verification and Validation in Computational Fluid Dynamics and Heat Transfer”, ASME V&V 20-2009.

[3.3.6] “Safety Analysis Report on the HI-STAR 180 Package”, USNRC Docket 71-9325.

[3.3.7] “Effective Thermal Properties of HI-STAR 180D Fuel Assemblies”, Holtec Report HI-2125201, Latest Revision (Holtec Proprietary).

[3.4.1] “Thermal Evaluations of HI-STAR 180D in Transport”, Holtec Report HI-2125241, Latest Revision, (Holtec Proprietary).

[3.4.2] “Thermal Measurements in a Series of Large Pool Fires”, Sandia Report SAND85 – 0196 TTC – 0659 UC 71, (August 1971).

CHAPTER 4: CONTAINMENT

4.0 INTRODUCTION

This chapter demonstrates the HI-STAR 180D cask containment system compliance with the permitted activity release limits specified in 10CFR71 for both normal and hypothetical accident conditions of transport [4.0.1]. Satisfaction of the containment criteria, expressed as the leakage rate acceptance criterion, ensures that the loaded HI-STAR 180D cask will not exceed the allowable radionuclide release rates.

The containment system for the HI-STAR 180D cask consists of the components, seals and welds identified in the drawing package in Section 1.3 and also in Figures 4.1.1, 4.1.2, and 4.1.3. Both the inner and outer closure lids are containment system components whose closure joints must be tested prior to shipment.

Chapter 2 of this SAR shows that all containment system components are maintained within their code-allowable stress limits and metallic seals remain compressed during all normal and hypothetical accident conditions of transport as defined in 10CFR71.71 and 10CFR71.73. Chapter 3 of this SAR shows that the peak containment system component temperatures and pressures are within the design basis limits for all normal and hypothetical accident conditions of transport as defined in 10CFR71.71 and 10CFR71.73. Since both the containment system is shown to remain intact and the temperature and pressure design bases are not exceeded, the design basis leakage rates are not exceeded during normal or hypothetical accident conditions of transport.

The HI-STAR 180D cask is subjected to a fabrication leakage rate test before the first loading. The fabrication leakage rate test is performed at the factory in accordance with ANSI N14.5-2014 [4.0.2] as part of the HI-STAR 180D cask acceptance testing. The HI-STAR 180D cask is also subjected to a pre-shipment leakage rate test after each cask loading and closure. The pre-shipment leakage rate test is performed in accordance with ANSI N14.5 by the user as final acceptance testing of the HI-STAR 180D cask containment system. The metallic seals of the HI-STAR 180D cask are to be replaced and retested for each cask loading and closure.

Additional requirements and clarification are provided in Section 4.4, Chapter 2 and Chapter 8.

4.1 DESCRIPTION OF THE CONTAINMENT SYSTEM

The containment system for the HI-STAR 180D cask consists of the containment shell, the containment base plate, the containment closure flange, the inner closure lid, the outer closure lid, inner and outer closure lid bolts, the inner closure lid port covers and port cover bolts, the outer closure lid access port plug, and their respective metallic seals and welds as specified in the drawing package in Section 1.3. The containment boundary and containment system components are shown in Figure 4.1.1 with additional detail on the inner and outer closure lids provided in Figures 4.1.2 and 4.1.3, respectively.

The containment system components for the HI-STAR 180D system are designed and fabricated in accordance with the requirements of ASME Code, Section III, Subsection NB [4.1.1], to the maximum extent practicable as clarified in Chapter 2 of this SAR. Chapter 1 specifies design criteria for the containment system. Section 2.1 provides the applicable code requirements. Exceptions to specific code requirements with complete justifications are presented in Table 2.1.14

4.1.1 Containment Vessel

The cask containment vessel consists of components which form the inner containment space and expanded containment inter-lid space. The inner containment space is used to house the internal basket designs which hold spent nuclear fuel. The containment vessel is represented by the containment shell, containment base plate, containment closure flange, and inner and outer closure lids. These are the main containment system components that create an enclosed cylindrical cavity for the containment of the enclosed radiological contents. The materials of construction for the containment vessel are specified in the drawing package in Section 1.3. No valve or pressure relief device is specified on the HI-STAR 180D containment system.

4.1.2 Containment Penetrations

The cask containment system penetrations include the inner closure lid vent and drain ports, and the outer closure lid access port. Each penetration has redundant metallic seals. The containment penetrations are designed and tested to ensure that the radionuclide release rates specified in 10CFR71.51 will not be exceeded.

4.1.3 Seals and Welds

The cask uses a combination of seals and welds designed and tested to provide containment during normal transport conditions, and during and after hypothetical accident conditions of transport. Seals and welds are individually discussed below.

The seals and welds provide for a containment system which is securely closed and, cannot be opened unintentionally or by an internal pressure within the package as required in 10CFR71.43(c).

4.1.3.1 Containment Seals

The containment system seals are designed and fabricated to meet the design requirements of the HI-STAR 180D cask specified in subparagraph 2.2.1.1.6 and in accordance with the manufacturer's recommendations. Chapter 7 describes the operating procedures required for proper seal function. Seal and closure details are provided in the drawing package in Section 1.3 and Appendix 8.A.

4.1.3.1.1 Inner Closure Lid

The cask inner closure lid uses two concentric metallic seals to form the closure with the containment closure flange surface. In the inner closure lid, the inner seal is the containment seal. To protect the sealing surfaces against corrosion, a stainless steel weld overlay is provided during manufacturing on both the inner closure lid and the mating containment closure flange. The inner closure lid inner seal is tested for leakage through an inter-seal test port. The inter-seal test port provides access to the volume between the two metallic lid seals. Following leakage rate testing of the inner closure lid inner seal, a threaded plug with a metallic seal is installed in the inter-seal test port hole to provide redundant closure. On the inner closure lid, the outer metallic seal provides redundant closure.

Closure of the inner closure lid vent and drain ports is achieved via a bolted port cover with two concentric metallic seals. In both port covers, the inner seal is the containment seal. The metallic seals are compressed between the underside of the port cover and the inner closure lid to form the seal. The vent and drain port cover inner seals are tested for leakage through an inter-seal test port in the port cover. The inter-seal test port provides access to the volume between the two metallic port cover seals. On the inner closure lid port covers, the outer metallic port seal provides redundant closure.

The inner closure lid containment boundary and redundant boundary sealing surfaces are not subject to corrosion due to the presence of the outer closure lid and inter-lid cavity helium backfill. In any case, the seal materials of construction are highly corrosion resistant.

4.1.3.1.2 Outer Closure Lid

The cask outer closure lid uses two concentric metallic seals to form the closure with the containment closure flange surface. In the outer closure lid, the inner seal is the containment seal. To protect the sealing surfaces against corrosion, a stainless steel weld overlay is provided during manufacturing on both the outer closure lid and mating containment closure flange. In the outer closure lid, the containment boundary seal is tested for leakage through an inter-seal test port. The inter-seal test port provides access to the volume between the two metallic lid seals. Following leakage rate testing of the outer closure lid inner seal, a threaded plug with a metallic seal is installed in the inter-seal test port hole to provide redundant closure. On the outer closure lid, the outer metallic seal provides redundant closure.

Closure of the outer closure lid access port is achieved via a threaded access port plug with a single metallic seal. The access port plug seal is the containment seal. The metallic seal is compressed between the underside of the threaded access port plug head and the outer closure lid to form the seal. The access port plug seal is independently tested for leakage to verify containment performance. A bolted access port cover, with a metallic seal, is installed over the access port plug to provide redundant closure.

The outer closure lid containment sealing surfaces are not subject to corrosion due to the presence of redundant closure features that prevent exposure to the environment external to the cask. In any case, the seal materials of construction are highly corrosion resistant.

4.1.3.2 Containment Welds

The cask containment system welds consists of full penetration welds forming the containment shell, the full penetration weld connecting the containment shell to the containment closure flange, and the full penetration weld connecting the containment base plate to the containment shell. All containment system boundary welds are fabricated and inspected in accordance with ASME Code Section III, Subsection NB. The weld details and examinations are shown in the drawing package in Section 1.3.

4.1.4 Closure Lids

The cask inner and outer closure lids are secured using multiple closure bolts around the perimeter. Torquing of closure lid bolts compresses the concentric metallic seals between the closure lids and the containment closure flange forming the closure lid seal.

Closure of the inner closure lid vent and drain port cover plates are provided using multiple port cover plate closure bolts around the perimeter. Torquing of the port cover bolts compresses the port cover plate concentric metallic seals between the port cover plate and the inner closure lid to form the port seal.

Closure of the outer closure lid access port is provided by a single threaded plug and seal installed in the penetration. Torquing of outer closure lid access port plug compresses the metallic seal between the outer closure lid access port plug and the outer closure lid to form the port seal. The access port cover plate, containing a single metallic seal, is installed with multiple perimeter port cover closure bolts.

Bolt torquing patterns, lubrication requirements, and torque values are provided in Table 7.1.1. The torque values are established to maintain leaktight containment during normal and accident conditions of transport. Torque values for the inner and outer closure lid bolts preclude separation of the closure lids from the containment closure flange as clarified in Chapter 2. The closure lid bolts cannot be opened unintentionally or by a pressure that may arise within the package.

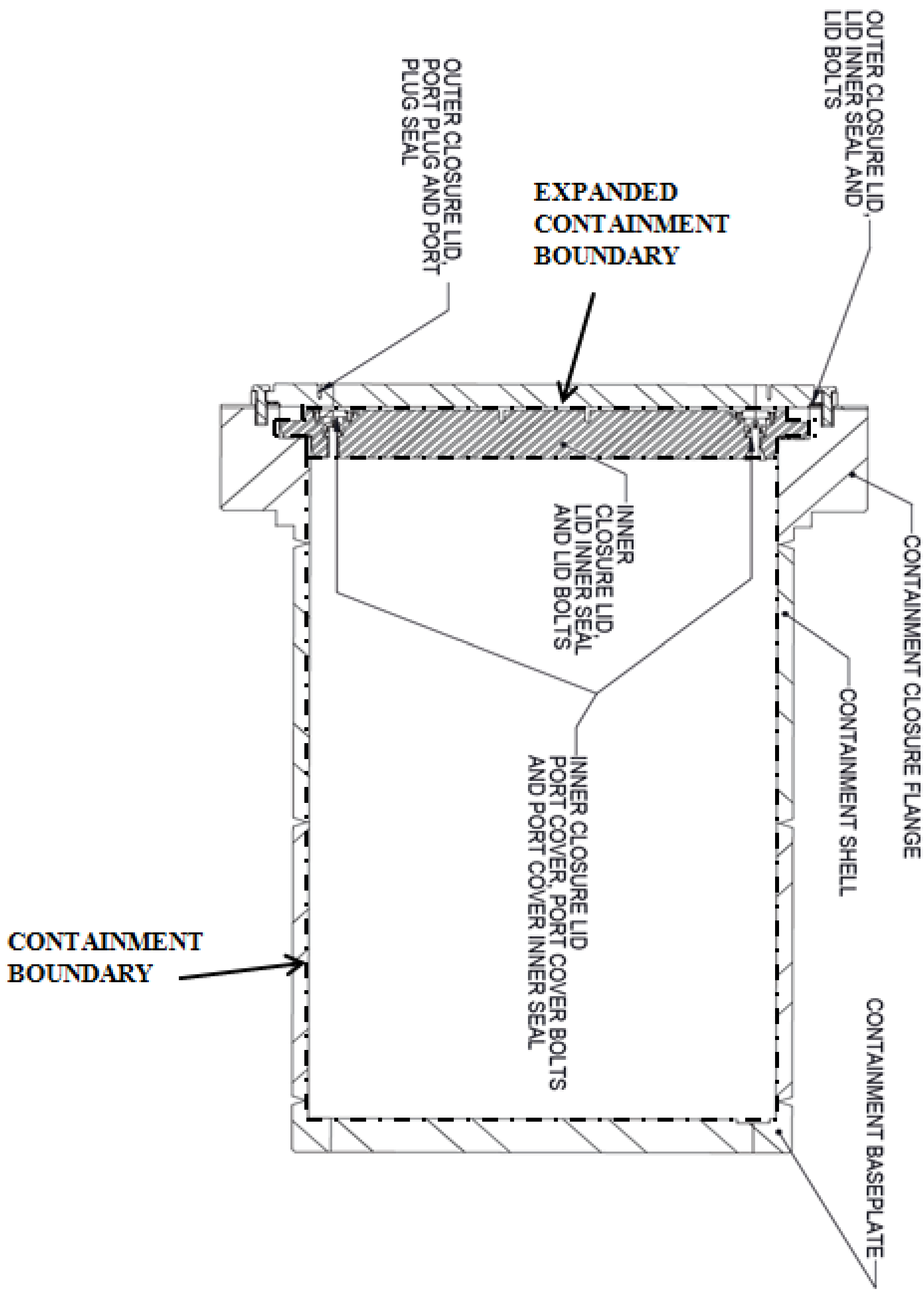

Figure 4.1.1: PICTORIAL VIEW OF HI-STAR 180D CASK CONTAINMENT BOUNDARY ANDCONTAINMENT SYSTEM COMPONENTS

Note 1: All assembly welds are identified in the drawing package in Section 1.3.

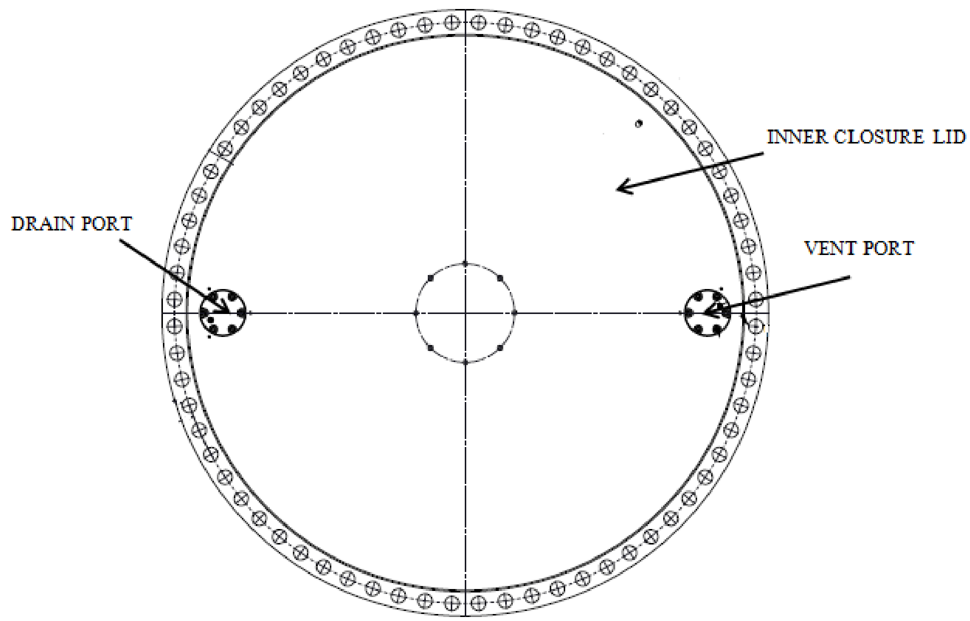

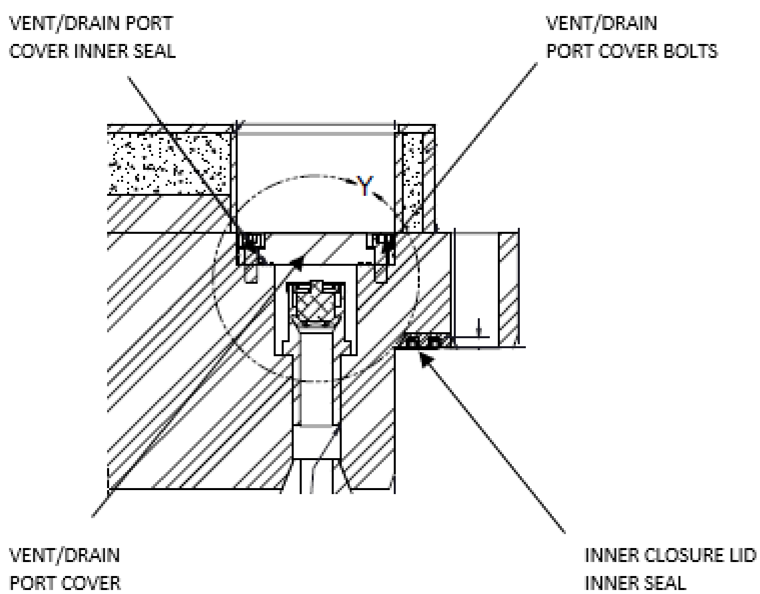

Figure 4.1.2: PICTORIAL VIEW OF HI-STAR 180D INNER CLOSURE LID CONTAINMENT BOUNDARY AND CONTAINMENT SYSTEM COMPONENTS

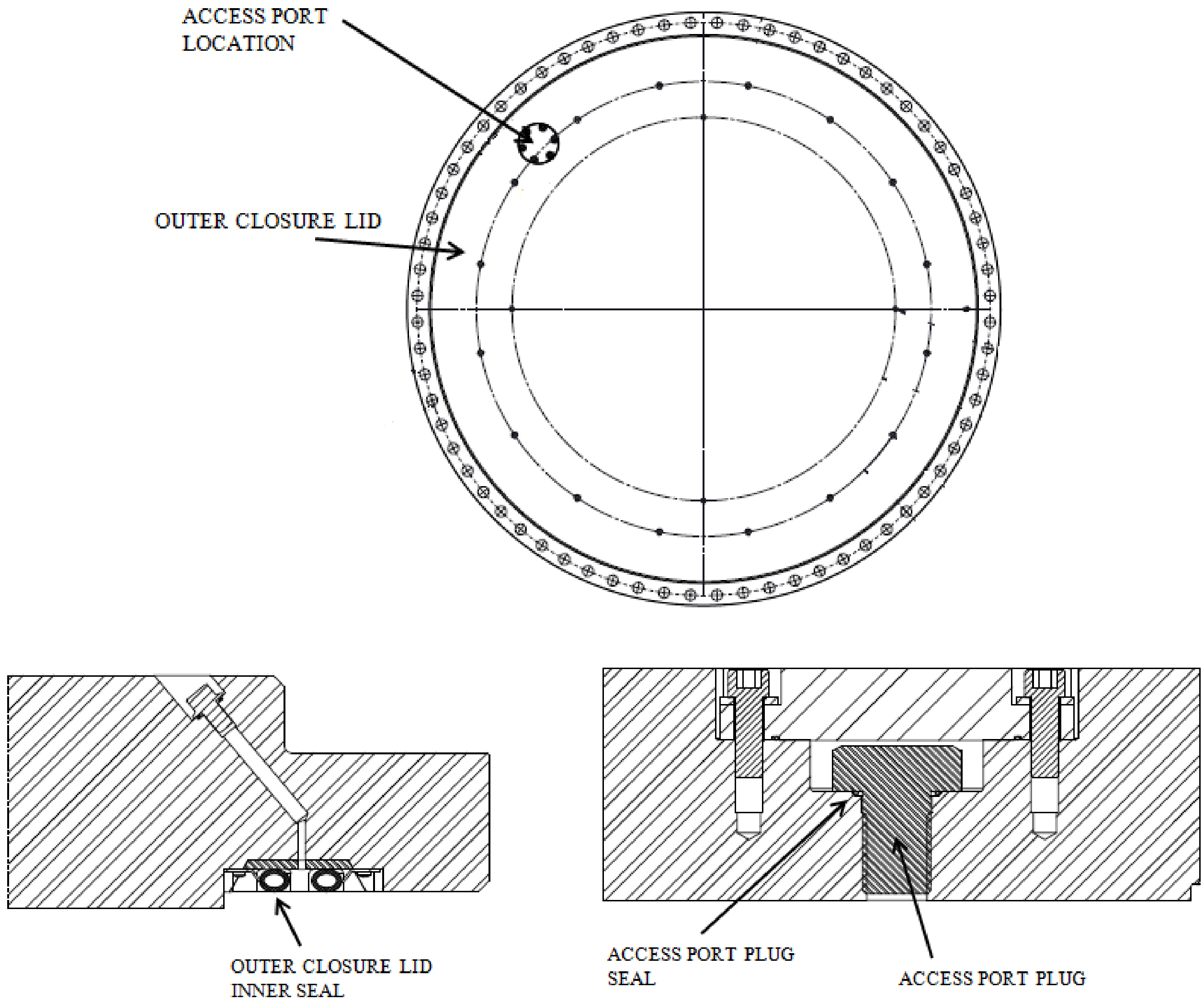

Figure 4.1.3: PICTORIAL VIEW OF HI-STAR 180D OUTER CLOSURE LID EXPANDED CONTAINMENT BOUNDARY AND CONTAINMENT SYSTEM COMPONENTS

4.2 CONTAINMENT UNDER NORMAL CONDITIONS OF TRANSPORT

Section 2.6 of this SAR shows that all containment system components are maintained within their code-allowable stress limits and the metallic seals remain compressed during all normal conditions of transport as defined in 10CFR71.71 [4.0.1]. Section 3.1 of this SAR shows that all containment system components are maintained within their peak temperature and pressure limits for all normal conditions of transport as defined in 10CFR71.71. Since the containment system remains intact without exceeding temperature and pressure limits, the design basis leakage rate (see Table 8.1.1) will not be exceeded during normal conditions of transport.

4.2.1 Containment Criteria

The leaktight criteria as defined by ANSI N14.5 shall be used for all containment system leakage tests. Compliance with the leaktight criteria of ANSI N14.5 precludes any significant release of radioactive materials and ensures that the radionuclide release rates specified in 10CFR71.51(a)(1) will not be exceeded during normal conditions of transport. Therefore, no containment analyses are performed for normal conditions of transport. Containment allowable leakage rate criteria and the type of tests specified are provided in Table 8.1.1 and Table 8.1.2.

4.2.2 Leak Test Sensitivity

The sensitivity for the leakage test instrument shall be equal to one-half of the allowable leakage rate in accordance with ANSI N14.5 (also see Table 8.1.1).

4.3 CONTAINMENT UNDER HYPOTHETICAL ACCIDENT CONDITIONS OF TRANSPORT

Section 2.7 of this SAR shows that all containment system components are maintained within their code-allowable stress limits and the metallic seals remain compressed during all hypothetical accident conditions of transport as defined in 10CFR71.73 [4.0.1]. Section 3.1 of this SAR shows that all containment system components are maintained within their peak temperature and pressure limits for all hypothetical accident conditions of transport as defined in 10CFR71.73. Since the containment system remains intact without exceeding temperature and pressure limits, the design basis leakage rate (see Table 8.1.1) will not be exceeded during hypothetical accident conditions of transport.

4.3.1 Containment Criteria

The leaktight criteria as defined by ANSI N14.5 shall be used for all containment system leakage tests. Compliance with the leaktight criteria of ANSI N14.5 precludes any significant release of radioactive materials and ensures that the radionuclide release rates specified in 10CFR71.51(a)(2) will not be exceeded during hypothetical accident conditions of transport. Therefore, no containment analyses are performed for hypothetical accident conditions of transport. Containment allowable leakage rate criteria and the type of tests specified are provided in Table 8.1.1 and Table 8.1.2.

4.3.2 Leak Test Sensitivity

The sensitivity for the leakage test instrument shall be equal to one-half of the allowable leakage rate in accordance with ANSI N14.5 (also see Table 8.1.1).

4.4 LEAKAGE RATE TESTS FOR TYPE B PACKAGES

All leakage rate testing of the cask containment system shall be performed in accordance with the guidance in ANSI N14.5. Table 8.1.2 provides the containment system components to be tested and the type of leakage test to be performed for post-fabrication, pre-shipment, periodic, and maintenance qualification.

4.4.1 Fabrication Leakage Rate Test

The fabrication leakage rate test demonstrates that the containment system, as fabricated, provides the required level of containment. The fabrication leakage test for the HI-STAR 180D package is performed at the fabrication facility to ensure that the welded enclosure vessel will maintain its containment function.

Additionally, after fabrication of all components, the inner and outer closure lids are installed and the mechanical seals are tested to ensure that the fit-up of the inner and outer closure lids with the containment flange will meet the leakage rate acceptance criteria after fuel loading.

4.4.2 Pre-Shipment Leakage Rate Test

The pre-shipment leakage rate test demonstrates that the containment system closure has been properly performed. The initial pre-shipment leakage rate test is performed by the user before shipment, after the contents are loaded and the containment system is assembled. The pre-shipment leakage rate test remains valid for 1 year.

4.4.3 Periodic Leakage Rate Test

The periodic leakage rate test demonstrates that the containment system closure capabilities have not deteriorated over an extended period of use. A periodic leakage rate test is only required if the most current leakage rate test occurred more than twelve months prior to package transport. Periodic leakage rate testing is performed by the user before each shipment if the previous leakage rate test has expired. The periodic leakage rate test remains valid for 1 year.

4.4.4 Maintenance Leakage Rate Test

The maintenance leakage rate test demonstrates that the containment system provides the required level of containment after undergoing maintenance, repair and or containment component replacement; and shall be performed prior to returning a package to service.

CHAPTER 4 REFERENCES

The following generic industry and Holtec produced references may have been consulted in the preparation of this document. Where specifically cited, the identifier is listed in the SAR text or table.

[4.0.1] 10CFR71. "Packaging and Transportation of Radioactive Materials," Title 10 of the Code of Federal Regulations, Office of the Federal Register, Washington, D.C.

[4.0.2] ANSI N14.5-2014. "American National Standard for Radioactive Materials- Leakage Tests on Packages for Shipment."

[4.1.1] American Society of Mechanical Engineers (ASME), Boiler and Pressure Vessel Code, Section III, Division 1, Subsection NB, Class 1 Components, 2007 Edition, 2008 Addenda.

CHAPTER 5 - SHIELDING EVALUATION

5.0 INTRODUCTION

The shielding analysis of the HI-STAR 180D Package to demonstrate compliance with 10CFR71.47 and 10CFR71.51 is presented in this chapter. The HI-STAR 180D is designed to accommodate two baskets, the F-32 and F-37, containing up to 32 and 37 PWR fuel assemblies, respectively.

In order to offer the user flexibility in fuel loading, the HI-STAR 180D offers several different loading patterns, where different positions in the basket are qualified for different burnup/cooling time/enrichment combinations. The loading patterns used for shielding evaluations are described in Appendix 7.D. All loading patterns have been analyzed and found to be acceptable compared to the regulatory limits.

The transport index in 10CFR71 is defined as the number determined by multiplying the radiation level in milliSievert per hour (mSv/h) at one meter from the external surface of the package by 100. Since the HI-STAR 180D has been designed to meet a dose rate limit of 0.1 mSv/h at 2 meters from the surface of the vehicle, the dose rate at 1 meter from the package could be greater than 0.1 mSv/h and the transport index could exceed 10. Therefore, the HI-STAR 180D loaded with design basis fuel must be shipped by exclusive use shipment as discussed in Section 1.1.

The shielding analyses were performed with MCNP-5 1.51 [5.1.1] developed by Los Alamos National Laboratory (LANL). The source terms for the design basis fuels were calculated with the SAS2H [5.1.2] and ORIGEN-S [5.1.3] sequences from the SCALE 5.1 systems. These are principally the same codes that were used in Holtec's approved Storage and Transportation FSARs and SAR under separate docket numbers [5.1.4]. Detailed descriptions of the MCNP models and the source term calculations are presented in Sections 5.3 and 5.2, respectively.

Finally, the analysis methods, models and acceptance criteria utilized in the safety evaluation documented in this chapter mirror those used in the SAR for HI-STAR 180 certified in Docket #71-9325.

This chapter contains the following information:

- A description of the shielding features of the HI-STAR 180D.
- A description of the source terms.
- A general description of the shielding analysis methodology.
- A description of the analysis assumptions and results for the HI-STAR 180D.
- Analyses for the HI-STAR 180D's content and results to show that the 10CFR71.47 dose rate limits are met during normal conditions of transport and that the 10CFR71.51 dose rate limit is not exceeded following hypothetical accident conditions.

5.1 DESCRIPTION OF SHIELDING DESIGN

5.1.1 Design Features

The principal design features of the HI-STAR 180D packaging with respect to radiation shielding consist of the fuel basket and basket support structures, the cask including the lid, the cask body, and the central steel structures of the impact limiters. The main shielding is provided by the cask body. The cask body steel, the lids and base plate provide the main gamma shielding, while the neutron shielding is provided by the Holtite neutron absorber embedded in those parts. In the radial direction, the neutron absorber is located in two overlapping rows of pockets near the outer surface of the cask. The fuel basket and the basket supports maintain the fuel assemblies in a fixed position within the package, and also provide additional gamma shielding. Any shielding effect of the crushable impact limiter material and its surrounding steel skin is neglected for both normal and accident conditions. The dimensions of the shielding components are shown in the drawing package in Section 1.3. The shielding material densities are listed in Table 5.3.2.

5.1.2 Summary of Maximum Radiation Levels

The burnup and cooling time combinations specified in Appendix 7.D were determined strictly based on the shielding analysis in this chapter. Each combination was independently analyzed and it was verified that the calculated dose rates were less than the regulatory limits. In this subsection, only the results for the bounding loading patterns that produce the highest dose rates at the surface and at 2 m under normal conditions, and at 1 m under accident conditions are presented. Dose rates for additional configurations are presented in Section 5.4.

The dose rates listed in the tables in this subsection are maximum values, considering axial, radial and azimuthal variations as applicable. This is achieved by specifying a reasonably fine grid of dose locations around the cask, and selecting the highest values. Details on dose locations are provided in Subsection 5.3.3.

The dose rates listed in this subsection are based on a number of conservative assumptions. However, they do not explicitly account for any uncertainties except for the inherent uncertainties of the Monte Carlo calculations, which are listed in the results tables. It is to be noted that the conservative assumptions used in the analyses may compensate for all the uncertainties in the calculations. Therefore, in Subsection 5.4.6, additional calculations are performed using a best estimate approach instead of the conservative assumptions, and then adding the effect of the major uncertainties. These calculations result in dose rates that are equivalent to or less than those listed in this subsection. This provides further assurance that the dose rates listed here are reasonable and conservative.

5.1.2.1 Normal Conditions

As discussed in Section 1.1, HI-STAR 180D will be transported by exclusive use shipment and complies with 10CFR71.47(b).

Dose rates are calculated on the cask surface, at locations shown in Figure 5.1.1. Dose locations 1A and 3A are used to calculate the dose rates on the flange between the ends of the impact limiter's skirts and the cask radial neutron shield. Results are presented in Tables 5.1.1 and 5.1.2 for the F-32 and F-37 basket, respectively.

All values are below 2 mSv/h, therefore showing that the HI-STAR 180D complies with 10CFR71.47(b)(1). It should be noted that the additional conditions stated in 10CFR71.47(b)(1)(i) through (iii) (closed vehicle; fixed position; no loading/unloading) do not have to be met by the HI-STAR 180D, since the surface dose rate do not exceed 2 mSv/h.

The calculated dose rates on the surface of the cask are below 2 mSv/h. Therefore, dose rates at any point on the outer surface of the vehicle will also be below 2 mSv/h. The HI-STAR 180D therefore complies with 10CFR71.47(b)(2).

The maximum dose rates for the HI-STAR 180D have been calculated at a distance of 2 m from impact limiter surfaces, for the locations shown in Figure 5.1.1. At 2 m, locations corresponding to 1A and 3A on the surface are included in locations 1 and 3. Results are presented in Tables 5.1.3 and 5.1.4 for the F-32 and F-37 basket, respectively, showing that all dose rates at that distance are below 0.1 mSv/h. Consequently, the dose rates at 2 m from the outer edges of the vehicle will also be below 0.1 mSv/h. The HI-STAR 180D therefore complies with 10CFR71.47(b)(3).

Dose rates have been calculated to determine the distance necessary to comply with the 0.02 mSv/hr requirement specified in 10CFR71.47(b)(4) for any normally occupied space. The results presented in Tables 5.1.5 and 5.1.6 for the F-32 and F-37 basket, respectively, identify the distances necessary from Dose Locations 4 and 5 (the top and bottom of the HI-STAR 180D, see Figure 5.1.1) for which exposed personnel of private carriers must maintain in order to meet the 0.02 mSv/h requirement. Therefore, if the normally occupied space of the vehicle is at a distance less than the values specified in Tables 5.1.5 and 5.1.6, radiation dosimetry is required for personnel to comply with 10CFR71.47(b)(4).

The analyses summarized in this section demonstrate HI-STAR 180D's compliance with the 10CFR71.47(b) limits.

5.1.2.2 Hypothetical Accident Conditions

The hypothetical accident conditions of transport presented in Section 2.7 have two bounding consequences that affect the shielding materials. These are the damage to the neutron shield as a result of the design basis fire, and damage to the impact limiters and lead slump as a result of the 9-meter (30 foot) drop. Conservatively, the shielding analysis of the hypothetical accident condition assumes the neutron shield is completely destroyed and replaced by a void and the impact limiters steel buttress plate is only present. This is a conservative assumption since some portion of the neutron shield would be expected to remain after the fire, and the impact limiters have been shown through the calculations in Chapter 2 to remain attached following impact.

Throughout the hypothetical accident condition the axial location of the fuel will remain practically fixed within the baskets (see Subparagraph 5.3.1.2). Chapter 2 shows that the HI-STAR 180D package remains significantly unaltered throughout the hypothetical accident conditions. Localized damage of the cask outer surface could be experienced during the pin puncture, and small localized deformations of the basket might be possible during drop accidents. However, such localized deformations will have a negligible impact on the dose rate at 1 meter from the surface. The dose rate at 1 meter are determined assuming the neutron shielding is completely lost due to the fire accident event.

Figure 5.1.2 shows the dose locations at 1 meter from the surface for the conditions of the HI-STAR 180D Package after the postulated accident. Corresponding maximum dose rates are listed in Tables 5.1.7 and 5.1.8 for the F-32 and F-37 basket, respectively. All values in these tables are below the regulatory limit of 10 mSv/h.

Analyses summarized in this section demonstrate the HI-STAR 180D Package's compliance with the 10CFR71.51 radiation dose limit.

TABLE 5.1.1

MAXIMUM DOSE RATES ON THE SURFACE OF THE HI-STAR 180D PACKAGE WITH THE F-32 BASKET FOR NORMAL CONDITIONS

Dose Point† Location	[PROPRIETARY INFORMATION WITHHELD PER 10 CFR 2.390]			Totals (mSv/h)	Uncertainty in Totals (%)†††	10 CFR 71.47 Limit (mSv/h)	Loading Pattern
1				1.0520	0.70	2	
1A				1.4076	1.54	2	
2				0.4650	1.57	2	
3				0.6787	0.43	2	
3A				0.4940	1.92	2	
4				0.0497	0.43	2	
5				0.4562	0.54	2	

† Refer to Figure 5.1.1.

††† Calculational Uncertainty from MCNP, expressed as total relative error in percent for one standard deviation.

TABLE 5.1.2

MAXIMUM DOSE RATES ON THE SURFACE OF THE HI-STAR 180D PACKAGE WITH THE F-37 BASKET FOR NORMAL CONDITIONS

Dose Point[†] Location	[PROPRIETARY INFORMATION WITHHELD PER 10 CFR 2.390]			Totals (mSv/h)	Uncertainty in Totals (%)[†††]	10 CFR 71.47 Limit (mSv/h)	Loading Pattern
1				1.0337	0.71	2	
1A				1.3930	1.57	2	
2				0.4316	1.42	2	
3				0.6367	0.48	2	
3A				0.4828	1.64	2	
4				0.0497	0.46	2	
5				0.4332	0.36	2	

† Refer to Figure 5.1.1.

††† Calculational Uncertainty from MCNP, expressed as total relative error in percent for one standard deviation.

TABLE 5.1.3

MAXIMUM DOSE RATES AT 2 METERS FROM THE HI-STAR 180D PACKAGE WITH THE F-32 BASKET FOR NORMAL CONDITIONS

Dose Point† Location	[PROPRIETARY INFORMATION WITHHELD PER 10 CFR 2.390]			Totals (mSv/h)	Uncertainty in Totals (%)†††	10 CFR 71.47 Limit (mSv/h)	Loading Pattern
1				0.0680	0.70	0.1	
2				0.0808	0.72	0.1	
3				0.0541	1.14	0.1	
4				0.0107	2.42	0.1	
5				0.0815	1.08	0.1	

† Refer to Figure 5.1.1.

††† Calculational Uncertainty from MCNP, expressed as total relative error in percent for one standard deviation.

TABLE 5.1.4

MAXIMUM DOSE RATES AT 2 METERS FROM THE HI-STAR 180D PACKAGE WITH THE F-37 BASKET FOR NORMAL CONDITIONS

Dose Point[†] Location	[PROPRIETARY INFORMATION WITHHELD PER 10 CFR 2.390]			Totals (mSv/h)	Uncertainty in Totals (%)[†††]	10 CFR 71.47 Limit (mSv/h)	Loading Pattern
1				0.0749	0.59	0.1	
2				0.0813	0.49	0.1	
3				0.0568	0.74	0.1	
4				0.0107	1.03	0.1	
5				0.0827	0.81	0.1	

[†] Refer to Figure 5.1.1.

[†††] Calculational Uncertainty from MCNP, expressed as total relative error in percent for one standard deviation.

TABLE 5.1.5

DISTANCES FOR THE 0.02 mSv/h DOSE RATE REQUIREMENT FOR THE HI-STAR 180D PACKAGE WITH THE F-32 BASKET FOR NORMAL CONDITIONS

Dose Point† Location	Distance (meters)	[PROPRIETARY INFORMATION WITHHELD PER 10 CFR 2.390]			Totals (mSv/h)	Uncertainty in Totals (%)†††	10 CFR 71.47 Limit (mSv/h)	Loading Pattern
4	2				0.0107	2.42	0.02	
5	6				0.0199	2.18	0.02	

† Refer to Figure 5.1.1.

††† Calculational Uncertainty from MCNP, expressed as total relative error in percent for one standard deviation.

TABLE 5.1.6

DISTANCES FOR THE 0.02 mSv/h DOSE RATE REQUIREMENT FOR THE HI-STAR 180D PACKAGE WITH THE F-37 BASKET FOR NORMAL CONDITIONS

Dose Point† Location	Distance (meters)	[PROPRIETARY INFORMATION WITHHELD PER 10 CFR 2.390]			Totals (mSv/h)	Uncertainty in Totals (%)†††	10 CFR 71.47 Limit (mSv/h)	Loading Pattern
4	2				0.0107	1.03	0.02	
5	6				0.0201	1.64	0.02	

† Refer to Figure 5.1.1.

††† Calculational Uncertainty from MCNP, expressed as total relative error in percent for one standard deviation.

TABLE 5.1.7

MAXIMUM DOSE RATES AT 1 METER FROM THE HI-STAR 180D PACKAGE WITH THE F-32 BASKET FOR ACCIDENT CONDITIONS

Dose Point† Location	[PROPRIETARY INFORMATION WITHHELD PER 10 CFR 2.390]			Totals (mSv/h)	Uncertainty in Totals (%)†††	10 CFR 71.51 Limit (mSv/h)	Loading Pattern
1				3.4199	0.11	10	
2				4.0633	0.50	10	
3				2.3284	0.10	10	
4				0.5806	0.50	10	
5				3.5228	0.29	10	

† Refer to Figure 5.1.2.

††† Calculational Uncertainty from MCNP, expressed as total relative error in percent for one standard deviation.

TABLE 5.1.8

MAXIMUM DOSE RATES AT 1 METER FROM THE HI-STAR 180D PACKAGE WITH THE F-37 BASKET FOR ACCIDENT CONDITIONS

Dose Point† Location	[PROPRIETARY INFORMATION WITHHELD PER 10 CFR 2.390]			Totals (mSv/h)	Uncertainty in Totals (%)†††	10 CFR 71.51 Limit (mSv/h)	Loading Pattern
1				3.5208	0.17	10	
2				4.2530	0.70	10	
3				2.3984	0.15	10	
4				0.5783	0.63	10	
5				3.3868	0.36	10	

† Refer to Figure 5.1.2.

††† Calculational Uncertainty from MCNP, expressed as total relative error in percent for one standard deviation.

FIGURE 5.1.1: [PROPRIETARY INFORMATION WITHHELD PER 10 CFR 2.390]

FIGURE 5.1.2: [PROPRIETARY INFORMATION WITHHELD PER 10 CFR 2.390]

5.2 SOURCE SPECIFICATION

The principal sources of radiation in the HI-STAR 180D are:

- Gamma radiation originating from the following sources (see Subsection 5.2.1)

  1. Decay of radioactive fission products
  2. Secondary photons from neutron capture in fissile and non-fissile nuclides
  3. Hardware activation products generated during core operations

- Neutron radiation originating from the following sources (see Subsection 5.2.2)

  1. Spontaneous fission
  2. α,n reactions in fuel materials
  3. Secondary neutrons produced by fission from subcritical multiplication
  4. γ,n reactions (this source is negligible)

The neutron and gamma source terms were calculated with the SAS2H [5.1.2] and ORIGEN-S [5.1.3] modules of the SCALE 5.1 system using the 44-group library.

The assemblies to be qualified for transportation in the HI-STAR 180D contain UO_2 assemblies. A description of the design basis fuel assemblies for the source term calculations is provided in Table 5.2.1 and Table 5.2.2.

[

PROPRIETARY INFORMATION WITHHELD PER 10 CFR 2.390

]

Appendix 7.D specifies the burnup, cooling time and enrichment combinations for spent nuclear fuel that were analyzed for transport in the HI-STAR 180D.

[

PROPRIETARY INFORMATION WITHHELD PER 10 CFR 2.390

]

The following Subsections 5.2.1 and 5.2.2 describe the calculation of the gamma and neutron source terms. Reference [5.2.1] discusses the uncertainties associated with the

SAS2H/ORIGEN-S calculations related to reactor input parameters, decay heat generation, and source term calculations.

[PROPRIETARY INFORMATION WITHHELD PER 10 CFR 2.390]

5.2.1 Gamma Source

Table 5.2.3 provides the gamma source in MeV/s and photons/s as calculated with SAS2H and ORIGEN-S for a subset of burnup and cooling time combinations from Appendix 7.D.

NUREG-1617 [5.2.2] states that "In general, only gammas from approximately 0.8 MeV-2.5 MeV will contribute significantly to the external radiation levels."

[

PROPRIETARY INFORMATION WITHHELD PER 10 CFR 2.390

]

ORIGEN-S was used to calculate a ^{60}Co activity level for the desired burnup and decay time. The methodology used to determine the activation level was developed from Reference [5.2.3] and is described here.

1. The activity of the ^{60}Co from ^{59}Co, steel and inconel is calculated using ORIGEN-S. The flux used in the calculation was the in-core fuel region flux at full power.

2. The activity calculated in Step 1 for the region of interest was modified by the appropriate scaling factors listed in Table 5.2.4. These scaling factors were taken from Reference [5.2.3].

Table 5.2.5 provides the ^{60}Co activity utilized in the shielding calculations in the non-fuel regions of the assemblies for a subset of burnup and cooling time combinations from Appendix 7.D.

[
PROPRIETARY INFORMATION WITHHELD PER 10 CFR 2.390
]

5.2.2 Neutron Source

It is well known that the neutron source strength for a UO_2 assembly increases as enrichment decreases, for a constant burnup and decay time. This is due to the increase in Pu content in the fuel that increases the inventory of other transuranium nuclides such as Cm. The gamma source also varies with enrichment, although only slightly.

[PROPRIETARY INFORMATION WITHHELD PER 10 CFR 2.390]

The neutron sources calculated are listed in Table 5.2.6 in neutrons/s for a subset of burnup and cooling time combinations from Appendix 7.D.

[
PROPRIETARY INFORMATION WITHHELD PER 10 CFR 2.390
]

TABLE 5.2.1

[PROPRIETARY INFORMATION WITHHELD PER 10 CFR 2.390]

TABLE 5.2.2

[PROPRIETARY INFORMATION WITHHELD PER 10 CFR 2.390]

TABLE 5.2.3

CALCULATED GAMMA SOURCE PER ASSEMBLY FOR SELECTED BURNUP AND COOLING TIMES

Lower Energy	**Upper Energy**	48,000 MWd/MtU 1.75 Year Cooling 4.25 wt% ^{235}U		51,000 MWd/MtU 5.5 Year Cooling 4.25 wt% ^{235}U		52,000 MWd/MtU 3.08 Year Cooling 4.25 wt% ^{235}U		54,000 MWd/MtU 4.5 Year Cooling 4.25 wt% ^{235}U		55,000 MWd/MtU 4.75 Year Cooling 4.25 wt% ^{235}U	
(MeV)	(MeV)	(MeV/s)	(Photons/s)	(MeV/s)	(Photons/s)	(MeV/s)	(Photons/s)	(MeV/s)	(Photons/s)	(MeV/s)	(Photons/s)
0.45	0.7	2.49E+15	4.34E+15	1.24E+15	2.15E+15	1.93E+15	3.36E+15	1.53E+15	2.66E+15	1.50E+15	2.60E+15
0.7	1.0	1.29E+15	1.52E+15	3.92E+14	4.62E+14	8.83E+14	1.04E+15	5.85E+14	6.89E+14	5.55E+14	6.53E+14
1.0	1.5	2.84E+14	2.27E+14	9.24E+13	7.39E+13	1.86E+14	1.49E+14	1.27E+14	1.02E+14	1.22E+14	9.75E+13
1.5	2.0	3.97E+13	2.27E+13	6.54E+12	3.74E+12	1.86E+13	1.06E+13	9.80E+12	5.60E+12	9.06E+12	5.18E+12
2.0	2.5	5.79E+13	2.57E+13	2.63E+12	1.17E+12	1.92E+13	8.53E+12	6.01E+12	2.67E+12	4.92E+12	2.19E+12
2.5	3.0	1.52E+12	5.51E+11	1.26E+11	4.58E+10	6.54E+11	2.38E+11	2.59E+11	9.40E+10	2.22E+11	8.06E+10
Total		4.17E+15	6.14E+15	1.73E+15	2.69E+15	3.04E+15	4.56E+15	2.26E+15	3.46E+15	2.19E+15	3.36E+15

TABLE 5.2.4

[PROPRIETARY INFORMATION WITHHELD PER 10 CFR 2.390]

TABLE 5.2.5

CALCULATED ^{60}Co SOURCE PER ASSEMBLY FOR SELECTED BURNUP AND COOLING TIMES

Location	48,000 MWd/MtU 1.75Year Cooling 4.25 wt% ^{235}U **(Photons/s)**	51,000 MWd/MtU 5.5 Year Cooling 4.25 wt% ^{235}U **(Photons/s)**	52,000 MWd/MtU 3.08 Year Cooling 4.25 wt% ^{235}U **(Photons/s)**	54,000 MWd/MtU 4.5 Year Cooling 4.25 wt% ^{235}U **(Photons/s)**	55,000 MWd/MtU 4.75 Year Cooling 4.25 wt% ^{235}U **(Photons/s)**
Bottom nozzle	7.00E+12	2.07E+13	1.34E+13	1.86E+13	1.57E+13
Active fuel zone	1.98E+12	1.76E+13	1.14E+13	1.58E+13	1.34E+13
Plenum	4.79E+12	8.74E+12	5.66E+12	7.86E+12	6.64E+12
Top nozzle	5.15E+12	1.60E+13	1.04E+13	1.44E+13	1.22E+13

TABLE 5.2.6

CALCULATED NEUTRON SOURCE PER ASSEMBLY FOR BOUNDING BURNUPS AND COOLING TIMES

Lower Energy (MeV)	**Upper Energy (MeV)**	48,000 MWd/MtU 1.75 Year Cooling 4.25 wt% ^{235}U **(Neutrons/s)**	51,000 MWd/MtU 5.5 Year Cooling 4.25 wt% ^{235}U **(Neutrons/s)**	52,000 MWd/MtU 3.08 Year Cooling 4.25 wt% ^{235}U **(Neutrons/s)**	54,000 MWd/MtU 4.5 Year Cooling 4.25 wt% ^{235}U **(Neutrons/s)**	55,000 MWd/MtU 4.75 Year Cooling 4.25 wt% ^{235}U **(Neutrons/s)**
1.0E-01	4.0E-01	2.53E+07	2.69E+07	3.18E+07	3.47E+07	3.68E+07
4.0E-01	9.0E-01	5.52E+07	5.87E+07	6.94E+07	7.55E+07	8.01E+07
9.0E-01	1.4	5.52E+07	5.86E+07	6.93E+07	7.54E+07	7.99E+07
1.4	1.85	4.41E+07	4.68E+07	5.53E+07	6.02E+07	6.38E+07
1.85	3.0	8.26E+07	8.72E+07	1.03E+08	1.12E+08	1.19E+08
3.0	6.43	7.51E+07	7.93E+07	9.37E+07	1.02E+08	1.08E+08
6.43	20.0	7.11E+06	7.57E+06	8.95E+06	9.74E+06	1.03E+07
Totals		3.45E+08	3.65E+08	4.31E+08	4.69E+08	4.97E+08

5.3 SHIELDING MODEL

The shielding analysis of the HI-STAR 180D was performed with MCNP 5 1.51 [5.1.1]. MCNP is a Monte Carlo transport code that offers a full three-dimensional combinatorial geometry modeling capability including such complex surfaces as cones and tori. This means that no gross approximations were required to represent the HI-STAR 180D in the shielding analysis. MCNP-5 is essentially the same code that is used for the shielding calculations of Holtec's other approved dry storage and transportation systems under separate dockets.

The MCNP model of the HI-STAR 180D Package for normal conditions has the neutron shield and impact limiters in place. The MCNP model for the hypothetical accident condition replaces the neutron shield with void and removes part of the impact limiters (all parts except the buttress plates) and includes lead slump. The shielding effect of the crush material in the impact limiters was conservatively neglected in all MCNP models. However, credit was taken for the outer dimensions of the impact limiters under normal conditions, i.e. the axial 2 m dose locations are based on the distance from the skin around the crush material, and axial surface dose locations are the impact limiters cover plates.

[

PROPRIETARY INFORMATION WITHHELD PER 10 CFR 2.390

]

5.3.1 Configuration of Shielding and Source

5.3.1.1 Shielding Configuration

Section 1.3 provides the drawings that describe the HI-STAR 180D Packaging. These drawings were used to create the MCNP models used in the radiation transport calculations. The drawing package also illustrates the HI-STAR 180D on a typical transport vehicle with a personnel barrier installed. The vehicle and barrier were not considered in the MCNP model, i.e. the outer dimensions of the vehicle are conservatively assumed to be identical to the outer dimensions of the package as modeled for normal conditions. Figures 5.3.1 and 5.3.2 show the cross sectional views of the HI-STAR 180D cask loaded with F-37 and F-32 baskets respectively, as they were modeled in MCNP. The figures were created with the MCNP plotter and are drawn to scale. The figures illustrate the annular monolithic cylinders that are utilized to house the radial Holtite. Figure 5.3.3 shows the MCNP model of the F-32 and F-37 baskets. Figure 5.3.4 shows a cross sectional view of the HI-STAR 180D. Figure 5.3.5 is an axial representation of the HI-STAR 180D cask. Figures 5.3.6 and 5.3.7 provide the as-modeled views of the impact limiters during normal conditions. The crush material in the impact limiter is not shown in Figure 5.3.6 because it was conservatively neglected in the MCNP calculations.

The conditions and tests specified in 10CFR 71.71 for normal conditions have no effect on the configuration of the cask. Therefore no additional considerations are necessary for these conditions and tests.

During the MCNP modeling process a few modeling simplifications were made. The major simplifications between model and drawings are listed and discussed here.

F-32 and F-37 Basket Modeling Simplifications

1. [
PROPRIETARY INFORMATION WITHHELD PER 10 CFR 2.390
]

2. The holes in the basket shims are modeled with squared rather than rounded corners. This is conservative since it neglects a small amount of material in the analyses.

HI-STAR Modeling Simplifications

1. [
PROPRIETARY INFORMATION WITHHELD PER 10 CFR 2.390
]

2. The annular monolithic cylinders are modeled as one casting rather than multiple castings stacked on top of one another. This is acceptable since the gap between the castings is small, and the castings overlap to prevent any significant streaming.

3. In the modeling of the impact limiters, only the steel portions, shown in Figure 5.1.1, were represented. Conservatively, the crush material of the impact limiters was not modeled.

4. The trunnions are not explicitly modeled.

5. The bolts utilized for closure of the inner and outer lid are not modeled, but rather the bolt hole locations are modeled as a solid material.

6. Penetrations in the two lids were not modeled. This is acceptable since these penetrations are not aligned and are covered by the port covers, and additionally by the steel structure of the impact limiter. Any streaming through these penetrations would therefore have a negligible effect.

7. All empty spaces in and around the cask are represented by voids in the model. This is acceptable, since any absorption and scattering in air would have a very small effect in comparison to the dose rates at the close distances analyzed here.

8. Deleted.

9. Conservatively, only the buttress plate and radial shielding (radial spacers and skirts) of the top impact limiter are modeled for normal conditions.

10. [PROPRIETARY INFORMATION WITHHELD PER 10 CFR 2.390]

11. [

PROPRIETARY INFORMATION WITHHELD PER 10 CFR 2.390

]

12. [
PROPRIETARY INFORMATION WITHHELD PER 10 CFR 2.390

]

5.3.1.2 Fuel and Source Configuration

In the model homogenized regions represent the fuel. Calculations on a similar cask design were performed to determine the acceptability of homogenizing the fuel assembly versus explicit modeling. Based on these calculations it can be concluded that homogenization of the fuel assembly is acceptable without loss of accuracy.

[

PROPRIETARY INFORMATION WITHHELD PER 10 CFR 2.390

]

5.3.1.3 Streaming Through Radial Steel Ribs

The HI-STAR 180D cask utilizes Holtite as a neutron absorber in radial and axial directions.

[

PROPRIETARY INFORMATION WITHHELD PER 10 CFR 2.390

]

5.3.2 Material Properties

Composition and densities of the various materials used in the HI-STAR 180D shielding analyses are given in Table 5.3.2. The density of the lead is reduced to a conservative amount that bounds the effect of engineered gaps. Holtite-B Material Compositions and densities are presented in Table 5.3.3. Further information on the Holtite and Metamic neutron absorbers is provided in Section 1.2. All of the materials and their actual geometries are represented in the MCNP model. All steel in the cask was modeled as carbon steel.

[

PROPRIETARY INFORMATION WITHHELD PER 10 CFR 2.390

]

[

PROPRIETARY INFORMATION WITHHELD PER 10 CFR 2.390

]

Section 3.4 demonstrates that all materials used in the HI-STAR 180D remain at or below their design temperatures during all normal conditions. Therefore, the shielding analysis does not address changes in the material density or composition as a result of temperature changes.

During normal operations, the depletion of B-10 in the Metamic and the Holtite neutron shield is negligible. Based on calculations prepared for a similar cask model, the fraction of B-10 atoms that are depleted in 50 years is less than 1E-6 in both the Metamic and Holtite. Therefore, the shielding analysis does not need to address any changes in the composition of the Metamic or Holtite as a result of neutron absorption.

5.3.3 Tally Specifications

The dose rate values listed in Tables 5.1.1 through 5.1.8, with corresponding dose point locations illustrated in Figures 5.1.1 and 5.1.2, are computed using MCNP volume tallies. In radial direction, the dose locations are represented by cylindrical rings with a thickness of 1 cm or 2 cm each at the surface, at 1 m and at 2 m from the surface, and outer edge of the impact limiter, respectively. In axial direction they are cylindrical disks with a thickness of 2 cm at various distances from the cask. Further details are discussed below.

Radial Tallies

- Dose Locations 2
  This dose location captures the maximum dose rate around the radial shield cylinder, i.e. the axial section of the cask [

PROPRIETARY INFORMATION WITHHELD PER 10 CFR 2.390

]

- Dose Locations 1 and 3
  These are the dose locations adjacent to the impact limiter skirt surrounding the upper and lower forgings of the cask. [
  PROPRIETARY INFORMATION WITHHELD PER 10 CFR 2.390
  ]

- Dose Locations 1A and 3A
  These are the dose locations adjacent to the gap between the impact limiter skirt and the radial shield cylinder, [PROPRIETARY INFORMATION WITHHELD PER 10 CFR 2.390].

<u>Axial Tallies</u>

The tally volumes located on the top and bottom surfaces, 1 meter and 2 meter positions of the cask were composed the following way:

- Dose Locations 4 and 5
  In axial direction, the tally volumes are circular disks that are divided into radial sections, each about 23 cm wide.

The dose locations for both radial and axial tallies are also described in Section 5.4.4.

TABLE 5.3.1

[PROPRIETARY INFORMATION WITHHELD PER 10 CFR 2.390]

TABLE 5.3.2

[PROPRIETARY INFORMATION WITHHELD PER 10 CFR 2.390]

TABLE 5.3.2 (CONTINUED)

[PROPRIETARY INFORMATION WITHHELD PER 10 CFR 2.390]

TABLE 5.3.3

[PROPRIETARY INFORMATION WITHHELD PER 10 CFR 2.390]

FIGURE 5.3.1: [PROPRIETARY INFORMATION WITHHELD PER 10 CFR 2.390]

FIGURE 5.3.2: [PROPRIETARY INFORMATION WITHHELD PER 10 CFR 2.390]

FIGURE 5.3.3: [PROPRIETARY INFORMATION WITHHELD PER 10 CFR 2.390]

FIGURE 5.3.4: [PROPRIETARY INFORMATION WITHHELD PER 10 CFR 2.390]

FIGURE 5.3.5: [PROPRIETARY INFORMATION WITHHELD PER 10 CFR 2.390]

FIGURE 5.3.6: [PROPRIETARY INFORMATION WITHHELD PER 10 CFR 2.390]

FIGURE 5.3.7: [PROPRIETARY INFORMATION WITHHELD PER 10 CFR 2.390]

FIGURE 5.3.8: [PROPRIETARY INFORMATION WITHHELD PER 10 CFR 2.390]

FIGURE 5.3.9: [PROPRIETARY INFORMATION WITHHELD PER 10 CFR 2.390]

FIGURE 5.3.10: [PROPRIETARY INFORMATION WITHHELD PER 10 CFR 2.390]

5.4 SHIELDING EVALUATION

5.4.1 Methods

A number of conservative assumptions are applied throughout the shielding calculations. These assumptions will assure that the actual dose rates will always be below the calculated dose rates, and below the regulatory limits.

[

PROPRIETARY INFORMATION WITHHELD PER 10 CFR 2.390

]

The MCNP-5 code [5.1.1] was used for all of the shielding analyses. MCNP is a continuous energy, three-dimensional, coupled neutron-photon-electron Monte Carlo transport code. Continuous energy cross-section data is represented with sufficient energy points to permit linear-linear interpolation between these points. Cross section libraries are based on ENDF/B-V and ENDF/B-VI, except for Sn isotopes where the ENDL92 library is used, and uranium isotopes where LANL/T16 libraries are used. These are the default libraries for the MCNP code version used for the shielding analyses. The large user community has extensively benchmarked MCNP against experimental data. References [5.4.2], [5.4.3], and [5.4.4] are three examples of the benchmarking that has been performed. MCNP-5 is essentially the same code that has been used as the shielding code in all of Holtec's dry storage and transportation analyses. Note also that the principal approach in the shielding analysis here is identical to the approach in licensing applications previously reviewed and approved by the USNRC.

[

PROPRIETARY INFORMATION WITHHELD PER 10 CFR 2.390

]

[

PROPRIETARY INFORMATION WITHHELD PER 10 CFR 2.390

]

[

PROPRIETARY INFORMATION WITHHELD PER 10 CFR 2.390

]

[

PROPRIETARY INFORMATION WITHHELD PER 10 CFR 2.390

]

5.4.2 Input and Output Data

[

PROPRIETARY INFORMATION WITHHELD PER 10 CFR 2.390

]

5.4.3 Flux-to-Dose-Rate Conversion

[

PROPRIETARY INFORMATION WITHHELD PER 10 CFR 2.390

]

5.4.4 External Radiation Levels

Tables 5.1.1 and 5.1.2 provide the maximum dose rates on the surface of the package during normal transport conditions for the HI-STAR 180D with design basis fuel. Tables 5.1.3 and 5.1.4 list the maximum dose rate 2 m from the outer edge of the impact limiter during normal conditions. The burnup and cooling time combinations chosen for the tables in that section were the combinations that resulted in maximum dose rates for the normal operation on the surface and at 2 m from the outer edge of the impact limiter, as specified in the regulatory requirements. These combinations may not be all from the same loading condition, but show the highest dose rate at each individual dose location. However, the loading patterns corresponding to the maximum dose rates are also listed in the tables.

Figure 5.1.1 shows the dose locations on the surface and the condition of the HI-STAR 180D Package during normal transport. Each of these dose locations has a corresponding location at 2 m from the outer edge of the impact limiter except 1A and 3A. 1A and 3A locations are covered by 1 and 3 at 2 m. The azimuthal dose values are taken from the dose point locations that are shown in Figure 5.3.4. [

PROPRIETARY INFORMATION WITHHELD PER 10 CFR 2.390

]

Dose locations 1, 2 and 3 shown in Figure 5.1.1 and Figure 5.1.2 do not correspond to single dose locations. Rather the dose rates for multiple axial and azimuthal segments were calculated and the highest value was chosen for the corresponding dose location. Dose location 2 is

comprised of axial segments that range from the bottom of the monolithic cylinders to the top of the monolithic cylinders (the length of the Holtite pockets). The highest dose rate of these axial segments was chosen as the value for dose location 2. Dose location 1 corresponds to the axial extension of the lower impact limiter that spans between the bottom of the Holtite pockets and the crushable structure of the impact limiter. Dose location 3 corresponds to the axial extension of the upper impact limiter that spans between the crushable structure of the impact limiter and the top of the Holtite pockets. Dose locations 1A and 3A represent the small gap between the end of the impact limiter's skirt and neutron shield cylinders. Dose location 4 corresponds to the surface location directly above the radial rib plates in the top impact limiter, and dose location 5 corresponds to the location directly below the radial rib plates in the bottom impact limiter.
Detailed results are listed in Tables 5.4.2 through 5.4.5. These tables show the highest total dose rates at each dose location for each pattern in each basket. Table 5.4.2 presents the dose rates for both the F-32 and F-37 baskets on the surface of the cask for normal condition using all the bounding loading patterns, while Table 5.4.3 shows the same at 2 m.

The dose rates calculated to determine the distances necessary to comply with the 0.02 mSv/hr requirement specified in 10CFR71.47(b)(4) for any normally occupied space are presented in Table 5.4.4 for all the bounding patterns.

Table 5.4.5 presents the maximum dose rates at 1 m from the surface of the cask during hypothetical accident conditions for both the F-32 and F-37 baskets for all the bounding loading patterns.

5.4.5 Fuel Reconfiguration

The licensing approach for HBF reconfiguration is discussed in Section 1.4. The structural analyses of fuel rods in Section 2.11 show that the fuel is expected to remain essentially undamaged during the hypothetical accident conditions. The design basis calculations for the hypothetical accident conditions therefore use the same model to represent fuel as the calculations for normal conditions. The current subsection presents additional calculations to show that even if some fuel reconfigurations should occur, the dose rates would still be expected to remain below the regulatory limits.

[

PROPRIETARY INFORMATION WITHHELD PER 10 CFR 2.390

]

[

PROPRIETARY INFORMATION WITHHELD PER 10 CFR 2.390

]

The results from the three scenarios described above along with a nominal reference case for accident conditions are shown in Table 5.4.6.

[

PROPRIETARY INFORMATION WITHHELD PER 10 CFR 2.390

]

5.4.6 Effect of Uncertainties

The design basis calculations presented in Section 5.1 and Subsection 5.4.4 are based on a range of conservative assumptions, but do not explicitly account for uncertainties in the methodologies, codes and input parameters, that is, it is assumed that the effect of uncertainties is small compared to the numerous conservatisms in the analyses.

[

PROPRIETARY INFORMATION WITHHELD PER 10 CFR 2.390

]

[

PROPRIETARY INFORMATION WITHHELD PER 10 CFR 2.390

]

5.4.7 Additional Sentivity Analyses

5.4.7.1 Neutron Axial Profile

[

PROPRIETARY INFORMATION WITHHELD PER 10 CFR 2.390

]

The methodology and the results of the analysis are provided in Appendix J in [5.4.6]. It is shown the the regulatory dose rate limits are met.

5.4.7.2 Determination of Dose Rate from All Alternative Patterns

The difficulties of defining acceptable loading patterns stem from the fact that defining a single bounding loading pattern would be *impractical* but *possible*. A single bounding pattern could simply be constructed by selecting, for each basket location, the combination of the lowest cooling time, lowest enrichment, and highest burnup. However, this would result in a much higher dose rate than that for any real expected loading configuration, and as a result, would require design changes that would exceed the given dimensional and weight limitations of the cask, or require a cask with a lower capacity which then would require a larger number of casks. Specifying a single bounding pattern (or a small set of such patterns) for a given fuel population would be difficult (or even impossible) to achieve within the limitations of an already optimized cask design. The reason is that the bounding pattern (pattern that results in the largest dose rate) would most likely be different for each location around the cask. To overcome this problem, a method is developed and documented in Appendix J in [5.4.6] to determine dose rates from all alternative patterns for all tally locations, where high dose rates are expected, at the surface and 2 m from the package. It is shown the the regulatory dose rate limits are met.

5.4.7.3 Source Probability in MCNP Input File

To evaluate the combined effect of the revised nonlinear relationship between burnup and source terms, an MCNP calculation has been performed with source terms applied directly in MCNP input file thus eliminating the approximation related to the axial burnup profile.

The analysis and results are provided in Appendix J in [5.4.6]. It is shown the the regulatory dose rate limits are met.

5.4.7.4 Lead Slump Analysis

The lead slump is considered for the accident condition of transport [5.4.6]. The MCNP model for the accident condition includes the following assumptions:

[

PROPRIETARY INFORMATION WITHHELD PER 10 CFR 2.390

]

TABLE 5.4.1 (a)

[PROPRIETARY INFORMATION WITHHELD PER 10 CFR 2.390]

TABLE 5.4.1 (b)

FLUX-TO-DOSE CONVERSION FACTORS
(FROM [5.4.1])

Gamma Energy (MeV)	(mSv/h)/ (photon/cm^2-s) †
0.01	3.96E-05
0.03	5.82E-06
0.05	2.90E-06
0.07	2.58E-06
0.1	2.83E-06
0.15	3.79E-06
0.2	5.01E-06
0.25	6.31E-06
0.3	7.59E-06
0.35	8.78E-06
0.4	9.85E-06
0.45	1.08E-05
0.5	1.17E-05
0.55	1.27E-05
0.6	1.36E-05
0.65	1.44E-05
0.7	1.52E-05
0.8	1.68E-05
1.0	1.98E-05
1.4	2.51E-05
1.8	2.99E-05
2.2	3.42E-05

† Values have been multiplied by 10 to convert rem, as given in [5.4.1], to mSv

TABLE 5.4.1 (b) (CONTINUED)

FLUX-TO-DOSE CONVERSION FACTORS
(FROM [5.4.1])

Gamma Energy (MeV)	(mSv/h)/ (photon/cm^2-s) †
2.6	3.82E-05
2.8	4.01E-05
3.25	4.41E-05
3.75	4.83E-05
4.25	5.23E-05
4.75	5.60E-05
5.0	5.80E-05
5.25	6.01E-05
5.75	6.37E-05
6.25	6.74E-05
6.75	7.11E-05
7.5	7.66E-05
9.0	8.77E-05
11.0	1.03E-04
13.0	1.18E-04
15.0	1.33E-04

† Values have been multiplied by 10 to convert rem, as given in [5.4.1], to mSv

TABLE 5.4.1 (b) (CONTINUED)

FLUX-TO-DOSE CONVERSION FACTORS
(FROM [5.4.1])

Neutron Energy (MeV)	Quality Factor	(mSv/h)/(n/cm^2-s) †, ††
2.5E-8	2.0	3.67E-05
1.0E-7	2.0	3.67E-05
1.0E-6	2.0	4.46E-05
1.0E-5	2.0	4.54E-05
1.0E-4	2.0	4.18E-05
1.0E-3	2.0	3.76E-05
1.0E-2	2.5	3.56E-05
0.1	7.5	2.17E-04
0.5	11.0	9.26E-04
1.0	11.0	1.32E-03
2.5	9.0	1.25E-03
5.0	8.0	1.56E-03
7.0	7.0	1.47E-03
10.0	6.5	1.47E-03
14.0	7.5	2.08E-03
20.0	8.0	2.27E-03

† Values have been multiplied by 10 to convert mrem, as given in [5.4.1], to mSv

†† Includes the Quality Factor

TABLE 5.4.2

TOTAL DOSE RATES ON THE
SURFACE OF THE HI-STAR 180D PACKAGE FOR NORMAL CONDITIONS
WITH THE F-32 AND F-37 Basket

Dose Point[††] Location	**Total Dose Rate (mSv/h)**		
	Loading Pattern, F-32		
	A	**B**	
1	1.0225	1.0520	
1A	1.3632	1.4076	
2	0.3502	0.4650	
3	0.6787	0.6348	
3A	0.4940	0.4827	
4	0.0497	0.0455	
5	0.4562	0.3949	
	Loading Pattern, F-37		
	A	**B**	**C**
1	0.9342	0.9683	1.0337
1A	1.3086	1.3821	1.3930
2	0.3445	0.4316	0.4107
3	0.6157	0.6243	0.6367
3A	0.4535	0.4611	0.4828
4	0.0488	0.0496	0.0497
5	0.4332	0.4269	0.4249
10CFR71.47 Limit (mSv/h)	2	2	2

†† Refer to Figure 5.1.1.

TABLE 5.4.3

TOTAL DOSE RATES AT
TWO METERS FROM THE HI-STAR 180D PACKAGE FOR NORMAL CONDITIONS
WITH THE F-32 AND F-37 BASKET

Dose Point[††] Location	**Total Dose Rate (mSv/h)**		
	Loading Pattern, F-32		
	A	**B**	
1	0.0674	0.0680	
2	0.0669	0.0808	
3	0.0468	0.0541	
4	0.0107	0.0097	
5	0.0815	0.0744	
	Loading Pattern, F-37		
	A	**B**	**C**
1	0.0689	0.0741	0.0749
2	0.0685	0.0792	0.0813
3	0.0474	0.0565	0.0568
4	0.0106	0.0107	0.0107
5	0.0827	0.0799	0.0778
10CFR71.47 Limit (mSv/h)	0.1	0.1	0.1

†† Refer to Figure 5.1.1.

TABLE 5.4.4

DISTANCES FOR THE 0.02 mSv/h DOSE RATE REQUIREMENT
FOR THE HI-STAR 180D PACKAGE FOR NORMAL CONDITIONS
WITH THE F-32 AND F-37 BASKET

Loading Pattern	**Dose Point[††] Location**	**Distance (Meters)**	**Total Dose Rate (mSv/h)**	**Dose Point Location**	**Distance (Meters)**	**Total Dose Rate (mSv/h)**
F-32						
A	4	2	0.0107	5	6	0.0199
B		2	0.0097		6	0.0184
F-37						
A	4	2	0.0106	5	7 Note 1	0.0148
B		2	0.0107		6	0.0197
C		2	0.0107		6	0.0197
10CFR71.47 Limit (mSv/h)			0.02	10CFR71.47 Limit (mSv/h)		0.02

Note. The values for 7 meters are calculated using the inverse square law.

[††] Refer to Figure 5.1.1.

TABLE 5.4.5

TOTAL DOSE RATES AT
ONE METER FROM THE HI-STAR 180D PACKAGE FOR ACCIDENT CONDITIONS
WITH THE F-32 AND F-37 BASKET

Dose Point[††] Location	**Total Dose Rate (mSv/h)**		
	Loading Pattern, F-32		
	A	**B**	
1	3.4199	3.1887	
2	4.0633	3.7553	
3	2.3284	2.1806	
4	0.5806	0.5254	
5	3.5228	3.1407	
	Loading Pattern, F-37		
	A	**B**	**C**
1	3.3380	3.4978	3.5208
2	4.0415	4.2530	4.2309
3	2.2837	2.3954	2.3984
4	0.5747	0.5770	0.5783
5	3.3868	3.3589	3.3254
10CFR71.51 Limit (mSv/h)	10	10	10

[††] Refer to Figure 5.1.2.

TABLE 5.4.6

TOTAL DOSE RATES AT 1 METER FROM THE HI-STAR 180D PACKAGE FOR HYPOTHETICAL FUEL RECONFIGURATION ACCIDENT CONDITIONS WITH THE F-37 BASKET

Dose Point† Location	**Total Dose Rate†† (mrem/hr)**				
	Configuration, F-37				
	Nominal Reference Case (see Table 5.1.8)	Scenario 1: Flat Axial Profile, Increased Fuel Density	Scenario 2: Compressed Axial Profile, Increased Fuel Density	Scenario 3: Decreased Fuel Density, Source Strength	10 CFR 71.51 Limit (mSv/h)
1	3.52	4.23	3.12	2.25	10
2	4.25	3.67	5.23	2.67	10
3	2.40	0.97	3.95	1.57	10
4	0.58	0.17	1.37	0.40	10
5	3.39	7.73	2.22	2.55	10

† Refer to Figure 5.1.2.

†† See Subsection 5.4.5 for description of calculations.

TABLE 5.4.7

[PROPRIETARY INFORMATION WITHHELD PER 10 CFR 2.390]

TABLE 5.4.8

[PROPRIETARY INFORMATION WITHHELD PER 10 CFR 2.390]

TABLE 5.4.9

[PROPRIETARY INFORMATION WITHHELD PER 10 CFR 2.390]

Table 5.4.10

[PROPRIETARY INFORMATION WITHHELD PER 10 CFR 2.390]

Table 5.4.11

[PROPRIETARY INFORMATION WITHHELD PER 10 CFR 2.390]

Table 5.4.12

[PROPRIETARY INFORMATION WITHHELD PER 10 CFR 2.390]

CHAPTER 5 REFERENCES

The following generic industry and Holtec produced references may have been consulted in the preparation of this document. Where specifically cited, the identifier is listed in the SAR text or table. Active Holtec Calculation Packages which are the repository of all relevant licensing and design basis calculations are annotated as “latest revision”. Submittal of the latest revision of such Calculation Packages to the USNRC and other regulatory authorities during the course of regulatory reviews is managed under the company’s Configuration Control system. Supporting documents submitted to the USNRC with the HI-STAR 180D LAR 9367-2 have been italicized.

[5.1.1] X-5 Monte Carlo Team, “MCNP – A General Monte Carlo N-Particle Transport Code, Version 5,” *LA-UR-03-1987*, Los Alamos National Laboratory (2003).

[5.1.2] I.C. Gauld and O.W. Hermann, "SAS2: A Coupled One-Dimensional Depletion and Shielding Analysis Module," ORNL/TM-2005/39, Revision 5.1, , Oak Ridge National Laboratory, November 2006.

[5.1.3] I.C. Gauld, O.W. Hermann, and R.M. Westfall, "ORIGEN-S: SCALE System Module to Calculate Fuel Depletion, Actinide Transmutation, Fission Product Buildup and Decay, and Associated Radiation Source Terms," ORNL/TM-2005/39, Version 5.1, Oak Ridge National Laboratory, November 2006.

[5.1.4] HI-STAR 100 SAR, Rev. 12, October 2007 (Docket 71-9261), and HI-STORM FSAR, Rev. 7, August 2008 (Docket 72-1014).

[5.1.5] B.L. Broadhead, “Recommendations for Shielding Evaluations for Transport and Storage Packages,“ NUREG/CR-6802 (ORNL/TM-2002/31), Oak Ridge National Laboratory, May 2003.

[5.2.1] HI-STAR 180 SAR, latest revision, HI-2073681, Holtec International.

[5.2.2] NUREG-1617, SRP for Transportation Packages for Spent Nuclear Fuel, USNRC, Washington, DC, March 2000.

[5.2.3] A. Luksic, "Spent Fuel Assembly Hardware: Characterization and 10CFR 61 Classification for Waste Disposal," PNL-6906-vol. 1, Pacific Northwest Laboratory, June 1989.

[5.2.4] M. D. DeHart and O. W. Hermann, “An Extension of the Validation of SCALE (SAS2H) Isotopic Predictions for PWR Spent Fuel,” ORNL/TM-13317, Oak Ridge National Laboratory, September 1996.

[5.2.5] O. W. Hermann, et al., “Technical Support for a Proposed Decay Heat Guide Using SAS2H/ORIGEN-S Data,” NUREG/CR-5625, ORNL-6698, Oak Ridge National Laboratory, September 1994.

[5.4.1] "American National Standard Neutron and Gamma-Ray Flux-to-Dose Rate Factors", ANSI/ANS-6.1.1-1977.

[5.4.2] D. J. Whalen, et al., "MCNP: Photon Benchmark Problems," LA-12196, Los Alamos National Laboratory, September 1991.

[5.4.3] D. J. Whalen, et al., "MCNP: Neutron Benchmark Problems," LA-12212, Los Alamos National Laboratory, November 1991.

[5.4.4] J. C. Wagner, et al., "MCNP: Criticality Safety Benchmark Problems," LA-12415, Los Alamos National Laboratory, October 1992.

[5.4.5] *Holtec International Report HI-2125229, "The Radiation Source Term Calculations for HI-STAR 180D", Latest Revision. (Holtec Proprietary)*

[5.4.6] *Holtec International Report HI-2125255, "Shielding Analysis for the HI-STAR 180D", Latest Revision. (Holtec Proprietary)*

Appendix 5.A

[PROPRIETARY INFORMATION WITHHELD PER 10 CFR 2.390]

Appendix 5.B

[PROPRIETARY INFORMATION WITHHELD PER 10 CFR 2.390]

Appendix 5.C

[PROPRIETARY INFORMATION WITHHELD PER 10 CFR 2.390]

CHAPTER 6 CRITICALITY EVALUATION

6.0 INTRODUCTION

This chapter documents the criticality evaluation of the HI-STAR 180D Cask for the packaging and transportation of radioactive materials (spent nuclear fuel) in accordance with 10CFR71. The results of this evaluation demonstrate that an infinite number of HI-STAR 180D Packages with variations in internal and external moderation remain subcritical with subcriticality margin, respectively, of at least 0.02Δk for misload conditions and greater than 0.05Δk under all the other conditions. This corresponds to a criticality safety index (CSI) of zero (0.0) and demonstrates compliance with criticality requirements in USNRC Interim Staff Guidance (ISG) - 8, Rev. 3, 10 CFR 71.55 and 10 CFR 71.59 for normal and hypothetical accident conditions of transport.

In addition to demonstrating that the criticality safety acceptance criteria are satisfied, this chapter describes the HI-STAR 180D design structures and components important to criticality safety. It also provides limiting fuel characteristics. With the cask and fuel description, this chapter gives data in sufficient detail to allow the criticality evaluation of the package.

Finally, the analysis methods, models and acceptance criteria utilized in the safety evaluation documented in this chapter mirror those used in the SAR for HI-STAR 180 certified in Docket #71-9325.

6.1 DESCRIPTION OF CRITICALITY DESIGN

6.1.1 Design Features

The containment system of the HI-STAR 180D is a cylindrical shell with a flat bottom and flat bolted lids at the top. Inside the containment system, fuel assemblies are placed in a basket structure to maintain their location.

The following basket designs are available for use in the HI-STAR 180D:

- a 32-cell basket (F-32), designed for fresh undamaged PWR UO_2 fuel assemblies with a specified maximum enrichment.

- a 37-cell basket (F-37), designed for fresh or spent undamaged PWR UO_2 fuel assemblies. UO_2 assemblies are specified with a maximum enrichment and minimum burnup. two configurations are analyzed:
    - Spent fuel assemblies are stored in all positions of the basket;
    - Fresh fuel assemblies are stored in one region which is at the periphery of the basket; spent fuel assemblies are stored in the remaining positions.

For general details of these baskets see the description and drawings in Section 1.3. Sketches showing the basket details that are important for criticality safety are shown in Section 6.3.1 of this chapter.

Criticality safety of the HI-STAR 180D depends on the following principal design features:

- The inherent geometry of the fuel basket design within the cask. Both basket designs contain flux traps for criticality control. The difference between the two baskets lies in the number and thickness of these flux traps. This allows a different number of fuel assemblies in the baskets;

- The incorporation of permanent fixed neutron-absorbing material in the fuel basket structure. The baskets are completely manufactured from Metamic-HT, an aluminum and B_4C composite material. All assemblies are therefore completely surrounded by neutron absorbing material;

- Administrative limits on the maximum enrichment (F-32 and F-37) and minimum average assembly burnup (F-37). The burnup credit methodology for the F-37 basket is described in detail in Appendix 6.B of this chapter, and implements an actinides-only approach, i.e. neglects the effect of fission products;

- The ability of the cask to prevent water inleakage under accident conditions. As a result of this characteristic, any potential reconfiguration of high burnup fuel under accident condition would be inconsequential from a criticality perspective; and

- The cask is equipped with a double lid system. The additional lid provides additional assurance that water will not enter the containment system under accident conditions. The cask therefore remains dry and the reactivity is very low under any accident conditions. Any fuel reconfiguration under accident conditions would therefore have a negligible effect on the reactivity of the cask.

Applicable codes, standards, and regulations, or pertinent sections thereof, include the following:

- U.S. Code of Federal Regulations, “Packaging and Transportation of Radioactive Materials,” Title 10, Part 71.

- NUREG-1617, “Standard Review Plan for Transportation Packages for Spent Nuclear Fuel” USNRC, Washington D.C., March 2000.

- U.S. Code of Federal Regulations, “Prevention of Criticality in Fuel Storage and Handling," Title 10, Part 50, Appendix A, General Design Criterion 62.

- USNRC Standard Review Plan, NUREG-0800, Section 9.1.2, “New and Spent Fuel Storage”, Rev. 4, March 2007.

- USNRC Interim Staff Guidance 19 (ISG-19), Revision 0, “Moderator Exclusion under Hypothetical Accident Conditions and Demonstrating Subcriticality of Spent Fuel under the Requirements of 10 CFR 71.55(e)”.

- USNRC Interim Staff Guidance - 8 (ISG-8), Revision 3, “Burnup Credit in the Criticality Safety Analyses of PWR Spent Fuel in Transportation and Storage Casks”.

6.1.2 Summary Table of Criticality Evaluations

The principal calculational results address the following conditions:

- A single package, under the conditions of 10 CFR 71.55(b), (d), and (e);
- An array of undamaged packages, under the conditions of 10 CFR 71.59(a)(1); and
- An array of damaged packages, under the conditions of 10 CFR 71.59(a)(2)

Results are summarized in Table 6.1.1 for the most reactive configurations and fuel condition. The table contains the maximum k_{eff}, and the uncertainty for each case. The results are conservatively evaluated for the worst combination of manufacturing tolerances (as identified in Section 6.3), and including the calculational bias, uncertainties, and calculational statistics. For package arrays, an infinite number of packages are analyzed. The maximum k_{eff} value for all cases is below the limit of 0.95 recommended in NUREG-1617 (for misload conditions, the limit is 0.98 based on ISG-8, rev 3, see Appendix 6.F). The results therefore demonstrate that the HI-STAR 180D Package is in full compliance with 10CFR71 (71.55(b), (d), and (e) and 71.59(a)(1) and (a)(2)). Table 6.1.2 presents the burnup requirement for the F-37 basket for the different loading configurations. Figure 7.D.2 in Appendix 7.D shows basket locations in the F-37 basket referenced in Table 6.1.2.

To assure the true reactivity will always be less than the calculated reactivity, the following conservative assumptions were made:

- The baskets are assumed to contain the most reactive fuel authorized to be loaded into a specific basket design.
- No credit is taken into account for the build-up of fission product neutron poisons.
- The criticality analyses assume up to 90% of the manufacturer's minimum Boron-10 content for the neutron absorber, with acceptance criteria as specified in Subsection 8.1.
- The maximum UO_2 effective pellet density (including uncertainty, dishes and chamfers) provided in Table 6.2.1 is used for the fuel stack density in all criticality analyses. Therefore, the actual fuel density will be less.
- For fresh fuel, no credit is taken for the ^{234}U and ^{236}U in the fuel.
- When flooded, the moderator is assumed to be water at a temperature corresponding to the highest reactivity within the expected operating range (i.e., water density of 1.000 g/cc).
- Neutron absorption in minor structural members is neglected.
- The worst hypothetical combination of tolerances (most conservative values within the range of acceptable values), as identified in Section 6.3, is assumed.
- When flooded, the fuel rod pellet-to-clad gap regions are assumed to be flooded.
- Regarding the position of assemblies in the basket, configurations with centered and eccentric positioning of assemblies in the fuel storage locations are considered.
- No credit is taken into account for poison material in the fuel assembly.
- No credit is taken into account for dissolved boron in the cask cavity or surrounding loading or storage area.
- The burnup credit methodology for the F-37 contains significant additional conservative assumptions specific to burnup credit, the most significant assumption is crediting only major

actinides, i.e. neglecting all fission products and minor actinides. See more details in Appendix 6.B.

6.1.3 Criticality Safety Index

The calculations for package arrays are performed for infinite arrays of HI-STAR 180D Packages under flooded conditions and results are below the NUREG-1617 limit of 0.95, i.e. N is infinite. Therefore, the criticality safety index (CSI) is zero (0.0).

Table 6.1.1
SUMMARY OF THE CRITICALITY RESULTS
TO DEMONSTRATE COMPLIANCE WITH 10CFR71.55 AND 10CFR71.59

F-32				
Configuration	% Internal Moderation	% External Moderation	Applicable Requirement	Maximum k_{eff}[2]
Single Package, unreflected	100%	0%	n/a	0.9213
Single Package, fully reflected	100%	100%	10CFR71.55 (b) and (d)	0.9219
Containment, fully reflected	100%	100%		0.9211
Single Package, Damaged	0%	100%	10CFR71.55 (e)	0.3721
Infinite Array of Undamaged Packages	0%	0%	10CFR71.59 (a)(1)	0.3821
Infinite Array of Damaged Packages	0%	100%	10CFR71.59 (a)(2)	0.3759

F-37[1]				
Configuration	% Internal Moderation	% External Moderation	Applicable Requirement	Maximum k_{eff}[2]
Single Package, unreflected	100%	0%	n/a	0.9413
Single Package, fully reflected	100%	100%	10CFR71.55 (b) and (d)	0.9411
Containment, fully reflected	100%	100%		0.9407
Single Package, Damaged	0%	100%	10CFR71.55 (e)	0.3725
Infinite Array of Undamaged Packages	0%	0%	10CFR71.59 (a)(1)	0.3814
Infinite Array of Damaged Packages	0%	100%	10CFR71.59 (a)(2)	0.3758

Note:
1 The results of Configuration 1 described in Table 6.1.2 are presented.
2 The maximum k_{eff} is equal to the sum of the calculated k_{eff}, three standard deviations, the code bias, and the uncertainty in the code bias. For all cases, the standard deviation is from 0.0001 to 0.0003. The combined bias and bias uncertainty is 0.0056 for the F-32, and 0.0198 for the F-37.

Table 6.1.2

Burnup Requirements for UO_2 fuel the F-37 Basket

Configuration	Fresh UO_2 Fuel[1]	Spent UO_2 Fuel	
	Region (see Figure 7.D.2)	Region (see Figure 7.D.2)	Minimum Assembly Burnup for UO_2 Assemblies with an Initial Enrichment up to 4.55 wt% ^{235}U. (GWd/mtU)
1	-	1,2,3,4,5,6,7,8,9	See Table 7.D.6
2	5	1,2,3,4,6,7,8,9	See Table 7.D.6

Note:
1. Maximum permissible initial enrichment of fresh UO_2 fuel is 4.55 wt% ^{235}U.

6.2 FISSILE MATERIAL CONTENT

6.2.1 General

The HI-STAR 180D contains up to 37 fuel assemblies. The maximum amount of uranium is about 275 kg per assembly. The maximum amount of uranium per cask is therefore about 10.2 t (metric). The nominal UO_2 pellet density is 10.55 g/cm^3. The maximum enrichment including uncertainty of UO_2 fuel is 4.55 wt% ^{235}U. All fuel is in solid metal oxide form and is dry.

6.2.2 Fuel Parameters

The various fuel assemblies to be qualified all have similar principal characteristics, such as array size and number of fuel rods and guide tubes, which are listed in Table 6.2.1. However, they may differ in some of the details, such as fuel rod and guide tube dimensions. Previous studies [6.2.1] have shown that the bounding conditions correspond to:

- Maximum Active Length;
- Maximum Pellet OD;
- Maximum Clad ID;
- Minimum Clad OD / Thickness;
- Minimum Guide Tube Thickness; and
- Minimum Instrument Tube Thickness.

These bounding dimensions are listed in Table 6.2.1. To show that small variations in the parameters are bounded by the dimensions listed in Table 6.2.1, various dimensional variations are analyzed. The analyzed cases, together with the calculated k_{eff} for the F-37 and the F-32 basket are listed in Table 6.2.2. The results show that the reference case has larger or statistically equivalent results in comparison to other cases. Consistent with previous work, the dimensions from the reference case are used in all further analyses. All calculations in Table 6.2.2 were performed for UO_2 fuel with an initial enrichment of 4.55 wt%. For the results for the F-37 basket, a burnup of 15 GWd/mtU is used (see Appendix 6.B). For the calculations with burned fuel in the F-37 basket, both the depletion and criticality calculations use the modified fuel parameters in each case.

TABLE 6.2.1

FUEL CHARACTERISTICS

Parameter	Value
Fuel Rod Array	14 x14
Number of Fuel Rods	179
Number of Guide Tubes and Instrument Tubes	17
Active Length (Max)	242.8 cm
Clad Material	Zr-based (Zr4)
Guide and Instrument Tube Material	Zr-based (Zr4)
Pellet OD (Max)	0.9344 cm
Clad Thickness (Min)	0.057 cm
Clad OD (Min)	1.068 cm
Guide Tube Thickness (Min)	0.036 cm
Instrument Tube Thickness (Min)	0.0525 cm
Rod Pitch (Nom)	1.412 cm
^{235}U Enrichment (Max)	4.55 wt%
Effective UO_2 Pellet Density (Max)	10.66 g/cm^3

TABLE 6.2.2
REACTIVITY EFFECT OF VARIATIONS IN FUEL DIMENSIONS
(all dimensions are in centimeters)

Variation	Pellet OD	Clad ID	Clad Thickness	Clad OD	Guide Tube Thickness	Instrument Tube Thickness	F-32 Basket 4.55 wt% Enrichment		F-37 Basket, 4.55 wt% Enrichment 15 GWD/MtU	
							Calculated k_{eff}	Difference to Reference	Calculated k_{eff}	Difference to Reference
Reference	0.9344 (max)	0.954	0.057 (min)	1.068 (min)	0.036 (min)	0.0525 (min)	0.9148	-	0.9206	-
1	**0.908 (min)**	**0.928**	**0.07**	1.068	0.036	0.0525	0.9101	-0.0047	0.9139	-0.0067
2	0.9344	**0.968 (max)**	0.057	**1.082 (max)**	0.036	0.0525	0.9144	-0.0004	0.9201	-0.0005
3	**0.908**	**0.9172**	**0.0824 (max)**	**1.082**	0.036	0.0525	0.8988	-0.0160	0.9046	-0.0160
4	0.9344	0.954	0.057	1.068	0.036	**0.0635 (max)**	0.9154	0.0006	0.9208	0.0002
5	0.9344	0.954	0.057	1.068	**0.053 (max)**	0.0525	0.9136	-0.0012	0.9188	-0.0018
6	0.908	**0.948**	**0.062**	**1.072**	**0.043**	0.0525	0.9150	0.0002	0.9187	-0.0019

Note:
1. The standard deviation (σ) of the calculations is about 0.0003.

6.3 GENERAL CONSIDERATIONS

In compliance with the requirements of 10CFR71.31(a)(1), 10CFR71.33(a)(5), and 10CFR71.33(b), this section provides a description of the HI-STAR 180D in sufficient detail to identify the package accurately and provide a sufficient basis for the evaluation of the package.

6.3.1 Model Configuration

Figures 6.3.1 through 6.3.4 show representative cross sections of the criticality models for the two baskets. Figure 6.3.1 shows a single cell from the basket. The cells are identical for both baskets, except for the width of the flux trap. Figures 6.3.2 and 6.3.3 show the entire F-32 and F-37 basket, respectively. Figure 6.3.4 shows a sketch of the calculational model in the axial direction.

Full three-dimensional calculations were used, assuming the axial configuration shown in Figure 6.3.4, and conservatively neglecting the absorption in the cask neutron shielding material (Holtite). Although the neutron absorber integral to the cell walls cover the full basket length, which is much longer than the active fuel length, they are assumed to only cover the active fuel length in the calculations.

The calculational model explicitly defines the fuel rods and cladding, the guide tubes, the water gaps and neutron absorber walls of the basket cells. Under normal conditions of transport, when the cask is dry, the resultant reactivity with the design basis fuel is very low (k_{eff} < 0.5). For the flooded condition, water was also assumed to be present in the fuel rod pellet-to-clad gap regions (see Subsection 6.3.4.3).

The basket geometry can vary due to manufacturing tolerances and due to potential deflections of basket walls as the result of accident conditions. The basket tolerances are defined on the drawings in Chapter 1. The structural acceptance criteria for the basket during accident conditions is that the permanent deflection of the basket panels is limited to 0.5 mm on average (see Table 2.7.9 in Chapter 2). The analyses in Chapter 2 demonstrate that permanent deformations of the basket walls during accident conditions are far below this limit. In fact, the analyses show that the vast majority of the basket panels remain elastic during and after the accident, and therefore show no permanent deflection whatsoever, and that any deformation is limited to small localized areas. Nevertheless, it is conservatively assumed that 2 adjacent cell walls in each cell are deflected to the maximum extent possible over their entire length and width, i.e. that the cell ID is increased or reduced by 0.5 mm. Similarly, it is assumed for all flux traps that their thickness is reduced by 0.5 mm. Stated differently, the tolerances were increased by 0.5 mm to account for the potential deflections of basket walls during accident conditions. MCNP5 was used to determine the manufacturing tolerances and deflections that produced the most adverse effect on criticality. After the reactivity effect (positive effect with an increase in reactivity; or negative effect with a decrease in reactivity) of the manufacturing tolerances was determined, the criticality analyses were performed using the worst case conditions in the direction which would increase reactivity. For simplification, the same worst case conditions are used for both normal and accident conditions. An evaluation of the various possible dimensional combinations was performed using MCNP5, with fuel assemblies centered in the fuel storage locations. Calculated k_{eff} results (which do not include the bias, uncertainties, or calculational statistics), along with the selected dimensions, for a number of dimensional combinations are shown in Table 6.3.1 for both baskets. The cell ID is evaluated for minimum, nominal and maximum values. The wall thickness and flux trap width are evaluated for nominal and minimum values. Note that the calculations of the F-37 basket were performed with spent fuel at an enrichment of 4.55 wt% and burnup of 15 GWD/MtU, which are based on the burnup requirement of Configuration 1 listed in Table 6.1.2.

Based on the calculations, the conservative dimensional assumptions listed in Table 6.3.2 were determined for the basket designs. Because the reactivity effect (positive or negative) of the manufacturing tolerances is not assembly dependent, these dimensional assumptions were employed for all criticality analyses.

The basket is manufactured from individual slotted panels. The panels are expected to be in direct contact with each other (see Drawings in Chapter 1). However, to show that small gaps between panels would have essentially no effect on criticality, calculations are performed with a postulated 2 mm gap between panels, repeated in the axial direction every 270 mm. These calculations were performed for all cases in Table 6.1.1 with full water density, assuming the 2 mm gap in all panels. Cases with no water were not evaluated, since under this condition the METAMIC is largely ineffective and the reactivity is very low. The results are summarized in Tables 6.3.15, where the calculated k_{eff} are compared between the cases with and without the gap. For the calculated k_{eff} values, the table also shows the average difference for both the F-32 and F-37 basket. The results indicate that there is no significant reactivity effect when the gap is considered, given that the uncertainty of each calculated k_{eff} difference at a 95/95 level is about 0.0008 delta-k, i.e. more than two times the average difference of about 0.0003 delta-k. Therefore, since the METAMIC gap has an insignificant effect, all further calculations are performed without any gaps.

Variations of other parameters, namely fuel density and water temperature in the cask, were analyzed using CASMO-5. The results are presented in Table 6.3.3, and show that the maximum fuel density and the minimum water temperature (corresponding to a maximum water density) are bounding. These conditions are therefore used in all further calculations.

Calculations documented in Chapter 2 show that the baskets stay within the applicable structural limits during all normal and accident conditions. Furthermore, the neutron poison material is an integral and non-removable part of the basket material, and its presence is therefore not affected by the accident conditions. Except for the potential deflection of the basket walls that is already considered in the criticality models, damage to the cask under accident conditions is limited to damage to the neutron absorber on the outside of the cask. However, this external absorber is already neglected in the calculational models. Other parameters important to criticality safety are fuel burnup and enrichment, which are not affected by the hypothetical accident conditions. The calculational models of the cask and basket for the accident conditions are therefore identical to the models for normal conditions, and no separate models need to be developed for accident conditions.

There are, however, differences between the normal and accident models in terms of internal and external water density and external reflections. The effect of these conditions is discussed in Section 6.3.4.

Additionally, studies are performed to evaluate the potential effect of fuel reconfiguration during accident conditions. These are presented in Section 6.3.5.

6.3.2 Material Properties

Composition of the various components of the principal designs of the HI-STAR 180D Package is listed in Table 6.3.4. In this table only the composition of fresh fuel is listed. For a discussion on the composition of spent fuel for burnup credit see Appendix 6.B.

The HI-STAR 180D is designed such that the fixed neutron absorber will remain effective for a period greater than 60 years, and there are no credible means to lose it. A detailed physical description, historical applications, unique characteristics, service experience, and manufacturing quality assurance of the fixed neutron absorber are provided in Subsection 1.2.1.6.

The continued efficacy of the fixed neutron absorber is assured by acceptance testing, documented in Subsection 8.1.5.4, to validate the ^{10}B (poison) concentration in the fixed neutron absorber. In addition, based on calculations prepared for a similar cask model, the fraction of ^{10}B atoms destroyed during the service life in the fixed neutron absorber by neutron absorption is negligible (less than 10^{-6}). Therefore, there is no need to provide a surveillance or monitoring program to verify the continued efficacy of the neutron absorber.

The only materials affected by the accident conditions are the Holtite neutron absorber on the outside of the cask, and the impact limiters. None of these materials are considered in the criticality model. Therefore, material properties of the materials used in the criticality analyses are not affected by the accidents.

6.3.3 Computer Codes and Cross Section Libraries

MCNP5-1.51 and CASMO-5 Version 2.00.00 are used for the criticality analyses of the HI-STAR 180D Cask for the packaging and transportation of radioactive materials. Both codes were installed and validated on the Holtec International's computer following the documentations provided by the code developers.

The principal code for the criticality analysis is the general three-dimensional continuous energy Monte Carlo N-Particle code MCNP5 [6.3.1] developed at the Los Alamos National Laboratory. MCNP5 was selected because it has been extensively used and verified and has all of the necessary features for this analysis. MCNP5 design basis calculations used continuous energy cross-section data, based on ENDF/B-VII, as distributed with the code.

The convergence of a Monte Carlo criticality problem is sensitive to the following parameters: (1) number of histories per cycle, (2) the number of cycles skipped before averaging, (3) the total number of cycles and (4) the initial source distribution. The MCNP5 criticality output contains a great deal of useful information that may be used to determine the acceptability of the problem convergence. Calculations used a minimum of 20,000 simulated histories per cycle, a minimum of 400 cycles were skipped before averaging, a minimum of 400 cycles were accumulated, and the initial source was specified as uniform over the fueled regions (assemblies). Convergence is ensured by confirming that the source distribution converged using the Shannon entropy [6.3.1], as implemented in MCNP5. .

CASMO-5 [6.3.2 – 6.3.3] was used for determining some incremental reactivity effects (see Section 6.3.1). Although CASMO has been extensively benchmarked, these calculations are used only to establish direction of reactivity. This allows the MCNP5 calculational model to use the worst combination of tolerances. Additionally, CASMO-5 was used to determine the isotopic composition of spent fuel for burnup credit in the HI-STAR 180D (see Appendix 6.B).

6.3.4 Demonstration of Maximum Reactivity

6.3.4.1 Internal and External Moderation

The regulations in 10CFR71.55 include the requirement that the package remains subcritical when assuming moderation to the most reactive credible extent. The regulations in 10CFR71.59 require subcriticality for package arrays under different moderation conditions. Subsections 6.3.4.1.1 through 6.3.4.4 present various studies to confirm or identify the most reactive configuration or moderation condition. Specifically, the following conditions are analyzed:

- Reduced internal and external water density for single packages (6.3.4.1.1) and package arrays (6.3.4.1.2);
- Variation in package to package distance in package arrays (6.3.4.1.2);
- Partial internal flooding of package (6.3.4.2);
- Flooding of pellet to cladding gap of the fuel rods (6.3.4.3); and
- Preferential flooding, i.e. uneven flooding inside the package, (6.3.4.4).

The calculations that specifically demonstrate compliance with the individual requirements of 10CFR71.55 and 10CFR71.59 are presented in Sections 6.4 through 6.6.

Regarding the effect of low moderator density it is noted that with a neutron absorber present (i.e., the neutron poison integral to the walls of the storage compartments), the phenomenon of a peak in reactivity at a hypothetical low moderator density (sometimes called "optimum" moderation) does not occur to any significant extent. In a definitive study, Cano, et al. [6.3.4] has demonstrated that the phenomenon of a peak in reactivity at low moderator densities does not occur when strong neutron absorbing material is present or in the absence of large water spaces between fuel assemblies. Nevertheless, calculations for a single reflected cask and for infinite arrays of casks were made to confirm that the phenomenon does not occur with low density water inside or outside the HI-STAR 180D.

As discussed in Chapter 2, the cask is designed so that water inleakage under accident conditions is not considered credible. The main purpose of this design characteristic is to ensure that any potential reconfiguration of high burnup fuel under accident conditions is inconsequential from a criticality perspective. The calculations to demonstrate compliance with 10CFR71.55 and 10CFR71.59 under accident conditions are therefore performed with an internally dry cask. Nevertheless, the studies performed in the following subsections that determine the optimum moderation conditions still conservatively consider internal water moderation under accident conditions.

The behavior of the package under different internal moderation conditions is predominantly a function of the neutron poison and its distribution, and of the fuel and basket geometry, which determines the distribution of the water in the cask. These aspects are essentially identical between the F-37 and the F-32 basket. Specifically,

- Both baskets use the same neutron poison material in the basket, with the same wall thickness and neutron poison loading in the basket walls.
- Both baskets use the same cell dimensions, and contain fuel with identical dimensions. The amount of water in and directly around each fuel assembly in each cell is therefore identical between the two baskets.
- Both baskets use flux traps, only with differences in the thickness and number of flux traps.

Most studies with different moderator densities are therefore only performed for the F-32 basket, and the conclusions are directly applicable to both baskets. Exceptions are calculations for partial flooding of the cask, where calculations for both F-32 and F-37 are performed.

6.3.4.1.1 Single Package Evaluation

The calculational model for a single package consists of the HI-STAR Cask surrounded by a hexagonal box filled with water. The neutron absorber on the outside of the HI-STAR is neglected, since it might be damaged under accident conditions, and since it is conservative to replace the neutron absorber (Holtite) with a neutron reflector (water). The minimum water thickness on each side of the cask is 30 cm, which effectively represents full water reflection. The outer surfaces of the surrounding box are conservatively set to be fully reflective, which effectively models a three dimensional array of casks with a minimum surface to surface distance of 60 cm. The calculations with internal and external moderators of various densities are shown in Table 6.3.6. For comparison purposes, a calculation for a single, unreflected cask (Case 1) is also included in Table 6.3.6. At 100% external moderator density, Case 2 corresponds to a single, fully-flooded cask, fully reflected by water. Figure 6.3.5 plots calculated k_{eff} values as a function of internal moderator density for 100% external moderator density (i.e., full water reflection).

Results listed in Table 6.3.6 and plotted in Figure 6.3.5 support the following conclusions:

- The calculated k_{eff} for a fully-flooded cask is independent of the external moderator (the small variations in the listed values are due to statistical uncertainties which are inherent to the calculational method (Monte Carlo)); and

- Reducing the internal moderation results in a monotonic reduction in reactivity, with no evidence of any optimum moderation. Thus, the fully flooded condition corresponds to the highest reactivity, and the phenomenon of optimum low-density moderation does not occur and is not applicable to the HI-STAR 180D.

6.3.4.1.2 Evaluation of Package Arrays

In terms of reactivity, the normal conditions of transport (i.e., no internal or external moderation) are bounded by the hypothetical accident conditions of transport. Therefore, the calculations in this section evaluate arrays of HI-STAR 180D Packages under hypothetical accident conditions (i.e., internal and external moderation by water to the most reactive credible extent and no neutron shield present).

In accordance with 10CFR71.59 requirements, calculations were performed to simulate an infinite three-dimensional square array of internally fully-flooded (highest reactivity) casks with varying cask spacing and external moderation density. The maximum k_{eff} results of these calculations are listed in Table 6.3.7 and confirm that the individual casks in a square-pitched array are independent of external moderation and cask spacing.

To further investigate the reactivity effects of array configurations, calculations were also performed to simulate an infinite three-dimensional hexagonal (triangular-pitched) array of internally fully-flooded (highest reactivity) casks with varying cask spacing and external moderation density. The maximum k_{eff} results of these calculations are listed in Table 6.3.8 and confirm that the individual casks in a hexagonal (triangular pitched) array are effectively independent of external moderation and cask spacing.

To assure that internal moderation does not result in increased reactivity, hexagonal array calculations were also performed for 10% internal moderator with 10% and 100% external moderation for varying cask spacing. Maximum k_{eff} results are summarized in Table 6.3.9 and confirm the very low values of k_{eff} for low values of internal moderation.

The results presented thus far indicate that neutronic interaction between casks is not enhanced by the neighboring casks, or the water between the neighboring casks, and thus, the most reactive arrangement of casks corresponds to a tightly packed array with the cask surfaces touching. Therefore, calculations were performed for an infinite hexagonal (triangular pitched) array of touching casks (neglecting the Holtite neutron shield). These calculations were performed for the internally flooded (highest reactivity) and internally dry conditions, with and without external flooding. The results of these calculations are listed in Table 6.3.10. In all cases, the maximum k_{eff}

values are shown to be in close agreement to that of a single, internally flooded, unreflected cask and are below the NUREG-1617 limit of 0.95.

The calculations demonstrate that the thick steel wall of the overpack is more than sufficient to preclude neutron coupling between casks, consistent with the findings of Cano, et al [6.3.4]. Neglecting the Holtite neutron shielding in the calculational model provides further assurance of conservatism in the calculations.

6.3.4.2 Partial Flooding

To demonstrate that the HI-STAR 180D would remain subcritical if water were to leak into the containment system, as required by 10CFR71.55, calculations in this section address partial flooding in the HI-STAR 180D and demonstrate that the fully flooded condition is the most reactive.

The reactivity changes during the flooding process were evaluated for the F-32 in both the vertical and horizontal positions. For these calculations, the cask is partially filled (at various levels) with full density (1.0 g/cm^3) water and the remainder of the cask is filled with steam consisting of ordinary water at partial density (0.002 g/cm^3). Results of these calculations are shown in Table 6.3.11.

Additional calculations are performed for the F-37, with burned fuel in the cask, and the cask in the vertical orientation. The burned fuel is modeled with the bounding axial burnup distribution (see Appendix 6.B, Section 6.B.4.1). This is to address potential concerns that the lower burned end sections of the fuel could have a noticeable effect on the maximum k_{eff} value. The calculations are based on configuration 1 (see Table 6.1.2). The water level is set to multiples of the axial burnup profile segment, consistent with the discretization of the axial burnup profile listed in Table 6.B.7 of Appendix 6.B, and calculations are performed from 2.38 cm to 121.4 cm covered with water. The results are presented in Table 6.3.16. The table also shows the reference case with the fully flooded cask.

In all cases, for both the F-32 and F-37, the reactivity increases monotonically as the water level rises, confirming that the most reactive condition is fully flooded. The fully flooded case therefore represents the bounding condition for all basket types.

6.3.4.3 Clad Gap Flooding

The reactivity effect of flooding the fuel rod pellet-to-clad gap regions, in the fully flooded condition, has been investigated. Table 6.3.12 presents maximum k_{eff} values that demonstrate the positive reactivity effect associated with flooding the pellet-to-clad gap regions. These results confirm that it is conservative to assume that the pellet-to-clad gap regions are flooded. For all cases that involve flooding, the pellet-to-clad gap regions are assumed to be flooded.

6.3.4.4 Preferential Flooding

Preferential flooding of the baskets is not possible because flow holes are present on all four walls of each basket cell and on the two flux trap walls at both the top and bottom of the basket. The flow holes are sized to ensure that crud deposits cannot block them. Therefore, the basket cannot be preferentially flooded.

6.3.4.5 Eccentric Positioning of Assemblies in Fuel Storage Cells

In this subsection, studies are presented to determine the reactivity effect of eccentric positioning of fuel assemblies in the fuel storage cells, and the conditions with the highest maximum k_{eff} are identified.

To conservatively account for eccentric fuel positioning in the fuel storage cells, three different configurations are analyzed, and the results are compared to determine the bounding configuration:

- Cell Center Configuration: All assemblies centered in their fuel storage cell;
- Basket Center Configuration: All assemblies in the basket are moved as closely to the center of the basket as permitted by the basket geometry; and
- Basket Periphery Configuration: All assemblies in the basket are moved furthest away from the basket center, and as closely to the periphery of the basket as possible.

The results are presented in Table 6.3.5. The table shows the maximum k_{eff} value for centered and the two eccentric configurations for each condition, and the difference in k_{eff} between the centered and eccentric positioning. The results and conclusions are summarized as follows:

- For both the F-32 and F-37 basket, the cell centered configuration results in the highest reactivity.

Therefore, all further calculations, including those that demonstrate compliance with 10CFR71 requirements, are performed with assemblies centered in the basket cells.

6.3.5 Potential Fuel Reconfiguration

6.3.5.1 Potential Fuel Reconfiguration under Accident Conditions

The cask is designed to remain internally dry under any accident conditions. Therefore, any fuel reconfiguration under accident conditions would be of no consequences. Additionally, the evaluation of the fuel performance under accident conditions presented in Chapter 2 indicate that no fuel damage, and hence no fuel reconfiguration would be expected, even for high burnup fuel. Nevertheless, as a defense-in-depth, analyses are performed assuming coinciding fuel reconfiguration and flooding of the cask, as mentioned in Chapter 1, Section 1.4.

Due to uncertainties of the cladding material properties after irradiation for high burnup fuel, there is the concern of cladding failures of such fuel under transport accident conditions. However, the fuel rods are supported by the grid spacers at regular distances along the length of the assembly. These will limit the extent and location of any clad damage. For a side drop, the most likely failure would be from shear loads, where the rod would break right next to the grid spacers, resulting in rod segments about the length of the grid spacer distance. These segments are confined to the assembly section between the grid straps. For an end drop, rods could fail from buckling loads near the dropped end. This could lead to rod segments that are again confined to the spaces between the grid straps. More substantial relocation of rod segments is not expected, since this would require a failure of the entire assembly structure, which is not expected under the loads in a transport accident. Rods breaking into smaller pieces is also not expected, since once the rod is broken, the inner pressure is relieved, which reduces the clad stresses. Also, significant losses of fuel pellets from rods are not expected, since the gap between fuel pellet and clad is typically closed in spent fuel due to the expansion of the fuel pellets during irradiation. To model the discussed credible damage to fuel rods, and show the potential reactivity effect of such damages, the following models are used:

- To model the behavior of larger broken rod segments, all rods in the assemblies are moved randomly by a certain distance within the array. The distance is chosen so that neighboring rods are able to touch each other. 10 different calculations were performed with different random locations of the rods. Results of the calculations are listed in Table 6.3.13. On average for the ten calculations, the reactivity is reduced by 0.0008 delta-k compared to the reference case. Only three of the 10 calculations show an increase of the reactivity compared to the reference case, and the differences are all within 3 standard deviations from the reference case. This shows that this type of assembly damage has a negligible effect on the reactivity of the package.

- To model the behavior of smaller rod segments, it is assumed that within the space between two grid straps, rods from the upper section fall into the lower section. This reduces the fuel amount in the upper section, while at the same time increasing the fuel amount in the lower section. The total fuel amount remains unchanged. This is modeled by dividing the active zone of each assembly into 5 axial sections, each with a length of about 486 mm. Each section is then again subdivided in an upper and lower section of 243 mm length. The fuel in each upper section is reduced by replacing selected rods with water, while the fuel in each lower section is increased by replacing water rods with fuel rods. Four configurations are analyzed, with 4, 8, 12 and 17 rods relocated between the sections. Results of the calculations are listed in Table 6.3.14. The maximum difference of all four cases is 0.0021 delta-k from the reference case. However, results listed in Table 6.1.1 show that the remaining safety margin to the NUREG-1617 limit of 0.95 is about 0.0280 delta-k for F-32 basket and around 0.0090 delta-k for F-37 basket, with further additional margins for the F-37 basket based on conservative assumptions of the burnup credit methodology discussed in Appendix 6.B. Therefore, the reactivity effect of local relocation of fuel rod segments is still small compared to the safety margin and does not have a significant impact.

- To model a situation where rods bend but not break under an axial impact, a study is performed assuming the so-called “bird caging” condition. In this condition it is assumed that within the space between any two grid straps, the rod array in the upper section is expanded, while in the lower section the array is compressed. The fuel amount remains unchanged in both the upper and lower sections. Similar to the cases listed in Table 6.3.14, this is modeled by dividing the active zone of each assembly into 5 axial sections, each with a length of about 486 mm. Each section is then again subdivided in an upper and lower section of 243 mm length. Results of the calculations are listed in Table 6.3.17. Results show that the reactivity remain unchanged in comparison to the reference case, which further indicate that the fuel reconfiguration does not have significant impact on the reactivity of the package.

- Additionally, to supplement and enhance the defense in depth evaluation of the fuel reconfiguration, the safety case for a new type of fuel assembly deformation [6.3.5] (referred herein as the second “bird caging” scenario) is documented. Specifically, since there are 5 grid spacers along the active fuel, the active length is divided into 4 segments, conservatively assuming that 25% of the fuel is located within the lowest inter-grid zone. It is expected that the maximum possible expansion of the rod array within a basket cell results in a maximum increase of the reactivity, because the fuel assembly is undermoderated. Nevertheless, three cases with various expansion of the rod array in the lowest inter-grid zone (1.6%, 4.8% and 8.0% increase of the fuel rod pitch) are considered to prove that the maximum possible expansion is bounding. The rod array in the rest of the fuel assembly remains undamaged. The modelling is therefore consistent with [6.3.5].

  The reactivity effect of the second “bird caging” scenario is analyzed for both the F-32 and F-37 fuel baskets. The F-32 basket is loaded with fresh UO_2 fuel with an initial enrichment of 4.55 wt%, while the F-37 basket is loaded with spent UO_2 fuel assemblies in Configuration 1 with an initial enrichment of 4.55 wt% and fuel burnup of 15 GWd/mtU (see Table 7.D.6). The uniform, artificial and the plant-specific axial burnup profiles (see Table 6.B.7) are considered for spent fuel in the F-37 basket. The results of the calculations are presented in Table 6.3.20 and Table 6.3.21 for F-32 and F-37 fuel basket, respectively.

  The results show that the second “bird caging” condition increases the reactivity both in the F-32 and in the F-37 basket. Since there is large margin in the F-32 basket, the reactivity of the cask with the postulated bird caging condition is still below the USNRC NUREG-1617 limit of 0.95. The reactivity in the F-37 basket exceeds the limit of 0.95 but it is still below the limit of 0.98 specified in ISG-8, rev 3, which is often used as a limit for the accident conditions. Note that the cask is designed to remain dry under any accident conditions, so any fuel reconfiguration would be of no consequences. Also, there are a few conservative assumptions, such as actinide-only burnup credit, conservative artificial axial profile and relatively small burnup for the postulated fuel reconfiguration. The concerns about fuel damage are principally related to high burnup fuel (HBF) defined as fuel with an assembly average burnup of about 45 GWd/mtU or more. To justify that the available criticality safety margin more than offsets the reactivity increase due to the second “bird caging” scenario, a supplementary calculation for the F-37 fuel basket has been performed assuming coinciding flooding of the cask and the second “bird caging” condition, but with the credit of all isotopes (all actinides and fission product) from the CASMO-5 depletion calculations. The results, presented in Table 6.3.22, show that the reactivity is well below the limit of 0.95.

Further it is important to recognize that the concerns about fuel damage are principally related to high burnup fuel (HBF). The burnup requirements for the 37 assembly basket are much lower, no more than 18 GWd/mtU, which creates additional margin for the fuel of concern. To estimate this margin, additional calculations are performed for fuel with a burnup of 45 GWd/mtU. Results are presented in Table 6.3.18 and show that the maximum k_{eff} is only about 0.85 for Configuration 1 and 0.88 for Configuration 2, compared to a design basis value of about 0.94.

In summary, the evaluations show that even if fuel damage as a result of accident conditions is postulated, the maximum k_{eff} would remain well below the NUREG-1617 limit.

6.3.5.2 Potential Fuel Reconfiguration under Normal Conditions

In Chapter 2, fuel performance was also evaluated under normal conditions of loading, transport and unloading, and it is concluded that no damage to the fuel is expected under those conditions, and hence no effect on the maximum k_{eff} of the system. Nevertheless, the evaluations performed for the accident conditions discussed in the previous subsection can also be used here as additional defense-in-depth, since all those evaluations were performed under fully flooded conditions, i.e. consistent with normal conditions. Based on this, if there would be any fuel damage under normal condition, the effect on the maximum k_{eff} would also be negligible, and the maximum k_{eff} would also remain well below the NUREG-1617 limit of 0.95.

6.3.6 Partial Loading

Each basket cell is completely surrounded by the basket walls containing neutron absorber material (B_4C). Under a partial loading situation, i.e. where one or more basket location are not occupied with fuel, the amount of fissile material is obviously reduced. Also, under the bounding condition of a fully flooded cask, the amount of water is increased. This will result in an increased moderation of neutrons in the empty cell locations. This increased moderation will increase the effectiveness of the surrounding thermal neutron absorber. Described differently, the now empty cell locations will act as additional flux traps. Therefore, due to the reduced amount of fissile material, and the increased neutron absorption, the reactivity of the package under partial loading conditions will be reduced, and will always be bound by the fully loaded conditions. No further evaluations of this condition are therefore necessary.

6.3.7 Evaluation of the Basket Shim Design

The design basis calculations are performed with aluminum basket shims, while the drawings in Chapter 1 show the basket shim as a compound, with the center section made of aluminum, and top and bottom sections, made of stainless steel. Additionally, the design basis model for F-32 basket has basket shims with an opening of about 4.7 cm, while the drawing shows an opening of 10 cm. The impact of these simplifications on reactivity are expected to be minor, since the maximum multiplication factor is dominated by the axial center of the basket that is relatively far from the top and bottom ends of the basket. To determine the reactivity effect of the steel in the basket shim, studies are performed for both the F-32 and F-37 baskets, assuming that the top and bottom 40 cm of the active length in the basket shim is changed to steel. This is a conservative approach since the assumed length of steel along the active fuel region is larger than the steel length from the drawing in Chapter 1. Additionally, basket shim openings of 10 cm were considered for F-32 basket. The results of the calculations are listed in Table 6.3.19 and show that the differences are below two times the standard deviation, indicating that the results are statistically equivalent. Therefore, the considered simplifications as well as the design basis calculations are acceptable.

Table 6.3.1

MCNP5 EVALUATION OF BASKET TOLERANCES AND DEFLECTIONS

Cell ID	**Cell Wall Thickness**	**Flux Trap**	**MCNP5 Calculated k_{eff}**
F-32, 4.55 wt%			
nominal (206 mm)	nominal (15 mm)	nominal (32 mm)	0.9085
nominal (206 mm)	minimum (14.5 mm)	nominal (32 mm)	0.9092
nominal (206 mm)	nominal (15 mm)	minimum (30.5 mm)	0.9102
maximum (208.5 mm)	minimum (14.5 mm)	minimum (30.5 mm)	**0.9148**
nominal (206 mm)	minimum (14.5 mm)	minimum (30.5 mm)	0.9121
minimum (203.5 mm)	minimum (14.5 mm)	minimum (30.5 mm)	0.9082
F-37, 4.55 wt%, 15 GWD/MtU			
nominal (206 mm)	nominal (15 mm)	nominal (28 mm)	0.9161
nominal (206 mm)	minimum (14.5 mm)	nominal (28 mm)	0.9178
nominal (206 mm)	nominal (15 mm)	minimum (26.5 mm)	0.9183
maximum (208.5 mm)	minimum (14.5 mm)	minimum (26.5 mm)	**0.9206**
nominal (206 mm)	minimum (14.5 mm)	minimum (26.5 mm)	0.9199
minimum (203.5 mm)	minimum (14.5 mm)	minimum (26.5 mm)	0.9187

Table 6.3.2

BASKET DIMENSIONAL ASSUMPTIONS

Basket Type	Cell ID	Cell Wall Thickness	Flux Trap
F-32	Maximum (208.5 mm)	Minimum (14.5 mm)	Minimum (30.5 mm)
F-37	Maximum (208.5 mm)	Minimum (14.5 mm)	Minimum (26.5 mm)

Table 6.3.3

CASMO-5 CALCULATIONS FOR EFFECT OF TOLERANCES AND TEMPERATURE

Changes in Parameters	Δk Maximum Tolerance F-32	Action/Modeling Assumption
Change UO_2 Density Nominal UO_2 Density	Ref. -0.0014	Assume max UO_2 density
Increase in Temperature 20°C 40°C 70°C 100°C	 Ref. -0.0034 -0.0102 -0.0188	Assume 20°C
10% Void in Moderator 20°C with no void 20°C 100°C	 Ref. -0.0413 -0.0597	Assume no void

Table 6.3.4

COMPOSITION OF THE MAJOR COMPONENTS OF THE HI-STAR 180D PACKAGE

HI-STAR 180D		
UO_2 4.55% ENRICHMENT, DENSITY 10.66 g/cm^3		
Nuclide	**Atom Fraction**	**Wt. Fraction**
^{16}O	6.6662E-01	1.185E-01
^{235}U	1.5355E-02	4.011E-02
^{238}U	3.1803E-01	8.414E-01
COMMON MATERIALS		
ZR CLAD, DENSITY 6.550 g/cm^3		
Nuclide	**Atom Fraction**	**Wt. Fraction**
^{90}Zr	5.1450E-01	5.0706E-01
^{91}Zr	1.1220E-01	1.1181E-01
^{92}Zr	1.7150E-01	1.7278E-01
^{94}Zr	1.7380E-01	1.7891E-01
^{96}Zr	2.8000E-02	2.9438E-02
MODERATOR (H_2O), DENSITY 1.000 g/cm^3		
Nuclide	**Atom Fraction**	**Wt. Fraction**
^{1}H	6.6659E-01	1.1189E-01
^{2}H	7.6666E-05	2.5717E-05
^{16}O	3.3252E-01	8.8580E-01
^{17}O	8.1000E-04	2.2932E-03
ALUMINUM, DENSITY 2.7 g/cm^3		
Nuclide	**Atom Fraction**	**Wt. Fraction**
^{27}Al	1.0000E+00	1.0000E+00

Table 6.3.4 (continued)

COMPOSITION OF THE MAJOR COMPONENTS OF THE HI-STAR 180D PACKAGE

COMMON MATERIALS		
METAMIC DENSITY 2.6 g/cm^3, 9% B_4C		
Nuclide	**Atom Fraction**	**Wt. Fraction**
^{10}B	3.0741E-02	1.2888E-02
^{11}B	1.2484E-01	5.7546E-02
^{12}C	3.8906E-02	1.9566E-02
^{27}Al	8.0551E-01	9.1000E-01
STAINLESS STEEL, DENSITY 7.840 g/cm^3		
Nuclide	**Atom Fraction**	**Wt. Fraction**
^{50}Cr	8.7562E-03	7.9057E-03
^{52}Cr	1.6886E-01	1.5854E-01
^{53}Cr	1.9147E-02	1.8323E-02
^{54}Cr	4.7661E-03	4.6471E-03
^{55}Mn	2.0151E-02	2.0012E-02
^{54}Fe	3.9984E-02	3.8986E-02
^{56}Fe	6.2766E-01	6.3464E-01
^{57}Fe	1.4495E-02	1.4919E-02
^{58}Fe	1.9291E-03	2.0202E-03
^{58}Ni	6.4170E-02	6.7204E-02
^{60}Ni	2.4718E-02	2.6778E-02
^{61}Ni	1.0745E-03	1.1835E-03
^{62}Ni	3.4259E-03	3.8352E-03
^{64}Ni	8.7247E-04	1.0082E-03

Table 6.3.5

REACTIVITY EFFECTS OF ECCENTRIC POSITIONING OF CONTENT IN BASKET CELLS

Basket	**Content centered (Reference)**	**Content moved towards center of basket**		**Content moved towards basket periphery**		**Bounding Configuration**
	Calculated k_{eff}	**Calculated k_{eff}**	**k_{eff} Difference to Reference**	**Calculated k_{eff}**	**k_{eff} Difference to Reference**	
F-32	0.9148	0.9131	-0.0017	0.9113	-0.0035	Cell Centered
F-37	0.9206	0.9197	-0.0009	0.9163	-0.0043	Cell Centered

Table 6.3.6

MAXIMUM REACTIVITIES WITH REDUCED WATER DENSITIES FOR CASK ARRAYS

	Water Density		MCNP5 Results		
Case Number	Internal	External	HI-STAR 180D		
			Max. k_{eff}	1 σ	EALF (eV)
1	100%	single cask	0.9213	0.0003	0.3698
2	100%	100%	0.9219	0.0003	0.3688
3	100%	70%	0.9216	0.0003	0.3696
4	100%	50%	0.9216	0.0003	0.3698
5	100%	20%	0.9224	0.0003	0.369
6	100%	10%	0.9216	0.0003	0.3692
7	100%	5%	0.9221	0.0003	0.3692
8	100%	0%	0.9228	0.0003	0.3689
9	70%	0%	0.7963	0.0003	0.8918
10	50%	0%	0.6882	0.0002	2.6113
11	20%	0%	0.4938	0.0002	104.45
12	10%	0%	0.4369	0.0002	1236.7
13	5%	0%	0.4175	0.0001	6155
14	10%	100%	0.4318	0.0001	1361.3

Note:

1. This table is for an infinite hexagonal array of casks with 60 cm spacing between cask surfaces.
2. All values are maximum k_{eff} which include the bias, uncertainties, and calculational statistics, evaluated for the worst case combination of manufacturing tolerances.

Table 6.3.7

REACTIVITY EFFECTS OF SPACING AND EXTERNAL MODERATOR DENSITY FOR SQUARE ARRAYS OF HI-STAR 180D CASKS

Cask-to-Cask External Spacing (cm)					
External Moderator Density (%)	2	10	20	40	60
5	0.9219	0.9221	0.9222	0.9215	0.9216
10	0.9219	0.9218	0.9222	0.9220	0.9218
20	0.9220	0.9218	0.9220	0.9221	0.9224
50	0.9218	0.9221	0.9212	0.9224	0.9213
100	0.9221	0.9221	0.9222	0.9219	0.9219

Note:

1. All values are maximum k_{eff} which include the bias, uncertainties, and calculational statistics, evaluated for the worst case combination of manufacturing tolerances.
2. The standard deviation (σ) of the calculations is about 0.0003.

Table 6.3.8

REACTIVITY EFFECTS OF SPACING AND EXTERNAL MODERATOR DENSITY FOR HEXAGONAL (TRIANGULAR-PITCHED) ARRAYS OF HI-STAR 180D CASKS

	Cask-to-Cask External Spacing (cm)				
External Moderator Density (%)	2	10	20	40	60
5	0.9222	0.9222	0.9222	0.9219	0.9221
10	0.9213	0.9217	0.9222	0.9219	0.9216
20	0.9221	0.9218	0.9223	0.9216	0.9224
50	0.9219	0.9222	0.9221	0.9219	0.9216
100	0.9222	0.9214	0.9223	0.9219	0.9219

Note:

1. All values are maximum k_{eff} which include the bias, uncertainties, and calculational statistics, evaluated for the worst case combination of manufacturing tolerances.
2. The standard deviation (σ) of the calculations is about 0.0003.

Table 6.3.9

REACTIVITY EFFECTS OF SPACING AND EXTERNAL MODERATOR DENSITY FOR HEXAGONAL (TRIANGULAR-PITCHED) ARRAYS OF HI-STAR 180D CASKS INTERNALLY FLOODED WITH WATER OF 10% FULL DENSITY

Cask-to-Cask External Spacing (cm)					
External Moderator Density (%)	2	10	20	40	60
10	0.4345	0.4333	0.4327	0.4321	0.4319
100	0.4324	0.4324	0.4322	0.4318	0.4318

Note:

1. All values are maximum k_{eff} which include the bias, uncertainties, and calculational statistics, evaluated for the worst case combination of manufacturing tolerances.
2. The standard deviation (σ) of the calculations is about 0.0003.

Table 6.3.10

CALCULATIONS FOR HEXAGONAL (TRIANGULAR-PITCHED) ARRAYS OF TOUCHING CASKS WITH HI-STAR 180D

HI-STAR 180D		
Internal Moderation (%)	External Moderation (%)	Maximum k_{eff}
0	0	0.3984
0	100	0.3924
100	0	0.9226
100	100	0.9216

Note:

1. All values are maximum k_{eff} which include bias, uncertainties, and calculational statistics, evaluated for the worst case combination of manufacturing tolerances.
2. The standard deviation (σ) of the calculations is about 0.0003.

Table 6.3.11

REACTIVITY EFFECTS OF PARTIAL CASK FLOODING
FOR HI-STAR 180D WITH THE F-32 BASKET

Flooded Condition (% Full)	Vertical Orientation	Horizontal Orientation
25	0.8770	0.8383
50	0.9109	0.9162
75	0.9186	0.9181
100	0.9213	0.9213

Notes:

1. All values are maximum k_{eff} which include bias, uncertainties, and calculational statistics, evaluated for the worst case combination of manufacturing tolerances.
2. The standard deviation (σ) of the calculations is about 0.0003.

Table 6.3.12

REACTIVITY EFFECT OF FLOODING THE PELLET-TO-CLAD GAP FOR HI-STAR 180D

Pellet-to-Clad Condition	**HI-STAR 180D**
dry	0.9134
flooded	0.9213

Notes:

1. All values are maximum k_{eff} which includes bias, uncertainties, and calculational statistics, evaluated for the worst case combination of manufacturing tolerances.
2. The standard deviation (σ) of the calculations is about 0.0003.

Table 6.3.13

REACTIVITY EFFECT OF RANDOM ROD REPOSITIONING IN THE F-32 BASKET AS A RESULT OF AN ACCIDENT

Configuration	**Maximum k_{eff}**	**Difference to Reference**
Reference	0.9213	-
Random Rod Pattern #1	0.9190	-0.0023
Random Rod Pattern #2	0.9206	-0.0007
Random Rod Pattern #3	0.9192	-0.0021
Random Rod Pattern #4	0.9216	0.0003
Random Rod Pattern #5	0.9201	-0.0012
Random Rod Pattern #6	0.9219	0.0006
Random Rod Pattern #7	0.9206	-0.0007
Random Rod Pattern #8	0.9220	0.0007
Random Rod Pattern #9	0.9204	-0.0009
Random Rod Pattern #10	0.9191	-0.0022
	Average Difference	-0.0008

Notes:

1. All values are maximum k_{eff} which includes bias, uncertainties, and calculational statistics, evaluated for the worst case combination of manufacturing tolerances.
2. The standard deviation (σ) of the calculations is about 0.0003.

Table 6.3.14

REACTIVITY EFFECT OF RELOCATED ROD SEGMENTS IN THE F-32 BASKET AS A RESULT OF AN ACCIDENT

Configuration	**Maximum k_{eff}**	**Difference to Reference**
Reference	0.9213	-
4 Segments relocated	0.9230	0.0017
8 Segments relocated	0.9234	0.0021
12 Segments relocated	0.9226	0.0013
17 Segments relocated	0.9215	0.0002

Notes:

1. All values are maximum k_{eff} which includes bias, uncertainties, and calculational statistics, evaluated for the worst case combination of manufacturing tolerances.
2. The standard deviation (σ) of the calculations is about 0.0003.

Table 6.3.15

REACTIVITY EFFECT OF GAPS BETWEEN BASKET PANELS
(CALCULATED k_{eff} VALUES)

Condition	**Design Basis Case, No Gap (from Table 6.1.1)**	**2 mm gap every 270 mm in all panels**	**Difference in Calculated k_{eff}**
F-32 – Single Cask Unreflected	0.9148	0.9150	0.0002
F-32 – Single Cask Fully Reflected	0.9154	0.9151	-0.0003
F-32 – Containment Fully Reflected	0.9146	0.9143	-0.0003
F-37 – Single Cask Unreflected	0.9206	0.9201	-0.0005
F-37 – Single Cask Fully Reflected	0.9204	0.9205	0.0001
F-37 – Containment Fully Reflected	0.9200	0.9192	-0.0008
Average Difference	-	-	-0.0003

Notes:

1. All values are calculated k_{eff} values
2. The standard deviation (σ) of the calculations is about 0.0003 for all calculations.

Table 6.3.16
REACTIVITY EFFECTS OF PARTIAL CASK FLOODING FOR HI-STAR 180D WITH THE F-37 BASKET

HI-STAR 180D, F-37 BASKET	
Flooded Condition (Number of axial sections flooded at the bottom)	Maximum k_{eff}
1	0.4235
2	0.5565
3	0.6613
4	0.7312
5	0.7785
6	0.8117
7	0.8360
8	0.8543
9	0.8683
10	0.8789
11	0.8872
12	0.8948
13	0.8996
14	0.9048
15	0.9084
16	0.9113
17	0.9147
18	0.9171
19	0.9195
20	0.9212
21	0.9230
22	0.9239
23	0.9255
24	0.9264
25	0.9275
26	0.9288
52 (all)	0.9388

Notes:
1. All values are maximum k_{eff} which include bias, uncertainties, and calculational statistics, evaluated for the worst case combination of manufacturing tolerances.
2. The standard deviation (σ) of the calculations is about 0.0003.

Table 6.3.17

REACTIVITY EFFECT OF BIRD CAGING CONDITION IN THE F-32 BASKET AS A RESULT OF AN ACCIDENT

Configuration	**Maximum k_{eff}**	**Difference to Reference**
Reference	0.9213	-
Bird caging condition	0.9213	0.0000

Notes:

1. All values are maximum k_{eff} which includes bias, uncertainties, and calculational statistics, evaluated for the worst case combination of manufacturing tolerances.
2. The standard deviation (σ) of the calculations is about 0.0003.

Table 6.3.18

REACTIVITY OF DESIGN BASIS CASES WITH HIGH BURNUP FUEL (45GWD/MTU) IN THE F-37 BASKET

Configuration (see Table 6.1.2)	Maximum k_{eff}	
	Plant Specific Axial Burnup Profile	Axially Constant Burnup
1	0.8457	0.8483
2	0.8773	0.8801

Notes:

1. All values are maximum k_{eff} which includes bias, uncertainties, and calculational statistics, evaluated for the worst case combination of manufacturing tolerances.
2. The standard deviation (σ) of the calculations is about 0.0003.

Table 6.3.19

REACTIVITY EFFECTS OF THE BASKET SHIM DESIGN

Configuration	**Maximum k_{eff}**	**Difference to Reference**
	F-32 Basket	
Aluminum Shim (Reference)	0.9213	-
Aluminum Shim with 40 cm of Steel at Top and Bottom of the Active Length	0.9217	0.0004
	F-37 Basket	
Aluminum Shim (Reference)	0.9413	-
Aluminum Shim with 40 cm of Steel at Top and Bottom of the Active Length	0.9414	0.0001

Notes:

1. All values are maximum k_{eff} which includes bias, uncertainties, and calculational statistics, evaluated for the worst case combination of manufacturing tolerances.
2. The standard deviation (σ) of the calculations is about 0.0003.

TABLE 6.3.20

REACTIVITY EFFECT OF THE SECOND BIRD CAGING CONDITION IN THE F-32 BASKET

Description	**Maximum k_{eff}**	**Difference to Reference**
Reference	0.9213	Ref.
Bird-Caging, Case 1 (1.6%)	0.9232	0.0019
Bird-Caging, Case 2 (4.8%)	0.9293	0.0080
Bird-Caging, Case 3 (8.0%)	0.9364	0.0151

Notes:

1. The standard deviation (σ) of the calculations is about 0.0003.

TABLE 6.3.21

REACTIVITY EFFECT OF THE SECOND BIRD CAGING CONDITION IN THE F-37 BASKET

Axial Profile	**Uniform**		**Artificial**		**Plant-Specific**	
Description	**Maximum k_{eff}**	**Difference to Reference**	**Maximum k_{eff}**	**Difference to Reference**	**Maximum k_{eff}**	**Difference to Reference**
Reference	0.9413	Ref.	0.9366	Ref.	0.9388	Ref.
Bird-Caging, Case 1 (1.6%)	0.9429	0.0015	0.9435	0.0069	0.9411	0.0022
Bird-Caging, Case 2 (4.8%)	0.9501	0.0087	0.9599	0.0234	0.9507	0.0119
Bird-Caging, Case 3 (8.0%)	0.9602	0.0189	0.9728	0.0362	0.9615	0.0227

Notes:

1. The standard deviation (σ) of the calculations is about 0.0003.

TABLE 6.3.22

CRITICALITY SAFETY MARGIN OF THE SECOND BIRD CAGING CONDITION, CASE 3 (8.0%) IN THE F-37 BASKET

Axial Profile	**Uniform**	**Artificial**	**Plant-Specific**
Description	**Maximum k_{eff}**	**Maximum k_{eff}**	**Maximum k_{eff}**
Major Actinides (from Table 6.3.21 for comparison purposes)	0.9602	0.9728	0.9615
All Actinides and Fission Products	0.9121	0.9370	0.9163

Notes:

1. The standard deviation (σ) of the calculations is about 0.0003.

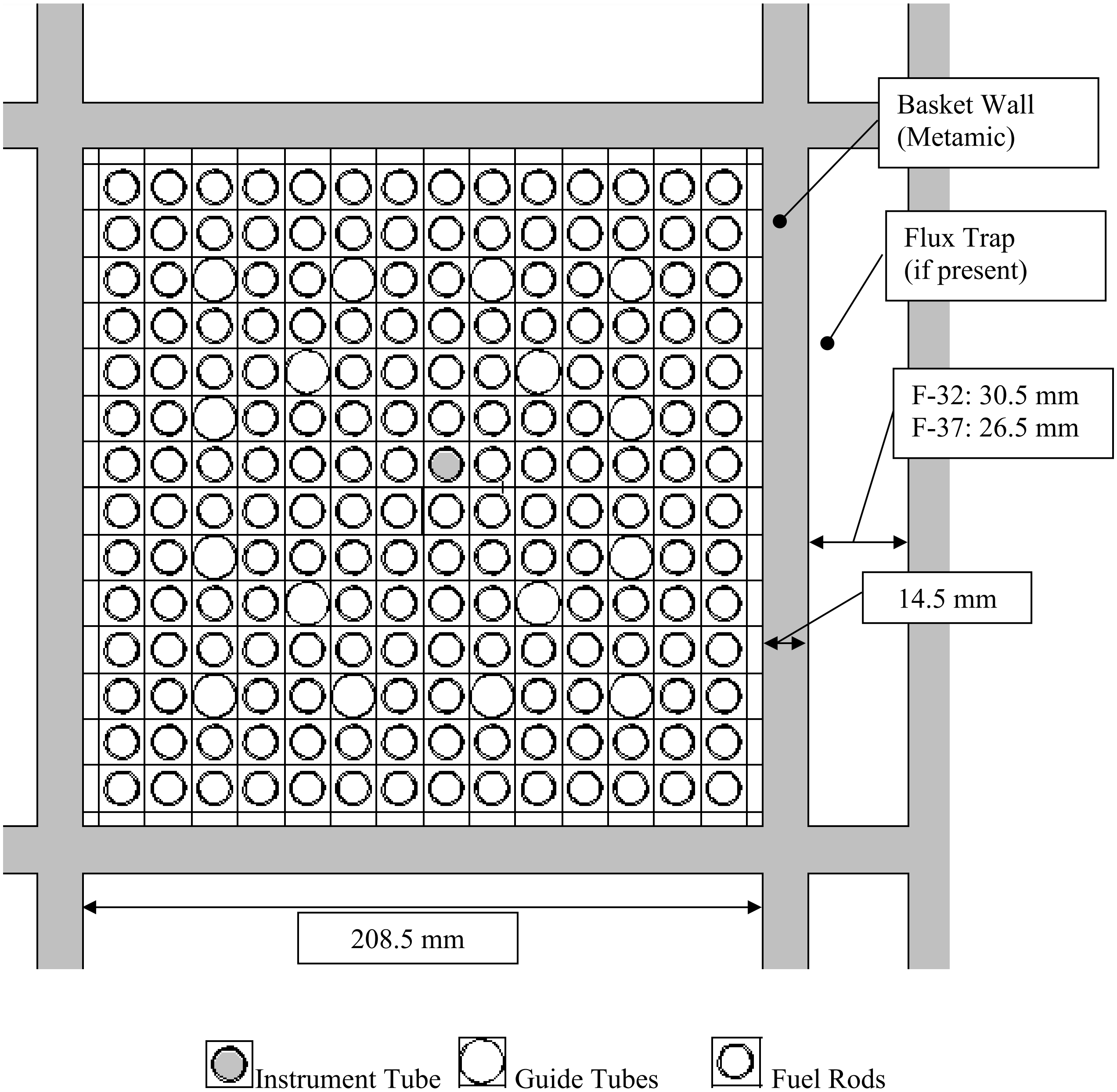

NOTE: THESE DIMENSIONS WERE CONSERVATIVELY USED FOR CRITICALITY ANALYSIS (SEE CHAPTER 1 FOR TRUE DIMENSIONS).

FIGURE 6.3.1 – TYPICAL CELL IN THE CALCULATIONAL MODEL (PLANAR CROSS-SECTION) WITH REPRESENTATIVE FUEL

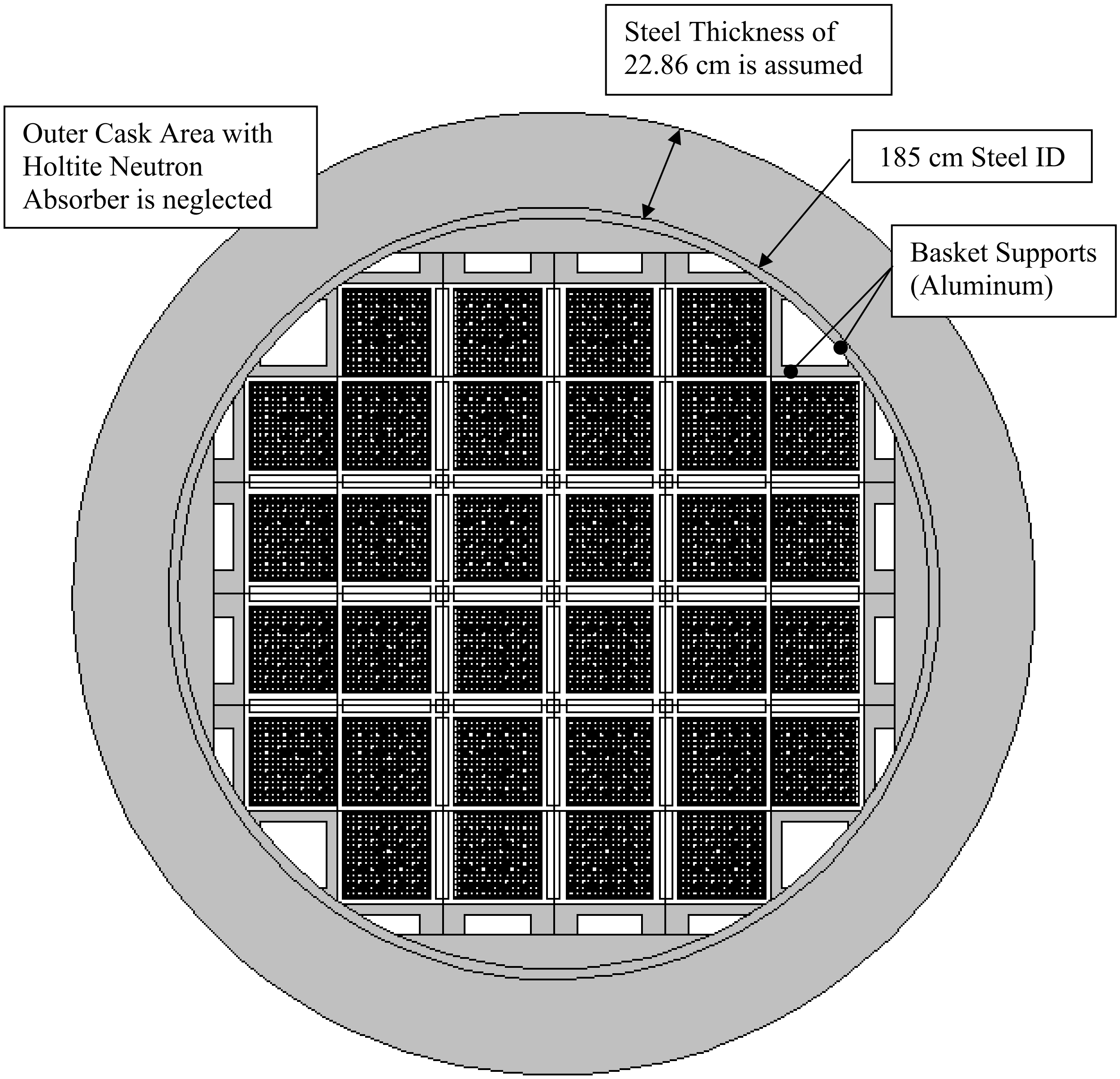

NOTE: THESE DIMENSIONS WERE CONSERVATIVELY USED FOR CRITICALITY ANALYSIS (SEE CHAPTER 1 FOR TRUE DIMENSIONS).

FIGURE 6.3.2 CALCULATION MODEL (PLANAR CROSS-SECTION) OF THE F-32

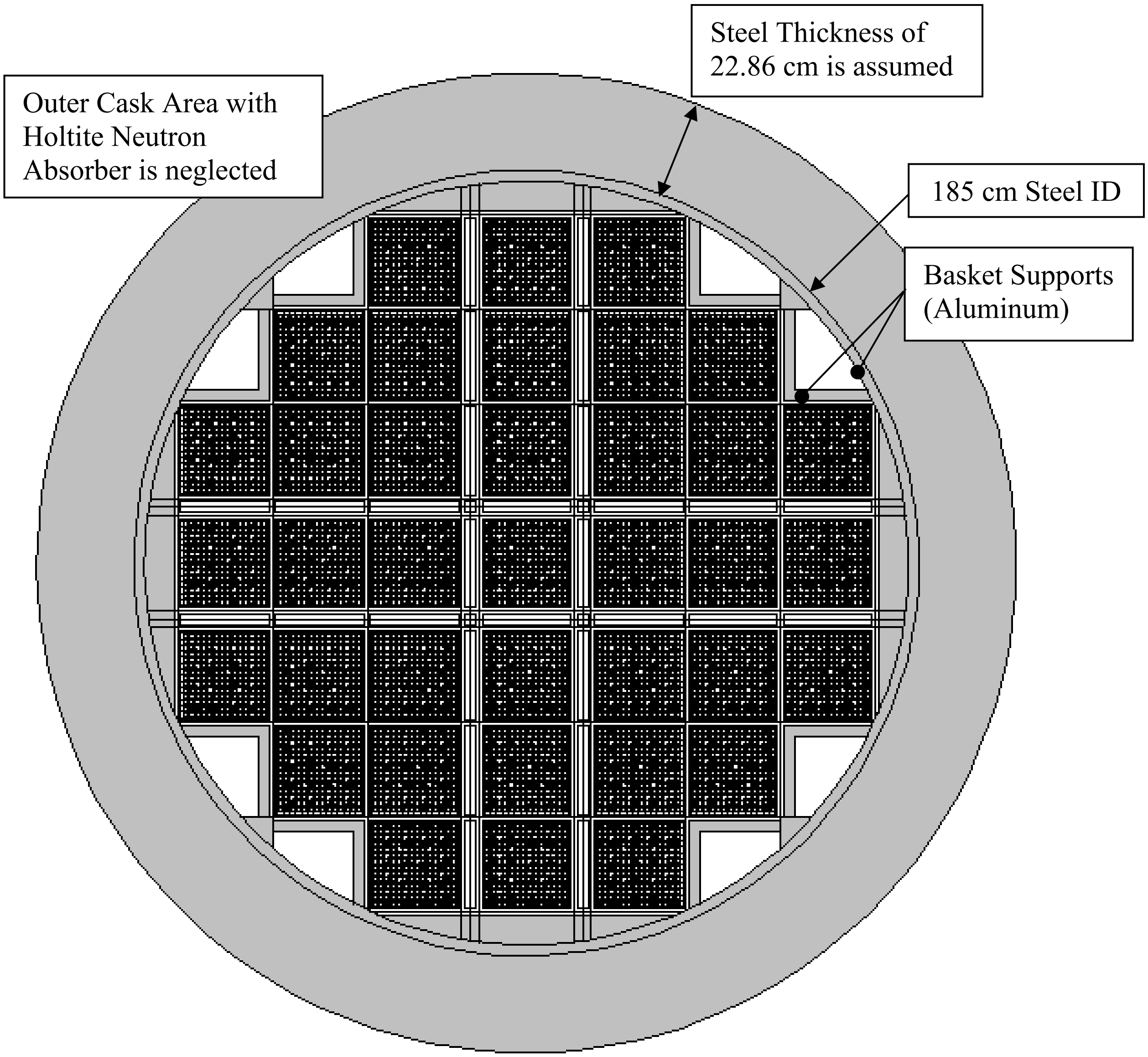

NOTE: THESE DIMENSIONS WERE CONSERVATIVELY USED FOR CRITICALITY ANALYSIS (SEE CHAPTER 1 FOR TRUE DIMENSIONS).

FIGURE 6.3.3 CALCULATION MODEL (PLANAR CROSS-SECTION) OF THE F-37

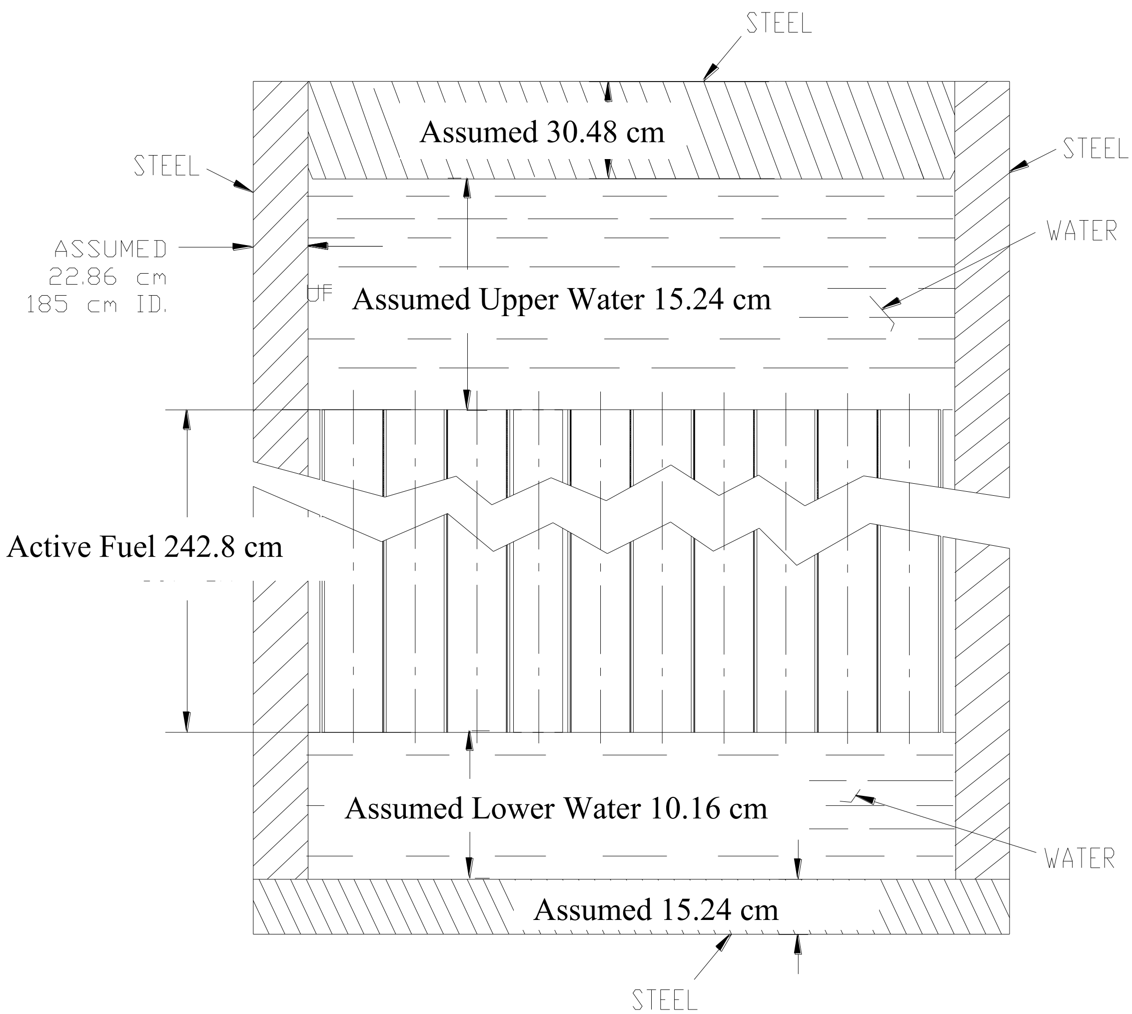

FIGURE 6.3.4 SKETCH OF THE CALCULATIONAL MODEL IN THE AXIAL DIRECTION

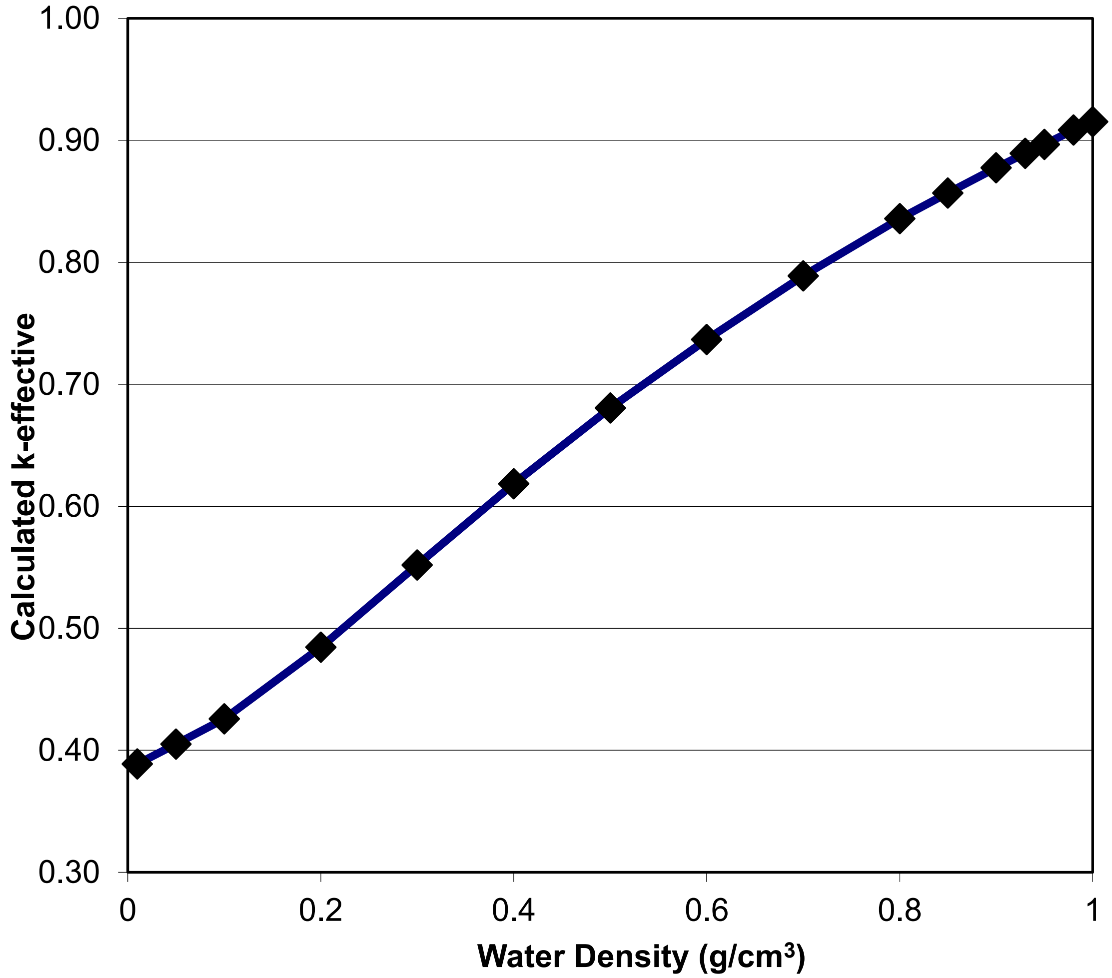

Figure 6.3.5: Calculated k_{eff} as a Function of Internal Moderator Density

6.4 SINGLE PACKAGE EVALUATION

6.4.1 Configuration

The calculations in this section demonstrate that a single HI-STAR 180D Package remains subcritical for all credible conditions of moderation, and that the package fulfills all requirements of 10CFR71.55.

In modeling the single package, the following considerations are applied:

- The bounding geometric and temperature assumptions identified in Tables 6.3.2 and 6.3.3 are used
- The assemblies are centered in the cell locations, which results in the highest k_{eff} as demonstrated in Section 6.3.4.5
- The pellet to clad gap is assumed to be flooded (see Section 6.3.4.3)
- The baskets are assumed to be loaded with fuel of the maximum permissible reactivity, i.e.
    - The F-32 basket is loaded with fresh UO_2 fuel with an initial enrichment of 4.55 wt%. This bounds all spent fuel.
    - The F-37 basket is loaded with fresh and spent UO_2 fuel assemblies using one of the two configurations defined in Table 6.1.2. The fresh assemblies are limited to certain basket positions, depending on the configuration, and are modeled with an initial enrichment of 4.55 wt%. The spent fuel assemblies are modeled with an initial enrichment of 4.55 wt% and with their minimum permissible burnup listed in Table 6.1.2.

Normal Conditions

The studies in sections 6.3.4.1 through 6.3.4.4 demonstrate that the moderation by water to the most reactive credible extent corresponds to the internally fully flooded condition of the basket, with the pellet-to-clad gap in the fuel rods also flooded with water. The external moderation has a statistically negligible effect.

Under normal condition, water is assumed to leak into the package, consistent with 10 CFR 71.55. Flooding with full density water is assumed, since this is the bounding condition as shown in Section 6.3.4.

To demonstrate compliance with 10CFR71.55 under normal conditions, the following calculations are performed for the HI-STAR 180D design:

- Single containment with full internal and external water moderation. The full external water moderation is modeled as water with a thickness of about 300 cm. The containment system corresponds to the 64 mm inner shell of the cask. This case addresses the requirement of 10CFR71.55 (b).

- Single cask with full internal and external water moderation. As for the single containment, the full external water moderation is modeled as water with a thickness of about 300 cm. The external neutron moderator (Holtite) is conservatively neglected in the model.

To satisfy the requirements of 10CFR71.55 (b)(1), the calculations are performed

- with the bounding basket dimensions as determined in Section 6.3.1 for each basket; and,
- with fuel positioned in the center of each cell, as discussed in Section 6.3.4.5.

The maximum k_{eff} values for all these cases, calculated with 95% probability at the 95% confidence level, are listed in Table 6.4.1 for the F-32 basket and in Table 6.4.2 for the F-37 basket. Overall, these results confirm that the effective multiplication factor (k_{eff}), including all biases and uncertainties at a 95-percent confidence level, does not exceed 0.95 under normal conditions of transport.

Additional calculations (CASMO-5) at elevated temperatures confirm that the temperature coefficients of reactivity are negative as shown in Table 6.3.3. This confirms that the calculations are conservative.

<u>Accident Conditions</u>

The analyses presented in Chapter 2 and Chapter 3 demonstrate that the damage resulting from the hypothetical accident conditions of transport are limited to a loss of the neutron shield material as a result of the hypothetical fire accident. Because the criticality analyses do not take credit for the neutron shield material (Holtite), this condition has no effect on the criticality analyses.

The HI-STAR 180D is designed for high burnup fuel (HBF), i.e. for fuel with burnups larger than 45 GWd/mtU. For fuel of this burnup, there are concerns that the fuel cladding could be damaged under accident conditions, with a potential effect on reactivity. Chapter 2 demonstrates that the cask remains leaktight under all credible accident conditions. Further, the second lid provides additional assurance that water will not leak into the containment as a result of an accident. The package therefore satisfies the intent of USNRC ISG 19, and flooding of the containment system under accident condition is not considered in the design basis analyses.

In summary, the hypothetical transport accidents have no adverse effect on the geometric form of the package contents important to criticality safety, and thus, are limited to the effects on internal and external moderation evaluated in Subsection 6.3.4.1.

To demonstrate compliance with 10CFR71.55 under accident conditions, the following calculations are performed for the HI-STAR 180D design:

- Single cask, internally dry, with full external water moderation. As for the single cask under normal conditions, the full external water moderation is modeled as water with a thickness of about 300 cm. Fuel is modeled as undamaged, since any small rearrangements of fuel as a result of the accident would have a negligible effect, compared to the safety margin for this condition. The external neutron moderator is conservatively neglected in the model. This case addresses the requirement of 10CFR71.55 (e).

As additional assurance that the package remains subcritical under accident conditions, studies were performed for some credible damaged fuel configurations under accident conditions with a fully flooded containment boundary. These studies, presented in Section 6.3.5, show that even under the assumption of fuel damage and flooding, the package remains subcritical in the accident.

6.4.2 Results

In calculating the maximum reactivity, the analysis uses the following equation:

$$k_{eff}^{max} = k_c + K_c \sigma_c + Bias + \sigma_B$$

where:

- ⇒ k_c is the calculated k_{eff} under the worst combination of tolerances;
- ⇒ K_c is the K multiplier for a one-sided statistical tolerance limit with 95% probability at the 95% confidence level [6.4.1]. Each final k_{eff} value calculated by MCNP5 is the result of averaging 400 (or more) cycle k_{eff} values, and thus, is based on a sample size of 400. In general, if the samples are exactly distributed by normal distribution with a known mean and uncertainty, then the single sided tolerance limit for 95% probability is about 1.65 times the standard deviation. However, when the standard deviation is based on a limited sample size the tolerance factor depends on the sample size, the K multiplier is 2.0 for a sample size of about 66 samples for the 95/95 level, and reduces further for larger sample sizes. For this analysis a value of 3.0 was assumed for the K multiplier, which is larger (more conservative) than the value corresponding to a sample size of 400;
- ⇒ σ_c is the standard deviation of the calculated k_{eff}, as determined by the computer code (MCNP5);
- ⇒ ***Bias*** is the systematic error in the calculations (code dependent) determined by comparison with critical experiments; and
- ⇒ σ_B is the standard error of the bias (which includes the K multiplier for 95% probability at the 95% confidence level).

Appendix 6.A presents the critical experiment benchmarking for fresh UO_2 fuel and the derivation of the corresponding bias and standard error of the bias (95% probability at the 95% confidence level). See Appendix 6.B, Section 6.B.3, for the critical experiment benchmarking for spent fuel.

The results are listed in Table 6.4.1 for the F-32 basket and in Table 6.4.2 for the F-37 basket. For the F-37 basket, both 2 configurations defined in Table 6.1.2 are analyzed for an internally flooded, unreflected cask. Configuration 1 is selected as the configuration analyzed to show compliance with 10CFR71.55, and for the evaluations of package arrays in the following sections 6.5 and 6.6.

Table 6.4.1

HI-STAR 180D SINGLE PACKAGE WITH F-32 BASKET

Configuration	% Internal Moderation	% External Moderation	Max. k_{eff}	1 σ	EALF (eV)
Single Package, fully reflected	100%	100%	0.9219	0.0003	0.3688
Containment, fully reflected	100%	100%	0.9211	0.0003	0.3696
Single Package, Damaged	0%	100%	0.3721	0.0001	129750

Note:

1. The maximum k_{eff} is equal to the sum of the calculated k_{eff}, three standard deviations, the code bias, and the uncertainty in the code bias.

Table 6.4.2

HI-STAR 180D SINGLE PACKAGE WITH F-37 BASKET

Configuration	% Internal Moderation	% External Moderation	Max. k_{eff}	1 σ	EALF (eV)
Single Package, Unreflected:					
Configuration 1, 15 GWd/mtU	100%	0%	0.9413	0.0003	0.3917
Configuration 2, 18 GWd/mtU	100%	0%	0.9392	0.0003	0.3861
Configuration 1, 15 GWd/mtU:					
Single Package, fully reflected	100%	100%	0.9411	0.0003	0.3922
Containment, fully reflected	100%	100%	0.9407	0.0003	0.3920
Single Package, Damaged	0%	100%	0.3725	0.0001	160200

Note:

1. The maximum k_{eff} is equal to the sum of the calculated k_{eff}, three standard deviations, the code bias, and the uncertainty in the code bias.

6.5 EVALUATION OF PACKAGE ARRAYS UNDER NORMAL CONDITIONS OF TRANSPORT

6.5.1 Configuration

Studies in Subsection 6.3.4 show that the spacing and external moderator densities have a negligible effect on the reactivity of the package. Therefore, any external condition can be used to represent the most reactive configuration. To represent package arrays under normal conditions, a hexagonal array of touching casks, infinite in lateral and axial direction, internally and externally dry, is modeled. All other modeling assumptions are identical to the modeling assumptions for the single package under normal conditions. The analyses are performed for both baskets. This addresses the requirement of 10CFR71.59 (a) (1) and the determination of the criticality safety index according to 10CFR71.59 (b).

6.5.2 Results

The results are presented in Table 6.5.1, and show that the maximum k_{eff} is well below the NUREG-1617 limit of 0.95for both baskets. Since an unlimited number of packages can be placed in an array, the value of N is infinite, and the CSI is therefore zero (0).

Table 6.5.1

HI-STAR 180D PACKAGE ARRAYS UNDER NORMAL CONDITIONS

Configuration	% Internal Moderation	% External Moderation	Max. k_{eff}	1 σ	EALF (eV)
F-32	0%	0%	0.3821	0.0001	111800
F-37, Configuration 1	0%	0%	0.3814	0.0001	137450

Note:

1. The maximum k_{eff} is equal to the sum of the calculated k_{eff}, three standard deviations, the code bias, and the uncertainty in the code bias.

6.6 PACKAGE ARRAYS UNDER HYPOTHETICAL ACCIDENT CONDITIONS

6.6.1 Configuration

Studies in Subsection 6.3.4 show that the spacing and external moderator density has a negligible effect on the reactivity of the package. Therefore, any external condition can be used to represent the most reactive configuration. To represent package arrays under accident conditions, a hexagonal array of touching casks, infinite in lateral and axial direction, internally dry with full external water reflection, is modeled. This model is consistent with the model for the single cask under accident condition, and recognizes the fact that water intrusion under accident condition is not considered credible. This calculation addresses the requirement of 10CFR71.59 (a)(2)

6.6.2 Results

The results are presented in Table 6.6.1, and show that the maximum k_{eff} is well below the NUREG-1617 limit of 0.95 for both baskets. Since an unlimited number of packages can be placed in an array, the value of N is infinite, and the CSI is therefore zero (0).

Table 6.6.1

HI-STAR 180D PACKAGE ARRAYS UNDER ACCIDENT CONDITIONS

Configuration	% Internal Moderation	% External Moderation	Max. k_{eff}	1 σ	EALF (eV)
F-32	0%	100%	0.3759	0.0001	122430
F-37, Configuration 1	0%	100%	0.3758	0.0001	150630

Note:

1. The maximum k_{eff} is equal to the sum of the calculated k_{eff}, three standard deviations, the code bias, and the uncertainty in the code bias.

6.7 FISSILE MATERIAL PACKAGES FOR AIR TRANSPORT

Not Applicable. The HI-STAR 180D package will not be transported by air.

6.8 BENCHMARK EVALUATIONS

Benchmark calculations have been made on selected critical experiments, chosen, insofar as possible, to bound the range of variables in the cask designs. The most important parameters are (1) the enrichment, (2) the cell spacing, and (3) the ^{10}B loading of the neutron absorber panels. Other parameters, within the normal range of cask and fuel designs, have a smaller effect, but are also included. Detailed benchmark calculations are presented in Appendix 6.A.

The benchmark calculations were performed with the same computer codes and cross-section data, described in Section 6.3, that were used to calculate the k_{eff} values for the cask. Further, all calculations were performed on the same computer hardware, specifically, personal computers under Microsoft Windows.

Additional isotopic benchmark calculations performed for the burnup methodology for the HI-STAR 180D are presented in Appendix 6.B.

CHAPTER 6 REFERENCES

The following generic industry and Holtec produced references may have been consulted in the preparation of this document. Where specifically cited, the identifier is listed in the SAR text or table. Active Holtec Calculation Packages which are the repository of all relevant licensing and design basis calculations are annotated as "latest revision". Submittal of the latest revision of such Calculation Packages to the USNRC and other regulatory authorities during the course of regulatory reviews is managed under the company's Configuration Control system. Supporting documents submitted to the USNRC with the HI-STAR 180D LAR 9367-2 have been italicized.

[6.2.1] Holtec International Report HI-951251, Safety Analysis Report HI-STAR 100 Cask System, USNRC Docket 71-9261, latest revision.

[6.3.1] X-5 Monte Carlo Team, MCNP - A General Monte Carlo N-Particle Transport Code, Version 5, LA-UR-03-1987, Los Alamos National Laboratory, April 2003 (Revised 2/1/2008).

[6.3.2] "CASMO-5/CASMO5M A Fuel Assembly Burnup Program Methodology Manual", SSP-08/405, Rev. 1, Studsvik Scandpower, Inc.

[6.3.3] "CASMO-5 A Fuel Assembly Burnup Program, Users Manual," SSP-07/431, Rev. 4, Studsvik Scandpower, Inc..

[6.3.4] J.M. Cano, R. Caro, and J.M Martinez-Val, "Supercriticality Through Optimum Moderation in Nuclear Fuel Storage*," Nucl. Technol.*, 48, 251-260, (1980).

[6.3.5] "Criticality Specialists and Nuclear Engineers Working Towards a Harmonised Approach to Criticality Assessments of Transport Packages", PATRAM 2007, Abstract #217, WNTI, October 2007.

[6.4.1] M.G. Natrella, "Experimental Statistics", National Bureau of Standards, Handbook 91, August 1963.

[6.4.2] *Holtec International Report HI-2125174, "Criticality Analysis for the HI-STAR 180D Cask", latest revision. (Holtec Proprietary).*

Appendix 6.A

[PROPRIETARY INFORMATION WITHHELD PER 10 CFR 2.390]

Appendix 6.B

[PROPRIETARY INFORMATION WITHHELD PER 10 CFR 2.390]

Appendix 6.C

[PROPRIETARY INFORMATION WITHHELD PER 10 CFR 2.390]

Appendix 6.D

[PROPRIETARY INFORMATION WITHHELD PER 10 CFR 2.390]

Appendix 6.E

[PROPRIETARY INFORMATION WITHHELD PER 10 CFR 2.390]

Appendix 6.F

[PROPRIETARY INFORMATION WITHHELD PER 10 CFR 2.390]

CHAPTER 7: PACKAGE OPERATIONS

7.0 INTRODUCTION

This chapter provides a summary description of the essential elements and minimum requirements necessary to prepare the package for shipment and to ensure that it operates in a safe and reliable manner under normal and accident conditions of transport pursuant to the provisions of 10CFR71 [7.1.4], as described in this SAR. The information presented in this chapter, along with the technical basis of the package design described in Chapters 2 through 6 will be used by Holtec International's Site Services organization to develop more detailed generic procedures for users of the HI-STAR 180D Package. Equipment specific operating details such as valve manipulation, onsite cask transporter handling methods etc, will be provided to individual users of the HI-STAR 180D package based on the specific ancillary equipment selected by the user and the configuration of the site. It is the user's responsibility to utilize the information provided in this chapter, (treating it as an inviolable set of operation elements that must be included in the detailed operating procedures). In addition, the user must consult the conditions of the NRC issued Certificate of Compliance (CoC), equipment-specific operating instructions, and the plant's working procedures and apply them to develop the site-specific written loading, unloading, and handling procedures to ensure that the package is operated in accordance with the CoC and all applicable government regulatory requirements. The following generic criteria shall be used to qualify that the site-specific operating procedures are acceptable for use:

- All heavy load handling instructions are in keeping with the guidance in industry standards, and Holtec's proprietary rigging manual.
- A careful technical evaluation of all potential modes of loss of load stability has been performed and accepted by Holtec International's site services organization.
- Procedures are in conformance with the essential elements and conditions of this Chapter and the CoC.
- The operational steps are ALARA.
- Procedures contain provisions for documenting successful execution of all safety significant steps for archival reference.
- Holtec's lessons learned database has been consulted to incorporate all applicable lessons learned from prior cask handling and loading evolutions.
- Procedures contain provisions for classroom and hands-on training and for a Holtec approved personnel qualification process to insure that all operations personnel are adequately trained.
- The procedures are sufficiently detailed and articulated to enable craft labor to execute them in *literal compliance* with their content.

The operations described in this chapter assume that the fuel will be loaded into or unloaded from the HI-STAR cask submerged in a spent fuel pool. With some modifications, the information presented herein can be used to develop site-specific procedures for loading or unloading fuel into the system within a hot cell or other remote handling facility.

US Department of Transportation (USDOT) transportation regulations in 49CFR parts 172 [7.1.1] and 173 [7.1.2] applicable to the transport of the HI-STAR 180D package as well as USNRC regulations in 10CFR20 [7.1.3], are only addressed in this chapter to the extent required to ensure compliance with 10CFR71 regulations and to provide a more complete package operation description. Applicable 49CFR and 10CFR20 regulations, including those explicitly called out in 10CFR 71.5, shall be complied with for package use in the US and/or for US package export and import. For transport outside US territory and under the approval or jurisdiction of one or more foreign competent authorities, other requirements such as the ADR, "European Agreement Concerning the International Carriage of Dangerous Goods by Road" and the RID, "European Agreement Concerning the International Carriage of Dangerous Goods by Rail" may be imposed in place of the 49CFR. It is the user's responsibility to comply with the latest revision of these transportation regulations as required by the applicable competent authority.

Users shall develop or modify existing programs and procedures to account for the transport operation of the HI-STAR 180D. Written procedures are required and will be developed or modified to account for such items as handling and storage of systems, structures and components identified as *important-to-safety*, heavy load handling, specialized instrument calibration, special nuclear material accountability, fuel handling procedures, training, equipment and process qualifications. Users shall implement controls to ensure that the lifted weights do not exceed the cask lifting trunnion design limit. Users shall implement controls to monitor the time limit for the removal of the cask from the spent fuel pool to the commencement of cask draining to prevent boiling. Users shall also implement controls to ensure that the cask cannot be subjected to a fire event in excess of design limits during loading operations.

For the determination of Time-To-Boil time limits or the determination of cyclic vacuum drying time limits, thermal evaluations may implement Fluent 3D models that are the same or consistent with the models used for safety analysis. Alternatively, other demonstrably conservative and appropriately benchmarked models may be utilized.

The procedures in this chapter contain generic ALARA notes and warnings to alert users to radiological issues. Actions identified with these notes and warnings are not mandatory and shall be implemented based on a determination by radiation protection.

Appendix 7.A provides general operational weights and illustrations of typical operations of the HI-STAR 180D Package. Additional general weight information may be provided in the drawing package referenced in the CoC.

Appendix 7.D provides content conditions of the HI-STAR 180D Package.

Appendix 7.E provides burnup verification conditions of the HI-STAR 180D Package.

Control of the package operation shall be performed in accordance with the user's Quality Assurance (QA) program to ensure critical steps are not overlooked and that the cask has been confirmed to meet all requirements of the CoC before being released for shipment.

Fuel assembly selection and verification shall be performed by the user in accordance with written, approved procedures that ensure that only SNF assemblies authorized in the CoC are loaded into the HI-STAR 180D cask. Fuel assembly selection, and some aspects of assembly verification, are typically performed well in advance of the actual loading date, specifically with respect to the selection and verification of the assemblies to meet the definition of undamaged fuel in the CoC. A typical approach to show compliance with the CoC definition of undamaged fuel may include the following steps:

- During reactor operation, the water chemistry is monitored. If no indication of fuel leakage is detected, all assemblies unloaded from the core are considered undamaged.
- If indication of leakage is found in the water during reactor operation, the population of the assemblies in the core that may have the leak may be narrowed down by a more detailed evaluation of the leaked isotopes.
- Once unloaded, further examination, such as sipping, may be performed to clearly identifying the leaking assembly or assemblies, out of the population identified.
- Once leaking assemblies are identified, they may simply be considered not meeting the CoC requirements and excluded from the selection, or further tests are performed to identify the extent of cladding damage.

Fuel handling shall be performed in accordance with written site-specific procedures.

7.1 PACKAGE LOADING

The HI-STAR 180D Package is used to load and transport spent fuel. The essential elements required to prepare the HI-STAR 180D Package for fuel loading, to load the fuel, to ready the cask for transport as a Transport Package are described below.

7.1.1 Preparation for Loading

1. If the HI-STAR 180D Packaging has previously been used to transport spent fuel, the HI-STAR 180D is received and the personnel barrier, if attached, is removed and security seals, if used, are inspected to verify there was no tampering and that they match the corresponding shipping documents.
2. The HI-STAR 180D Packaging is visually receipt inspected to verify that there are no outward visual indications of impaired physical conditions except for superficial marks and dents. Any issues are identified to site management. Any road dirt is washed off and any foreign material is removed.
3. Radiological surveys are performed in accordance with 49CFR173.443 [7.1.2] and 10CFR20.1906 [7.1.3]. If necessary, the HI-STAR 180D Packaging is decontaminated to meet survey requirements and/or notifications are made to affected parties.
4. The impact limiters, if attached, are removed and a second visual inspection to verify that there are no outward visual indications of impaired physical condition is performed.
5. The trunnion hole plugs, if installed, are removed and the cask trunnions are installed. The cask is upended and the neutron shield relief devices are inspected to confirm that they are installed, intact, and not covered by tape or any other covering.
6. The cask lids are removed and used seals are removed and discarded. If equipped, the neutron shield pressure relief device(s) on the inner closure lid is inspected to confirm it is installed, intact, and not covered by tape or any other covering.
7. The containment closure flange inner and outer lid sealing surfaces are inspected for damage that may compromise the performance of the seal. Any damage to the sealing surfaces is repaired by welding and/or polishing/machining damaged areas as necessary. If the cask sealing surface is weld repaired, the sealing surfaces are faced with corrosion resistant veneers.
8. The inner and outer closure lid bolts are inspected for distortion and damaged threads and any suspect bolts are replaced.
9. Any foreign material is removed from inside the cask and the basket panels are visually checked to verify they are not damaged.

7.1.2 Loading of Contents

7.1.2.1 Fuel Loading Operations

ALARA Note:
A bottom protective cover may be attached to the cask bottom or placed in the designated preparation area or spent fuel pool. This will help prevent embedding contaminated particles in the cask bottom surface and ease the decontamination effort. Waterproof tape placed over empty bolt holes, and bolt plugs may also reduce the time required for decontamination. Wetting the components that enter the spent fuel pool may reduce the amount of decontamination work to be performed later.

1. The cask containment closure flange sealing surfaces are covered with a protective cover or a protective funnel. Caps or plugs are installed on the neutron shielding enclosure pressure relief devices. The cask storage cavity is filled with either spent fuel pool water or clean borated water and the cask is lowered into the spent fuel pool for fuel loading. The cask cavity may be filled by pumping water into the cask or by lowering the cask in the spent fuel pool and allowing water to overflow into the cask cavity.

2. Prior to loading the fuel, the user identifies the fuel to be loaded and the fuel is independently verified that it meets the conditions of the CoC and this chapter. The pre-selected assemblies are loaded into the cask and a visual verification of the assembly identification is performed. Any additional information required to be documented by Appendix 7.D for the shipping manifest must be recorded. If equipped, the neutron shield pressure relief device(s) on the inner closure lid is verified to be undamaged prior to fuel loading or prior becoming inaccessible by the outer closure lid installation.

3. While still underwater, the containment closure flange seal protection device is removed. The containment closure flange sealing surfaces for the inner closure lid are inspected to verify they are free of particulate matter or damage that might affect the seal performance. Any particulate matter or damage that would prevent a seal is remedied. Prior to placing the inner lid in the water its sealing surfaces are inspected to verify they are free of particulate matter or damage that might affect seal performance. Any particulate matter or damage that would prevent a seal is remedied. New seals are installed in the inner closure lid and the lid is then lowered into the water and installed on the cask. The lid is visually inspected to confirm it is properly seated. The user performs a site-specific Time-to-Boil evaluation to determine a time limitation to ensure that water boiling will not occur in the cask prior to the start of draining operations. If it appears that the Time-to-Boil limit will be exceeded prior to draining operations, the user shall take appropriate action to either replace the water in the cask cavity with an inert gas, circulate water through the cask cavity to reset the Time-to-Boil clock, or return the cask to the spent fuel pool and remove the lid to allow for natural water circulation. Inner closure lid bolts may be installed at any time after the inner closure lid is installed but before the cask is dried.

ALARA Note:
Activated debris may have settled on flat surfaces of the cask during fuel loading. Cask surfaces suspected of carrying activated debris should be kept under water until a preliminary dose rate scan clears the cask for removal. To reduce decontamination time, the cask surfaces should be kept wet until decontamination begins.

4. The lift attachment is engaged to the cask lifting trunnions and the cask is raised out of the spent fuel pool after being cleared by Radiation Protection. As the cask is raised out of the spent fuel pool, the lift attachment and cask are sprayed with clean water to help remove contamination.
5. The accessible areas of the bottom of the cask and the cask bottom protective cover, if used, are decontaminated, the cask is placed in the designated preparation area and the lift attachment is removed. The top surfaces and accessible areas of the cask are decontaminated. Caps or plugs are removed from the neutron shielding enclosure pressure relief devices.
6. At the discretion of Radiation Protection, dose rates are measured at the inner closure lid and around the cask body to confirm appropriate radiological control.
7. The lid vent line is opened to prevent cask pressurization and temporary shielding (if used) is installed.
8. Any standing water is removed from the inner and outer closure lid bolt holes in the closure flange. The inner closure lid bolts are installed and torqued after the vent line is opened and before the cask cavity is drained. Bolt torque requirements and recommended tightening procedure are provided in Table 7.1.1 and Figure 7.1.1, respectively. The user may attach security seals to the inner closure lid bolts at this time.

ALARA Warning:
Personnel should remain clear of the drain lines any time water is being pumped or purged from the cask. Radiological crud, suspended in the water, may create a radiation hazard to workers. Dose rates will rise as water is drained from the cask. Continuous dose rate monitoring is recommended.
Caution:
An inert gas must be used any time the fuel is not covered with water to prevent oxidation of the fuel cladding. The fuel cladding is not to be exposed to air at any time during loading operations.

9. For moderate or high burnup fuel, the Forced Helium Dehydration (FHD) System is connected to the cask and used to remove moisture from the cask cavity. There is no

time limit on FHD drying. As the water is drained from the cask, an inert gas is introduced into the cask to prevent oxidation of the fuel cladding. After the bulk water has been removed, the helium exiting the FHD demoisturizer is cooled to the temperature or dew point given in Table 7.1.2 and circulated through the duration given in Table 7.1.2 to ensure that the cask cavity is suitably dry.

10. Optionally, a vacuum drying system is connected to the cask and used to remove moisture from the cask cavity. The user performs a site-specific evaluation to determine whether cyclic vacuum drying and time limits are necessary to ensure the vacuum drying criteria is met. Users shall refer to Table 7.1.2 and Table 7.1.3 for vacuum drying criteria. As the water is drained from the cask, an inert gas is introduced into the cask to prevent oxidation of the fuel cladding. The cask cavity is vacuum dried. Once it is demonstrated that the cask cavity pressure meets the pressure criterion given in Table 7.1.2 for the duration given in Table 7.1.2, with the valve closed, it shall be considered dry.

11. The cask cavity is backfilled to the requirements in Table 7.1.4 and the port caps/plugs are closed.

12. With the inner closure lid inter-seal test port plug removed, (that will be located beneath the outer closure lid access port) the inner closure lid inter-seal space is dried. The inner closure lid inner seal is leak tested through its respective inter-seal test ports in accordance with the test requirements and acceptance criteria provided in Chapter 8. Unacceptable leakage rates may require cleaning or repair of the sealing surfaces and replacement of the seals prior to retesting of the seals. The leak testing of the inner closure lid main seal may be performed immediately after the lid bolts are installed and torqued such that if a leak is detected, the cask does not need to be reflooded. If the cask is to be transported within 12 months of closure and leakage testing, the inner closure lid inter-seal test port plugs are installed with new seals.

13. The sealing surfaces on the inner closure lid port covers and the respective mating surfaces of the inner closure lid port covers are inspected for signs of damage. Any damage that would prevent a seal is remedied and new seals are installed. The space beneath the port covers are backfilled to the requirements in Table 7.1.4. The port cover bolts are torqued. Bolt torque requirements and recommended tightening procedure are provided in Table 7.1.1 and Figure 7.1.1, respectively. The vent and drain port cover plate inner seals are leak tested through their respective inter-seal test port in accordance with test requirements and acceptance criteria provided in Chapter 8. Unacceptable leakage rates may require cleaning or repair of the sealing surfaces and replacement of the seals prior to retesting of the seals. If the cask is to be transported within 12 months of closure and leakage testing, the inner closure lid port cover inter-seal test port plugs are installed with new seals.

7.1.2.2 Cask Closure

1. The inter-seal test port plug(s) of the inner closure lid and the inter-seal test port plugs of the inner closure lid port covers are installed with new seals and torqued. The containment closure flange outer sealing surface protective cover is removed. The

containment closure flange sealing surfaces for the outer closure lid are inspected to verify they are free of particulate matter or damage that might affect the seal performance. Any particulate matter or damage that would prevent a seal is remedied. The sealing surfaces for the outer closure lid are inspected for signs of damage or particulate matter that might affect the seal performance. Any particulate matter or sealing surface damage that would prevent a seal is remedied. The user ensures that the inner closure lid inter-seal test port plug(s) are installed. The outer closure lid is installed using new seals. The outer closure lid bolts are installed and torqued. Bolt torque requirements and recommended tightening procedure are provided in Table 7.1.1 and Figure 7.1.1, respectively. The user may attach security seals to the outer closure lid bolts at this time.

2. The inter-lid space is dried, evacuated and backfilled to the requirements in Table 7.1.4.
3. The outer closure lid access port plug, fitted with a new seal, is torqued to the requirements in Table 7.1.1.
4. The outer closure lid inner-seal and outer closure lid access port plug seal are leak tested in accordance with the test requirements and acceptance criteria in Chapter 8. Unacceptable leakage rates may require cleaning or repair of the sealing surfaces and replacement of the seals prior to retesting of the seals.
5. The outer closure lid access port cover is installed with a seal and port cover bolts are torqued. The outer closure lid inter-seal test port plug(s) is installed with new seal and torqued.

7.1.3. Preparation for Transport

1. If more than twelve months have elapsed since the performance of the leakage tests described in Section 7.1.2.2, a periodic leakage test shall be performed as follows:
   a. If installed, the outer closure lid is removed and the inner closure lid inter-seal test port plug(s) and inner closure lid port cover inter-seal test port plugs are removed. The inner closure lid inner seal and vent and drain port cover plate inner seals are leak tested in accordance with the test requirements and acceptance criteria in Chapter 8. Unacceptable leakage rates may require cleaning or repair of the sealing surfaces and replacement of the seals prior to retesting of the seals.
   b. The inner closure lid inter-seal test port plug(s) and inner closure lid port cover inter-seal test port plugs are installed with new seals.
   c. The sealing surfaces for the outer closure lid are inspected for signs of damage or particulate matter that might affect the seal performance. Any particulate matter or sealing surface damage that would prevent a seal is remedied. The outer closure lid is installed using new seals. The outer closure lid bolts are installed and torqued. Bolt torque requirements and recommended tightening procedure are provided in Table 7.1.1 and Figure 7.1.1, respectively. The user may attach security seals to the outer closure lid bolts at this time.

d. The inter-lid space is dried, evacuated and backfilled to the requirements in Table 7.1.4.

e. The outer closure lid access port plug, fitted with a new seal, is torqued to the requirements in Table 7.1.1. The outer closure lid inner-seal and outer closure lid access port plug seal are leak tested in accordance with the test requirements and acceptance criteria in Chapter 8. Unacceptable leakage rates may require cleaning or repair of the sealing surfaces and replacement of the seals prior to retesting of the seals.

f. The outer closure lid access port cover is installed with a seal and port cover bolts are torqued. The outer closure lid inter-seal test port plug(s) is installed with new seal and torqued.

2. The cask neutron shield pressure relief devices are visually verified to be undamaged.

ALARA Warning:
Dose rates around the unshielded bottom end of the cask may be higher than other locations around the cask. After the cask is downended on the transport frame, the bottom impact limiter should be installed promptly. Personnel should remain clear and exercise other appropriate ALARA controls when working around the bottom end of the cask.

3. The cask is moved to the transport location, downended, and placed on the transport vehicle.

4. A visual inspection for signs of impaired condition is performed. Any non-satisfactory conditions are remedied.

5. Contamination surveys are performed per 49CFR173.443. If necessary, the cask is further decontaminated to meet the survey requirements.

6. The cask trunnions are removed and the trunnion hole plugs are installed. The radial spacers and impact limiters are installed on the cask and the impact limiter bolts/nuts are torqued. Bolt/Nut torque requirements and recommended tightening procedure are provided in Table 7.1.1 and Figure 7.1.1, respectively.

7. The tie-down system is installed, a cover is installed over at least one of the access tubes on the top impact limiter, and a security seal is installed on the top impact limiter. Security seal serial number(s) are recorded in the shipping documents.

8. Final radiation surveys of the package surfaces per 10CFR71.47 [7.1.4] and 49CFR173.443 [7.1.2] are performed and if necessary, the HI-STAR 180D Packaging is further decontaminated to meet the survey requirements. Survey results are recorded in the shipping documents.

9. For packages containing HBF, the final radiation survey shall include the dose rate measurements required by the post-shipment fuel integrity acceptance test specified in

Chapter 8, Subsection 8.1.8 of this SAR. The final location of measurements and the measurements shall be recorded in the shipping documents.

10. The surface temperatures of the accessible areas of the package are measured if to confirm temperatures are within 10CFR71.43 requirements, if the personnel barrier will not be used.
11. For packages containing HBF, surface temperatures are measured as required by the post-shipment fuel integrity acceptance test specified in Chapter 8, Subsection 8.1.8 of this SAR. The final location of measurements, ambient conditions (air temperature, date, time of day, and description of daylight (sunny, cloudy, overcast, in-shade or night time)) and the measurements shall be recorded in the shipping documents. Package surfaces shall be dry at the time of temperature measurements.
12. The personnel barrier is installed. The personnel barrier is optional if the package surface temperature and the dose rates without the personnel barrier are within 10CFR71.43 and 10CFR71.47 requirements, respectively; and no applicable 49CFR requirements are violated.
13. The assembled package is given a final inspection to verify that the following conditions for transport have been met (inspection steps may be performed in any order):
    a. Verify that required radiation survey results are properly documented on the shipping documentation.
    b. Perform a cask surface temperature check. The accessible surfaces of the Transport Package (impact limiters and personnel barrier) shall not exceed the exclusive use temperature limits of 49CFR173.442.
    c. Verify that all required leakage testing has been performed, the acceptance criteria have been met, and the results have been documented on the shipping documentation.
    d. Verify that the receiver has been notified of the impending shipment and that the receiver has the appropriate procedures and equipment available to safely receive and handle the Transport Package (10CFR20.1906(e)).
    e. Verify that the carrier has the written instructions and a list of appropriate contacts for notification of accidents or delays.
    f. Verify that the carrier has written instructions that the shipment is to be Exclusive Use in accordance with 49CFR173.441.
    g. Verify that route approvals and notification to appropriate agencies have been completed.
    h. Verify that the appropriate labels have been applied in accordance with 49CFR172.403 [7.1.1].
    i. Verify that the appropriate placards have been applied in accordance with 49CFR172.500.

j. Verify that all required information is recorded on the shipping documentation including information required by Appendix 7.D.

Following the above checks, the Transport Package is released for transport.

Table 7.1.1

HI-STAR 180D Package Torque Requirements (Note 6)

Fastener (See Note 1)	**Recommended Torque (N-m), τ** (See Note 2)	**Minimum Total Bolt Preload** kN (See Note 7)	**Comments**
Inner Closure Lid Bolts	1st Pass: Wrench Tight Intermediate Pass: 30% to 45% of final torque value Final Pass: See Note 3	42,600	See Figure 7.1.1 and Notes 4 and 5. Intermediate pass is final pass for empty but previously used packages
Outer Closure Lid Bolts	1st Pass: Wrench Tight Intermediate Pass: 30% to 45% of final torque value Final Pass: See Note 3	28,700	See Figure 7.1.1 and Notes 4 and 5. Intermediate pass is final pass for empty but previously used packages
Inner Closure Lid Port Cover Bolts	See Note 3	110	None
Outer Closure Lid Access Port Plug	See Note 3	22	None
Top Impact Limiter Attachment Bolts/Nuts	"Snug Tight"	N/A	None
Bottom Impact Limiter Attachment Bolts/Nuts	"Snug Tight"	N/A	None

Notes continued on next page:

Table 7.1.1

HI-STAR 180D Package Torque Requirements (continued)

Notes:

1. Fasteners shall be cleaned and inspected for damage or excessive wear (replaced if necessary) and coated with a light layer of lubricant, such as Fel-Pro Chemical Products, N-5000, Nuclear Grade Lubricant.
2. For conversion from Newton-meter (N-m) to foot pounds (ft-lb) divide by 1.356.
3. The nominal bolt torque, τ, is given by the semi-empirical formula (derived from Shigley, et. al.[1]),

   $\tau = (P_B)(K)(d)$

   where, K = Torque coefficient

   The torque coefficient, K, varies depending on bolt lubricant used (e.g. extremely effective lubricants such as Bowman Anti-Sieze have a K value = 0.12).

   P_B = Minimum Bolt Preload.

   d = Nominal bolt diameter (soft conversion between metric and US units is permitted)

   Fastener sizes are provided in the drawing package referenced in the CoC.
4. Detorquing shall be performed by turning the bolts counter-clockwise in 1/3 turn +/- 30 degrees increments per pass for three passes. The bolts may then be removed.
5. Values listed are for the minimum number of passes permitted. Additional intermediate passes are permitted.
6. For empty packages, alternate torque requirements may be used with Holtec approval.
7. To determine individual bolt preload required, divide the total shown by the number of bolts for the lid/cover.

[1] Shigley J. D. and Mischke C. R., "Mechanical Engineering Design", 5th Edition, pp 346-347, Mc Graw Hill (1989).

Table 7.1.2

Cask Drying Method and Dryness Criteria

Fuel Burnup (MWD/MTU)	**Heat Load (kW)**	**Method of Moisture Removal**
All Fuel Assembly Burnups	Up to design basis cask heat load in Table 7.D.1 Q_{DB}	Forced Helium Dehydration
		Vacuum Drying (Note 3)
Recommended Dryness Criteria (Note 1 and 2)		
Forced Helium Dehydration	Temperature or dew point of gas exiting the FHD demoisturizer, T_{FHD}	≤ -5.0°C (22.9°F)
	Duration of gas circulation at T_{FHD}	≥ 30 minutes
Vacuum Drying (continuous and cyclic)	Cask cavity vacuum pressure, P_{VAC}	≤ 0.4kPa (3 Torr)
	Duration of isolated cask cavity at P_{VAC}	≥ 30 minutes

Notes:
1. Alternate dryness criteria following the guidance of NUREG 1617, NUREG 1536, PNL-6365 (Knoll, 1987) may be permitted with Holtec approval.
2. Users shall refer to Table 7.1.3 for additional cask drying criteria.
3. Time limits may be applicable.

Table 7.1.3

Criteria Applicable to Cask Drying Operations

Criterion	Specification
Fuel Cladding Temperature Limit	400ºC (752ºF) (High Burnup Fuel)
	570°C (1058°F) (Moderate Burnup Fuel)
Fuel Cladding Temperature Excursion During Cycling	According to the guidance contained in ISG-11 Revision 3 or latest revision
Thermal Cycling	According to the guidance contained in ISG-11 Revision 3 or latest revision

Table 7.1.4

Cask Backfill Requirements

Cask Space	**Reference Pressure or Pressure Range**
Cask Cavity Space (Notes 1 and 2)	20 kPa (2.9 psia) to 200 kPa (29 psia) absolute pressure
Cask Inter-Lid Space (Notes 1 and 3)	0 kPa (0 psig) to 17.2 kPa (2.5 psig) gauge pressure
Inner Closure Lid Port Space	atmospheric
Recommended Backfill Gas	
Type	Helium
Reference Purity	99.99% Nom.

Notes:

1. The reference pressure is based on a reference cask space bulk temperature of ≥ 21.1ºC (70ºF)
2. Following cask drying operations, the gas temperature inside the cask cavity will be higher than 21.1ºC (70ºF); therefore, direct measurement of the gas temperature is not required. Use of pressure gauges to confirm that the cask cavity pressure is within the pressure range is sufficient to establish the proper backfill conditions.
3. For ambient temperatures above 21.1ºC (70ºF), the gas temperature in the inter-lid cavity will be higher than 21.1ºC (70ºF); therefore, direct measurement of the gas temperature is not required. Use of pressure gauges to confirm that the inter-lid cavity pressure is sufficient to establish the proper backfill conditions. For ambient temperatures below 21.1ºC (70ºF), the pressure range shown above may be adjusted based on the ratio between ambient temperature and 21.1ºC (70ºF) using the ideal gas law. Use of pressure gauges to confirm that the inter-lid cavity pressure is between the adjusted limits is sufficient to establish the proper backfill conditions.

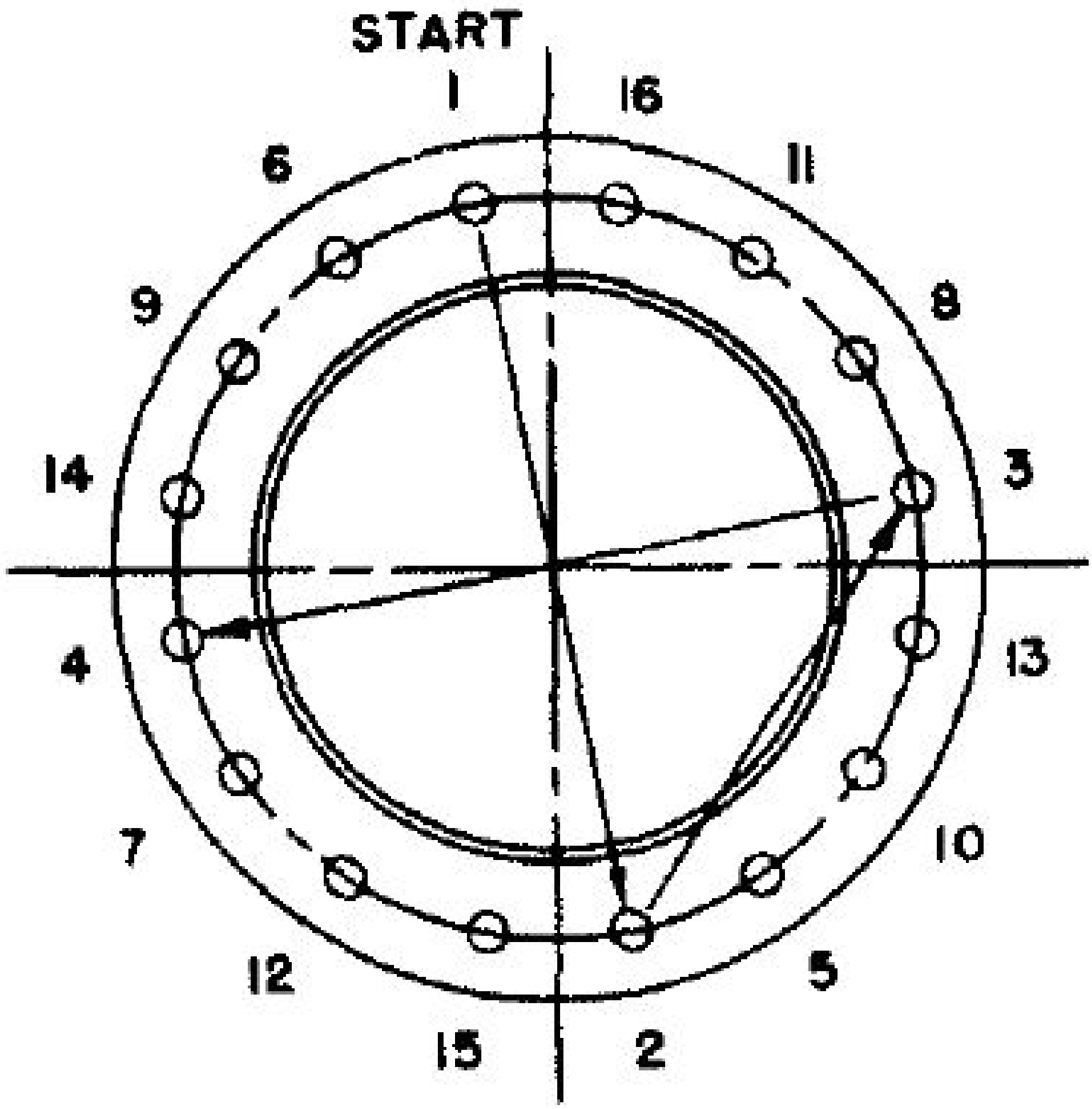

Note: It is important that all bolted joints be tightened uniformly and in a diametrically staggered pattern as illustrated above. Due to the large diameter of the closure lids and other factors, the standard star pattern with added flexibility is permitted with Holtec approval. Tools designed to torque more than one bolt at a time (e.g. bolts 1 and 2 simultaneously) may be implemented and are recommended as good ALARA practice. Alternate patterns shall be approved by Holtec.

FIGURE 7.1.1

RECOMMENDED BOLT TIGHTENING PROCEDURE

7.2 PACKAGE UNLOADING

In the event that the HI-STAR 180D Package needs to be unloaded, the essential elements required to prepare the package for fuel unloading, to cool the stored fuel assemblies in the cask, to flood the internal cavity, to remove the lids and bolts, to unload the spent fuel assemblies, and to recover the cask are described below.

7.2.1 Receipt of Package from Carrier

1. The HI-STAR 180D Package is received from the carrier and inspected to verify that there are no outward visual indications of impaired physical conditions except for superficial marks and dents. Any issues are identified to site management.
2. The personnel barrier, if used, is removed and the security seal installed on the top impact limiter is inspected to verify there was no tampering and that it matches the corresponding shipping documents.
3. Radiological surveys are performed in accordance with 49CFR173.443 [7.1.2] and 10CFR20.1906 [7.1.3]. If necessary, the HI-STAR 180D Packaging is decontaminated to meet survey requirements and notifications are made to affected parties. For packages containing HBF, the radiation survey shall include the dose rate measurements required by the post-shipment fuel integrity acceptance test specified in Chapter 8, Subsection 8.1.8 of this SAR. The location of measurements shall correspond to the same locations recorded for Subsection 7.1.3. The measurements shall be recorded in the shipping documents.
4. For packages containing HBF, surface temperature measurements shall include the surface temperature measurements required by the post-shipment fuel integrity acceptance test specified in Chapter 8, Subsection 8.1.8 of this SAR. The location of measurements shall correspond to the same locations recorded for Subsection 7.1.3. Ambient conditions (air temperature, date, time of day and description of daylight (sunny, cloudy, overcast, in-shade or night time)) and the measurements shall be recorded in the shipping documents. Package surfaces shall be dry at the time of temperature measurements.

ALARA Warning:
Dose rates around the unshielded bottom end of the HI-STAR 180D cask may be higher that other locations around the cask. After the impact limiter is removed, the cask should be upended promptly. Personnel should remain clear of the bottom of the unshielded cask and exercise other appropriate ALARA controls.

5. The impact limiters and tie-down system are removed. The radial spacers are removed from the top and bottom of the cask.

6. The cask is visually inspected to verify there are no outward visual indications of impaired physical conditions and a radiation survey and a removable contamination survey are performed to establish appropriate radiological controls. Any issues are identified to site management.

7. The trunnion hole plugs, if used, are removed and the cask trunnions are installed. The cask is upended and returned to the fuel building or other unloading area.

8. The cask is placed in the designated preparation area.

7.2.2 Removal of Contents

1. The outer lid access port cover is removed and a gas sample is drawn from the inter-lid space to determine radiological conditions.

2. The inter-lid space gas is handled in accordance with Radiation Protection directions and the outer closure lid is removed.

3. The inner closure lid port covers are removed to access the vent and drain ports.

ALARA Warning:
Gas sampling is performed to assess the condition of the fuel cladding. If a leak is discovered in the fuel cladding, the user's Radiation Control organization may require special actions to vent the cask cavity.
Caution:
An inert gas must be used any time the fuel is not covered with water to prevent oxidation of the fuel cladding. The fuel cladding is not to be exposed to air at any time during unloading operations.

4. A temporary attachment is connected to the vent port to open the vent port tube cap/plug and a gas sample from inside the cask cavity is collected. A gas sample analysis is performed to assess the condition of the fuel assembly cladding. As necessary during preparation for lid removal, the gas inside the cask cavity is handled/vented to an approved location. Depending on cask cavity pressure, the cavity may require additional backfill or venting to equalize its pressure to atmospheric.

5. If the cask is to be unloaded under water, the cask is filled with water at a controlled rate to minimize thermal shock to the fuel assemblies and to avoid over-pressurizing the cask from the formation of steam. The effluent is directed to the spent fuel pool or other approved discharge point.

6. If the cask is not immediately moved to the spent fuel pool, water is circulated through the cask to cool the contents and allow for establishment of a Time-To-Boil time limit. The user performs a site-specific Time-to-Boil evaluation to determine a time limitation to ensure that water boiling will not occur in the cask prior to placement of the cask in the spent fuel pool. If it appears that the Time-to-Boil limit will be exceeded prior to

placement of the cask in the spent fuel pool, the user shall take appropriate action to circulate water through the cask cavity to reset the Time-to-Boil clock.

7. Inner closure lid bolts may be removed at any time from after the internal cavity pressure is equalized until the time the inner closure lid is to be removed. In addition, the inner closure lid bolts are removed either before the cask is placed in the spent fuel pool or other fuel unloading area or after placement of the cask in one of these areas.

ALARA Note:
Wetting the components that enter the spent fuel pool may reduce the amount of decontamination work to be performed later.

8. The lift attachment is engaged to the lifting trunnions and the cask is placed in the spent fuel pool or other appropriate unloading area. The inner closure lid is removed.

9. All fuel assemblies are returned to the spent fuel storage racks and the cask fuel cells are vacuumed to remove any assembly debris and crud.

10. The fuel cells are inspected for any remaining items to be removed as appropriate.

ALARA Warning:
Activated debris may have settled on flat surfaces of the cask during fuel unloading. Surfaces suspected of carrying activated debris should be kept under water until a preliminary dose rate scan clears the cask for removal. To reduce contamination of the cask, the surfaces of the cask and lift yoke should be kept wet until decontamination can begin.

11. The cask is returned to the designated preparation area and any water is pumped back into the spent fuel pool, liquid radwaste system or other approved location as necessary.

12. The cask is decontaminated as directed by site Radiation Protection personnel. Outer surfaces of the cask are decontaminated to remove surface contamination to the level necessary to allow for proper cask transport, loading, or storage as applicable.

7.3 PREPARATION OF EMPTY PACKAGE FOR TRANSPORT

7.3.1 Overview of Empty Package Transport

The essential elements and minimum requirements for preparing an empty package (previously used) for transport are similar to those required for transporting the loaded package with some differences. A survey for removable contamination is performed to verify that the removable contamination on the internal and external surfaces of the cask is ALARA and that the limits of 49CFR173.428 [7.1.2] and 10CFR71.87(i) [7.1.4] are met. At the user's discretion, impact limiters and/or personnel barrier are installed. The procedures provided herein describe the installation of the impact limiters and personnel barrier. These steps may be omitted, as appropriate.

7.3.2 Preparation for Empty Package Shipment

1. The containment closure flange inner closure lid sealing surface protector is removed from the cask, if necessary.

2. The cask is surveyed for contamination and verified to be empty and contain less than 15 gm U-235 in accordance with 49CFR173.421(a)(5).

3. The inner closure lid is installed and the bolts are torqued. See Table 7.1.1 for torque requirements.

4. The inner closure lid port covers are installed if necessary.

5. The containment flange outer closure lid sealing surface protector is removed, if necessary, the outer closure lid is installed, and the bolts are torqued. See Table 7.1.1 for torque requirements. If desired, a security seal may be attached to the outer closure lid bolts.

6. The outer closure lid access port plug and access port cover are installed if necessary.

7. The cask is downended and positioned on the transport equipment.

8. A final inspection of the cask is performed and includes the following:

   - A final survey for removable contamination on the accessible external surfaces of the cask in accordance with 49CFR173.443(a). If necessary, the cask is decontaminated to meet the survey requirements.

   - A radiation survey of the cask to confirm that the radiation levels on any external surface of the cask do not exceed the levels required by 49CFR173.421(a)(2). Any issues are identified to site management and the cask is decontaminated as directed by site radiation protection.

   - A visual inspection of the cask to verify that there are no outward visual indications of impaired physical condition except for superficial marks and dents and that the empty package is securely closed in accordance with 49CFR173.428(b).

- Verification that the cask neutron shield pressure relief devices are installed, are intact and are not covered by tape or other covering.

9. If necessary, the cask trunnions are removed, the trunnion hole plugs are installed, the radial spacers are installed, the impact limiters are installed and the impact limiter bolts/nuts are torqued. (See Table 7.1.1 for torque requirements.)

10. If desired, a security seal is installed on the top impact limiter.

11. Final radiation surveys of the empty package surfaces are performed per 10CFR71.47, and 49CFR173.428(a).

12. If desired, the personnel barrier and personnel barrier locks are installed and the personnel barrier keys are transferred to the carrier.

13. A final check to ensure that the empty package is ready for release is performed and includes the following checks:

    - Verification that the receiver has been notified of the impending shipment.
    - Verification that any labels previously applied in conformance with Subpart E of 49CFR172 [7.1.1] have been removed, obliterated, or covered and the "Empty" label prescribed in 49CFR172.450 is affixed to the packaging in accordance with 49CFR173.428(e).
    - Verification that the empty package for shipment is prepared in accordance with 49CFR173.422.
    - Verification that all required information is recorded on the shipping documentation.

14. The empty package is then released for transport.

7.4 OTHER OPERATIONS

There are no other operations for the HI-STAR 180D Package with regard to provisions for any special operational controls (e.g., route, weather, shipping time restrictions, etc.). Essential operations and conditions are detailed in this chapter.

CHAPTER 7 REFERENCES

The following generic industry and Holtec produced references may have been consulted in the preparation of this document. Where specifically cited, the identifier is listed in the SAR text or table.

[7.1.1] U.S. Code of Federal Regulations, Title 49 “Transportation”, Part 172 "Hazardous Materials Table, Special Provisions, Hazardous Materials Communications, Emergency Response Information, Training Requirements and Security Plans."

[7.1.2] U.S. Code of Federal Regulations, Title 49 “Transportation”, Part 173, "Shippers – General Requirements for Shipments and Packagings,"

[7.1.3] U.S. Code of Federal Regulations, Title 10, “Energy”, Part 20 "Standards for Protection against Radiation".

[7.1.4] U.S. Code of Federal Regulations, Title 10, “Energy”, Part 71 "Packaging and Transportation of Radioactive Material".

APPENDIX 7.A

GENERAL WEIGHTS AND ILLUSTRATIONS OF TYPICAL LOADING OPERATIONS

Table 7.A.1: General Weights of HI-STAR 180D

Item	**Value** (kg)
Maximum Gross Transport Weight of HI-STAR 180D Package (no Personnel Barrier) – Note 1	125,000
Nominal Empty Packaging Weight (with F-37 Fuel Basket and no Personnel Barrier) – Note 2 and 3	106,200
Nominal Empty Cask (with F-37 Fuel Basket) – Note 2 and 3	80,900
Nominal Empty Cask (no basket or shims) – Note 2	73,000

Notes:

1. The Maximum Gross Transport Weight is a condition of the CoC.
2. Weight is representative based upon CAD models and provided for information only. Weights include cask lids and bolting. Lifting, handling and tie down evaluations shall be performed using bounding weights.
3. The weight of the F-32 fuel basket with basket shims is less than the weight of the F-37 fuel basket with basket shims.

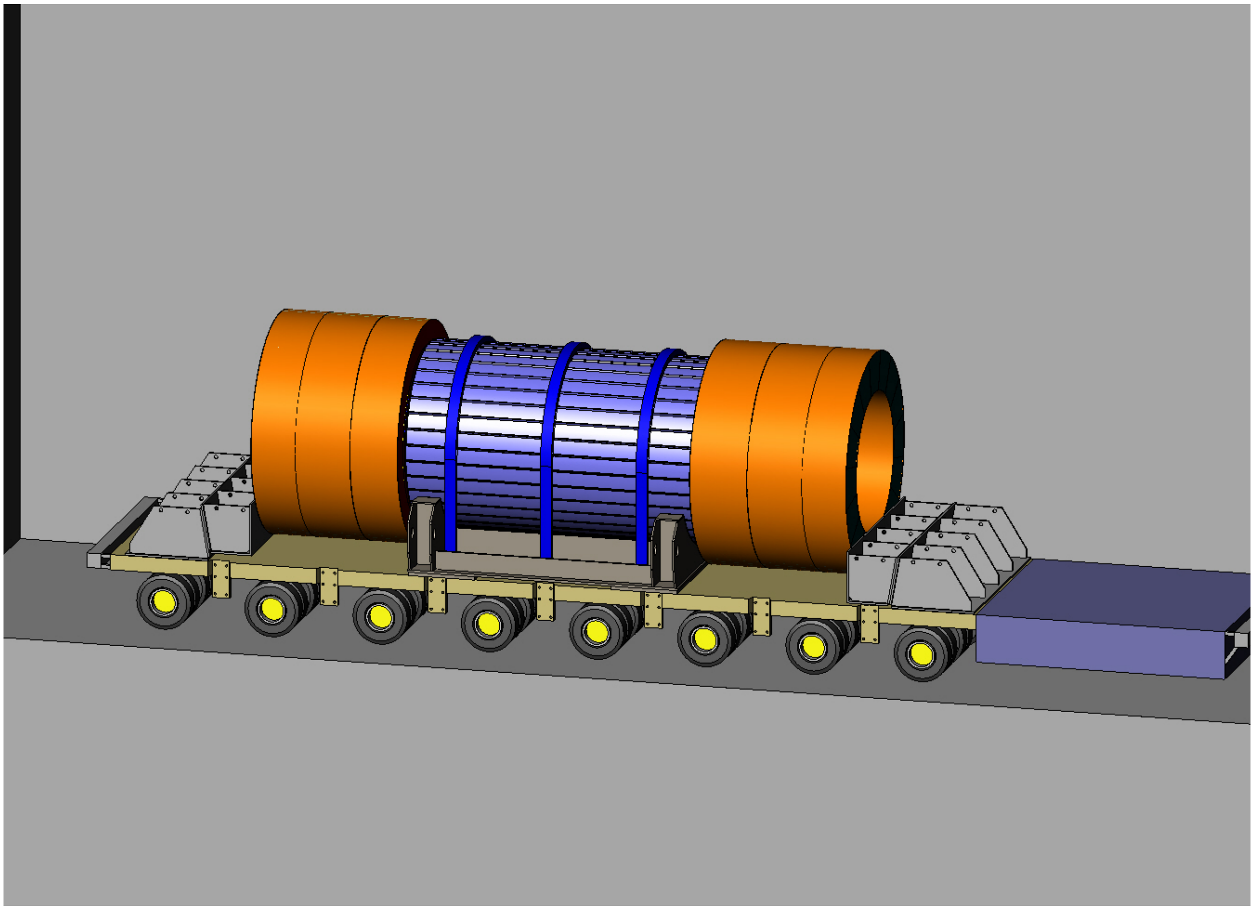

FIGURE 7.A.1: GENERAL ARRANGEMENT OF THE HI-STAR 180D ON A TRANSPORT VEHICLE WITH IMPACT LIMITER, AND TIE-DOWNS ATTACHED. PERSONNEL BARRIER NOT INSTALLED (EXAMPLE ONLY, SHOWN FOR ILLUSTRATION ONLY)

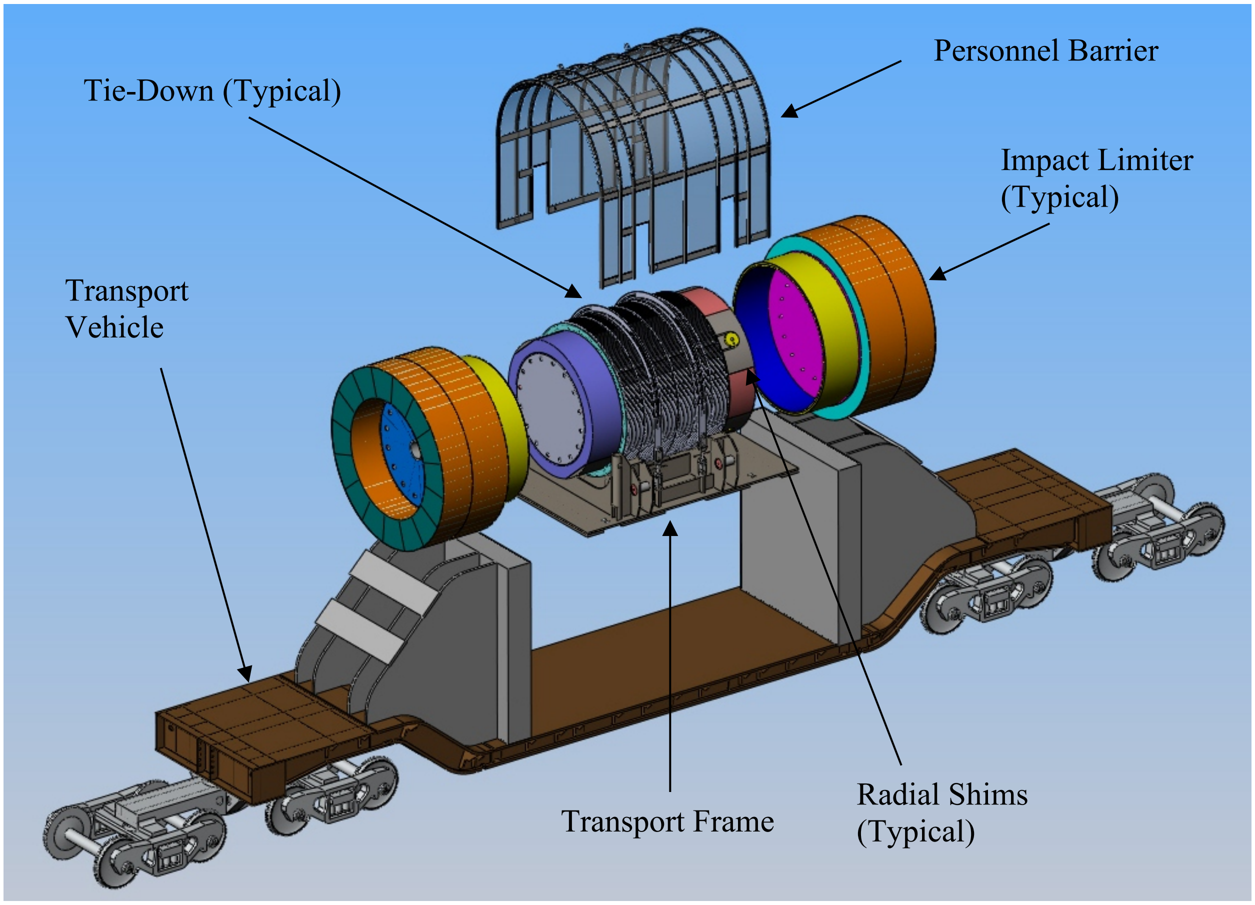

FIGURE 7.A.2: HI-STAR 180D TRANSPORT ASSEMBLY ON RAIL CAR (EXAMPLE ONLY, SHOWN FOR ILLUSTRATION ONLY)

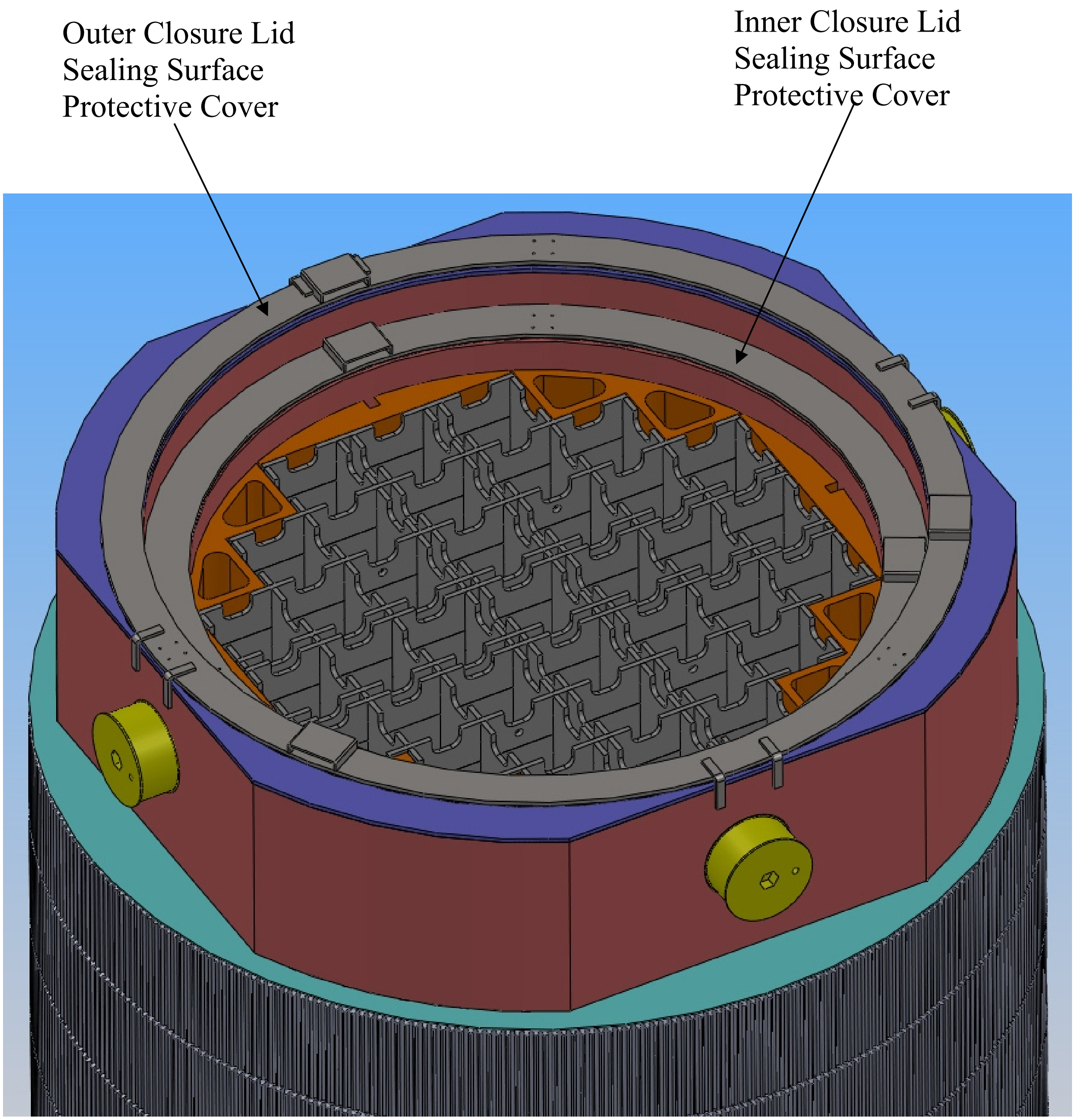

FIGURE 7.A.3: HI-STAR 180D SHOWN WITH INNER AND OUTER CLOSURE LIDS REMOVED AND SEALING SURFACE PROTECTIVE COVERS INSTALLED ON THE CONTAINMENT CLOSURE FLANGE (SEALING SURFACE PROTECTORS SHOWN FOR EXAMPLE ONLY AND MAY VARY IN ACTUAL CONFIGURATION DETAILS)

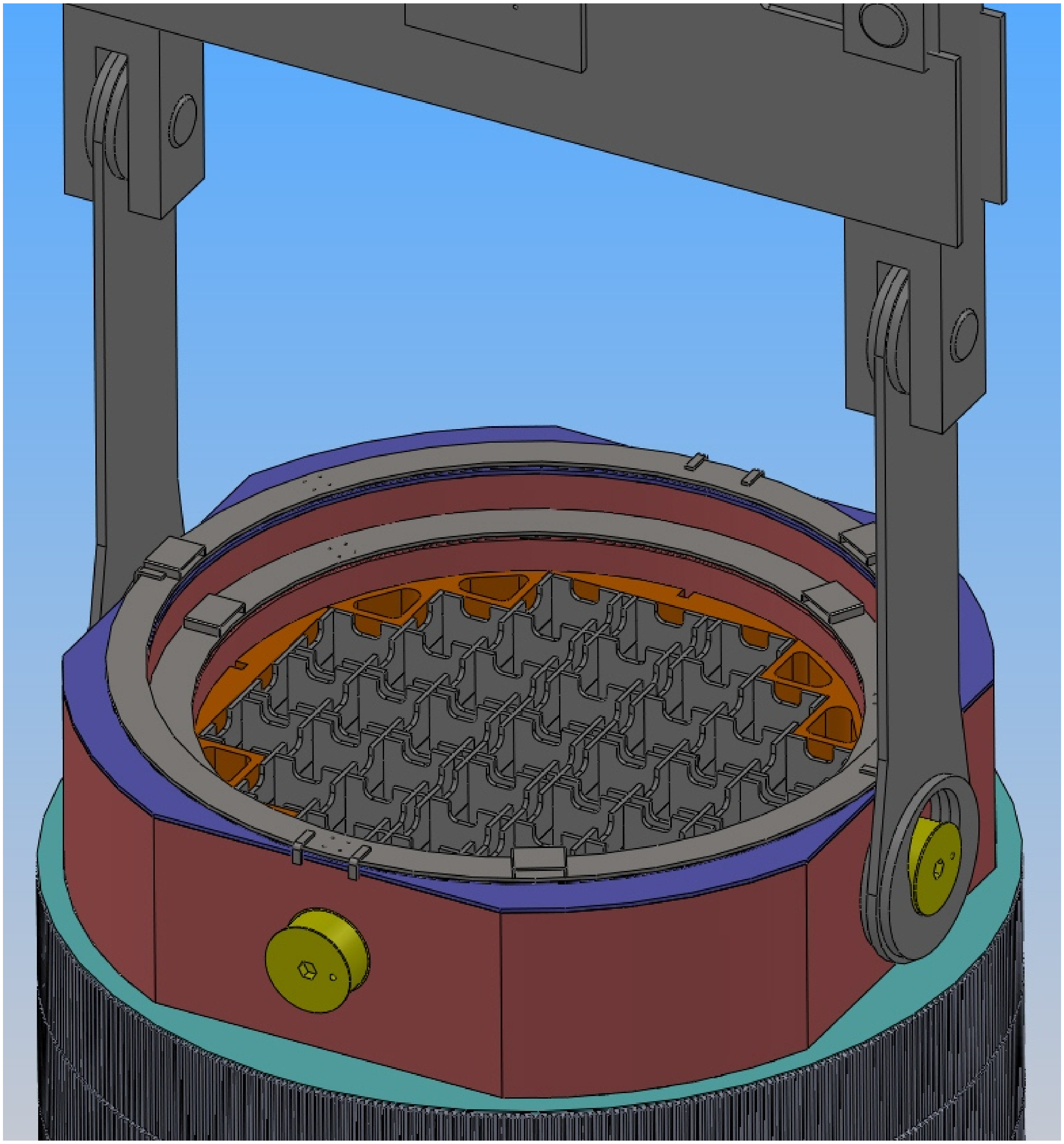

FIGURE 7.A.4: HI-STAR 180D SHOWN BEING LOADED INTO THE SPENT FUEL POOL (LIFTING ATTACHMENTS ARE SHOWN FOR ILLUSTRATIVE PURPOSES ONLY, FINAL CONFIGURATION OF LIFT ATTACHMENTS WILL BE DETERMINED BASED ON PLANT SYSTEMS)

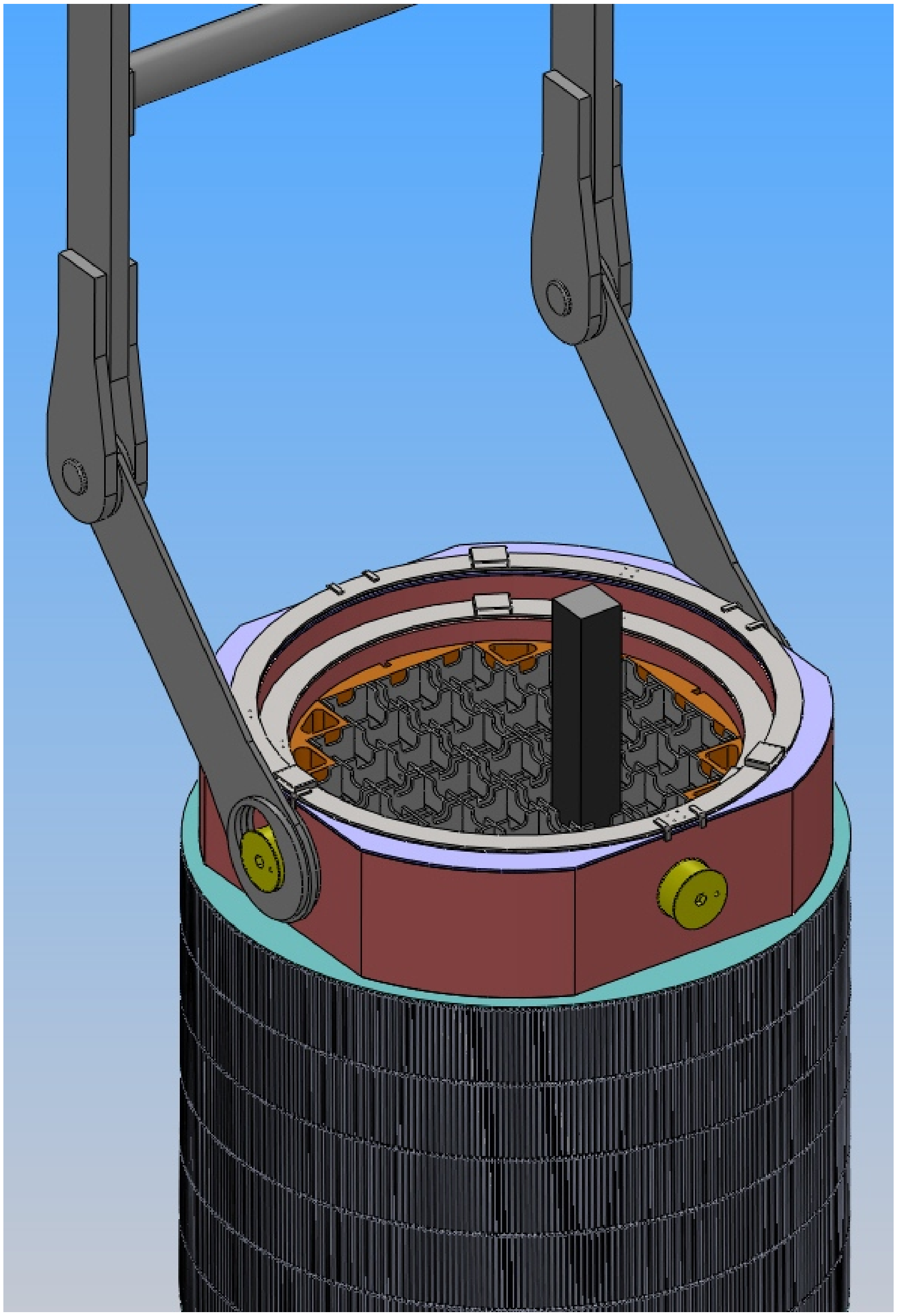

FIGURE 7.A.5: SPENT FUEL ASSEMBLY LOADING IN THE HI-STAR 180D (EXAMPLE ONLY, SHOWN FOR ILLUSTRATION ONLY)

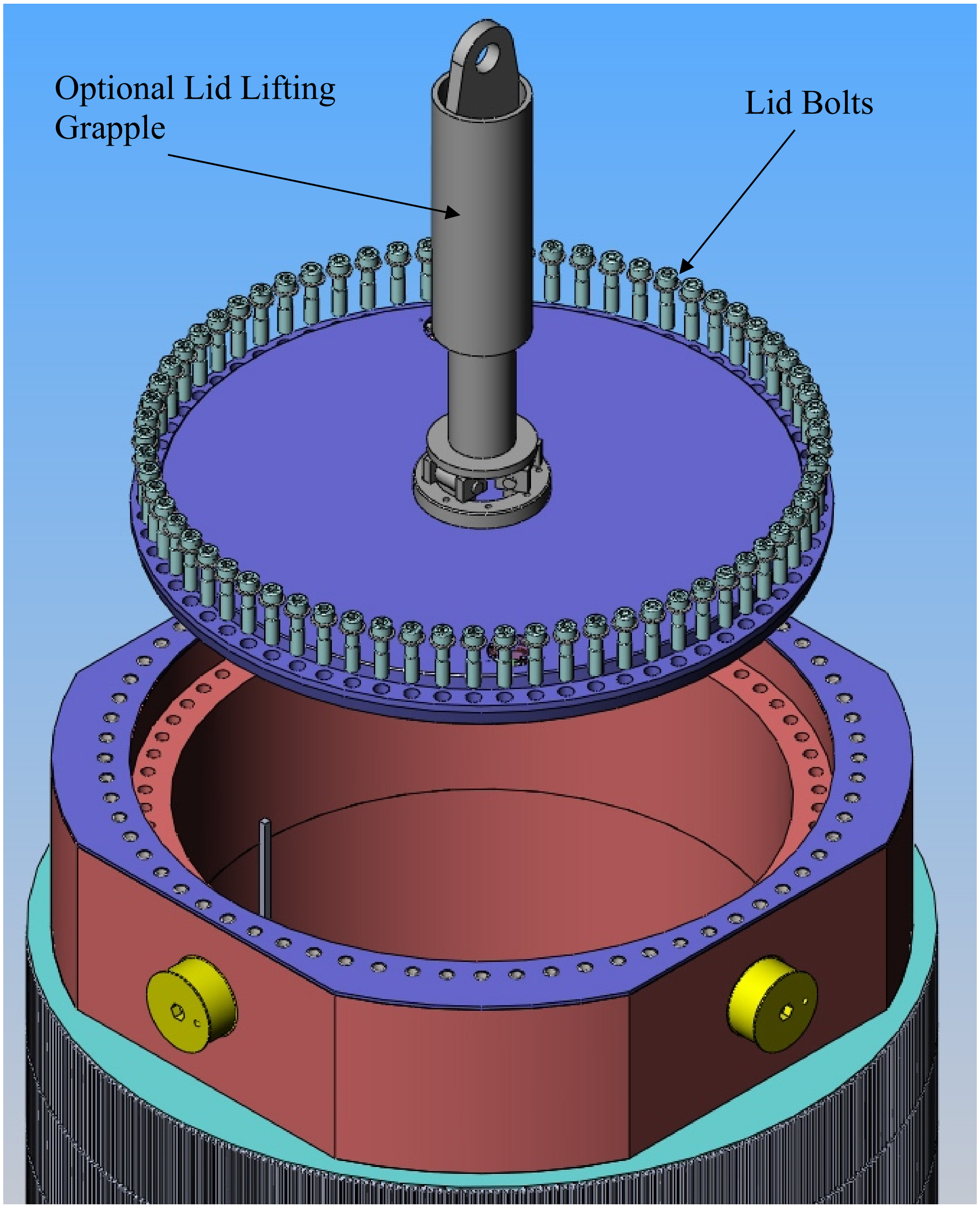

FIGURE 7.A.6: HI-STAR 180D INNER CLOSURE LID, BOLTS AND OPTIONAL LID LIFTING GRAPPLE ASSEMBLY (EXAMPLE ONLY, SHOWN FOR ILLUSTRATION ONLY)

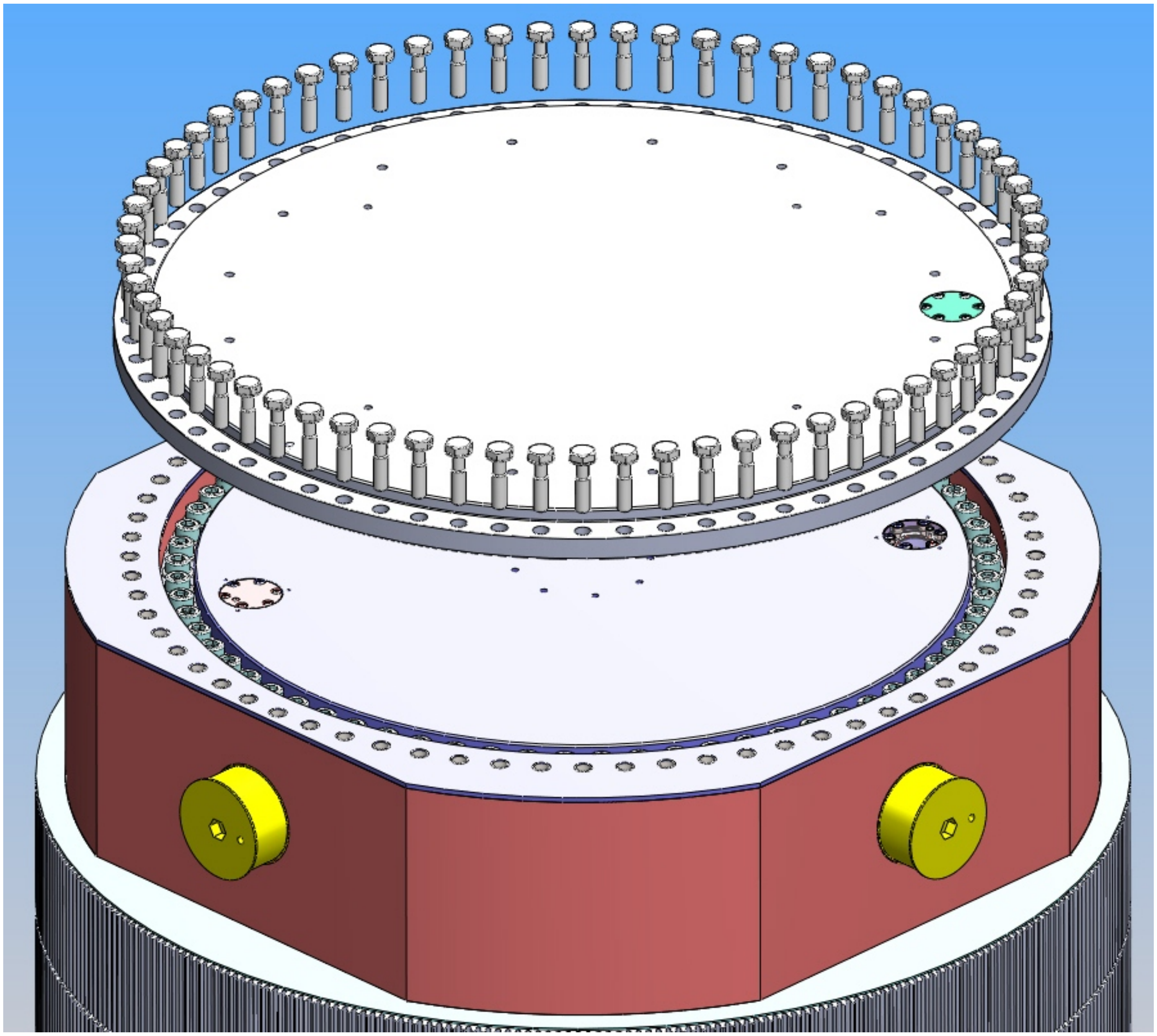

FIGURE 7.A.7: HI-STAR 180D OUTER CLOSURE LID EXPLODED VIEW (EXAMPLE ONLY, SHOWN FOR ILLUSTRATION ONLY)

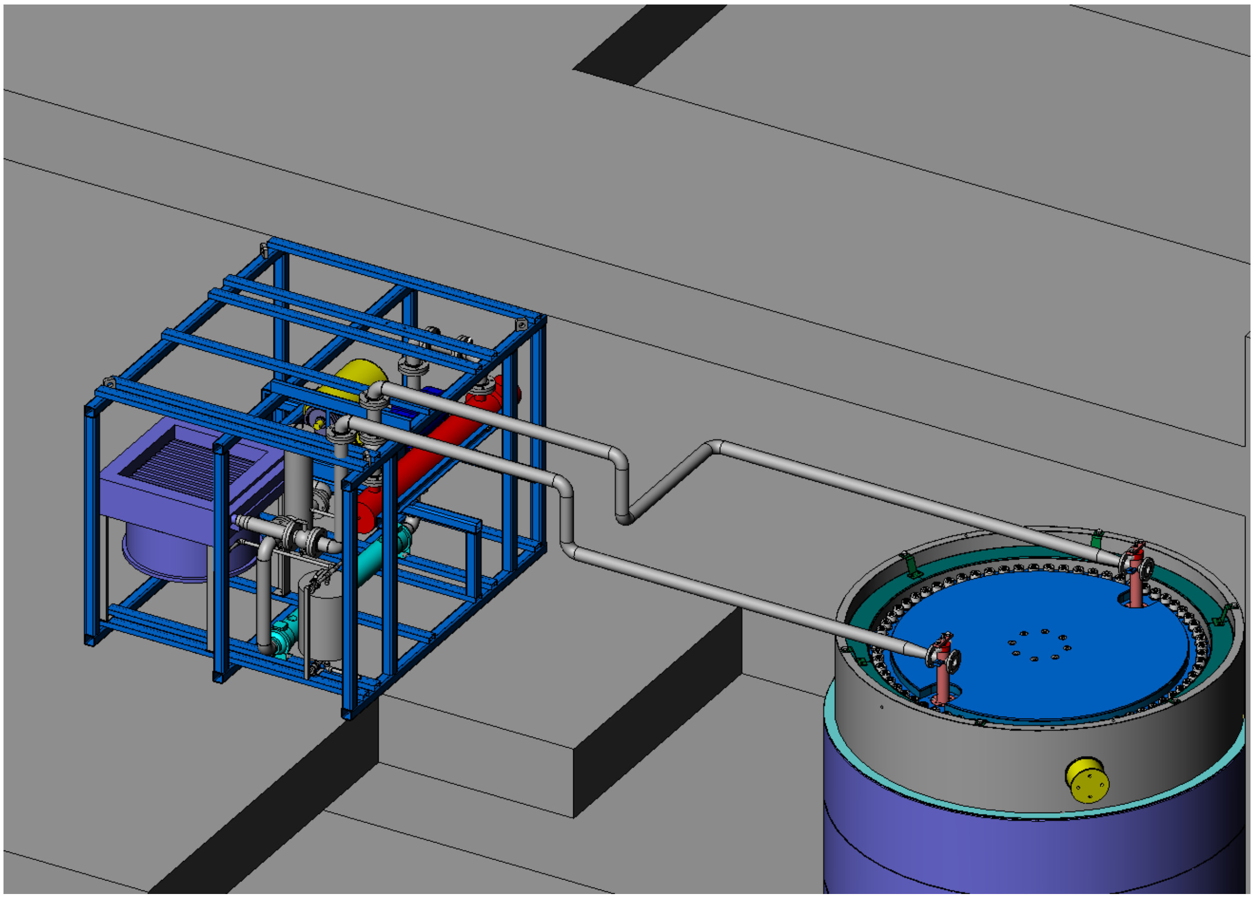

FIGURE 7.A.8: HI-STAR 180D SHOWN DURING DEWATERING, DRYING AND BACKFILL OPERATIONS (EXAMPLE CONFIGURATION FOR ILLUSTRATION ONLY, ACTUAL CONFIGURATION IS DEPENDENT UPON PLANT SYSTEMS)

APPENDIX 7.B AND APPENDIX 7.C

Intentionally Not Used

APPENDIX 7.D

CONTENT CONDITIONS OF THE HI-STAR 180D PACKAGE

Note: This Appendix is an integral part of the Certificate of Compliance (CoC) of the package.

Table 7.D.1

PWR Fuel Assembly Characteristics

Fuel Assembly Type	14x14
No. of Fuel Rod Locations	179
Design Initial Heavy Metal Mass (kg)	275 Max.
Fuel Rod Clad O.D. (mm)	≥10.68 Nom.
Fuel Rod Clad I.D. (mm)	≤9.68 Nom.
Fuel Pellet Dia. (mm)	≤9.344 Nom.
Fuel Rod Pitch (mm)	≤14.12 Nom.
Active Fuel Length (mm)	≤2428 Nom.
No. of Guide and/or Instrument Tubes	17
Guide/Instrument Tube Thickness (mm)	≥0.36 Nom. (Guide) ≥0.525 Nom. (Instrument)
Length of Longest Unirradiated Fuel Assembly (mm)	2926 Nom.
Minimum Cooling Time for Assemblies	Per Table 7.D.2 (F-32) or Table 7.D.3 (F-37)
Maximum Fuel Assembly Mass (kg)	400
Maximum Fuel Assembly Initial Enrichment	4.55 wt% ^{235}U
Maximum Overall Cask Heat Load (kW)	F-32: 33.08 F-37: 36.4

Note: All dimensions are design nominal values. Maximum and minimum dimensions are specified to bound variations in design nominal values

Table 7.D.2: F-32 Loading Pattern

Loading Pattern A for the F-32 Basket					
Region	Maximum Decay Heat Load per Assembly (kW)	Maximum Burnup (GWd/mtU)	Minimum Enrichment (wt%)	Minimum Cooling Time (years)	Alternative Fuel Specification (Table 7.D.4)
1	1	55	4.25	6	F-32-A1
2	1	55	4.25	6	F-32-A2
3	1	55	4.25	6	F-32-A3
4	1	55	4.25	6	F-32-A4
5	1	55	4.25	6	F-32-A5
6	1	55	4.25	6	F-32-A6
7	1	55	4.25	6	F-32-A7
8	1	55	4.25	6	F-32-A8

Loading Pattern B for the F-32 Basket						
Region	Maximum Decay Heat Load per Assembly (kW)		Maximum Burnup (GWd/mtU)	Minimum Enrichment (wt%)	Minimum Cooling Time (years)	Alternative Fuel Specification (Table 7.D.4)
	Option 1S	Option 2S				
1	1.46	1.45	53.5	4.25	3.83	F-32-B1
2	0.85	0.87	53.5	4.25	4.42	F-32-B2
3	0.6	0.8	48	4.25	7.50	F-32-B3
4	0.85	0.8	54	4.25	8.50	F-32-B4
5	1.35	1.15	51	4.25	3.42	F-32-B5
6	0.85	0.87	54	4.25	6.5	F-32-B6
7	0.85	0.8	40	4.25	3.42	F-32-B7
8	1.46	1.45	54.5	4.25	3.25	F-32-B8

Table 7.D.3: F-37 Loading Pattern

Loading Pattern A for the F-37 Basket					
Region	Maximum Decay Heat Load per Assembly (kW)	Maximum Burnup (GWd/mtU)	Minimum Enrichment (wt%)	Minimum Cooling Time (years)	Alternative Fuel Specification (Table 7.D.4)
1	0.85	50	4.25	5	F-37-A1
2	1	55	4.25	5	F-37-A2
3	0.85	50	4.25	5	F-37-A3
4	0.85	50	4.25	5	F-37-A4
5	0.85	50	4.25	5	F-37-A5
6	1	55	4.25	5	F-37-A6
7	0.85	50	4.25	5	F-37-A7
8	0.85	50	4.25	5	F-37-A8
9	1	55	4.25	5	F-37-A9

Loading Pattern B for the F-37 Basket						
Region	Maximum Decay Heat Load per Assembly (kW)		Maximum Burnup (GWd/mtU)	Minimum Enrichment (wt%)	Minimum Cooling Time (years)	Alternative Fuel Specification (Table 7.D.4)
	Option 1S	Option 2S				
1	1.45	1.46	27.5	4.25	1.75	F-37-B1
2	1	1.2	54	4.25	4.50	F-37-B2
3	0.7	0.7	54	4.25	9.50	F-37-B3
4	0.4	0.45	30	4.25	4.08	F-37-B4
5	0.85	0.5	51	4.25	5.50	F-37-B5
6	1.35	1.35	53.5	4.25	3.17	F-37-B6
7	0.7	0.7	48	4.25	6.50	F-37-B7
8	0.85	1.1	54.5	4.25	6.00	F-37-B8
9	1.25	1.25	54.5	4.25	3.67	F-37-B9

Table 7.D.3: F-37 Loading Pattern (continued)

Loading Pattern C for the F-37 Basket						
Region	Maximum Decay Heat Load per Assembly (kW)		Maximum Burnup (GWd/mtU)	Minimum Enrichment (wt%)	Minimum Cooling Time (years)	Alternative Fuel Specification (Table 7.D.4)
	Option 1S	Option 2S				
1	1.45	1.46	52	4.25	3.08	F-37-C1
2	1	1.2	47.5	4.25	2.08	F-37-C2
3	0.7	0.7	45	4.25	2.00	F-37-C3
4	0.4	0.45	40	4.25	6.00	F-37-C4
5	0.85	0.5	40	4.25	3.50	F-37-C5
6	1.35	1.35	48.5	4.25	2.50	F-37-C6
7	0.7	0.7	45	4.25	3.58	F-37-C7
8	0.85	1.1	45.5	4.25	3.25	F-37-C8
9	1.25	1.25	45	4.25	2.25	F-37-C9

Table 7.D.4: Alternative Fuel Specifications (F-32-A)

Maximum Burnup	Minimum Enrichment	F-32-A1	F-32-A2	F-32-A3	F-32-A4	F-32-A5	F-32-A6	F-32-A7	F-32-A8
(MWd/mtU)	(wt% ^{235}U)	Cooling Time in Years							
55000	4.25	6	6	6	6	6	6	6	6
55000	4.5	5.5	4.5	4.75	6	5.5	4.5	6	5.5
54500	4.25	--	5.5	5.5	--	--	5.5	--	--
54500	4.5	--	4.08	4.33	5.5	4.92	4	5.5	--
54000	4.25	5.5	4.92	--	--	5.5	4.83	--	5.5
54000	4.5	5	3.67	4	--	4.67	3.67	--	4.92
53500	4.25	--	4.42	4.67	--	--	4.42	--	--
53500	4.5	4.83	3.33	3.75	--	4.5	3.33	--	4.83
53000	4.25	--	4	4.25	5.5	4.83	4	5.5	--
53000	4.5	4.67	3.08	3.42	--	4.33	3	--	4.67
52500	4.25	4.92	3.67	3.92	--	4.58	3.58	--	4.92
52500	4.5	4.5	2.83	3.17	5	4.17	2.75	--	4.5
52000	4.25	4.75	3.25	3.67	--	4.42	3.25	--	4.75
52000	4.5	4.42	2.58	3	4.92	4	2.58	4.92	4.42
51500	4.25	4.58	3	3.42	--	4.25	3	--	4.58
51500	4.5	4.33	2.33	2.75	4.83	3.92	2.33	4.83	4.25
51000	4.25	4.5	2.75	3.17	5	4.08	2.75	5	4.42
51000	4.5	4.17	2.17	2.58	4.75	3.75	2.17	4.75	4.17
50500	4.25	4.33	2.5	2.92	4.83	4	2.5	4.92	4.33
50500	4.5	4.08	2	2.42	4.67	3.67	2	4.67	4.08
50000	4.25	4.25	2.33	2.75	4.75	3.83	2.33	4.83	4.25
50000	4.5	4	1.92	2.33	4.58	3.58	1.92	4.58	4
49500	4.25	4.17	2.17	2.58	4.67	3.75	2.08	4.75	4.08
49500	4.5	3.92	1.75	2.17	4.5	3.5	1.75	4.5	3.92
49000	4.25	4	2	2.42	4.58	3.58	2	4.67	4
49000	4.5	3.83	--	2.08	4.42	3.42	--	--	3.83
48500	4.25	3.92	1.83	2.25	4.5	3.5	1.83	4.58	3.92
48500	4.5	3.75	--	1.92	4.33	3.33	--	4.42	3.75
48000	4.25	3.83	1.75	2.08	4.42	3.42	1.75	4.5	3.83
48000	4.5	3.67	--	1.83	4.25	3.25	--	4.33	3.67
47500	4.25	3.75	--	2	4.33	3.33	--	4.42	3.75
47500	4.5	3.58	--	1.75	--	3.17	--	4.25	3.58

Table 7.D.4: Alternative Fuel Specifications (F-32-A)

Maximum Burnup	Minimum Enrichment	F-32-A1	F-32-A2	F-32-A3	F-32-A4	F-32-A5	F-32-A6	F-32-A7	F-32-A8
(MWd/mtU)	(wt% ^{235}U)	Cooling Time in Years							
47000	4.25	3.67	--	1.92	--	3.25	--	4.33	3.67
47000	4.5	3.5	--	--	4.17	3.08	--	--	3.5
46500	4.25	--	--	1.83	4.25	3.17	--	4.25	3.58
46500	4.5	--	--	--	4.08	3	--	4.17	--
46000	4.25	3.58	--	1.75	4.17	3.08	--	--	3.5
46000	4.5	3.42	--	--	--	--	--	4.08	3.42
45500	4.25	3.5	--	--	4.08	--	--	4.17	--
45500	4.5	3.33	--	--	4	2.92	--	--	3.33
45000	4.25	3.42	--	--	--	3	--	4.08	3.42
45000	4.5	--	--	--	3.92	2.83	--	4	--
40000	4.25	3	--	--	3.58	2.5	--	3.67	2.92
40000	4.5	2.92	--	--	3.58	2.42	--	3.58	2.92
39000	4.25	2.92	--	--	3.5	2.42	--	3.58	--
39000	4.5	2.83	--	--	3.5	--	--	3.5	2.83
35000	4.25	2.67	--	--	3.25	2.25	--	3.33	2.67
35000	4.5	2.58	--	--	3.25	2.17	--	3.25	2.58
30000	4.25	2.42	--	--	3	2	--	3.08	2.42
30000	4.5	2.42	--	--	3	2	--	3	2.33
27500	4.25	2.25	--	--	2.92	1.92	--	2.92	2.25
27500	4.5	2.25	--	--	2.92	1.83	--	2.92	2.25
25000	4.25	2.17	--	--	2.75	1.75	--	2.83	2.17
25000	4.5	2.17	--	--	2.75	1.75	--	2.83	2.17
22500	4.25	2.08	--	--	2.67	--	--	2.67	2.08
22500	4.5	2.08	--	--	2.67	--	--	2.67	2.08
21500	4.25	--	--	--	2.58	--	--	--	2
21500	4.5	2	--	--	2.58	--	--	--	2
21000	4.25	2	--	--	--	--	--	--	--
21000	4.5	--	--	--	--	--	--	2.58	--
20000	4.25	--	--	--	--	--	--	2.58	--
20000	4.5	--	--	--	2.5	--	--	--	--
15500	4.25	1.75	--	--	2.33	--	--	2.33	1.75
15500	4.5	1.75	--	--	2.33	--	--	2.33	1.75

Table 7.D.4: Alternative Fuel Specifications*† (F-32-A continued)

Maximum Burnup	Minimum Enrichment	F-32-A1	F-32-A2	F-32-A3	F-32-A4	F-32-A5	F-32-A6	F-32-A7	F-32-A8
(MWd/mtU)	(wt% ^{235}U)	Cooling Time in Years							
15000	4.25	--	--	--	2.25	--	--	--	--
15000	4.5	--	--	--	2.25	--	--	--	--
10500	4.25	--	--	--	1.92	--	--	2	--
10500	4.5	--	--	--	1.92	--	--	2	--

* A dash in the table means that the burnup/enrichment combination is bounded by a higher burnup at the same enrichment. For example, the first dash under F-32-A3 means that a 54000/4.25 assembly would have a cooling time requirement of 5.5 years since this is the cooling time for a 54500/4.25 assembly.

† Double asterisks "**" in the table means not permitted for loading.

Table 7.D.4: Alternative Fuel Specifications (F-32-B)

Maximum Burnup	Minimum Enrichment	F-32-B1	F-32-B2	F-32-B3	F-32-B4	F-32-B5	F-32-B6	F-32-B7	F-32-B8
(MWd/mtU)	(wt% ^{235}U)	Cooling Time in Years							
55000	4.25	5.5	6	**	10	6.5	8.5	9.5	3.58
55000	4.5	3.92	4.5	**	8	4.58	6	7.5	3.17
54500	4.25	4.67	5.5	**	9	5.5	7.5	9	3.25
54500	4.5	3.58	4.08	**	7.5	4.25	5.5	7	3.08
54000	4.25	4.25	4.92	**	8.5	5	6.5	8	--
54000	4.5	3.25	3.67	**	7	3.83	4.92	6.5	--
53500	4.25	3.83	4.42	**	8	4.58	6	7.5	3.17
53500	4.5	3.17	3.33	**	6.5	3.67	4.5	6	3
53000	4.25	3.5	4	**	7.5	4.17	5.5	7	3.08
53000	4.5	3.08	3.08	**	6	3.5	4.08	5.5	2.92
52500	4.25	3.25	3.67	**	6.5	3.75	4.83	6.5	3
52500	4.5	--	2.83	**	5.5	3.42	3.67	--	--
52000	4.25	3.17	3.25	**	6	3.58	4.42	6	--
52000	4.5	3	2.58	**	--	3.33	3.33	--	2.83
51500	4.25	3.08	3	**	5.5	3.5	4	5.5	2.92
51500	4.5	2.92	2.33	12	5	3.25	3.08	4.92	--
51000	4.25	3	2.75	**	--	3.42	3.58	--	2.83
51000	4.5	--	2.17	11	4.83	3.17	2.83	4.75	2.75
50500	4.25	--	2.5	**	--	3.33	3.25	5	--
50500	4.5	2.83	2	10	4.67	3.08	2.58	4.58	--
50000	4.25	2.92	2.33	11.5	4.92	3.25	3	4.83	2.75
50000	4.5	--	1.92	9	4.5	3	2.42	4.42	2.67
49500	4.25	--	2.17	10.5	4.75	3.17	2.75	4.67	--
49500	4.5	2.75	1.75	8	4.33	--	2.25	4.25	--
49000	4.25	2.83	2	9.5	4.58	3.08	2.5	4.5	2.67
49000	4.5	--	--	7.5	4.25	2.92	2.08	4.17	2.58
48500	4.25	2.75	1.83	8.5	4.42	3	2.33	4.33	--
48500	4.5	2.67	--	7	4.17	2.83	1.92	4.08	--
48000	4.25	--	1.75	7.5	4.25	2.92	2.17	4.25	2.58
48000	4.5	--	--	6.5	4.08	2.75	1.83	--	2.5
47500	4.25	2.67	--	7	4.17	2.83	2	4.08	--
47500	4.5	2.58	--	6	4	--	1.75	4	--

Table 7.D.4: Alternative Fuel Specifications (F-32-B continued)

Maximum Burnup	Minimum Enrichment	F-32-B1	F-32-B2	F-32-B3	F-32-B4	F-32-B5	F-32-B6	F-32-B7	F-32-B8
(MWd/mtU)	(wt% ^{235}U)	Cooling Time in Years							
47000	4.25	--	--	6.5	4.08	--	1.83	--	2.5
47000	4.5	--	--	5.5	--	2.67	--	3.92	2.42
46500	4.25	2.58	--	6	4	2.75	1.75	4	--
46500	4.5	--	--	4.92	3.92	--	--	--	--
46000	4.25	--	--	5.5	--	2.67	--	3.92	--
46000	4.5	2.5	--	4.5	3.83	2.58	--	3.83	--
45500	4.25	--	--	--	3.92	--	--	--	2.42
45500	4.5	--	--	4.25	--	--	--	--	2.33
45000	4.25	2.5	--	4.67	--	2.58	--	3.83	--
45000	4.5	2.42	--	3.92	3.75	2.5	--	3.75	--
44500	4.25	--	--	4.33	3.83	--	--	--	2.33
44500	4.5	--	--	3.67	--	--	--	--	--
44000	4.25	2.42	--	4.08	3.75	2.5	--	3.75	--
44000	4.5	--	--	3.42	3.67	2.42	--	3.67	2.25
43500	4.25	--	--	3.75	--	--	--	--	--
43500	4.5	2.33	--	3.25	--	--	--	--	--
43000	4.25	--	--	3.5	3.67	2.42	--	3.67	2.25
43000	4.5	--	--	3.08	3.58	2.33	--	3.58	--
42500	4.25	2.33	--	3.33	--	--	--	--	--
42500	4.5	--	--	2.92	--	--	--	--	2.17
42000	4.25	--	--	3.17	3.58	2.33	--	3.58	--
42000	4.5	2.25	--	2.75	3.5	2.25	--	3.5	--
41500	4.25	--	--	3	--	--	--	--	2.17
41500	4.5	--	--	2.67	--	--	--	--	--
40000	4.25	2.25	--	2.5	3.5	2.25	--	3.42	--
40000	4.5	2.17	--	2.25	3.42	2.17	--	3.42	2.08
39500	4.25	2.17	--	2.42	3.42	2.17	--	--	2.08
39500	4.5	--	--	2.17	3.33	--	--	3.33	--
39000	4.25	--	--	2.33	--	--	--	--	--
39000	4.5	--	--	2.08	--	2.08	--	--	--
35000	4.25	2	--	1.75	3.17	1.92	--	3.17	1.92
35000	4.5	2	--	1.75	3.08	1.92	--	3.08	1.92

Table 7.D.4: Alternative Fuel Specifications (F-32-B continued)

Maximum Burnup	Minimum Enrichment	F-32-B1	F-32-B2	F-32-B3	F-32-B4	F-32-B5	F-32-B6	F-32-B7	F-32-B8
(MWd/mtU)	(wt% ^{235}U)	Cooling Time in Years							
30000	4.25	1.83	--	--	2.92	1.75	--	2.92	1.75
30000	4.5	1.83	--	--	2.92	1.75	--	2.92	1.75
28000	4.25	1.75	--	--	2.83	--	--	2.83	--
28000	4.5	1.75	--	--	2.83	--	--	2.83	--
27500	4.25	--	--	--	--	--	--	--	--
27500	4.5	--	--	--	2.75	--	--	2.75	--
25000	4.25	--	--	--	2.67	--	--	2.67	--
25000	4.5	--	--	--	2.67	--	--	2.67	--
22500	4.25	--	--	--	2.58	--	--	2.58	--
22500	4.5	--	--	--	2.58	--	--	2.58	--
22000	4.25	--	--	--	--	--	--	--	--
22000	4.5	--	--	--	2.5	--	--	2.5	--
21500	4.25	--	--	--	2.5	--	--	2.5	--
21500	4.5	--	--	--	--	--	--	--	--
20000	4.25	--	--	--	2.42	--	--	2.42	--
20000	4.5	--	--	--	2.42	--	--	2.42	--
16000	4.25	--	--	--	2.25	--	--	2.25	--
16000	4.5	--	--	--	2.25	--	--	2.25	--
15000	4.25	--	--	--	2.17	--	--	2.17	--
15000	4.5	--	--	--	2.17	--	--	2.17	--
10500	4.25	--	--	--	1.83	--	--	1.83	--
10500	4.5	--	--	--	1.83	--	--	1.83	--

Table 7.D.4: Alternative Fuel Specifications (F-37-A)

Maximum Burnup	Minimum Enrichment	F-37-A1	F-37-A2	F-37-A3	F-37-A4	F-37-A5	F-37-A6	F-37-A7	F-37-A8	F-37-A9
(MWd/mtU)	(wt% ^{235}U)	Cooling Time in Years								
55000	4.25	11	5	**	**	11	5	**	11	5
55000	4.5	9	3.83	12	11	9.5	4.33	11.5	9.5	4.42
54500	4.25	10.5	4.58	**	**	10.5	4.75	**	10.5	4.75
54500	4.5	8.5	3.5	11	10	8.5	4.17	10.5	8.5	4.25
54000	4.25	9.5	4.17	**	11.5	10	4.5	12	10	4.5
54000	4.5	8	3.25	10	9	8	4	9.5	8	4.08
53500	4.25	9	3.75	11.5	10.5	9	4.33	11	9	4.33
53500	4.5	7.5	2.92	9	8	7.5	3.83	8.5	7.5	3.92
53000	4.25	8.5	3.42	10.5	9.5	8.5	4.17	10.5	8.5	4.17
53000	4.5	7	2.75	8	7	7	3.75	8	7	3.83
52500	4.25	8	3.17	10	9	8	4	9.5	8	4
52500	4.5	6	2.5	7	6	6.5	3.58	7	6.5	3.67
52000	4.25	7	2.92	9	8	7.5	3.83	8.5	7.5	3.92
52000	4.5	5.5	2.33	6	5.5	6	3.5	6	6	3.58
51500	4.25	6.5	2.67	8	7	7	3.67	7.5	6.5	3.75
51500	4.5	--	2.17	5.5	5	5.5	3.42	5.5	5.5	3.5
51000	4.25	6	2.5	7	6	6	3.58	6.5	6	3.67
51000	4.5	4.92	2	4.75	4.75	5	3.33	4.58	5	3.42
50500	4.25	5.5	2.25	6	5.5	5.5	3.5	6	5.5	3.58
50500	4.5	4.75	1.92	4.25	4.5	4.92	3.25	4.17	4.92	3.33
50000	4.25	5	2.17	5	4.92	5	3.33	4.92	5	3.42
50000	4.5	4.67	1.75	3.92	4.25	4.75	3.17	3.83	4.83	3.25
49500	4.25	4.83	2	4.58	4.67	4.92	3.25	4.5	4.92	3.33
49500	4.5	4.58	--	3.58	4.08	4.67	3.08	3.5	4.75	3.17
49000	4.25	4.75	1.83	4.17	4.42	4.83	3.17	4.08	4.83	3.25
49000	4.5	4.42	--	3.25	3.83	4.58	3	3.17	4.67	3.08
48500	4.25	4.58	1.75	3.75	4.17	4.75	3.08	3.67	4.75	3.17
48500	4.5	4.33	--	3	3.67	4.5	2.92	2.92	4.58	3
48000	4.25	4.5	--	3.42	4	4.58	3	3.33	4.67	3.08
48000	4.5	4.25	--	2.83	3.5	4.42	2.83	2.75	4.5	2.92
47500	4.25	4.33	--	3.17	3.75	4.5	2.92	3.08	4.58	--
47500	4.5	4.17	--	2.58	3.33	4.33	--	2.5	--	--

Table 7.D.4: Alternative Fuel Specifications (F-37-A continued)

Maximum Burnup	Minimum Enrichment	F-37-A1	F-37-A2	F-37-A3	F-37-A4	F-37-A5	F-37-A6	F-37-A7	F-37-A8	F-37-A9
(MWd/ mtU)	(wt% ^{235}U)	Cooling Time in Years								
47000	4.25	4.25	--	2.92	3.58	4.42	--	2.83	--	3
47000	4.5	4.08	--	2.42	3.25	4.25	2.75	2.33	4.42	2.83
46500	4.25	4.17	--	2.67	3.42	4.33	2.83	2.58	4.5	2.92
46500	4.5	4	--	2.25	3.08	--	2.67	2.17	4.33	2.75
46000	4.25	4.08	--	2.5	3.33	--	2.75	2.42	4.42	2.83
46000	4.5	3.92	--	2.17	3	4.17	--	2	4.25	--
45500	4.25	4	--	2.33	3.17	4.25	2.67	2.25	4.33	--
45500	4.5	3.83	--	2	2.83	4.08	2.58	1.92	--	2.67
45000	4.25	3.92	--	2.17	3	4.17	--	2.08	4.25	2.75
45000	4.5	3.75	--	1.92	2.75	4	2.5	1.83	4.17	--
40000	4.25	3.33	--	1.75	2.08	3.67	2.25	1.75	3.83	2.33
40000	4.5	3.25	--	1.75	2	3.58	2.17	1.75	3.75	2.25
39000	4.25	3.25	--	--	2	3.58	2.17	--	3.75	2.25
39000	4.5	3.17	--	--	1.83	3.5	2.08	--	3.67	--
35000	4.25	3	--	--	1.75	3.25	1.92	--	3.5	2.08
35000	4.5	2.92	--	--	1.75	3.25	1.92	--	3.42	2
30000	4.25	2.67	--	--	--	3	1.75	--	3.17	1.83
30000	4.5	2.67	--	--	--	3	1.75	--	3.17	1.83
27500	4.25	2.58	--	--	--	2.92	--	--	3.08	1.75
27500	4.5	2.58	--	--	--	2.83	--	--	3.08	1.75
25000	4.25	2.5	--	--	--	2.75	--	--	3	--
25000	4.5	2.42	--	--	--	2.75	--	--	2.92	--
22500	4.25	2.33	--	--	--	2.67	--	--	2.83	--
22500	4.5	2.33	--	--	--	2.67	--	--	2.83	--
22000	4.25	--	--	--	--	2.58	--	--	--	--
22000	4.5	--	--	--	--	2.58	--	--	--	--
21000	4.25	--	--	--	--	--	--	--	2.75	--
21000	4.5	2.25	--	--	--	--	--	--	2.75	--
20000	4.25	2.25	--	--	--	2.5	--	--	--	--
20000	4.5	--	--	--	--	2.5	--	--	--	--

Table 7.D.4: Alternative Fuel Specifications (F-37-A continued)

Maximum Burnup	Minimum Enrichment	F-37-A1	F-37-A2	F-37-A3	F-37-A4	F-37-A5	F-37-A6	F-37-A7	F-37-A8	F-37-A9
(MWd/mtU)	(wt% ^{235}U)	Cooling Time in Years								
15500	4.25	2	--	--	--	2.25	--	--	2.5	--
15500	4.5	2	--	--	--	2.25	--	--	2.5	--
15000	4.25	--	--	--	--	--	--	--	2.42	--
15000	4.5	--	--	--	--	--	--	--	2.42	--
10500	4.25	1.75	--	--	--	1.92	--	--	2.08	--
10500	4.5	1.75	--	--	--	1.92	--	--	2.08	--

Table 7.D.4: Alternative Fuel Specifications (F-37-B)

Maximum Burnup	Minimum Enrichment	F-37-B1	F-37-B2	F-37-B3	F-37-B4	F-37-B5	F-37-B6	F-37-B7	F-37-B8	F-37-B9
(MWd/ mtU)	(wt% ^{235}U)	Cooling Time in Years								
55000	4.25	**	6	11	**	8.5	4.08	**	6	4
55000	4.5	11	4.17	8.5	**	6.5	3.17	**	5.5	3.25
54500	4.25	**	5	10	**	7.5	3.67	**	--	3.67
54500	4.5	10.5	3.75	8	**	--	3.08	**	4.92	3.17
54000	4.25	12	4.5	9.5	**	7	3.33	**	5.5	3.42
54000	4.5	10	3.42	7.5	**	6	3	**	4.67	3.08
53500	4.25	11	4.08	8.5	**	6.5	3.17	**	--	3.17
53500	4.5	9	3.17	7	**	--	2.92	**	4.5	3
53000	4.25	10.5	3.75	8	**	6	3.08	**	4.83	3.08
53000	4.5	8.5	2.92	6	**	5.5	2.83	**	4.33	2.92
52500	4.25	9.5	3.42	7	**	--	3	**	4.67	3
52500	4.5	8	2.67	5.5	**	--	--	**	4.17	2.83
52000	4.25	9	3.08	6.5	**	5.5	2.92	**	4.42	2.92
52000	4.5	7.5	2.5	4.92	**	--	2.75	11.5	4.08	2.75
51500	4.25	8.5	2.83	6	**	--	2.83	**	4.33	--
51500	4.5	7	2.33	4.5	**	4.92	2.67	10.5	3.92	--
51000	4.25	8	2.67	5.5	**	--	2.75	12	4.17	2.83
51000	4.5	6.5	2.17	4.08	**	4.75	2.58	9.5	3.83	2.67
50500	4.25	7	2.42	4.83	**	5	2.67	11	4	2.75
50500	4.5	6	2	3.75	**	4.58	--	8.5	3.75	2.58
50000	4.25	6.5	2.25	4.33	**	4.83	--	10	3.92	2.67
50000	4.5	5.5	1.92	3.42	**	4.5	2.5	7.5	3.67	--
49500	4.25	6	2.08	3.92	**	4.67	2.58	9	3.75	--
49500	4.5	4.67	1.75	3.08	**	4.42	2.42	7	3.5	2.5
49000	4.25	5.5	2	3.58	**	4.58	2.5	8	3.67	2.58
49000	4.5	4.25	--	2.92	**	4.25	--	6	3.42	--
48500	4.25	4.92	1.83	3.25	**	4.42	--	7	3.58	2.5
48500	4.5	3.92	--	2.67	**	4.17	2.33	5.5	--	2.42
48000	4.25	4.5	1.75	3	**	4.33	2.42	6.5	3.5	--
48000	4.5	3.58	--	2.5	**	4.08	--	4.92	--	2.33
47500	4.25	4.08	--	2.75	**	4.25	2.33	6	3.42	2.42
47500	4.5	3.33	--	2.33	**	4	2.25	4.5	3.33	--

Table 7.D.4: Alternative Fuel Specifications (F-37-B continued)

Maximum Burnup	Minimum Enrichment	F-37-B1	F-37-B2	F-37-B3	F-37-B4	F-37-B5	F-37-B6	F-37-B7	F-37-B8	F-37-B9
(MWd/mtU)	(wt% ^{235}U)	Cooling Time in Years								
47000	4.25	3.75	--	2.58	**	4.17	--	5.5	--	--
47000	4.5	3.08	--	2.17	**	3.92	--	4.08	--	--
46500	4.25	3.5	--	2.42	**	4.08	2.25	4.75	3.33	2.33
46500	4.5	2.92	--	2	**	3.83	2.17	3.75	3.25	2.25
46000	4.25	3.25	--	2.25	**	4	--	4.33	--	--
46000	4.5	2.75	--	1.92	**	--	--	3.42	--	--
45500	4.25	3	--	2.08	**	3.92	2.17	3.92	3.25	2.25
45500	4.5	2.58	--	1.83	**	3.75	2.08	3.17	--	2.17
45000	4.25	2.83	--	2	**	3.83	--	3.58	--	--
45000	4.5	2.42	--	1.75	**	3.67	--	2.92	3.17	--
40000	4.25	2.25	--	1.75	9.5	3.33	1.83	1.83	3	1.92
40000	4.5	2.17	--	--	8.5	3.25	1.83	1.75	2.92	1.92
39000	4.25	2.17	--	--	8.5	3.25	--	1.75	2.92	--
39000	4.5	--	--	--	8	--	1.75	--	--	1.83
35000	4.25	2	--	--	6	3	1.75	--	2.75	1.75
35000	4.5	2	--	--	5.5	3	--	--	2.75	1.75
30000	4.25	1.83	--	--	4.08	2.75	--	--	2.58	--
30000	4.5	1.83	--	--	3.92	2.75	--	--	2.5	--
27500	4.25	1.75	--	--	3.58	2.67	--	--	2.42	--
27500	4.5	1.75	--	--	3.42	2.67	--	--	2.42	--
25000	4.25	--	--	--	3.08	2.58	--	--	2.33	--
25000	4.5	--	--	--	3	2.58	--	--	2.33	--
22500	4.25	--	--	--	2.75	2.42	--	--	2.25	--
22500	4.5	--	--	--	2.67	2.42	--	--	2.25	--
22000	4.25	--	--	--	2.67	--	--	--	--	--
22000	4.5	--	--	--	2.58	--	--	--	--	--
21500	4.25	--	--	--	2.58	--	--	--	--	--
21500	4.5	--	--	--	--	--	--	--	--	--
21000	4.25	--	--	--	--	--	--	--	2.17	--
21000	4.5	--	--	--	2.5	2.33	--	--	2.17	--

Table 7.D.4: Alternative Fuel Specifications (F-37-B continued)

Maximum Burnup (MWd/ mtU)	Minimum Enrichment (wt% ^{235}U)	F-37-B1	F-37-B2	F-37-B3	F-37-B4	F-37-B5	F-37-B6	F-37-B7	F-37-B8	F-37-B9
		Cooling Time in Years								
20000	4.25	--	--	--	2.42	2.33	--	--	--	--
20000	4.5	--	--	--	2.42	--	--	--	--	--
15500	4.25	--	--	--	1.92	2.08	--	--	1.92	--
15500	4.5	--	--	--	1.92	2.08	--	--	1.92	--
15000	4.25	--	--	--	1.83	--	--	--	--	--
15000	4.5	--	--	--	1.83	--	--	--	--	--
10500	4.25	--	--	--	1.75	1.75	--	--	1.75	--
10500	4.5	--	--	--	1.75	1.75	--	--	1.75	--

Table 7.D.4: Alternative Fuel Specifications (F-37-C)

Maximum Burnup	Minimum Enrichment	F-37-C1	F-37-C2	F-37-C3	F-37-C4	F-37-C5	F-37-C6	F-37-C7	F-37-C8	F-37-C9
(MWd/mtU)	(wt% ^{235}U)	Cooling Time in Years								
55000	4.25	4.75	7.5	11	**	9.5	6.5	**	6.5	6
55000	4.5	3.67	6	8.5	**	8	4.67	**	5.5	4.58
54500	4.25	4.33	7	10	**	9	6	**	6	5.5
54500	4.5	3.33	5.5	8	**	7.5	4.25	**	4.92	4.17
54000	4.25	3.92	6.5	9.5	**	8.5	5.5	**	5.5	4.92
54000	4.5	3.17	4.83	7.5	**	7	3.83	**	4.67	3.83
53500	4.25	3.58	6	8.5	**	8	4.58	**	--	4.5
53500	4.5	3.08	4.42	7	**	6	3.5	**	4.5	3.5
53000	4.25	3.25	5.5	8	**	7	4.17	**	4.83	4.08
53000	4.5	3	4	6	**	5.5	3.17	**	4.33	3.25
52500	4.25	3.08	4.75	7	**	6.5	3.75	**	4.67	3.75
52500	4.5	--	3.67	5.5	**	--	2.92	**	4.17	3
52000	4.25	--	4.33	6.5	**	6	3.42	**	4.42	3.42
52000	4.5	2.92	3.33	4.92	**	--	2.75	11.5	4.08	2.75
51500	4.25	3	3.92	6	**	5.5	3.17	**	4.33	3.17
51500	4.5	--	3.08	4.5	**	4.92	2.67	10.5	3.92	--
51000	4.25	2.92	3.58	5.5	**	--	2.83	12	4.17	2.92
51000	4.5	2.83	2.83	4.08	**	4.75	2.58	9.5	3.83	2.67
50500	4.25	--	3.25	4.83	**	5	2.67	11	4	2.75
50500	4.5	--	2.67	3.75	**	4.58	--	8.5	3.75	2.58
50000	4.25	2.83	3	4.33	**	4.83	--	10	3.92	2.67
50000	4.5	2.75	2.5	3.42	**	4.5	2.5	7.5	3.67	--
49500	4.25	--	2.75	3.92	**	4.67	2.58	9	3.75	--
49500	4.5	--	2.33	3.08	**	4.42	2.42	7	3.5	2.5
49000	4.25	2.75	2.58	3.58	**	4.58	2.5	8	3.67	2.58
49000	4.5	2.67	2.17	2.92	**	4.33	--	6	3.42	--
48500	4.25	--	2.42	3.25	**	4.42	--	7	3.58	2.5
48500	4.5	--	2	2.67	12	4.25	2.33	5.5	--	2.42
48000	4.25	2.67	2.25	3	**	4.33	2.42	6.5	3.5	--
48000	4.5	2.58	1.92	2.5	11.5	4.17	--	4.92	--	2.33
47500	4.25	--	2.08	2.75	12	4.25	2.33	6	3.42	2.42
47500	4.5	--	1.75	2.33	11	--	2.25	4.5	3.33	--

Table 7.D.4: Alternative Fuel Specifications (F-37-C continued)

Maximum Burnup	Minimum Enrichment	F-37-C1	F-37-C2	F-37-C3	F-37-C4	F-37-C5	F-37-C6	F-37-C7	F-37-C8	F-37-C9
(MWd/mtU)	(wt% ^{235}U)	Cooling Time in Years								
47000	4.25	2.58	1.92	2.58	11.5	--	--	5.5	--	--
47000	4.5	2.5	--	2.17	10.5	4.08	--	4.08	--	--
46500	4.25	--	1.83	2.42	11	4.17	2.25	4.75	3.33	2.33
46500	4.5	--	--	2	10	4	2.17	3.75	3.25	2.25
46000	4.25	--	1.75	2.25	10.5	4.08	--	4.33	--	--
46000	4.5	--	--	1.92	9.5	3.92	--	3.42	--	--
45500	4.25	2.5	--	2.08	10	4	2.17	3.92	3.25	2.25
45500	4.5	2.42	--	1.83	9	--	2.08	3.17	--	2.17
45000	4.25	--	--	2	--	--	--	3.58	--	--
45000	4.5	--	--	1.75	--	3.83	--	2.92	3.17	--
40000	4.25	2.25	--	1.75	6	3.5	1.83	1.83	3	1.92
40000	4.5	2.17	--	--	5.5	3.42	1.83	1.75	2.92	1.92
39000	4.25	2.17	--	--	5.5	3.42	--	1.75	2.92	--
39000	4.5	--	--	--	4.92	3.33	1.75	--	--	1.83
35000	4.25	2	--	--	3.92	3.17	1.75	--	2.75	1.75
35000	4.5	2	--	--	3.67	3.08	--	--	2.75	1.75
30000	4.25	1.83	--	--	2.83	2.92	--	--	2.58	--
30000	4.5	1.83	--	--	2.75	2.83	--	--	2.5	--
27500	4.25	1.75	--	--	2.5	2.75	--	--	2.42	--
27500	4.5	1.75	--	--	2.42	2.75	--	--	2.42	--
25000	4.25	--	--	--	2.25	2.67	--	--	2.33	--
25000	4.5	--	--	--	2.17	2.67	--	--	2.33	--
22500	4.25	--	--	--	2	2.58	--	--	2.25	--
22500	4.5	--	--	--	1.92	2.58	--	--	2.25	--
22000	4.25	--	--	--	1.92	2.5	--	--	--	--
22000	4.5	--	--	--	--	2.5	--	--	--	--
21500	4.25	--	--	--	--	--	--	--	--	--
21500	4.5	--	--	--	1.83	--	--	--	--	--
21000	4.25	--	--	--	1.83	--	--	--	2.17	--
21000	4.5	--	--	--	--	--	--	--	2.17	--

Table 7.D.4: Alternative Fuel Specifications (F-37-C continued)

Maximum Burnup	Minimum Enrichment	F-37-C1	F-37-C2	F-37-C3	F-37-C4	F-37-C5	F-37-C6	F-37-C7	F-37-C8	F-37-C9
(MWd/ mtU)	(wt% ^{235}U)	Cooling Time in Years								
20000	4.25	--	--	--	1.75	2.42	--	--	--	--
20000	4.5	--	--	--	1.75	2.42	--	--	--	--
15500	4.25	--	--	--	--	2.17	--	--	1.92	--
15500	4.5	--	--	--	--	2.17	--	--	1.92	--
15000	4.25	--	--	--	--	--	--	--	--	--
15000	4.5	--	--	--	--	--	--	--	--	--
10500	4.25	--	--	--	--	1.83	--	--	1.75	--
10500	4.5	--	--	--	--	1.83	--	--	1.75	--

Table 7.D.5

Regions for Regionalized Loading

Region Number	Cell Numbers	
	F-32 (see Figure 7.D.1)	F-37 (see Figure 7.D.2)
1	3,11,22,30	2,16,22,36
2	8,12,21,25	6,17,21,32
3	13,14,19,20	12,18,20,26
4	4,5,28,29	19
5	6,9,24,27	1,3,9,15,23,29,35,37
6	7,15,18,26	5,7,31,33
7	1,10,23,32	11,13,25,27
8	2,16,17,31	4,8,30,34
9	N/A	10,14,24,28

Table 7.D.6

Burnup Requirements for F-37 Basket

Configuration	Regions (Figure 7.D.2)	Minimum Assembly Burnup for UO_2 Assemblies with an Initial Enrichment up to 4.55 wt% ^{235}U. (GWd/mtU)
1	1,2,3,4,5,6,7,8,9	15
2	1,2,3,4,6,7,8,9	18

Notes:

1. All regions not listed above for a given Configuration can be loaded with fresh UO_2 fuel with an enrichment of up to 4.55 wt% ^{235}U.
2. Fixed Burnup Requirements are used for all qualified spent UO_2 assemblies which have enrichment range from 4.25 wt% ^{235}U to 4.55 wt% ^{235}U.
3. See Appendix 7.E for burnup verification requirements.

Table 7.D.7: In-Core Operating Requirements

Parameter	Requirement
Assembly Average Specific Power, MW/MtU	≤ 54.45
Assembly Average Moderator Temperature, K	≤ 601
Average Soluble Boron Concentration, ppm	≤ 900

Notes:

1. These requirements only apply to assemblies that need to meet the burnup requirements in Table 7.D.6.
2. For each assembly, the parameters Soluble Boron Concentration (SBC), Specific Power (SP), and Moderator Temperature (MT) must be calculated and compared to the requirements using the following equations. In these equations, and the symbols used therein, the subscript i denotes the cycle. The summation (∑) in these equation is to be performed over all cycles i that the assembly was in the core.

   Soluble Boron:

   $SB = \sum (SB_i * B_i) / \sum B_i$

   Assembly Average Specific Power:

   $SP = \sum B_i / \sum T_i$

   Assembly Average Moderator Temperature:

   $MT = \sum (B_i*(CIT_i + CFC_i * (COT_i\text{-}CIT_i))) / \sum B_i$

   where:

   B_i = Assembly-average burnup for cycle i
   BC_i = Core-average burnup for cycle i
   SB_i = Average In-Core Soluble Boron Concentration for cycle i
   T_i = Length of Cycle
   CITi = Core Inlet Temperature
   COT_i = Core Outlet temperature
   CFC_i = B_i/BC_i with Correction Factor; if $CFC_i<1$ then set $CFC_i = 1$

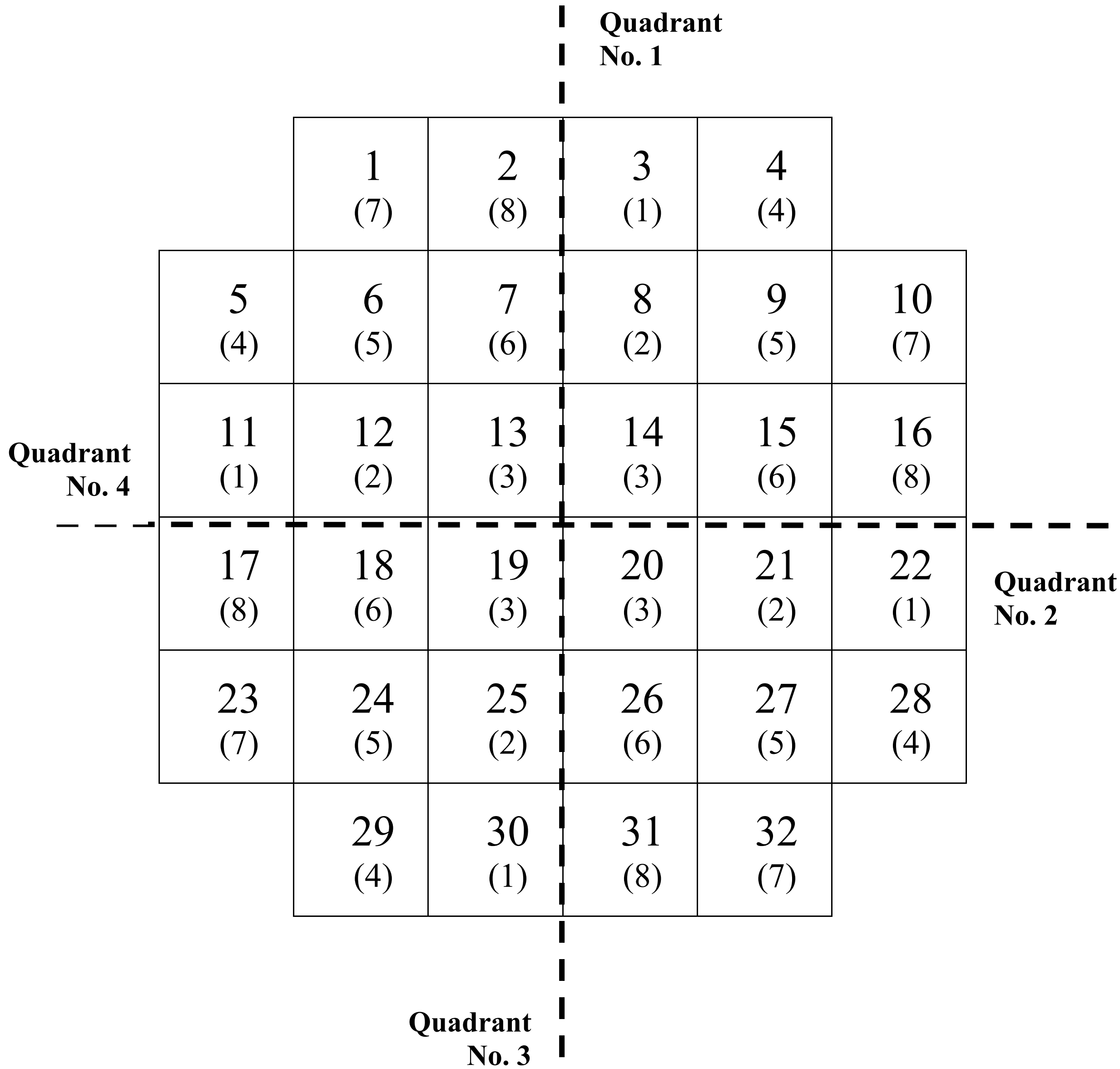

Notes: 1. Numbers in parenthesis denote region number.
2. All quadrants are rotationally symmetric by region number.

FIGURE 7.D.1: F-32 FUEL BASKET STORAGE CELL NUMBERING AND BASKET QUADRANT IDENTIFICATION

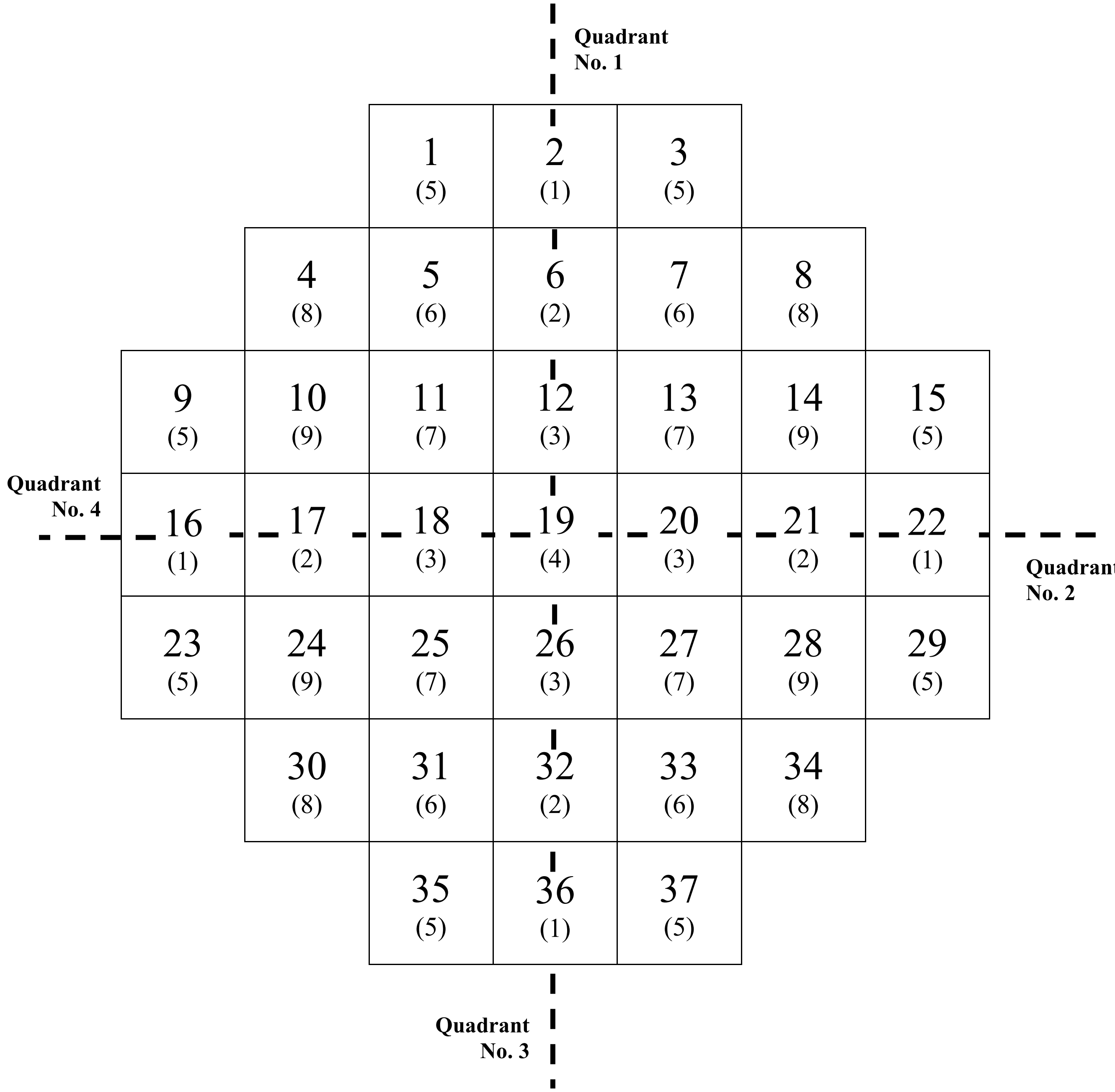

Notes: 1. Numbers in parenthesis denote region number.
2. All quadrants are symmetric by region number at two lines of symmetry.

FIGURE 7.D.2: F-37 FUEL BASKET STORAGE CELLS NUMBERING AND BASKET QUADRANT IDENTIFICATION

APPENDIX 7.E

BURNUP VERIFICATION CONDITIONS OF THE HI-STAR 180D PACKAGE

For those spent fuel assemblies that need to meet the burnup requirements specified in Table 7.D.6, a burnup verification shall be performed in accordance with either Method A or Method B described below.

Method A: Burnup Verification Through Quantitative Burnup Measurement

For each assembly in the F-37 where burnup credit is required, the minimum burnup is determined from the burnup requirement applicable to the configuration chosen for the cask (see Table 7.D.6). A measurement is then performed that confirms that the fuel assembly burnup exceeds this minimum burnup. The measurement technique may be calibrated to the reactor records for a representative set of assemblies. The assembly burnup value to be compared with the minimum required burnup should be the measured burnup value as adjusted by reducing the value by a combination of the uncertainties in the calibration method and the measurement itself.

Method B: Burnup Verification Through an Administrative Procedure and Qualitative Measurements

Depending on the location in the basket, assemblies loaded into a specific F-37 basket can either be fresh, or have to meet a single minimum burnup value. The assembly burnup value to be compared with the minimum required burnup should be the reactor record burnup value as adjusted by reducing the value by the uncertainties in the reactor record value. An administrative procedure shall be established that prescribes the following steps, which shall be performed for each cask loading:

- Based on a review of the reactor records, all assemblies in the spent fuel pool that have a burnup that is below the minimum required burnup of the loading curve for the cask to be loaded are identified.
- After the cask loading, but before the release for shipment of the cask, the presence and location of all those identified assemblies is verified, except for those assemblies that have been loaded as fresh assemblies into the cask.

Additionally, for all assemblies to be loaded that are required to meet a minimum burnup, a measurement shall be performed that verifies that the assembly is not a fresh assembly. This measurement is not applicable if reactor records show that at the time of fuel loading, no fresh fuel assemblies were present in the spent fuel pool.

CHAPTER 8: ACCEPTANCE TESTS AND MAINTENANCE PROGRAM

8.0 INTRODUCTION

This chapter identifies the acceptance tests and maintenance program to be conducted on the HI-STAR 180D Package to verify that the structures, systems and components (SSCs) classified as *important-to-safety* have been fabricated, assembled, inspected, tested, accepted, and maintained in accordance with the requirements set forth in this Safety Analysis Report (SAR), all applicable regulatory requirements, and the Certificate of Compliance (CoC). The acceptance criteria and maintenance program described in this chapter is in full compliance with the requirements of 10CFR Part 71 Subpart G [8.0.1].

8.1 ACCEPTANCE TESTS

In this section the inspections and acceptance tests to be performed on the HI-STAR 180D Package prior to its use are summarized. These inspections and tests provide assurance that the HI-STAR 180D Package has been fabricated, assembled and accepted for use and loading under the conditions specified in Chapter 7 of this SAR and the USNRC issued CoC in accordance with the requirements of 10CFR Part 71.

8.1.1 Visual Inspections and Measurements

The HI-STAR 180D Package shall be assembled in accordance with the drawing package referenced in the CoC. Dimensional tolerances that define the limits on the dimensions critical to the licensing basis analysis are included in these drawings. Fabrication drawings provide additional dimensional tolerances necessary to ensure fit-up of parts as well as compliance with the design conditions. A fabrication sampling plan shall be made and controls shall be exercised to ensure that the packaging conforms to the dimensions and tolerances specified on the licensing and fabrication drawings. These dimensions are subject to independent confirmation and documentation in accordance with the Holtec QA program approved in NRC Docket No. 71-0784.

The following shall be verified as part of visual inspections and measurements:

- Visual inspections and measurements shall be made to ensure that the packaging effectiveness is not significantly reduced. Any *important-to-safety* component found to be under the minimum thickness requirement shall be repaired or replaced as required.
- Visual inspections shall be made to verify that neutron absorber panels, basket shims and anti-rotation bars are present as required by cask and basket design.
- The packaging shall be visually inspected to ensure it is conspicuously and durably marked with the proper markings/labels in accordance with 10CFR71.85(c).
- The packaging shall be inspected for cleanliness and preparation for shipping in accordance with written and approved procedures.

The visual inspection and measurement results for the HI-STAR 180D Package shall become part of the final quality documentation package.

8.1.2 Weld Examination

The examination of HI-STAR 180D Package welds shall be performed in accordance with the drawing package referenced in the CoC and applicable codes and standards in Table 2.1.15, including alternatives as specified in Table 2.1.14**.** Weld examinations and repairs shall be performed as specified below. All code and Metamic-HT weld inspections shall be performed in accordance with written and approved procedures by personnel qualified in accordance with SNT-TC-1A [8.1.2]. All required inspections, examinations, and tests shall become part of the final quality documentation package.

The following specific weld requirements shall be followed in order to verify fabrication in accordance with the drawings.

1. Containment boundary welds including any attachment welds (and temporary welds to the containment boundary) shall be examined in accordance with ASME Code Section V, with acceptance criteria per ASME Code Section III, Subsection NB, Article NB-5300. Examinations, Visual (VT), Radiographic (RT), and Liquid Penetrant (PT) or Magnetic Particle (MT), apply to these welds as defined by the code. These welds shall be repaired in accordance with the requirements of the ASME Code Section III, Article NB-4450 and examined after repair in the same manner as the original weld. Weld overlays for cask sealing surfaces shall be VT and PT examined to insure that a leakage path between the containment space and the outside environment that may violate the specified cask leak tightness criterion is detected and eliminated. Although ASME Code Section III, Subsection NB does not require visual examination of welds, the welds will be visually examined to ensure conformance with the fabrication drawings (e.g. proper geometry, workmanship etc.).

2. Structural welds in the cask and impact limiter (excluding those listed above) shall be examined in accordance with ASME Code Section V, with acceptance criteria per ASME Code Section III, Subsection NF, Article NF-5300. These welds shall be repaired in accordance with ASME Code Section III, Article NF-4450 and examined after repair in the same manner as the original weld. These weld requirements are not applicable to NITS welds (e.g. seal welds) on the cask and impact limiters.

3. Basket welds shall be examined and repaired in accordance with NDE specified in the drawing package and with written and approved procedures developed specifically for welding Metamic-HT with acceptance criteria per ASME Section V, Article 1, Paragraph T-150 (2007 Edition). The basket welds, made by the Friction Stir Weld process, are classified as Category E per NG-3351.3 and belonging to Type VI in Table NG-3352-1. These weld requirements are not applicable to welds identified as NITS on the drawing package.

4. NITS welds shall be examined and repaired in accordance with written and approved procedures

8.1.3 Structural and Pressure Tests

The cask containment boundary will be tested by combination of methods (including helium leak test, pressure test, MT, and/or PT, as specified in this Chapter) to verify that it is free of cracks, pinholes, uncontrolled voids or other defects that could significantly reduce the effectiveness of the packaging.

8.1.3.1 Lifting Trunnions

Four top trunnions are provided for vertical lifting and handling of the loaded cask. The top trunnions are required to be designed, tested and inspected in accordance with ANSI N14.6 [8.1.3]. Two bottom trunnions are provided for rotation of the loaded or empty cask for downending/upending operations. Both top and bottom trunnions are rendered inoperable during package transport.

At least one pair of top lifting trunnions shall be tested in accordance with ANSI N14.6 at 300% of the maximum design service lifting load (the full weight of the loaded cask at a minimum). The second pair of top lifting trunnions may be tested in accordance to ANSI N14.6 at 150% of the maximum design service lifting load (the full weight of the loaded cask at a minimum) if used as redundant lifting attachments. Load tests may be performed in excess of the test loads specified above provided an engineering evaluation is performed to ensure trunnions or other cask components will not be damaged by the load test. The test load shall be applied for a minimum of 10 minutes. The accessible parts of the top trunnions (areas outside the cask), and the local cask areas shall then be visually examined to verify no deformation, distortion, or cracking has occurred. Any evidence of deformation (other than minor localized surface deformation due to contact pressure between lifting device and top trunnion), distortion or cracking of the trunnion or adjacent cask areas shall require replacement of the trunnion and/or repair of the cask. Following any replacements and/or major repair, as defined in ANSI N14.6, the load testing shall be re-performed and the components re-examined in accordance with the original procedure and acceptance criteria. Testing shall be performed in accordance with written and approved procedures. Certified material test reports verifying trunnion material mechanical properties meet ASME Code Section II requirements provide further verification of the trunnion load capabilities. Test results shall be documented and shall become part of the final quality documentation package.

8.1.3.2 Pressure Testing

Pressure testing of the HI-STAR 180D containment boundary (cavity space) and expanded containment boundary (inter-lid space) is required. The cask cavity shall be pressure tested in accordance with ASME Section III, Subsection NB, NB-6000 at a test pressure of not less than 150% of cask cavity maximum normal operating pressure per 10CFR71.85(b) or at a test pressure of 125% of the cask cavity design internal pressure; whichever is greater. The inter-lid space shall be pressure tested in accordance with ASME Section III, Subsection NB, NB-6000 at a test pressure of not less than the minimum test pressure applied to the cask cavity. All pressure testing shall be performed in accordance with written and approved procedures. The written and approved test procedure shall clearly define the test equipment arrangement. Pressure testing may be performed using a single temporary test seal on the lid. Test results shall be documented and shall become part of the final quality documentation package.

8.1.4 Leakage Tests

Leakage rate tests on the cask containment system shall be performed per written and approved procedures in accordance with the requirements of Chapter 7 and the requirements of ANSI N14.5, 2014 [8.1.6]. Tables 8.1.1 and 8.1.2 specify the allowable leakage rate and test sensitivity in terms of helium leak tightness as well as components to be tested for fabrication, pre-shipment, periodic and maintenance leakage rate tests.

A pre-shipment leakage rate test of cask containment seals is performed following loading of authorized contents into the cask. This pre-shipment leakage rate test is valid for 1 year or until the tested component(s) is opened or respective containment fasteners are untorqued.

Leakage rate testing procedures shall be approved by an American Society for Nondestructive Testing (ASNT) Level III specialist in leak testing for the nondestructive method(s) of leak testing for which the procedures are written. The written and approved test procedures shall clearly define the test equipment arrangement. Leakage rate testing shall be performed by personnel who are qualified and certified in accordance with the requirements of SNT-TC-1A [8.1.2]. Leakage rate testing shall be performed in accordance with a written quality assurance program.

In case of an unsatisfactory leakage rate, weld repair, seal surface repair/polishing and/or seal change and retest shall be performed until the test acceptance criterion is satisfied.

Leakage rate test results shall become part of the final quality documentation package.

8.1.5 Component and Material Tests

Cask closure seals are conservatively specified in the drawing package referenced in the CoC and in Appendix 8.A to provide a high degree of assurance of leak tightness under normal and accident conditions of transport. Seal tests under the most severe package service conditions including performance at pressure under high and low temperatures will not challenge the capabilities of these seals and thus are not required.

No other package components require individual testing. The following subsections present the required packaging material tests.

8.1.5.1 Impact Testing

To provide protection against brittle fracture under cold conditions, facture toughness test criteria of cask ferritic components, including containment boundary welds, are specified in Table 8.1.9 and Table 2.1.9. Code alternatives listed in Table 2.1.14 may apply. Exemption from fracture toughness testing as allowed by ASME Code Section III, Subsections NB and NF may apply.

Test results shall become part of the final quality documentation package.

8.1.5.2 Impact Limiter Crush Material Testing

Verification of the transport impact limiter crush material crush strength shall be accomplished by performance of a crush test of sample blocks. The verification tests shall be performed by the crush material supplier or other testing facility qualified for testing in accordance with the Holtec Nuclear QA program using standardized test methods such as ASTM D7336 [8.1.10]. Impact limiter crush material crush strength ranges are specified in the drawing package referenced in the CoC. In order to account for uncertainties and variations in crush material's crush strength with manufacturing methods and characterization methods, a minimum of five samples from each batch of crush material shall be tested to demonstrate that the crush strength falls within the acceptance criteria. The results of the tests shall be averaged, and the average value shall be compared to the acceptance criteria. Individual samples that vary more than 15% from the average shall be discarded and additional samples shall be tested to replace any missing data. The testing for crush strength shall demonstrate that the average crush strength falls within the specified acceptance criteria over the full operating temperature range. Acceptance of the material shall be through either batch testing over a range of temperatures or using established relationships between operating temperature and crush strength to tighten the acceptance criteria for tests at room temperature.

The certified test results shall be retained by Holtec International as archival record for each batch of impact limiter crush material manufactured and used. Test results shall be documented and shall become part of the final quality documentation package.

8.1.5.3 Neutron Shielding Material

Each manufactured lot of Holtite-B neutron shield material shall be tested to verify that boron carbide content, hydrogen density and bulk Holtite material density meet the requirements specified in Table 8.1.11. A manufactured lot is defined as the total amount of material used to make any number of mixed batches comprised of constituent ingredients from the same lot/batch identification numbers supplied by the constituent manufacturer. Testing shall be performed in accordance with written and approved procedures.

Test results for each manufactured lot of neutron shield material shall become part of the final quality documentation package.

Approved written procedures shall ensure that mix ratios and mixing methods are controlled in order to achieve proper material composition, boron concentration and distribution, and that emplacement is properly controlled.

8.1.5.4 Neutron Absorber Material

The manufacturing of Metamic-HT is governed by a set of quality validated standard procedures contained in the Metamic-HT Manufacturing Manual [8.1.8].

The key constituents of Metamic-HT, namely aluminum powder and Boron Carbide powder are procured under their respective purchasing specifications that define the required particle size distributions and set down the prohibited materials & impurities, as well as tolerable level of trace amounts of acceptable impurities. The purchasing specifications are defined and incorporated in the Metamic-HT Manufacturing Manual.

The manufacturing processes for Metamic-HT are defined in the Metamic-HT Manufacturing Manual. Metamic-HT panels will be manufactured to Holtec's purchase specification [8.1.9] that incorporates all requirements set forth in Chapter 8 of this SAR, the drawing package referenced in the CoC and the fabrication drawings. The supplier of raw materials must be qualified under Holtec's quality program for important to safety materials and components or alternatively each lot of raw material shall be tested in accordance with Table 8.1.3 requirements. The manufacturing of Metamic-HT is subject to all quality assurance requirements under Holtec International's NRC approved quality program.

The tests conducted on Metamic-HT to establish the compliance of the manufactured panels with Holtec's Purchasing Specification are intended to ensure that *critical characteristics* of the final product will meet the minimum guaranteed values (MGVs) set forth in Table 8.1.5. The tests are performed at both the raw material and manufactured panels stages of production with the former serving as the insurer of the properties in the final product and the latter serving the confirmatory function. The testing is conducted for each lot of raw material and finished panels as prescribed in Table 8.1.3. A lot is defined as follows:

> "Lot" means a population of an item that shares identical attributes that are central to defining a critical performance or operational characteristic required of it. Thus, a lot of boron carbide powder procured to a certified Purchasing Specification used in the manufacturing of Metamic-HT is the bulk quantity of the powder that has the same particle size distribution. A lot of finished panels drawn from a powder mix and manufactured in an extrusion run have identical aluminum and boron carbide characteristics and the same extrusion conditions.

The following tests are performed (see Table 8.1.3):

(i) Testing and certification of powder material

- All lots of aluminum and boron carbide powder shall be certified to meet particle size distribution and chemistry requirements in the Metamic-HT Manufacturing Manual.
- All lots of B_4C will be certified as containing Boron with the minimum isotopic B-10 per the boron carbide purchase specifications incorporated in the Metamic-HT Manufacturing Manual.
- Homogenized mixtures of Al powder(s) and boron carbide powder(s) from traceable lots, prepared for sintering and billet forming operations, shall have the minimum boron carbide wt% verified by wet chemistry testing of one sample from each lot of blended powders. The mixing/blending of the batch shall be controlled via approved procedures.

(ii) Testing of finished panels

The number of panels subject to testing shall be governed by Table 8.1.4. The panels that need to be tested per the statistical protocol of Table 8.1.4, hereafter referred to as test panels, shall be subject to the following evaluations:

- The Metamic-HT panels shall be tested for all mechanical properties in Table 8.1.5 in accordance with Table 8.1.4 sampling plan.

- The thickness of each panel will be measured using the procedure set down in the Metamic-HT Manufacturing Manual. The average measured value must meet the minimum basket wall requirements specified in the Drawing Package referenced in the CoC.
- One coupon from the test panel shall be subject to neutron attenuation testing to quantify the boron carbide content for compliance with the minimum requirement in Table 8.1.3 using written procedures.

(iii) Testing of Basket

- Metamic-HT basket welds shall be tested/inspected as stated in Section 8.1.2 using written procedures.

FSW Procedure Qualification, Welder Operator Qualification and Welded Coupon Test:

A. Procedure qualification and welder operator qualification of the Friction Stir Welding (FSW) process shall meet the following requirements:
   - The Procedure Qualification Record (PQR) shall meet the essential variable requirements of QW-267 [8.1.1].
   - The Weld Procedure Specification (WPS) shall meet the essential variable requirements of QW-267, QW-361.1(e) and QW-361.2 [8.1.1].
   - Welder operator performance qualifications shall meet the essential variable requirements of QW-361.2.
   - Welder operator may be qualified by volumetric NDE of a test coupon; or a coupon from their initial production welding within the limitations of QW-304 and QW-305 [8.1.1]; or by bend tests taken from a test coupon.
   - All welding by FSW process shall meet applicable requirements of ASME Section IX, 2013 Edition [8.1.1].

B. Procedure qualification of the Friction Stir Welding process may be accomplished by tensile testing the appropriate number of coupons per ASME Section IX (2007). Verification of weld soundness is performed by visual examination, radiography and bend testing per approved written procedures (bend testing emulates ASME Section IX). Bend test qualification of a representative weld sample emulating ASME Section IX paragraph QW 160 at a bend radius that produces at least 150% of the average tensile strain developed in the friction stir welded joint under the hypothetical free drop accident condition. The bend radius shall be recorded on the PQR. The bend test sample must meet the acceptance criteria of Section IX QW-163 and visual examination acceptance criteria of ASME Section III Subsection NG 5362 with any additional requirements per Holtec approved written procedure. In addition, at least one welded coupon from the population of Metamic-HT production panels used for manufacturing a fuel basket type must pass the criteria provided herein and shall be so documented in the Documentation Package of the manufactured fuel baskets.

Visual Inspection of Metamic-HT Panels:

Each plate of neutron absorber shall be visually inspected for damage such as scratches, cracks, burrs, foreign material embedded in the surfaces, voids, and delamination. Panels are also visually inspected for contamination on the surface as specified in the Metamic-HT Manufacturing Manual. Panels not meeting the acceptance criteria will be reworked or rejected. Unless basket is fabricated at the same factory manufacturing Metamic-HT, all panels shall be inspected before being shipped to the cask manufacturing facility where they may be subject to receipt inspection prior to installation.

8.1.6 Shielding Tests

A shielding effectiveness test must be performed prior to the first shipment as specified in the following paragraph.

Following the first fuel loading of each HI-STAR 180D package, a shielding effectiveness test shall be performed to verify the effectiveness of the shielding using written and approved procedures. Calibrated radiation detection equipment shall be used to take measurements at the surface of the HI-STAR package. Measurements shall be taken at three cross sectional planes through the radial shield and at four points along each plane’s circumference. The average measurement results from each sectional plane shall be compared to calculated values to assess the continued effectiveness of the shielding. The calculated values shall be representative of the loaded contents (e.g. fuel type, enrichment, burnup, cooling time, etc.). Measurements shall be documented and become part of the final quality documentation package.

8.1.7 Thermal Tests

The first fabricated HI-STAR cask shall be tested to confirm its heat transfer capability through the containment shell and monolithic shielding cylinders.

A thermal test performed for a similar cask design (e.g. HI-STAR 180 USNRC Docket 71-9325) may be used as proof of heat transfer capability in lieu of thermal testing of the HI-STAR 180D. In case of a proof with similar cask, an engineering evaluation between HI-STAR 180D and the previously-tested cask shall be documented and become part of the final quality documentation package.

The test shall be conducted after fabrication is complete. A test cover plate shall be used to seal the cask cavity. The cavity will be heated with steam.

Twelve (12) calibrated thermocouples shall be installed on the external walls of the cask using four thermocouples, equally spaced circumferentially, at three different elevations. Three calibrated thermocouples shall be installed on the internal walls of the cask in locations to be determined by procedure. Additional temperature sensors shall be used to monitor ambient temperature, steam supply temperature, and condensate drain temperature. The thermocouples shall be attached to strip chart recorders or other similar mechanism to allow for continuous monitoring and recording of temperatures during the test. Instrumentation shall be installed to monitor cask cavity internal pressure.

After the thermocouples have been installed, dry steam will be introduced through an opening in the test cover plate previously installed on the cask and the test initiated. Temperatures of the thermocouples, plus ambient, steam supply, and condensate drain temperature shall be recorded at hourly intervals until thermal equilibrium is reached. Appropriate criteria defining when thermal equilibrium is achieved shall be determined based on a variety of potential ambient test conditions and incorporated into the test procedure. In general, thermal equilibrium is expected approximately 12 hours after the start of steam heating. Air will be purged from the cask cavity via venting during the heatup cycle. During the test, the steam condensate flowing out of the cask drain shall be collected and the mass of the condensate measured with a precision weighing instrument.

Once thermal equilibrium is established, the final ambient, steam supply, and condensate drain temperatures and temperatures at each of the thermocouples shall be recorded. The strip charts, hand-written logs, or other similar readout shall be marked to show the point when thermal equilibrium was established and final test measurements were recorded. The final test readings along with the hourly data inputs and strip charts (or other similar mechanism) shall become part of the quality records documentation package for the HI-STAR 180D Package.

The heat rejection capability of the cask at test conditions shall be computed using the following formula:

$$Q_{hm} = (h_1 - h_2)\, m_c$$

Where:

Q_{hm} = Heat rejection rate of the cask (kW)

h_1 = Enthalpy of steam entering the cask cavity (KJ/kg)

h_2 = Enthalpy of condensate leaving the cask cavity (KJ/kg)

m_c = Average rate of condensate flow measured during thermal equilibrium conditions (kg/s)

Based on the HI-STAR 180D cask thermal model, a design basis minimum heat rejection capacity (Q_{hd}) shall be computed at the measured test conditions (i.e., steam temperature in the cask cavity and ambient air temperature). The thermal test shall be considered acceptable if the measured heat rejection capability is greater than the design basis minimum heat rejection capacity ($Q_{hm} > Q_{hd}$).

If the acceptance criteria above are not met, then the HI-STAR 180D Package shall not be accepted until the root cause is determined, appropriate corrective actions are completed, and the package is re-tested with acceptable results.

- Testing shall be performed in accordance with written and approved procedures similar to the Holtec standard procedure used for the test performed on the HI-STAR 100 overpack and documented in Holtec Document DOC-5014-03 [8.1.7].

8.1.8 Miscellaneous Tests

Post-Shipment Fuel Integrity Acceptance Test

For packages containing HBF, cask surface temperatures and cask surface dose rates shall be measured in accordance with the procedures in Chapter 7 as a practical means of monitoring the condition of the fuel assemblies. Fuel reconfiguration and significant fuel cladding damage is not expected after the transportation period of each shipment.

A total of six measurements of both temperature and dose rate shall be recorded before and after each shipment with the loaded cask configured horizontally with impact limiters and no personnel barrier. Three measurements are taken from each side of the package at least 45 degrees below the cask axial centerline (below the top cask trunnion, at or near the cask circumferential centerline and below the bottom cask trunnion).

The post-shipment surface temperature measurements should not exceed the pre-shipment surface temperature measurements by more than 5 degrees C when adjusted under the same ambient conditions. The temperature criteria may be adjusted to account for the difference in ambient conditions such as solar insolation.

The post-shipment surface dose rate measurements should not exceed the pre-shipment surface dose rate measurements by more than 10%.

Failed tests shall be reported to USNRC within one month of the post-shipment measurement and shall include a description of the package contents, any available engineering justification for failed test(s), and if applicable any special precautions that will be implemented prior to unloading the contents of the package. Package exhibiting tests results equal to or greater than twice the acceptance criteria shall not be unloaded without USNRC authorization.

No additional tests are required prior to using the packaging.

Table 8.1.1
Containment System Performance Specifications

Design Attribute	Design Rating
Leakage Rate Acceptance Criterion	$1x10^{-7}$ ref-cm^3/s air (Leaktight as defined by ANSI N14.5)
Leakage Rate Test Sensitivity	$5x10^{-8}$ ref-cm^3/s air (½ of the leakage rate acceptance criterion per ANSI N14.5)

Notes:

1. During leakage rate tests appropriate conversion factors will be employed using written and approved procedures to account for actual backfill/tracer gas. For helium as the tracer gas, the Leakage Rate Acceptance Criterion and Test Sensitivity are multiplied by a factor of 1.85.
2. “Leaktight” criteria define herein is applicable to Fabrication, Maintenance, Pre-shipment and Periodic leakage tests.

Table 8.1.2
Leakage Rate Tests For The HI-STAR 180D Containment System

Leakage Test	Components Tested	Type of Leakage Rate Test (from ANSI N14.5-2014, App. A)	Allowable Leakage Rate
Fabrication Leakage Rate Test	• Containment Shell • Containment Baseplate • Containment Closure Flange • Inner Closure Lid • Outer Closure Lid • Inner Closure Lid Vent and Drain Port Cover Plates • Containment Shell Welds • Containment Shell to Containment Baseplate Weld • Containment Shell to Containment Closure Flange Weld	A.5.3	Table 8.1.1
	• Inner Closure Lid Inner Seal	A.5.4	Table 8.1.1
	• Inner Closure Lid Vent/Drain Port Cover Inner Seal	A.5.4	Table 8.1.1
	• Outer Closure Lid Inner Seal	A.5.4	Table 8.1.1
	• Outer Closure Lid Access Port Plug Seal	A.5.4	Table 8.1.1
Pre-Shipment Leakage Rate Test	• Inner Closure Lid Inner Seal	A.5.4	Table 8.1.1
	• Inner Closure Lid Vent/Drain Port Cover Inner Seal	A.5.4	Table 8.1.1
	• Outer Closure Lid Inner Seal	A.5.4	Table 8.1.1
	• Outer Closure Lid Access Port Plug Seal	A.5.4	Table 8.1.1

Table 8.1.2 (Continued)
Leakage Rate Tests For The HI-STAR 180D Containment System

Leakage Test	Components Tested	Type of Leakage Rate Test (from ANSI N14.5-2014, App. A)	Allowable Leakage Rate
Maintenance Leakage Rate Test	• Containment Shell • Containment Baseplate • Containment Closure Flange • Inner Closure Lid • Outer Closure Lid • Inner Closure Lid Vent and Drain Port Cover Plates • Containment Shell Welds • Containment Shell to Containment Baseplate Weld • Containment Shell to Containment Closure Flange Weld	A.5.3	Table 8.1.1
	• Inner Closure Lid Inner Seal	A.5.4	Table 8.1.1
	• Inner Closure Lid Vent/Drain Port Cover Inner Seal	A.5.4	Table 8.1.1
	• Outer Closure Lid Inner Seal	A.5.4	Table 8.1.1
	• Outer Closure Lid Access Port Plug Seal	A.5.4	Table 8.1.1
Periodic Leakage Rate Test	• Inner Closure Lid Inner Seal	A.5.4	Table 8.1.1
	• Inner Closure Lid Vent/Drain Port Cover Inner Seal	A.5.4	Table 8.1.1
	• Outer Closure Lid Inner Seal	A.5.4	Table 8.1.1
	• Outer Closure Lid Access Port Plug Seal	A.5.4	Table 8.1.1

Note 1: For a Leakage Rate Acceptance Criterion specified in Table 8.1.1 as “Leaktight as defined by ANSI N14.5”, the summation of individual component leakage rates of the containment boundary of a package is not required.
Note 2: The welding and removal of temporary attachments to the bottom of the containment baseplate during fabrication and maintenance operations is permitted without reperformance of the fabrication or maintenance leakage rate test.

Table 8.1.3
Metamic-HT Production Testing Requirements

	Item Tested	Property Tested For	Frequency of Test	Purpose of Test	Acceptance Criterion
i.	B_4C powder (raw material) (see note 1)	Particle size distribution	One sample per lot	To verify material supplier's data sheet	Per Holtec's Purchasing Specification [8.1.9]
		Purity	One sample per lot	To verify material supplier's data sheet	ASTM C-750
ii.	Al Powder (raw material)	Particle Size Distribution	One sample per lot	To verify material supplier's data sheet	Per Holtec's Purchasing Specification [8.1.9]
		Purity	One sample per lot	To verify material supplier's data sheet	Must be 99% (min.) pure aluminum
iii.	B_4C/Al Mix	B_4C Content (by the wet chemistry method)	One sample per mixed/blended powders lot	To ensure wt.% B_4C requirements compliance	The weight density of B_4C must lie in the range of 10 to 11% Nom.

Table 8.1.3 (Continued)
Metamic-HT Production Testing Requirements

	Item Tested	Property Tested For	Frequency of Test	Purpose of Test	Acceptance Criterion
iv.	Finished Metamic-HT panel	Thickness and width, straightness, camber and bow	Holtec QA Program Sampling Plan	To ensure fabricability of the basket	Per Holtec's Purchasing Specification [8.1.9]
		Mechanical & Structural Properties in Table 8.1.5 (see Note 3)	Per Sampling Plan Table 8.1.4 (see note 2)	To ensure structural performance.	MGV per Table 8.1.5
		B_4C content by areal density measurements (neutron attenuation method)	One sample from a panel from each Metamic-HT manufactured lot	To ensure criticality safety	The B_4C content by weight shall be ≥ 10 wt. %
		B-10 areal density measured by Neutron Attenuation Method	One sample from a panel from each Metamic-HT manufactured lot	To ensure criticality safety	≥ 0.0565 grams B-10/cm^2

Notes:
1. The B_4C testing requirements apply if the raw material supplier is not in Holtec's Approved Vendor List.
2. Sampling Plan is included in the Metamic-HT Manufacturing Manual [8.1.8].
3. All properties shall be measured at room temperature on extruded coupons.

Table 8.1.4: Tier System for Metamic-HT Production Coupon Testing

Tier No. (Note 1)	Number of Extrusions Tested per Lot (Note 4)	Number of Continuous Lots that Must Pass to Drop Down to the Next Tier (Note 2 and 3)
1 (most sampling)	20 %	5
2	12.5 %	5
3	5 %	10
4 (least sampling)	1 %	N/A

Note 1: Tier No. 1 is associated with the most amount of required extrusion testing while Tier No. 4 is associated with the least amount of required extrusion testing. A test coupon (i.e. test sample) is taken from each extrusion that is required to be tested.

Note 2: The last column reflects the logic where in order to reduce sampling and ultimately achieve Tier No. 4, MGV properties must be met on a consistent basis. For example, if Tier No. 1 applies, then to achieve Tier No. 2, five lots in a row must pass. On the other hand, a stringent penalty applies as specified in Note 4.

Note 3: Testing shall be moved up the table to the next tier (a greater amount of sampling) if any MGV property (accounting for the application of the two replacement coupons per Note 4) fails in two consecutive lots. For example, if Tier No. 2 applies and an MGV property fails on two lots in a row then Tier No. 1 must be applied going forward.

Note 4: If a coupon fails with respect to any MGV property, then it may be replaced by two coupons from the extrusion that produced the failed coupon. If both of the replacement coupons pass the failed MGV property, then the lot can be accepted. If either of the replacement coupons is unsuccessful in meeting the failed MGV property, then the entire lot is rejected. An MGV on a coupon is not considered failed if the replacement coupons pass the failed MGV property. As an alternative to rejecting the entire lot, testing of the failed MGV value on all extrusions within the lot is permitted to isolate acceptable panels.

Table 8.1.5: Minimum Guaranteed Values of Metamic-HT Primary Properties

Property (Note 1)	Temperature, °C	Property Value (Note 2)	Property Type
Yield strength, σ_y (ksi)	Ambient 200/300/350 450	19.5 15.0/13.8/10.0 7.7	Primary
Tensile strength, σ_u (ksi)	Ambient 200/300/350 450	28.2 18.8/15.6/11.9 8.1	Primary
Young's Modulus, E (Msi)	Ambient 200/300/350 450	11.8 10.8/8.8/6.9 3.8	Primary
Area Reduction (%)	Ambient 200/300/350 450	20 17.9/14.2/12.9 7.8	Primary

Note 1: All properties are critical characteristics.
Note 2: Properties can be interpolated, use 40°C for ambient when interpolating.

Table 8.1.6: This table is intentionally not used

Table 8.1.7: This table is intentionally not used.

Table 8.1.8: This table is intentionally not used.

Table 8.1.9: Fracture Toughness Test Criteria: Containment System (Sheet 1 of 3)

Item	Material	Thickness mm (in.)	Qualification to LST of -29°C (-20°F) (Note 3)		Qualification to LST of -40°C (-40°F) (Note 3)	
			Charpy V-Notch Temperature	Drop Test Temperature (Note 1)	Charpy V-Notch Temperature	Drop Test Temperature (Note 1)
Weld Metal for NB Welds	As required	NA	$T_{NDT} \leq$ -74.7°C (-102.5°F) with testing and acceptance criteria per ASME Section III, Subsection NB, Article NB-2430 and Article NB-2330	Drop Test Not Required	$T_{NDT} \leq$ -85.8°C (-122.5°F) with testing and acceptance criteria per ASME Section III, Subsection NB, Article NB-2430 and Article NB-2330	Drop Test Not Required
Containment Shell	SA-203 E/ SA-350 LF3	64 (2.5)	$T_{NDT} \leq$ -74.7°C (-102.5°F) with testing and acceptance criteria per ASME Section III, Subsection NB, Article NB-2330	$T_{NDT} \leq$ -74.7°C (-102.5°F) per R.G. 7.11	$T_{NDT} \leq$ -85.8°C (-122.5°F) with testing and acceptance criteria per ASME Section III, Subsection NB, Article NB-2330	$T_{NDT} \leq$ -85.8°C (-122.5°F) per R.G. 7.11
Containment Closure Flange	SA-350 LF3	245 (9.6)	$T_{NDT} \leq$ -93.9°C (-137°F) with testing and acceptance criteria per ASME Section III, Subsection NB, Article NB-2330	$T_{NDT} \leq$ -93.9°C (-137°F) per R.G 7.12.	$T_{NDT} \leq$ -82.2°C (-116°F) with testing and acceptance criteria per ASME Section III, Subsection NB, Article NB-2330	$T_{NDT} \leq$ -82.2°C (-116°F) per fracture initiation criteria developed in the NUREG-CR-3826 (Notes 4 and 5)
Containment Baseplate	SA-203 E/ SA-350 LF3	151 (6)	$T_{NDT} \leq$ -89.4°C (-129°F) with testing and acceptance criteria per ASME Section III, Subsection NB, Article NB-2330	$T_{NDT} \leq$ -89.4°C (-129°F) per R.G 7.12.	$T_{NDT} \leq$ -71.7°C (-97°F) with testing and acceptance criteria per ASME Section III, Subsection NB, Article NB-2330	$T_{NDT} \leq$ -71.7°C (-97°F) per fracture initiation criteria developed in the NUREG-CR-3826 (Notes 4 and 5)

Table 8.1.9: Fracture Toughness Test Criteria: Containment System (Sheet 2 of 3)

Item	Material	Thickness mm (in.)	Qualification to LST of -29^{0}C (-20^{0}F) (Note 3)		Qualification to LST of -40^{0}C (-40^{0}F) (Note 3)	
			Charpy V-Notch Temperature	**Drop Test Temperature (Note 1)**	**Charpy V-Notch Temperature**	**Drop Test Temperature (Note 1)**
Inner Closure Lid	SA-203 E/ SA-350 LF3	254 (10)	$T_{NDT} \leq$ -94.4°C (-138°F) with testing and acceptance criteria per ASME Section III, Subsection NB, Article NB-2330	$T_{NDT} \leq$ -94.4°C (-138°F) per R.G. 7.12	$T_{NDT} \leq$ -83.3°C (-118°F) with testing and acceptance criteria per ASME Section III, Subsection NB, Article NB-2330	$T_{NDT} \leq$ -83.3°C (-118°F) per fracture initiation criteria developed in the NUREG-CR-3826 (Notes 4 and 5)
Outer Closure Lid	SA-203 E/ SA-350 LF3	135 (5.3)	$T_{NDT} \leq$ -88.3°C (-127°F) with testing and acceptance criteria per ASME Section III, Subsection NB, Article NB-2330	$T_{NDT} \leq$ -88.3°C (-127°F) per R.G. 7.12	$T_{NDT} \leq$ -69.4°C (-93°F) with testing and acceptance criteria per ASME Section III, Subsection NB, Article NB-2330	$T_{NDT} \leq$ -69.4°C (-93°F) per fracture initiation criteria developed in the NUREG-CR-3826 (Notes 4 and 5)

Table 8.1.9: Fracture Toughness Test Criteria: Containment System (Sheet 3 of 3)

Item	Material	Thickness mm (in.)	Qualification to LST of -29⁰C (-20⁰F) (Note 3)		Qualification to LST of -40⁰C (-40⁰F) (Note 3)	
			Charpy V-Notch Temperature	Drop Test Temperature (Note 1)	Charpy V-Notch Temperature	Drop Test Temperature (Note 1)
Inner Closure Lid Bolt	SA-564 630 / SA-705 630	42 (1.65)	Cv (lateral expansion): minimum 25 mils (per Table NB-2333-1) for each of three specimens. (Note 2) Min. test temperature = -29ºC	No requirements (per Table NB-2333-1)	Cv (lateral expansion): minimum 25 mils (per Table NB-2333-1) for each of three specimens. (Note 2) Min. test temperature = -40ºC	No requirements (per Table NB-2333-1)
Outer Closure Lid Bolt	SA-564 630 / SA-705 630	36 (1.41)	Cv (lateral expansion): minimum 25 mils (per Table NB-2333-1) for each of three specimens. (Note 2) Min. test temperature = -29ºC	No requirements (per Table NB-2333-1)	Cv (lateral expansion): minimum 25 mils (per Table NB-2333-1) for each of three specimens. (Note 2) Min. test temperature = -40ºC	No requirements (per Table NB-2333-1)

Notes:

1. Materials to be tested in accordance with ASTM E208-87a or subsequent edition.
2. An additional Charpy absorbed energy requirement of 5 ft-lb at -29ºC (-20ºF) or at -40⁰C (-40⁰F), depending on the desired cask LST qualification, is imposed on the closure lid bolts.
3. Per Reg. Guide 7.8 [2.1.4],the LST which applies to impactive loads is -29⁰C (-20⁰F). The cask may be qualified to either to an LST of either -29⁰C (-20⁰F) or -40⁰C (-40⁰F).
4. Component to undergo 100% volumetric examination to confirm absence of flaws which exceed the critical values as defined in NUREG/CR-3826 Table 3. 100% volumetric re-examination is required for cask components qualified per NUREG/CR-3826 following cask operations which result in impactive or impulsive loadings in excess of those defined in the normal conditions of transport.
5. In lieu of qualification per NUREG/CR-3826, qualification per R.G. 7.12 may be applied.

Table 8.1.10: This table is intentionally not used.

Table 8.1.11: Properties of Holtite-B for Shielding Function

Property (Note 1)	Property Value
Minimum Bulk Density, g/cm^3	1.248
Minimum Hydrogen Density, g/cm^3	0.1068
Minimum Boron Carbide Content, wt%	2
Other Requirements (See Note 2)	
Requirement	Value
Minimum Copper Content, wt%	10
Maximum Copper Content, wt%	12

Notes:
1. All properties are critical characteristics.
2. The copper content is specified to achieve the minimum bulk density.

8.2 MAINTENANCE PROGRAM

An ongoing maintenance program for the HI-STAR 180D Package will be prepared and issued prior to the delivery and first use of the HI-STAR 180D Package as a part of its O&M Manual. This document shall delineate the detailed inspections, testing, and parts replacement necessary to ensure continued radiological safety, proper handling, and containment performance of the HI-STAR 180D Package in accordance with 10CFR71 regulations, conditions in the Certificate of Compliance, and the design requirements and criteria contained in this Safety Analysis Report (SAR).

The HI-STAR 180D package is totally passive by design. There are no active components or systems required to assure the continued performance of its safety functions. As a result, only minimal maintenance will be required over its lifetime, and this maintenance would primarily result from weathering effects, and pre- and post-usage requirements for transportation. Typical of such maintenance would be the reapplication of corrosion inhibiting materials on accessible external surfaces, seal replacement, and leak testing following seal replacement. Such maintenance requires methods and procedures no more demanding than those currently in use at nuclear power plants.

A maintenance inspections and tests program schedule for the HI-STAR 180D Package is provided in Table 8.2.1.

8.2.1 Structural and Pressure Tests

No periodic structural or pressure tests on the packaging following the initial acceptance tests are required to verify continuing performance.

8.2.2 Leakage Tests

A pre-shipment leakage rate test of cask double closure lid containment seals is performed following fuel loading. This pre-shipment leakage rate test is valid for 1 year. If the pre-shipment leakage rate test expires, a periodic leakage rate test of the containment seals must be performed prior to transport. This periodic leakage rate test is valid for 1 year.

Maintenance leakage rate testing shall be performed prior to returning a package to service following maintenance, repair (such as a weld repair), or replacement of containment system components (such as containment seal replacement and/or removal of closure bolts/plugs). Only that portion of the containment system that is affected by the maintenance, repair or component replacement needs to be leak tested. Leakage rate tests on the cask containment system shall be performed per written and approved procedures in accordance with the requirements of ANSI N14.5.

Table 8.1.1 specifies the allowable leakage rate and test sensitivity in terms of helium leak tightness. Table 8.1.2 specifies the components subject to testing for fabrication, pre-shipment, periodic and maintenance leakage rate tests.

Leakage rate testing procedures shall be approved by an American Society for Nondestructive Testing (ASNT) Level III specialist in leak testing for the nondestructive method(s) of leak testing for which the procedures are written. The written and approved test procedures shall clearly define the test equipment arrangement. Leakage rate testing shall be performed by personnel who are qualified and certified in accordance with the requirements of SNT-TC-1A [8.1.2]. Leakage rate testing shall be performed in accordance with a written quality assurance program.

8.2.3 Component and Material Tests

8.2.3.1 Pressure Relief Devices

The neutron shield pressure relief devices shall be visually inspected for damage or indications of excessive corrosion prior to each transport of the HI-STAR 180D package. If the inspection determines an unacceptable condition, the neutron shield pressure relief devices shall be replaced. The neutron shield pressure relief devices shall be replaced periodically while the cask is in service as recommended by the manufacturer's O&M manual.

8.2.3.2 Shielding Materials

Periodic verification of the neutron shield integrity shall be performed within 5 years prior to shipment. The periodic verification shall be performed by radiation measurements with either loaded contents or a check source. Measurements shall be taken at three cross sectional planes through the radial shield and at four points along each plane's circumference. The average measurement results from each sectional plane shall be compared to calculated values to assess the continued effectiveness of the neutron shield. The calculated values shall be representative of the loaded contents (i.e., fuel type, enrichment, burnup, cooling time, etc…) or the particular check source used for the measurements.

8.2.3.3 Packaging Surfaces

Accessible external surfaces of the packaging (including impact limiters) shall be visually inspected for damage prior to each fuel loading to ensure that the packaging effectiveness is not significantly reduced. Visual inspections of the cask and impact limiters shall be performed for external surface coating and component damage including surface denting, surface penetrations, weld cracking, chipped or missing coating. Where necessary, cask coatings shall be reapplied. Damage shall be evaluated for impact on packaging safety and shall be repaired or replaced accordingly. Wear and tear from normal use will not impact cask safety. Repairs or replacement in accordance with written and approved procedures, as set down in the O&M manual, shall be required if unacceptable conditions are identified.

Prior to installation or replacement of a closure seal, the cask sealing surface shall be cleaned and visually inspected for scratches, pitting or roughness, and affected surface areas shall be polished smooth or repaired as necessary in accordance with written and approved procedures.

8.2.3.4 Packaging Fasteners

Cask closure fasteners and impact limiter fasteners shall be visually inspected for damage such as excessive wear, galling, or indentations on the threaded surfaces prior to installation. The severity of thread damage shall be evaluated per standard industry practice. Damaged fasteners shall be replaced accordingly. Damaged internal threads may be repaired per standard industry practice (e.g. threaded inserts). Any repair shall be evaluated to ensure ASME Code stress limits applicable to bolted closure joints are met. Any required material or manufacturing process testing would also be performed in accordance with ASME Section III, Subsection NB.

Bolting of both Inner and Outer Closure Lids, including Inner Closure Lid Port Covers, shall be replaced as guided by fatigue analysis per the provisions of Section III of the ASME Code. The maintenance program in Table 8.2.1 provides a bolt change out schedule to insure that the cumulative damage factor accumulated by a bolt shall be less than 1.0 with sufficient margin. One bolting cycle is the complete sequence of torquing and removal of bolts.

Containment Closure Flange internal threads for closure bolts have a maximum service life limit based on bolting cycles as determined by fatigue analysis per the provisions of Section III of the ASME Code. The bolting cycles specified in Table 8.2.1 shall not be exceeded. One bolting cycle is the complete sequence of torquing and removal of bolts.

8.2.3.5 Cask Trunnions and Trunnion Replacement Plugs

Cask trunnions shall be inspected prior to each fuel loading. The accessible parts of the trunnions (areas outside the cask), and the local cask areas shall be visually examined to verify no deformation, distortion, or cracking has occurred. Any evidence of deformation (other than minor localized surface deformation due to contact pressure between lifting device and trunnion), distortion or cracking of the trunnion or adjacent cask areas shall require repair or replacement of the trunnion and/or repair of the cask. Following any replacements and/or repair, the load testing shall be re-performed and the components re-examined in accordance with the original procedure and acceptance criteria.

8.2.3.6 Closure Seals

The HI-STAR 180D Packaging is equipped with metallic closure seals on the inner and outer closure lids and other penetration closure joints to ensure leak tightness. The closure seals are shipped from the factory pre-inspected and carefully packaged. Once installed and compressed, the seals should not be disturbed by removal of closure fasteners. Removal of closure fasteners requires replacement of closure seals and performance of a Maintenance Leakage Rate Test for closure seals classified as containment boundary seals. Closure seals are specified for long-term use and do not require additional maintenance.

8.2.3.7 Fuel Basket

No additional tests are required for the HI-STAR 180D fuel basket. Long-term fuel basket integrity has been ensured by fuel basket design and by extensive material testing. The essential fuel basket predicates including the effects of creep and irradiation, lateral deflection, protection against crack propagation and tearing, and B-10 area density, in conjunction with the minimum guaranteed values (MGVs) provided in Table 8.1.5 ensure that the fuel basket will meet its performance requirements.

8.2.4 Thermal Tests

For each package, a periodic thermal performance test shall be performed at least once within the 5 years prior to shipment to demonstrate that the thermal capabilities of the cask remain within its design basis.

This test may be performed immediately after a HI-STAR 180D Package is loaded with spent nuclear fuel. The in-service test is performed to verify a continued adequate rate of heat dissipation from the cask to the environment. Acceptable performance under test conditions ensures that design basis fuel cladding temperature limits to which the HI-STAR 180D Package is qualified under design basis heat loads will not be exceeded during transport.

Prior to performing the test, thermal equilibrium of the HI-STAR 180D Package shall be verified by measuring the temperature at a defined point near the mid-plane of the HI-STAR 180D Package at one hour intervals using a calibrated thermocouple or surface pyrometer. Appropriate criteria defining when thermal equilibrium is achieved shall be determined based on a variety of ambient test conditions and incorporated into the test procedure.

After thermal equilibrium is established, temperatures shall be measured and recorded using a calibrated thermocouple or surface pyrometer at four equally spaced circumferential locations at the mid height of the active fuel. The decay heat load and fuel cycle history of the fuel assemblies loaded in the HI-STAR 180D Package shall also be recorded. These records shall become part of the maintenance program quality records for the HI-STAR 180D Package.

The HI-STAR 180D Package is considered acceptable if the average measured surface to ambient temperature differential indicated in the procedure, when adjusted for environmental conditions, is not exceeded.

8.2.5 Miscellaneous Tests

No additional tests are required for the HI-STAR 180D Packaging, packaging components, or packaging materials.

Table 8.2.1
Maintenance Inspections and Tests Program Schedule

Task	Schedule
Cask surface visual inspection. (See Paragraph 8.2.3.3)	Prior to each fuel loading
Cask closure fasteners/bolts visual inspection (See Paragraph 8.2.3.4)	Prior to installation and/or prior to each transport
Cask trunnion visual inspection (See Paragraph 8.2.3.5.)	Prior to each fuel loading
Impact limiter and impact limiters fasteners visual inspection (See Paragraph 8.2.3.3 and 8.2.3.4)	Prior to installation and/or prior to each transport
Neutron shield pressure relief device visual inspection (See Paragraph 8.2.3.1)	Prior to each transport
Pre-shipment leakage test of containment system seals (See Subsection 8.2.2)	Following each fuel loading
Periodic leakage rate test of containment system seals (See Subsection 8.2.2)	Prior to off-site package transport if period from last test exceeds 1 year.
Seal replacement for Inner and Outer Closure Lids (See Paragraph 8.2.3.6)	Following removal of closure bolting
Bolt replacement (*Service Life*) for Inner and Outer Closure Lids (See Paragraph 8.2.3.4)	Every 225 bolting cycles for SA-564/705 630 Every 277 bolting cycles for SB-637
Bolt replacement (*Service Life*) for Inner Closure Lid Port Cover Bolts (See Paragraph 8.2.3.4)	558 bolting cycles for the bolt specified in drawing package referenced in the CoC.
Containment Closure Flange internal closure bolt thread *Service Life* (See Paragraph 8.2.3.4)	1000 bolting cycles for the bolt specified in drawing package referenced in the CoC.
Seal replacement for Outer Closure Lid Access Port Plug (See Paragraph 8.2.3.6)	Following removal of applicable access port plug
Seal replacement for Inner Closure Lid Port Covers (See Paragraph 8.2.3.6)	Following removal of applicable port cover fasteners
Neutron shield pressure relief device replacement (See Paragraph 8.2.3.1)	If required by the manufacturer's O&M manual
Shielding Test (See Paragraph 8.2.3.2)	Within 5 years prior to shipment
Thermal Test (See Subsection 8.2.4)	Within 5 years prior to shipment
Maintenance Leakage Rate Test (See Subsection 8.2.2)	Following maintenance, repair or replacement of containment system components

CHAPTER 8 REFERENCES

The following generic industry and Holtec produced references may have been consulted in the preparation of this document. Where specifically cited, the identifier is listed in the SAR text or table. Active Holtec Calculation Packages or Technical Reports, which are the repository of all relevant licensing and design basis calculations, are annotated as "latest revision". Submittal of the latest revision of such Calculation Packages to the USNRC and other regulatory authorities during the course of regulatory reviews is managed under the company's Configuration Control system.

[8.0.1] U.S. Code of Federal Regulations, Title 10, "Energy", Part 71, "Packaging and Transportation of Radioactive Materials."

[8.1.1] American Society of Mechanical Engineers, "Boiler and Pressure Vessel Code," Sections II, III, V, IX, and XI, 2007 Edition, 2008 Addenda (Section IX, 2013 for FSW only unless otherwise indicated).

[8.1.2] American Society for Nondestructive Testing, "Personnel Qualification and Certification in Nondestructive Testing," Recommended Practice No. SNT-TC-1A, Revision as required by the ASME Code [8.1.1] or as required by ANSI N14.5 [8.1.6].

[8.1.3] American National Standards Institute, Institute for Nuclear Materials Management, "American National Standard for Radioactive Materials - Special Lifting Devices for Shipping Containers Weighing 10,000 Pounds (4500 kilograms) or More", ANSI N14.6, September 1993.

[8.1.4] U.S. Nuclear Regulatory Commission, "Fracture Toughness Criteria of Base Material for Ferritic Steel Shipping Cask Containment Vessels with a Maximum Wall Thickness of 4 Inches (0.1m)," Regulatory Guide 7.11, June 1991.

[8.1.5] U.S. Nuclear Regulatory Commission, "Fracture Toughness Criteria of Base Material for Ferritic Steel Shipping Cask Containment Vessels with a Wall Thickness Greater than 4 Inches (0.1m) But Not Exceeding 12 Inches (0.3m)," Regulatory Guide 7.12, June 1991.

[8.1.6] American National Standards Institute, Institute for Nuclear Materials Management, "American National Standard for Radioactive Materials Leakage Tests on Packages for Shipment", ANSI N14.5, 2014.

[8.1.7] Holtec International Document DOC-5014-03, "Acceptance Testing of First HI-STAR Overpack (Thermal and He Leak Tests)", September 2006.

[8.1.8] "Metamic-HT Manufacturing Manual", Latest Revision, Holtec International (Holtec Proprietary).

[8.1.9] "Metamic-HT Purchasing Specification", Holtec Document ID PS-11, Latest Revision, (Holtec Proprietary).

[8.1.10] American Society for Testing and Materials, ASTM D7336 / D7336M-16, "Standard Test Method for Static Energy Absorption Properties of Honeycomb Sandwich Core Materials".

Appendix 8.A: CONTAINMENT BOUNDARY SEAL DATA

The information in Tables 8.A-1, 8.A-2, 8.A-3 and 8.A-4 provides the complete description of containment boundary seal options for the HI-STAR 180D package. The critical characteristics of containment seals include the Seal Cross Section Diameter, Groove Depth, Seating Load, Seal Springback, Minimum Seal/Groove radial clearance, Sealing Surface Finish Range, and Seal Materials and Material Combinations. Seal Seating Load and Springback are defined in Table 2.2.12. Springback is not specified for the inner closure lid port covers and outer lid access port plug since it is not essential to maintaining leaktightness in these joints. The approved seal designs and corresponding seal part/drawing numbers are defined in the tables that follow. Use of other seal designs or changes to critical characteristics as defined in the tables requires prior NRC approval.

Table 8.A-1 Inner Lid Seals

Seal Property	Seal Option 1	Seal Option 2
Seal Manufacturer	American Seal & Engineering	Technetics
Seal Part/Drawing Number	050545 / 050546	HN-200 / H-313506 & H-313507
Inner Seal Groove OD "ODg" (mm [inches])	1901.39 +0.64/-0.00 [74.858 +0.025/-0.000]	1901.70 +1.52/-0.00 [74.870 +0.060/-0.000]
Inner Seal, Seal OD "ODs" (mm [inches])	1899.51 +0.00/-1.02 [74.784 +0.000/-0.040]	1900.61 +/-0.25 [74.827 +/- 0.010]
Outer Seal Groove ID "IDg" (mm [inches])	1917.52 +0.00/-0.64 [75.493 +0.000/-0.025]	N/A
Outer Seal, Seal ID "IDs" (mm [inches])	1919.40 +1.02/-0.00 [75.567 +0.040/-0.000]	N/A
Outer Seal Groove OD "ODg" (mm [inches])	N/A	1951.48 +1.52/-0.00 [76.830 +0.060/-0.000]
Outer Seal Seal OD "ODs" (mm [inches])	N/A	1950.39 +/-0.25 [76.787 +/-0.010]
Groove Width "W" (mm [inches])	15.34 +1.52/-0.00 [0.604 +0.060/-0.000]	17.15 +/- 0.25 [0.675 +/- 0.010]
Groove Height "H" - Min/Max (mm [inches])	10.16 / 10.41 [0.400 / 0.410]	10.69 +/- 0.13 [0.421 +/- 0.005]
Seal Cross Section Diameter – Min / Max (mm [inches])	12.60 / 12.80 [0.496 / 0.504]	11.56 / 12.07 [0.455 / 0.475]
Seal Seating Load, +/-10% (N/mm [lbs/inch])	560 [3200]	545 [3100]
Surface Finish Requirement for Sealing Surfaces (μm [μin])	0.4c [16c]	1.6-3.2 c [63-125c]
Component Materials	Spring: X750 Jacket: X750 Plating: Silver	Spring: Nimonic 90 Lining: 304L Jacket: Silver

Table 8.A-2 Outer Lid Seals

Seal Property	Seal Option 1	Seal Option 2
Representative Seal Manufacturer	American Seal & Engineering	Technetics
Seal Part/Drawing Number	050547 / 050548	HN-200 / H-313504 & H-313505
Inner Seal Groove OD “ODg” (mm [inches])	2144.65 +0.76/-0.00 [84.435 +0.030/0.00]	2145.03 +1.52/-0.00 [84.450 +0.060/-0.000]
Inner Seal, Seal OD “ODs” (mm [inches])	2142.77 +0.00/-1.27 [84.361 +0.000/-0.050]	2143.94 +/-0.25 [84.407 +/-0.010
Outer Seal Groove ID “IDg” (mm [inches])	2160.91 +0.00/-0.76 [85.075 +0.000/-0.030]	N/A
Outer Seal, Seal ID “IDs” (mm [inches])	2162.78 +1.27/-0.00 [85.149 +0.050/-0.000]	N/A
Outer Seal Groove OD “ODg” (mm [inches])	N/A	2194.81 +1.52/-0.00 [86.410 +0.060/-0.000]
Outer Seal Seal OD “ODs” (mm [inches])	N/A	2193.72+/-0.25 [86.367+/-0.010]
Groove Width “W” (mm [inches])	15.34 +1.52/-0.00 [0.604 +0.060/-0.000]	17.15 +/- 0.25 [0.675 +/- 0.010]
Groove Height “H” - Min/Max (mm [inches])	10.16 / 10.41 [0.400 / 0.410]	10.69 +/- 0.13 [0.421 +/- 0.005]
Seal Cross Section Diameter – Min / Max (mm [inches])	12.60 / 12.80 [0.496 / 0.504]	11.56 / 12.07 [0.455 / 0.475]
Seal Seating Load +/-10% (N/mm [lbs/inch])	560 [3200]	545 [3100]
Surface Finish Requirement for Sealing Surfaces (μm [μin])	0.4c [16c]	1.6-3.2 c [63-125c]
Component Materials	Spring: X750 Jacket: X750 Plating: Silver	Spring: Nimonic 90 Lining: 304L Jacket: Silver

Table 8.A-3 Inner Port Cover Seals		
Seal Property	Seal Option 1	Seal Option 2
Seal Manufacturer	American Seal & Engineering	Technetics
Seal Part/Drawing Number	050332/050333	HN-100 / H-313508 & H-313509
Inner Seal Groove OD "ODg" (mm [inches])	92.84 +0.13/-0.00 [3.655 +0.005/-0.000]	93.73 +0.10/0.00 [3.690 +0.004/-0.000]
Inner Seal, Seal OD "ODs" (mm [inches])	92.50 +0.00/-0.23 [3.642 +0.000/-0.009]	93.42 +/-0.10 [3.678 +/-0.004]
Outer Seal Groove ID "IDg" (mm [inches])	103.17 +0.00/-0.13/ [4.062 +0.000/-0.005]	N/A
Outer Seal, Seal ID "IDs" (mm [inches])	103.50 +0.23/-0.00 [4.075 +0.009/-0.000]	N/A
Outer Seal Groove OD "ODg" (mm [inches])	N/A	109.50 +0.10/-0.00 [4.311 +0.004/0.000]
Outer Seal Seal OD "ODs" (mm [inches])	N/A	109.19 +/-0.10 [4.299 +/-0.004]
Groove Width "W" (mm [inches])	3.18 +0.76/-0.00 [0.125 +0.030/-0.000]	3.03 +0.76/-0.00 [0.119 +0.030/-0.000]
Groove Height "H" - Min/Max (mm [inches])	1.90 / 2.00 [0.075 / 0.079]	1.14 / 1.24 [0.045 / 0.049]
Seal Cross Section Diameter – Min / Max (mm [inches])	2.34 / 2.44 [0.092 / 0.096]	1.70/1.90 [0.067/0.075]
Seal Seating Load +/-10% (N/mm [lbs/inch])	148 [850]	151 [860]
Surface Finish Requirement for Sealing Surfaces (µm [µin])	0.4c [16c]	1.6-3.2 c [63-125c]
Component Materials	Spring: X750 Jacket: X750 Plating: Silver	Spring: Alloy 90 Jacket: Silver

Table 8.A-4 Outer Lid Access Port Plug Seal		
Seal Property	Seal Option 1	Seal Option 2
Seal Manufacturer	American Seal & Engineering	Technetics
Seal Part/Drawing Number	050415/050415 CAV	HN-100 / H-313510
Seal Groove OD “ODg” (mm [inches])	38.61 +0.10/-0.00 [1.520 +0.004/-0.000]	38.61 +0.10/-0.00 [1.520 +0.004/-0.00]
Seal OD “ODs” (mm [inches])	38.28 +0.00/-0.15 [1.507 +0.000/-0.006]	38.30 +/-0.10 [1.508 +/-0.004]
Seal Cross Section Diameter – Min / Max (mm [inches])	2.34 / 2.44 [0.092 / 0.096]	1.70/1.90 [0.067/0.075]
Groove Height “H” - Min/Max (mm [inches])	1.91 / 2.01 [0.075/0.079]	1.14 / 1.24 [0.045 / 0.049]
Seal Seating Load +/- 10% (N/mm [lbs/inch])	148 [850]	151 [860]
Surface Finish Requirement for Sealing Surfaces (µm [µin])	0.4c [16c]	1.6-3.2c [63-125c]
Component Materials	Spring: X750 Jacket: X750 Plating: Silver	Spring: Alloy 90 Jacket: Silver